



Department of Electrical & Electronics Engineering

Course Title: Electrical and Hybrid Vehicles (GR18A4014)

Following documents are available in Course File.

S.No.	Points	Yes	No
1	Institute and Department Vision and Mission Statements	√	
2	PEO & PO Mapping	√	
3	Academic Calendar	√	
4	Subject Allocation Sheet	√	
5	Class Time Table, Individual Timetable (Single Sheet)	√	
6	Syllabus Copy	√	
7	Course Handout	√	
8	CO-PO Mapping	√	
9	CO-Cognitive Level Mapping	√	
10	Lecture Notes	√	
11	Tutorial Sheets With Solution	√	
12	Soft Copy of Notes/Ppt/Slides	√	
13	Sessional Question Papers and Scheme of Evaluation	√	
14	Best, Average and Weak Answer Scripts for Each Sessional Exam. (Photocopies)	√	
15	Assignment Questions and Solutions	√	
16	Previous Question Papers	√	
17	Result Analysis	√	
18	Feedback From Students	√	
19	CO Attainment for All Mids.	√	
20	Remedial Action.		√

Course Instructor / Course Coordinator

Course Instructor / Course Coordinator)

DAVU SRINIVASA RAO
Assistant Professor
EEE Department



GOKARAJU RANGARAJU

INSTITUTE OF ENGINEERING AND TECHNOLOGY

Department of Electrical and Electronics Engineering

Vision of the Institute

To be among the best of the institutions for engineers and technologists with attitudes, skills and knowledge and to become an epicentre of creative solutions.

Mission of the Institute

To achieve and impart quality education with an emphasis on practical skills and social relevance

Vision of the Department

To impart technical knowledge and skills required to succeed in life, career and help society to achieve self sufficiency.

Mission of the Department

1. To become an internationally leading department for higher learning.
2. To build upon the culture and values of universal science and contemporary education.
3. To be a center of research and education generating knowledge and technologies which lay groundwork in shaping the future in the fields of electrical and electronics engineering.
4. To develop partnership with industrial, R&D and government agencies and actively participate in conferences, technical and community activities.



Department of Electrical and Electronics Engineering

This Programme is meant to prepare our students to professionally thrive and to lead. During their progression:

Graduates will be able to

- PEO 1:** Graduates will have a successful technical or professional careers, including supportive and leadership roles on multidisciplinary teams.
- PEO 2:** Graduates will be able to acquire, use and develop skills as required for effective professional practices.
- PEO 3:** Graduates will be able to attain holistic education that is an essential prerequisite for being a responsible member of society.
- PEO 4:** Graduates will be engaged in life-long learning, to remain abreast in their profession and be leaders in our technologically vibrant society.

Programme Outcomes (B.Tech. – EEE)

At the end of the Programme, a graduate will have the ability to

- PO-1:** Ability to apply knowledge of mathematics, science, and engineering.
- PO-2:** Ability to identify, formulate, analyze engineering problems using engineering sciences.
- PO-3:** Ability to design a system, component, or process to meet desired needs within realistic constraints such as economic, environmental, social, political, ethical, health and safety..
- PO-4:** Ability to design and conduct experiments, as well as to analyze and interpret data with valid conclusions.
- PO-5:** Ability to utilize experimental, statistical and computational methods and tools necessary for modelling engineering activities.
- PO-6:** Ability to apply reasoning informed by the relative knowledge to evaluate societal, health, safety, legal and cultural issues and tasks applicable to the professional engineering practice.
- PO-7:** Ability to adapt broad education necessary to understand the impact of engineering solutions and obtain sustainability in a global, economic, environmental, and societal context.
- PO-8:** Ability to discover ethical principles and bind to professional and ethical responsibility.
- PO-9:** Ability to function as an individual and in multi-disciplinary teams.
- PO-10:** Ability to communicate effectively on complex activities in engineering community and society.
- PO-11:** Ability to develop Project management principles and apply in various disciplinary environments.
- PO-12:** Recognition of the need for, and an ability to engage in life-long learning

Program Specific Outcomes(PSOs):

- PSO-1:** Graduates will interpret data and able to analyze digital and analog systems related to electrical and programming them.
- PSO-2:** Graduates will able to demonstrate, design and model electrical, electronic circuits, power electronics, power systems and electrical machines.



Gokaraju Rangaraju Institute of Engineering and Technology
(Autonomous)
Bachupally, Kukatpally, Hyderabad – 500 090, India

GRIET/DAA/1H/G/22-23

19 July 2022

Revised Academic Calendar
Academic Year 2022-23

IV B.Tech – First Semester

S. No.	EVENT	PERIOD	DURATION
1	Commencement of First Semester class work	04-07-2022	
2	I Spell of Instructions	04-07-2022 to 03-09-2022	9 Weeks
3	I Mid-term Examinations	05-09-2022 to 07-09-2022	3 Days
4	II Spell of Instructions	08-09-2022 to 11-11-2022	9 Weeks
5	II Mid-term Examinations	14-11-2022 to 16-11-2022	3 Days
6	Preparation	17-11-2022 to 23-11-2022	1 Week
7	End Semester Examinations (Theory/ Practical) Regular/ Supplementary	24-11-2022 to 14-12-2022	3 Weeks
8	Commencement of Second Semester, AY 2022-23	16-12-2022	

IV B.Tech – Second Semester

S. No.	EVENT	PERIOD	DURATION
1	Commencement of Second Semester class work	16-12-2022	
2	I Spell of Instructions	16-12-2022 to 13-02-2023	9 Weeks
3	I Mid-term Examinations	14-02-2023 to 16-02-2023	3 Days
4	II Spell of Instructions	17-02-2023 to 26-04-2023	10 Weeks
5	II Mid-term Examinations	27-04-2023 to 29-04-2023	3 Days
6	Preparation & Summer Vacation	01-05-2023 to 13-05-2023	2 Weeks
7	End Semester Examinations (Theory/ Practical) Regular / Supplementary	15-05-2023 to 03-06-2023	3 Weeks

J. Praveen



[Signature]

Dean Academic Affairs

Copy to Principal, All HoDs, CoE



GOKARAJU RANGARAJU
INSTITUTE OF ENGINEERING AND TECHNOLOGY
Department of Electrical and Electronics Engineering

Faculty Work load for the Academic Year 2022-23 / I SEM
Subject Allocation Sheet

S.No	Faculty	Designation	Faculty ID	YEAR (UG/PG)	Subject Name	No.of Sections	No. of Hours	Total (in Hrs)
2	Dr B Phaneendra Babu	Prof. & HOD	1563	II B.Tech	DCM	1	5	11
				II M.Tech	Dph 1	1	3	
				II M.Tech	DLED	1	3	
3	Dr.D G Padhan	Prof.	1283	III B.Tech	EHV	1	5	11
				I M.Tech	EHV	1	3	
				II M.Tech	IS	1	3	
4	Dr. J. Sridevi	Prof.	516	III B.Tech	PSA	1	6	11
				III B.Tech	PS Lab	1	5	
5	Dr T Suresh Kumar	Prof.	1494	II B.Tech	EMF	1	5	11
				I Mtech	PE Lab	1	3	
				I Mtech	MSPEC	1	3	
6	V.Vijaya Rama Raju	Asso. Prof.	361	II B.Tech	PGT	1	5	11
				II B.Tech	DCM Lab	1	6	
7	P Ravikanth	Asso. Prof.	1178	II B.Tech	PAE	1	5	14
				III B.Tech	NPTEL	1	3	
				IV B.Tech	ED Lab	1	6	
8	A Vinay Kumar	Asso. Prof.	881	IV B.Tech	HVE	2	10	16
				IV B.Tech	PWK	1	3	
				I M.Tech	PQ&FACTS	1	3	



GOKARAJU RANGARAJU
INSTITUTE OF ENGINEERING AND TECHNOLOGY
Department of Electrical and Electronics Engineering

9	Syed Sarfaraz Nawaz	Asso. Prof.	695	Electrical Maintenance Officer				
10	Dr Pakkiraiah B	Asso. Prof.	1593	III B.Tech	PE Lab	1	5	14
				I M.Tech	IPR	1	3	
				III B.Tech	PE Lab	1	6	
11	Dr D Naga Mallesara Rao	Asso. Prof.	1598	IV B.Tech	ED	2	10	16
				IV B.Tech	ED Lab	1	6	
12	Dr P Sri Vidya Devi	Asso. Prof.	931	III B.Tech	MC Lab	1	6	11
				IV B.Tech	PS-III	1	5	
13	Dr D Raveendhra	Asso. Prof.	1604	I M.Tech	MAEM	1	3	11
				I M.Tech	PQ Lab	1	3	
				III B.Tech	MC	1	5	
14	P.Praveen Kumar	Asst. Prof	609	I B.Tech	1 st Year BEE			
15	R. Anil Kumar	Asst. Prof	657	I B.Tech	I st Year BEE			
16	U Vijaya Lakshmi	Asst. Prof	692	II B.Tech	PAE Lab	1	6	15
				III B.Tech	PS Lab	1	6	
				I B.Tech	BEE Lab	1	3	
17	D Karuna Kumar	Asst. Prof	760	II B.Tech	CI	1	2	14
				IV B.Tech	ED Lab	1	6	
				I B.Tech	BEE Lab	2	6	
19	M Naga Sandhya Rani	Asst. Prof	882	III B.Tech	MC Lab	1	6	14
				II B.Tech	BEEE	1	5	
				IV B.Tech	PWK	1	3	
20	G Sandhya Rani	Asst. Prof	888	II B.Tech	ECA	1	5	14



GOKARAJU RANGARAJU
INSTITUTE OF ENGINEERING AND TECHNOLOGY
Department of Electrical and Electronics Engineering

				III B.Tech	PE Lab	1	6	
				IV B.Tech	PWK	1	3	
21	M Rekha	Asst. Prof	933	II B.Tech	DCM Lab	1	6	15
				III B.Tech	PE Lab	1	6	
				I B.Tech	BEE Lab	1	3	
22	V Usha Rani	Asst. Prof	1045	IV B.Tech	ED Lab	1	6	12
				III B.Tech	PS Lab	1	6	
23	P Prashanth Kumar	Asst. Prof	1055	I B.Tech	BEE	1	6	20
				IV B.Tech	PS-III	1	5	
				I B.Tech	BEE Lab	3	9	
24	K Sudha	Asst. Prof	1211	I B.Tech	1 st Year BEE			
25	M Prashanth	Asst. Prof	1279	II B.Tech	PAE Lab	1	6	14
				II B.Tech	VEGC	1	2	
				I B.Tech	BEE Lab	2	6	
26	D Srinivasa Rao	Asst. Prof	1540	IV B.Tech	EHV	2	10	13
				IV B.Tech	PWK	1	3	



Gokaraju Rangaraju Institute of Engineering and Technology

Department of Electrical and Electronics Engineering

GRIET/PRIN/06/G/01/22-23

BTech - EEE - A

Wef : 13th June 2022

IV Year - I Semester

DAY/ HOUR	10:20-11:15	11:15-12:10	12:10-01:05	01:05-01:40	01:40-02:30	02:30-03:20	03:20-04:10
MONDAY	HVE		ED	BREAK	PS-III		RB/DBMS
TUESDAY	PS-III		RB/DBMS		ED Lab/PW-I		
WEDNESDAY	PS-III	EHV			HVE		-
THURSDAY	ED		RB/DBMS		PW-I/ED Lab		
FRIDAY	RB/DBMS		Mentoring		EHV		HVE
SATURDAY	EHV	ED			PW-I		
Course Code	Course Name				Faculty Code	Faculty Name (Emp ID)	
GR18A4012	Power Systems-III (PS-III)			Dr PSVD	Dr. P. Srividya Devi (931)		
GR18A4013	Electroncis Design (ED)			Dr DSNM	Dr. D. S. Naga Malleswara Rao (1598)		
GR18A4014	Electrical and Hybrid Vehicles (EHV)			DSR	D. Srinivasa Rao (1540)		
GR18A4021	High Voltage Engineeering (HVE)			AVK	A Vinay Kumar (881)		
GR18A4022	Electronic Design Lab (ED Lab)			VUR/ DKK	V. Usharani/ D. Karuna Kumar (1045/760)		
GR18A4061	Project Work Phase - I (PW-I)			AVK/DSR	A. Vinay Kumar/D Srinivasa Rao (881/1540)		
GR18A4079/ GR18A2068	Robotics (RB)/ Data Base Management System (DBMS)			Dr. AAL/DS	Dr. A. Anitha Lakshmi (AAL) (944)/ D. Swathi (1681)		

ROOM NO	
Theory/Tutorial	4404
Lab	MP Phase I - 4404 ED Lab - 4407
Class Incharge:	M. N. Sandhya Rani

Almanac	
1st Spell of Instructions	13-06-2022 to 06-08-2022
1st Mid-term Examinations	08-08-2022 to 11-08-2022
2nd Spell of Instructions	12-08-2022 to 06-10-2022
2nd Mid-term Examinations	07-10-2022 to 11-10-2022
Preparation	12-10-2022 to 18-10-2022
End Semester Examinations (Theory/ Practicals) Regular / Supplementary	19-10-2022 to 08-11-2022

Time Table Coordinator

HOD

DAA



Gokaraju Rangaraju Institute of Engineering and Technology

Department of Electrical and Electronics Engineering

GRIET/PRIN/06/G/01/22-23

BTech - EEE - B

Wef : 13th June 2022

IV Year - I Semester

DAY/ HOUR	10:20-11:15	11:15-12:10	12:10-01:05	01:05-01:40	01:40-02:30	02:30-03:20	03:20-04:10
MONDAY	PS-III	EHV		BREAK	ED		RB/DBMS
TUESDAY	HVE		RB/DBMS		EHV		-
WEDNESDAY	PS-III		HVE		PW-I/ED Lab		
THURSDAY	PS-III	EHV	RB/DBMS		Mentoring	ED	
FRIDAY	RB/DBMS		ED		ED Lab/PW-I		
SATURDAY	HVE		PS-III		PW-I		
Course Code	Course Name				Faculty Code	Faculty Name (Emp ID)	
GR18A4012	Power Systems-III (PS-III)			PK	P. Prasanth Kumar (1055)		
GR18A4013	Electroncis Design (ED)			Dr DSNM	Dr. D. S. Naga Malleswara Rao (1598)		
GR18A4014	Electrical and Hybrid Vehicles (EHV)			DSR	D. Srinivasa Rao (1540)		
GR18A4021	High Voltage Engineeering (HVE)			AVK	A Vinay Kumar (881)		
GR18A4022	Electronic Design Lab (ED Lab)			PRK/Dr. DSNMR	P. Ravi Kanth/ Dr. D. S. Naga Malleswara Rao (1178/1598)		
GR18A4061	Project Work Phase - I (PW-I)			GSR/MNSR	G. Sandhya Rani/M. N. Sandhya Rani(888/882)		
GR18A4079/ GR18A2068	Robotics (RB)/ Data Base Management System (DBMS)			Dr. AAL/DS	Dr. A. Anitha Lakshmi (AAL) (944)/ D. Swathi (1681)		

ROOM NO	
Theory/Tutorial	4412
Lab	MP Phase I - 4412 ED Lab - 4407
Class Incharge:	M. N. Sandhya Rani

Almanac	
1st Spell of Instructions	13-06-2022 to 06-08-2022
1st Mid-term Examinations	08-08-2022 to 11-08-2022
2nd Spell of Instructions	12-08-2022 to 06-10-2022
2nd Mid-term Examinations	07-10-2022 to 11-10-2022
Preparation	12-10-2022 to 18-10-2022
End Semester Examinations (Theory/ Practicals) Regular / Supplementary	19-10-2022 to 08-11-2022

Time Table Coordinator

HOD

DAA



GOKARAJU RANGARAJU

INSTITUTE OF ENGINEERING AND TECHNOLOGY
Department of Electrical and Electronics Engineering

Faculty Name: D SRINIVASA RAO							
DAY/ HOUR	10.20- 11.15	11.15- 12.10	12.10- 1.05	1.05- 1.40	1.40- 2.30	2.30 - 3.20	3:20 -4.10
MONDAY				LUNCH			
TUESDAY							
WEDNESDAY	EHV						
THURSDAY							
FRIDAY					EHV		
SATURDAY	EHV						



**GOKARAJU RANGARAJU INSTITUTE OF ENGINEERING AND TECHNOLOGY
(Autonomous)**

Department of Electrical and Electronics Engineering

**ELECTRICAL AND HYBRID VEHICLES
(Professional Elective –III)**

**Course Code: GR18A4014
IV year I semester**

L:3 P:0 T:0 C:3

COURSE OBJECTIVES:

At the end of this course, the student should be able to

1. Explain basic concepts of electric traction.
2. Demonstrate Vehicle Brake Performance..
3. Analyze power flow control in hybrid drive-train topologies
4. Discuss electric components used in hybrid and electric vehicles.
5. Select the energy storage technology for Hybrid and Electric Vehicles.

COURSE OUTCOMES:

At the end of this course, students will demonstrate the ability to

1. Summarize various electric drive train topologies.
2. Explain Brake System of EV, HEV, and FCV.
3. Identify various hybrid drive-train topologies
4. Analyze the configuration and control of different motor drives.
5. Interpret the different possible ways of energy storage requirements in Hybrid and Electric Vehicles.

Syllabus:

UNIT 1: Introduction to Electric Traction:

Basic concept of electric traction, introduction to various electric drive train topologies, power flow control in electric drive-train topologies, fuel efficiency analysis.

UNIT 2: Braking fundamentals and Regenerative braking in Electric Vehicles:

General Description of Vehicle Movement, Vehicle Resistance, Dynamic Equation, Tire–Ground Adhesion and Maximum Tractive Effort, Power Train Tractive Effort and Vehicle Speed, Vehicle Power Plant and Transmission Characteristics, Brake Performance.

Braking Energy Consumed in Urban Driving, Braking Energy on Front and Rear Axles, Brake System of EV, HEV, and FCV- Parallel Hybrid Braking System, Fully Controllable Hybrid Brake System.

UNIT 3: Introduction to Conventional and Electric Vehicles:

History of hybrid and electric vehicles, social and environmental importance of hybrid and electric vehicles, impact of modern drive-trains on energy supplies.

Hybrid Electric Drive-trains: Basic concept of hybrid traction, introduction to various hybrid drive-train topologies, power flow control in hybrid drive-train topologies, fuel efficiency analysis.

Introduction to ICE vehicles, Introduction to pure EV's (BEV, FCV).

UNIT 4: Electric Propulsion unit:

Introduction to electric components used in hybrid and electric vehicles, Configuration and control of DC Motor drives, Configuration and control of Induction Motor drives, configuration and control of Permanent Magnet Motor drives, Configuration and control of Switch Reluctance Motor drives, drive system efficiency.

UNIT 5: Energy Storage Requirements in Hybrid and Electric Vehicles:

Introduction to Energy Storage Requirements in Hybrid and Electric Vehicles, Battery based energy storage and its analysis, Fuel Cell based energy storage and its analysis, Super Capacitor based energy storage and its analysis, Flywheel based energy storage and its analysis, Hybridization of different energy storage devices. Matching the electric machine and the internal combustion engine (ICE), Sizing the propulsion motor, sizing the power electronics, selecting the energy storage technology, Communications, supporting subsystems.

Text/Reference Books:

1. C. Mi, M. A. Masrur and D. W. Gao, "Hybrid Electric Vehicles: Principles and Applications with Practical Perspectives", John Wiley & Sons, 2011.
2. S. Onori, L. Serrao and G. Rizzoni, "Hybrid Electric Vehicles: Energy Management Strategies", Springer, 2015.
3. M. Ehsani, Y. Gao, S. E. Gay and A. Emadi, "Modern Electric, Hybrid Electric, and Fuel Cell Vehicles: Fundamentals, Theory, and Design", CRC Press, 2004.
4. T. Denton, "Electric and Hybrid Vehicles", Routledge, 2016.



GOKARAJU RANGARAJU

INSTITUTE OF ENGINEERING AND TECHNOLOGY

Department of Electrical and Electronics Engineering

Course Outcomes-Program Outcomes (POs) Relationship Matrix (Relationships are indicated by mark HIGH as “H” and MEDIUM as “M”)- COI

		P-Outcomes											
C-Outcomes		1	2	3	4	5	6	7	8	9	10	11	12
	1	M				M			M			M	
	2	M	M		M	M	M	M	H		M	H	H
	3	M				M					M	M	
	4	H	M	M	M	H	M		H	M	M	H	M
	5	M			M	H	M	H	M	M	H	M	M



GOKARAJU RANGARAJU
INSTITUTE OF ENGINEERING AND TECHNOLOGY
Department of Electrical and Electronics Engineering

Branch: EEE Subject Code: GR18A4014 Academic Year: 2022-23 Regulation: GR18 Year: IV Semester: I

ELECTRICAL AND HYBRID VEHICLES (GR18A4014)

L:3 T:0 P:0 C:3

Syllabus

UNIT 1: Introduction to Electric Traction:

Basic concept of electric traction, introduction to various electric drive train topologies, power flow control in electric drive-train topologies, fuel efficiency analysis.

UNIT 2: Braking fundamentals and Regenerative braking in Electric Vehicles:

General Description of Vehicle Movement, Vehicle Resistance, Dynamic Equation, Tire–Ground Adhesion and Maximum Tractive Effort, Power Train Tractive Effort and Vehicle Speed, Vehicle Power Plant and Transmission Characteristics, Brake Performance.

Braking Energy Consumed in Urban Driving, Braking Energy on Front and Rear Axles, Brake System of EV, HEV, and FCV- Parallel Hybrid Braking System, Fully Controllable Hybrid Brake System.

UNIT 3: Introduction to Conventional and Electric Vehicles:

History of hybrid and electric vehicles, social and environmental importance of hybrid and electric vehicles, impact of modern drive-trains on energy supplies.

Hybrid Electric Drive-trains: Basic concept of hybrid traction, introduction to various hybrid drive-train topologies, power flow control in hybrid drive-train topologies, fuel efficiency analysis. Introduction to ICE vehicles, Introduction to pure EV's (BEV, FCV).

UNIT 4: Electric Propulsion unit:

Introduction to electric components used in hybrid and electric vehicles, Configuration and control of DC Motor drives, Configuration and control of Induction Motor drives, configuration and control of Permanent Magnet Motor drives, Configuration and control of Switch Reluctance Motor drives, drive system efficiency.

UNIT 5: Energy Storage Requirements in Hybrid and Electric Vehicles:

Introduction to Energy Storage Requirements in Hybrid and Electric Vehicles, Battery based energy storage and its analysis, Fuel Cell based energy storage and its analysis, Super Capacitor based energy storage and its analysis, Flywheel based energy storage and its analysis, Hybridization of different energy storage devices. Matching the electric machine and the internal combustion engine (ICE), Sizing the propulsion motor, sizing the power electronics, selecting the energy storage technology, Communications, supporting subsystems.

Electric Traction

The action of pulling something over a surface (especially a road or a track) is known as **traction**. The action of drawing of vehicles by electric power derived from overhead wires, third rail, storage batteries or diesel generators mounted on the vehicles is known as **electric traction**. In simple words, the traction system which uses electric power for its operation is known as **electric traction**.

The electric traction system is widely used in electric trains, tramcars, trolley buses and hybrid vehicles, etc.

Advantages of Electric Traction

The major advantages of electric traction system over other types of traction (such as steam traction) are described below –

- **Cleanliness** – Electric traction is free from smoke and flue gases, etc.

Therefore, it is most suitable type of traction system to be used for underground and tubular railways.

- **Less starting time** – Electric locomotives can be starting without any loss of time.
- **Less maintenance cost & time** – The maintenance cost of an electric traction system is about half of that of steam traction system and also the time required for maintenance is quite low.

- **High starting torque** – The motor used in electric traction is DC series motor or AC series motor which has a very high starting torque. Hence, the electric locomotives has very high acceleration about 1.5 to 2.5 kmphps.
- **High traffic handling capacity** – As the electric locomotives have high acceleration which makes the traffic handling capacity almost double of that of the steam locomotive.
- **Require lesser terminal space** – As the electric traction has high traffic handling capacity. Therefore, it needs lesser terminal space because quicker disposal of passengers to destination is there and hence gathering is reduced.

Disadvantages of Electric Traction

In spite of the fact that the electric traction has so many advantages, it suffers from many disadvantages which are given below –

- Electric traction has high capital cost due to overhead equipment, so electric traction becomes uneconomical unless heavy traffic is to be handled.
- In electric traction, a power failure for few minutes causes distortion in traffic.
- Electric traction can be used only at the places which are electrified.
- Electric traction is tied to electric routes.
- Power lines for electric traction causes disturbance in neighboring communication lines.

- **A non-electric traction system** is a type of traction system that does not use electrical energy for the movement of a vehicle at any stage.
- Types of Non-Electric Traction System
- The most popular non-electric traction systems are –
- Steam Engine Drive
- Internal Combustion (IC) Engine Drive or Diesel Engine Drive
- **Steam Engine Drive**
- In the steam engine drives, the reciprocating steam engine is used for getting the required motive power. The steam engine drive is not used in these days due to various reasons. However, it is still employed for traction work in underdeveloped countries.

• Advantages of Steam Engine Drive

The advantages of steam engine drive based traction system include the following –

- Steam engine drives are simple in design.
- The maintenance of steam engine drives is easy and less costly.
- Steam engine drives provide easy speed control.
- Steam engine drives do not have interference with neighboring communication lines.
- The capital cost of steam engine drives is low. As these do not require track electrification.
- In case of steam engine drives, there is simplicity of connections between the cylinders and the driving wheels.
- In case of steam engine drives, the locomotive and train unit is self-contained. Hence, it is not tied to a route.
- This type of traction system is cheap for low density traffic areas.

Internal Combustion Engine Drive or Diesel Engine Drive

- The drive which uses an internal combustion (IC) engine or a diesel engine for getting the necessary motive power. The internal combustion engine drive is widely used in railway work. When IC engine drive operating at normal speed, it has an efficiency of about 25%.

- **Advantages of I.C. Engine Drive**

- The chief advantages of the internal combustion engine drive are as follows –
- The initial cost of installing diesel engine drive is low.
- As it is a self-contained unit, it is not tied to any route.
- The internal combustion engine locomotive can run on different track conditions.
- IC engine locomotive has higher efficiency than steam locomotive.
- In case of internal combustion engine locomotive, the braking system used is simple.
- IC engine drive has simple and easy speed control.

Electric and Hybrid Electric Vehicles



Course Content

- Unit 1

HISTORY OF HYBRID AND ELECTRIC VEHICLES

Social and environmental importance of hybrid and electric vehicles, Impact of modern drive-trains on energy supplies, Basics of vehicle performance, vehicle power source characterization, Transmission characteristics, Mathematical models to describe vehicle performance

- Unit 2

BASIC CONCEPT OF HYBRID TRACTION

Introduction to various hybrid drive-train topologies,
Power flow control in hybrid drive-train topologies,
Fuel efficiency analysis, braking fundamentals and
regenerative braking in EVs.

- Unit 3

INTRODUCTION TO ELECTRIC COMPONENTS USED IN HYBRID AND ELECTRIC VEHICLES

Configuration and control of DC Motor drives,
Configuration and control of Induction Motor
drives, configuration and control of Permanent
Magnet Motor Drives, Configuration and control
of Switch Reluctance Motor drives, drive system
efficiency

- Unit 4

MATCHING THE ELECTRIC MACHINE AND THE INTERNAL COMBUSTION ENGINE (ICE)

Sizing the propulsion motor, sizing the power
electronics Selecting the energy storage
technology, Communications, supporting
subsystems

- Unit 5

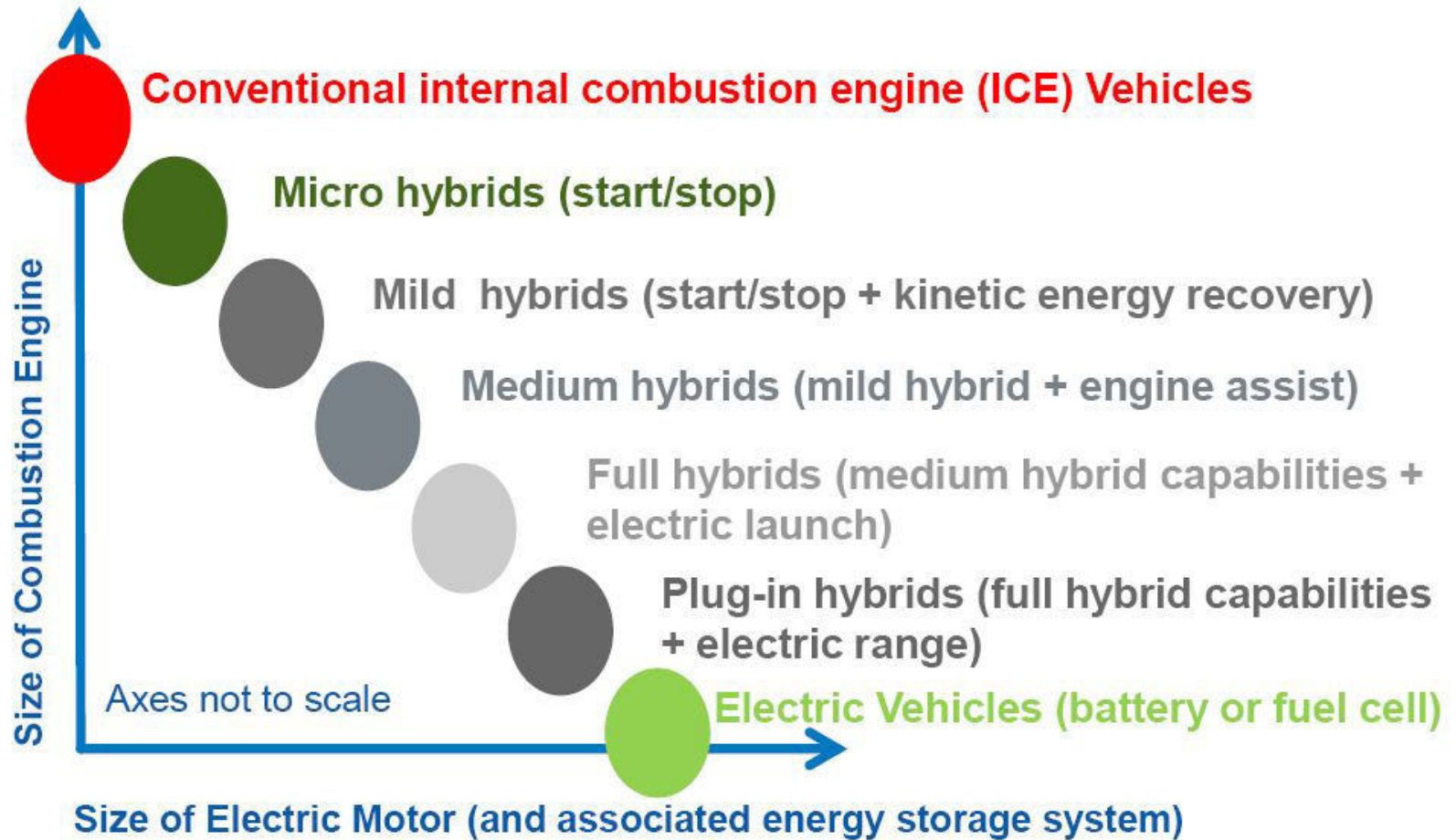
INTRODUCTION TO ENERGY MANAGEMENT AND THEIR STRATEGIES USED IN HYBRID AND ELECTRIC VEHICLE

Classification of different energy management strategies Comparison of different energy management strategies Implementation issues of energy strategies. Plug-in electric vehicles, Vehicle to grid (V2G) and G2V fundamentals.

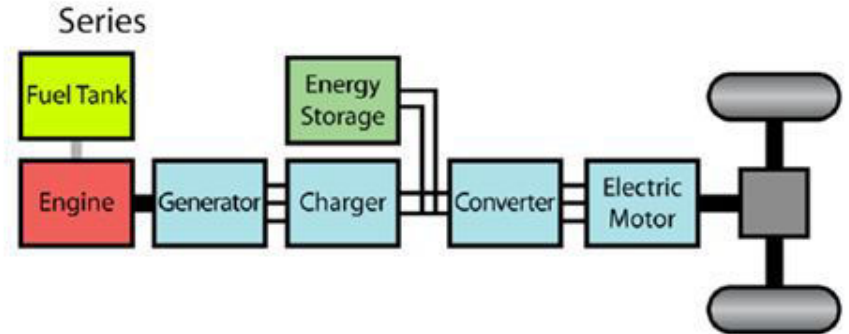
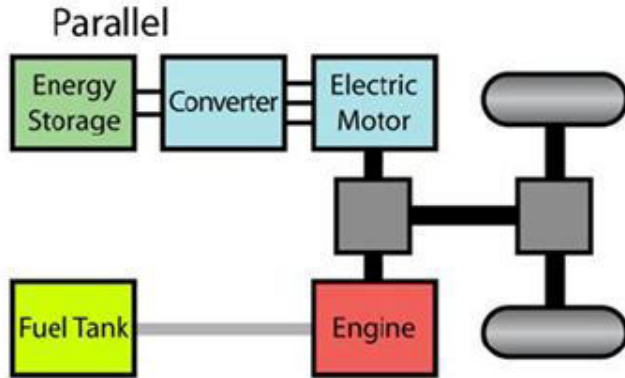
Unit-I and II

EV DriveTrain Topologies

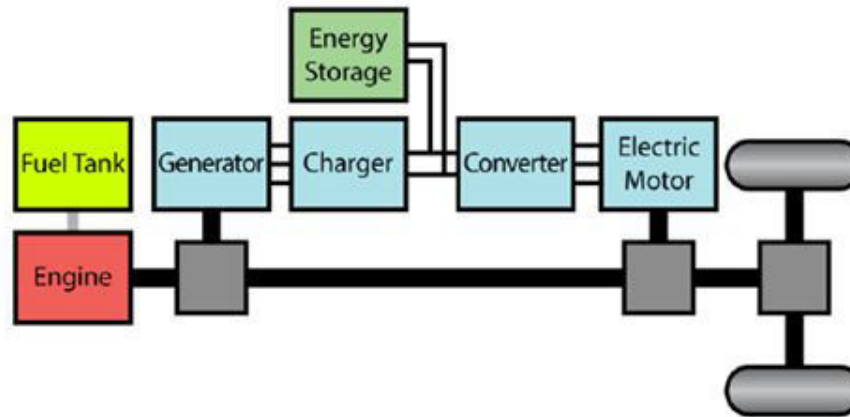
Overview Of Electric Drive Vehicle Technologies



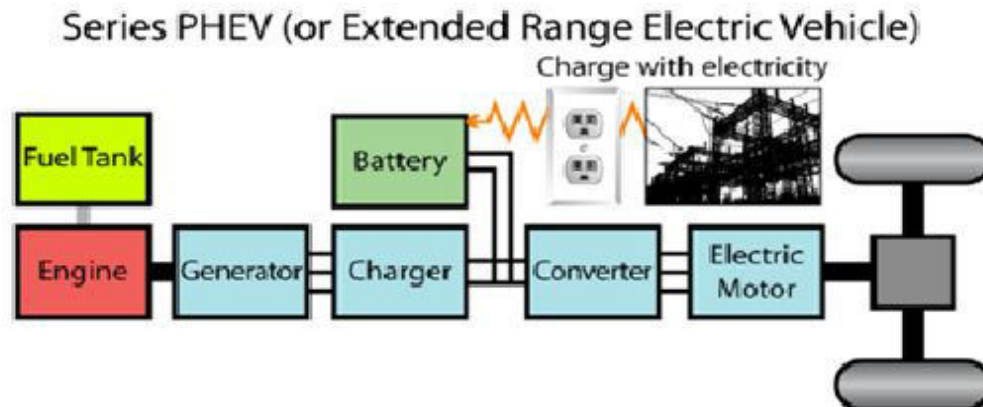
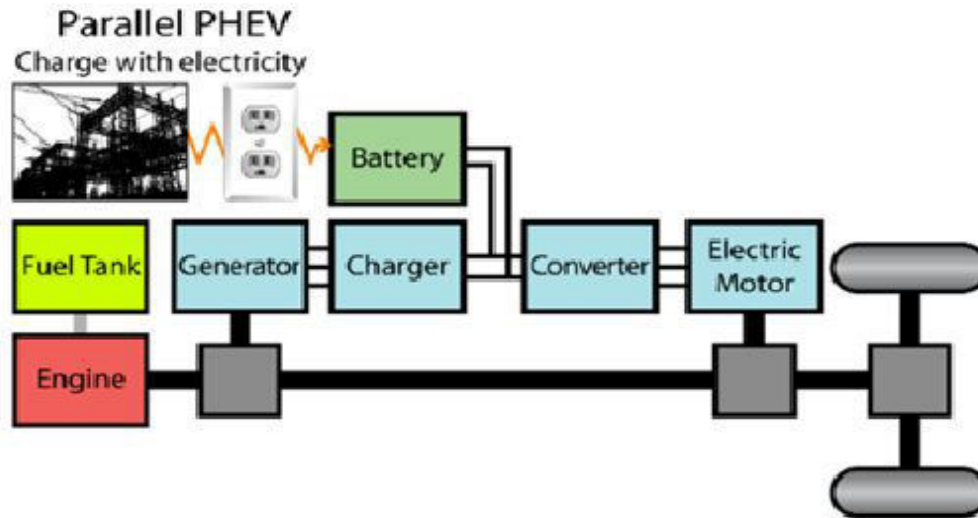
Hybrid Electric Vehicle Configurations



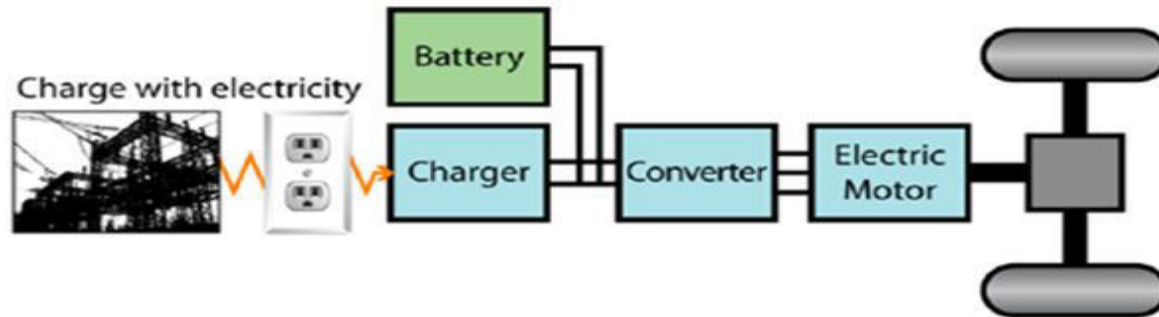
Parallel-Series



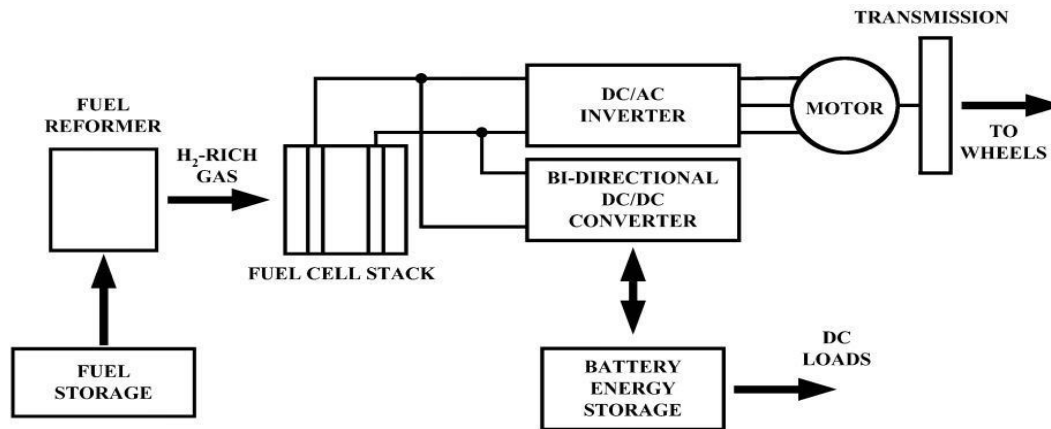
Plug-In Vehicle Configurations



EV configurations

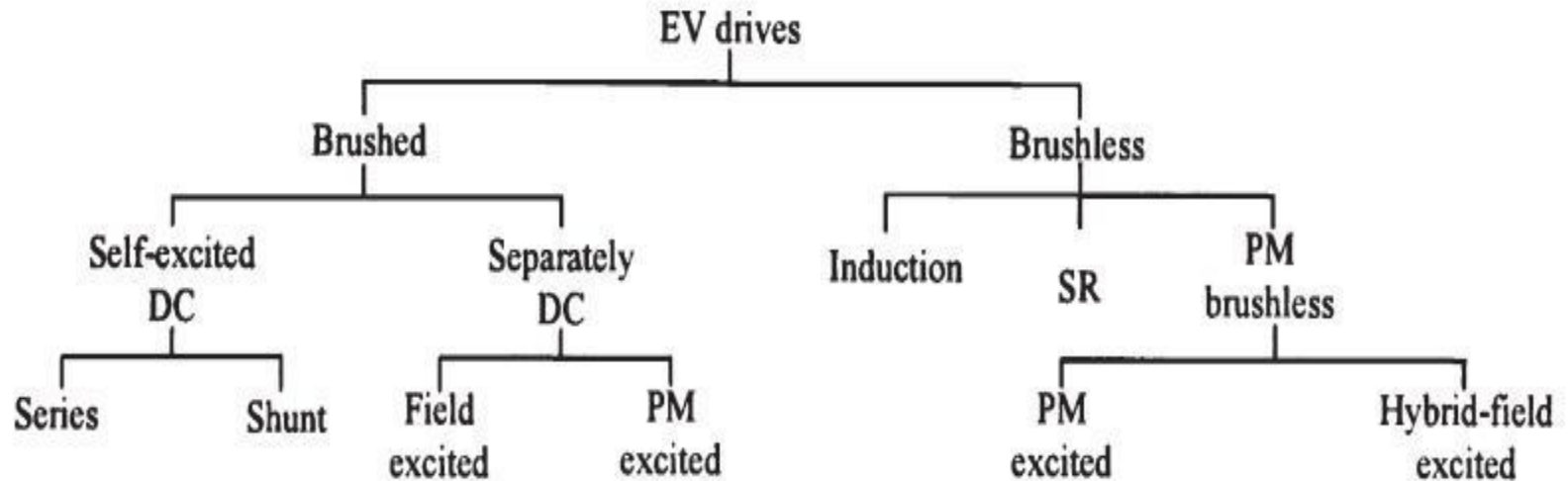


Battery Electric Vehicle



Fuel cell Electric Vehicle

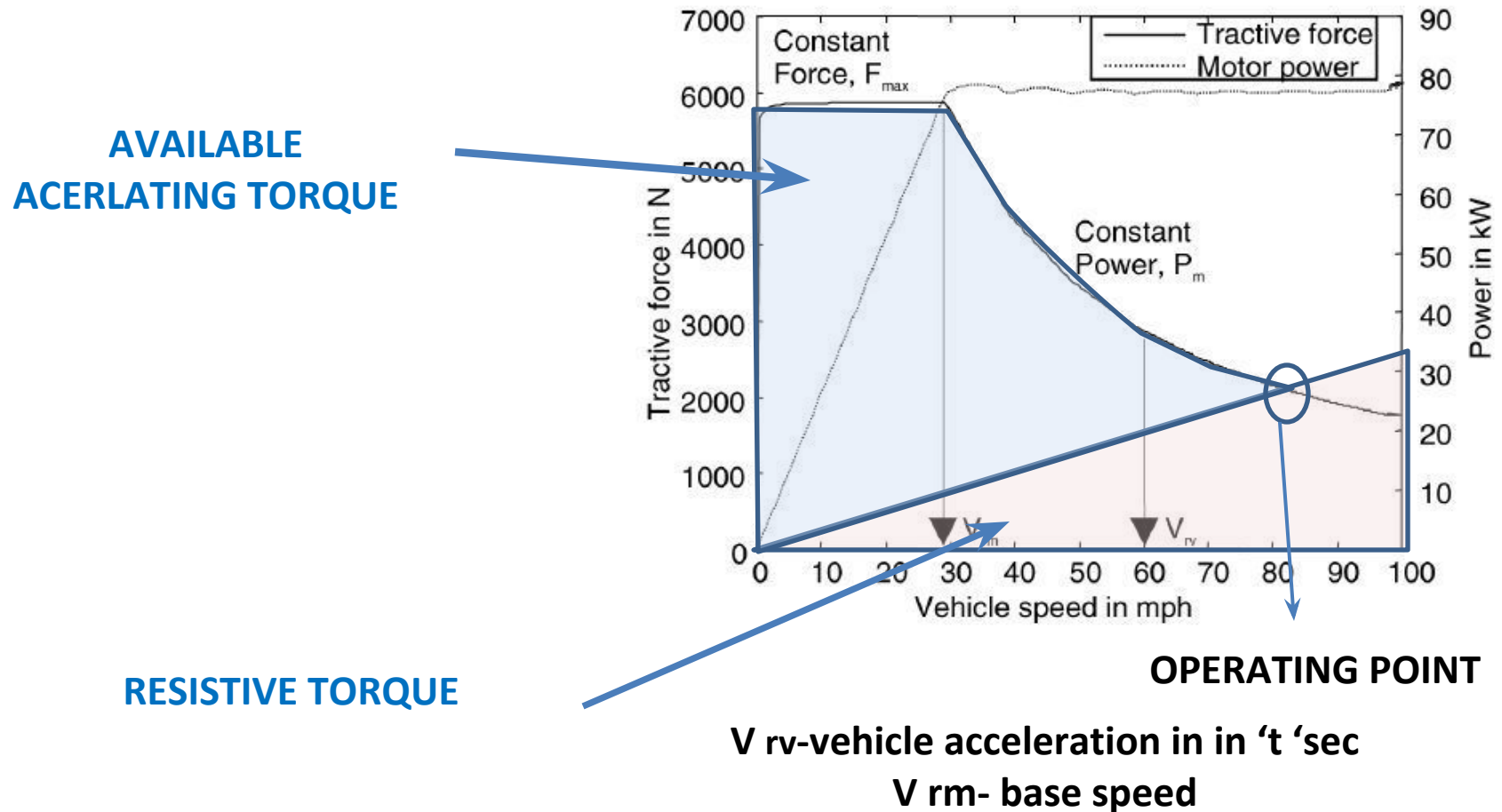
Classification of EV Drives



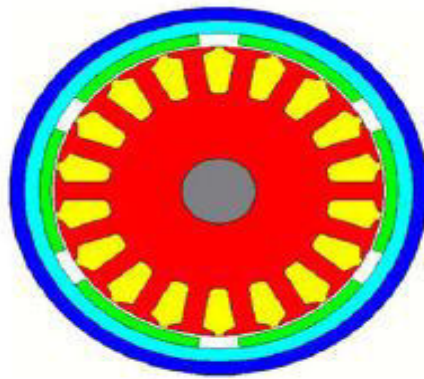
Characteristics for EV Motors

- ✓ High instant power and a high power density;
- ✓ High torque at low speeds for starting and climbing, as well as a high power at high speed for cruising
- ✓ Very wide speed range, including constant-torque and constant-power regions
- ✓ Fast torque response;
- ✓ High efficiency over the wide speed and torque ranges
- ✓ High efficiency for regenerative braking
- ✓ High reliability and robustness for various vehicle operating conditions
- ✓ Reasonable cost.

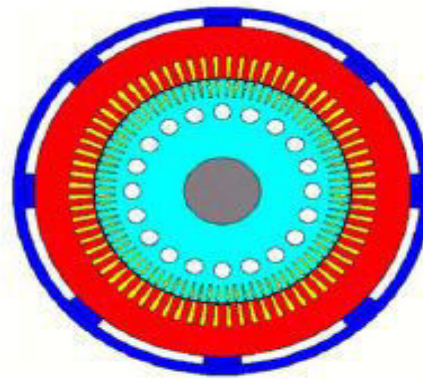
Typical EV Drive characteristics



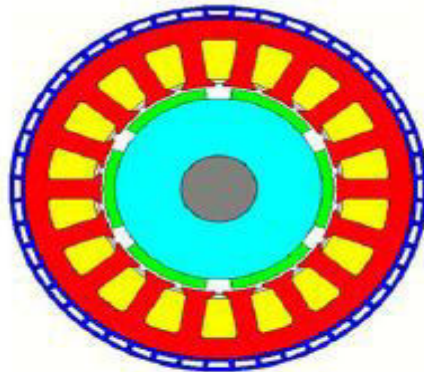
Different types of Electrical Machines Used In Electric Traction



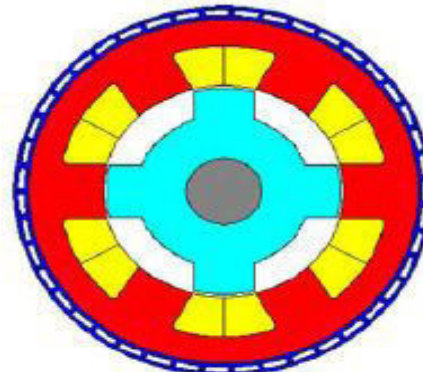
(a)



(b)



(c)



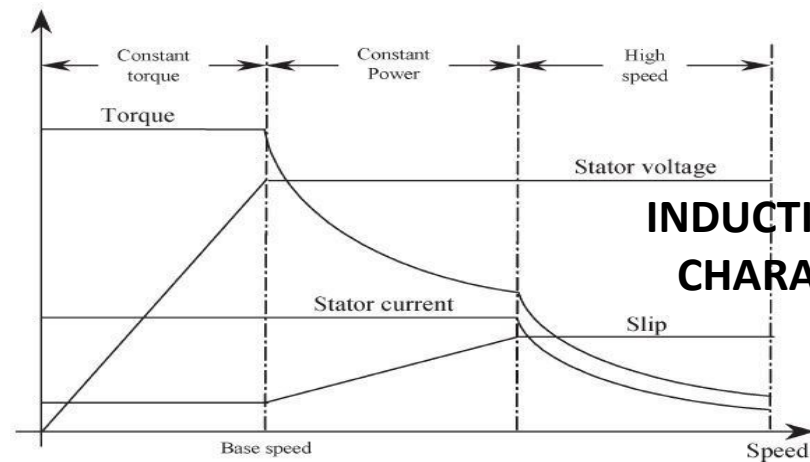
(d)

Industrial and traction motors.

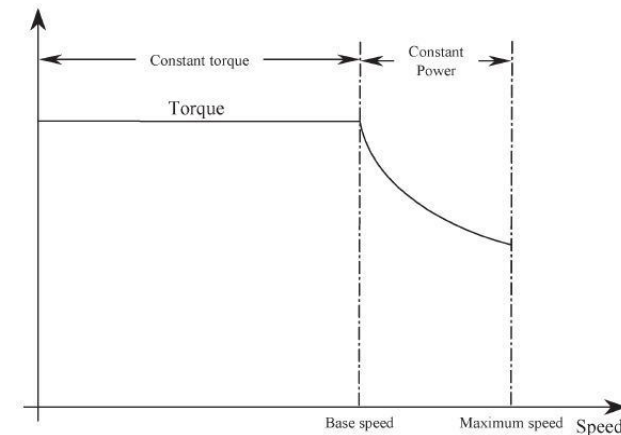
(a) DC motor (b) Induction Motor (c) PM brushless motor. (d) SRM.

✓ For the same maximum speed of the EV PM motor should design with higher base speed due to limited availability of constant power region.

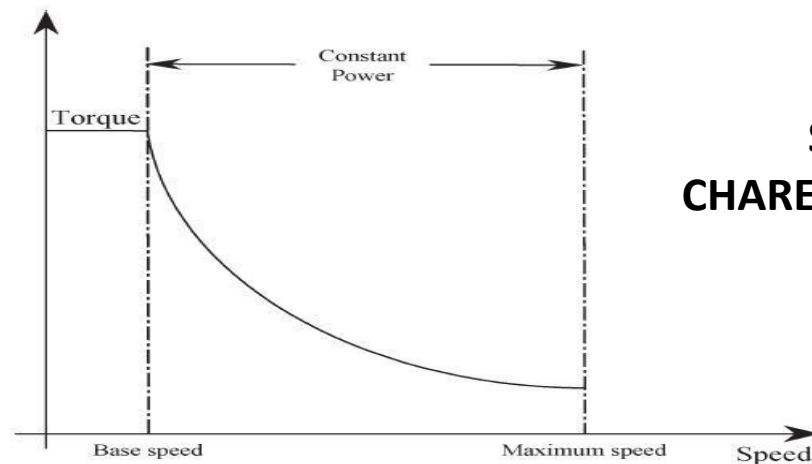
✓ Induction Motor and SRM are having more constant power region compared to PM Motor so motor base speed is less.



**INDUCTION MOTOR
CHARACTERISTIC**



**PM MOTOR
CHARACTERISTIC**


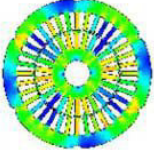
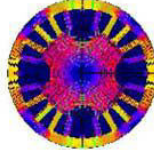
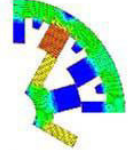






**SRM
CHARACTERISTIC**

Comparison of different Machines






	DC	IM	PM	SRM
Power Density	lowest	High	Highest	High
Efficiency	lowest	High	Highest	High
Controllability	High	Highest	High	Medium
Reliability	Medium	Highest	High	Highest
Technological maturity	Highest	Highest	High	High
Cost	High	Highest	Medium	High

Selection of EV Motor

<i>Propulsion Systems</i> <i>Characteristics</i>	 DC	 IM	 PM	 SRM
<i>Power Density</i>	2.5	3.5	5	3.5
<i>Efficiency</i>	2.5	3.5	5	3.5
<i>Controllability</i>	5	5	4	3
<i>Reliability</i>	3	5	4	5
<i>Technological maturity</i>	5	5	4	4
<i>Cost</i>	4	5	3	4
Σ Total	 22	 27	 25	 23





Evaluation of suitability of EV motor**

****The points are given relatively based on experience and knowledge, these points will vary based on technology developments and cost aspects.**

 PSA Peugeot-Citroën/Berlingo (France)	Dc Motor
 Holden/ECOMmodore (Australia)	Switched Reluctance Motor
 Nissan/Tino (Japan)	Permanent Magnet Synchronous Motor
 Honda/Insight (Japan)	Permanent Magnet Synchronous Motor
 Toyota/Prius (Japan)	Permanent Magnet Synchronous Motor

✓ Every machine has its own advantages and disadvantages for electric vehicle application based on based on load requirements .So one single machine cannot suffice all the needs.

✓ The different manufactures prefer different machines for traction based on evaluation criteria.

 Renault/Kangoo (France)	Induction Motor
 Chevrolet/Silverado (USA)	Induction Motor
 DaimlerChrysler/Durango (Germany/USA)	Induction Motor
 BMW/X5 (Germany)	Induction Motor

Examples of Light-Duty EDVs in the Market

Micro hybrids



CITROËN C3



Smart



BMW 1&3

Stop & Start

Mild hybrids



BMW ED



SATURN VEO



Saturn Aura

Medium hybrids



Chevy Malibu



Mercedes S400



Honda Insight

Full hybrids



Chevy Tahoe



Ford Fusion



Toyota Prius3

Plug-in hybrids



BYD F3DM



Toyota Prius 3



GM Volt

Electric



Honda FCX



Nissan Leaf



iMiev



Renault ZE

+ Electric Range

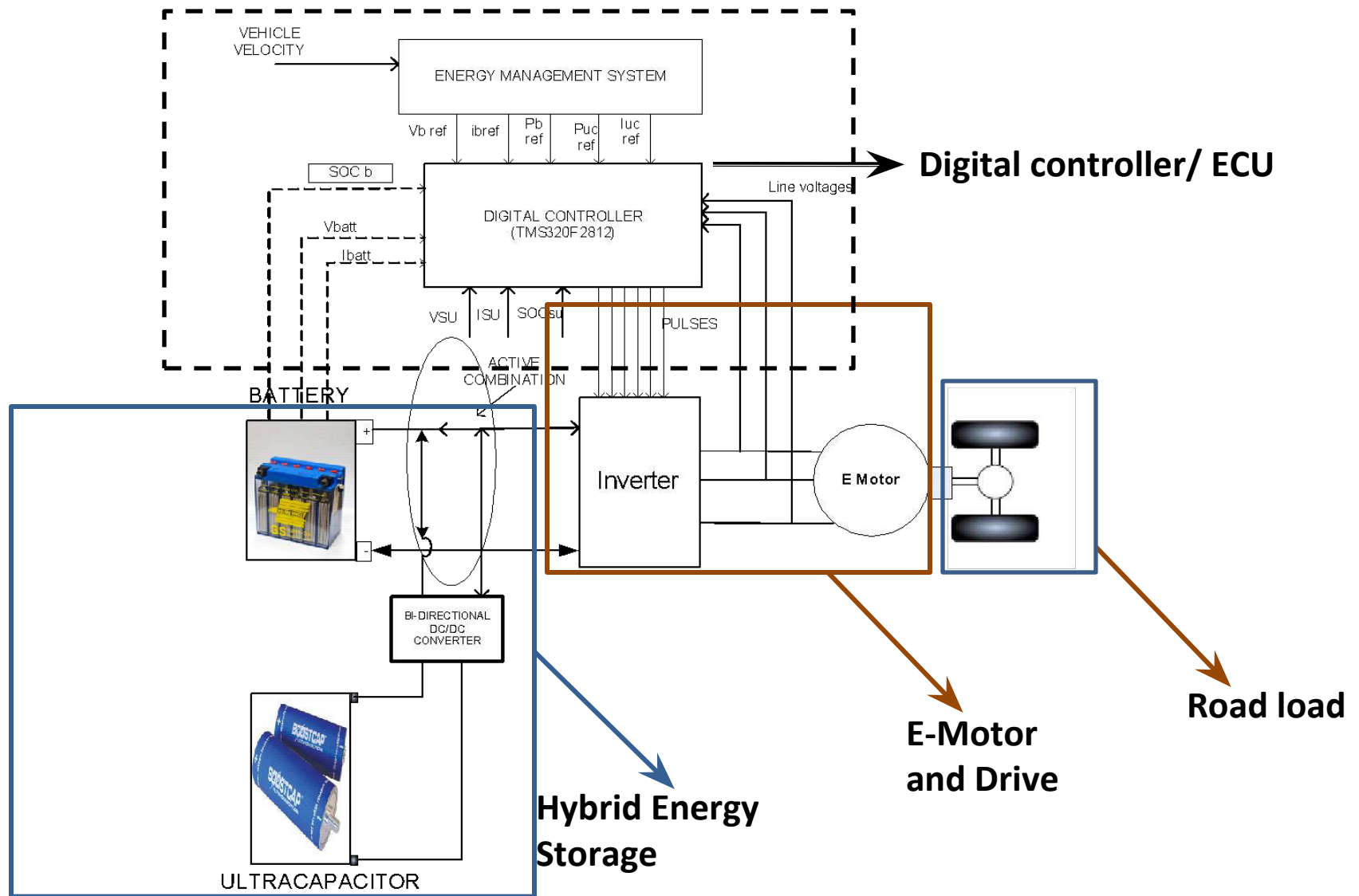
+ Electric Take-off or Launch

+ Engine Assistance

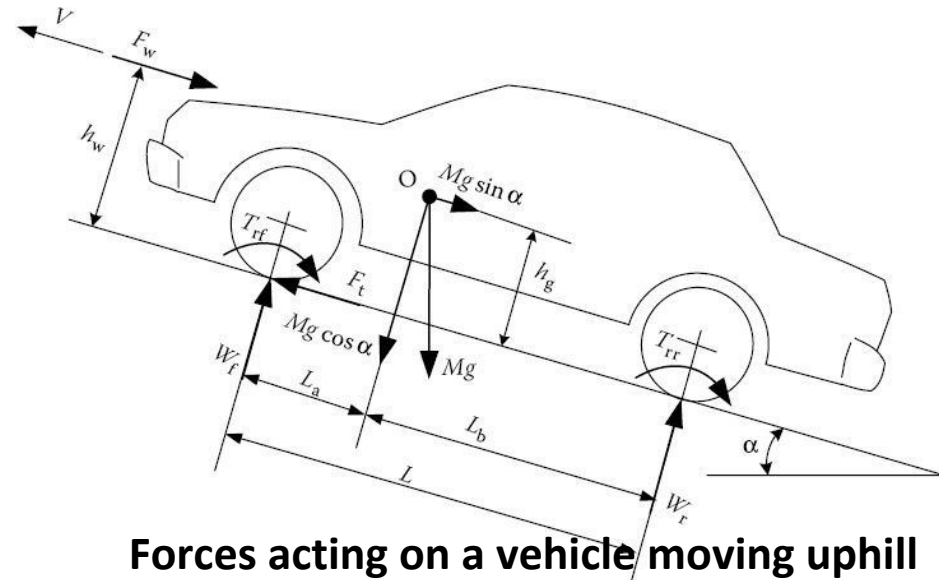
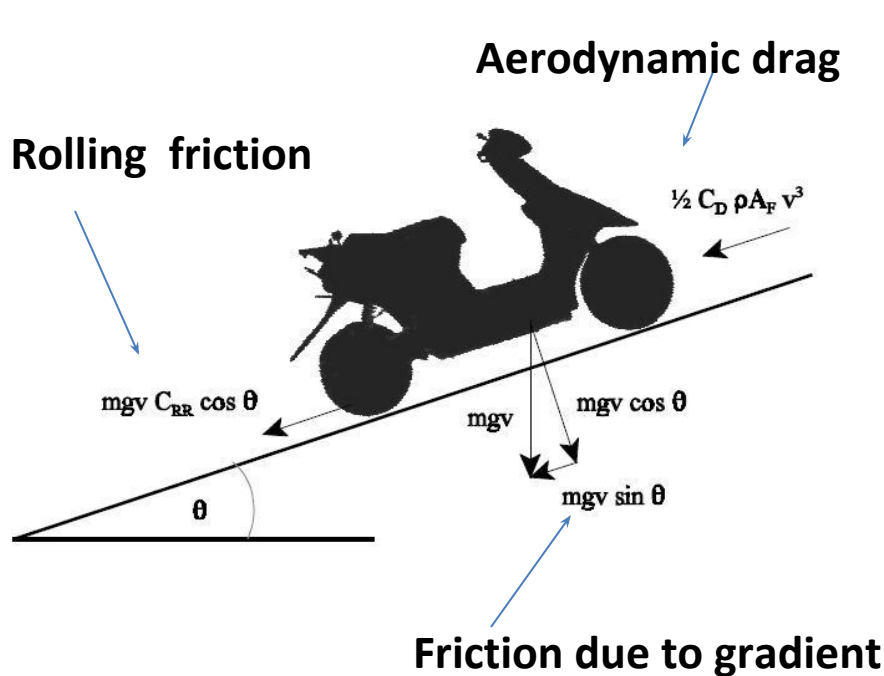
+ Kinetic Energy Recovery

ADAPTED FROM www.nrel.org

Electric vehicle schematic with hybrid battery system



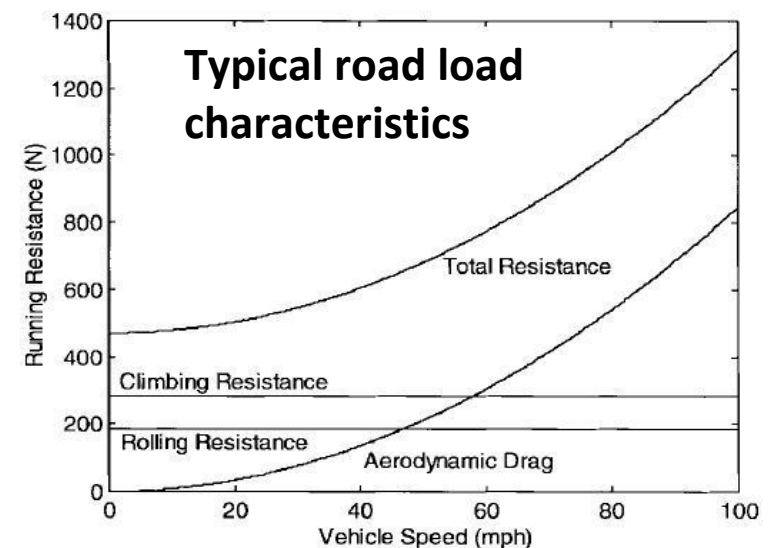
Vehicle load modeling



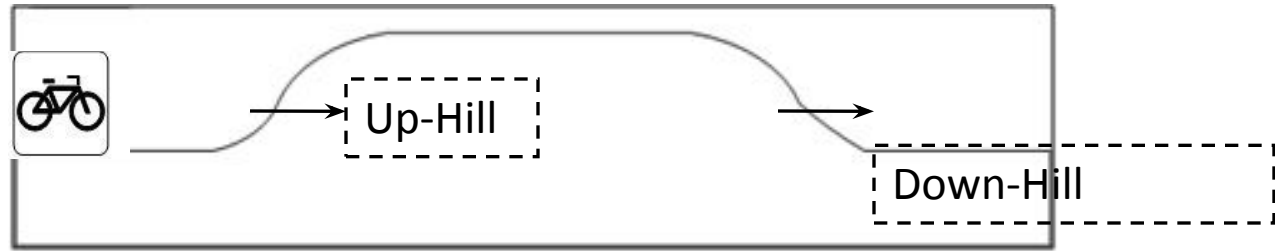
Forces acting on a vehicle moving uphill

Vehicle	C_{RR}	C_D	A_F (m ²)	curb weight (kg)	auxiliary power (W)
Electric Scooter	0.014	0.9	0.6	130	60
Roadster Bicycle	0.008	1.2	0.5	10	0
Motorcycle	unknown	0.6	0.8	300	unknown
Ford AIV Sable	0.0092	0.33	2.13	1291	500
PNGV Automobile	0.007	0.20	2.0	920	400

Typical modeling parameters for
Electric scooter



Vehicle Load Modelling



$$F=Ma$$

$$F_g = Mg \sin \theta$$

$$F_{air} = \frac{1}{2} \rho C_d A V^2$$

$$F_r = M g C_r \cos(\theta)$$

$$C_{roll} = 0.018$$

$$g = 9.81$$

$$\text{grad} = i = \text{flat road} = 0$$

$$GVW = 175$$

$$\text{Efficiency of drive} = 0.8$$

$$\text{Tyre radius} = R = 0.2032$$

$$V_w = 0$$

$$C_d = 0.92$$

$$A = 0.6$$

$$C_r = 1.23$$

◆ **M= Mass of the vehicle (kg)**

◆ **F= Resulting Force**

◆ **Fg= Gravitational force**

◆ **Fair= air Friction Force**

◆ **Fr=Wheel friction force**

$$\rho = \text{Air Density} (Kg / m^2)$$

◆ **Af= Frontal Area of vehicle**

◆ **Cd= Air friction coefficient**

◆ **Cr= wheels friction coefficient**

Load torque calculation for Electric two-Wheeler

- ❖ Consider vehicle is running with a velocity $V(t)$ then the power required by the system is

$$PL = Pa + Pr + Pair + Pg$$

$$PL = V(t) \left\{ 0.5 M_p a + M \left(g \sin \theta + \frac{M_d g \cos \theta}{f} \right) + \frac{M_d^2 g^2 \cos^2 \theta}{2 f^2} \right\}$$

- ❖ Assuming that the vehicle speed $v(t)$ is equal to the angular Speed W of wheels with radius R , torque of the traction system can be estimated as,

$$TL = Ta + Tg + Tair + Tr$$

$$TL = R \left\{ 0.5 M_p a + M \left(g \sin \theta + \frac{M_d g \cos \theta}{f} \right) + \frac{M_d^2 g^2 \cos^2 \theta}{2 f^2} \right\}$$

In a specific drive cycle, **the tractive effort of a vehicle on a flat road can be expressed as**

$$F_t = Mg f_r \cos \alpha + \frac{1}{2} \rho_a C_D A_f V^2 + M \delta \frac{dV}{dt}$$

- Energy consumption is an integration of the power output at the battery terminals.
- For propelling, the battery power output is equal to the resistance
- power and power losses in the transmission and motor drive, including power losses in the electronics.
- The power losses in transmission and motor drive are represented by their efficiencies η_t and η_m , respectively.

The battery power output can be expressed as

$$P_{b-out} = \frac{V}{\eta_t \eta_m} \left(Mg(f_r + i) + \frac{1}{2} \rho_a C_D A_f V^2 + M \delta \frac{dV}{dt} \right)$$

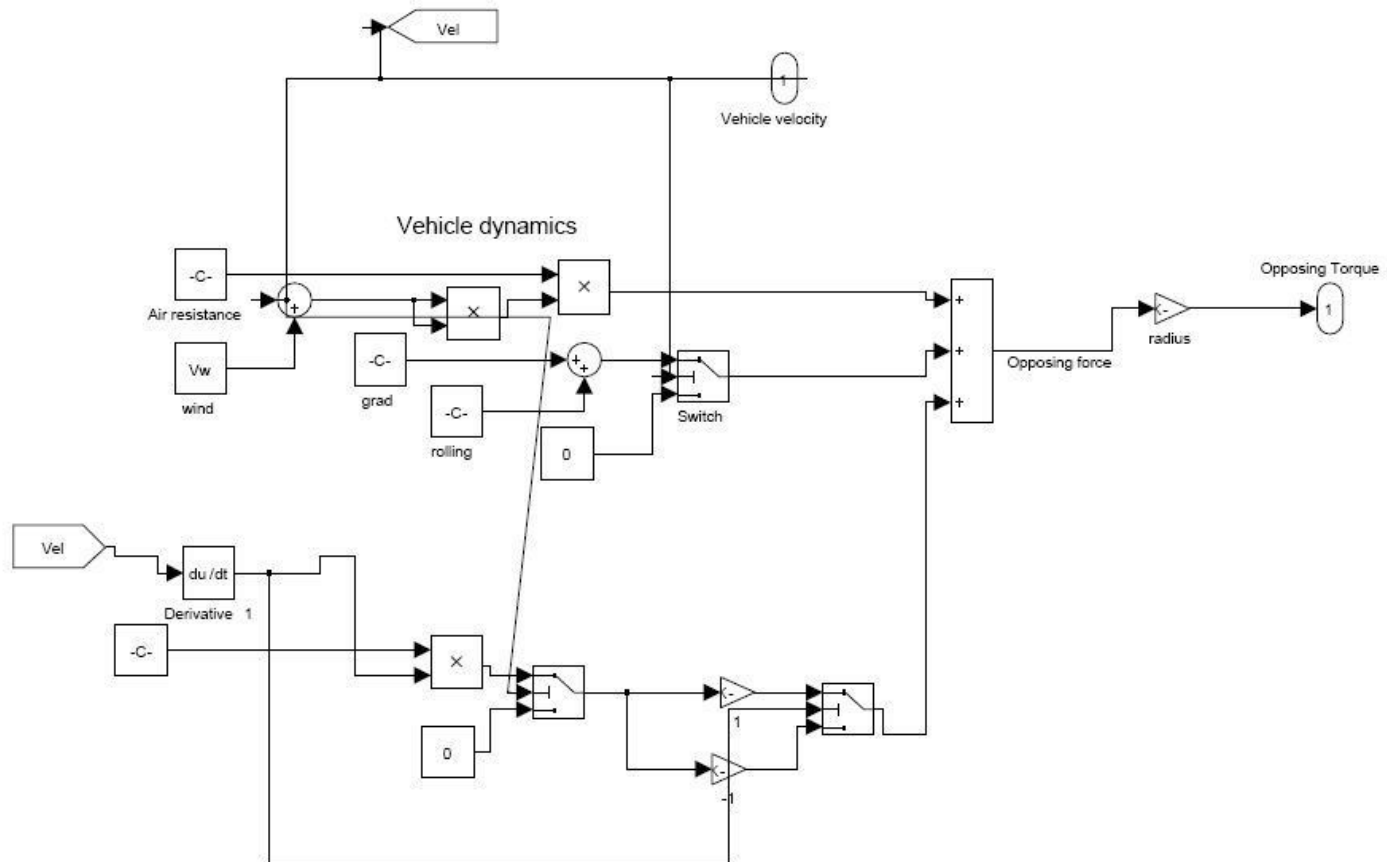
- The regenerative braking power at the battery terminals can also be expressed as

$$P_{b-in} = \frac{\alpha V}{\eta_t \eta_m} \left(Mg(f_r + i) + \frac{1}{2} \rho_a C_D A_f V^2 + M \delta \frac{dV}{dt} \right)$$

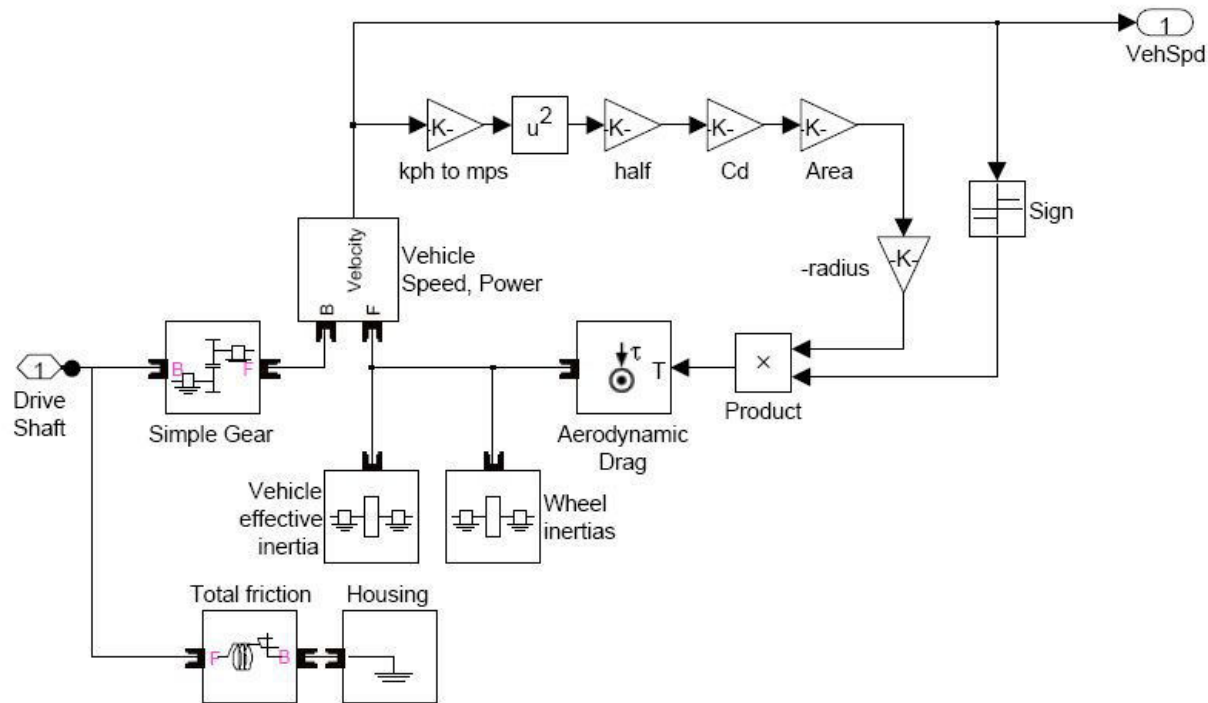
where road grade i or acceleration dV/dt or both are negative, and α ($0 < \alpha < 1$) is the percentage of the total braking energy that can be regenerated by the electric motor, called the regenerative braking factor. The regenerative braking factor α is a function of the applied braking strength and the design and control of the braking system, The net energy consumption from the batteries is

$$E_{out} = \int_{\text{traction}} P_{b-out} dt + \int_{\text{braking}} P_{b-in} dt$$

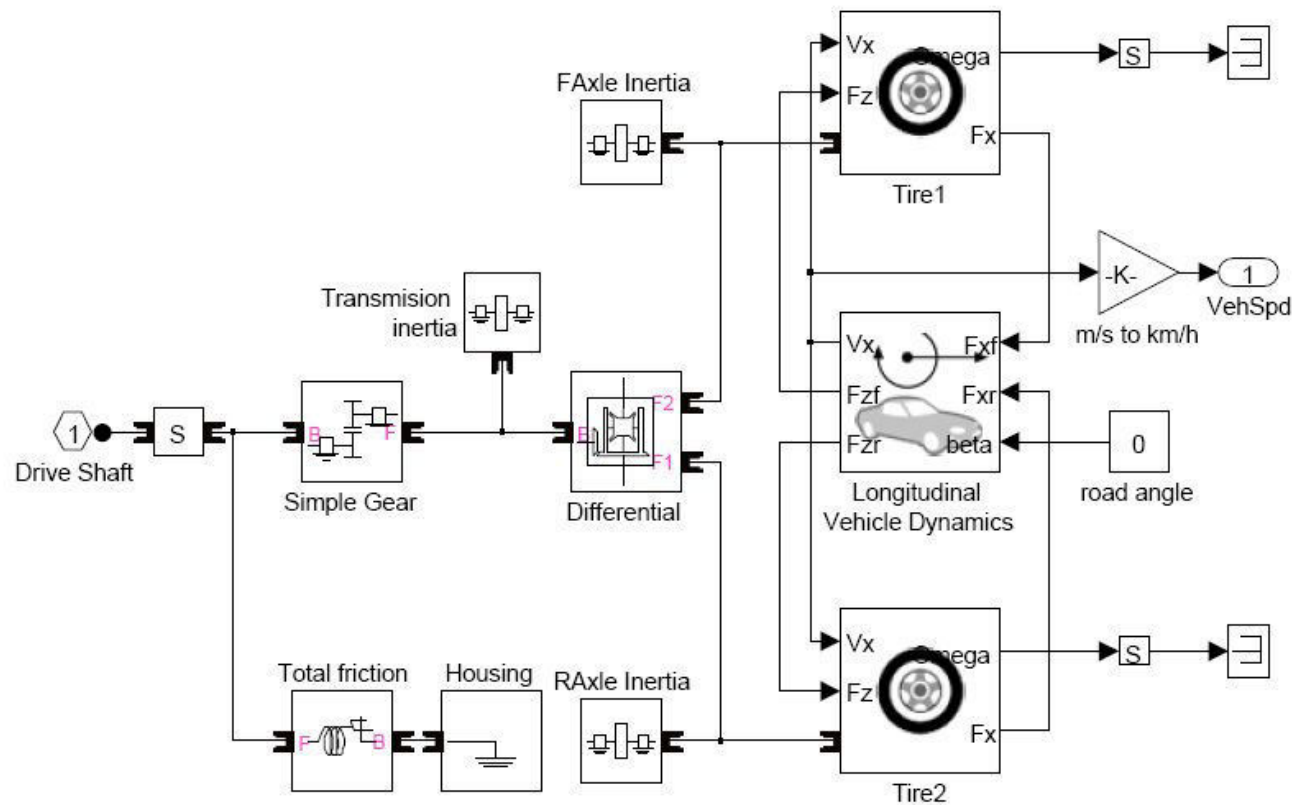
Vehicle load model in MATLAB/SIMULINK



Four wheeler simple load modeling(simscape)



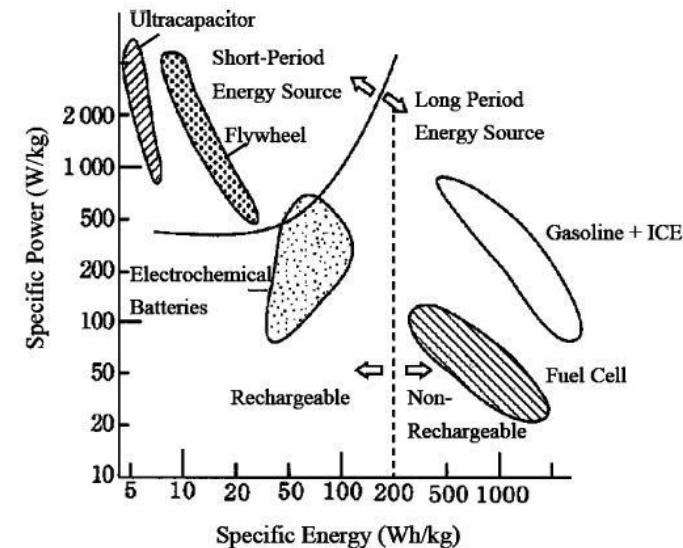
Four wheeler complete load modeling(simscape)



Battery modeling

CHARACTERISTICS OF BEV, HEV, AND FCV

Types of EVs	Battery EVs	Hybrid EVs	Fuel Cell EVs
Propulsion	<ul style="list-style-type: none"> Electric motor drives 	<ul style="list-style-type: none"> Electric motor drives Internal combustion engines 	<ul style="list-style-type: none"> Electric motor drives
Energy system	<ul style="list-style-type: none"> Battery Ultracapacitor 	<ul style="list-style-type: none"> Battery Ultracapacitor ICE generating unit 	<ul style="list-style-type: none"> Fuel cells Need battery / ultracapacitor to enhance power density for starting.
Energy source & infrastructure	<ul style="list-style-type: none"> Electric grid charging facilities 	<ul style="list-style-type: none"> Gasoline stations Electric grid charging facilities (for Plug In Hybrid) 	<ul style="list-style-type: none"> Hydrogen Hydrogen production and transportation infrastructure
Characteristics	<ul style="list-style-type: none"> Zero emission High energy efficiency Independence on crude oils Relatively short range High initial cost Commercially available 	<ul style="list-style-type: none"> Very low emission Higher fuel economy as compared with ICE vehicles Long driving range Dependence on crude oil (for non Plug In Hybrid) Higher cost as compared with ICE vehicles The increase in fuel economy and reduce in emission depending on the power level of motor and battery as well as driving cycle. Commercially available 	<ul style="list-style-type: none"> Zero emission or ultra low emission High energy efficiency Independence on crude oil (if not using gasoline to produce hydrogen) Satisfied driving range High cost Under development
Major issues	<ul style="list-style-type: none"> Battery and battery management Charging facilities Cost 	<ul style="list-style-type: none"> Multiple energy sources control, optimization and management. Battery sizing and management 	<ul style="list-style-type: none"> Fuel cell cost, cycle life and reliability Hydrogen infrastructure

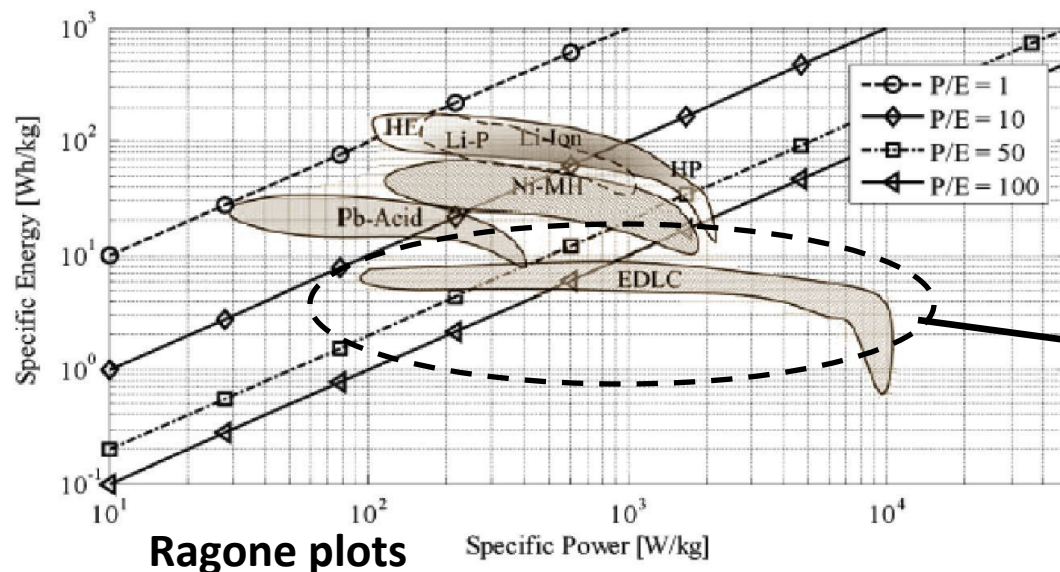


Characteristics of various energy sources

Characteristics of different vehicles and major challenges

Nominal parameters of EV batteries

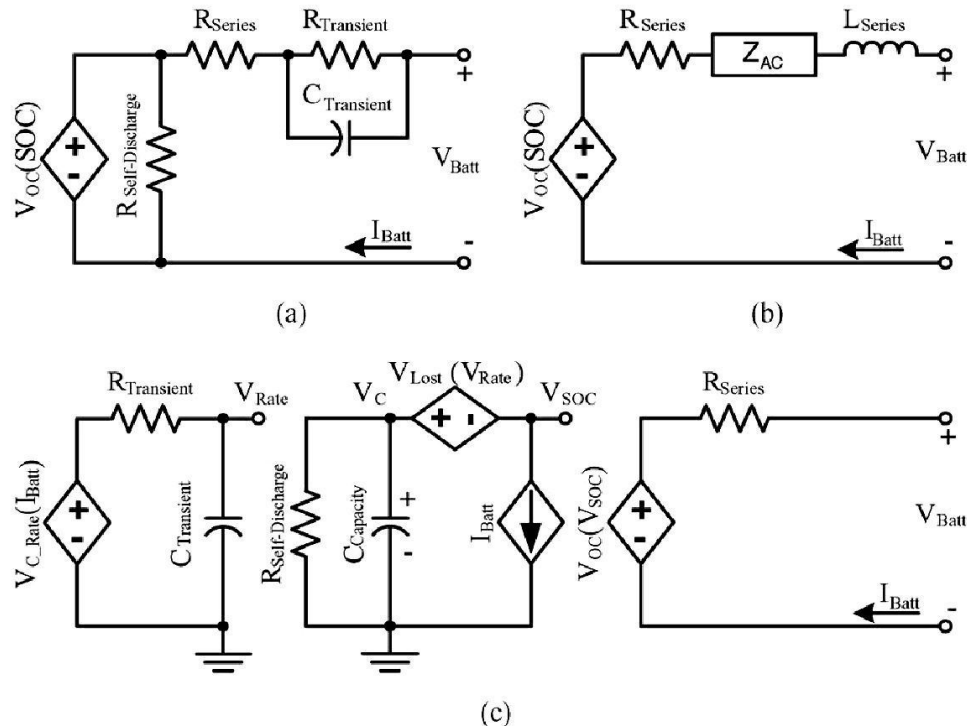
	Lead Acid	NiMH	ZEBRA	Lithium-ion
Specific energy	20-35 Wh/kg	50-70 Wh/kg	120 Wh/kg	100-200 Wh/kg
Energy density	50-90 Wh/l	150-200 Wh/l	180 Wh/l	150-250 Wh/l
Specific power	250 W/kg	< 1000 W/kg	180 W/kg	< 2000 W/kg
Nominal cell voltage	2.1 V	1.2 V	2.58 V	3.6 V
Temperature range	-20C to 60C	-20C to 50C	N.A.	-20C to 50C
Number of cycles @80% Depth Of Discharge	700	2000	1500	2000



Due to high energy density suitable for automotive applications

High pulse power applications

Battery Modelling



(a) thevenin (b) impedance and (c) runtime-based electrical battery models.

Battery Modelling

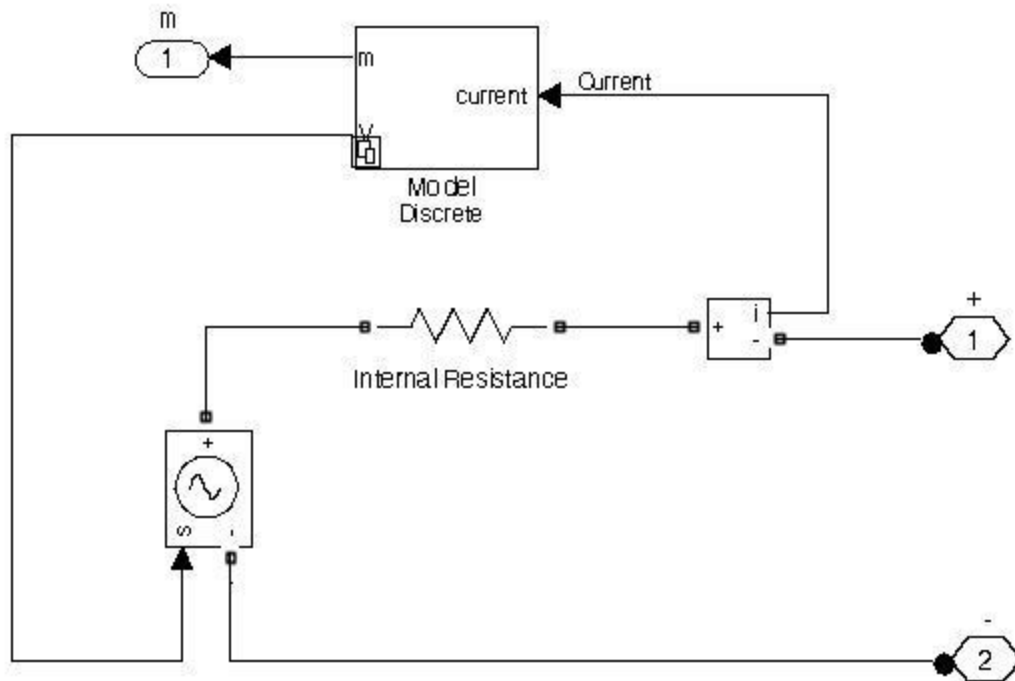
RITAR Battery Parameters used for simulation:

Battery voltage=48v

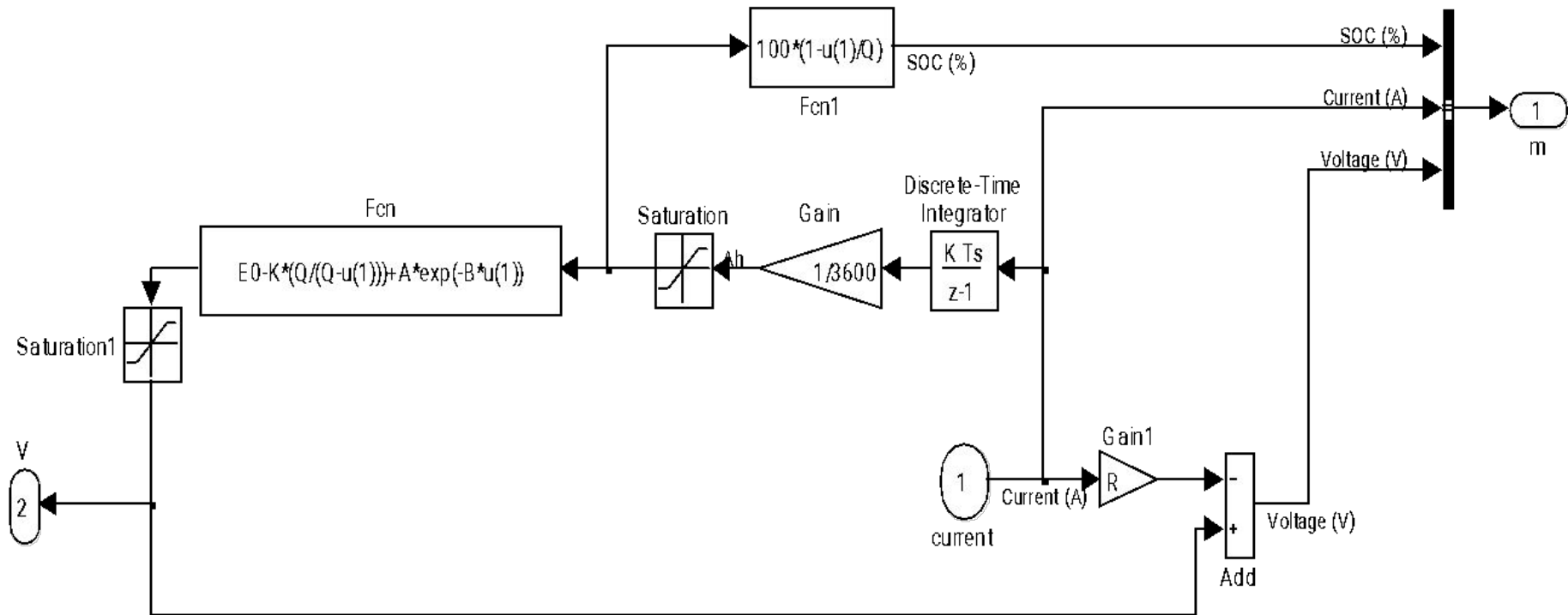
Battery capacity=20Ah

Internal Resistance=0.056Ohms

Initial State Of Charge=80%

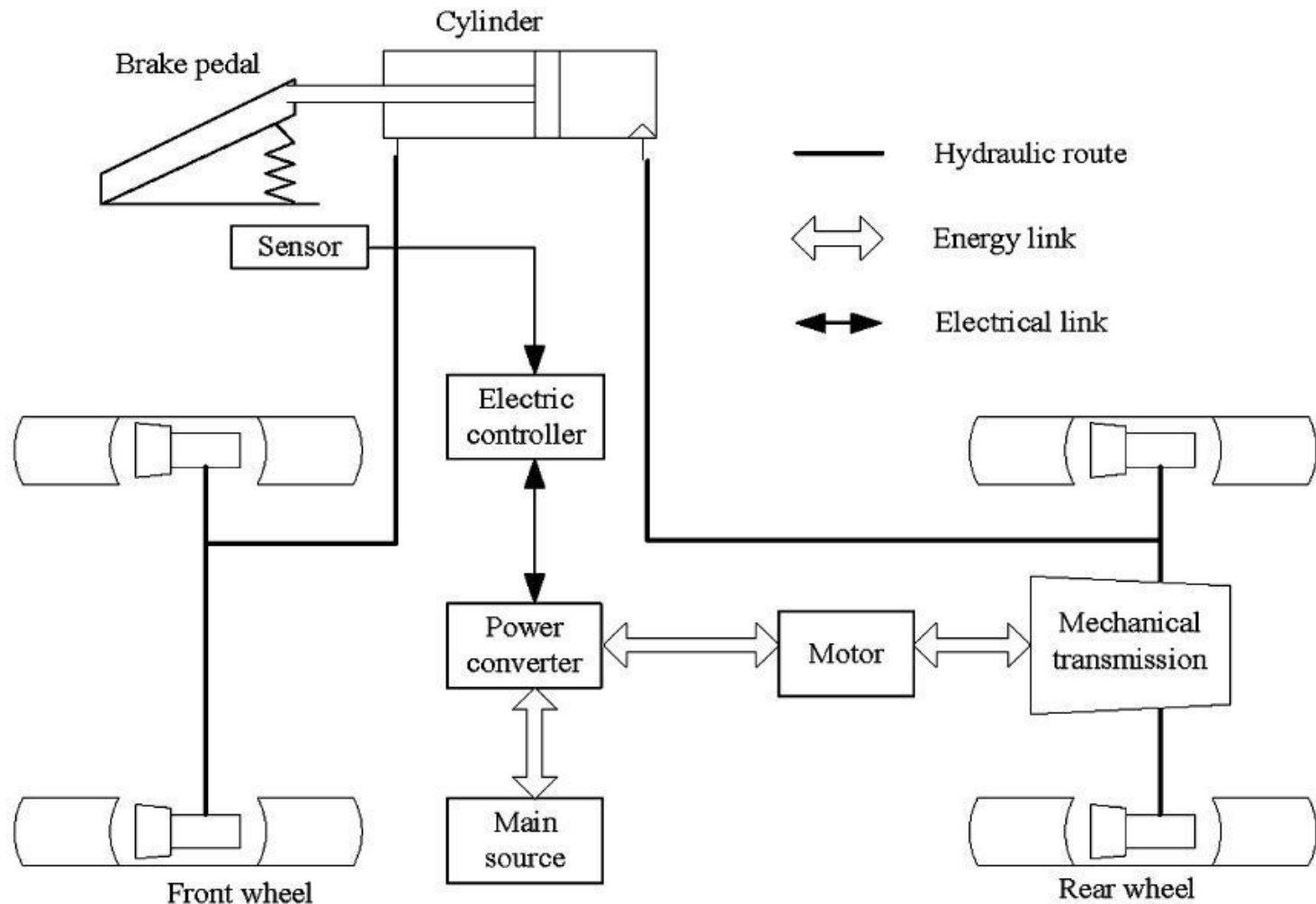


Battery Modelling

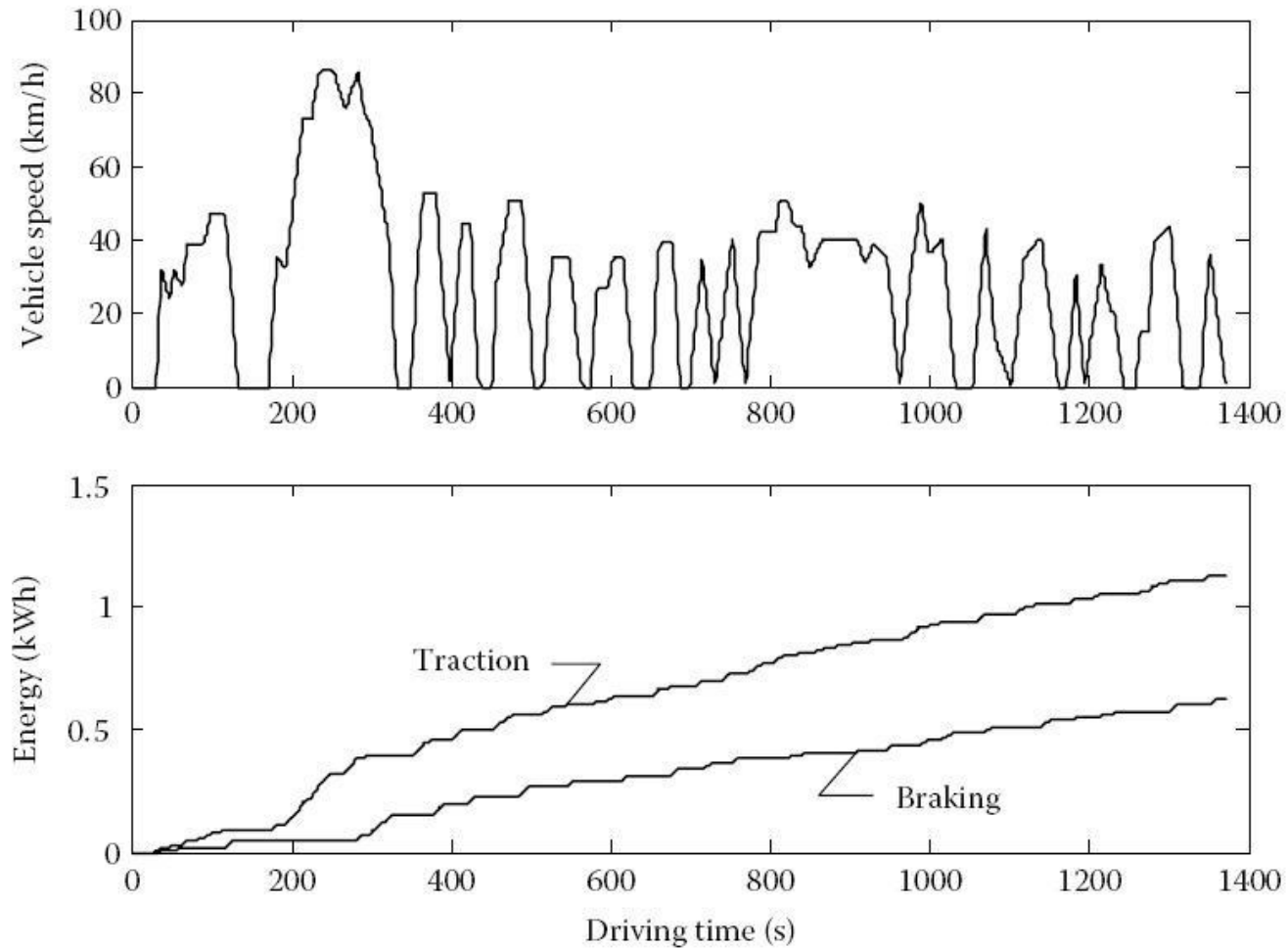


Different electrical braking schemes

The configuration of the braking system



Braking Energy Consumed in a Urban Driving Cycle



Traction and braking energy dissipation in an FTP75 urban driving cycle

Maximum Speed, Average Speed, Total, and Energies Dissipated by the Drag and Braking per 100km Traveling Distance in Different Drive Cycles

	FTP75 Urban	LA92	US06	New York	ECE15
Max. speed (km/h)	86.4	107.2	128.5	44.6	120
Ave. speed (km/h)	27.9	39.4	77.4	12.2	49.8
Traveling distance per cycle (km)	10.63	15.7	12.8	1.90	7.95
Traction energy (kWh)					
Per cycle	1.1288	2.3559	2.2655	0.2960	0.9691
Per km	1.1062	0.15	0.1769	0.1555	0.1219
Braking energy (kWh)					
Per cycle	0.6254	1.3666	0.9229	0.2425	0.3303
Per km	0.0589	0.0870	0.0721	0.1274	0.0416
Percentage of braking energy to traction energy	55.4	58.01	40.73	81.9	34.08



Kinetic Energy

OR

Kinetic Energy



Dynamic Braking

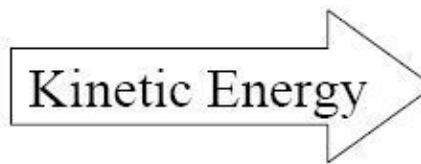


Regenerative Braking

Importance of regenerative braking in two-wheelers



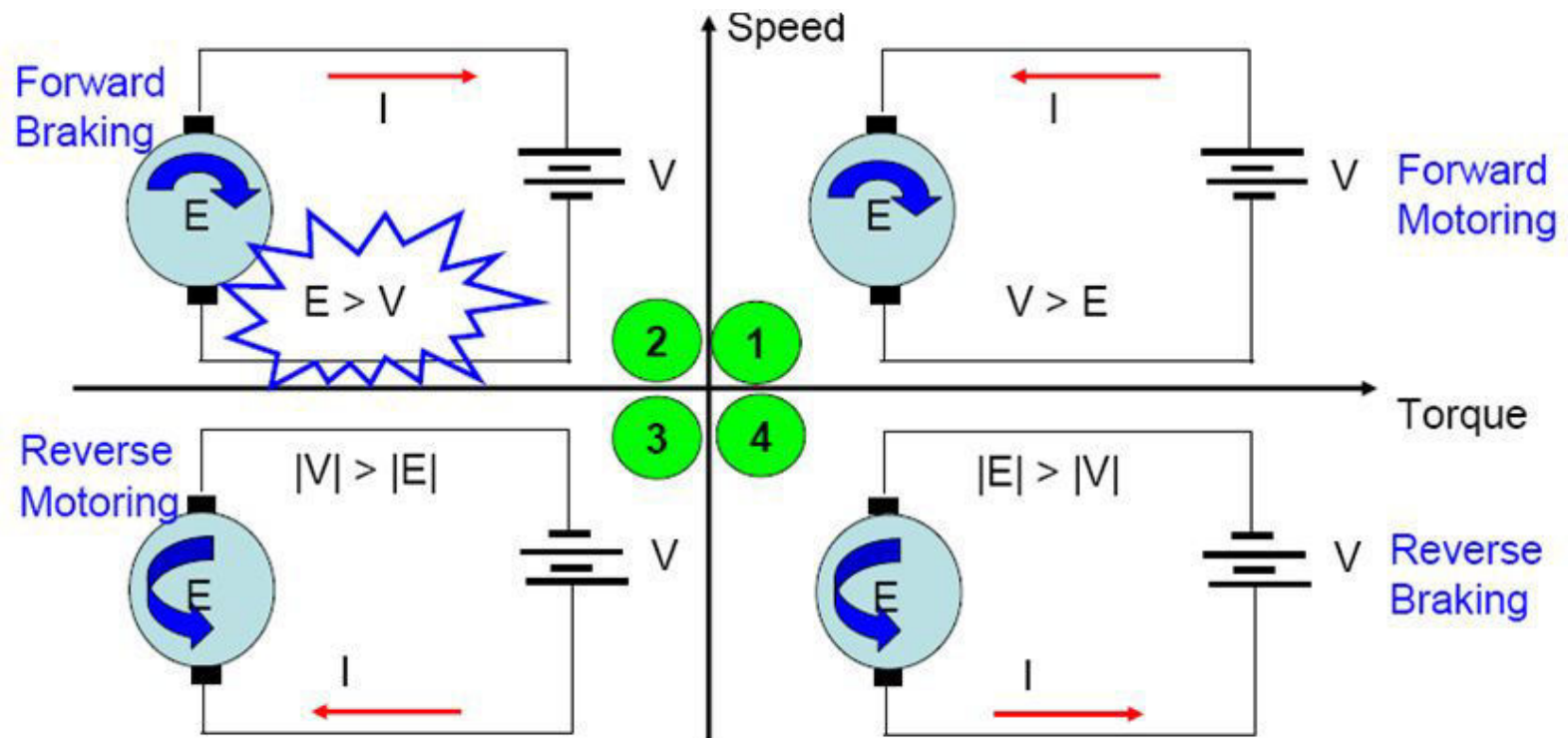
BLDC Hub Motor used
in e-bike application



While braking, energy
is stored in the battery

Regenerative braking stores energy back into the battery, while increasing the life of friction pads on brake shoe. However, to bring the bike to a complete stop, the mechanical brakes are required.

4-Quadrant Motor Operation



For a BLDC motor to operate in 2nd quadrant, the value of the back EMF generated by the BLDC motor should be greater than the battery voltage (DC bus voltage). This ensures that the direction of the current reverses, while the motor still runs in the forward direction.

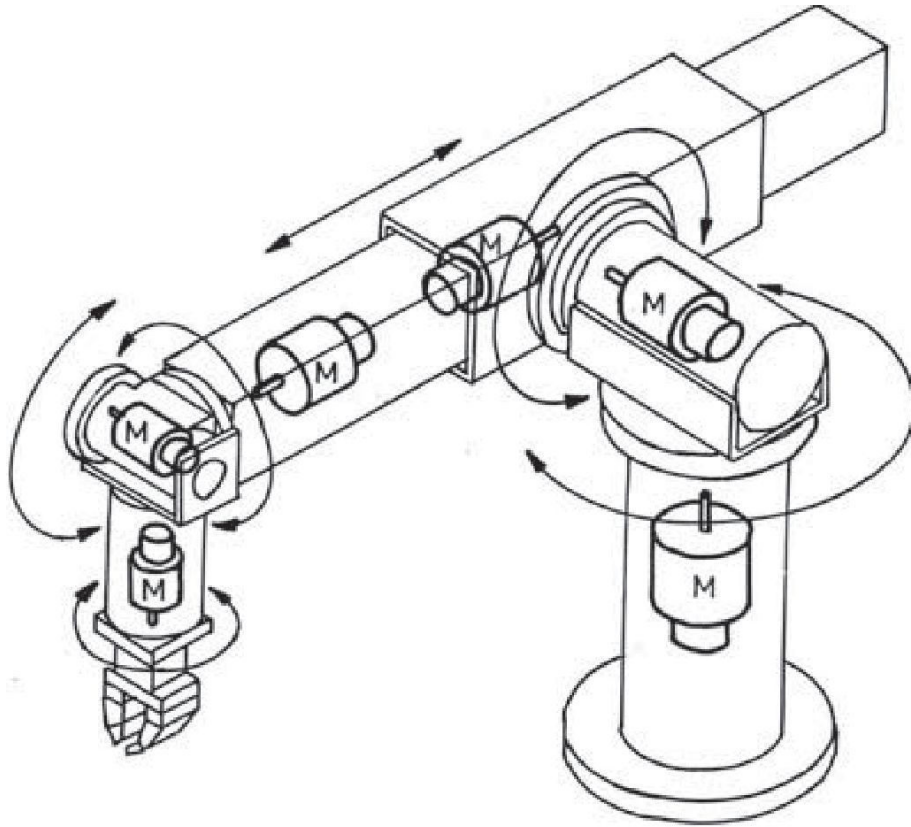
Unit -III

PM Machines and Control (PMBLDC and PMSM)

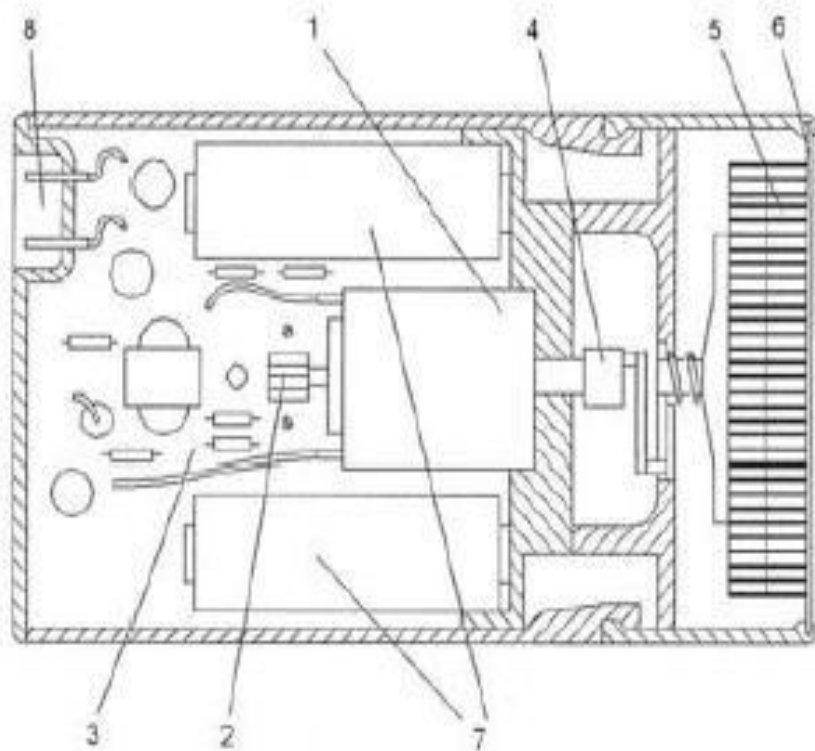
Application Areas

- House Hold appliances
 - Transportation (Electric)- Rail, Road, air transportation
 - Industry Automation (Robotics, Position control, etc)
 - Marine Applications (under water Vehicles, Ships)
 - Computers
 - Space Applications
 - Electric Power Generation
 - Medical Devices
 - Toys etc
-
- (80 % of the power is consumed by the electrical machines)

An Industrial Robot - Automation



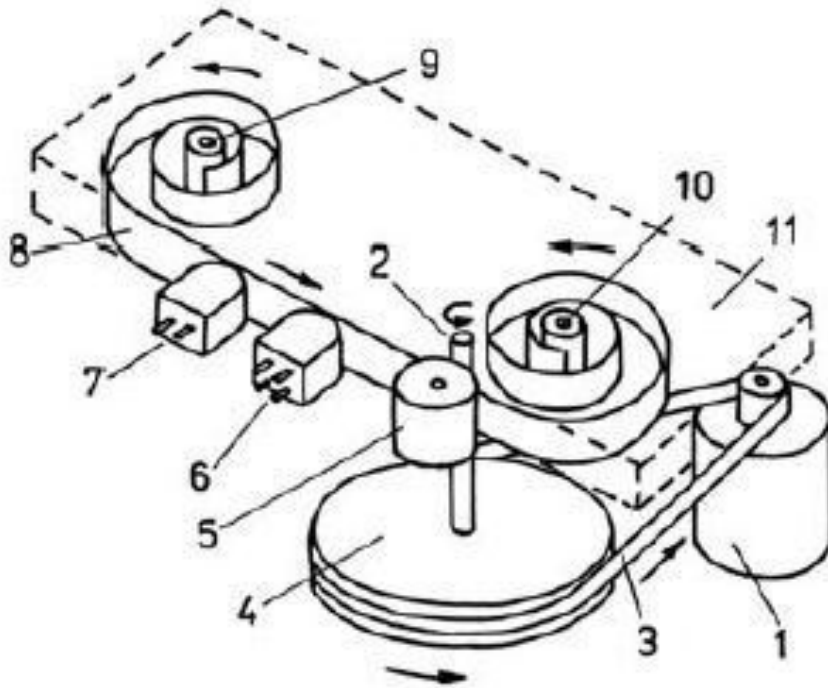
Low power Home appliances



Electric shaver with a PM brushless motor:

- 1 — PM brushless motor,
 - 2 — position sensor,
 - 3 — printed circuit board,
 - 4 — cam-shaft,
 - 5 — twizzer head,
 - 6 — platinum-coated shaving foil,
 - 7 — rechargeable battery,
 - 8 — input terminals
- 110/220 V.

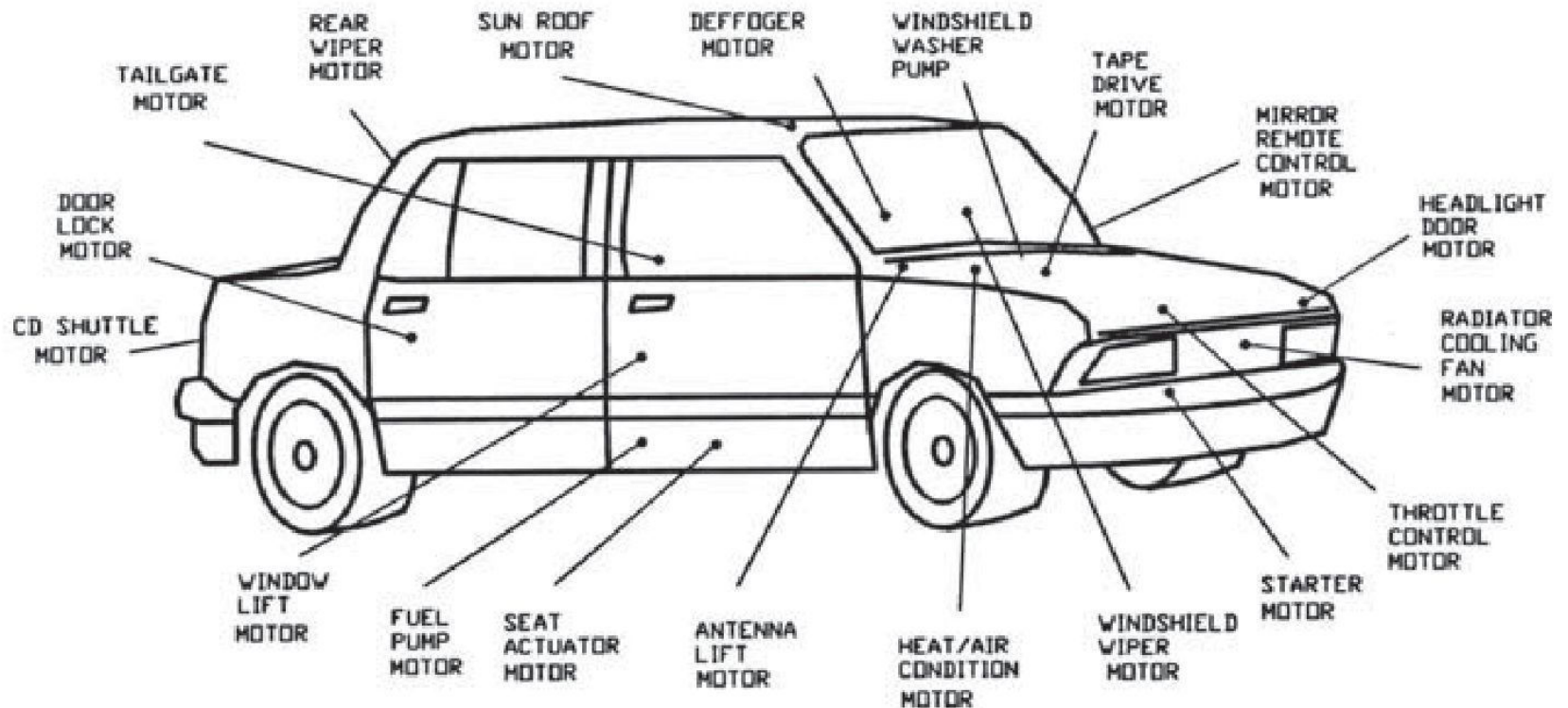
Computer Applications



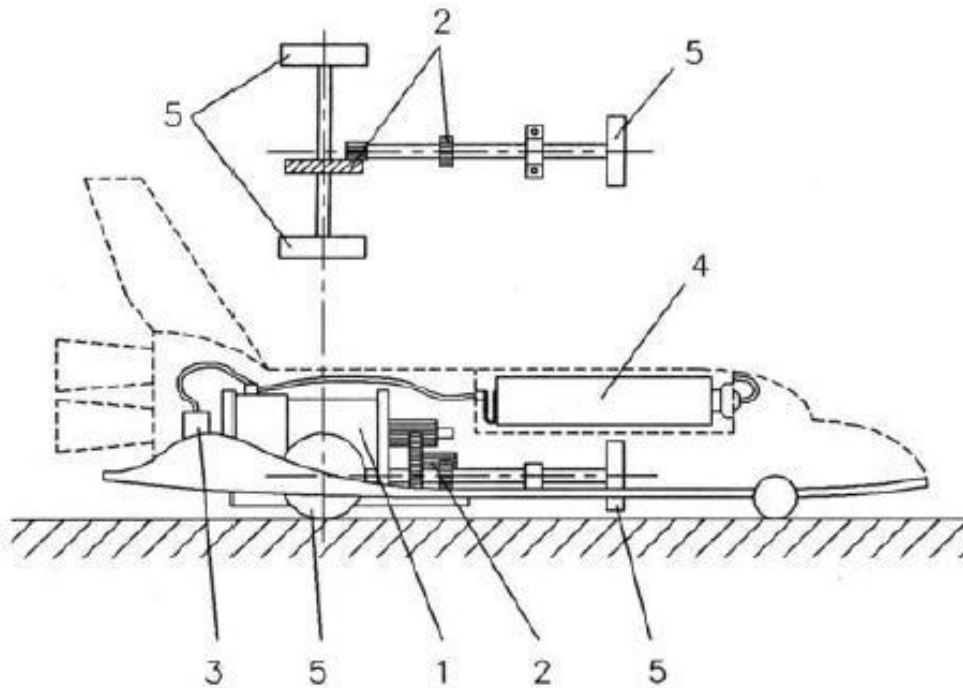
Cassette deck:

1 — PM motor,
2 — capstan, 3 — belt, 4 —
flywheel,
5 — pressure roller, 6 —
rec/play head, 7 — erase head,
8 — tape, 9 — supply reel
table, 10 — take-up reel table,
11 — cassette.

Motors used in CARS



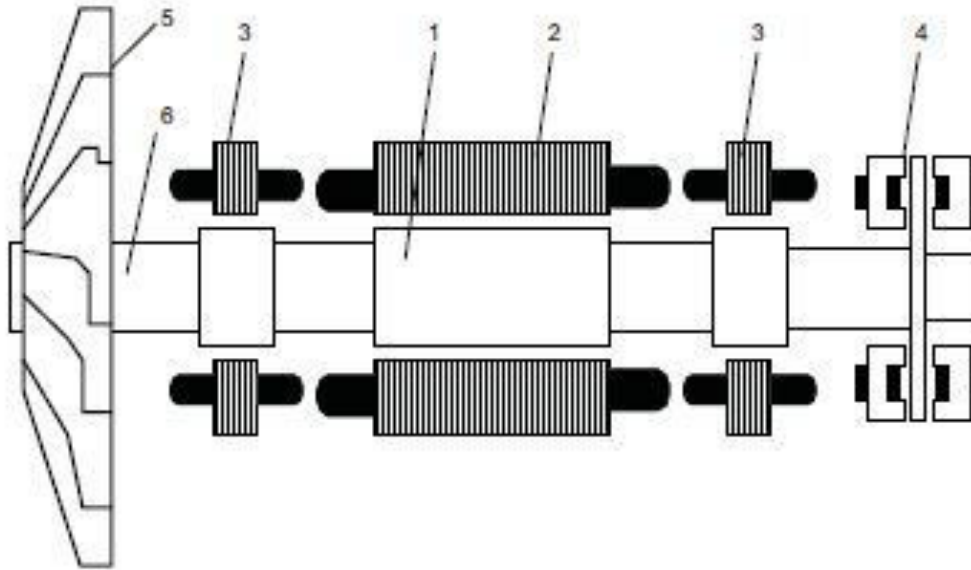
Space Applications



Toy space shuttle:

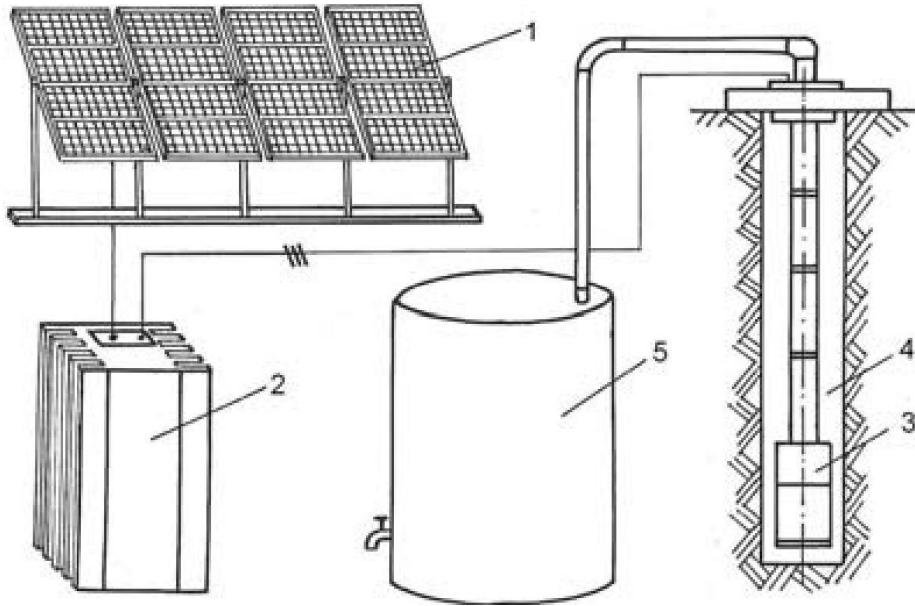
1 — PM d.c. commutator motor, 2 — transmission,
3 — on-off switch, 4 — 1.5-V battery, 5 — driven wheels.

Cooling application



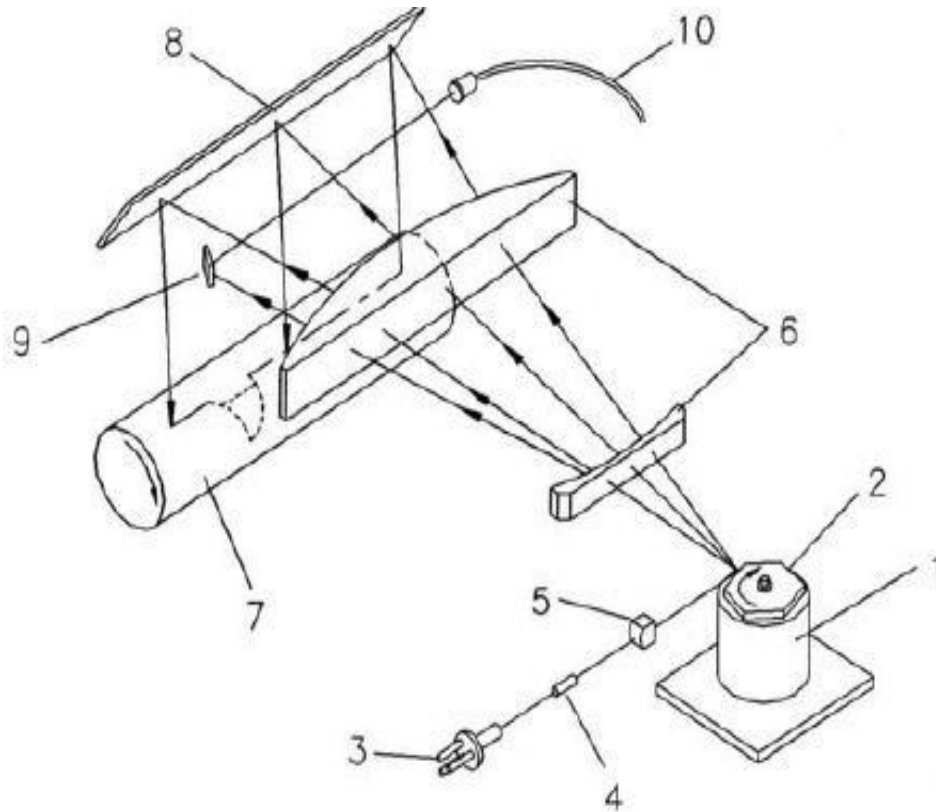
Centrifugal chiller compressor with high speed PM brushless motor and magnetic bearings: 1 — rotor with surface PMs and nonmagnetic can, 2 — stator, 3 — radial magnetic bearing, 4 — axial magnetic bearing, 5 — impeller, 6 — shaft.

Solar Water Pumping Applications



Water pumping system for a remote population center:
1 — solar panels,
2 — inverter, 3 — submersible
PM brushless motor-pump unit,
4 — well, 5 — water
storage tank.

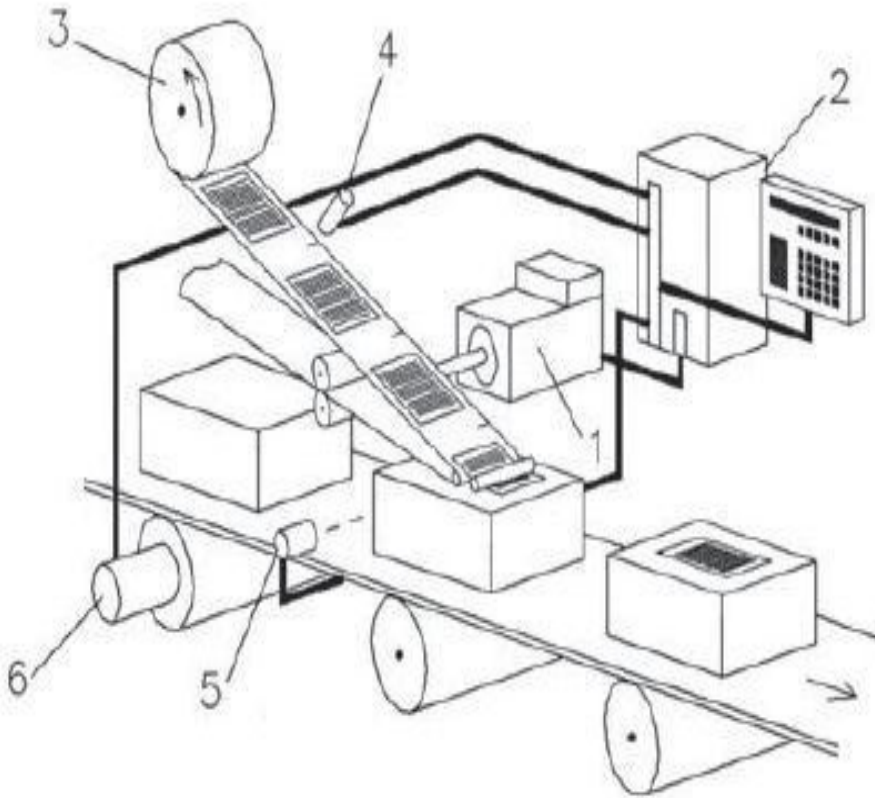
Printer Applications



Laser beam printer:

- 1 — stepping motor, 2 — scanner mirror,
- 3 — semiconductor laser,
- 4 — collimator lens,
- 5 — cylindrical lens,
- 6 — focusing lenses,
- 7 — photosensitive drum,
- 8 — mirror, 9 — beam detect mirror,
- 10 — optical fiber

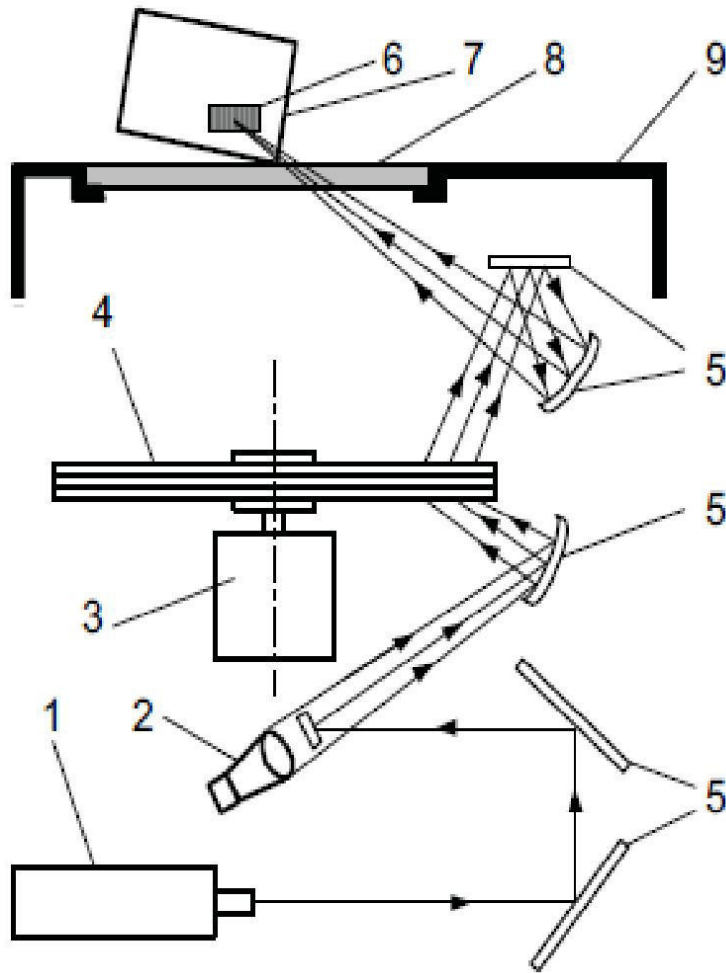
Position control application



Automatic labelling systems with a PM brushless motor:

- 1 — PM brushless motor servo drive,
- 2 — controller,
- 3 — spool of self-adhesive labels,
- 4 — registration mark sensor,
- 5 — box position sensor,
- 6 — conveyor speed encoder

Scanner Application



Bar code scanner:

- 1 — laser,
- 2 — photo decoder converting
laser beam
into electric signal,
- 3 — PM brushless motor,
- 4 — holographic three-layer disk,
- 5 — mirror,
- 6 — bar code,
- 7 — scanned object,
- 8 — scan window,
- 9 — housing.

Home appliances

High Power Appliances

- Refrigerators
- Air conditioners
- Washing machines
- Vaccum cleaners
- Mixers and Grinders
- Water coolers etc....
- fans

low Power Appliances

Electric Shavers

Blenders and coffee makers

Mixers and grinders(small power)

Hair Dryers

Control of PM BLDC Motors

OUTLINE

- Permanent Magnet Machines- Introduction, its Importance and Applications
- Constructional details
 - Stator and Rotor
 - PMSM Hub motor for EV application
- PMSM motor Operation using Hall Sensors
- Modelling of PMSM motor
- Speed control of PMSM motor
- PMSM motor Control in EV applications

Permanent Magnet Machines

❑ Permanent Magnet

The materials used for such motors have high **residual flux density** and high **coercivity**.

❑ Alnico magnets (Al, Ni, Co, Fe):

They are used in motors having ratings in the range of 1 kW to 150 kW.

❑ Ceramic (ferrite) magnets:

barium ferrite ($\text{BaO} \times 6\text{Fe}_2\text{O}_3$) and strontium ferrite ($\text{SrO} \times 6\text{Fe}_2\text{O}_3$)

❑ They are much economical in fractional kW motors.

Permanent magnets...

- **Rare-earth magnets:**

Made of **samarium cobalt (SmCo)** and **neodymium iron boron (NdFeB)** which have the highest energy product. Such magnetic materials are costly but are best economic choice for small as well as large motors.

- **NdFeB** magnets are mechanically very strong, not as brittle as **SmCo**.
- **In comparison with SmCo magnets, NdFeB magnets have low corrosion resistance.**

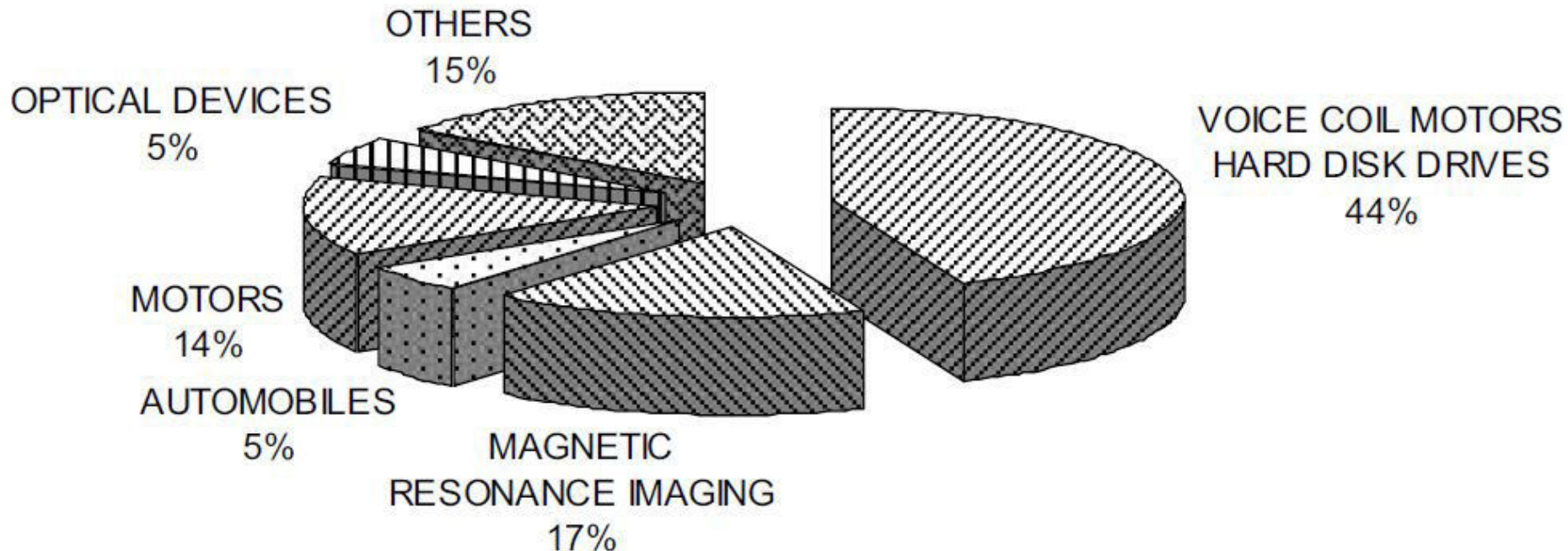
Permanent magnets...

- **NdFeB magnets cannot be used under the following conditions:**

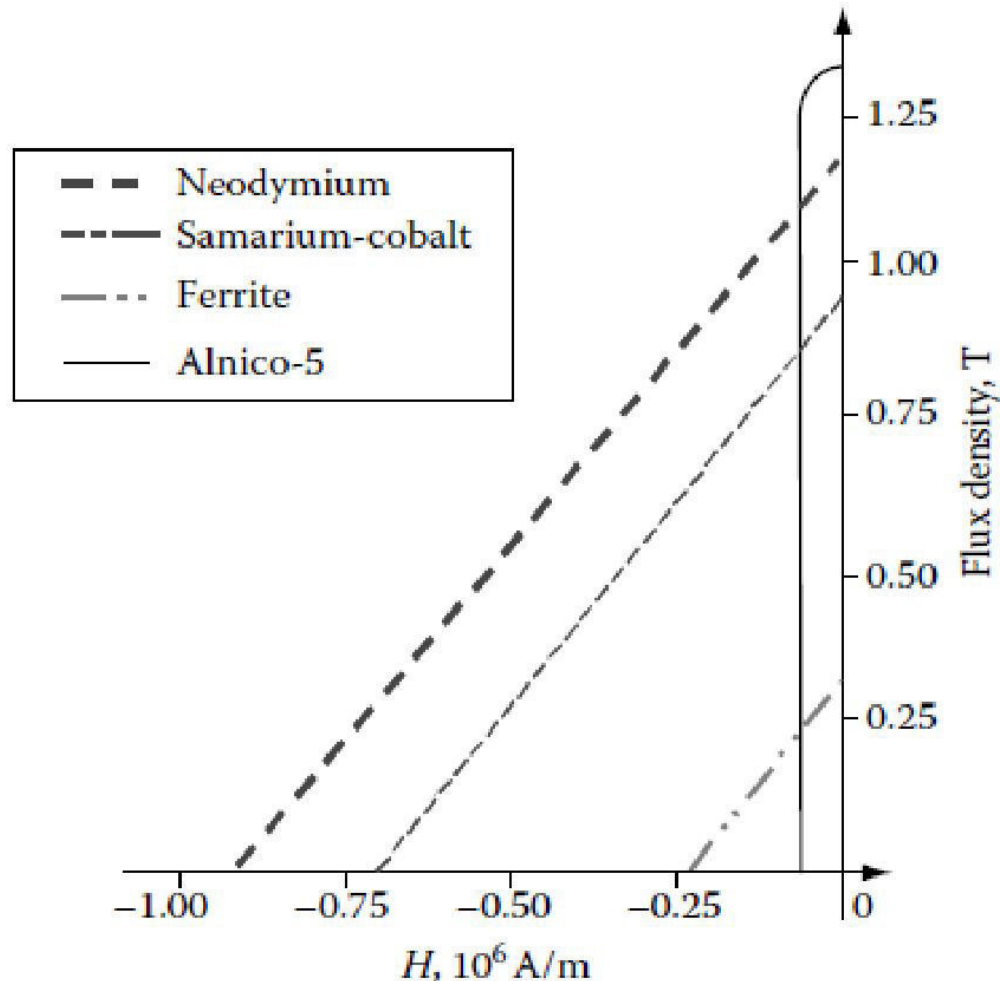
- ☐ in an acidic, alkaline, or organic solvent (unless hermetically sealed inside a can)
- ☐ in water or oil (unless hermetically sealed)
- ☐ in an electrically conductive liquid, such as electrolyte containing water.
- ☐ in a hydrogen-containing atmosphere, especially at elevated temperatures since hydrogenation causes the magnet material to disintegrate.
- ☐ in corrosive gasses, such as Cl, NH_3 (Ammonia), N_{ox} , etc.
- ☐ in the presence of radioactive rays (NdFeB magnets can be by radiation, mainly gamma ray)

Applications of Rare Earth magnets

- NdFeB magnets - US\$55 per kg (60 to 70% of the cost of SmCo)

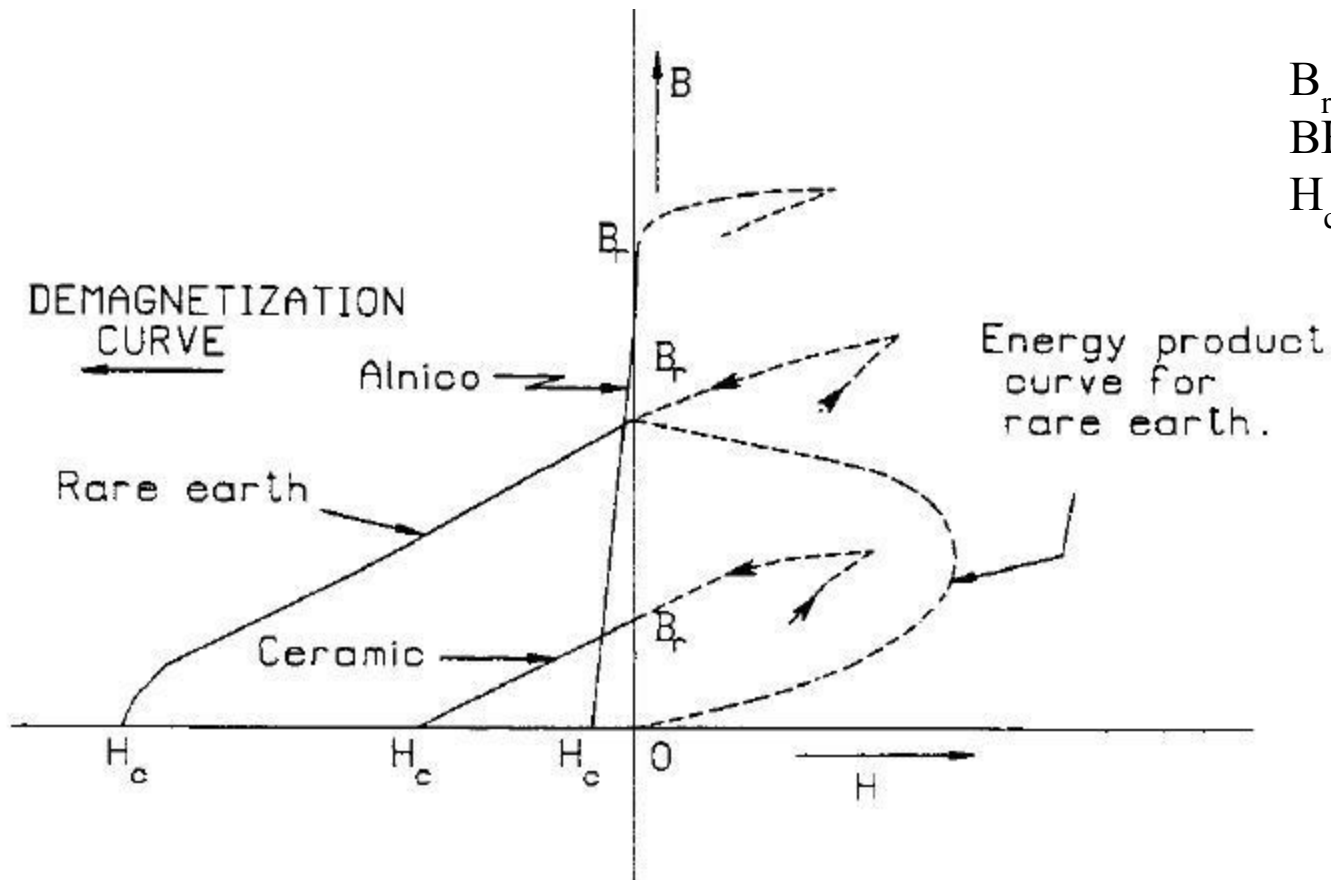


Demagnetization characteristics of Permanent Magnets



Second Quadrant B-H Characteristics of PMs

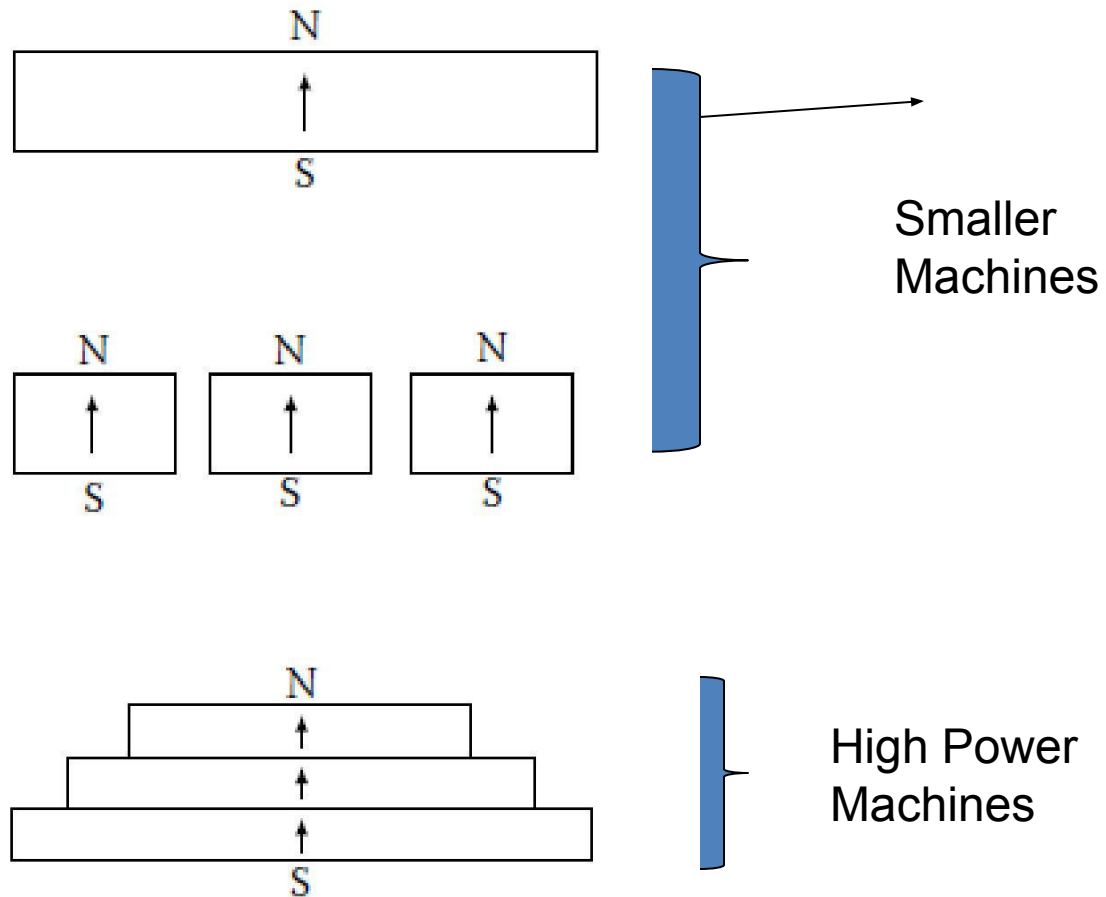
PM Charecterstics



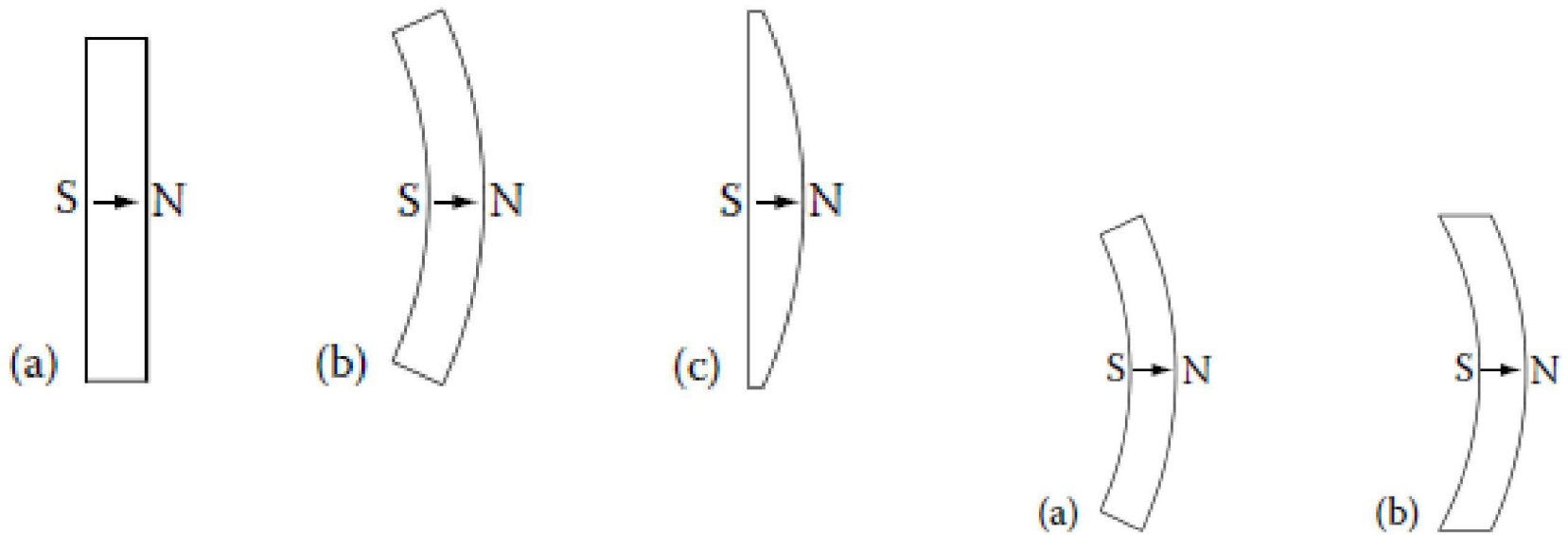
Typical demagnetization and energy-product curves of *three* permanent magnets

An ideal permanent magnetic material exhibits a **flat-topped, wide hysteresis curve** so that the residual magnetism stays at a high level when the applied field is removed.

Realization of magnet poles with one or multiple segments



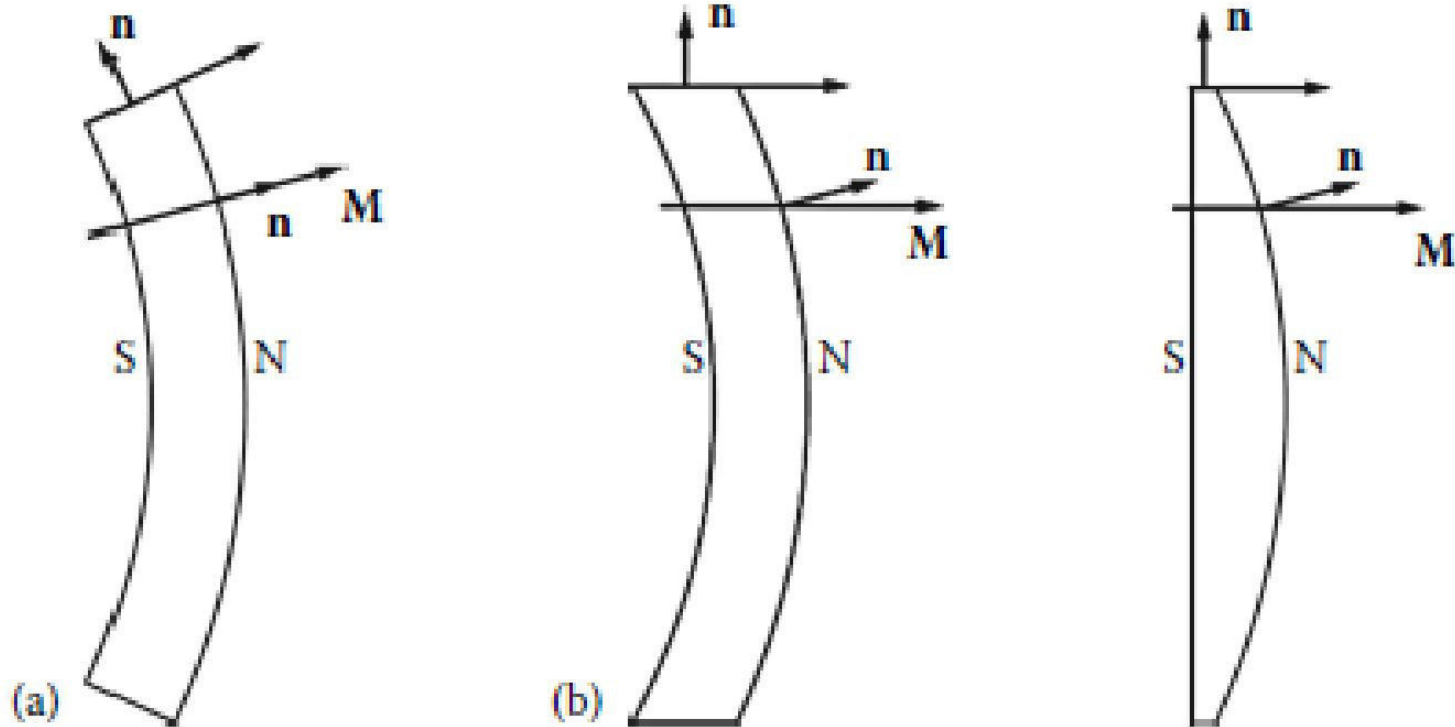
Types of magnets



(a) Rectangular; (b) radial; and (c) Bread-loaf

**(a) Surface radial magnet
and (b) surface parallel
magnet.**

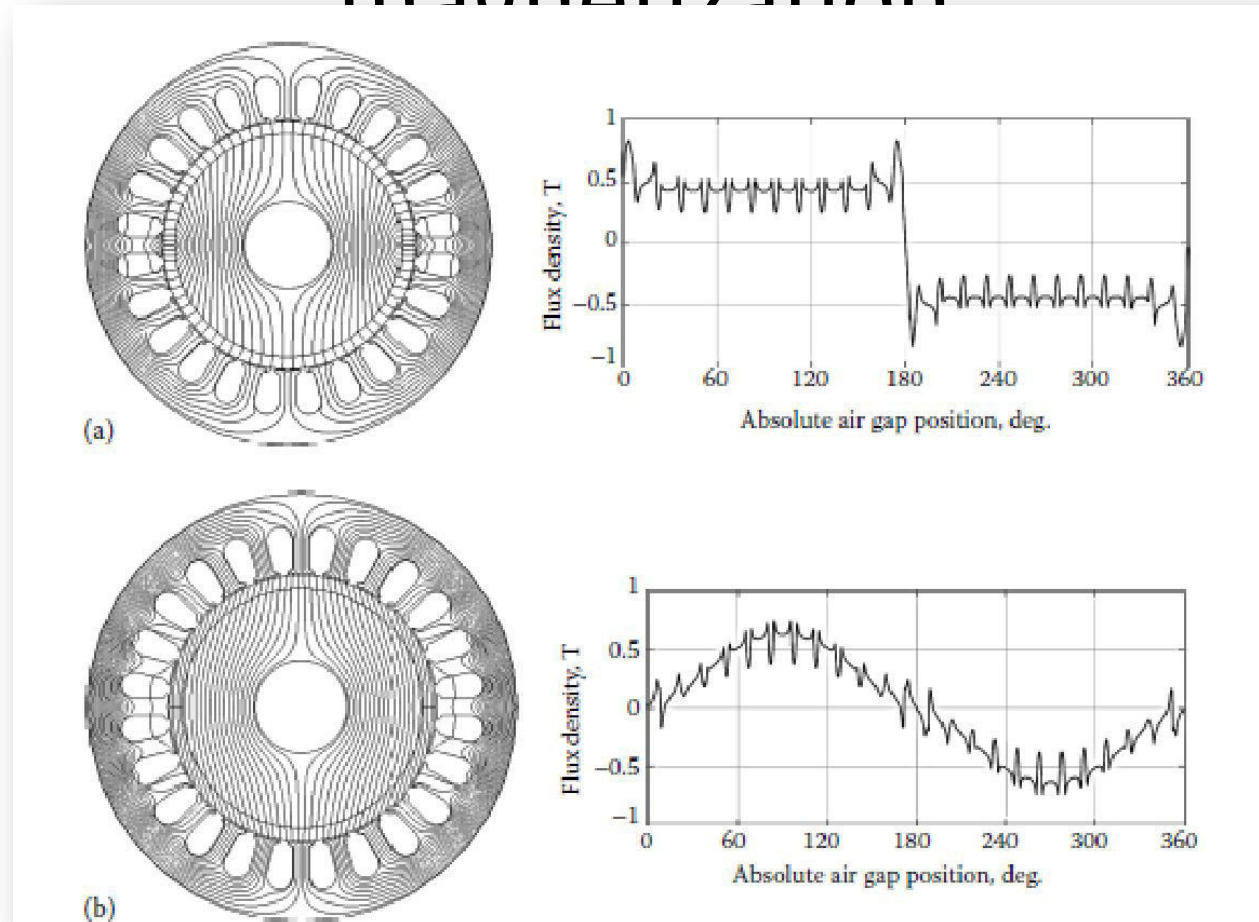
Types of magnetization



a) Radial magnetization and
(b) parallel magnetization

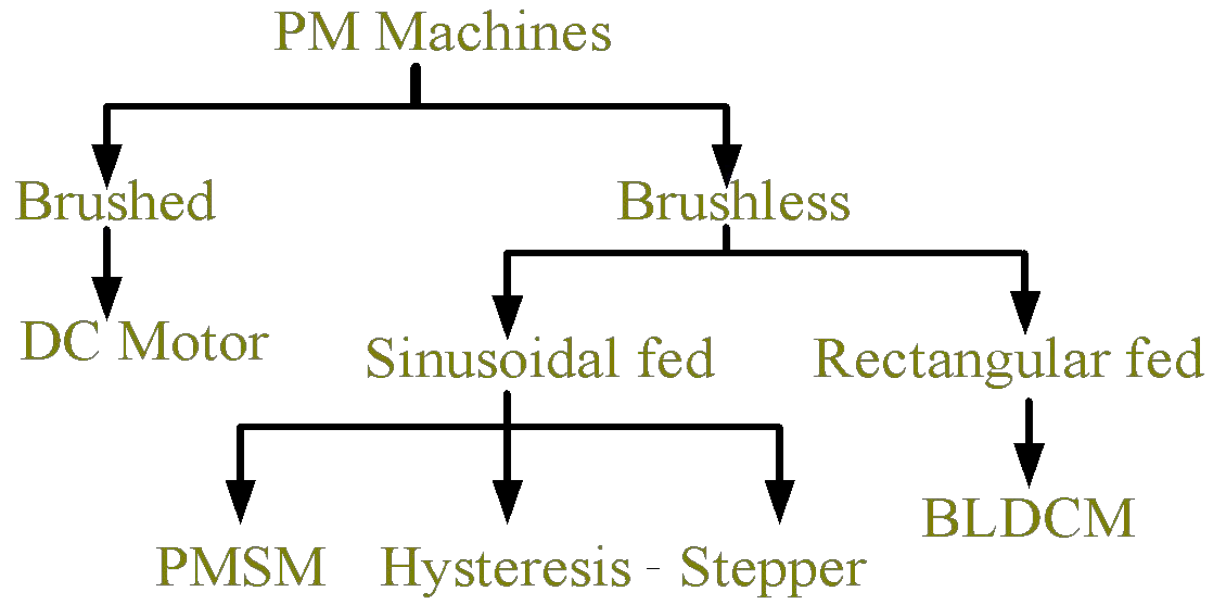
normal direction to the surface is
indicated by **vector \mathbf{n}**
and the magnetization **vector by \mathbf{M}**

Flux and Flux density based on magnetization

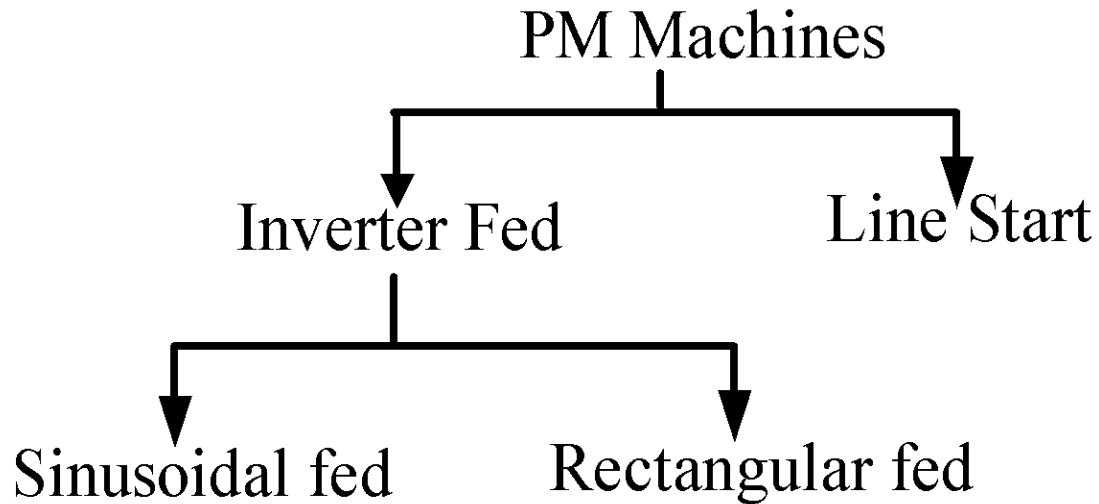


Flux and flux density versus rotor position for radially and parallel magnetized magnet machines. (a) Radially magnetized magnet machine. (b) Parallel magnetized magnet machine.

Classification of PM Machines (working principle based)

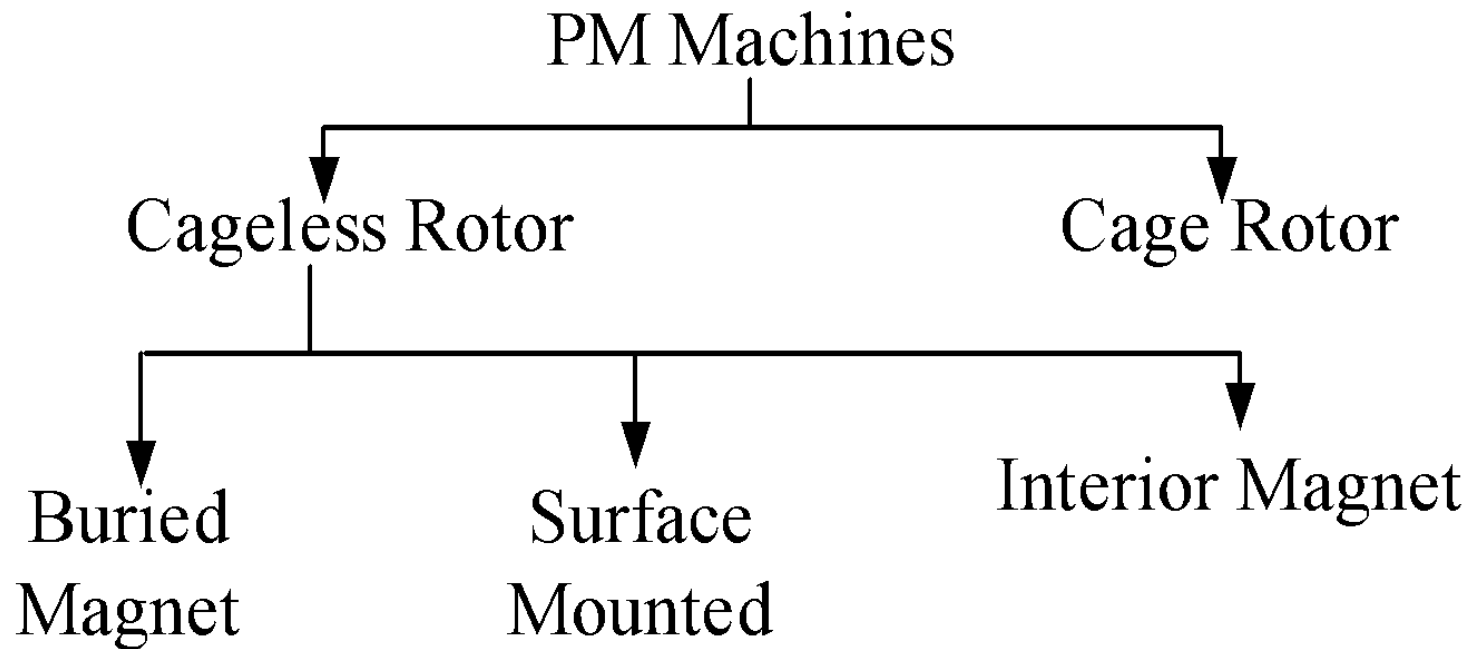


Classification of PM Machines (starting method based)

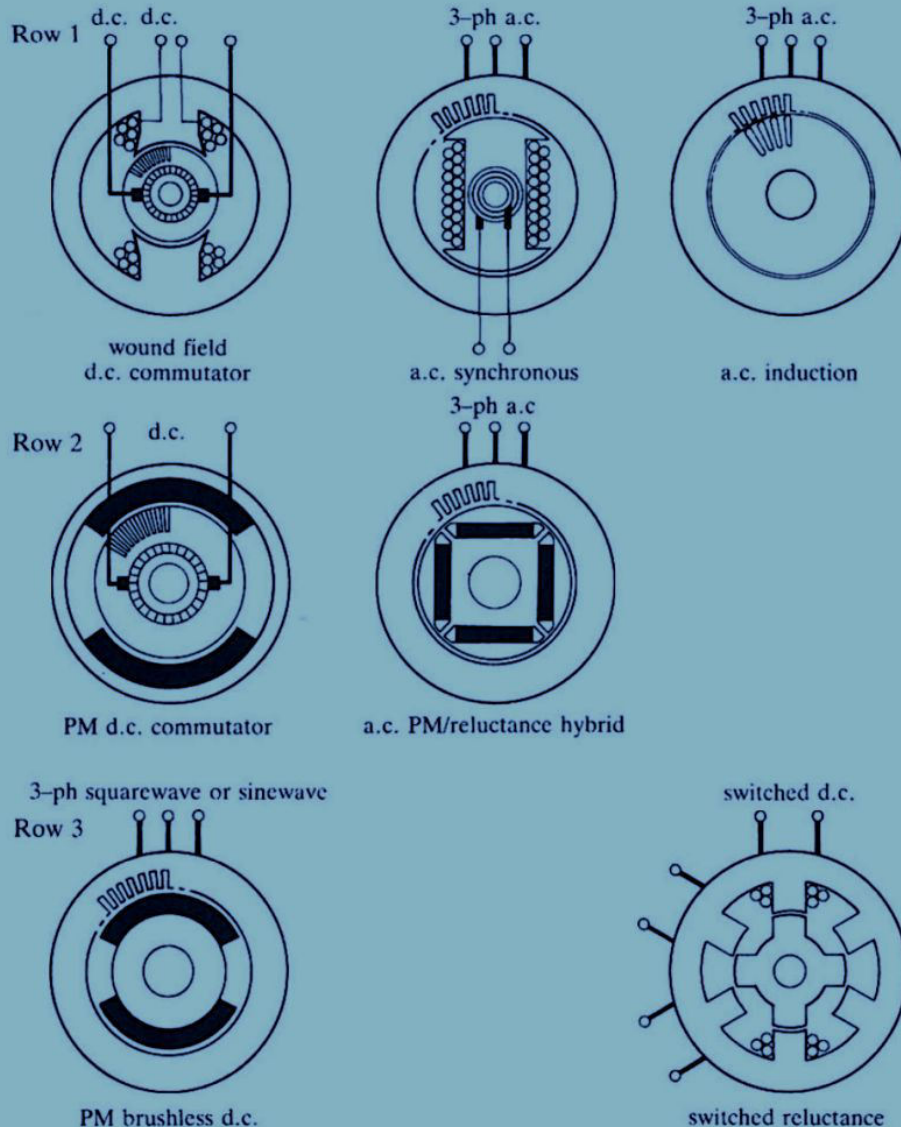


Classification of PM Machines

(Magnet Position based)



Evolution of Motors



Classical Motors :

- produce essentially constant instantaneous torque
- operate from pure dc, or ac sine wave supplies
- directly can start and run without electronic controllers

Efficient Motors:

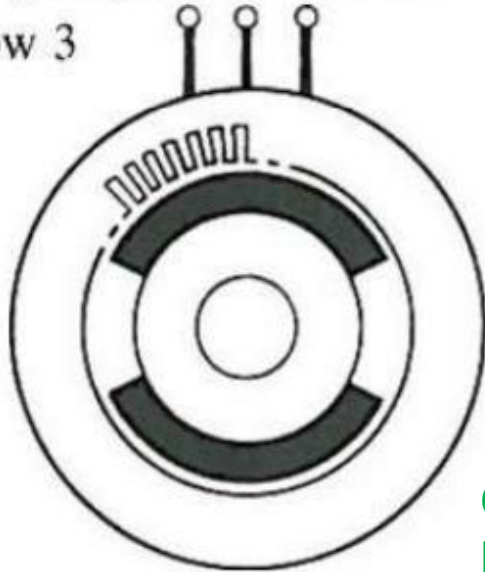
- Same characteristics of classical motors
- Magnetization is supplied by permanent magnets
- can start and run with/without electronic controllers

Efficient and Maintenance-Free Motors:

- Need electronic controllers to start and run
- Continuously rotating stepper motors
- Also called electronically commutated motors

Advanced Electronically commutated Motors

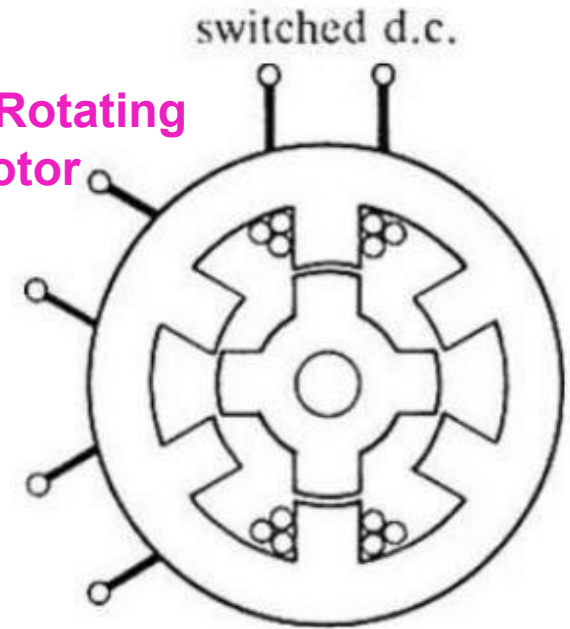
3-ph squarewave or sinewave
Row 3



PM brushless d.c.

Continuously rotating
PM Stepper motor

Continuously Rotating
VR Stepper motor



switched reluctance

- 3ph PMBL square wave motor resembles 6step – 3phase PM stepper motor.
- 3ph PMBL sine wave motor resembles 6step – 3phase PM stepper motor in micro-stepping mode.
- Switched reluctance motor resembles VR stepper motor.

Stator Configuration- PM machine



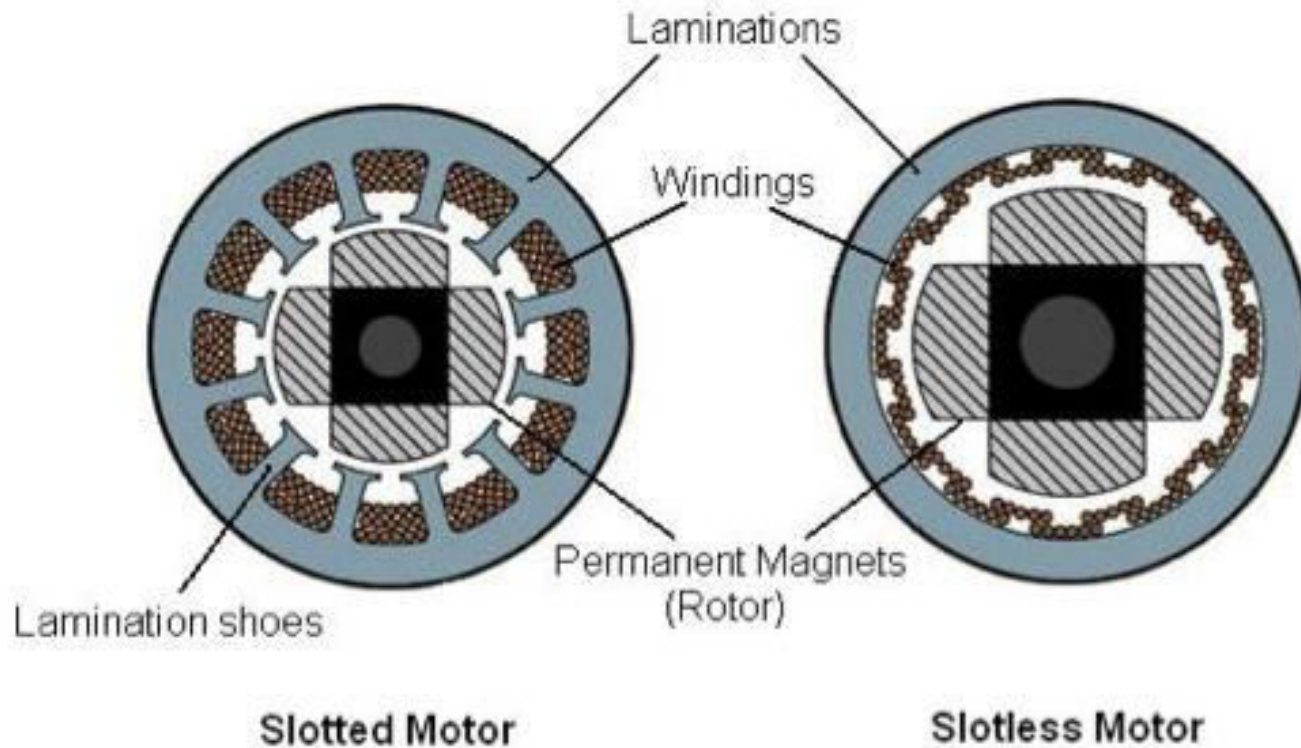
**Laminated steel stampings
of Stator**

Rotor Structure – PM machine

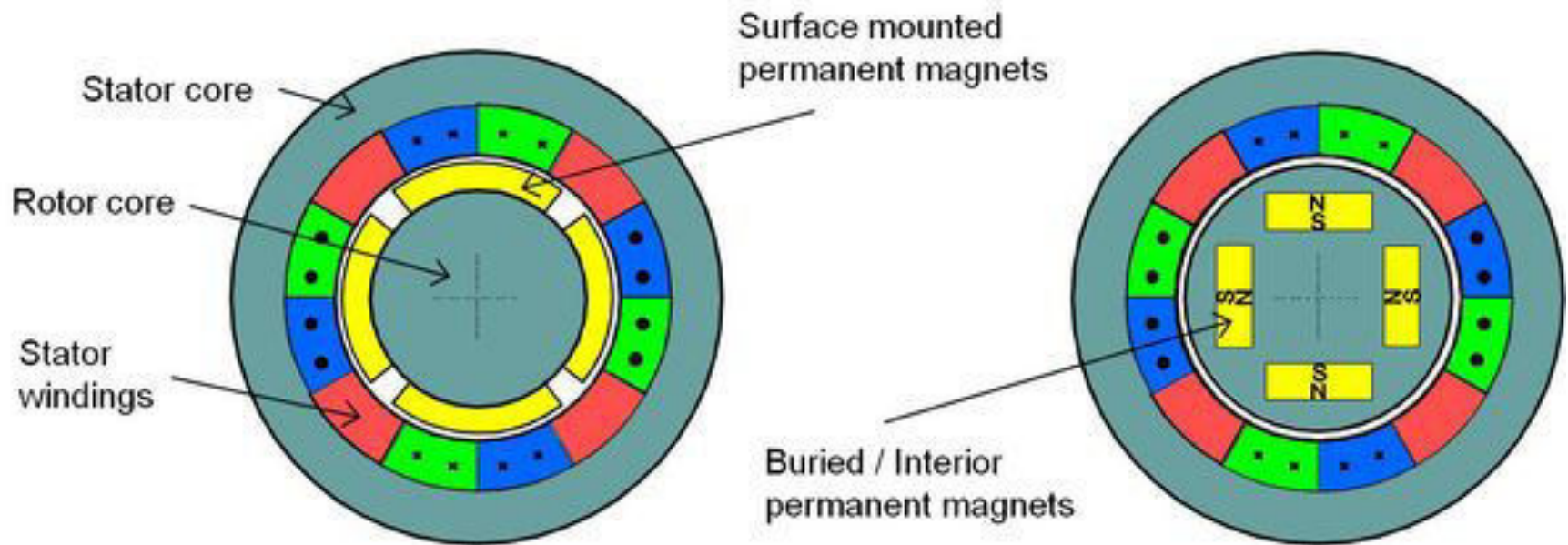


4-pole and 8-pole PM rotor

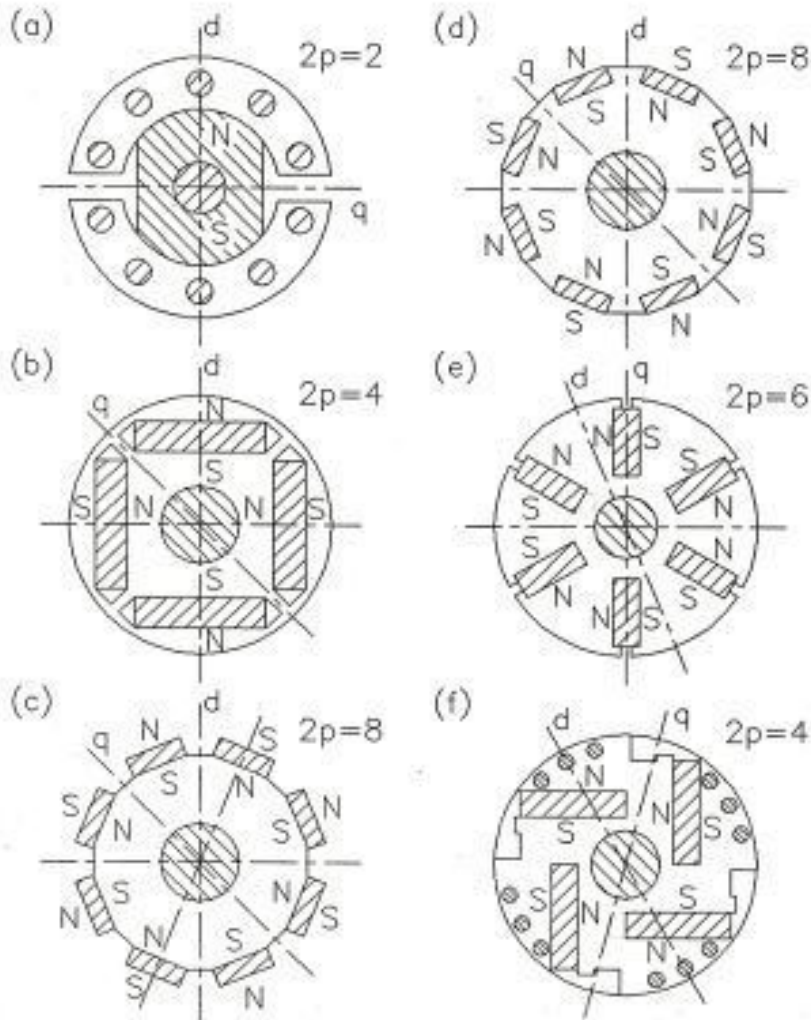
Slotted and Slot-less PM Machine



Rotor Configurations

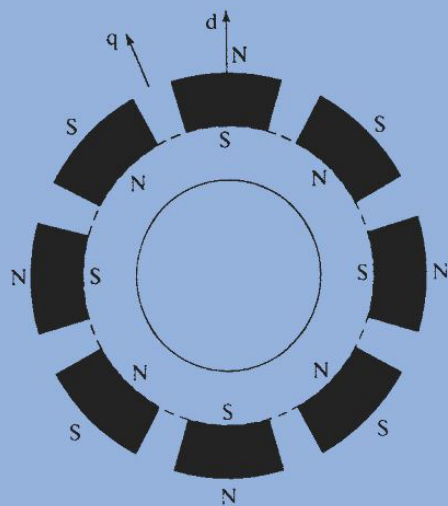


Different rotor configurations

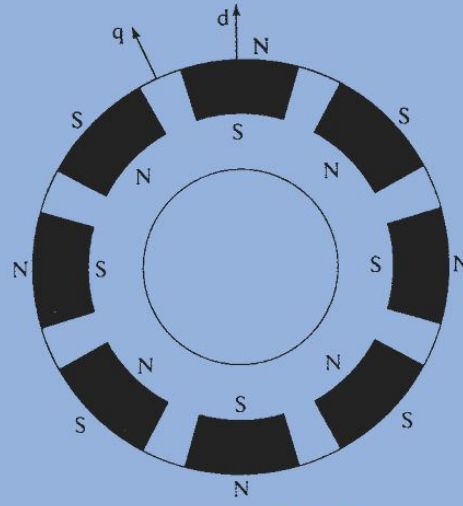


- ☐ classical (with salient poles, laminated pole shoes and a cage winding) (Fig.a),
- ☐ interior magnet rotor (Fig.b),
- ☐ surface magnet rotor (Fig.c),
- ☐ inset magnet rotor (Fig.d),
- ☐ rotor with buried magnets symmetrically distributed (Fig. e),
- ☐ rotor with buried magnets asymmetrically distributed (Fig.f)

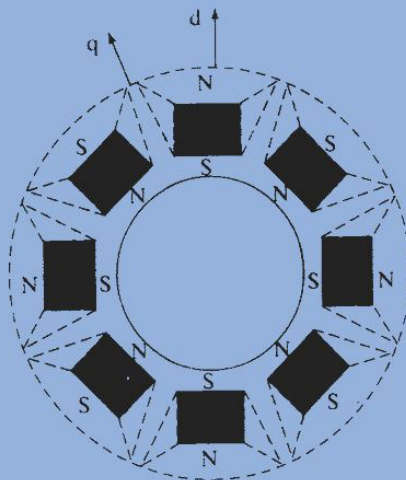
PM Motor Rotor configurations



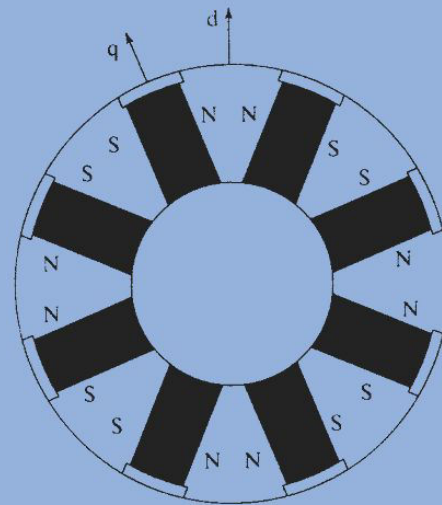
(i) Surface PM (SPM) synchronous machine



(ii) Surface inset PM (SIPM) synchronous machine



(iii) Interior PM (IPM) synchronous machine



(iv) Interior PM with circumferential orientation synchronous machine

Magnet Configurations:

- Surface mounted PM machine (SPM)
- Surface inset PM (SIPM) machine
- Interior permanent magnet machine (IPM)
- circumferential oriented PM machine

- Energy efficient
- Lesser audible noise
- Flat torque speed characteristics
- Better dynamic response
- Less maintenance and long motor life
- Higher output power per frame size
- Electronically commutated

Comparison of Brushless DC and Brushed DC Motor

Feature	PMBLDC motor	DC motor
Commutation	Electronically	Mechanical
Maintenance	Less because it does not have brushes and Commutator	High
Electrical Noise	less	High(arcs in brushes causes EMI in nearby Devices)
Life		
Speed/torque Characteristics	Moderately Flat	Flat (enables to operate in all regions)
Efficiency	High	Lowest
Motor Size	Low	Larger due to commutator and difficulty to remove heat
Speed Ranges	Can rotate at high speeds	Commutator limits the speed
Audible Noise	Less	More
Drive Complexity	Expensive	Simple and inexpensive
Control Requirements	A controller always required to rotate	No controller requirement for fixed speed and variable speed inexpensive drive can be used.
Cost	Higher (rotor has permanent magnets)	Lower

PMSM and PMBLDC motor

PMBLDCM

Square current fed Synchronous machine

Trapezoidal Back EMF

Stator flux position commutation each 60°

Only two phases are ON at a time

Mechanical power density is 15% higher than PMSM

Torque ripple at commutation

PMSM

Sine current fed synchronous machine

Sinusoidal Back EMF

Continuous stator flux position

All the three phases are ON at a time

Mechanical power density is lower than PMBLDCM

No Torque ripples

Comparison between motors used in electric vehicles

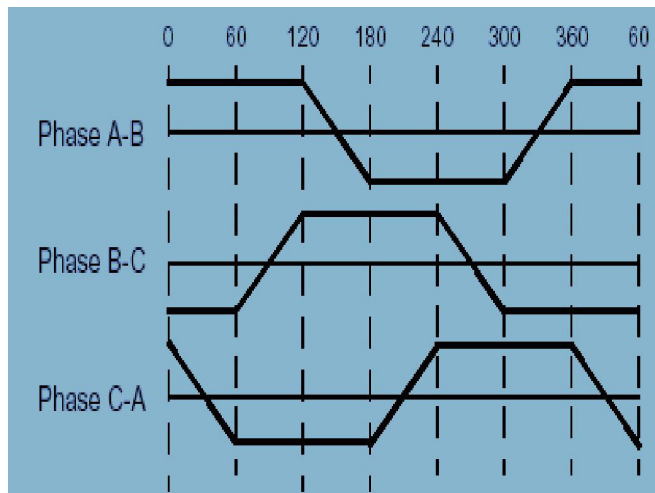
Motor type	DC motor	Induction motor	PM motor	Switched reluctance motor
Performance index				
Power density	Low	Intermediate	High	Very high
Peak efficiency (%)	<90	90–95	95–97	<90
Load efficiency (%)	80–87	90–92	85–97	78–86
Controllability	Simple	Complex	Hard for field-weakening	Complex
Reliability	Normal	Good	Excellent	Good
Heat dissipation	Bad	Bad	Good	Good
Size & weight	Big, Heavy	Normal, Normal	Small, Light	Small, Light
High-speed performance	Poor	Excellent	Good	Excellent
Construction	Slightly worse	Better	Slightly better	Excellent
Cost of motor (\$/kW)	10	8–10	10–15	6–10
Cost of controller	Low	High	High	Normal
Combination property	Slightly worse	Normal	Excellent	Better

PM BLDC

Motors

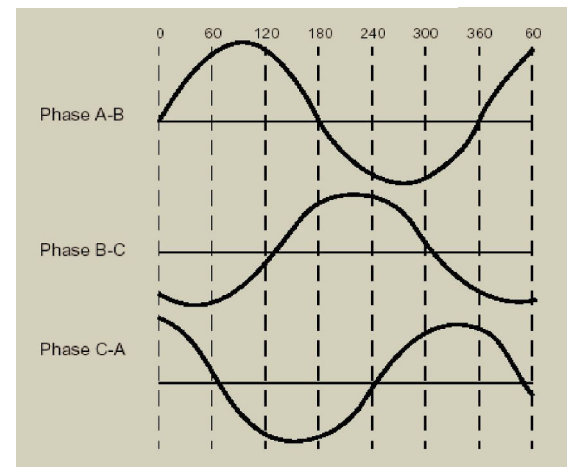
Permanent Magnet Brushless DC Motor

Trapezoidal Back EMF



Permanent Magnet Synchronous Motor

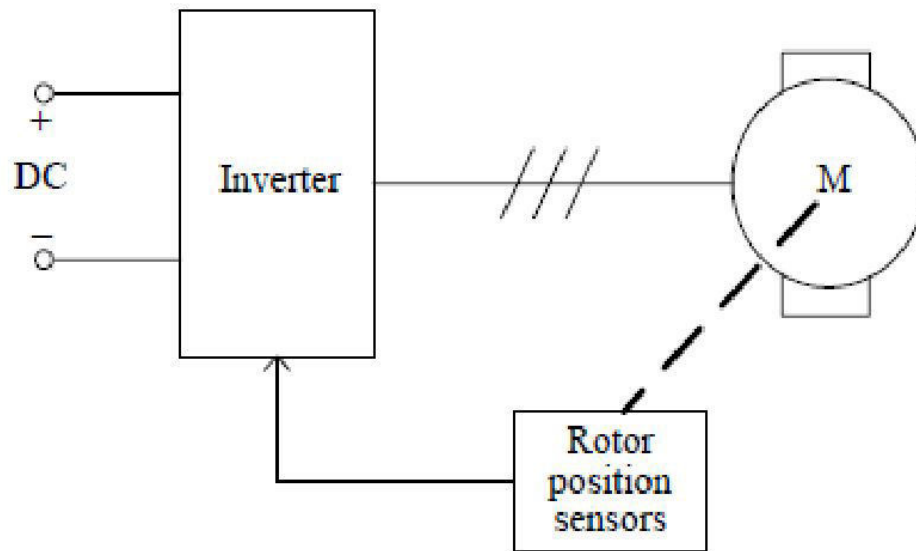
Sinusoidal Back EMF



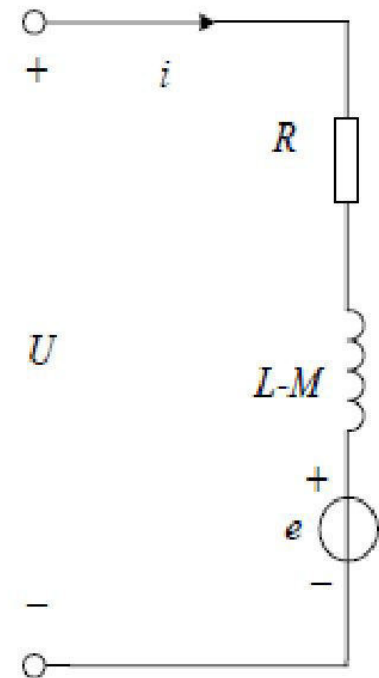
- ✓ Square wave / Quasi-square wave/ Trapezoidal motor
- ✓ In this motor the back emf is generally trapezoidal in shape and current in each phase is 120° quasi square wave in form
- ✓ The operation is more near to a 3-commutator segment DC motor with fixed field supply.
- ✓ Generally called a PM BLDC motor

- ✓ Sine wave motor:
- ✓ Currents and Voltages of phases are 120° displaced sine waves
- ✓ The operation is close to a synchronous motor with fixed field supply
- ✓ Generally called as PM synchronous motor, PMSM

Topology and equivalent circuit of BLDC motor



(a) Topology

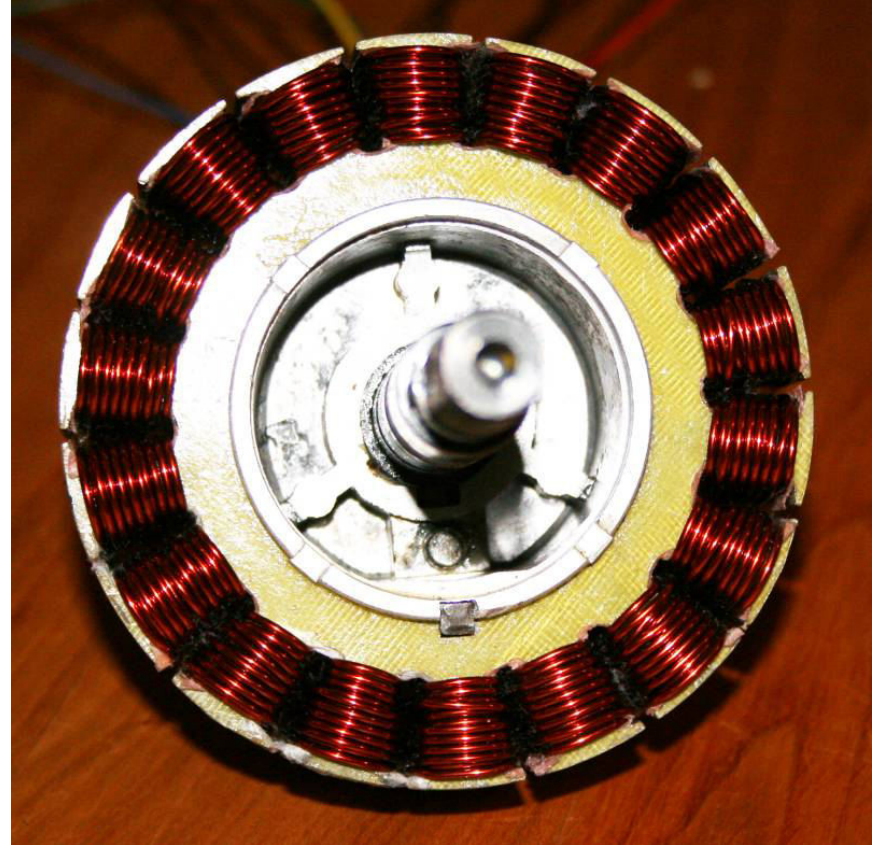


(b) Equivalent circuit

PM BLDC hub Motor

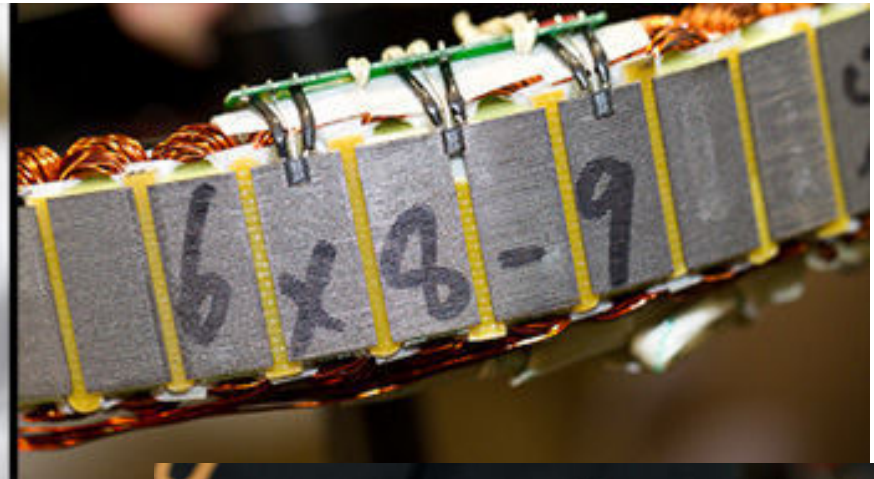
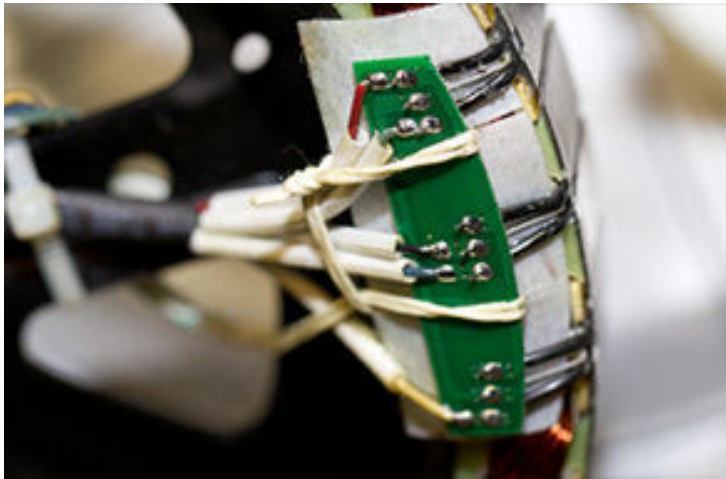


PM BLDC Hub Motor

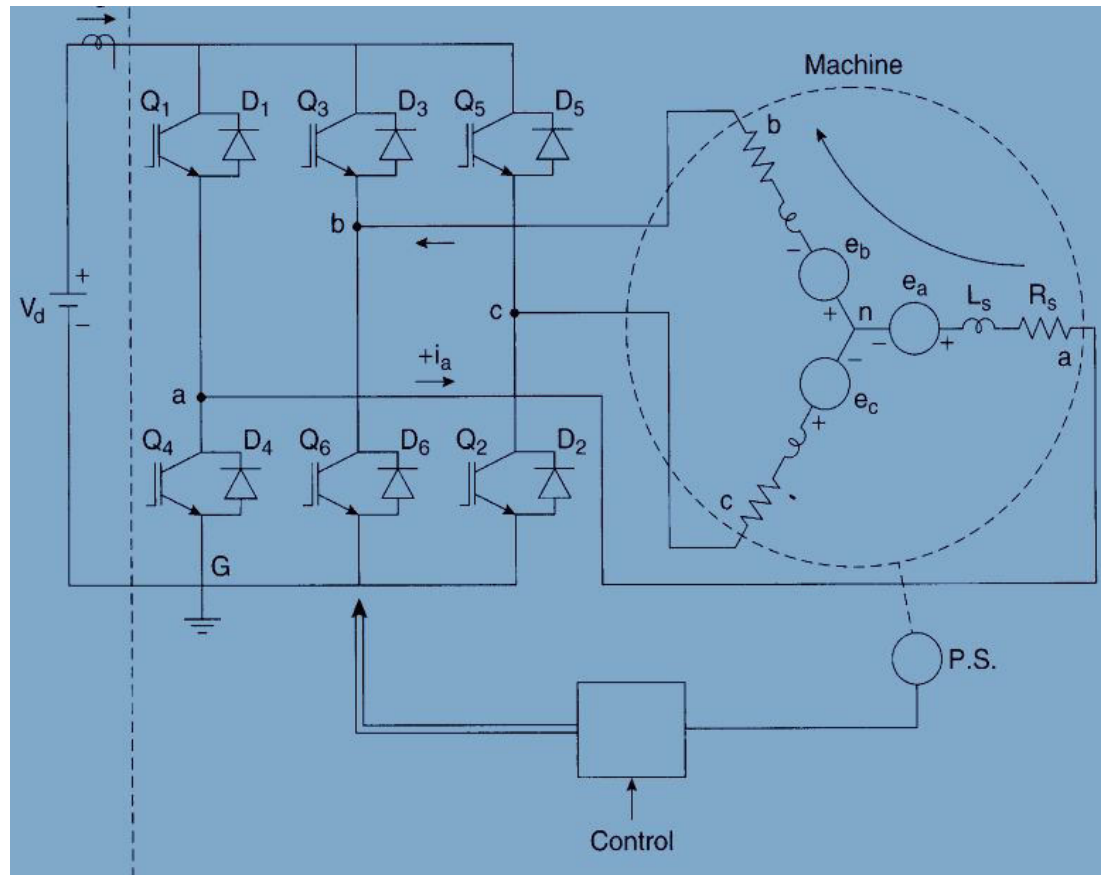


Before and after Rewinding

Placement of Hall effect Sensors



Drive circuit of PM BLDC Motor

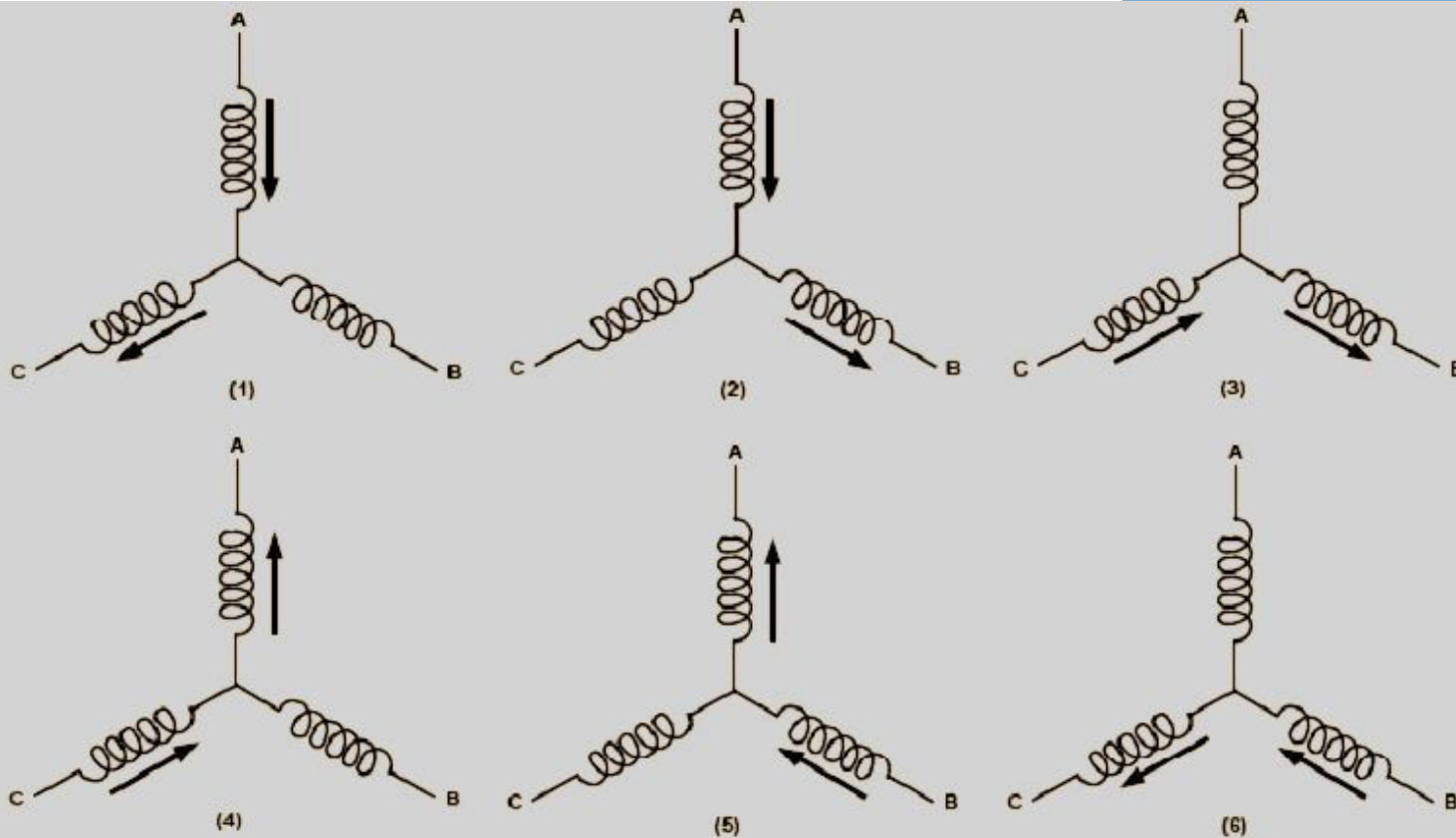
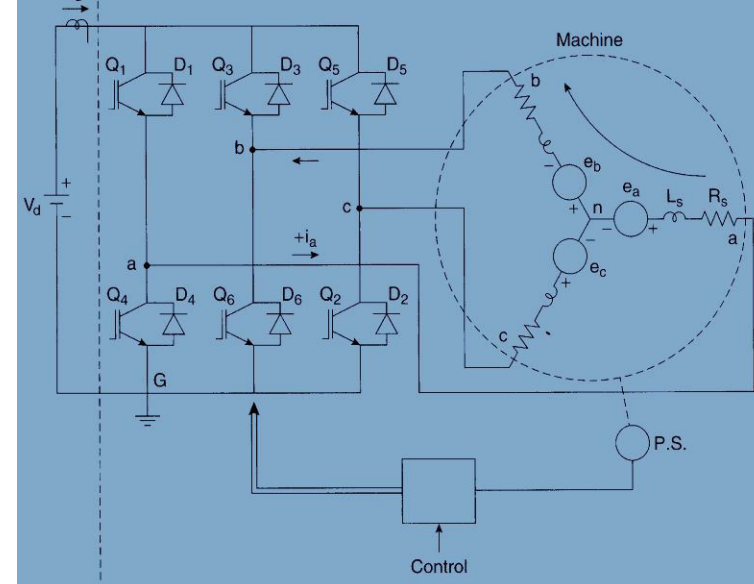


- * Needs position sensors, Position information is given to the control unit / decoder
- * Which intern generates switching pulses for the switches Corresponding phases turned off and turned in accordingly.
- * Any time, 2 (one top and one bottom) out of 6 switches are in conducting state

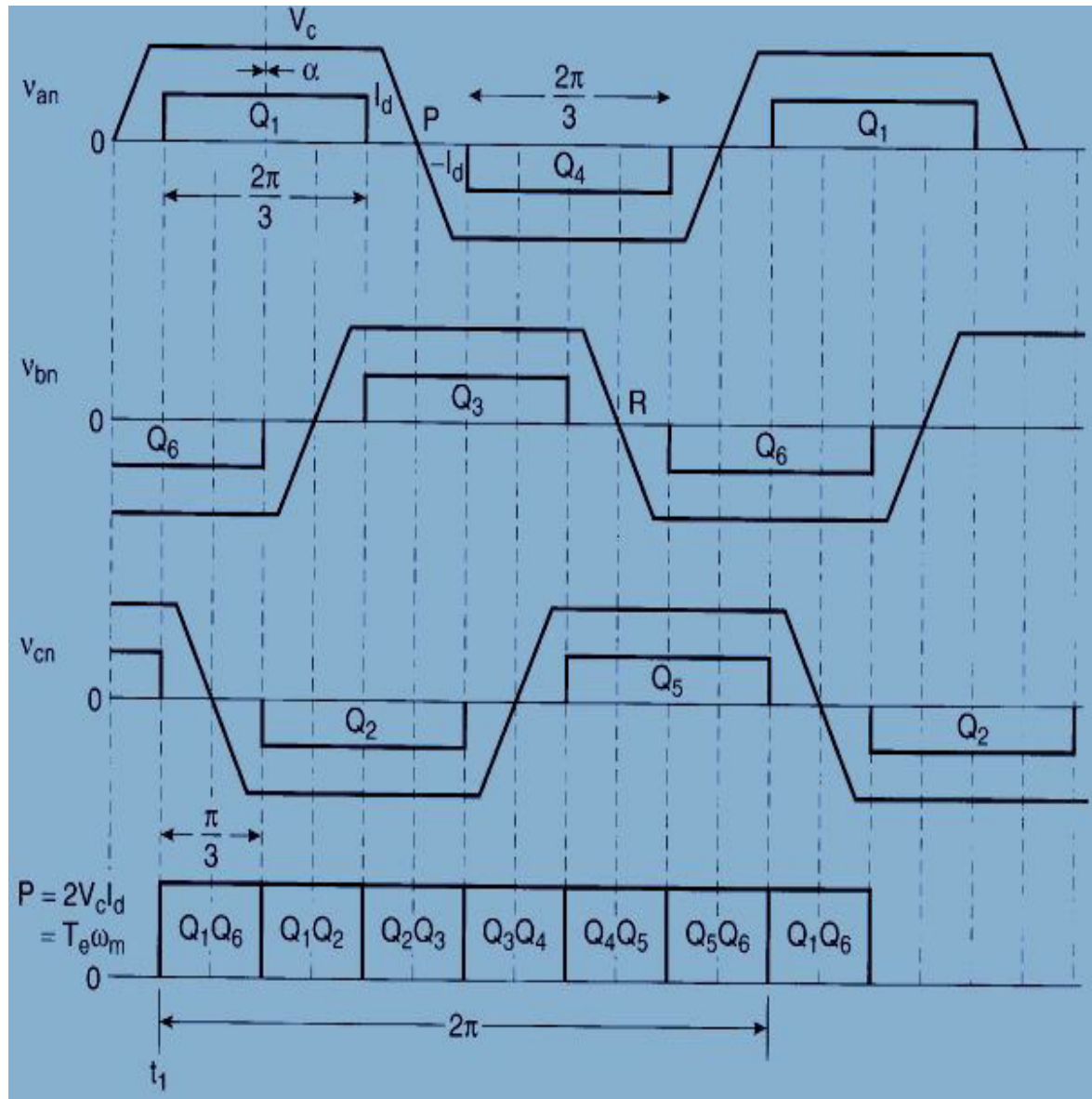
Switching states

For clockwise direction :
AC-BC-BA-CA-CB-AB-AC

For anti-clockwise direction
AC-AB-CB-CA-BA-BC-AC

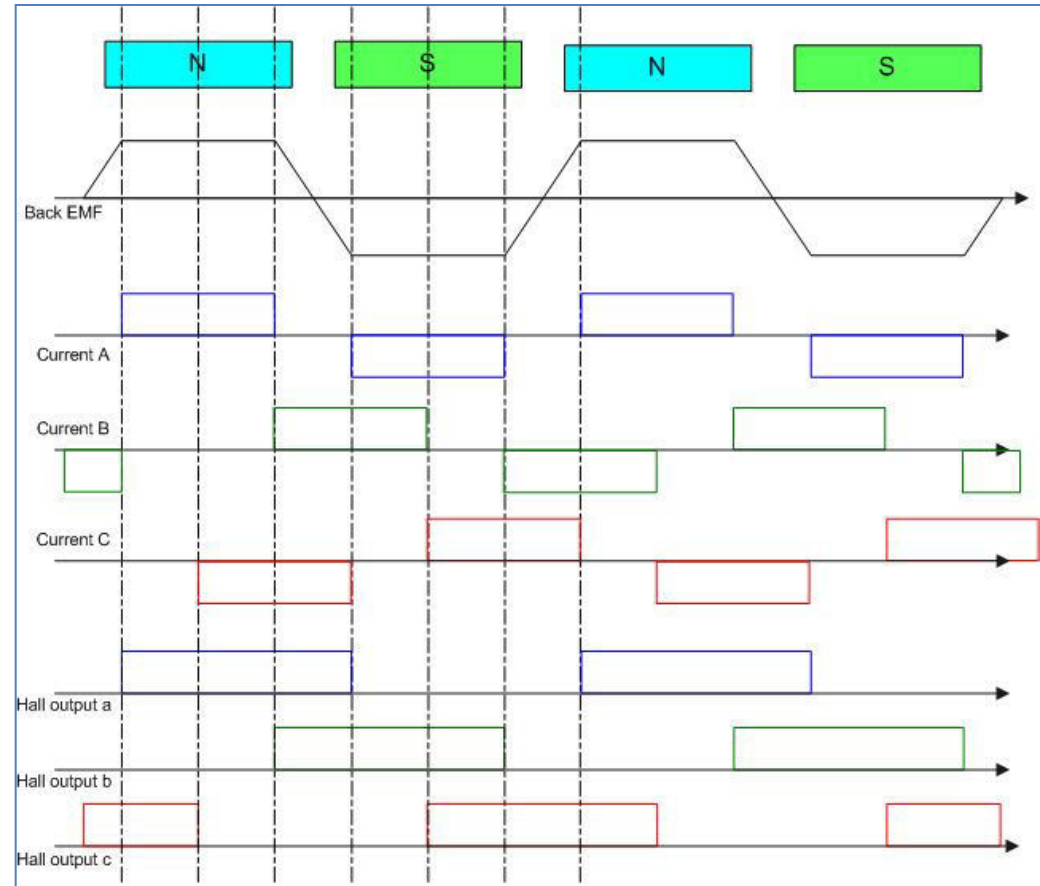
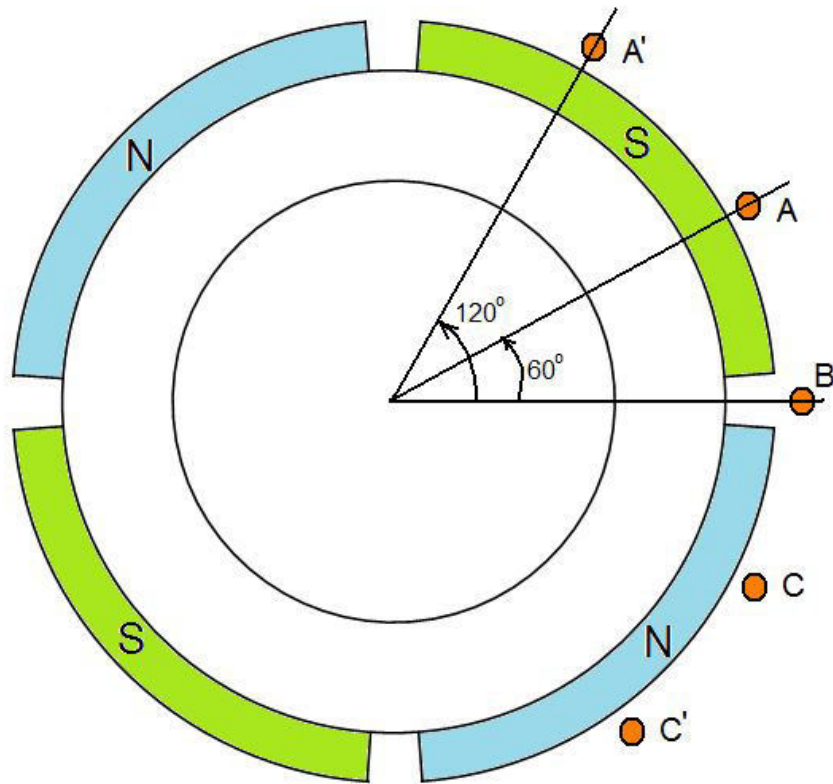


Position sensor requirements



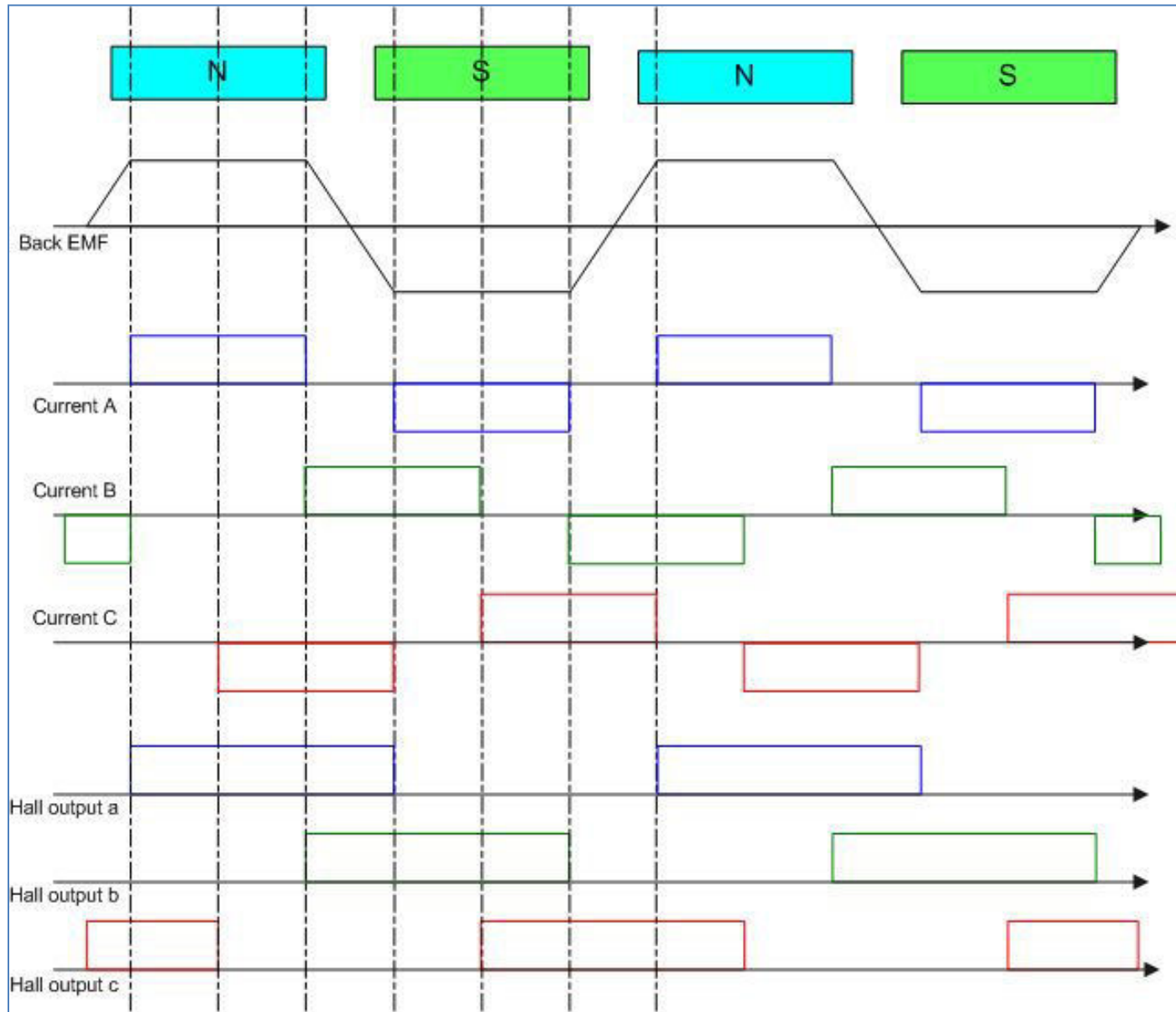
- The popularity of the PM BLDC machine is because of its control simplicity
- Only six discrete positions needed for a three-phase machine in each of the electrical cycle
- These signals generally generated using three Hall sensors displaced from each other by 120 electrical degrees

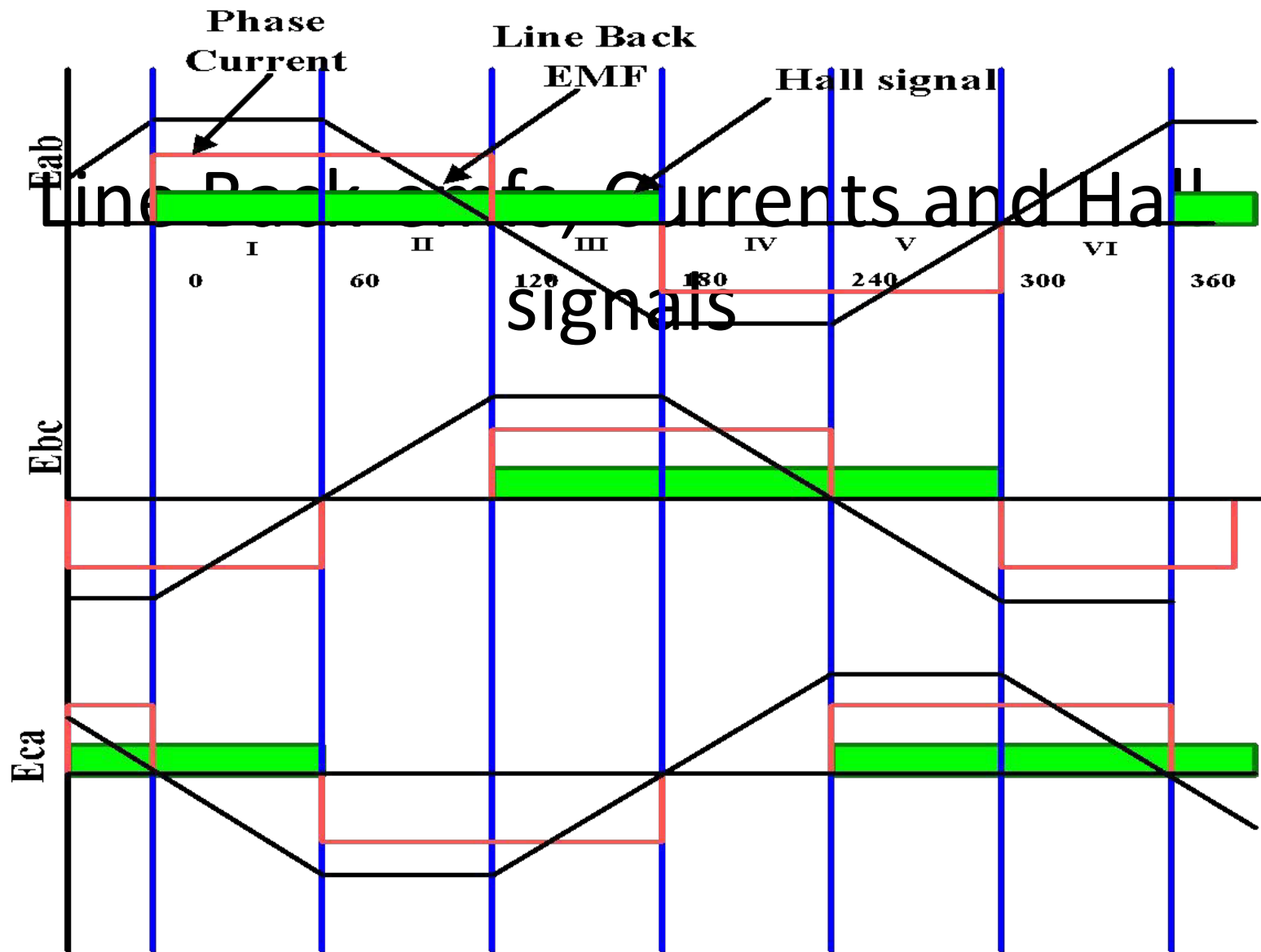
Hall sensors placement



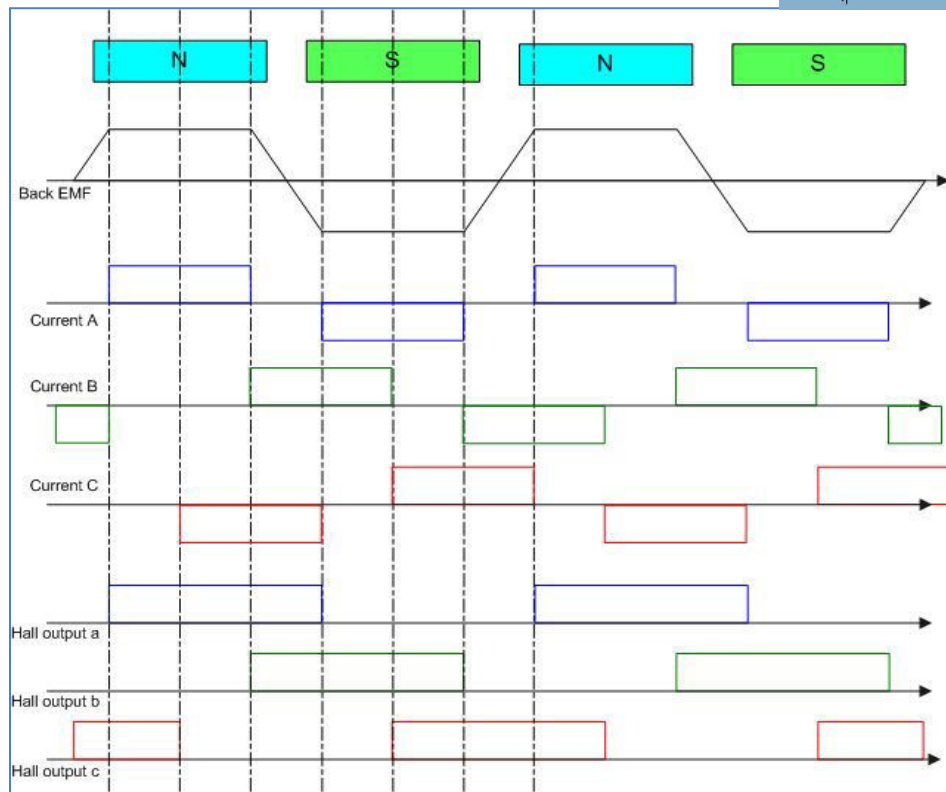
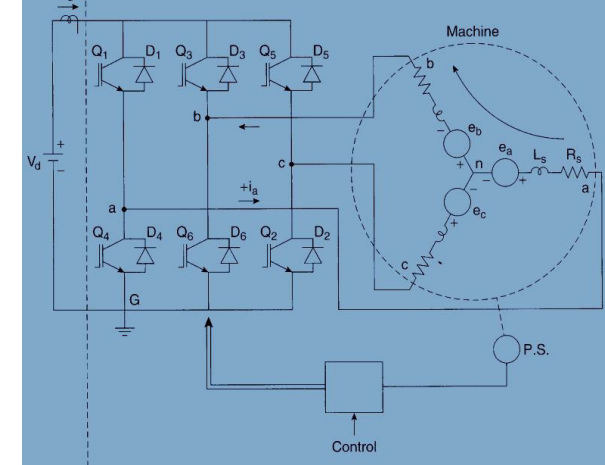
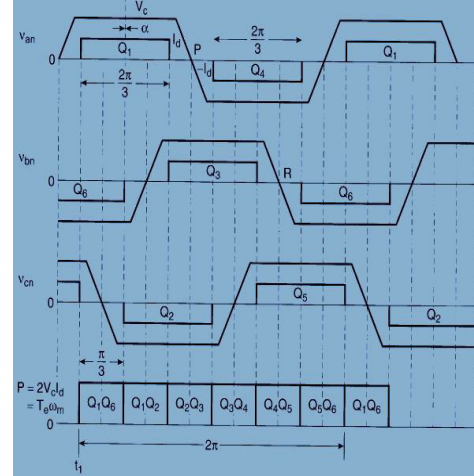
- We can Place hall sensors 120° (A'BC') apart or 60° (ABC) apart
- Placing 60° apart reduces the fixtures cost, slightly increases the logic circuitry

Hall Signals





Hall Sensors output decoding

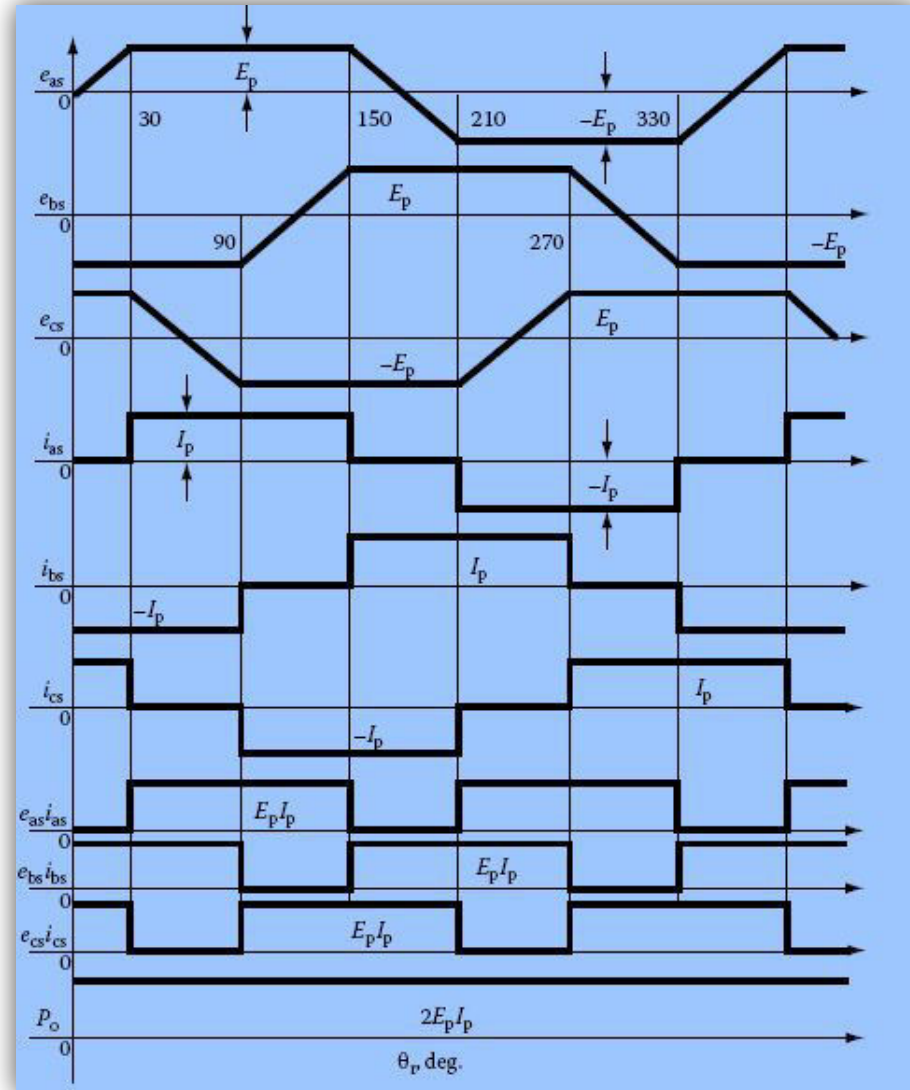


Ha	Hb	Hc	Q1	Q2	Q3	Q4	Q5	Q6
1	0	1	1	0	0	0	0	1
1	0	0	1	1	0	0	0	0
1	1	0	0	1	1	0	0	0
0	1	0	0	0	1	1	0	0
0	1	1	0	0	0	1	1	0
0	0	1	0	0	0	0	1	1

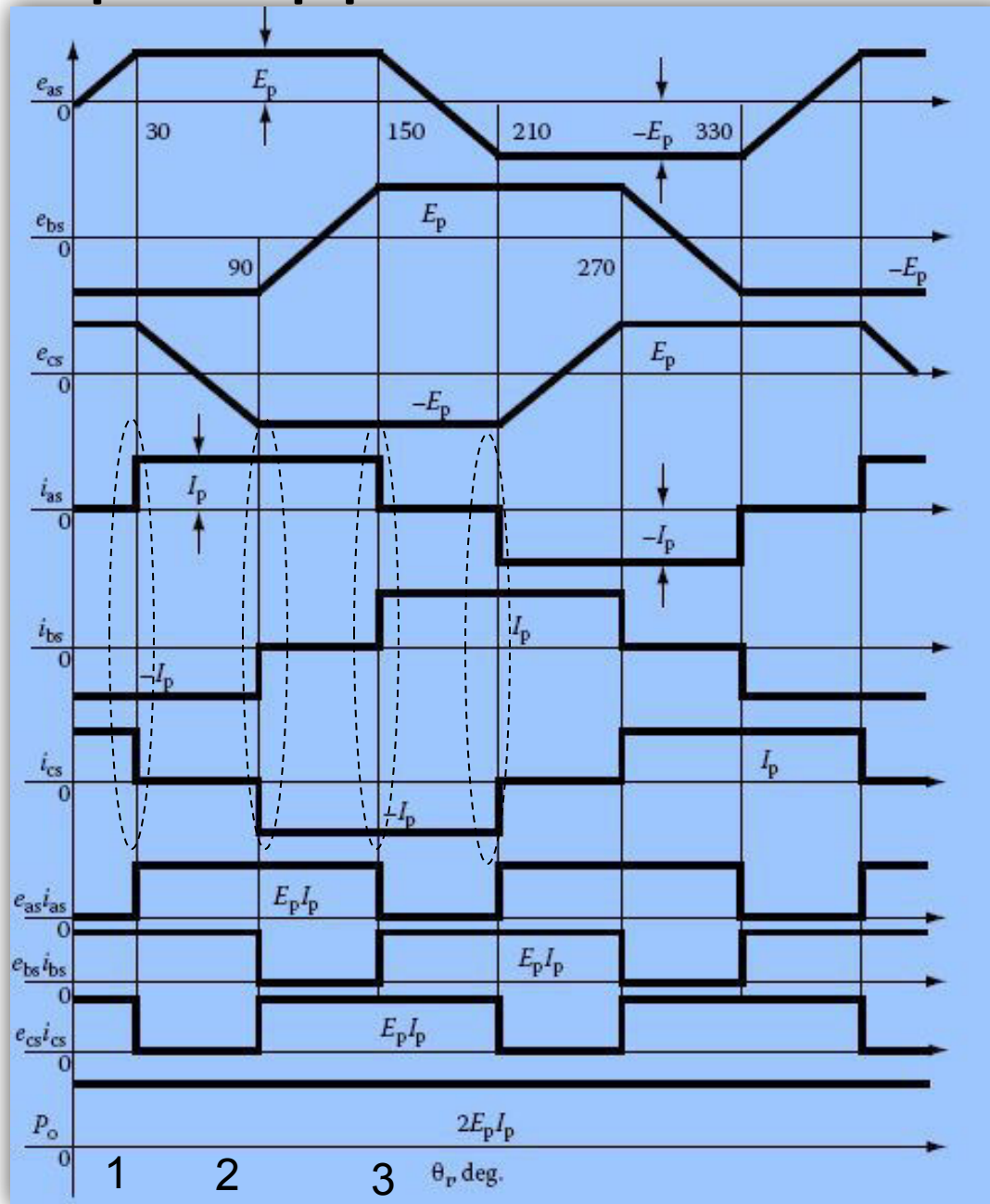
Q1	Q2	Q3	Q4	Q5	Q6
HaH'b	HaH'c	HbH'c	HbH'a	HcH'a	HcH'b

PMBL DC Motor waveforms

- The induced emfs have constant magnitude for electrical 120° both in the positive and negative half cycles,
- the power output can be uniform by exciting the rotor phases with 120° (electrical) wide currents as shown.
- But the currents cannot rise and fall in the motor windings in zero time and hence in actual operation, there are power pulsations during the turn on and turn off of the currents for each half cycle, which intern create torque ripples.



Torque ripples in BLDC motor



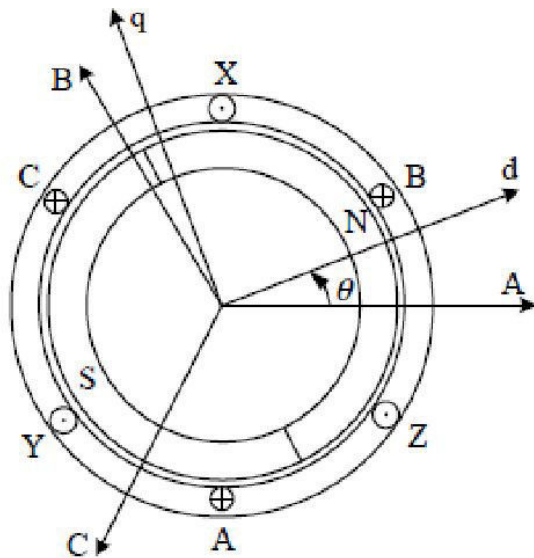
Torque ripple in PM BLDC Motor

- Deviation from ideal conditions introduces torque ripples
- Reasons for torque ripple is
 - Currents cannot rise and fall in the motor windings in zero time, which deviate from desired constant magnitude current commands produce commutation torques that are very significant in magnitude.
 - The deviations in the induced emf waveforms from a truly trapezoid of 120° in each half cycle.
 - Switching harmonics in the inverter output voltages generate harmonic currents which in turn result in switching harmonic torques
 - There are other kinds due to magnets and their assembly asymmetries, air gap eccentricity and cogging, etc.
- In low-performance applications, torque ripple hardly matters but in high-performance applications, it becomes unacceptable.

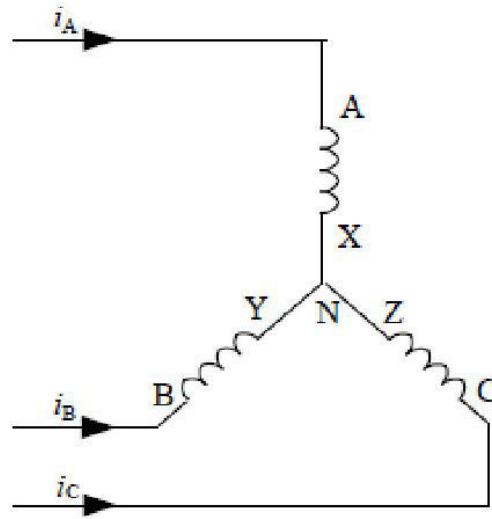
Modeling of PMBL DC Motor

- The flux distribution in PM brushless dc motor is trapezoidal and therefore the d–q rotor reference frames model not applicable.
- Due to the non-sinusoidal flux distribution, it is prudent to derive a model of the PMBL DC motor in phase variables.
- The derivation of this model is based on the assumptions
 - the induced currents in the rotor due to stator harmonic fields are neglected and
 - iron and stray losses are also neglected.
 - The motor is considered to have three phases even though for any number of phases the derivation procedure is valid.

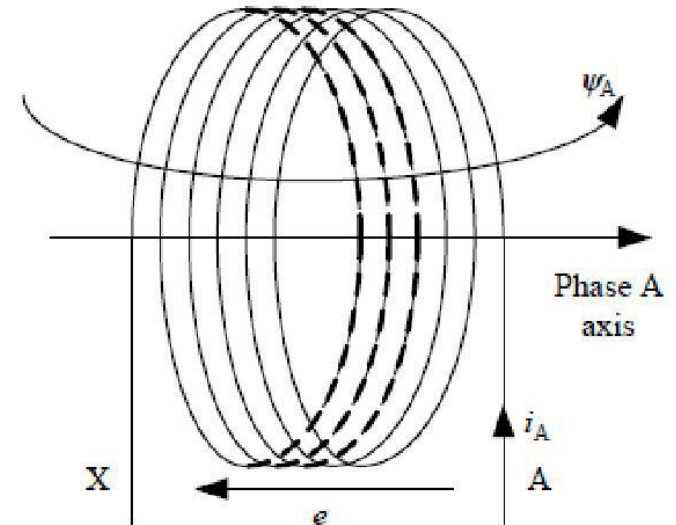
Mathematical Modelling Of PMBLDC Motor



(a) Structure of BLDC motor



(b) Connecting type of winding



(c) Provision of positive direction (Phase A)

Schematic diagram of the BLDC motor.

Assumptions in Modelling Of PMBLDC motor

- ☐ Ignore the core saturation, as well as the eddy current losses and the hysteresis losses.
- ☐ Ignore the armature reaction, and the distribution of air-gap magnetic field is thought to be a trapezoidal wave with a flat-top width of 120 electrical angle.
- ☐ Ignore the cogging effect and suppose the conductors are distributed continuously and evenly on the surface of the armature.
- ☐ Power switches and flywheel diodes of the inverter circuit have ideal switch features.

Mathematical Modelling..

- The phase voltage of each winding, which includes the resistance voltage drop and the induced EMF, can be expressed as

$$u_x = R_x i_x + e_{\psi x}$$

→ 1

u_x — phase voltage, in which subscript x denotes phase A, B and C;
 i_x — phase current; $e_{\psi x}$ — phase-induced EMF; R_x — phase resistance.
For three-phase symmetrical winding, there exists $R_a = R_b = R_c$.

The winding-induced EMF is equal to the change rate of the flux. Since the positive direction of induced EMF and flux linkage defined in Figure is opposite to that of the right-hand screw rule, the induced EMF can be written as

$$e_{\psi x} = - \frac{d\psi_x}{dt}$$

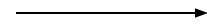
} → 2

Mathematical Modelling..

- Taking phase A for example, the flux is given as

$$\psi_A = L_A i_A + M_{AB} i_B + M_{AC} i_C + \psi_{pm}(\theta)$$

where



3

$\Psi_{pm}(\theta)$ — PM flux linkage of phase A;

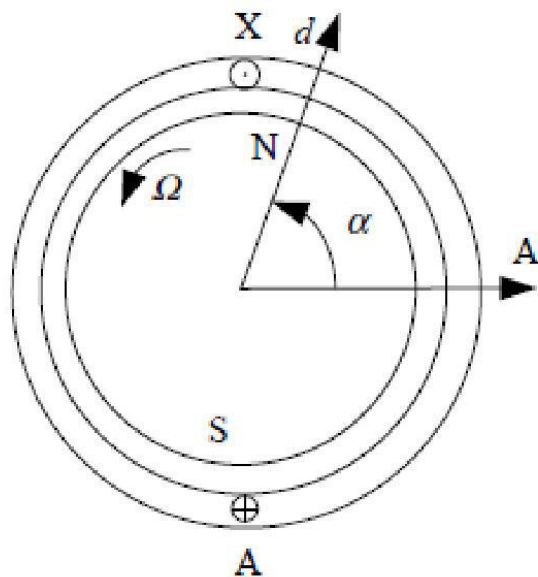
Θ — position angle of rotor, the angle between rotor d-axis and the axis of phase A;

L_a — self-inductance of phase A;

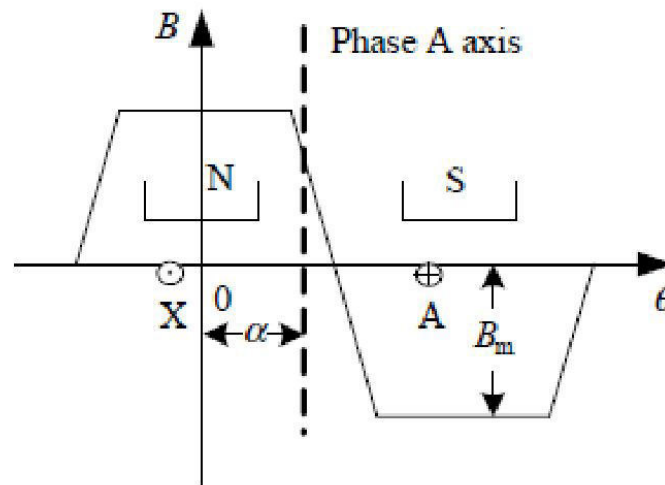
M_{AB} , M_{AC} — mutual inductance of phase A with phase B and phase C.

Mathematical Modelling..

- The magnitude of $\Psi_{pm}(\theta)$ depends on the magnetic field distribution of the PM in the air gap. The radial component of PM air-gap magnetic field distributes as a trapezoidal profile along the inner surface of the stator, is shown in Figure



(a) Rotor position

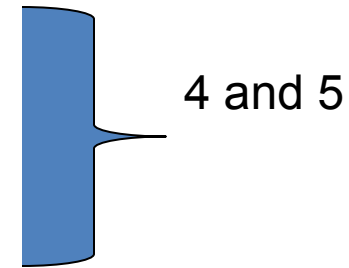


(b) Flux distribution

**PM Flux of
Phase A**

Mathematical Modelling..

- The magnitude of when the rotor rotates anticlockwise, the winding AX moves in the forward direction along the θ -axis. Then, the effective flux of phase A will change with regard to the rotor position. When the rotor position is α , the PM flux of phase A



where

$\Phi_{pm}(\alpha)$ — PM flux of phase A when the rotor position angle is α ;

$B(\theta)$ — PM rotor radial flux density in the air gap, which is in a trapezoidal distribution

along θ ; N — turns of winding;

S — product of rotor radius and effective length of conductors.

Mathematical Modelling..

- By substituting equations 2 to 5 in equation 1

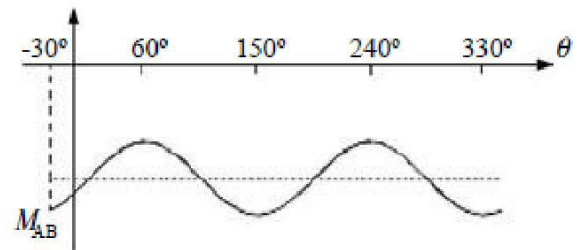
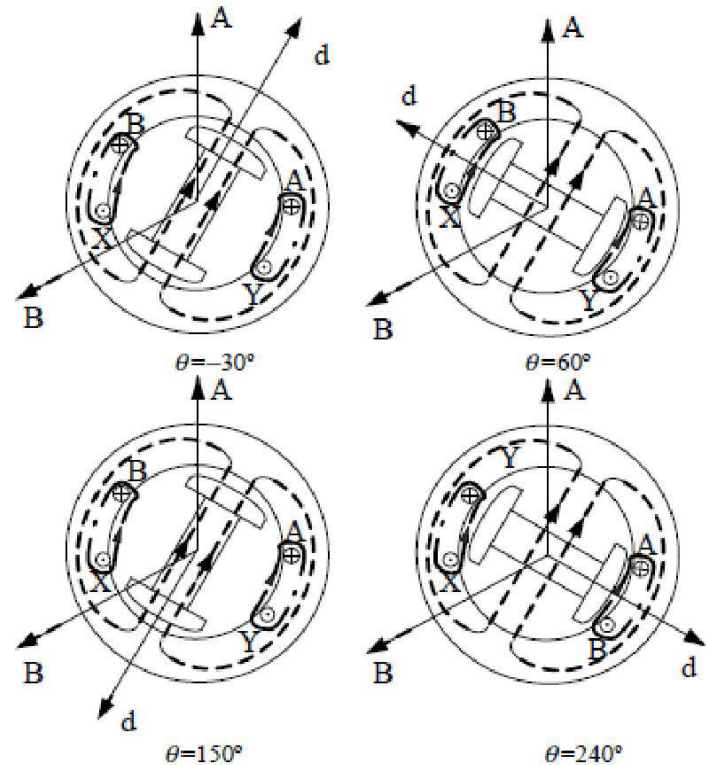
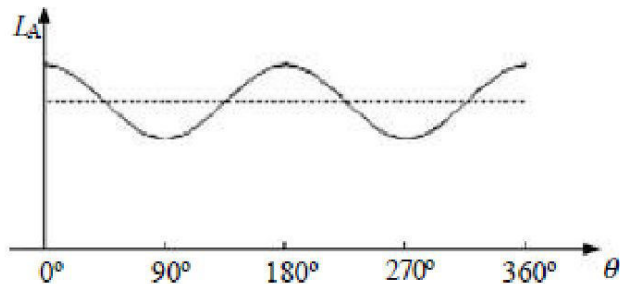
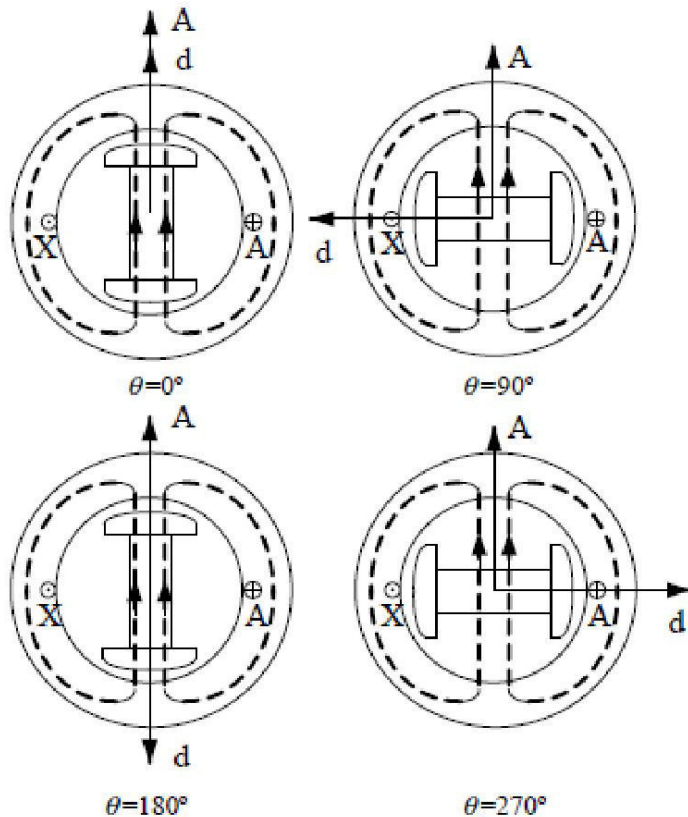
$$\begin{aligned}
 u_A &= Ri_A + \frac{d}{dt}(L_A i_A + M_{AB} i_B + M_{AC} i_C + \psi_{pm}) \\
 &= Ri_A + \frac{d}{dt}(L_A i_A + M_{AB} i_B + M_{AC} i_C) + \frac{d}{dt} \left[NS \int_{-\frac{\pi}{2} + \theta}^{\frac{\pi}{2} + \theta} B(x) dx \right] \\
 &= Ri_A + \frac{d}{dt}(L_A i_A + M_{AB} i_B + M_{AC} i_C) + e_A
 \end{aligned} \tag{6}$$

where E_a represents the back-EMF of phase A.

Equation (6) includes a derivative operation of the product of inductance and current, where the self-inductance and the mutual inductance of the winding is proportional to N^2 (N represents the number of turns) and the permeance of the corresponding magnetic circuit. That is

Mathematical Modelling..

- Effect of rotor saliency on inductances



Mathematical Modelling..

- Generally, the surface-mounted salient-pole rotor is used for BLDC motors. In this condition, the winding inductance will not change with the time. Further, as the three-phase stator windings are symmetrical, the self-inductances will be equal, and so as the mutual inductance.

$$L_A = L_B = L_C = L,$$

$$M_{AB} = M_{BA} = M_{BC} = M_{CB} = M_{AC} = M_{CA} = M \text{ and } i_a + i_b + i_c = 0$$

Substituting them into Equation (6), we can get

$$\begin{aligned} u_A &= R i_A + L \frac{di_A}{dt} + M \frac{di_B}{dt} + M \frac{di_C}{dt} + e_A \\ e_A &= \frac{d}{dt} \left[NS \int_{-\frac{\pi}{2} + \theta}^{\frac{\pi}{2} + \theta} B(x) dx \right] \\ &= NS \left[B\left(\frac{\pi}{2} + \theta\right) - B\left(-\frac{\pi}{2} + \theta\right) \right] \frac{d\theta}{dt} \\ &= NS\omega \left[B\left(\frac{\pi}{2} + \theta\right) - B\left(-\frac{\pi}{2} + \theta\right) \right] \end{aligned}$$

**W- Electrical
angular speed**

Mathematical Modelling..

- According to the distribution of magnetic density in the air gap as shown in Figure, together with $B(\theta)$ having a period of 2π and $B(\theta + \pi) = B(\theta)$, we can get

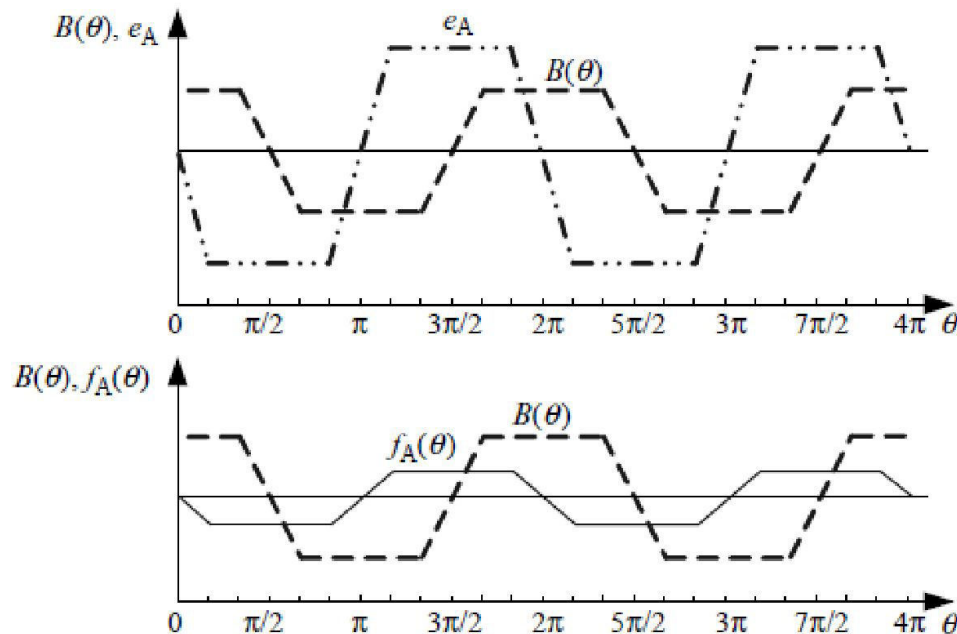
$$\begin{aligned}
 e_A &= NS\omega \left[B\left(\frac{\pi}{2} + \theta\right) - B\left(-\frac{\pi}{2} + \theta\right) \right] \\
 &= NS\omega \left[B\left(\frac{\pi}{2} + \theta\right) - B\left(\frac{\pi}{2} + \theta + \pi - 2\pi\right) \right] \\
 &= 2NS\omega B\left(\frac{\pi}{2} + \theta\right)
 \end{aligned}$$

$$e_A = 2NS\omega B_m f_A(\theta) = \omega \psi_m f_A(\theta)$$

B_m — maximum value of PM density distribution in air gap;
 ψ_m — maximum value of PM flux linkage of each winding, $\psi_m = 2NSB_m$

Mathematical Modelling..

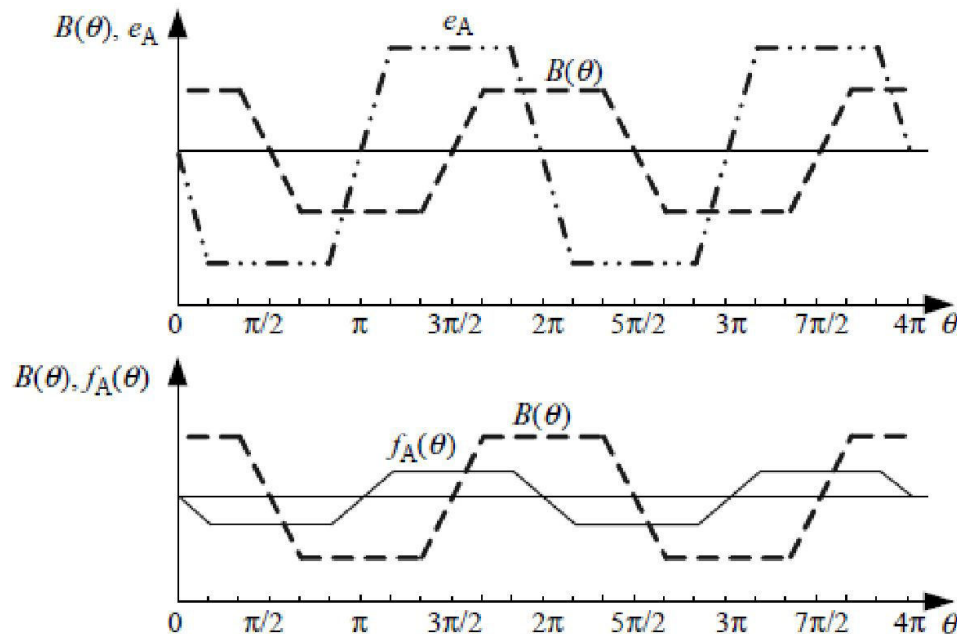
- Note that the $f_a(\theta)$ has a trapezoidal distribution with the rotor position, and its maximum and minimum values are, respectively, 1 and -1 . The corresponding waveform and its phase relationship with $B(\theta)$ and e_a are shown in Figure
- As for the three-phase symmetrical windings, there also exist $f_a(\theta) = f_b(\theta - 2\pi/3)$, and $f_c(\theta) = f_c(\theta + 2\pi/3)$.



Phase relationship between $B(\theta)$, e_a , and $f_a(\theta)$.

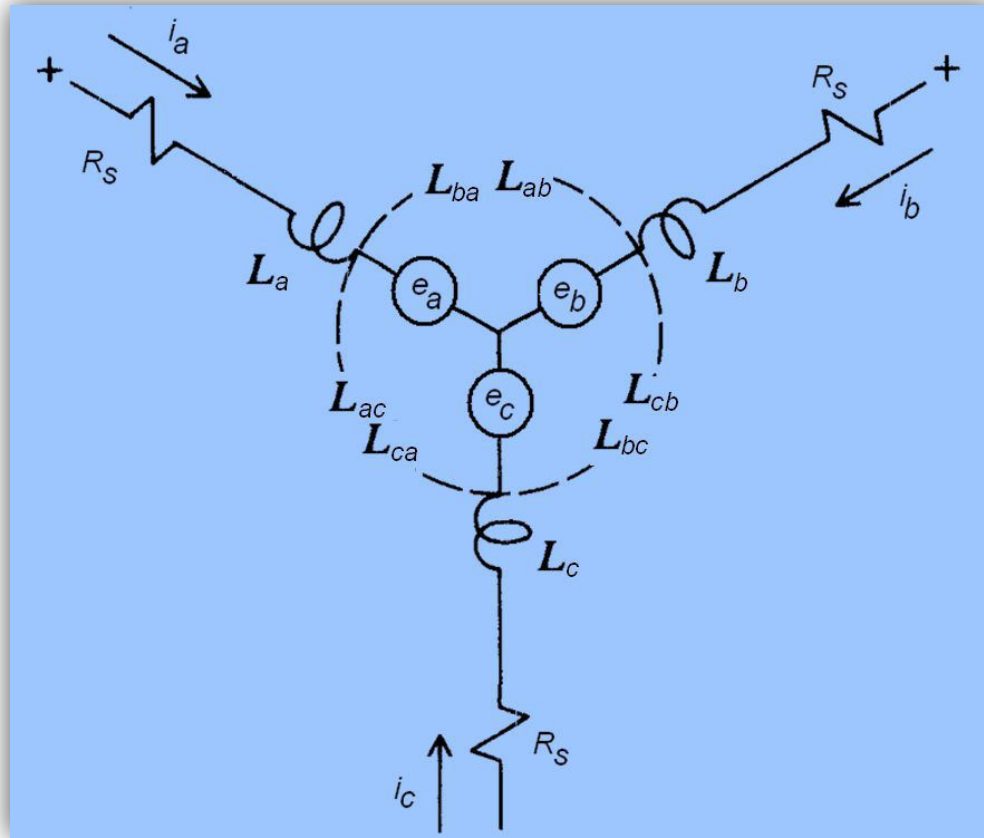
Mathematical Modelling..

- Note that the $f_a(\theta)$ has a trapezoidal distribution with the rotor position, and its maximum and minimum values are, respectively, 1 and -1 . The corresponding waveform and its phase relationship with $B(\theta)$ and e_a are shown in Figure
- As for the three-phase symmetrical windings, there also exist $f_a(\theta) = f_b(\theta - 2\pi/3)$, and $f_c(\theta) = f_c(\theta + 2\pi/3)$.



Phase relationship between $B(\theta)$, e_a , and $f_a(\theta)$.

Modeling of PM BLDC Motor



- Three phase star connected PM BLDC motor represented as shown.
- Each phase has
 - Resistance of winding
 - Self Inductance
 - Mutual inductance due to other windings
 - EMF induced due to relative motion PM flux and winding

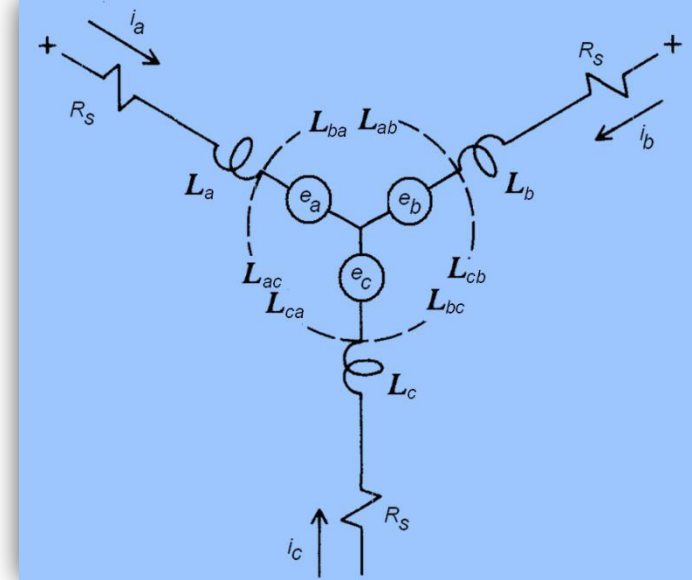
Equivalent Circuit of PM BLDC Motor

Modeling of PMBL DC Motor

The coupled circuit equations of the stator windings in terms of motor electrical constants are:

$$\begin{bmatrix} v_{as} \\ v_{bs} \\ v_{cs} \end{bmatrix} = \begin{bmatrix} R_s & 0 & 0 \\ 0 & R_s & 0 \\ 0 & 0 & R_s \end{bmatrix} \begin{bmatrix} i_{as} \\ i_{bs} \\ i_{cs} \end{bmatrix} + p \begin{bmatrix} L_{aa} & L_{ab} & L_{ac} \\ L_{ba} & L_{bb} & L_{bc} \\ L_{ca} & L_{cb} & L_{cc} \end{bmatrix} \begin{bmatrix} i_a \\ i_b \\ i_c \end{bmatrix} + \begin{bmatrix} e_{as} \\ e_{bs} \\ e_{cs} \end{bmatrix}$$

- Where R_s is the stator resistance per phase and it is assumed to be equal for all three phases.
- The induced emfs e_{as} , e_{bs} , and e_{cs} are all assumed to be trapezoidal.



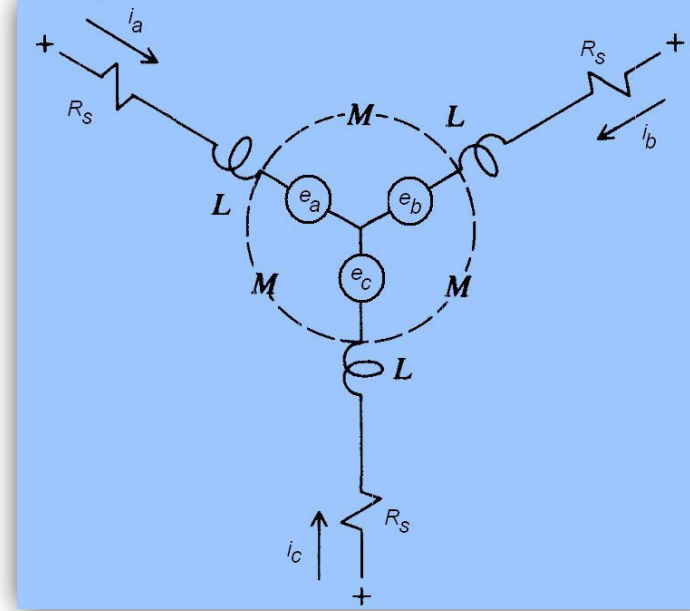
Modeling of PMBL DC Motor

- If there is no change in the rotor reluctance with angle, and assuming symmetric three phases, the self-inductances of all phases are equal and the mutual inductance between phases are equal to one another and they are denoted as
- Substituting L and M in the above equation we get,

$$L_{aa} = L_{bb} = L_{cc} = L$$

$$L_{ab} = L_{ba} = L_{ac} = L_{ca} = L_{bc} = L_{cb} = M$$

$$\begin{bmatrix} v_{as} \\ v_{bs} \\ v_{cs} \end{bmatrix} = R_s \begin{bmatrix} 1 & 0 & 0 \\ 0 & 1 & 0 \\ 0 & 0 & 1 \end{bmatrix} \begin{bmatrix} i_{as} \\ i_{bs} \\ i_{cs} \end{bmatrix} + \begin{bmatrix} L & M & M \\ M & L & M \\ M & M & L \end{bmatrix} p \begin{bmatrix} i_a \\ i_b \\ i_c \end{bmatrix} + \begin{bmatrix} e_{as} \\ e_{bs} \\ e_{cs} \end{bmatrix}$$



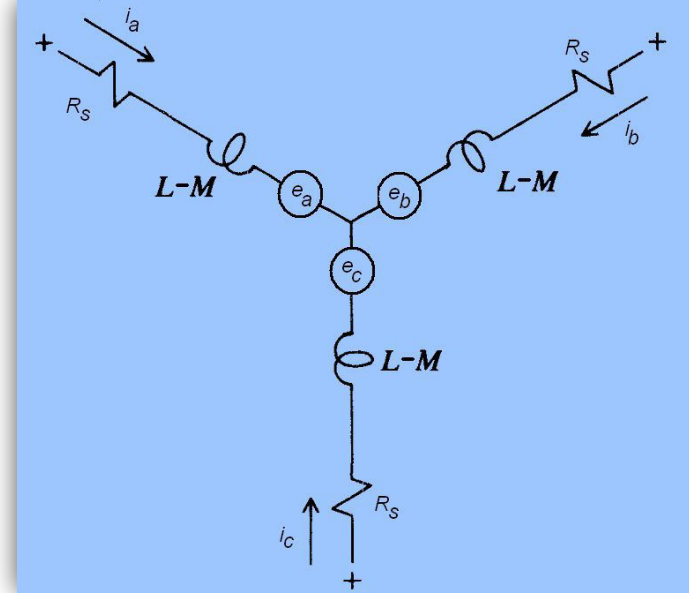
Modeling of PMBL DC Motor

In PMBLDC Motor

$$i_a + i_b + i_c = 0.$$

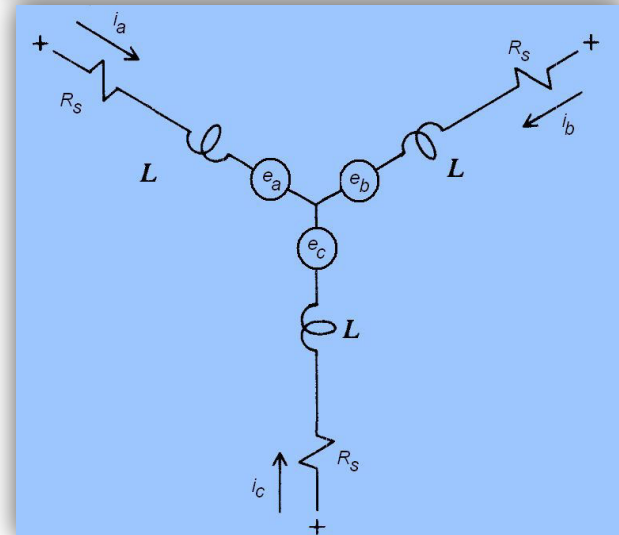
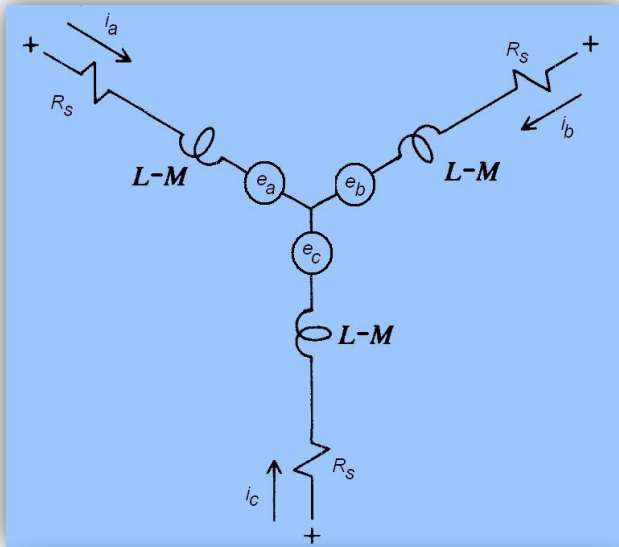
$$Mi_b + Mi_c = -Mi_a. \quad \text{Substituting in above equation}$$

$$\begin{bmatrix} v_{as} \\ v_{bs} \\ v_{cs} \end{bmatrix} = \begin{bmatrix} R_s & 0 & 0 \\ 0 & R_s & 0 \\ 0 & 0 & R_s \end{bmatrix} \begin{bmatrix} i_{as} \\ i_{bs} \\ i_{cs} \end{bmatrix} + \begin{bmatrix} (L-M) & 0 & 0 \\ 0 & (L-M) & 0 \\ 0 & 0 & (L-M) \end{bmatrix} p \begin{bmatrix} i_a \\ i_b \\ i_c \end{bmatrix} + \begin{bmatrix} e_{as} \\ e_{bs} \\ e_{cs} \end{bmatrix}$$



- The phase voltage equation is similar to that of the armature voltage equation of a dc machine.
- Resemblance to a dc machine and having no brushes and commutator are the reasons behind the machine being called a PM BLDC machine.

Modeling of PMBLDC Motor



- Where induced emfs e_a , e_b , and e_c are trapezoidal.
- Currents i_a , i_b and i_c are square shape
- V_c is average counter emf of each phase and I_d is DC link current
- Because of concentrated coils the mutual inductance is negligible.
- The power and electromagnetic torque is given by

$$P = e_a i_a + e_b i_b + e_c i_c = 2I_d V_C = T_e \omega_m$$

$$T_e = (e_a i_a + e_b i_b + e_c i_c) / \omega_m$$

Modeling of PMBL DC Motor

- The instantaneous-induced emfs can be stated as

$$e_{as} = f_{as}(\theta_r) \lambda_p \omega_m$$

Where $\lambda_p = \psi_m$

$$e_{bs} = f_{bs}(\theta_r) \lambda_p \omega_m$$

$$e_{cs} = f_{cs}(\theta_r) \lambda_p \omega_m$$

- where the functions $f_{as}(\theta_r)$, $f_{bs}(\theta_r)$, and $f_{cs}(\theta_r)$ have the same shape as e_{as} , e_{bs} , and e_{cs} with a maximum magnitude of ± 1 .
- The induced emfs do not have sharp corners but have rounded edges.
- It is because the emfs are the derivatives of the flux linkages and the flux linkages are continuous functions and fringing also makes the flux density functions smooth with no abrupt edges.

Modeling of PMBL DC Motor

- The electromagnetic torque is given by

$$T_e = [e_{as}i_{as} + e_{bs}i_{bs} + e_{cs}i_{cs}] \frac{1}{\omega_m} \quad (\text{N} \cdot \text{m})$$

- Substituting the induced instantaneous back-emfs in above equation with,

$$e_{as} = f_{as}(\theta_r)\lambda_p\omega_m$$

$$e_{bs} = f_{bs}(\theta_r)\lambda_p\omega_m$$

$$e_{cs} = f_{cs}(\theta_r)\lambda_p\omega_m$$

- Then the electromagnetic torque can be written as

$$T_e = \lambda_p [f_{as}(\theta_r)i_{as} + f_{bs}(\theta_r)i_{bs} + f_{cs}(\theta_r)i_{cs}] \quad (\text{N} \cdot \text{m})$$

$$T_e = p[\psi_m f_A(\theta)i_A + \psi_m f_B(\theta)i_B + \psi_m f_C(\theta)i_C]$$

P= no of pole pairs

$$T_e = 2p\psi_m i_A = K_T i$$

Kt = Torque constant, i= steady current

Modeling of PMBL DC Motor

- The equation of motion for a simple system with inertia J , friction coefficient B , and load torque T_l is
- The electrical rotor speed and position are related by

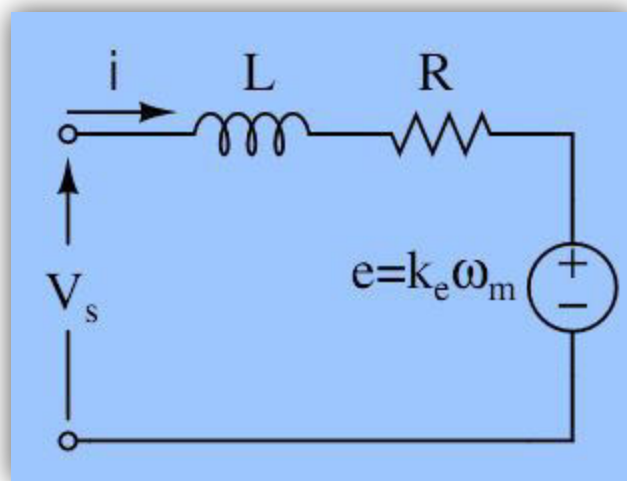
$$J \frac{d\omega_m}{dt} + B\omega_m = (T_e - T_l)$$

- where
 - P is the number of poles
 - $\frac{d\theta_r}{dt} = \frac{P}{2} \omega_m$
 - ω_m is the rotor speed in mechanical rad/s
 - θ_r is the rotor position in rad

PMBL DC Motor

MATLAB Implementation

DC Motor equations



$$V_s = Ri + L \frac{di}{dt} + e$$

$$T_e = k_f \omega_m + J \frac{d\omega_m}{dt} + T_L$$

$$e = k_e \omega_m$$

$$T_e = k_t \omega_m$$

PMBL DC Motor

MATLAB Implementation

Voltage and Torque equations

Where

V_{ab}, V_{bc}, V_{ca} is applied line voltages

i_a, i_b, i_c are phase currents

T_e – Electro magnetic torque

R – Resistance of winding

L – Inductance of winding

k_e – EMF Constant of machine

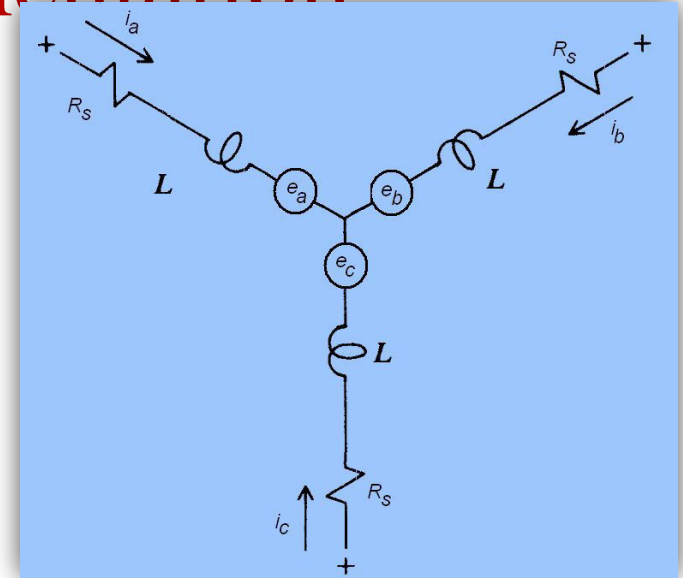
k_t – Torque Constant of machine

T_L – Load Torque

J – Inertia of machine

k_f/B – Friction factor

ω_m – speed of machine



$$v_{ab} = R(i_a - i_b) + L \frac{d}{dt}(i_a - i_b) + e_a - e_b$$

$$v_{bc} = R(i_b - i_c) + L \frac{d}{dt}(i_b - i_c) + e_b - e_c$$

$$v_{ca} = R(i_c - i_a) + L \frac{d}{dt}(i_c - i_a) + e_c - e_a$$

$$T_e = k_f \omega_m + J \frac{d\omega_m}{dt} + T_L.$$

PMBL DC Motor MATLAB Implementation

Back EMF and
Toque
Equations

$$\begin{aligned}e_a &= \frac{k_e}{2} \omega_m F(\theta_e) \\e_b &= \frac{k_e}{2} \omega_m F\left(\theta_e - \frac{2\pi}{3}\right) \\e_c &= \frac{k_e}{2} \omega_m F\left(\theta_e - \frac{4\pi}{3}\right)\end{aligned}$$

$$T_e = \frac{k_t}{2} \left[F(\theta_e) i_a + F\left(\theta_e - \frac{2\pi}{3}\right) i_b + F\left(\theta_e - \frac{4\pi}{3}\right) i_c \right]$$

$$F(\theta_e) = \begin{cases} 1, & 0 \leq \theta_e < \frac{2\pi}{3} \\ 1 - \frac{6}{\pi}(\theta_e - \frac{2\pi}{3}), & \frac{2\pi}{3} \leq \theta_e < \pi \\ -1, & \pi \leq \theta_e < \frac{5\pi}{3} \\ -1 + \frac{6}{\pi}(\theta_e - \frac{5\pi}{3}), & \frac{5\pi}{3} \leq \theta_e < 2\pi \end{cases}.$$

PMBL DC Motor MATLAB Implementation

□ The system in state space form as

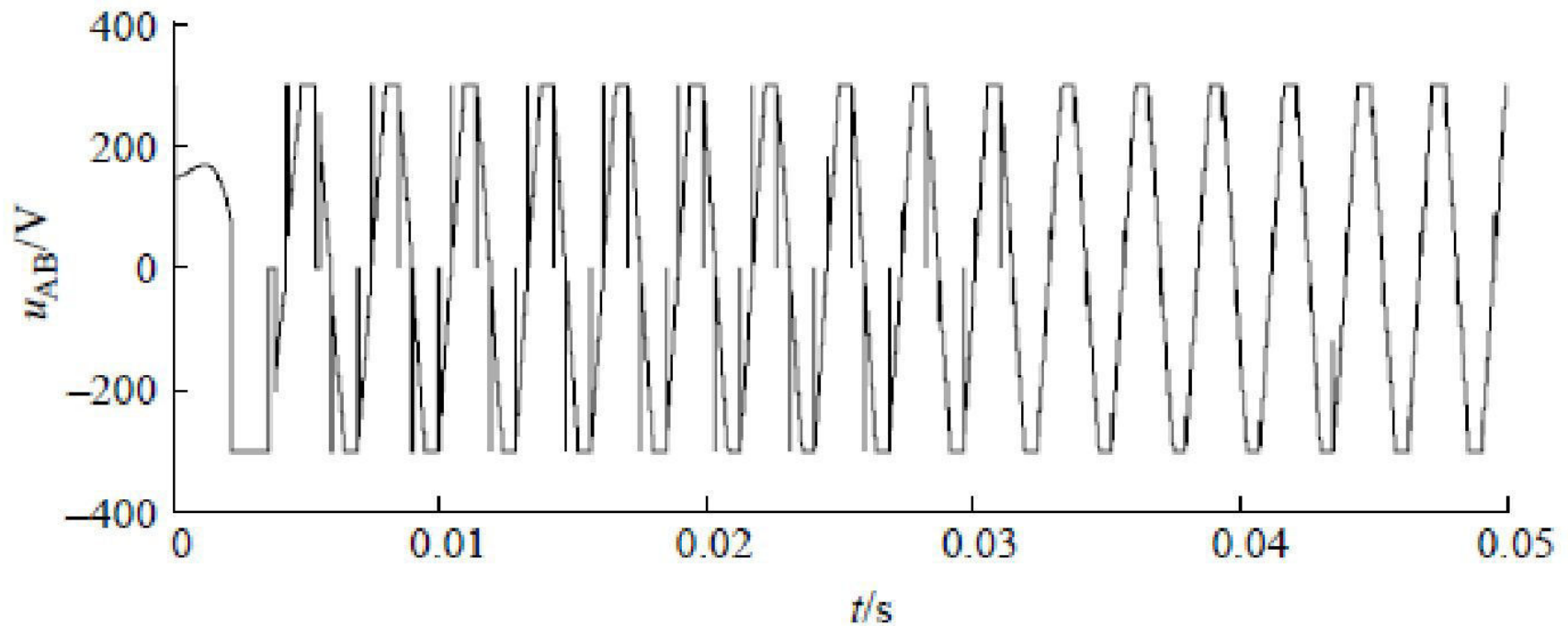
$$\dot{x} = Ax + Bu$$

$$\begin{pmatrix} i_a' \\ i_b' \\ \omega_m' \\ \theta_m' \end{pmatrix} = \begin{pmatrix} -\frac{R}{L} & 0 & 0 & 0 \\ 0 & -\frac{R}{L} & 0 & 0 \\ 0 & 0 & -\frac{k_f}{J} & 0 \\ 0 & 0 & 1 & 0 \end{pmatrix} \begin{pmatrix} i_a \\ i_b \\ \omega_m \\ \theta_m \end{pmatrix} + \begin{pmatrix} \frac{2}{3L} & \frac{1}{3L} & 0 \\ -\frac{1}{3L} & \frac{1}{3L} & 0 \\ 0 & 0 & \frac{1}{J} \\ 0 & 0 & 0 \end{pmatrix} \begin{pmatrix} v_{ab} - e_{ab} \\ v_{bc} - e_{bc} \\ T_e - T_L \end{pmatrix}$$

$$Y = Cx$$

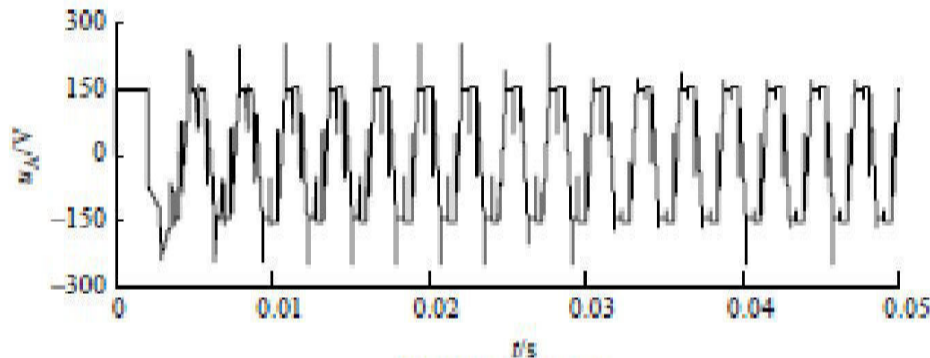
$$\begin{pmatrix} i_a \\ i_b \\ i_c \\ \omega_m \\ \theta_m \end{pmatrix} = \begin{pmatrix} 1 & 0 & 0 & 0 \\ 0 & 1 & 0 & 0 \\ -1 & -1 & 0 & 0 \\ 0 & 0 & 1 & 0 \\ 0 & 0 & 0 & 1 \end{pmatrix} \begin{pmatrix} i_a \\ i_b \\ \omega_m \\ \theta_m \end{pmatrix}$$

Dynamic performance of PM BLDC Motor – At No-load

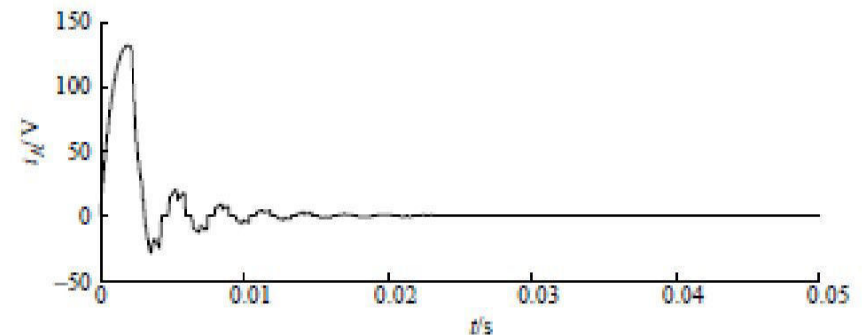


(a) Line voltage u_{AB}

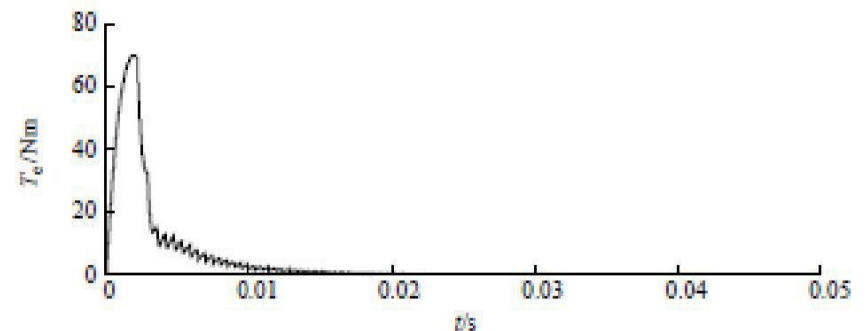
Dynamic performance of PM BLDC Motor at No-Load



(b) Phase voltage u_A

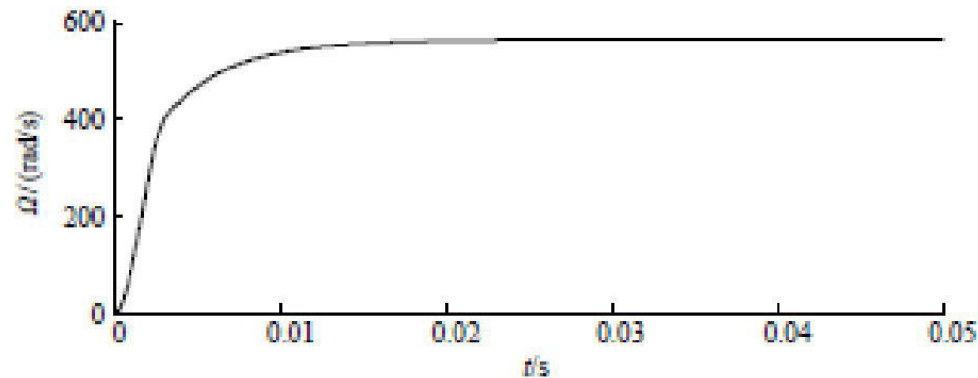


(c) Phase current i_A

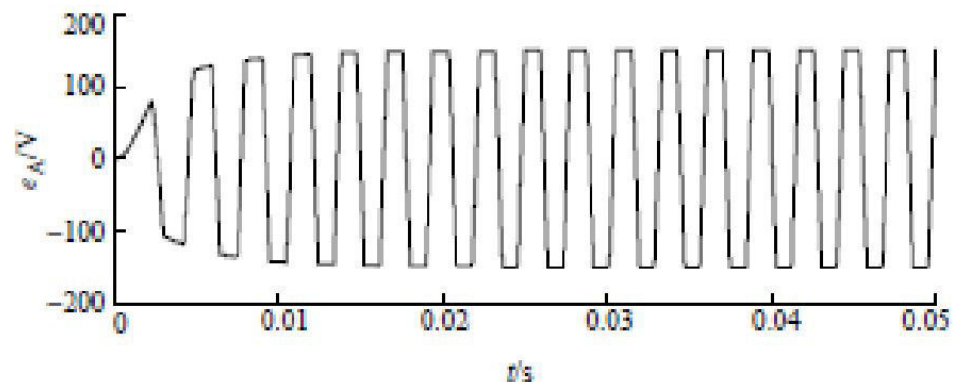


(d) Electromagnetic torque T_e

Dynamic performance of PM BLDC Motor at No-Load

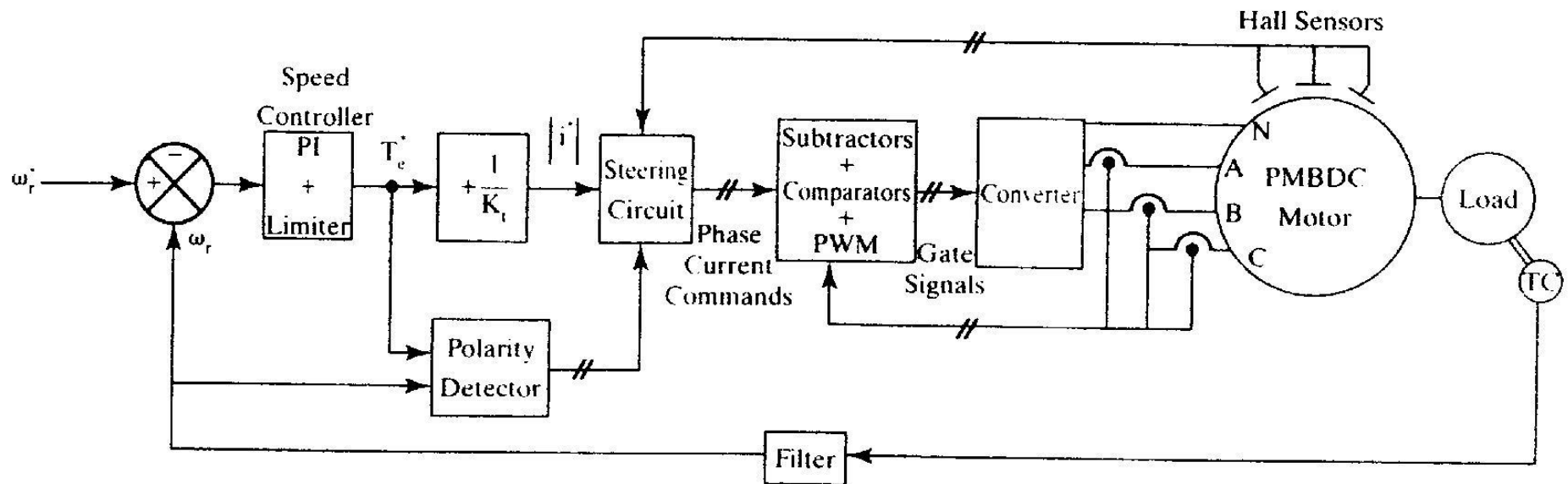


(e) Angular velocity Ω

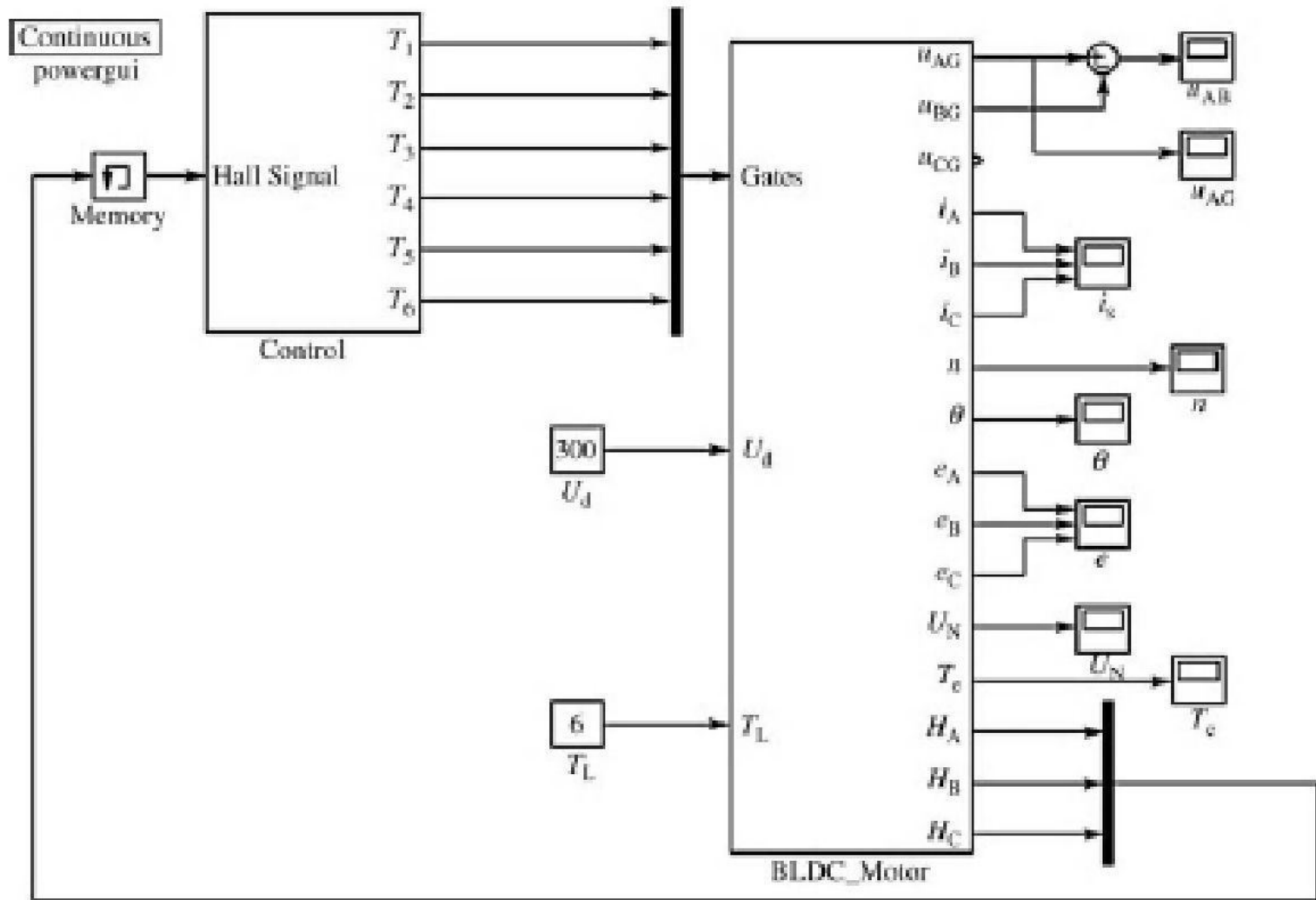


(f) Phase back-EMF e_A

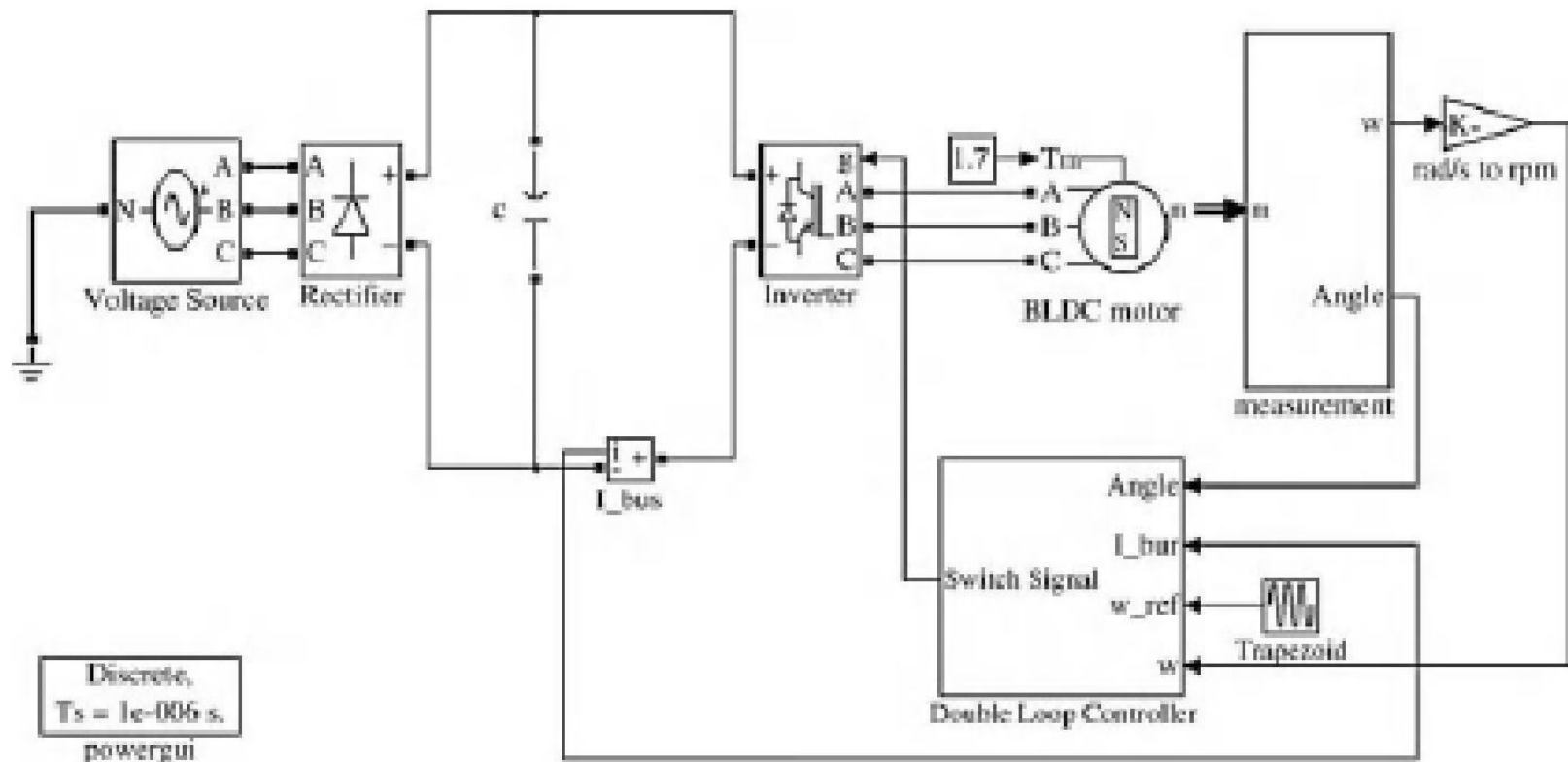
Speed Control of PM BLDC motor



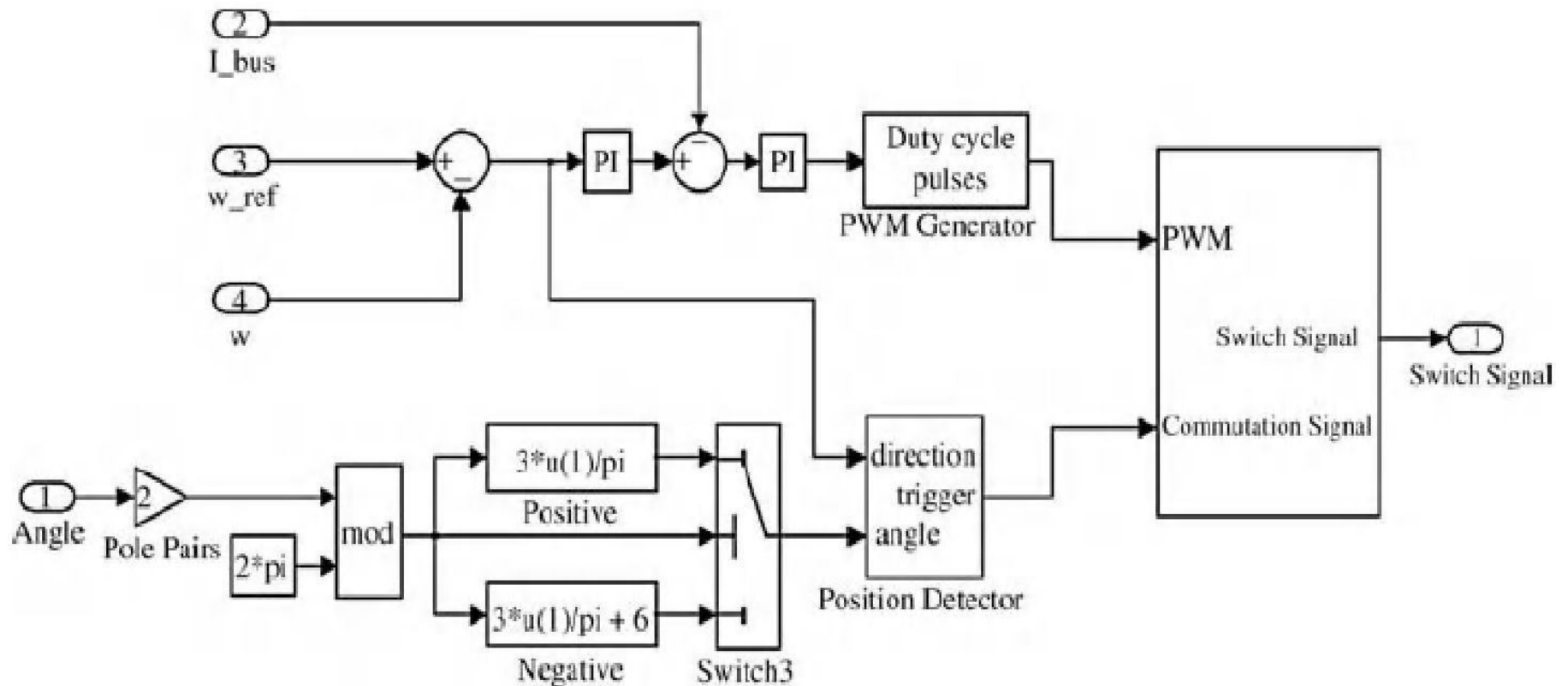
Simulation Based on S-function approach(MATLAB)



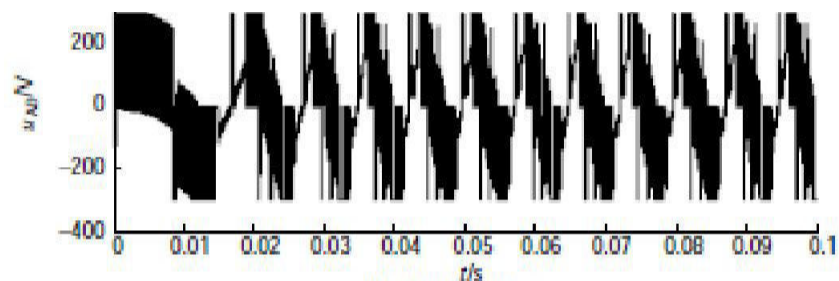
Simulation PMBLDC motor with Dual loop control



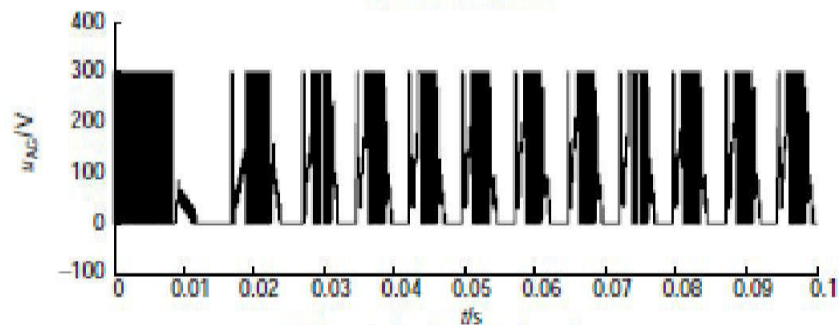
Dual loop control



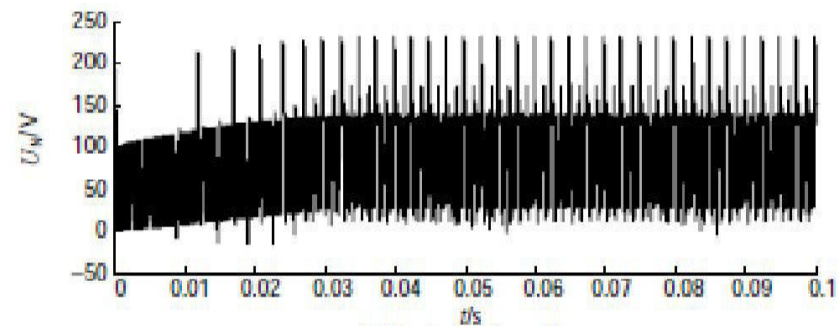
Simulation result



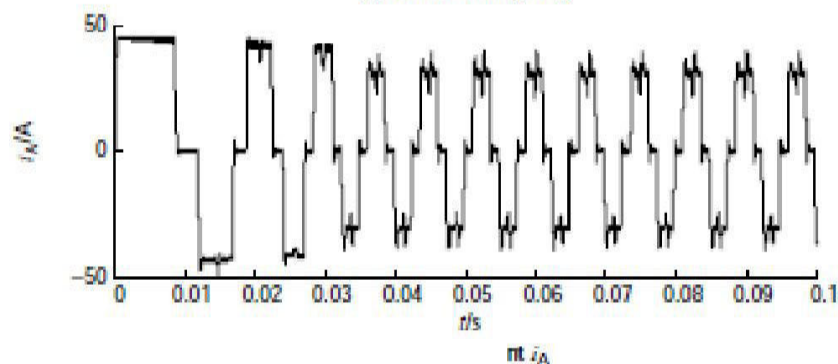
(a) Line voltage u_{AB}



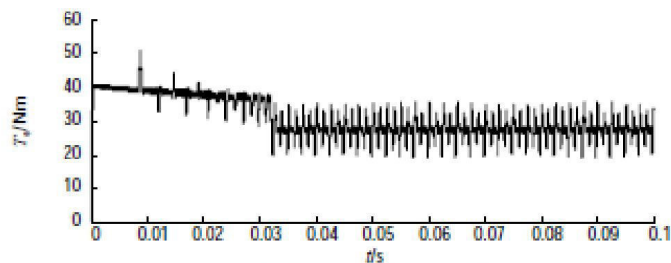
(b) Terminal voltage of phase A, u_{AG}



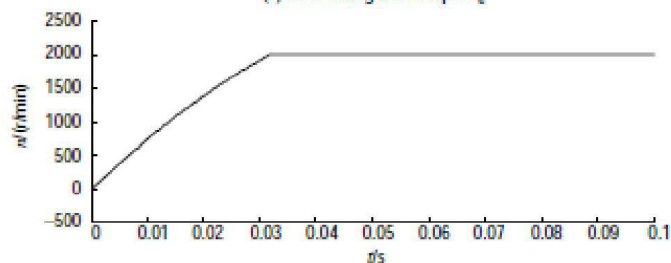
(c) Neutral voltage U_N



or i_A

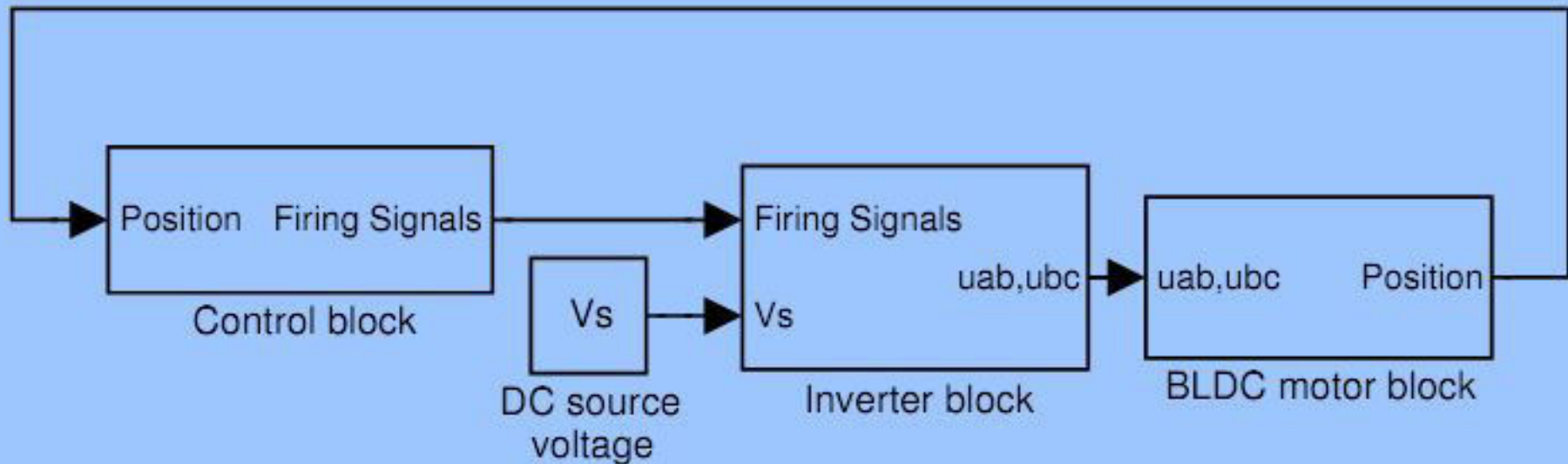


(e) Electromagnetic torque T_e



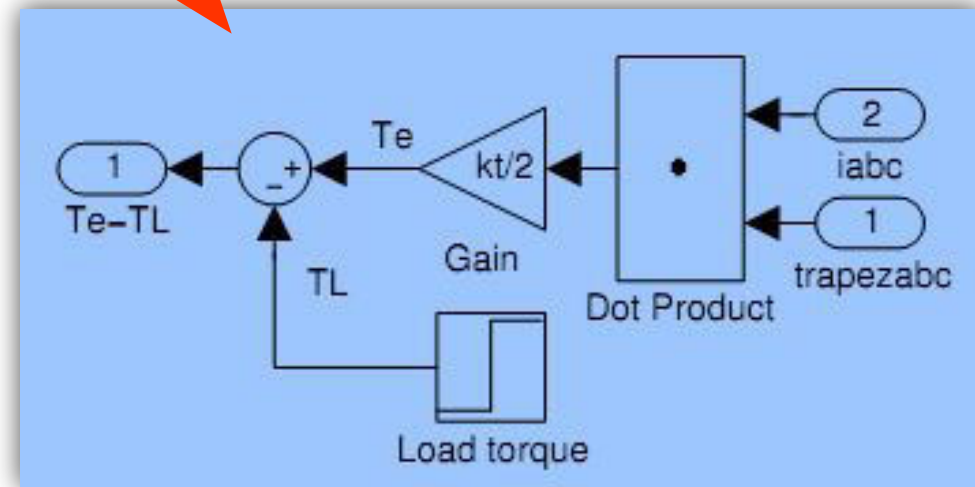
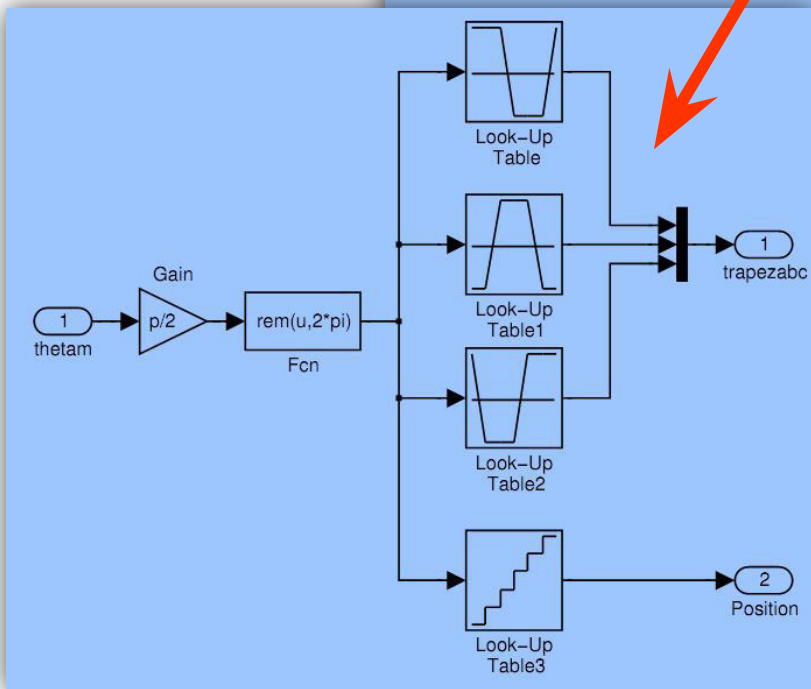
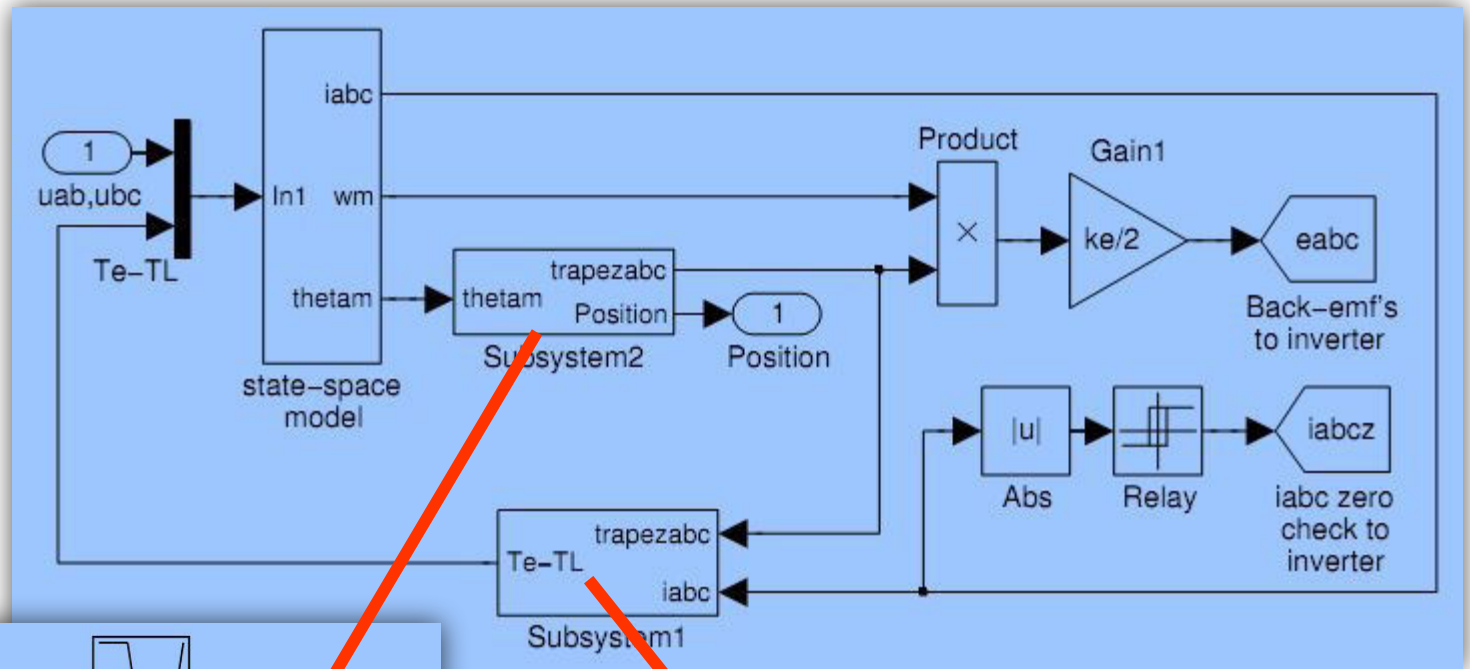
(f) Rotor speed n

PMBL DC Motor MATLAB Implementation

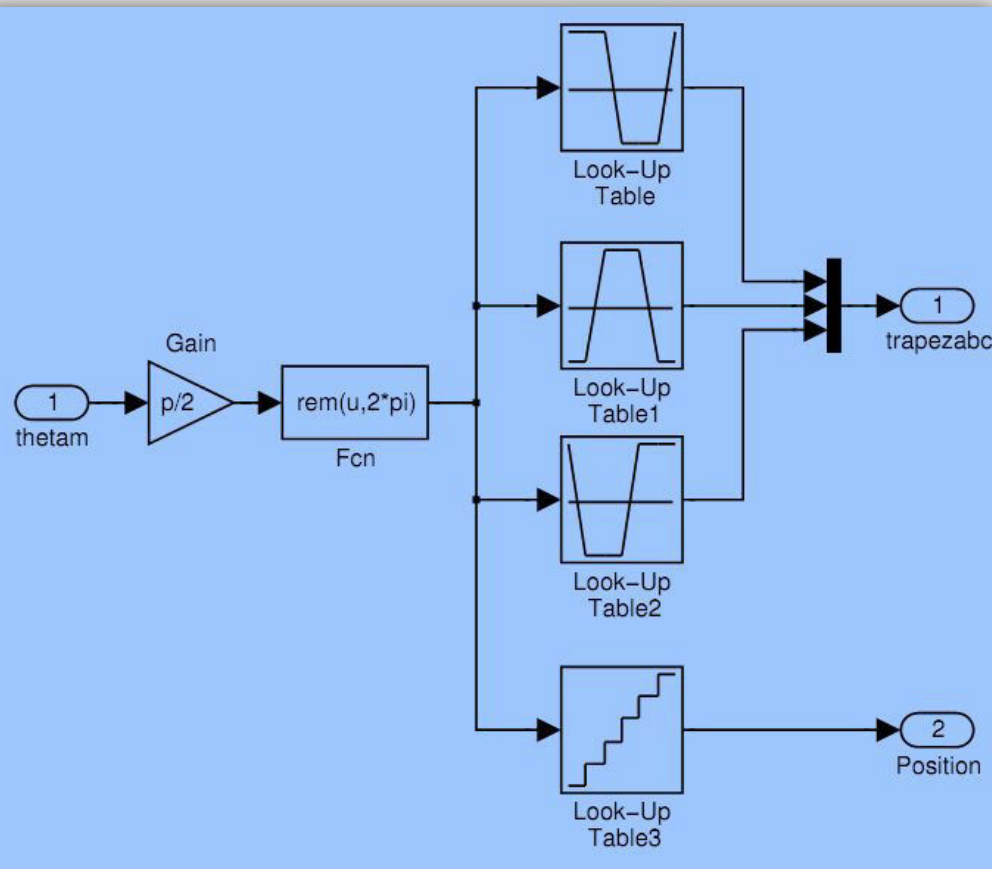


The figure shows over all implementation of PM BLDC Motor

BLDC Motor Model



PMBL DC Motor MATLAB Implementation



$$e_a = \frac{k_e}{2} \omega_m F(\theta_e)$$

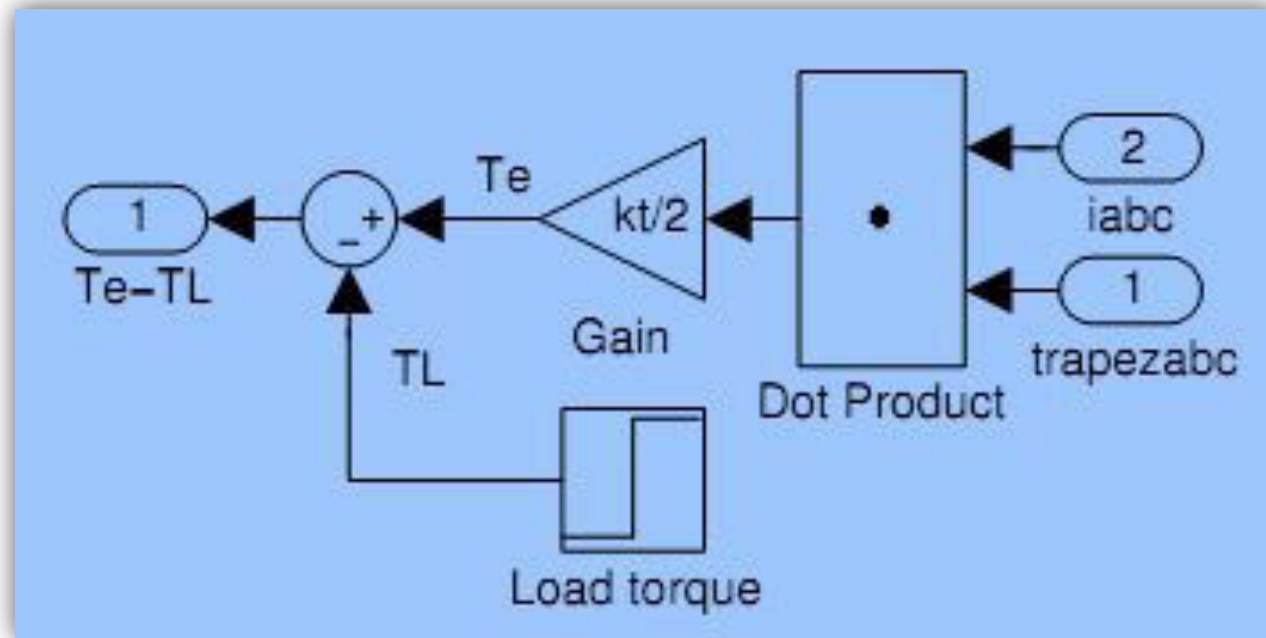
$$e_b = \frac{k_e}{2} \omega_m F(\theta_e - \frac{2\pi}{3})$$

$$e_c = \frac{k_e}{2} \omega_m F(\theta_e - \frac{4\pi}{3})$$

$$F(\theta_e) = \begin{cases} 1, & 0 \leq \theta_e < \frac{2\pi}{3} \\ 1 - \frac{6}{\pi}(\theta_e - \frac{2\pi}{3}), & \frac{2\pi}{3} \leq \theta_e < \pi \\ -1, & \pi \leq \theta_e < \frac{5\pi}{3} \\ -1 + \frac{6}{\pi}(\theta_e - \frac{5\pi}{3}), & \frac{5\pi}{3} \leq \theta_e < 2\pi \end{cases}$$

The block generate Back EMF based on position

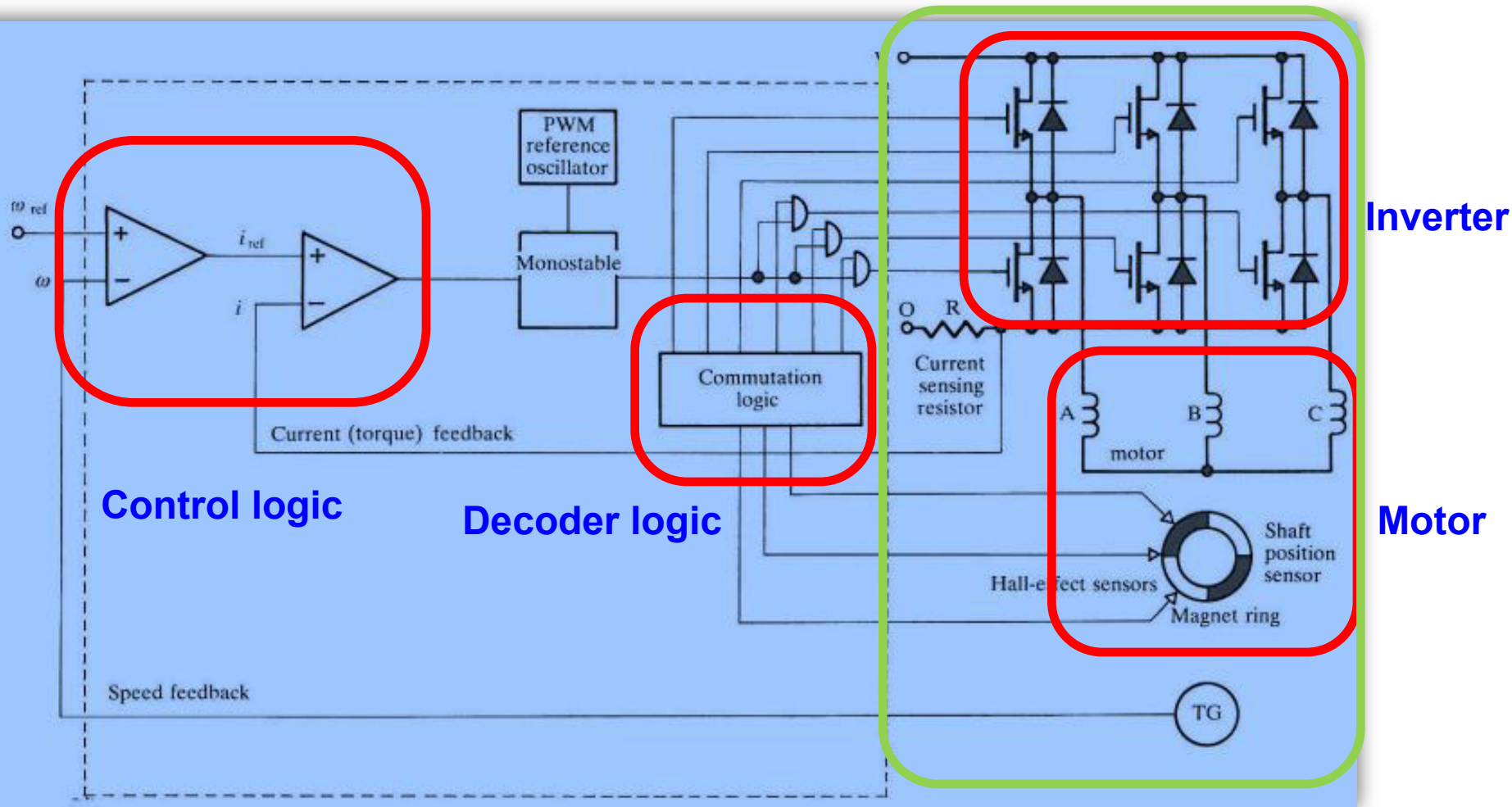
PMBL DC Motor MATLAB Implementation



$$T_e = \frac{k_t}{2} \left[F(\theta_e) i_a + F\left(\theta_e - \frac{2\pi}{3}\right) i_b + F\left(\theta_e - \frac{4\pi}{3}\right) i_c \right]$$

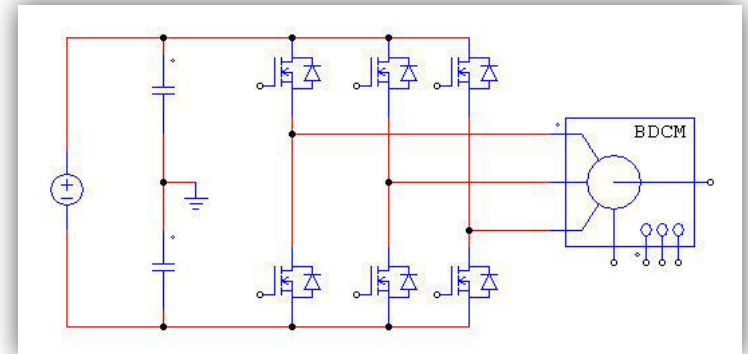
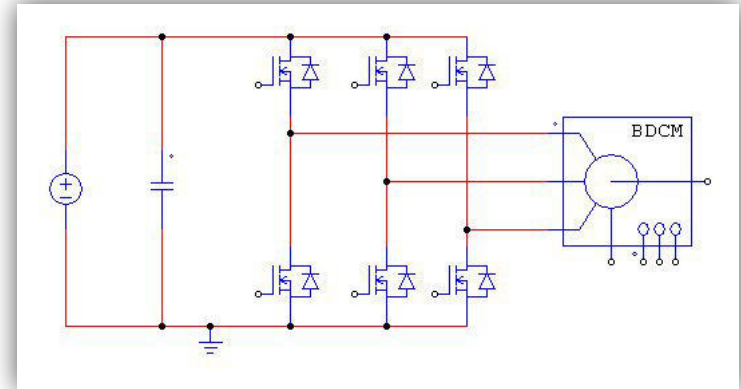
Block to calculate Torque based on currents

Basic PM BLDC Drive



Supply polarity

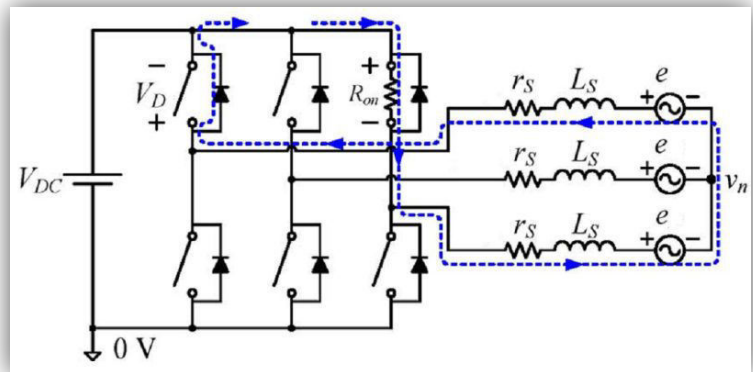
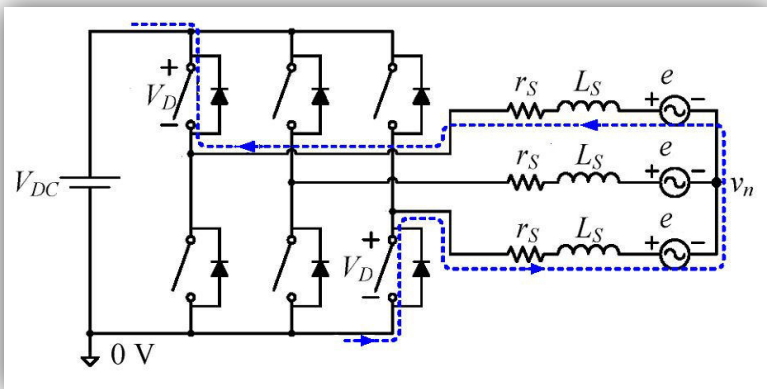
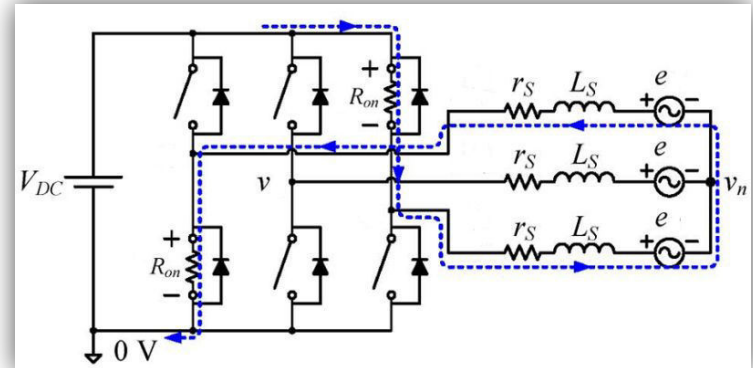
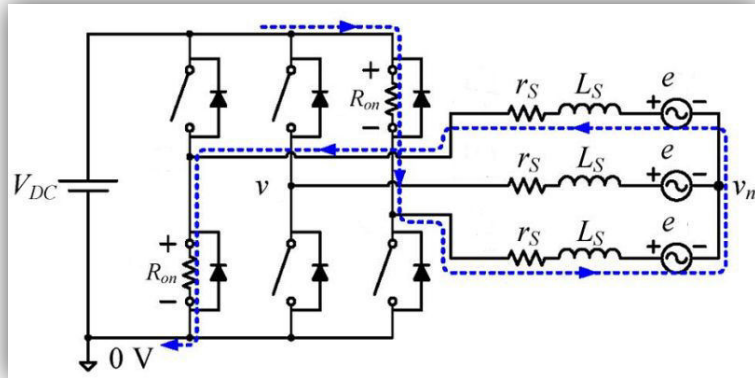
- **Unipolar supply drive:** One side of the inverter grounded, and is taken as reference terminal for control. In this case bottom switch can be directly driven, Top switch needs isolation/boost strapping is needed. This types of drives are used in battery based drives like Auto mobiles, small toys etc.
- **Bipolar supply drive:** Ground is created by split capacitor connection. Both top and bottom switches gate circuits need isolation circuit.



PWM Techniques

- Soft chopping (Unipolar PWM switching) drive
 - Out of two conducting switches one switch simply turn on based on position, PWM signal is given to other switch.
 - approach allows not only a control of the current and of the rate of change of the current but a minimization of the current ripple as well.
 - Based on the time instants at which PWM signals are applied to the switches, this can be classified in number of ways.
- Hard Chopping (Bipolar PWM switching) drive
 - Like other motors Induction motor, PMSM both phase transistors are driven by the same pulsed signal: the two transistors are switched-on and switched-off at the same time.
 - A disadvantage of hard chopping operation is that it increases the current ripple by a large factor, Increases switching losses in one switch in comparison with the soft chopping approach.

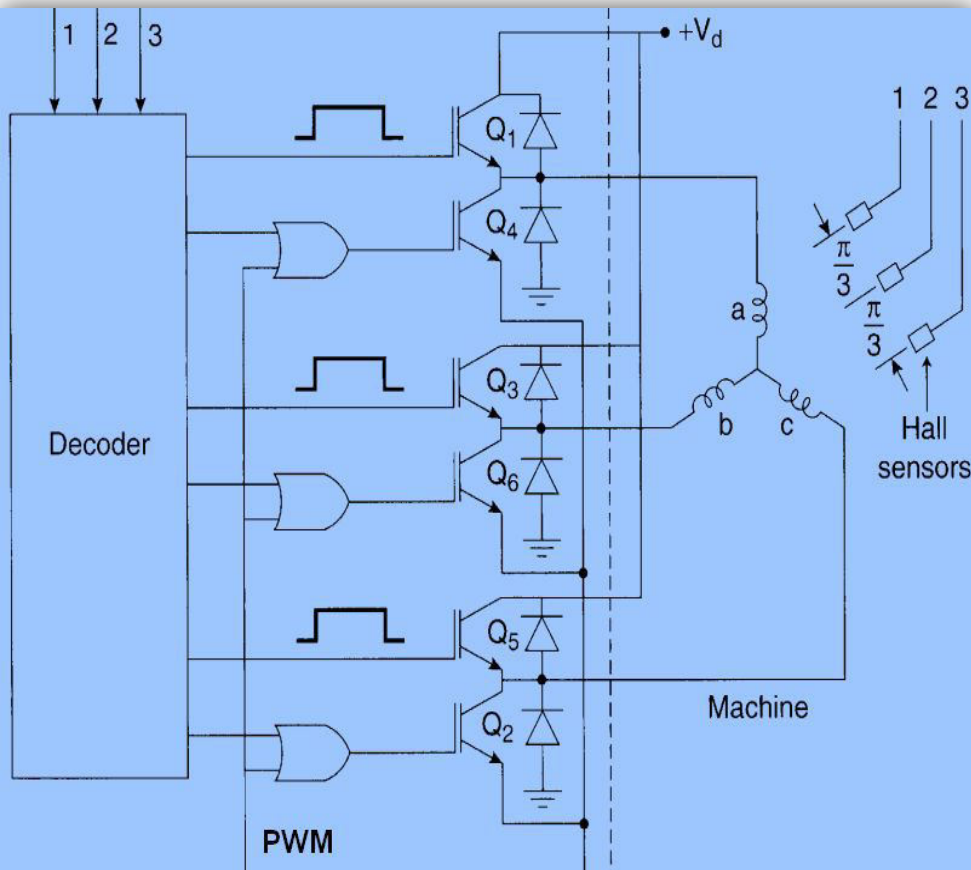
Hard and Soft chopping Modes



Top and Bottom switch is in chopping (Hard chopping)

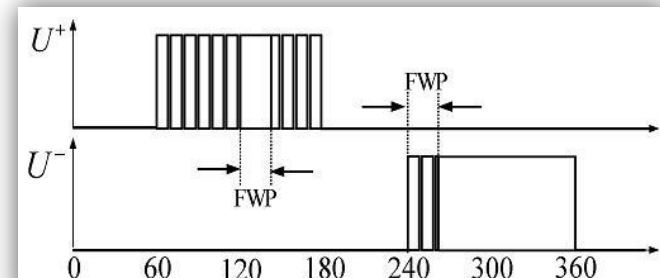
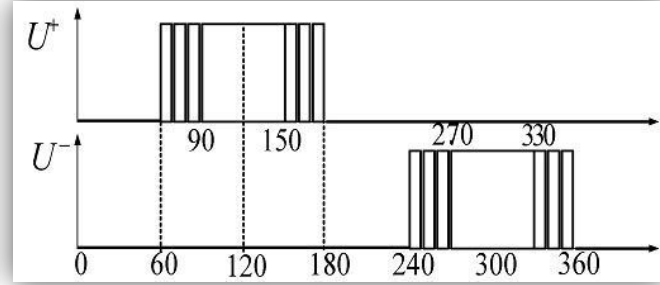
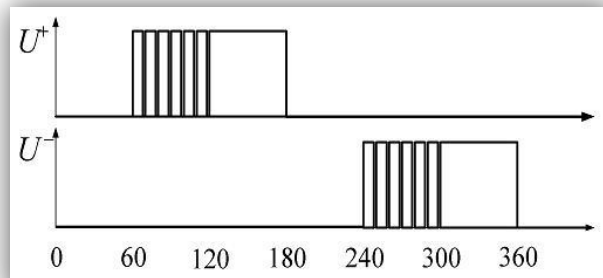
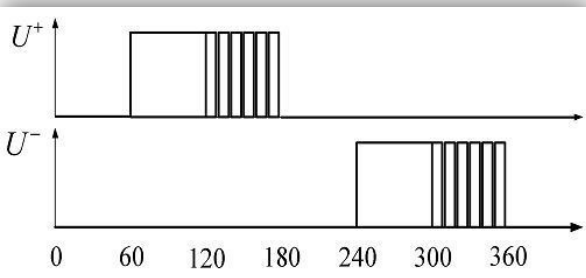
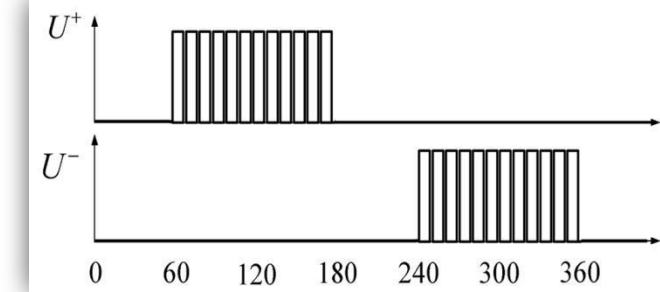
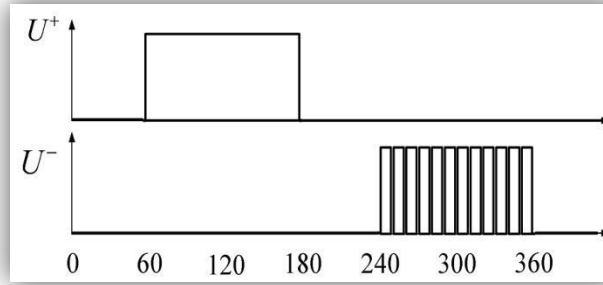
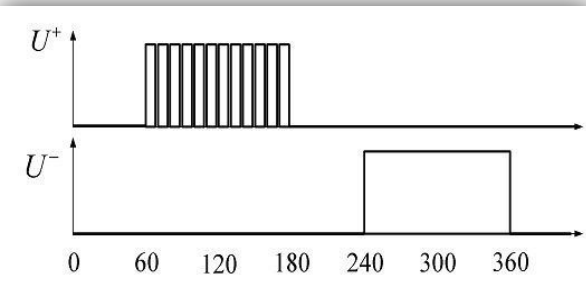
Top switch is on and Bottom is in chopping (Soft chopping)

Soft chopping implementation



- The circuit shown is case (c) implementation where Top switch is on and Bottom is in chopping mode.
- The hall signals 1,2,3 are given to the decoder, which generates signals to turn on switches, out of which three are directly given to top switches, other three are ANDed with PWM signal.

Different PWM Chopping methods



- Top and Bottom switch is in chopping (Hard switching)
- Top switch is in chopping and Bottom switch is on
- Top switch is on and Bottom is in chopping
- Top and Bottom switch is on for first half of on period
- Top and Bottom switch is in chopping for first half of on period
- Top and Bottom switch is on in the middle of on period
- Top switch is in chopping except Bottom switch is turning on

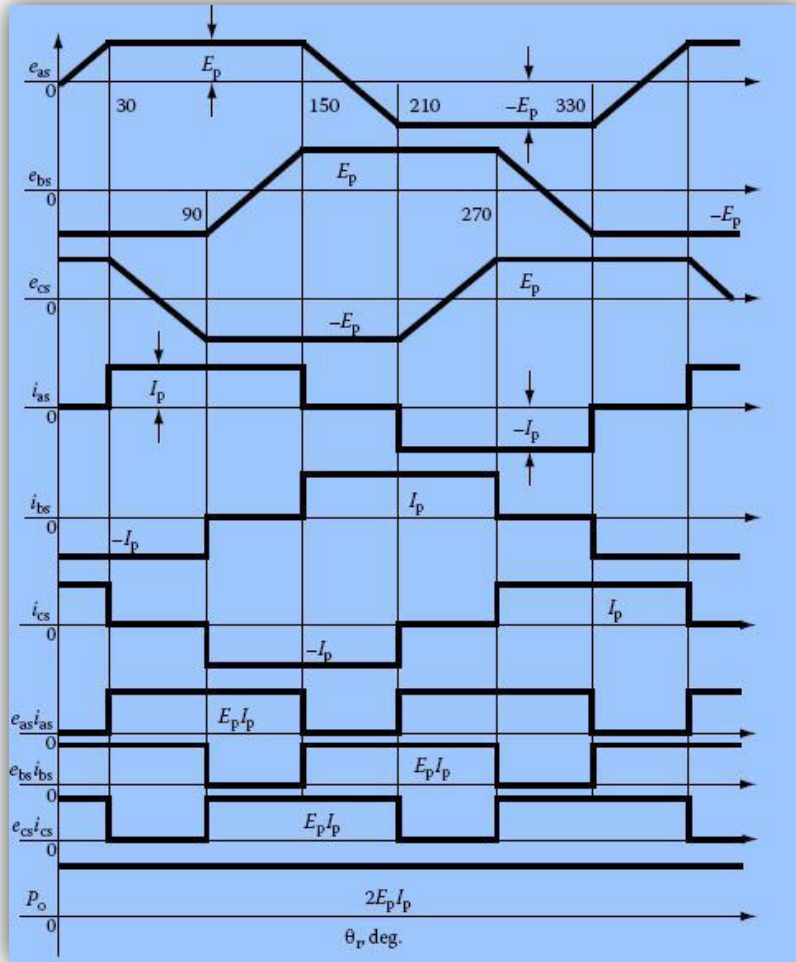
Like above in many other ways PWM can be implemented

Each of these techniques has its own pros and cons, some simplifies hardware, some reduces torque ripple, some eases sensor-less operation, etc. Example in case (b) implementation current sensing is easy and bottom switch can be directly driven.

Control of PM BLDC Motor

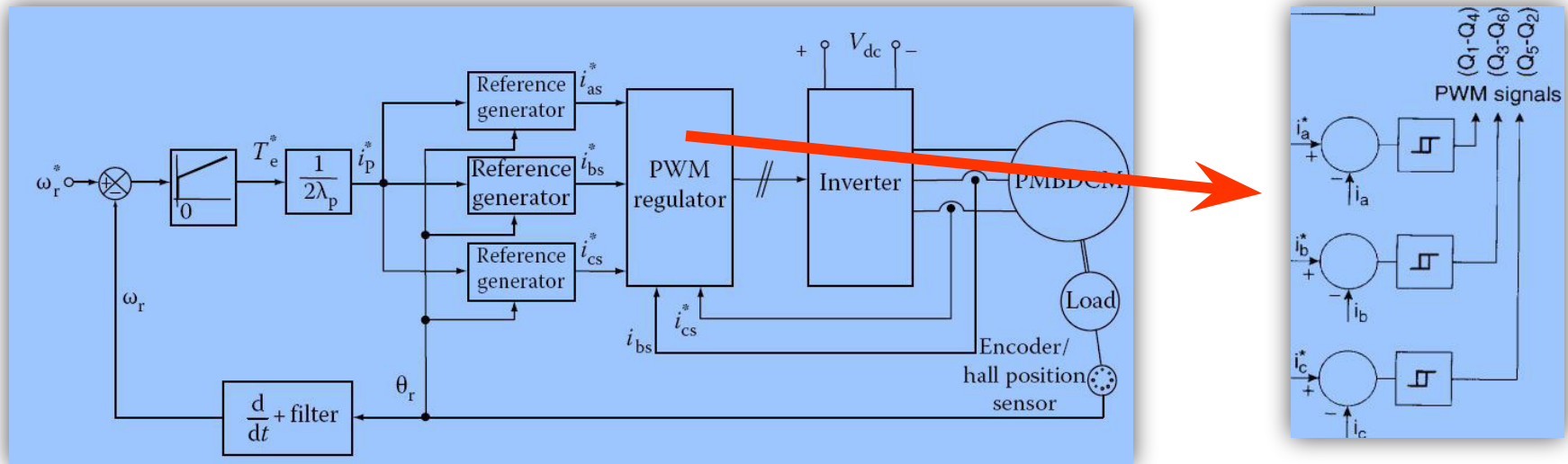
- What is control?
 - To make system respond in predetermined manner by some given input signals
- Why do we need controller?
 - It serves to govern in some predetermined manner the performance of an electric motor.
 - May be a manual or automatic means for
 - starting and stopping
 - Forward or reverse rotation
 - regulating the speed
 - regulating or limiting the torque
 - protecting against overloads and faults
 - Protecting from abnormalities

Requirement of Controller



- Motor Controller
 - Controlled starting
 - Limiting the max. current
 - Dynamic response
 - No torque ripple
 - Limiting the max torque
 - Braking
 - Regeneration
 - Efficient
 - Protection
 - Compact
 - Safety
 - Cheep
 - Etc ...

Control of PM BLDC Motor



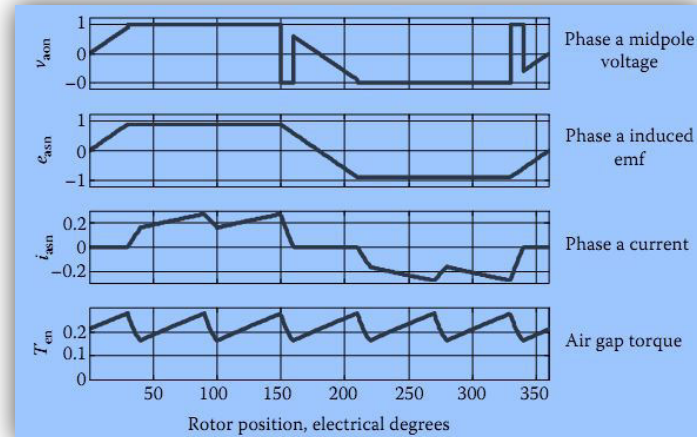
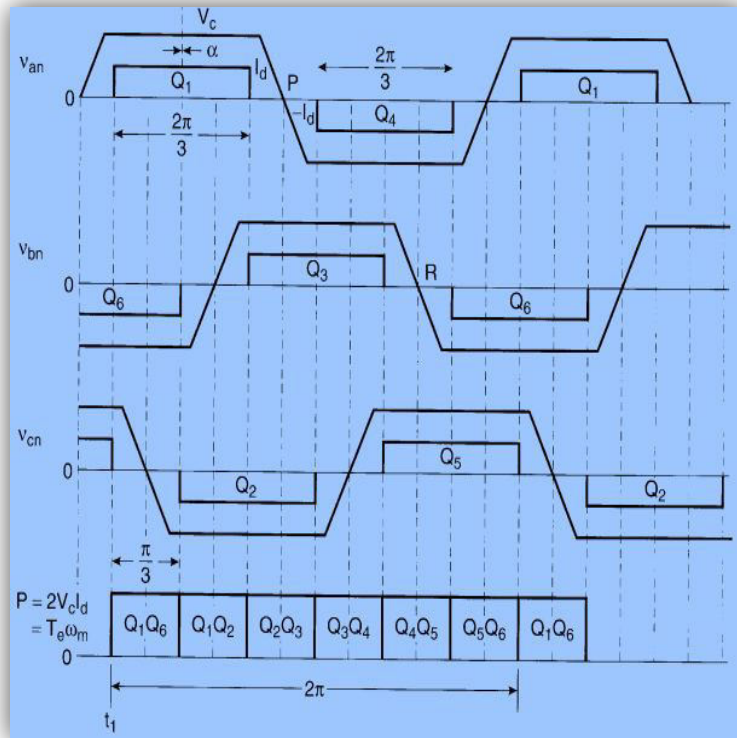
$$T_e^* = \lambda_p [f_{as}(\theta_r)i_{as}^* + f_{bs}(\theta_r)i_{bs}^* + f_{cs}(\theta_r)i_{cs}^*]$$

$$T_e^* = 2\lambda_p I_p^*$$

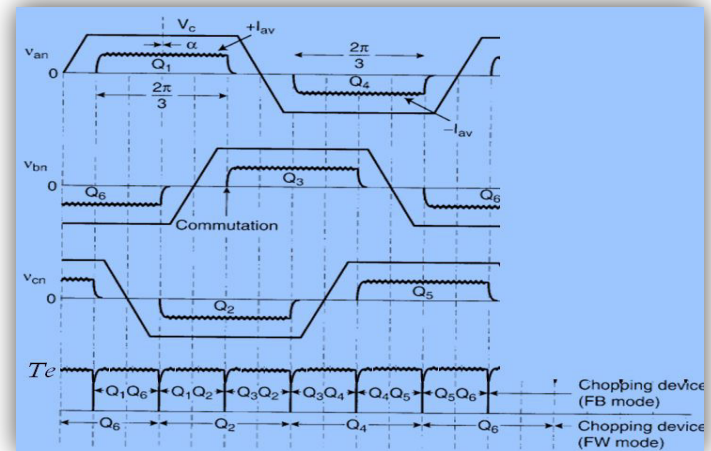
$$I_p^* = \frac{T_e^*}{2\lambda_p}$$

- The rotor speed is compared to its reference and the rotor speed error is amplified through the speed controller.
- The output of the speed controller provides the reference torque, T_e^* .
- The current magnitude command, I_p^* , is obtained from the torque expression

Control of PM BLDC Motor

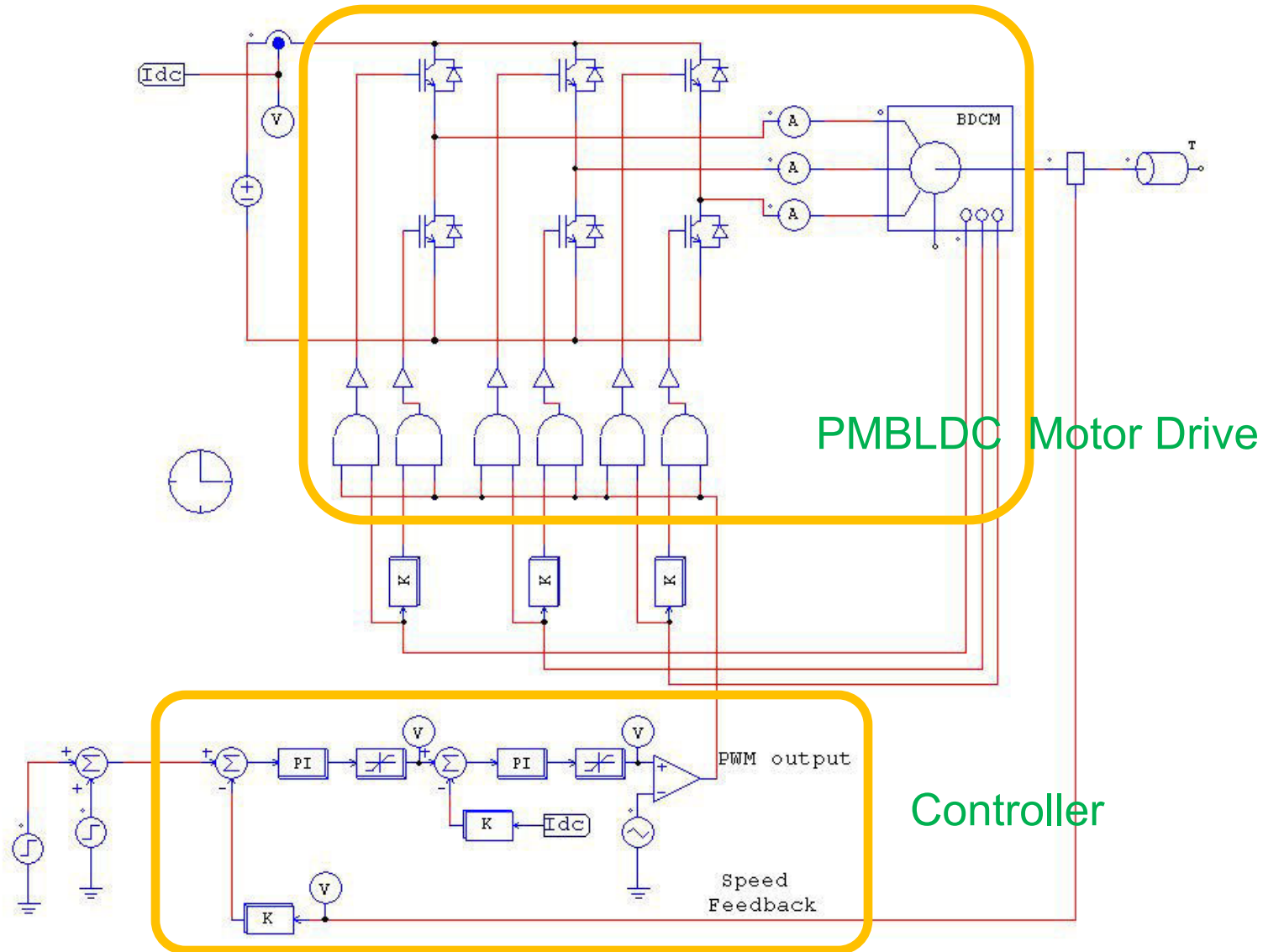


Voltage control

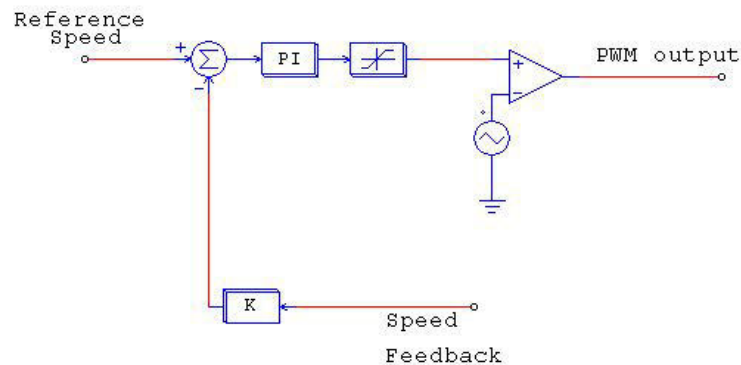


Current control

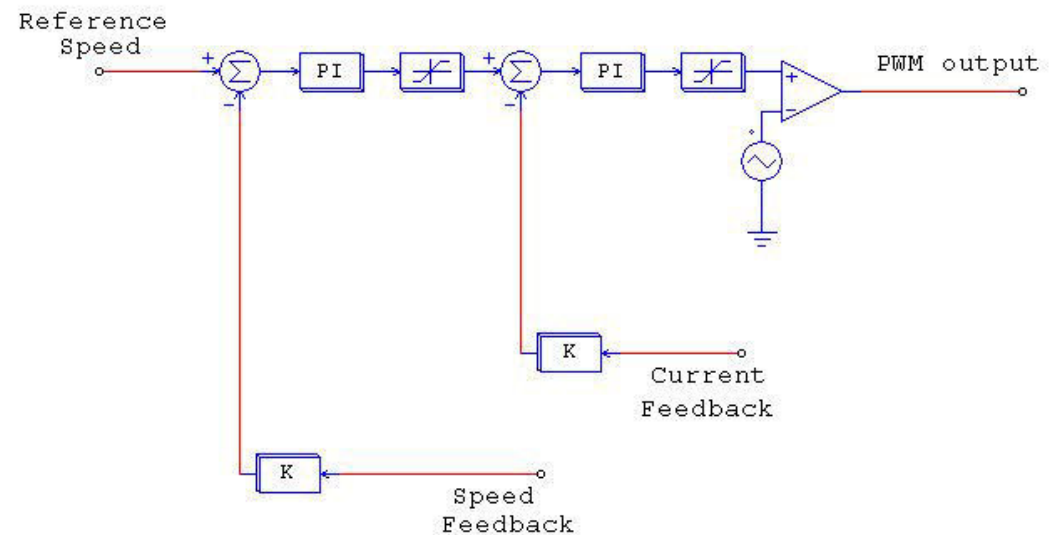
Control of PM BLDC Motor



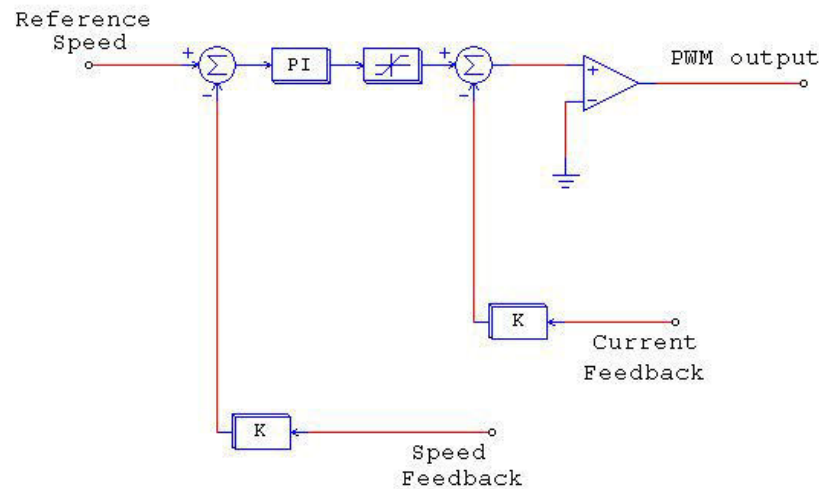
Control of PM BLDC Motor



Single loop speed control



Outer loop speed control and inner loop current control

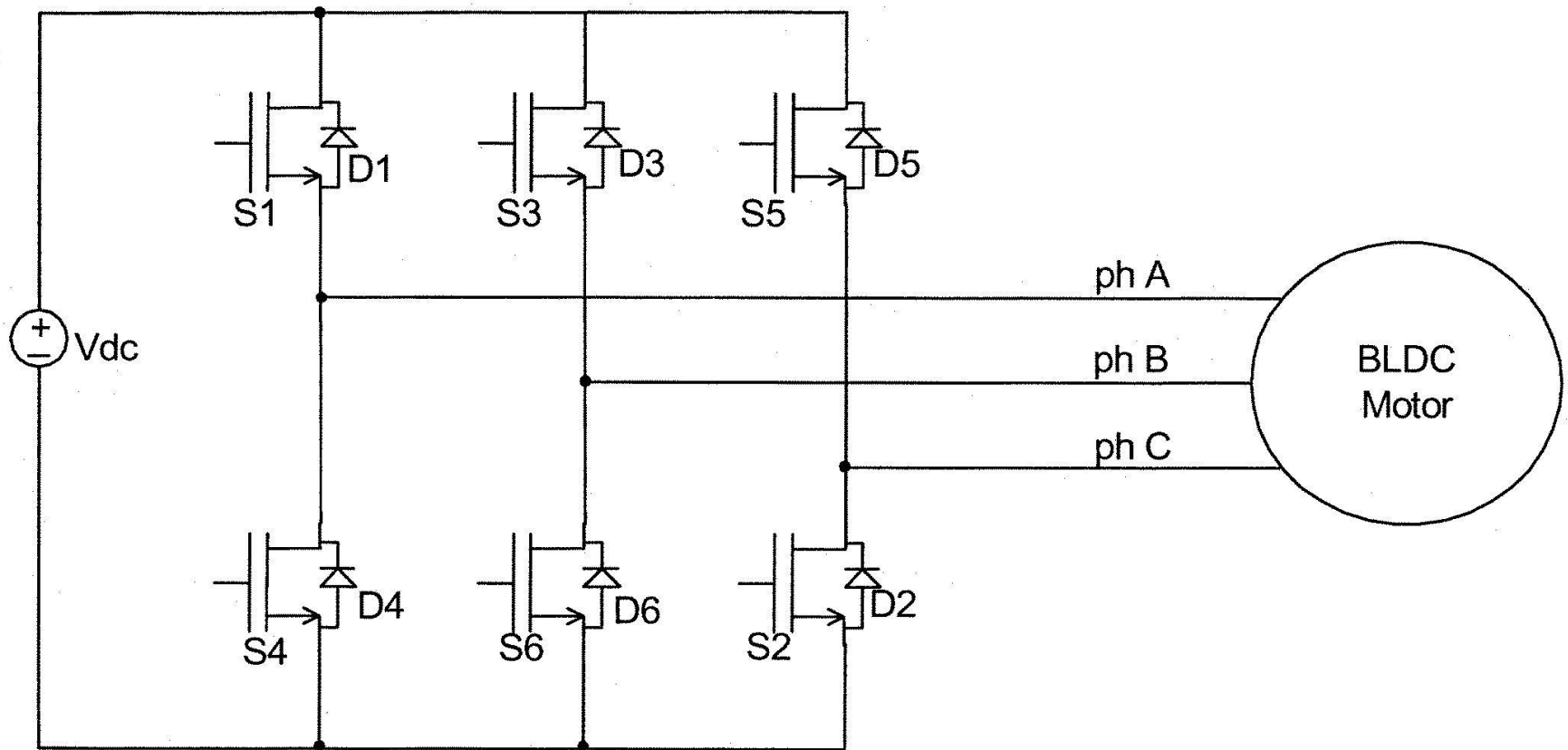


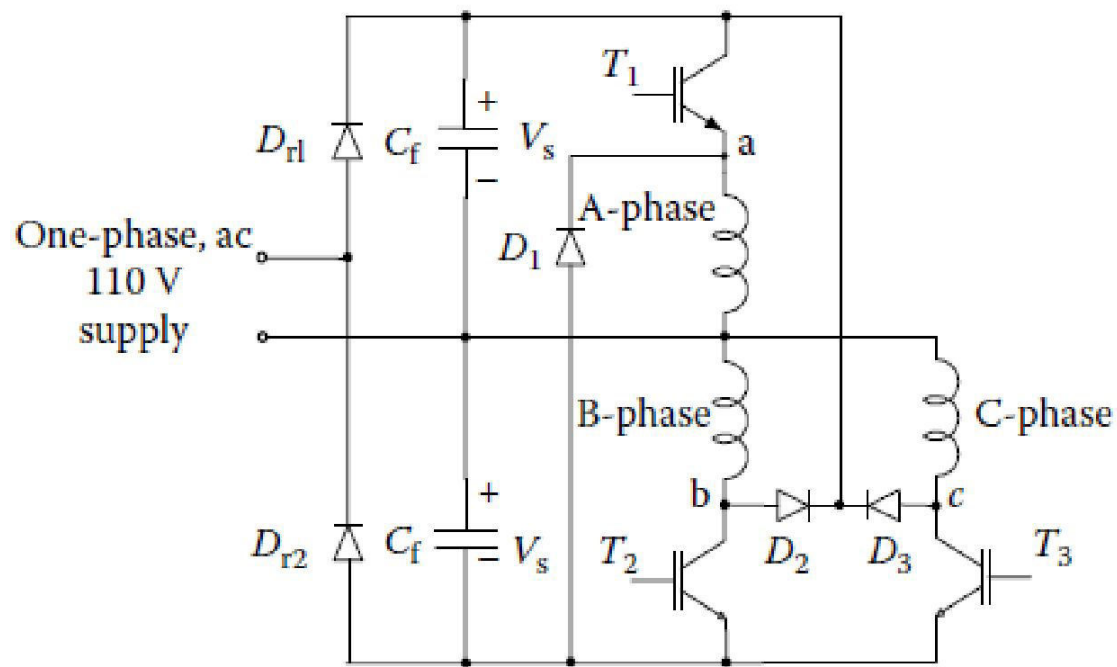
Outer loop speed control and inner loop Hys. current control

Converter Topologies Used IN PMBLDC Motor

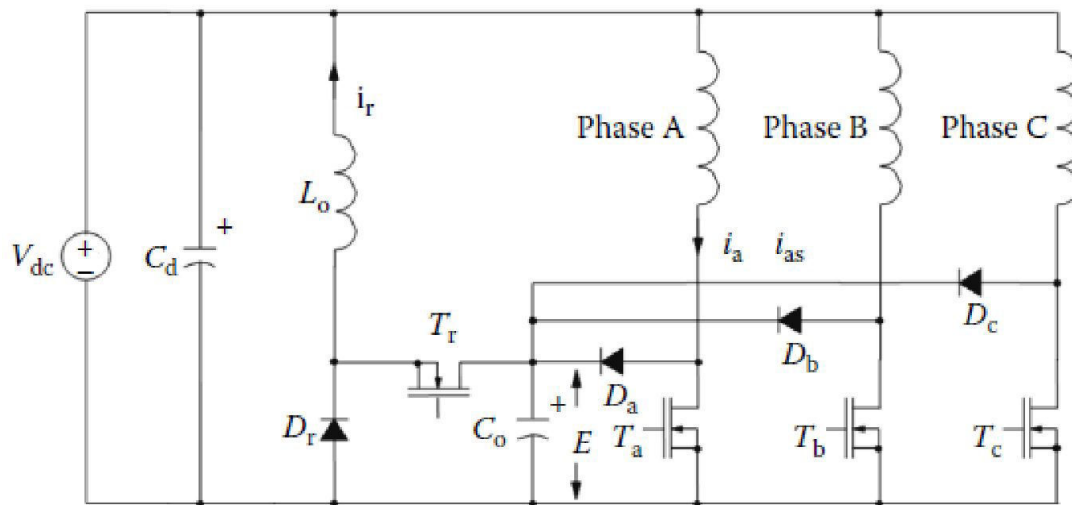
- **Conventional six-switch inverter used for BLDC motor drive**
- **Half-Wave PMBDCM Drives**
 - **Split supply converter topology**
 - **C-dump topology**
 - **Variable DC link converter topology**

Conventional / Optimal six-switch





**Split Supply Converter
motor drives**

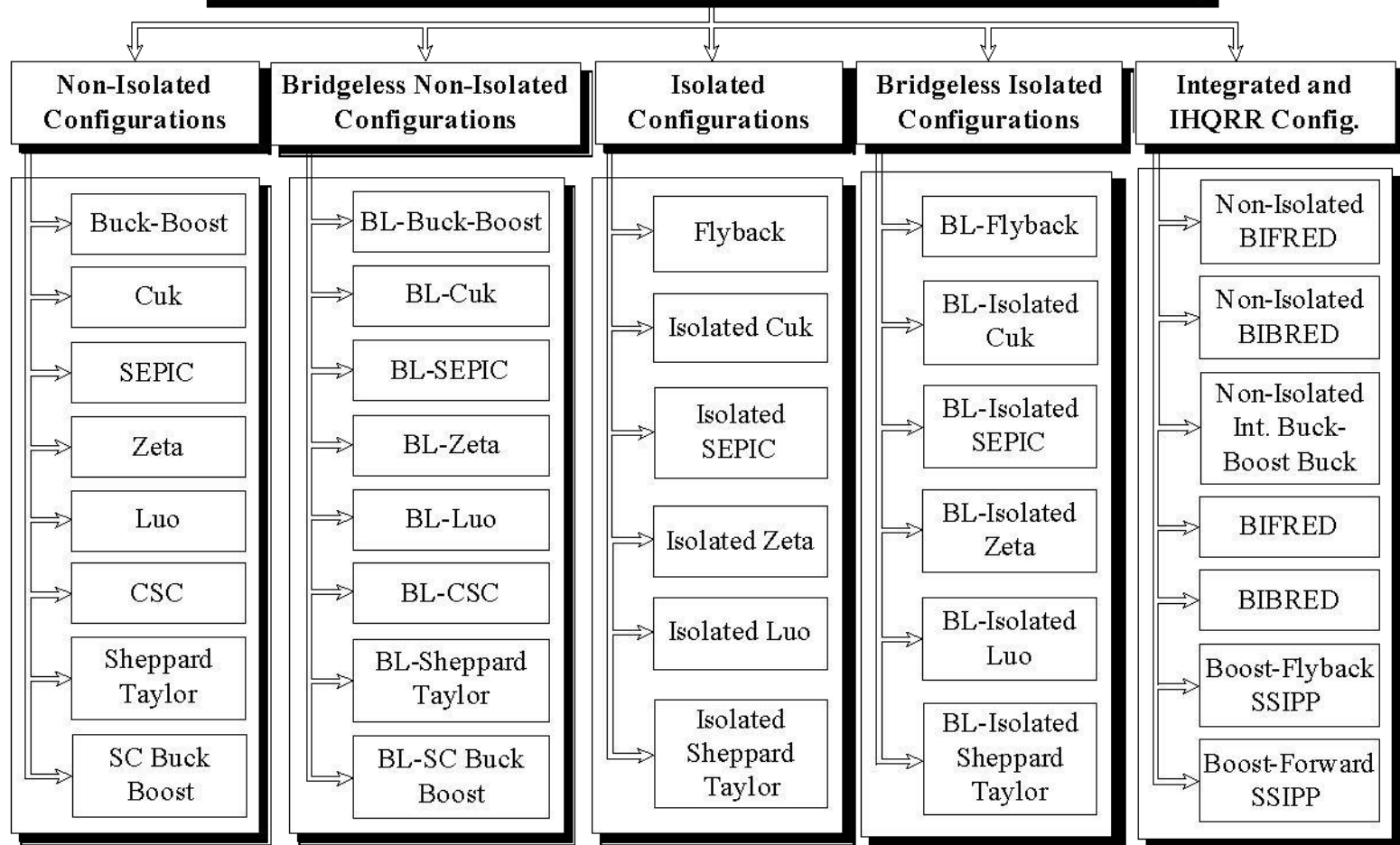


**C-Dump Converter
Topology**

Variable DC link topologies

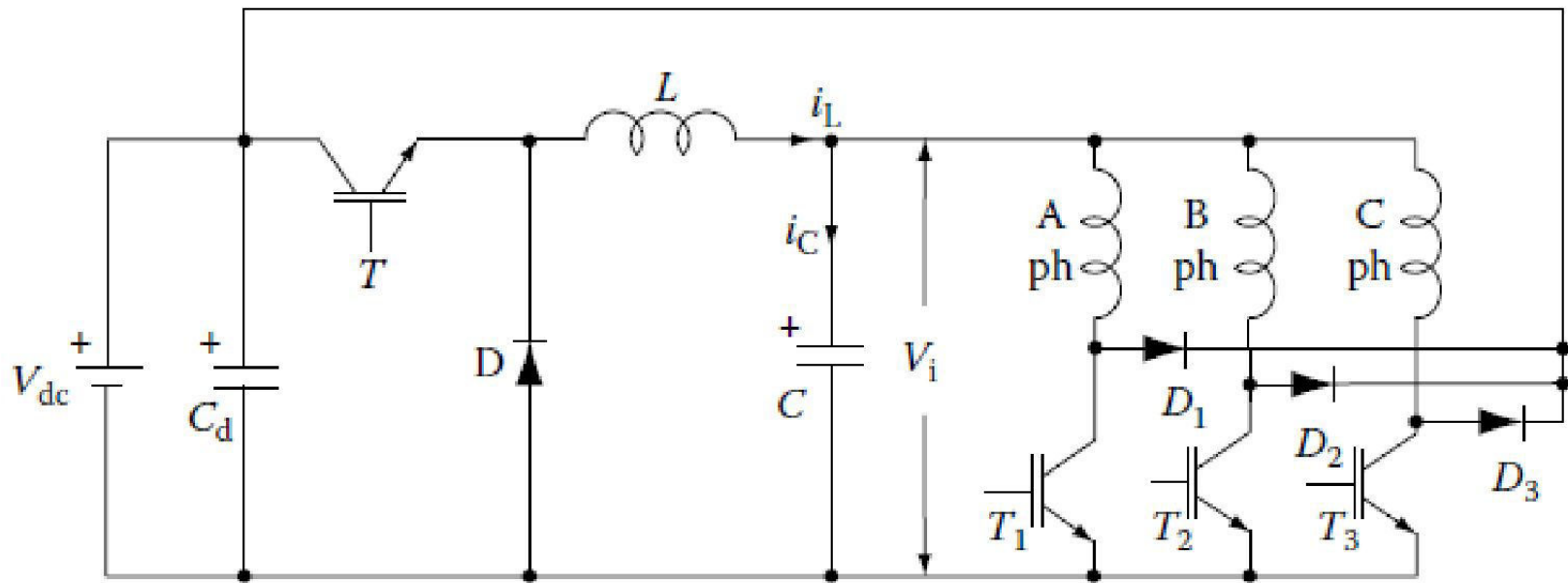
Half Wave BLDC motor drives

Converter Configurations for Feeding BLDC Motor Drive

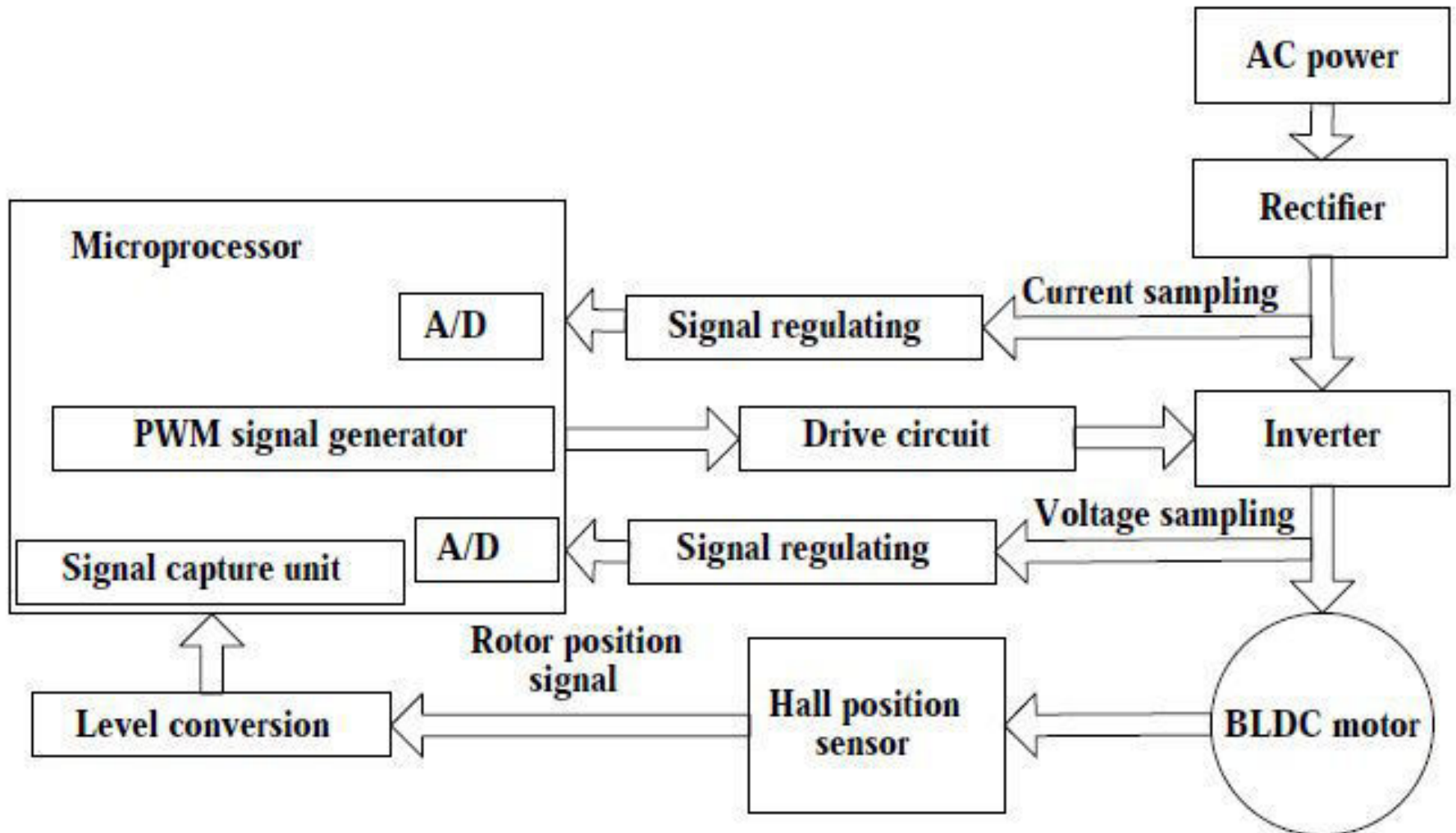


Variable DC link

Half Wave BLDC motor drives

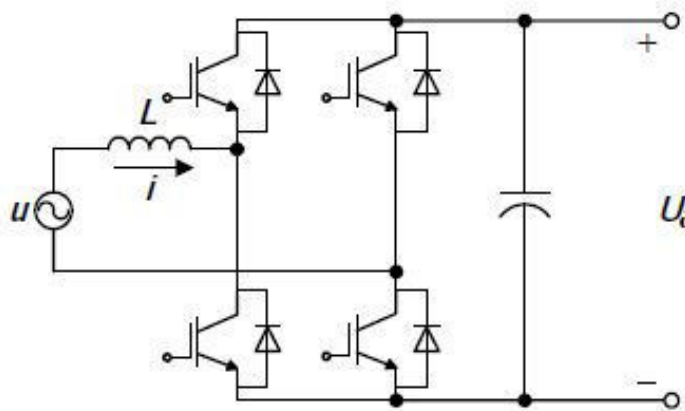


Realization of PM BLDC Motor Drives

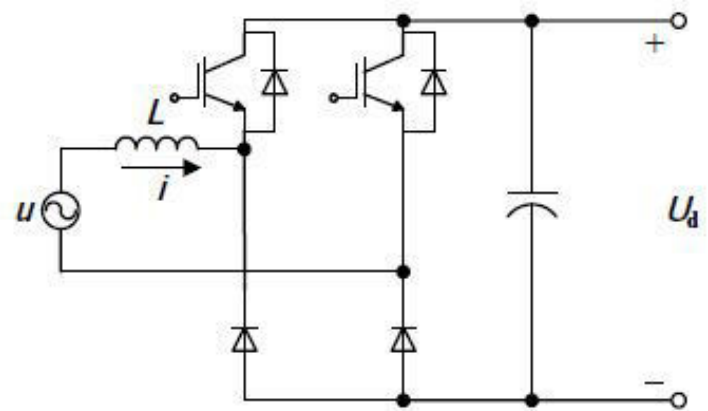


Hardware block diagram of a BLDC motor

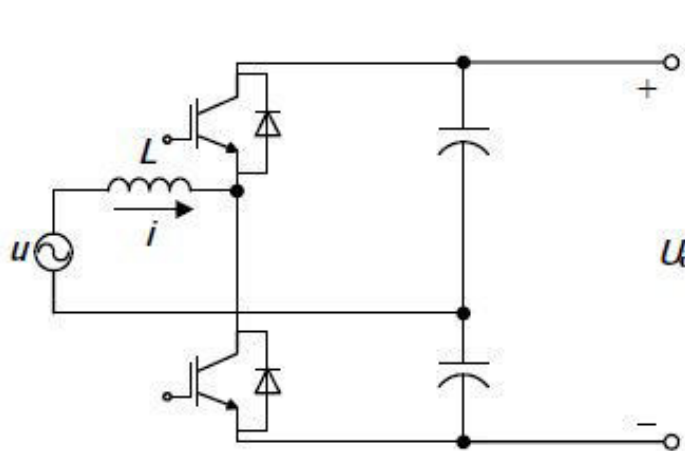
Common rectifier circuits



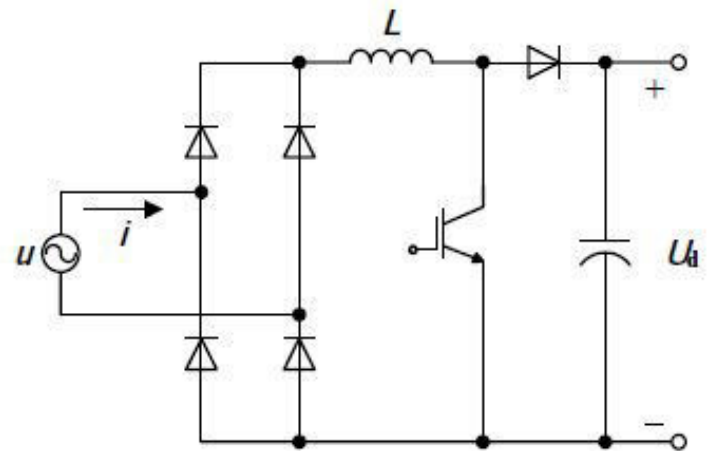
(a) Full-bridge rectifier circuit



(b) Half-bridge rectifier circuit

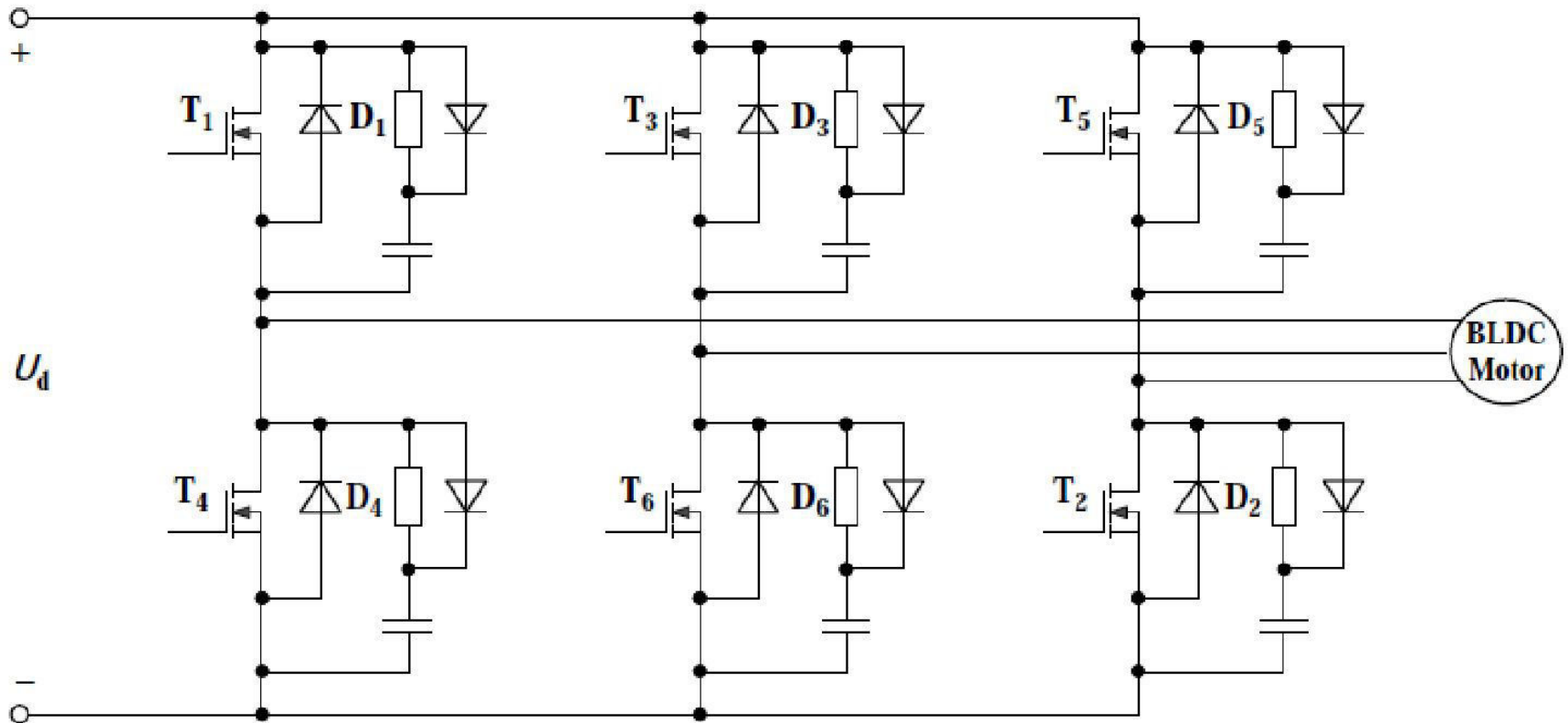


(c) Voltage-doubling rectifier circuit

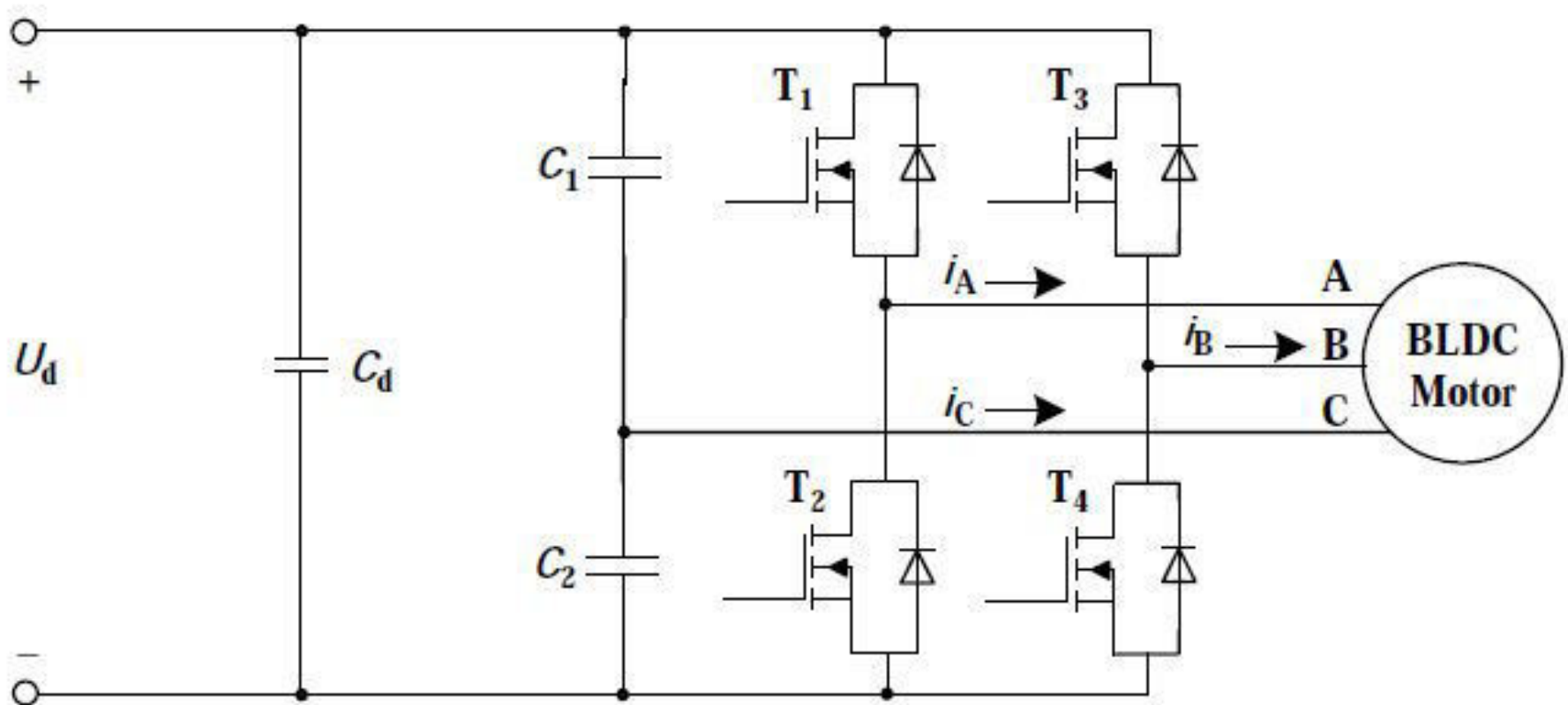


(d) Boost rectifier circuit

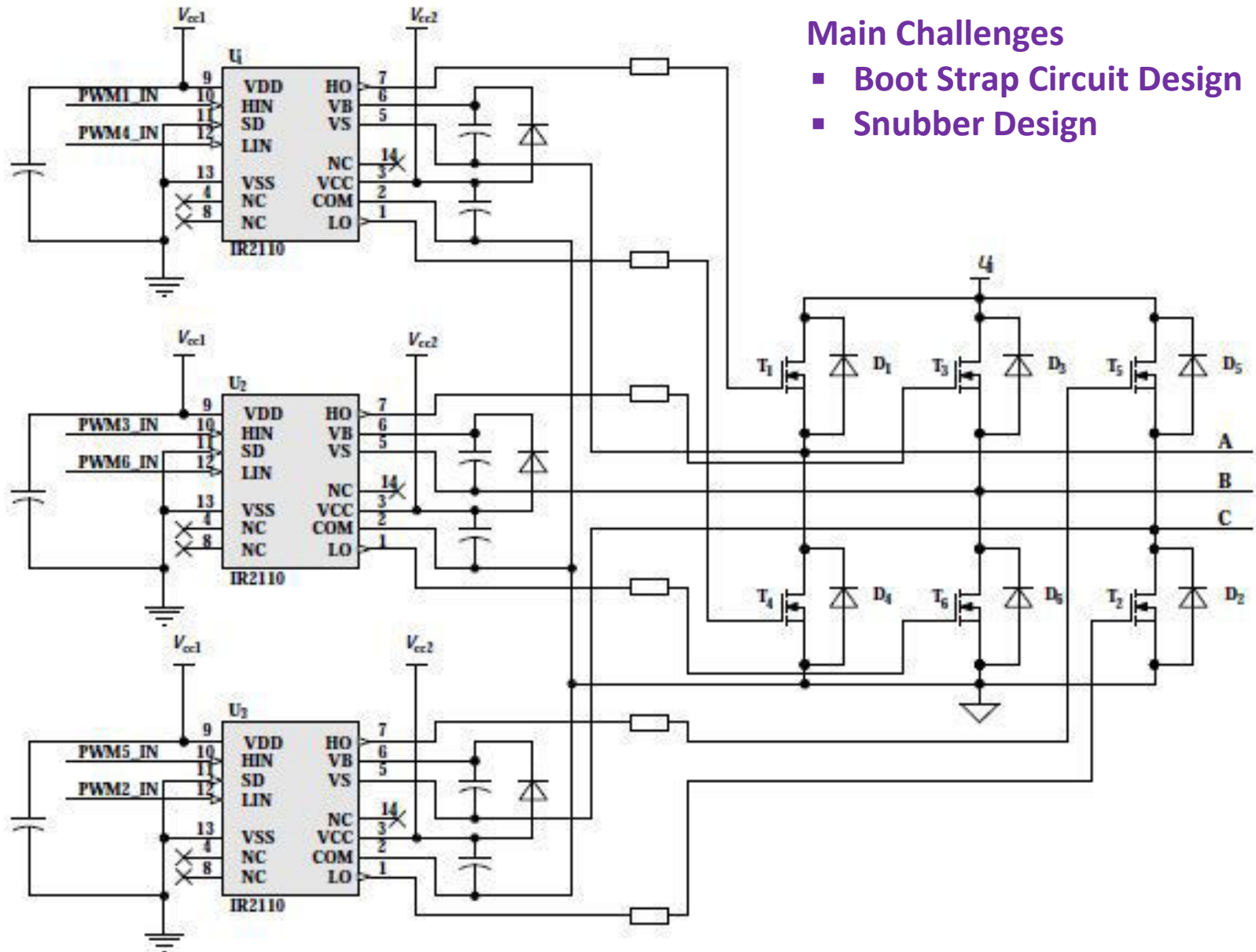
Three phase Bridge inverter circuit



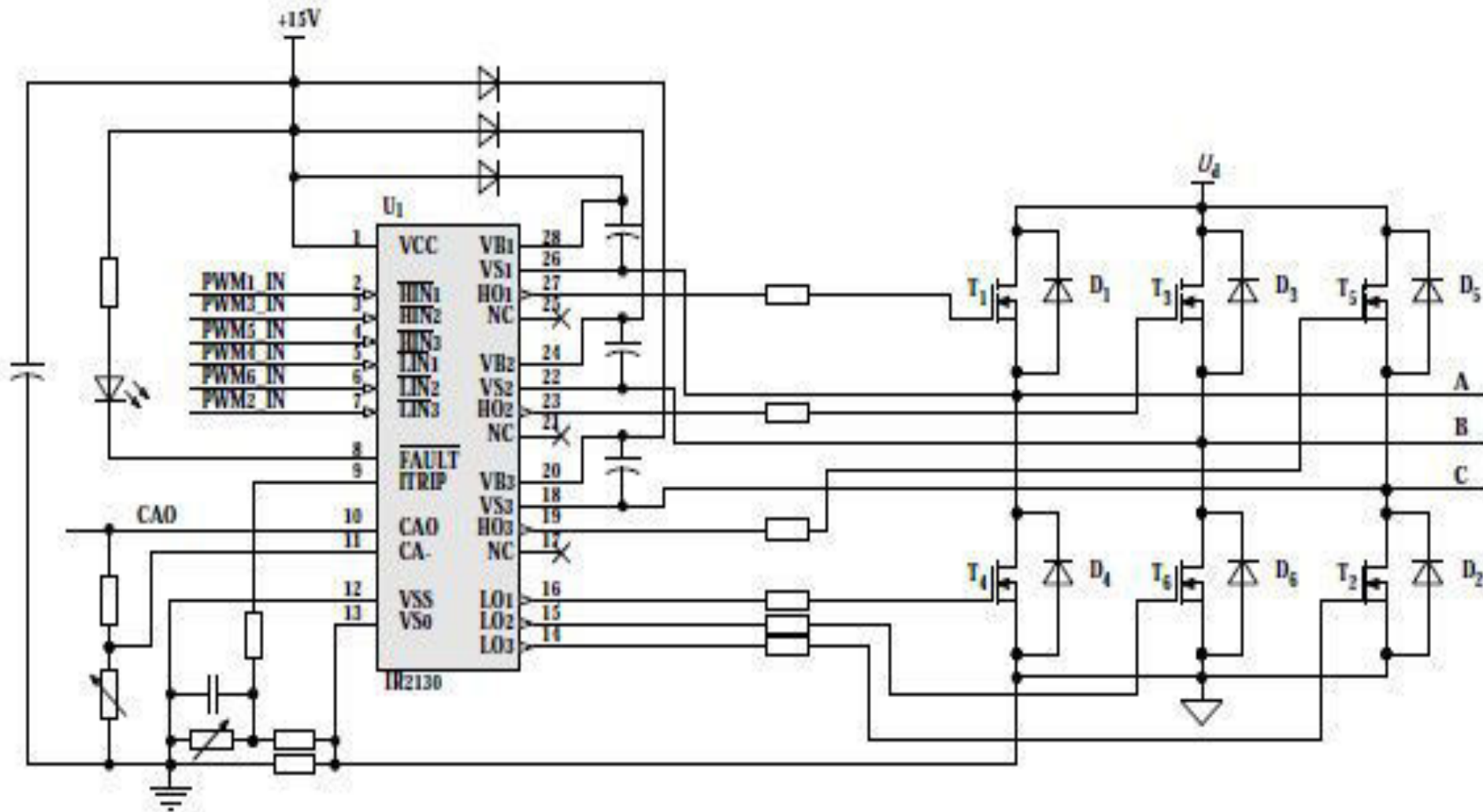
Inverter Circuit based on Four-Switch circuit



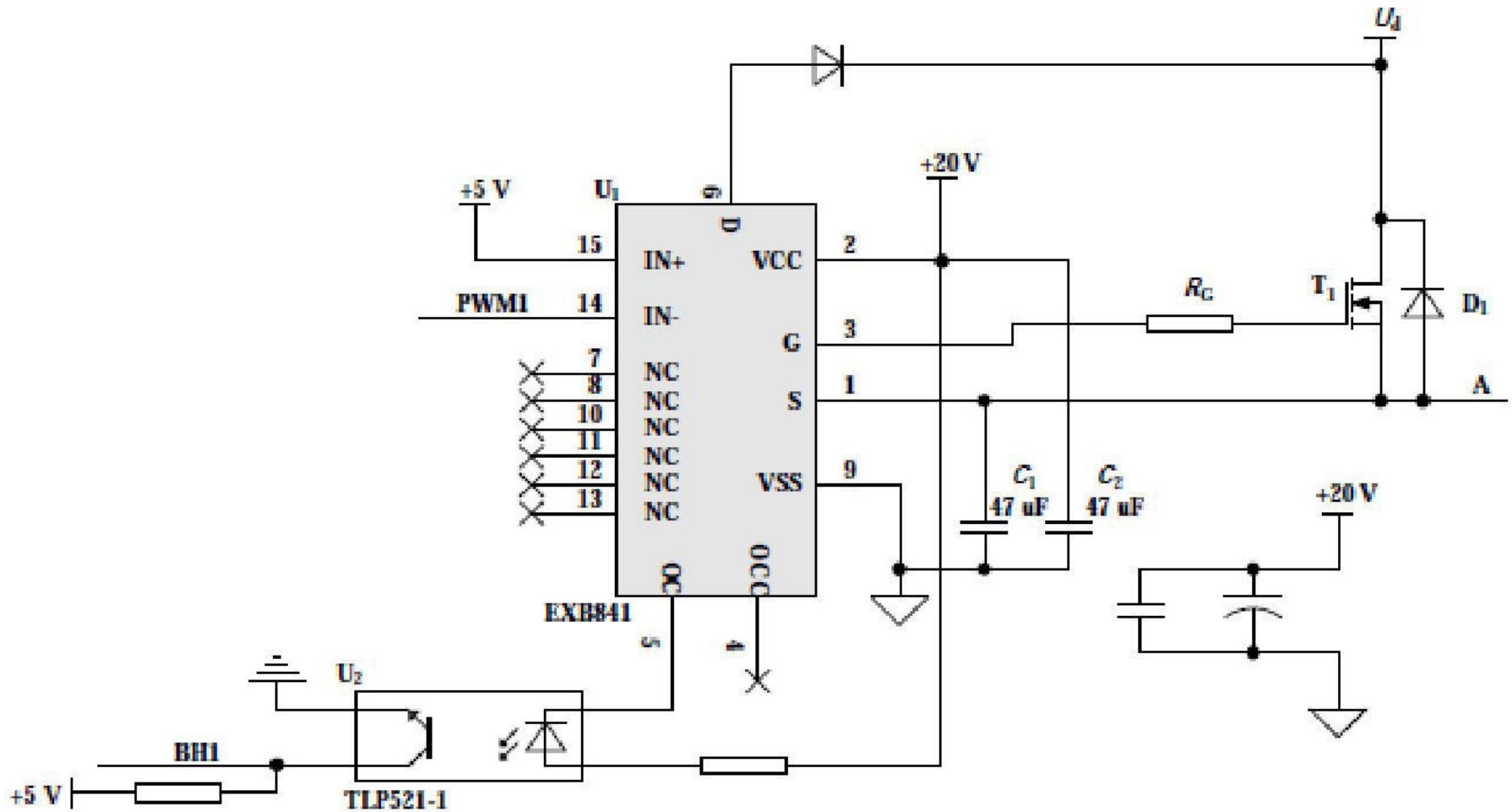
Driving Circuits of MOSFET (IR2110)



Driving Circuit of MOSFET based on IR2130

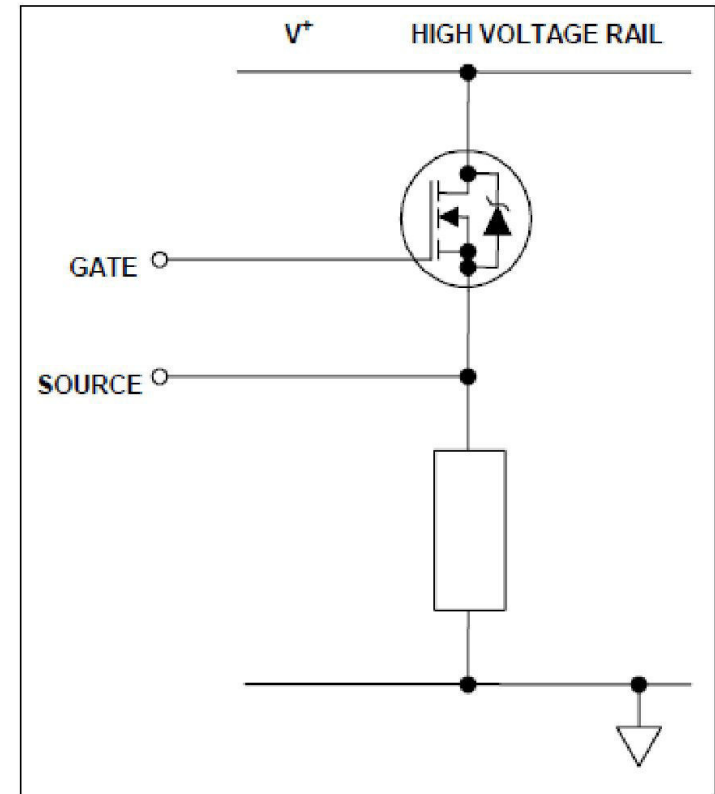


IGBT Driving Circuit based on EXB841



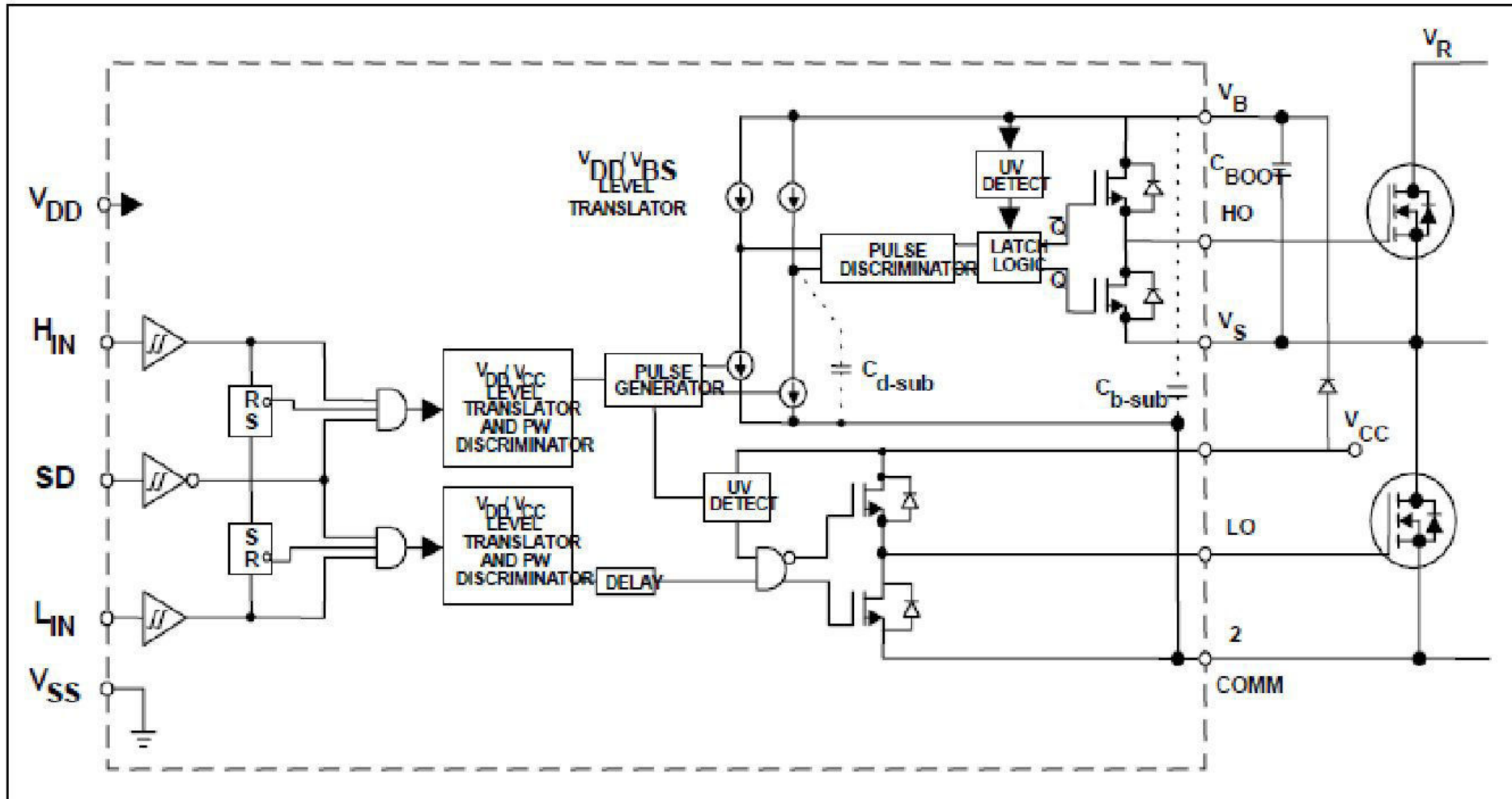
Boot –Strapping Circuit Design

- Gate voltage must be 10 V to 15 V higher than the source voltage. Being a high-side switch, such gate voltage would have to be higher than the rail voltage, which is frequently the highest voltage available in the system.
- The gate voltage must be controllable from the logic, which is normally referenced to ground. Thus, the control signals have to be level-shifted to the source of the high-side power device, which, in most applications, swings between the two rails.
- The power absorbed by the gate drive circuitry should not significantly affect the overall efficiency.

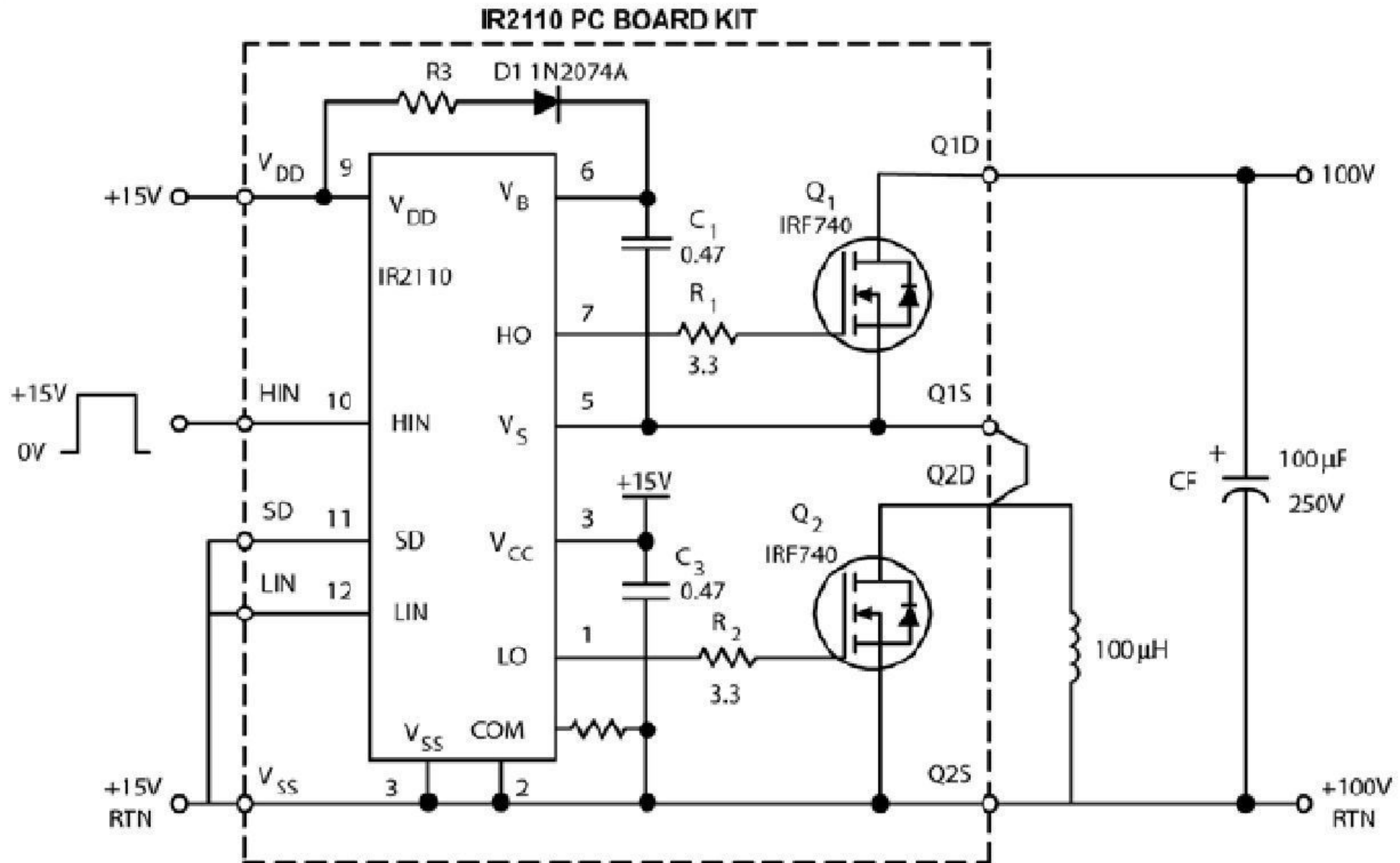


Power MOSFET in the High-Side Configuration

Block Diagram of the IRS2110

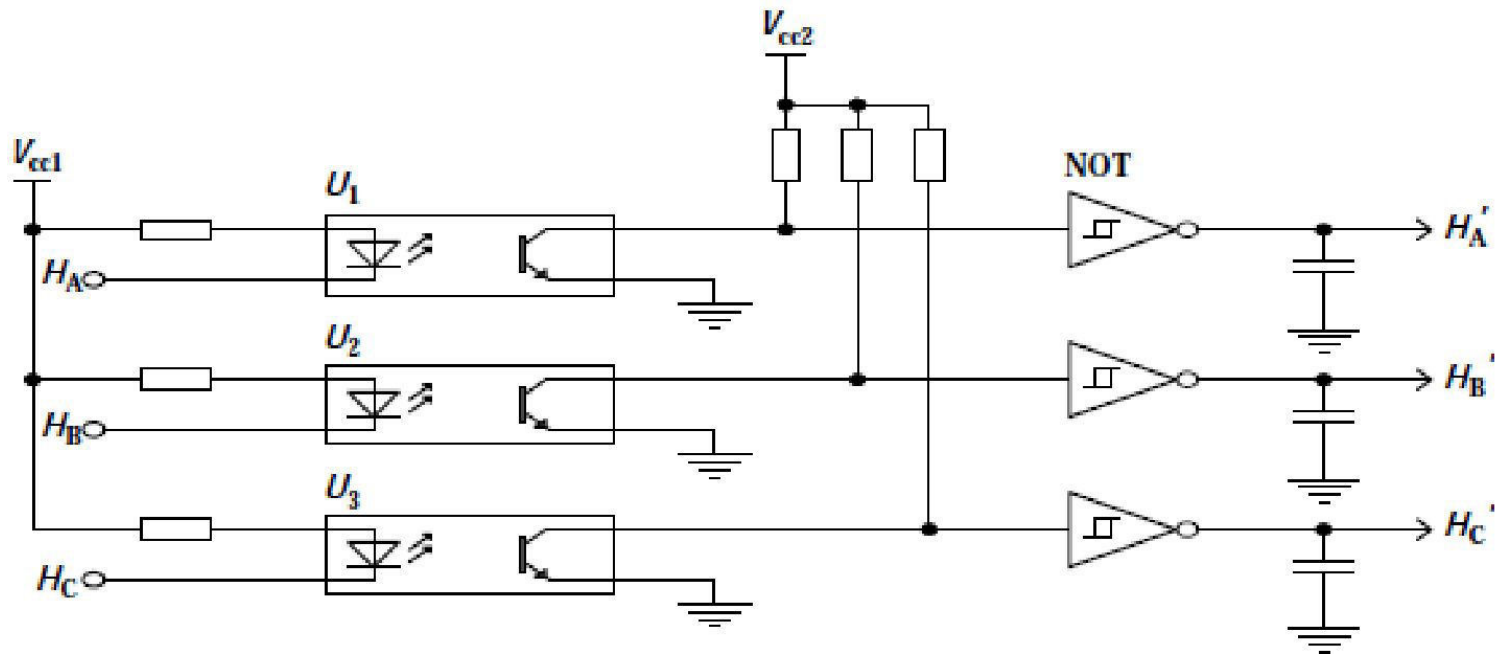
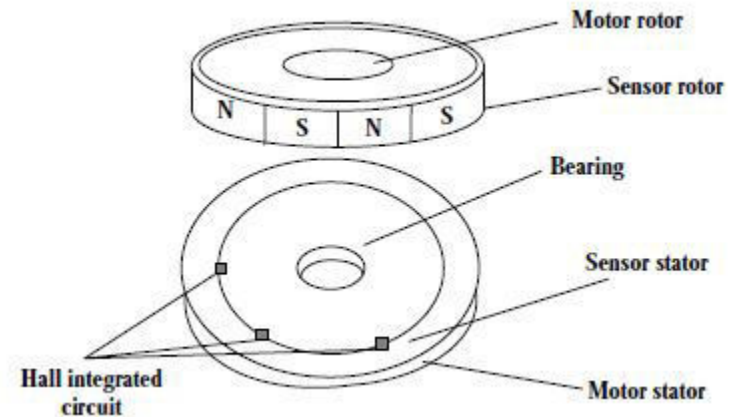


IR2110 Test Circuit



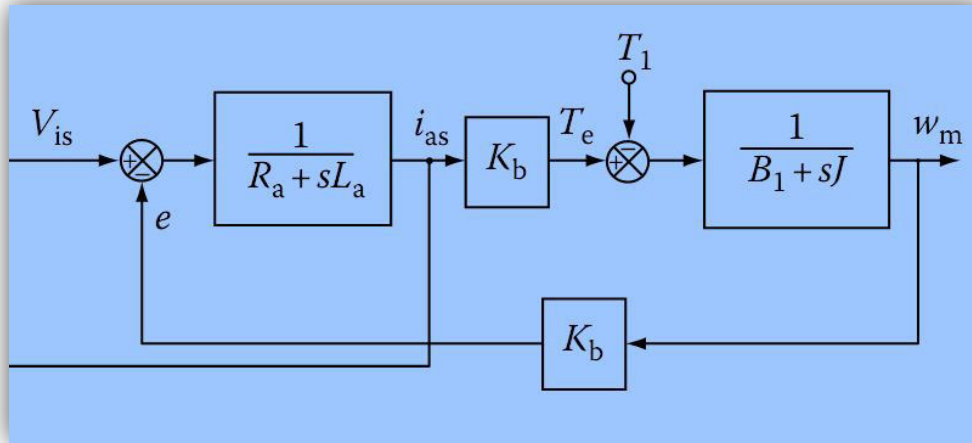
Rotor Position Sensor Circuit

Structure of a hall sensor



Rotor Position Detection Circuit

TRANSFER FUNCTION OF MACHINE AND LOAD



$$Z = 2 \{ R_s + s(L - M) \} = R_a + sL_a$$

$$R_a = 2R_s$$

$$L_a = 2(L - M)$$

$$v_{is} = (R_a + sL_a)i_{as} + e_{as} - e_{cs}$$

$$e_{as} = -e_{cs} = \lambda_p \omega_m$$

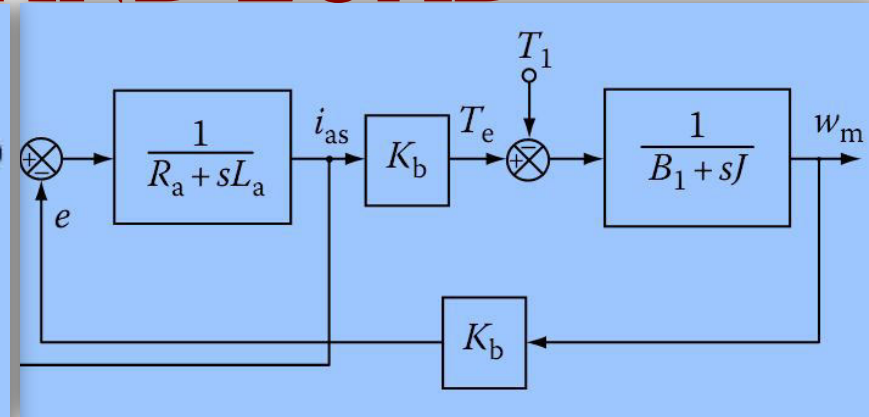
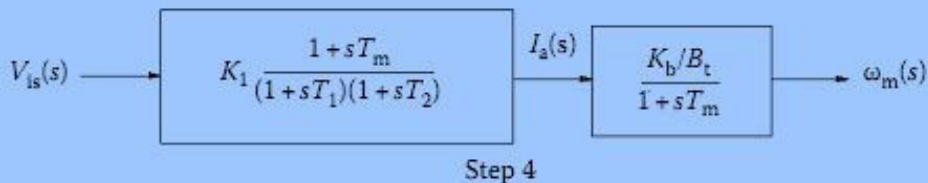
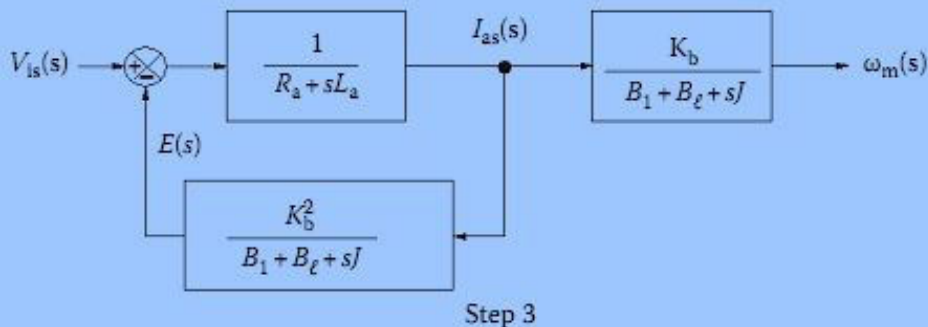
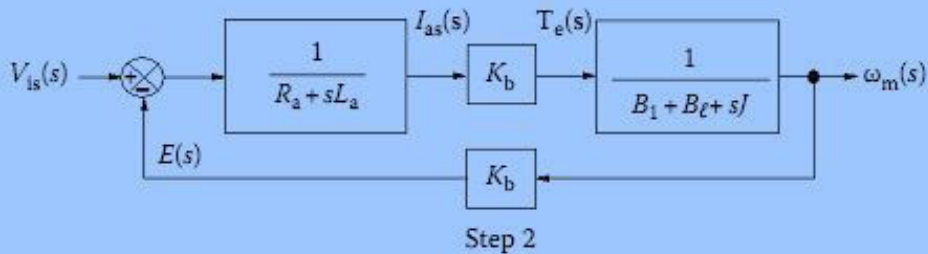
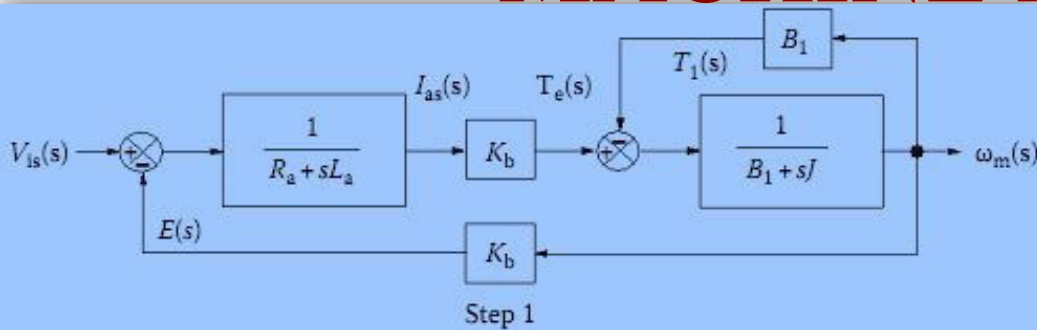
$$v_{is} = (R_a + sL_a)i_{as} + 2\lambda_p \omega_m = (R_a + sL_a)i_{as} + K_b \omega_m$$

$$T_e = 2\lambda_p i_{as} = K_b i_{as}, \text{ N} \cdot \text{m}$$

$$K_b = 2\lambda_p$$

$$T_1 = B_\ell \omega_m$$

TRANSFER FUNCTION OF MACHINE AND LOAD



$$\frac{\omega_m(s)}{V_{is}(s)} = \frac{\omega_m(s)}{I_{as}(s)} \cdot \frac{I_{as}(s)}{V_{is}(s)}$$

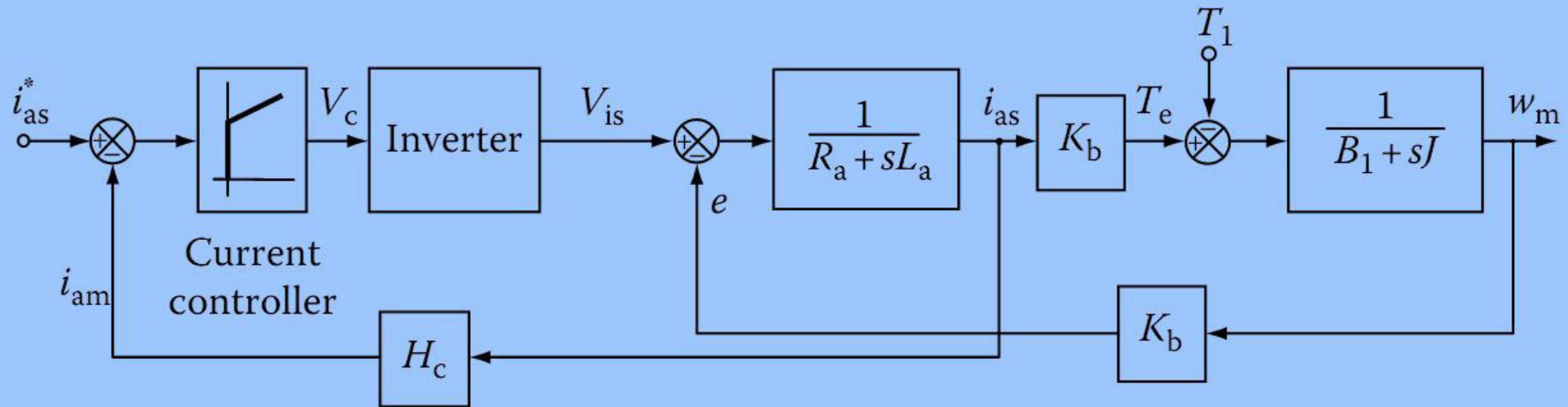
$$\frac{\omega_m(s)}{I_a(s)} = \frac{K_b}{B_t(1 + sT_m)} \quad B_t = B_1 + B_\ell$$

$$\frac{I_a(s)}{V_{is}(s)} = K_1 \frac{1 + sT_m}{(1 + sT_1)(1 + sT_2)} \quad T_m = \frac{J}{B_t}$$

$$-\frac{1}{T_1}, -\frac{1}{T_2} = -\frac{1}{2} \left[\frac{B_t}{J} + \frac{R_a}{L_a} \right] \pm \sqrt{\frac{1}{4} \left(\frac{B_t}{J} + \frac{R_a}{L_a} \right)^2 - \left(\frac{K_b^2 + R_a B_t}{J L_a} \right)}$$

$$K_1 = \frac{B_t}{K_b^2 + R_a B_t}$$

TRANSFER FUNCTION OF DRIVE



Inverter TF

$$G_r(s) = \frac{V_{is}(s)}{v_c(s)} = \frac{K_r}{1 + sT_r} \quad K_r = 0.65 \frac{V_{dc}}{V_{cm}}$$

Current Controller TF

K_c and T_c correspond to the gain and time constants

$$G_c(s) = \frac{K_c(1 + sT_c)}{sT_c} \quad T_r = \frac{1}{2f_c}$$

Speed Controller TF

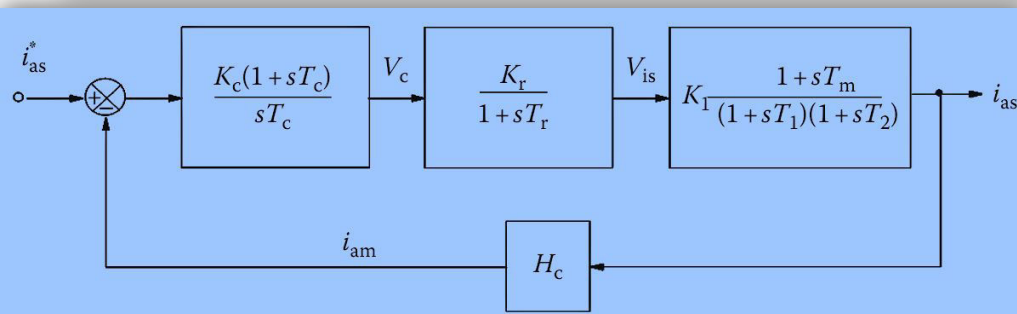
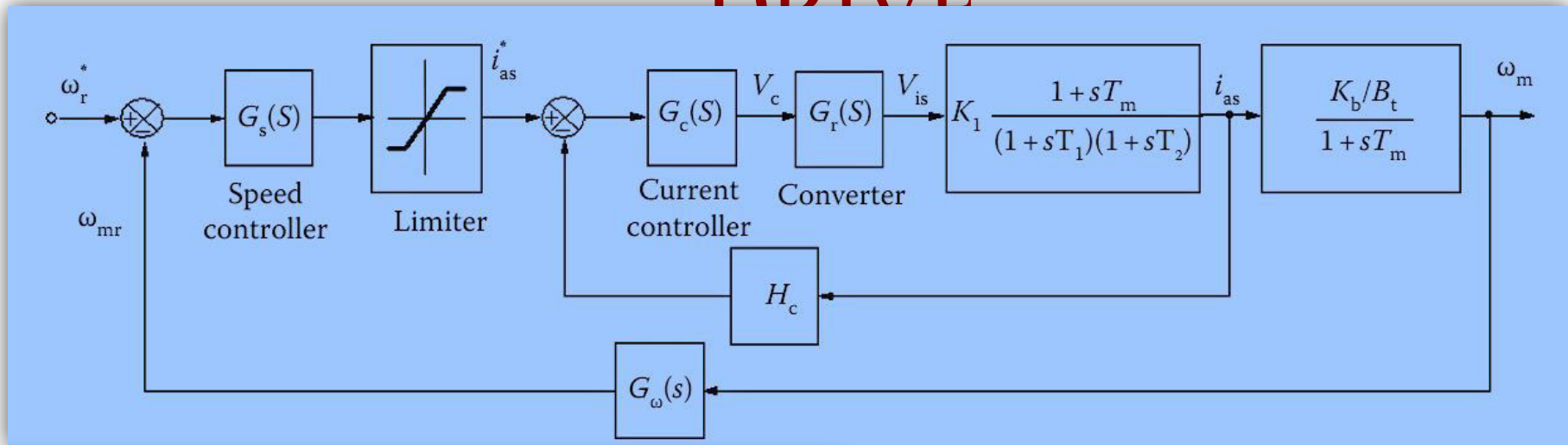
K_c and T_c correspond to the gain and time constants

$$G_s(s) = \frac{K_s(1 + sT_s)}{sT_s}$$

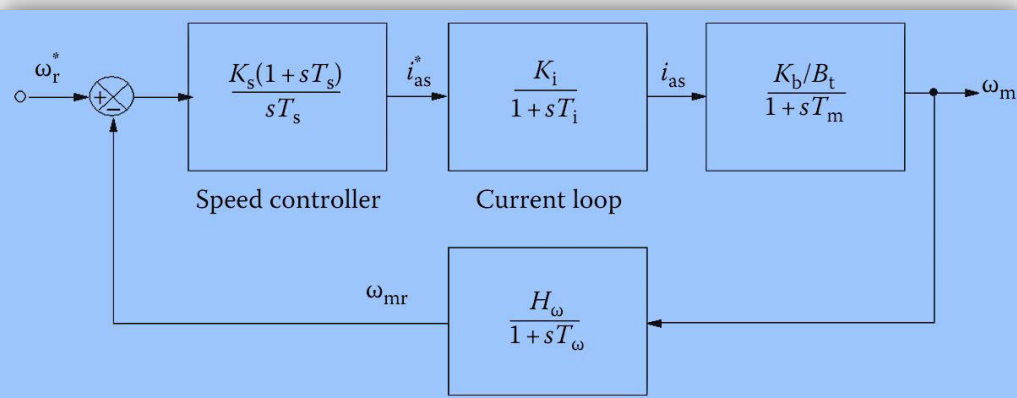
Speed feed back tacho TF

$$G_\omega(s) = \frac{K_\omega}{1 + sT_\omega} \quad \begin{array}{l} K_\omega \text{ is the gain} \\ T_\omega \text{ is the time constant} \end{array}$$

TRANSFER FUNCTION OF DRIVE



Inner current control loop.



Outer speed control loop

Sensorless Control of PMBLDC Motor

- The system needs position and current sensors for control
- *Elimination of both the sensors is desirable in many applications*
- *In the low-cost but high-volume applications from the cost and compact packaging points of view*
- *Reliability in other applications*
- *The current sensor is easier to accommodate*
- *Position sensor requires a considerable labor and spatial volume in the motor for its mounting.*
- *That makes it all the more important to do without the position sensor*

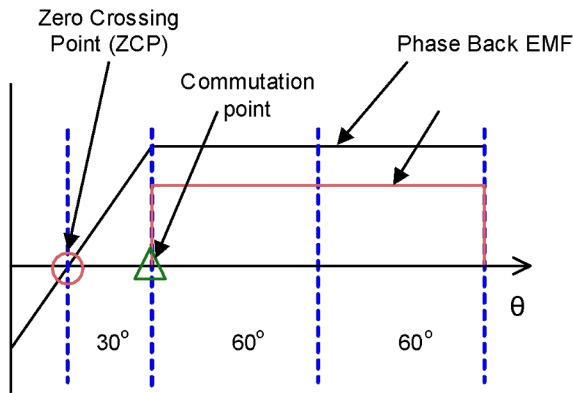
Sensorless Control of PM BLDC Motor

- ***Sensing induced emfs***
 - This method is based on emf sensed on phase terminals, one of the simple and widely used methods. This is explained in further slides
- ***Sensing coils (Flux based)***
 - Sensing coils in the machine can be installed inexpensively to obtain the induced emf signals. Otherwise calculate the flux linkage from the voltage equation from the terminal voltages, based on flux linkage and initial position can calculate position.
- ***Signal Injection method (Inductance)***
 - A high-frequency signal is injected to detect inductance, which is a function of rotor position for salient PM motors and the initial rotor position at standstill can be detected based on the incremental inductance calculation.
- ***Estimation using machine model (observer)***
 - The induced emf can be sensed from the machine model using the applied currents and voltages and machine parameters of resistance, self-inductance, and mutual inductance.
- ***Method based on artificial intelligent control***
 - Intelligent controllers such as neural network or fuzzy controllers can extract the rotor position and or the commutation positions from the machine variables such as current and flux linkages.

Sensorless Control Based on Back EMFs

(a) *Phase back EMF zero crossing*

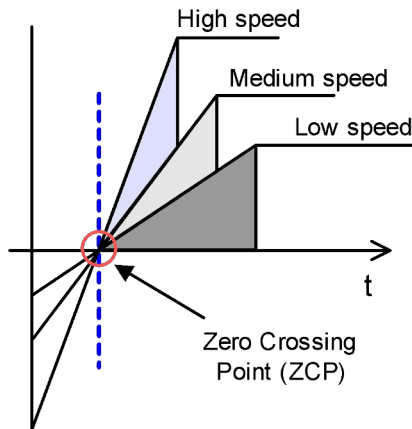
- Current commutation point is after 30° to zero crossing point (ZCP) of back EMF.
- LPFs will limit the high speed operation capability.
- Error during the transient period when the speed is accelerated or decelerated rapidly.



(a)

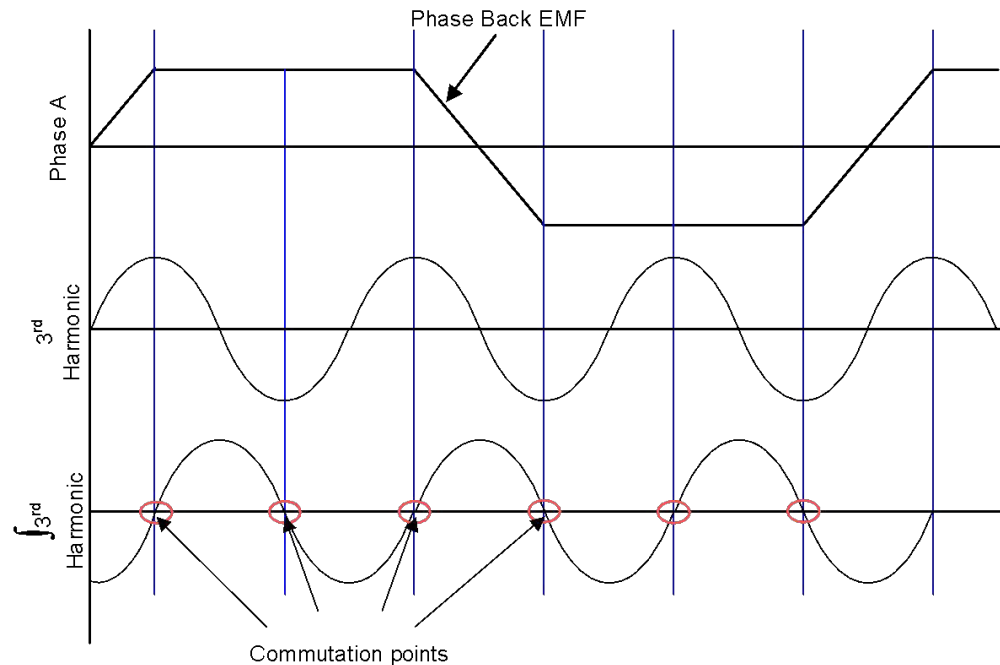
(b) *Back-EMF integration*

- Integrated area of the back EMF is approximately the same at all speeds.
- Low speed operation is poor due to the error accumulation.
- Offset voltage problems from the integration.



(b)

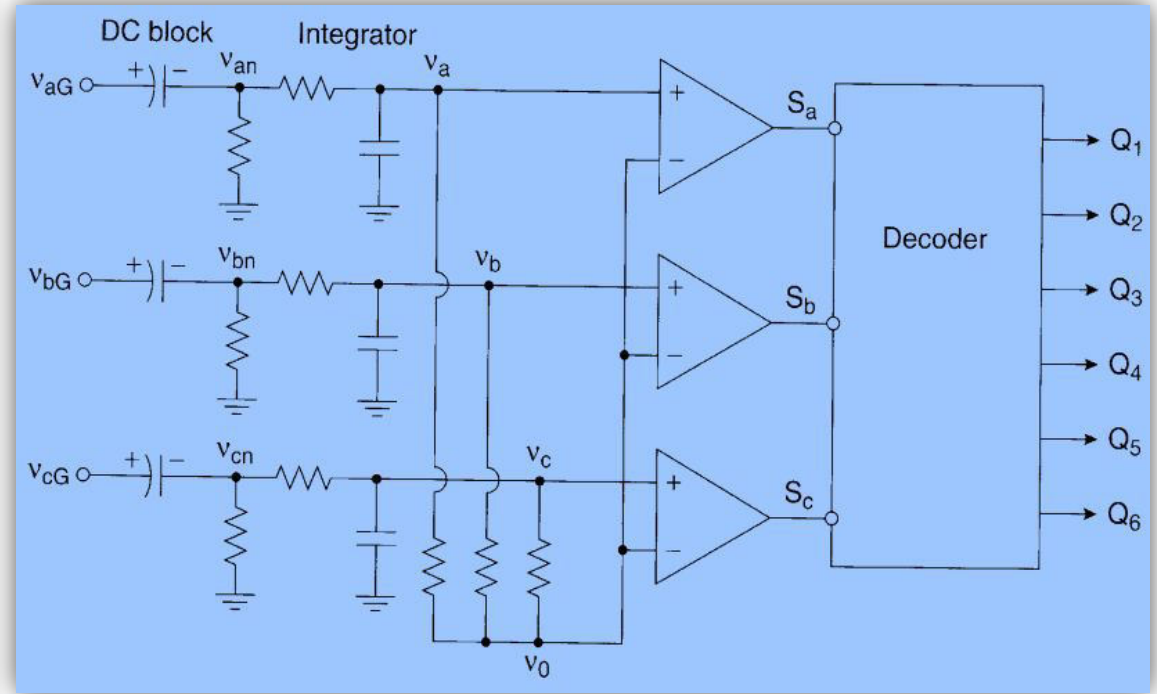
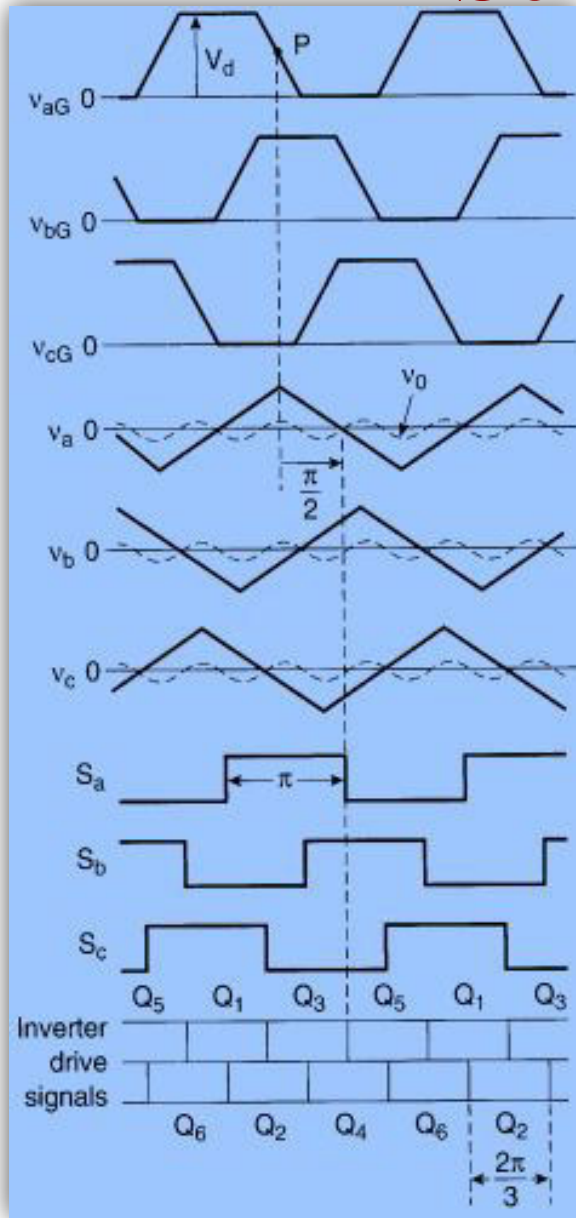
Sensorless Control of PM BLDC Motor



(c) *Third harmonic of the back EMF*

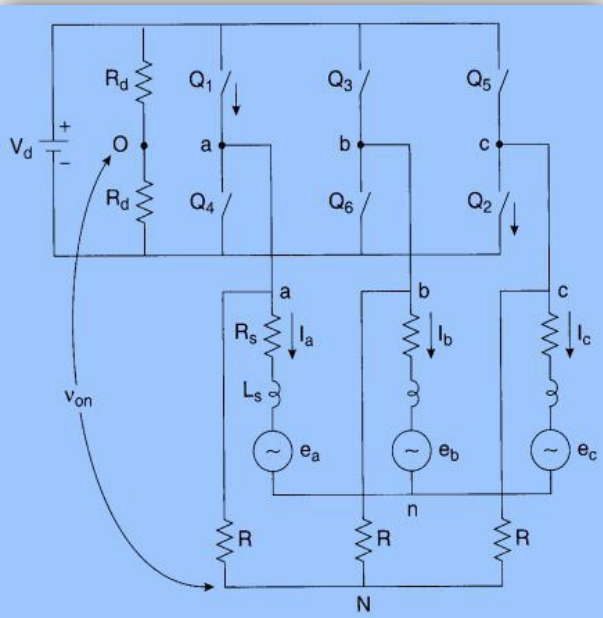
- Third harmonic content of the back EMF to determine the commutation instants.
- At low speed, the integration process can cause a serious position error, as noise and offset error from sensing can be accumulated for a relatively long period of time.

BACK EMF BASED Sensorless Control



This method uses two filter sections to pass a band of frequency.

Third harmonic Based Sensorless Control

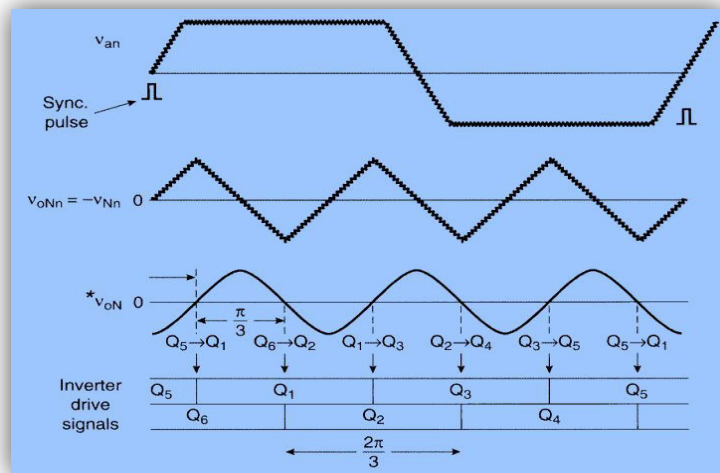


$$v_{an} = R_s i_a + L_s \frac{di_a}{dt} + e_a$$

$$e_a = E [\cos \omega_e t + K_3 \cos 3\omega_e t + K_5 \cos 5\omega_e t + \dots]$$

$$v_{an} + v_{bn} + v_{cn} = R_s (i_a + i_b + i_c) + L_s \left(\frac{di_a}{dt} + \frac{di_b}{dt} + \frac{di_c}{dt} \right) + (e_a + e_b + e_c)$$

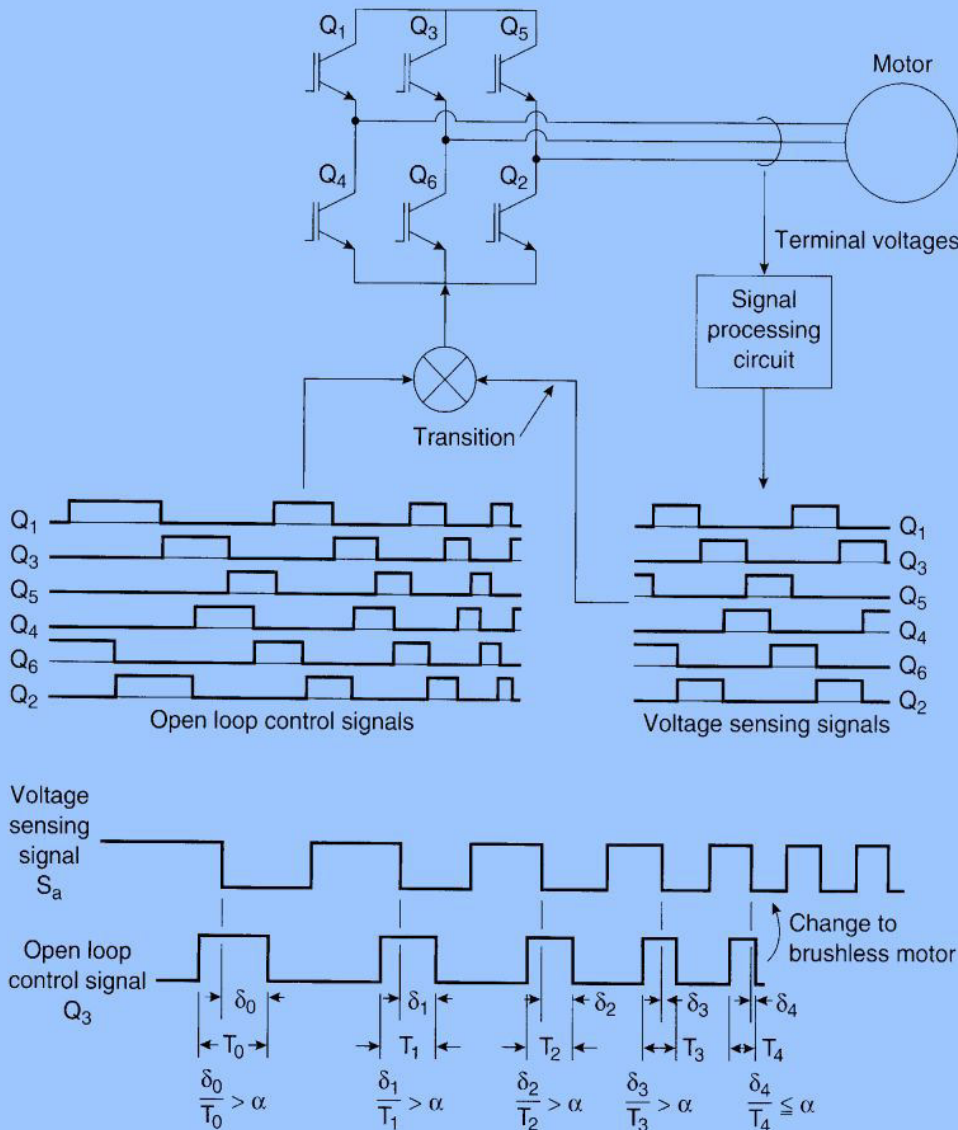
$$= 0 + 0 + 3EK_3 \cos 3\omega_e t + v_{hf}$$



A three-phase star-connected four wire system will allow the collection of the third harmonic-induced emf and this can be inexpensively instrumented with four resistors.

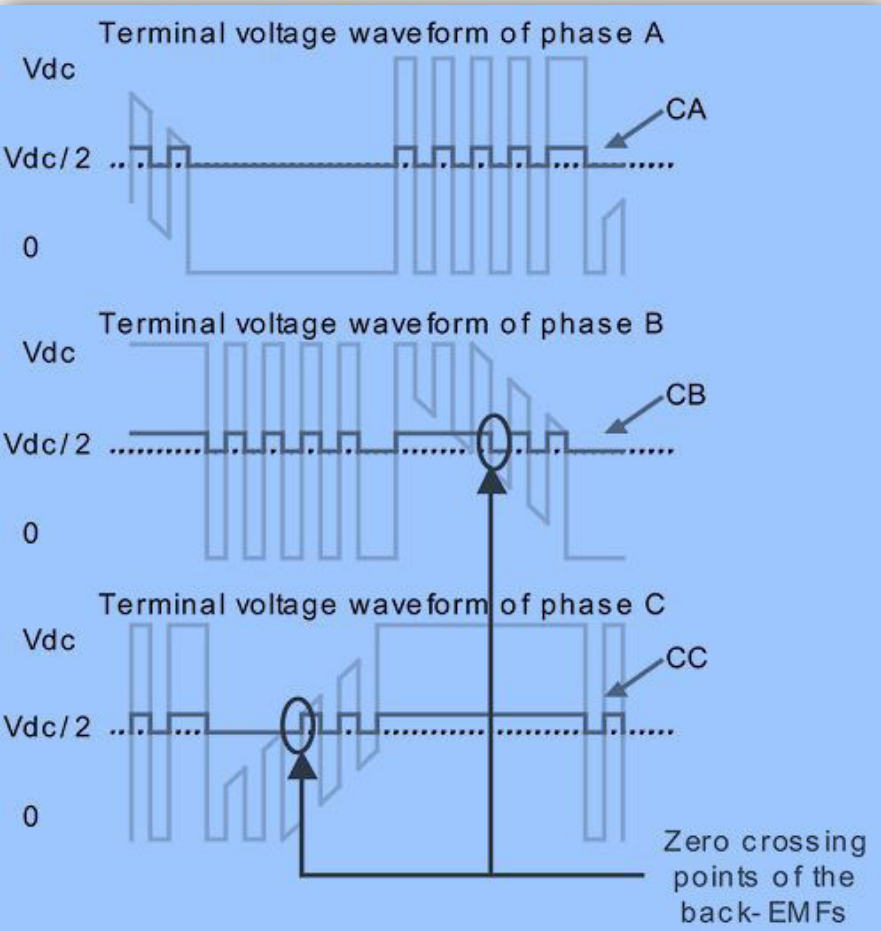
Starting OF PM BLDC Motor

Sensorless Control



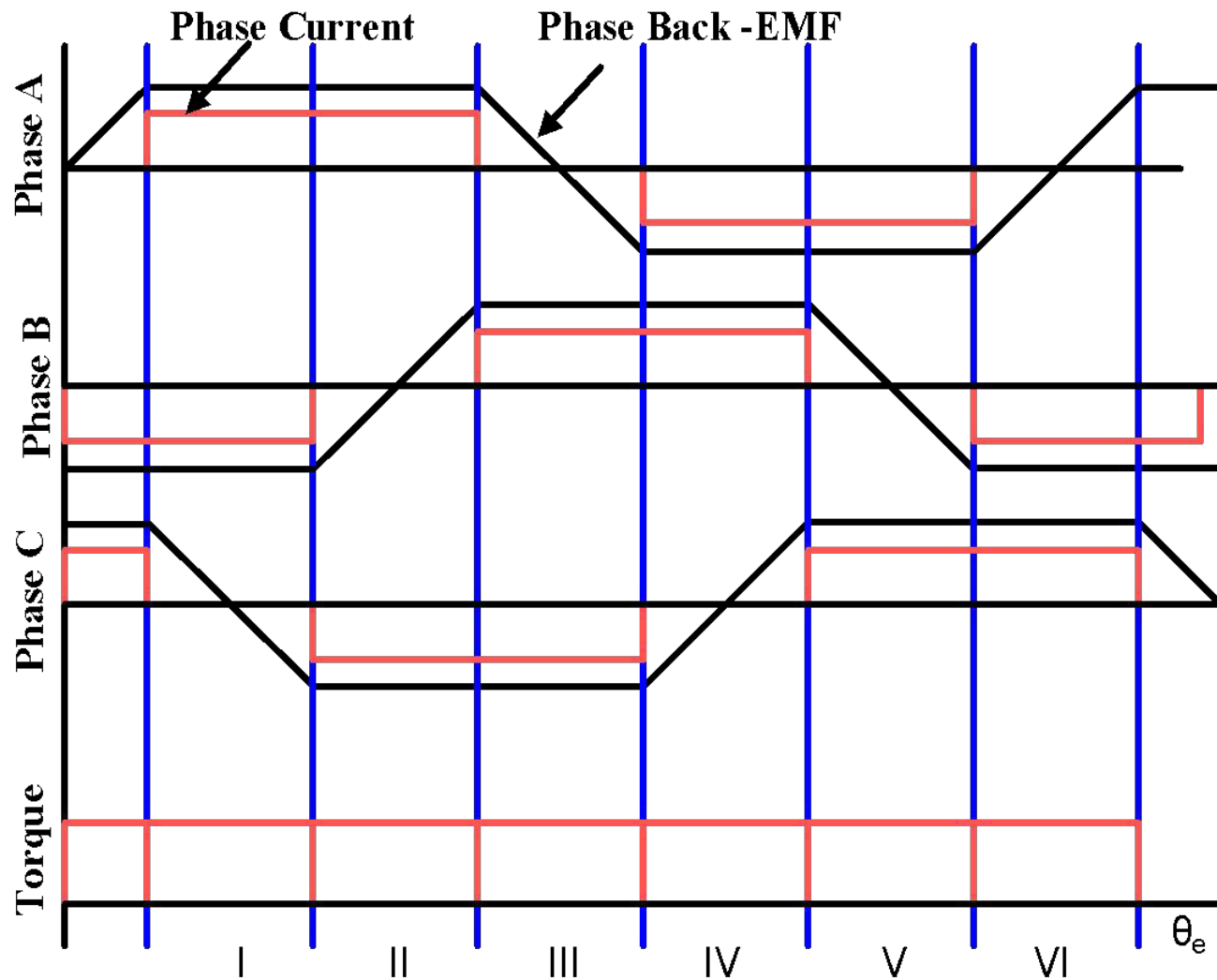
- The position information is not available, as there is no induced emf at zero speed.
- At standstill, Even at very low speeds, the induced emf may not be easily detectable.
- A method to generate the control signals at and around zero speed has to be incorporated for successful starting

Direct back emf BASED Sensorless Control

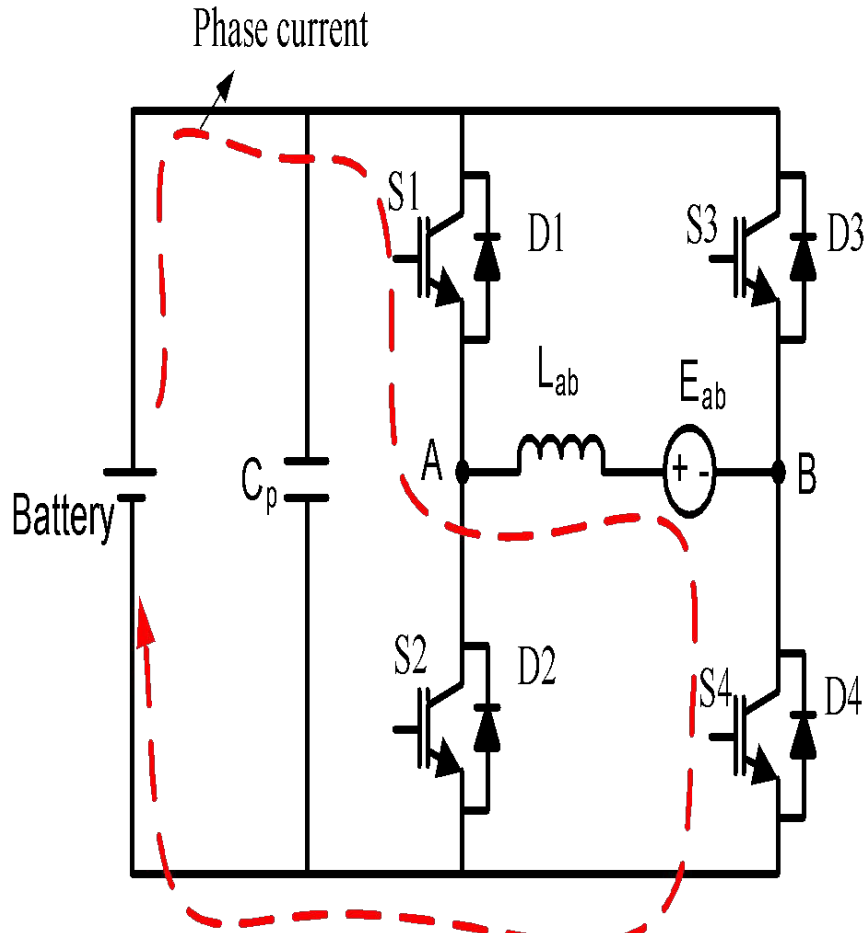


- One of the most commonly used methods for acquiring position information is to monitor the induced emf of the machine phases when they are not being energized.
- Phase is inactive for 33.33% of the time and only two phases conduct at any given time. During that time, the induced emf appears across the machine winding, which can be sensed and can detect zero crossing.
- Direct back emf sensing is one of the accurate method to sense the back emf zero crossing. This method don't use any filtering elements so response is fast.

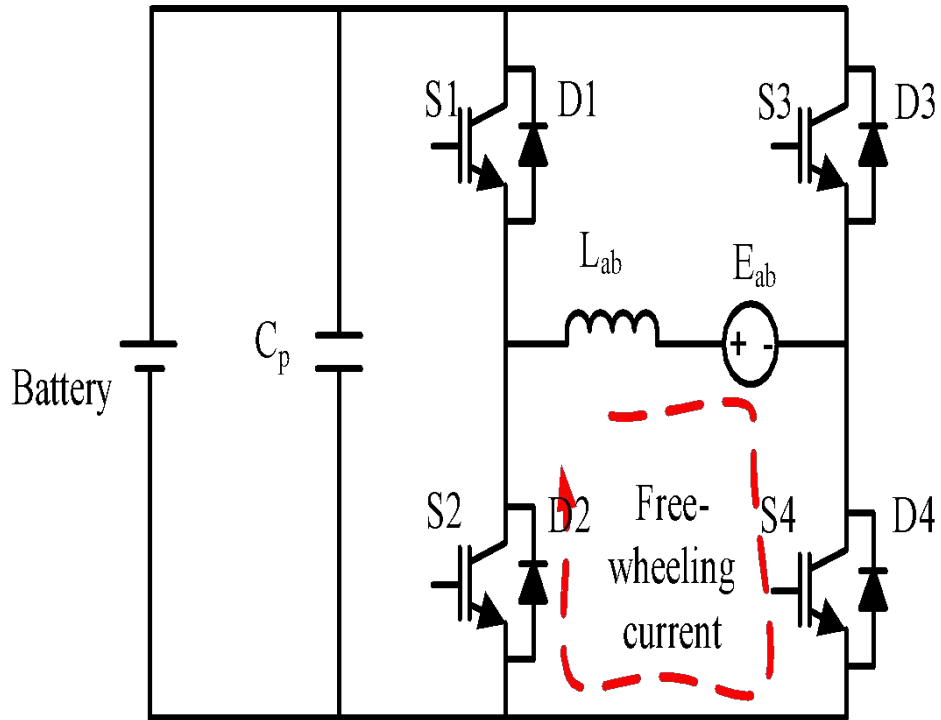
Thank you



Ideal back-EMF, phase current and developed torque profiles in a 3-phase PM BLDC motor



**When S1 and S4 are closed with PWM-ON
(State-I) for motoring mode**



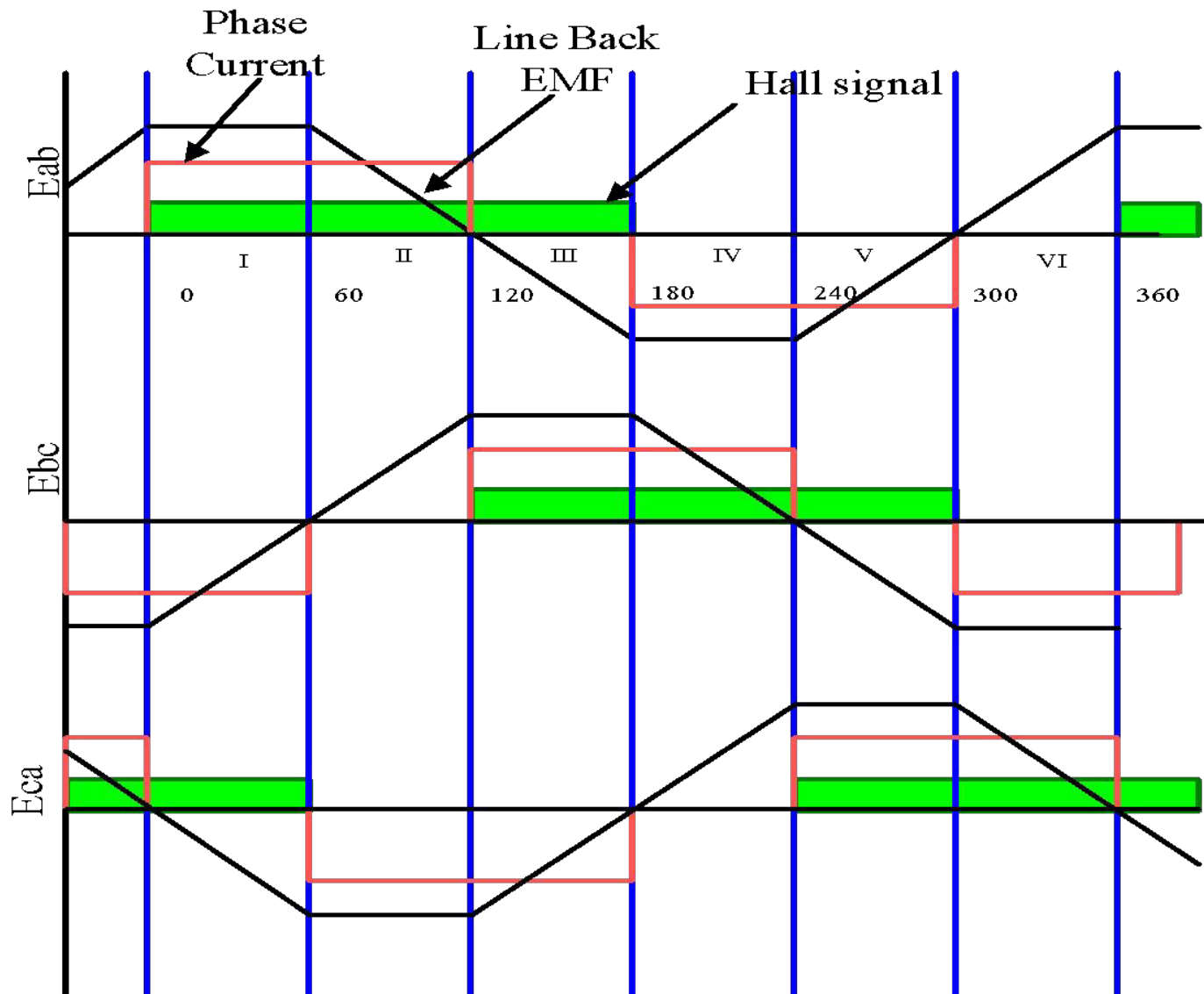
**When S4 only is closed (State-I) for
free-wheeling mode**

**Equivalent circuit of the 3-phase PM BLDC motor during the motoring
mode and free-wheeling modes**

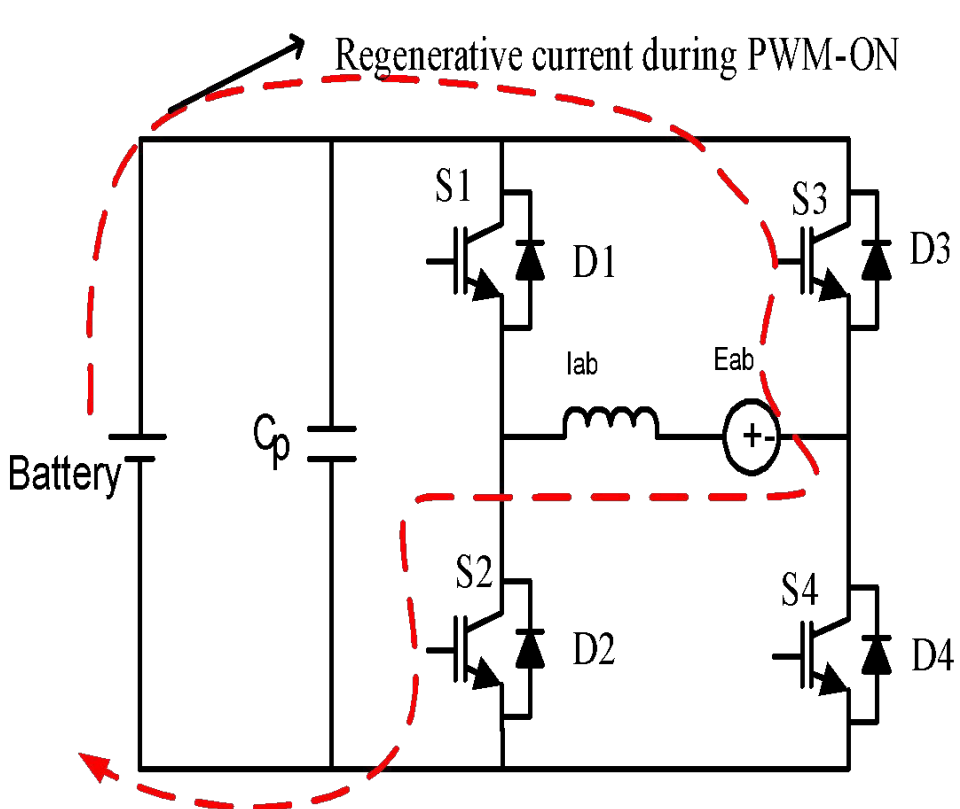
Regenerative braking mode

- Regenerative method of braking of an electric vehicle (EV) helps in efficient utilization of the battery power to increase the range of the vehicle

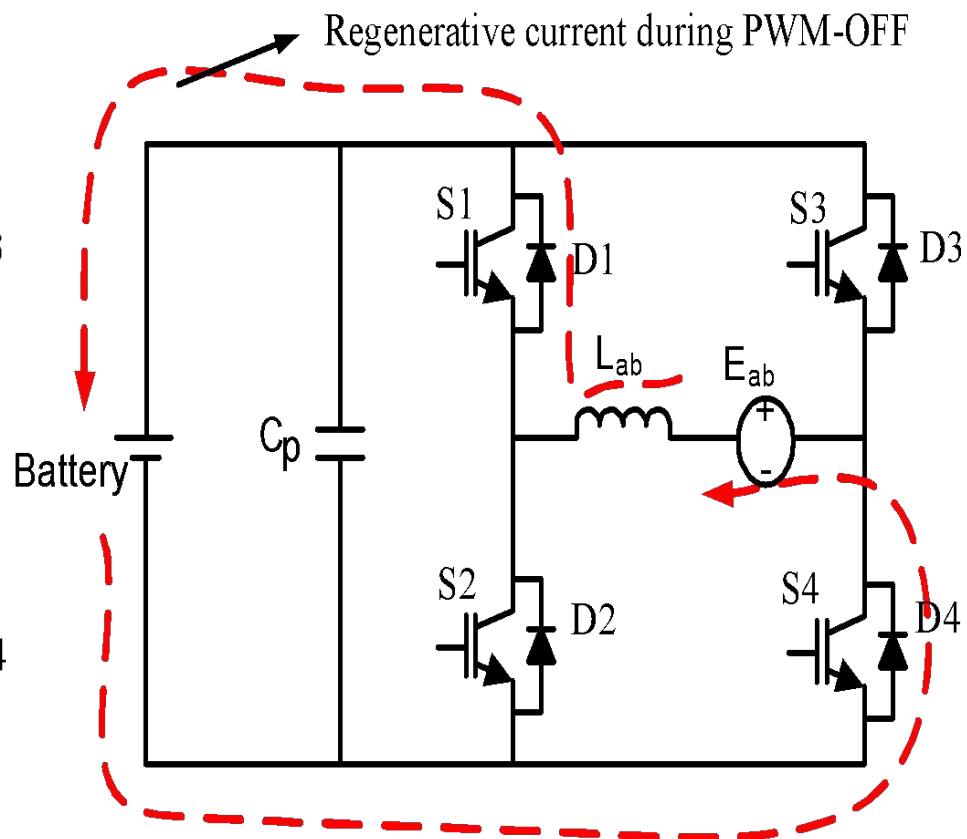
- Whenever ECU receives a brake signal, EV operation changes from the motoring mode to regenerative braking mode.
- Conventionally, in electric two-wheelers, energy during the braking mode is wasted as heat due to mechanical braking.
- **Regenerative braking** is employed in EVs to convert this mechanical energy into electrical energy so that it can be fed back to the battery or any other energy storage system such as ultra-capacitor, etc. and which can be utilized during high energy demands such as the starting and accelerating conditions of the EV. By the regeneration in EVs while braking, the range of the EV for a charge can be enhanced.



Regenerative braking strategy in a 3-phase PM BLDC motor using the line back-EMF



**When S2 and S3 are closed with PWM-ON
(State-I) for regenerative mode**



**When S2 and S3 are open with PWM-OFF
(state-I) for regenerative mode**

**Equivalent circuit of the 3-phase PM BLDC
motor during the regenerative mode**

Analysis in DCM and CCM modes

$$V_L = L_{ab} \times \frac{di_{ab}}{dt} \quad \& \quad L_{ab} \times \frac{\Delta i_L}{\Delta t}$$

Rearranging

$$\Delta i_L = \frac{V_L}{L} \Delta t$$

$$\Delta i_L (\text{on}) = \frac{(V_{bat} + E_{ab})}{L} \quad \text{on}$$

$$\Delta i_L (\text{Off}) = \frac{-V_{bat}}{L} \quad \text{off}$$

Under steady state condition

$$\Delta i_L (\text{on}) + \Delta i_L (\text{Off}) = 0$$

$$\frac{\Delta t_{\text{off}}}{\Delta t_{\text{on}}} = \frac{(V_{bat} + E_{ab})}{V_{bat}} = 1 + \frac{E_{ab}}{V_{bat}}$$

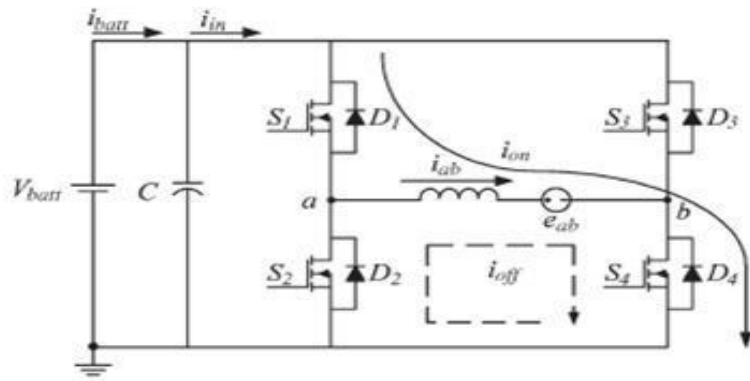
$$\frac{W_r}{W_b} = \frac{\Delta t_{\text{off}}}{\Delta t_{\text{on}}} = 1 + \frac{E_{ab}}{V_{bat}}$$

$$f_s = \left[1 + \frac{2 \times E_{ab}}{\Delta t_{bat} - E_{ab}} \right] * \frac{1}{2 \Delta t_{off}} \quad \text{Continuous conduction mode (CCM)}$$

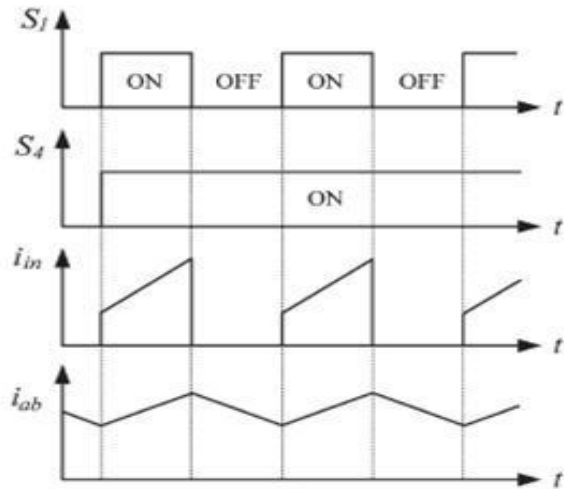
$$f_s = \left(1 + \frac{E_{ab}}{\Delta t_{bat}} \right) * \frac{1}{2 \Delta t_{off}} \quad \text{Discontinuous conduction mode (DCM)}$$

In both DCM and CCM modes time duration of energy regeneration (Δt_{off}) is dependent on the switching frequency and back-EMF. By assuming the switching frequency to be constant, the time for energy regeneration is directly proportional to back-EMF.

Regeneration process at 60 degrees (Method-1)



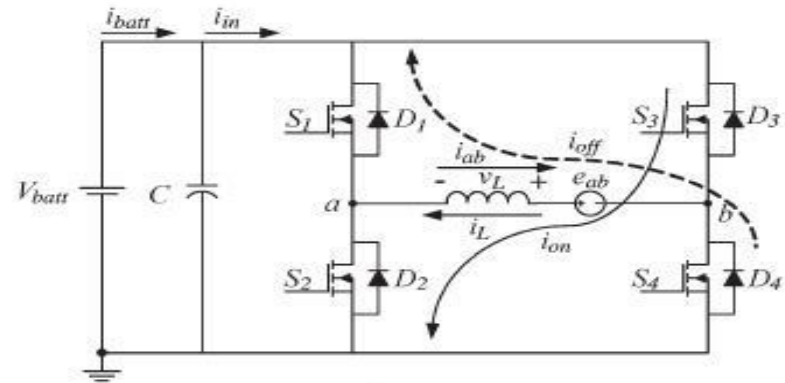
(a)



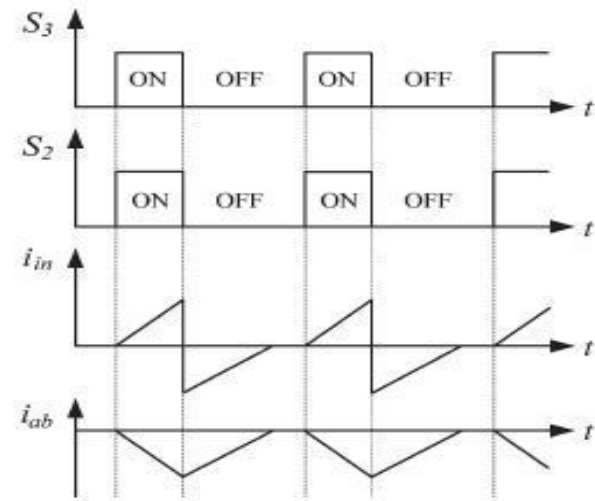
(b)

In Motoring Mode

a.)Equivalent circuit b) wave form of input and phase currents, switching signals



(a)

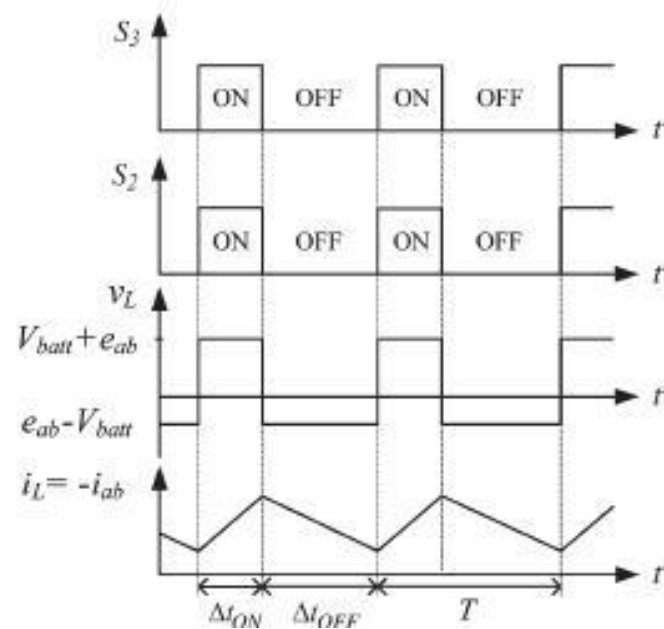
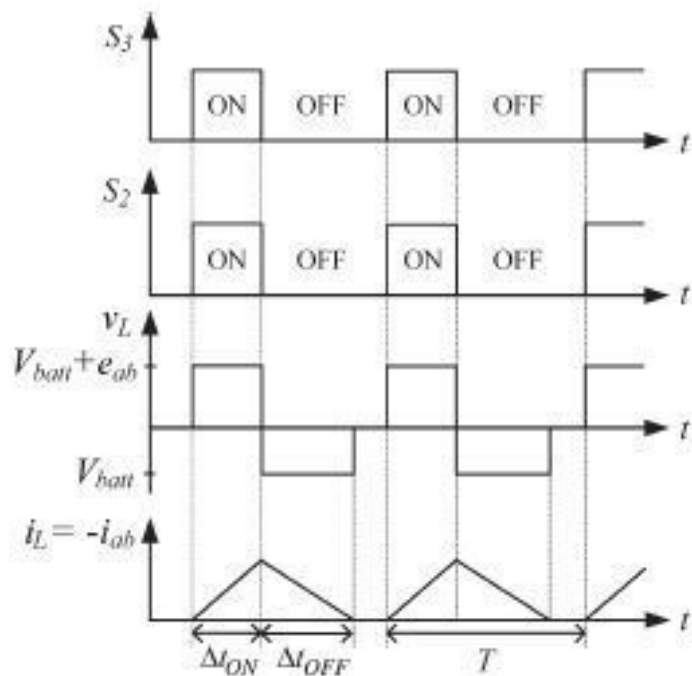


(b)

In Energy regenerative mode

a.)Equivalent circuit b) wave form of input and phase currents, switching signals

Method1 continued...



Waveforms of inductor voltage and current, switching signals of S_2 and S_3 . (a) DCM. (b) CCM

$$\frac{W_r}{W_t} = 1 + \frac{V_{EMF}}{V_{batt}}.$$

$$\frac{W_r}{W_t} = 1 + \frac{2 \times V_{EMF}}{V_{batt} - V_{EMF}}.$$

Analysis in DCM and CCM modes

$$V_L = L_{ab} \times \frac{di_{ab}}{dt} \quad \& \quad L_{ab} \times \frac{\Delta i_L}{\Delta t}$$

Rearranging

$$\Delta i_L = \frac{V_L}{L} \Delta t$$

$$\Delta i_L (\text{on}) = \frac{(V_{bat} + E_{ab})}{L} \quad \text{on}$$

$$\Delta i_L (\text{Off}) = \frac{-V_{bat}}{L} \quad \text{off}$$

Under steady state condition

$$\Delta i_L (\text{on}) + \Delta i_L (\text{Off}) = 0$$

$$\frac{\Delta t_{\text{off}}}{\Delta t_{\text{on}}} = \frac{(V_{bat} + E_{ab})}{V_{bat}} = 1 + \frac{E_{ab}}{V_{bat}}$$

$$\frac{W_r}{W_b} = \frac{\Delta t_{\text{off}}}{\Delta t_{\text{on}}} = 1 + \frac{E_{ab}}{V_{bat}}$$

$$f_s = \left[1 + \frac{2 \times E_{ab}}{\Delta t_{bat} - E_{ab}} \right] * \frac{1}{2 \Delta t_{off}} \quad \text{Continuous conduction mode (CCM)}$$

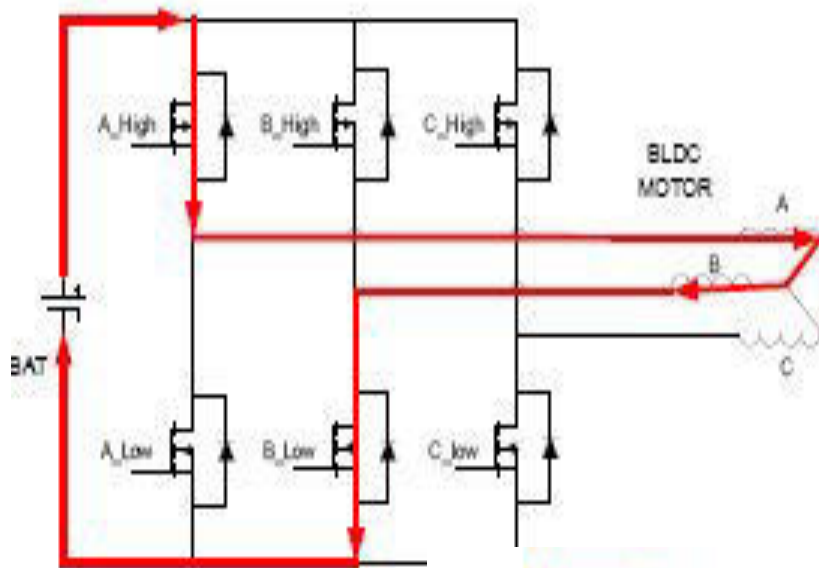
$$f_s = \left(1 + \frac{E_{ab}}{\Delta t_{bat}} \right) * \frac{1}{2 \Delta t_{off}} \quad \text{Discontinuous conduction mode (DCM)}$$

In both DCM and CCM modes time duration of energy regeneration (Δt_{off}) is dependent on the switching frequency and back-EMF. By assuming the switching frequency to be constant, the time for energy regeneration is directly proportional to back-EMF.

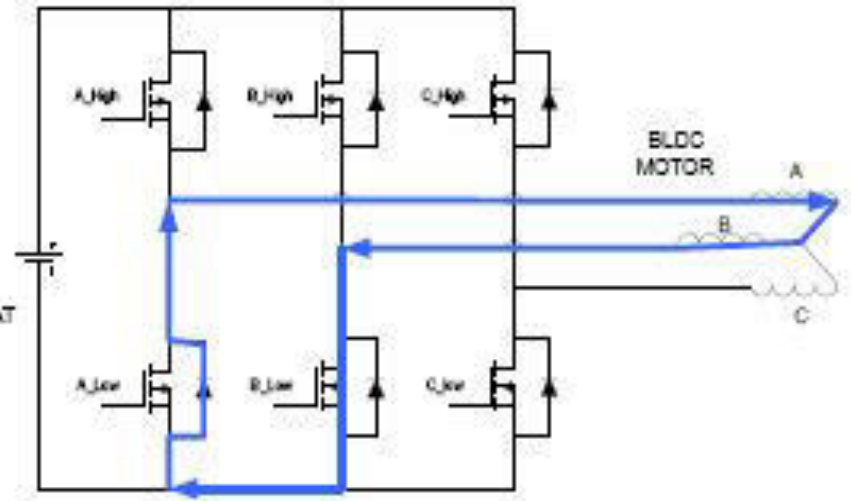
Regenerative braking switching sequence Method 1

Motoring mode				Regenerative mode		
Degrees	Phases conducting	Switches conducting	Hall decoding	Phases conducting	Switches conducting	Hall decoding
60	AB	Q1Q2	Ha hb-	BA	Q4Q5	Ha hb-
120	AC	Q2Q3	Ha hc-	CA	Q5Q6	Ha hc-
180	BC	Q3Q4	Hb hc-	CB	Q6Q1	Hb hc-
240	BA	Q4Q5	Hb ha-	AB	Q1Q2	Hb ha-
300	CA	Q5Q6	Hc ha-	AC	Q2Q3	Hc ha-
360	CB	Q6Q1	Hc hb-	BC	Q3Q4	Hc hb-

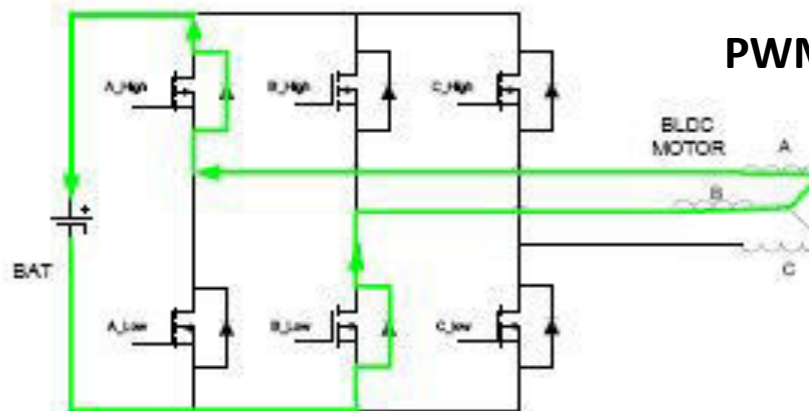
Regenerative braking in PM BLDC motor(Method2)



Motoring mode Mode



PWM -ON Mode

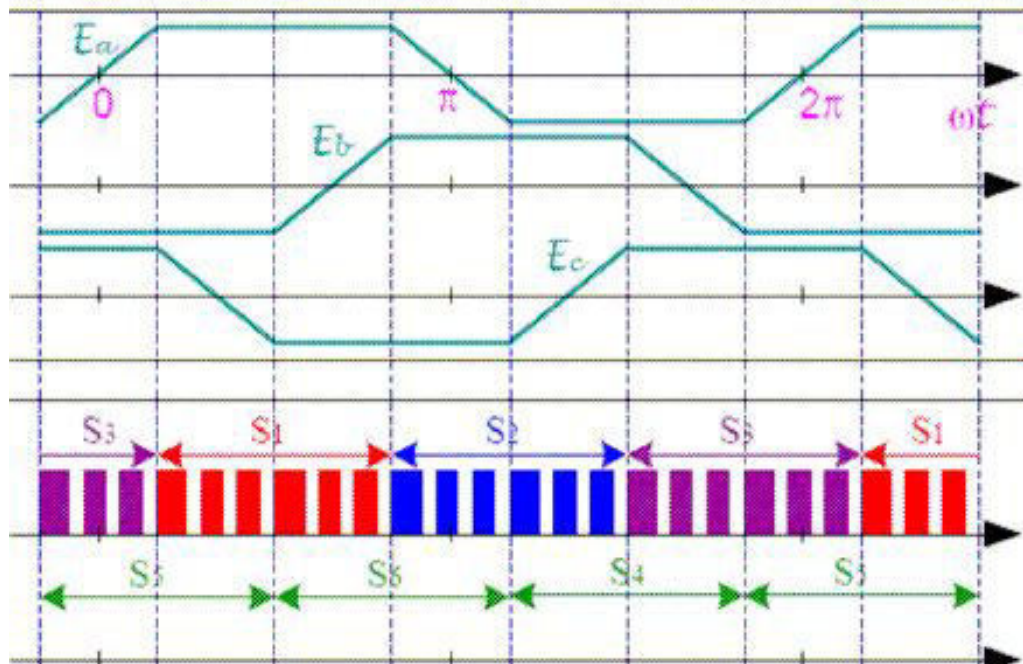


PWM - Off Mode

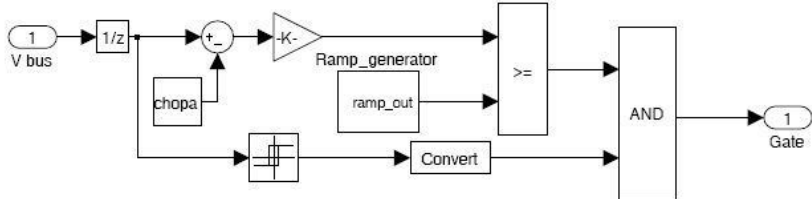
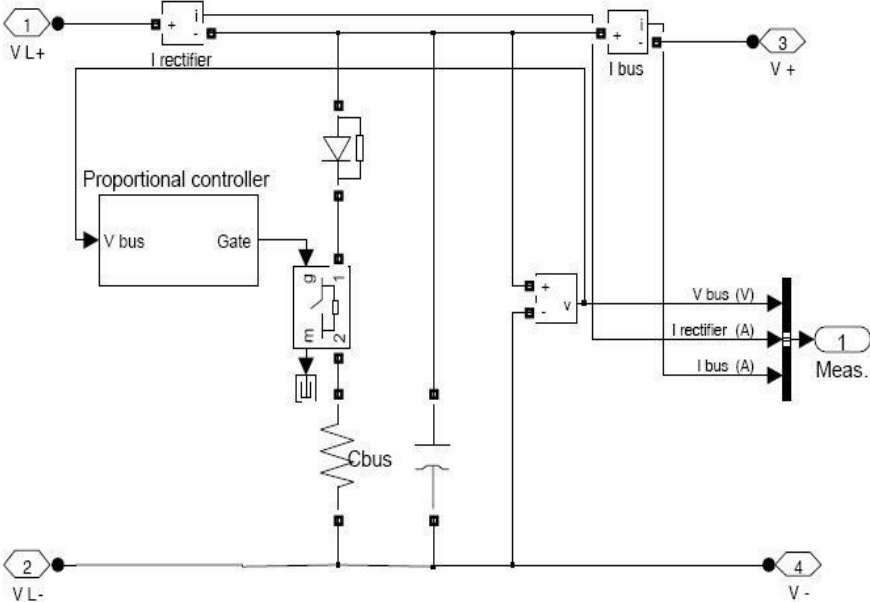
Switching logic in Method 2

Forward/Clockwise Regenerative Inverter Operation			
Step	PWM Switch	ON Switch	OFF Switch
1	A_Low	NIL	Remaining
2	C_Low	NIL	Remaining
3	C_Low	NIL	Remaining
4	B_Low	NIL	Remaining
5	B_Low	NIL	Remaining
6	A_Low	NIL	Remaining

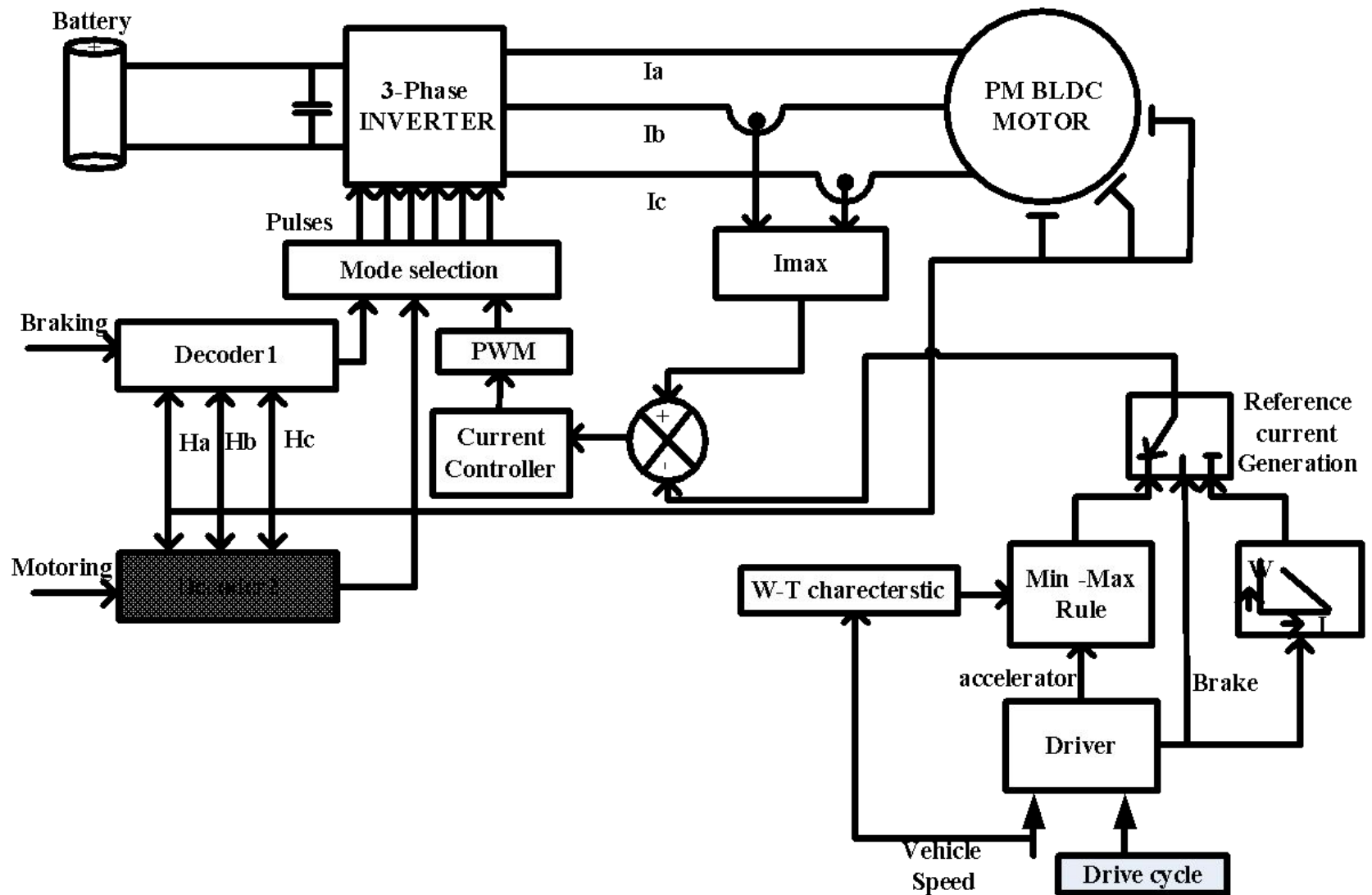
Reverse/Anticlockwise Regenerative Inverter Operation			
Step	PWM Switch	ON Switch	OFF Switch
1	B_Low	NIL	Remaining
2	C_Low	NIL	Remaining
3	C_Low	NIL	Remaining
4	A_Low	NIL	Remaining
5	A_Low	NIL	Remaining
6	B_Low	NIL	Remaining



Rheostatic braking



Electric two-wheeler schematic



Schematic of electric two-wheeler with regenerative braking and mechanical braking

Main components in Electric two-wheeler

The schematic shown represents electric two-wheeler with regenerative braking and motoring modes. Following are the main sections of the simulation model,

(a) Driver model

(b) Reference current generation

(c) Mode selection

(d) Battery

(e) PM BLDC hub Motor

(f) Current Controller

(g) Vehicle load modeling

System Parameters

Vehicle parameters

Rolling friction = $C_{roll} = 0.018$

Aero dynamic drag co-efficient = $C_d = 0.92$

A_f = frontal area of the vehicle = 0.6 m^2

V_w = wind velocity = 0 m/s

Gross vehicle weight = 175 kg

Gradient = 0°

Maximum vehicle Speed = 25 kmph.

Battery Parameters

Battery voltage = 48V

Battery internal resistance = 0.056 ohms

Initial state of charge (SOC) = 80%

PM BLDC hub motor Parameters

Number of poles = 46

Stator phase resistance = 0.18 ohms

Maximum peak current = 50 A

Study state current = 5A

Power rating = 350 W

Driver model

Driver model is a simple PI – controller

$K_P = 5$

$K_i = 1.1$

Current controller

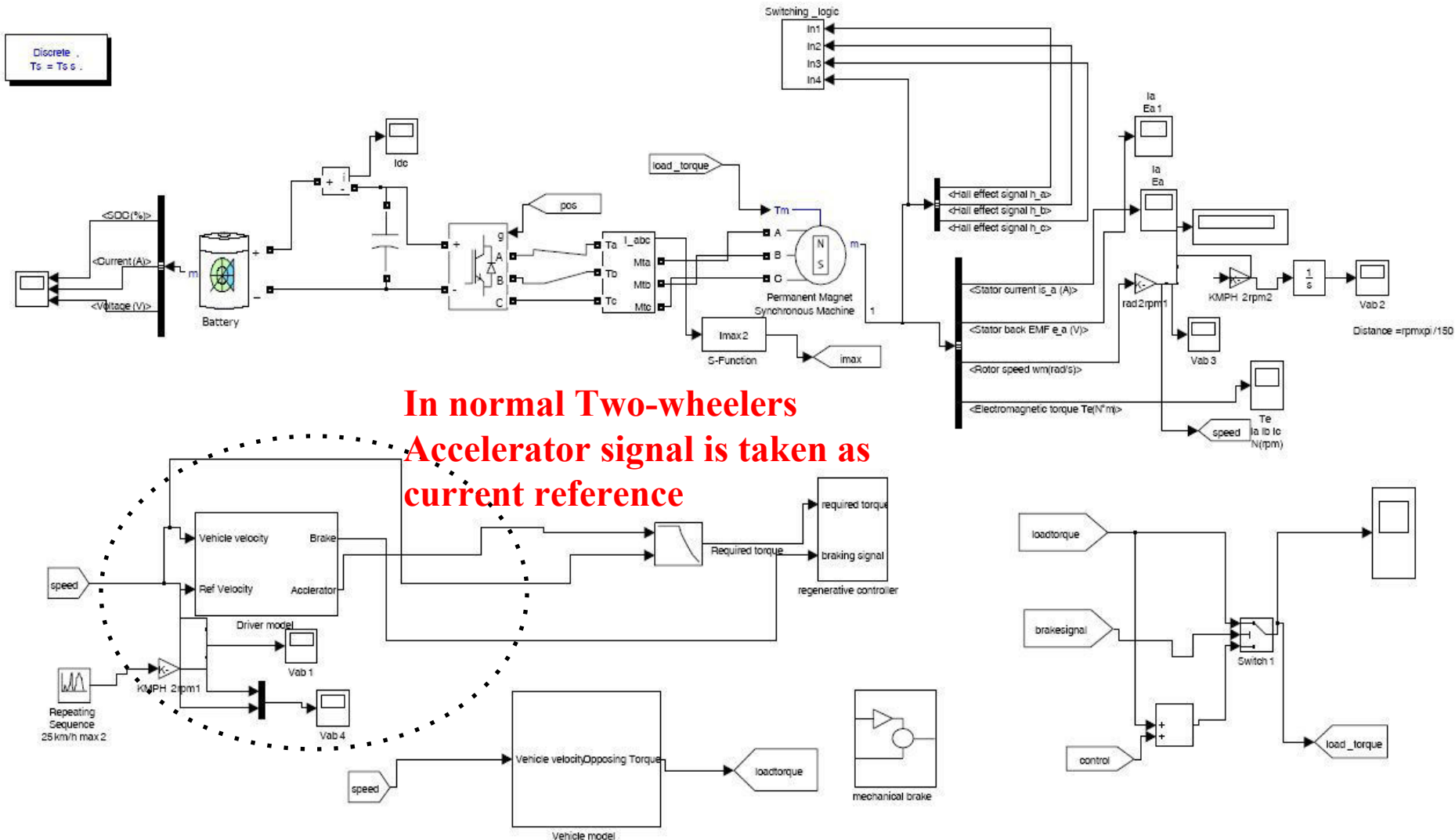
Current controller is a simple PI – controller

$K_P = 0.1$

$K_i = 0.1$

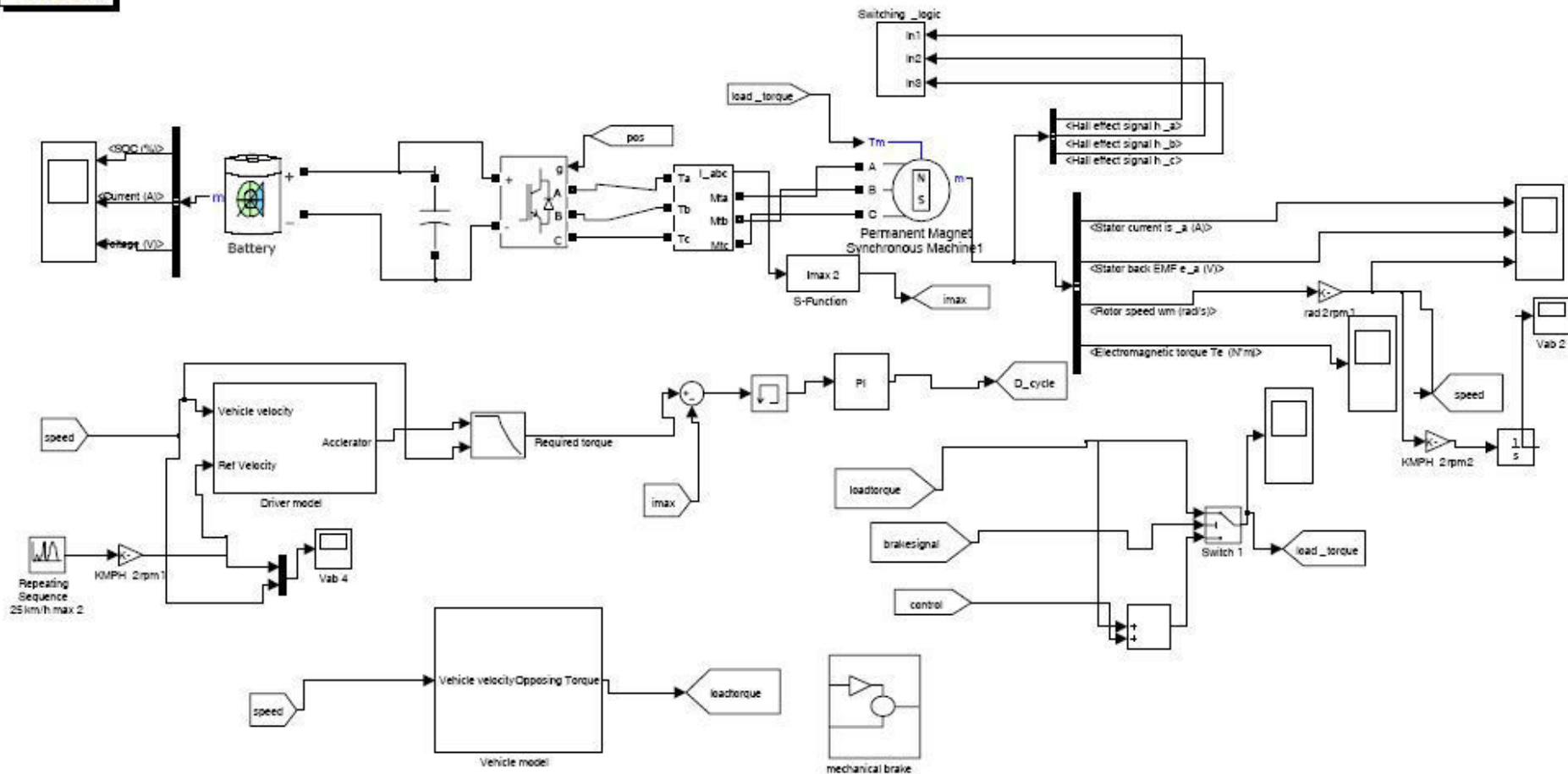
Simulation Model

Electric Two-wheeler Simulation Model With Regenerative Braking and Mechanical braking

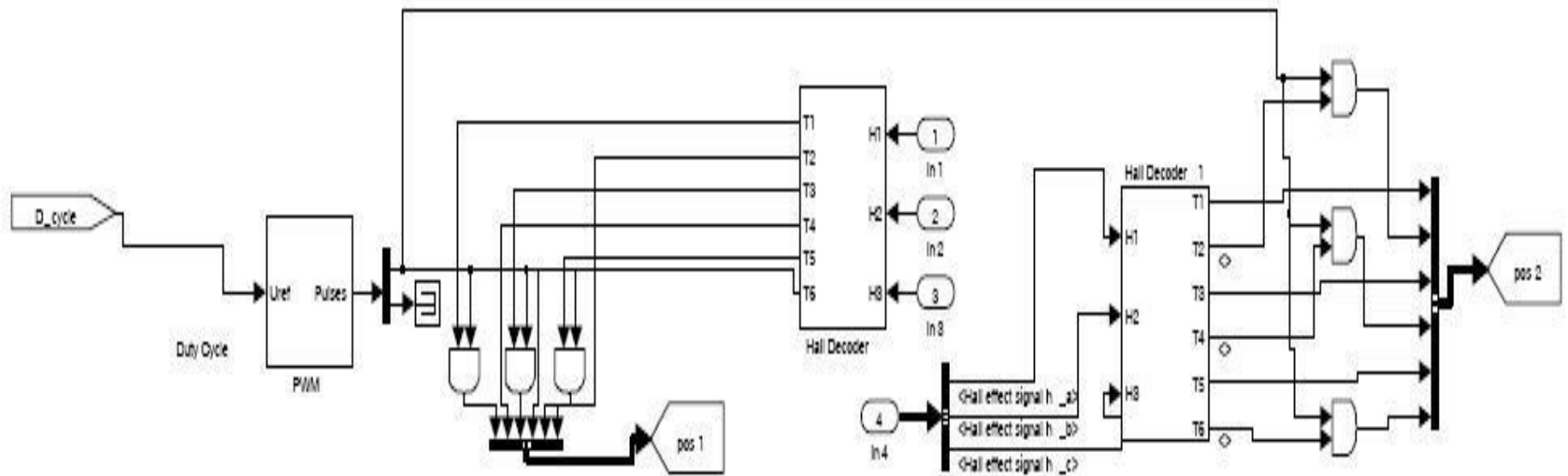


Electric Two-wheeler Simulation Model With Mechanical Braking

Discrete,
Ts = 1e-005 s.

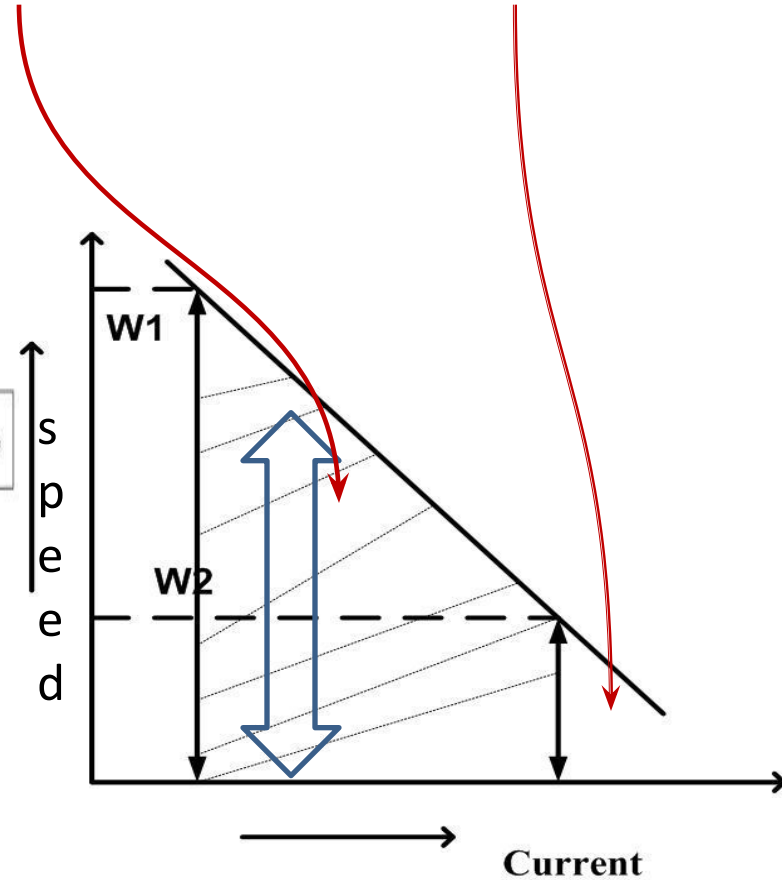
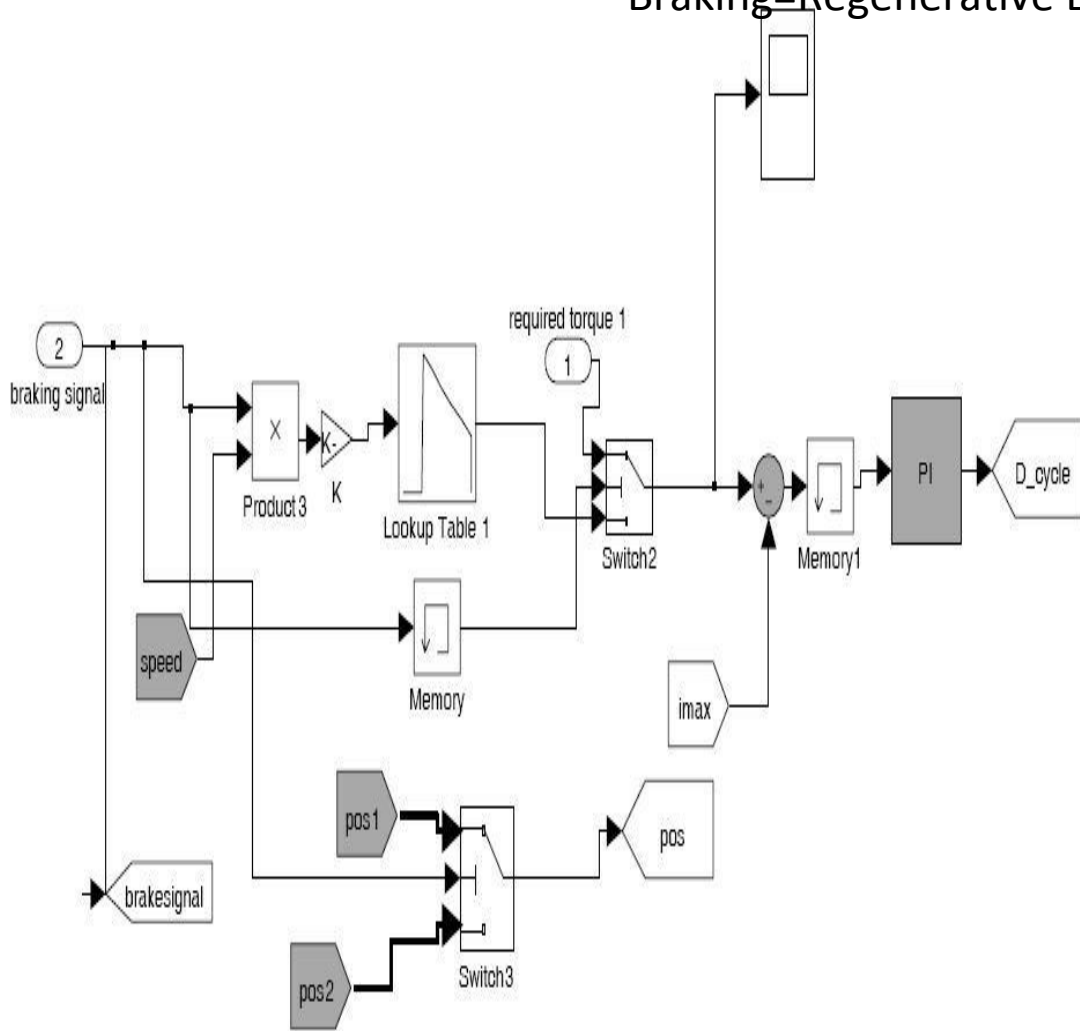


Pulse Generation Using Halls

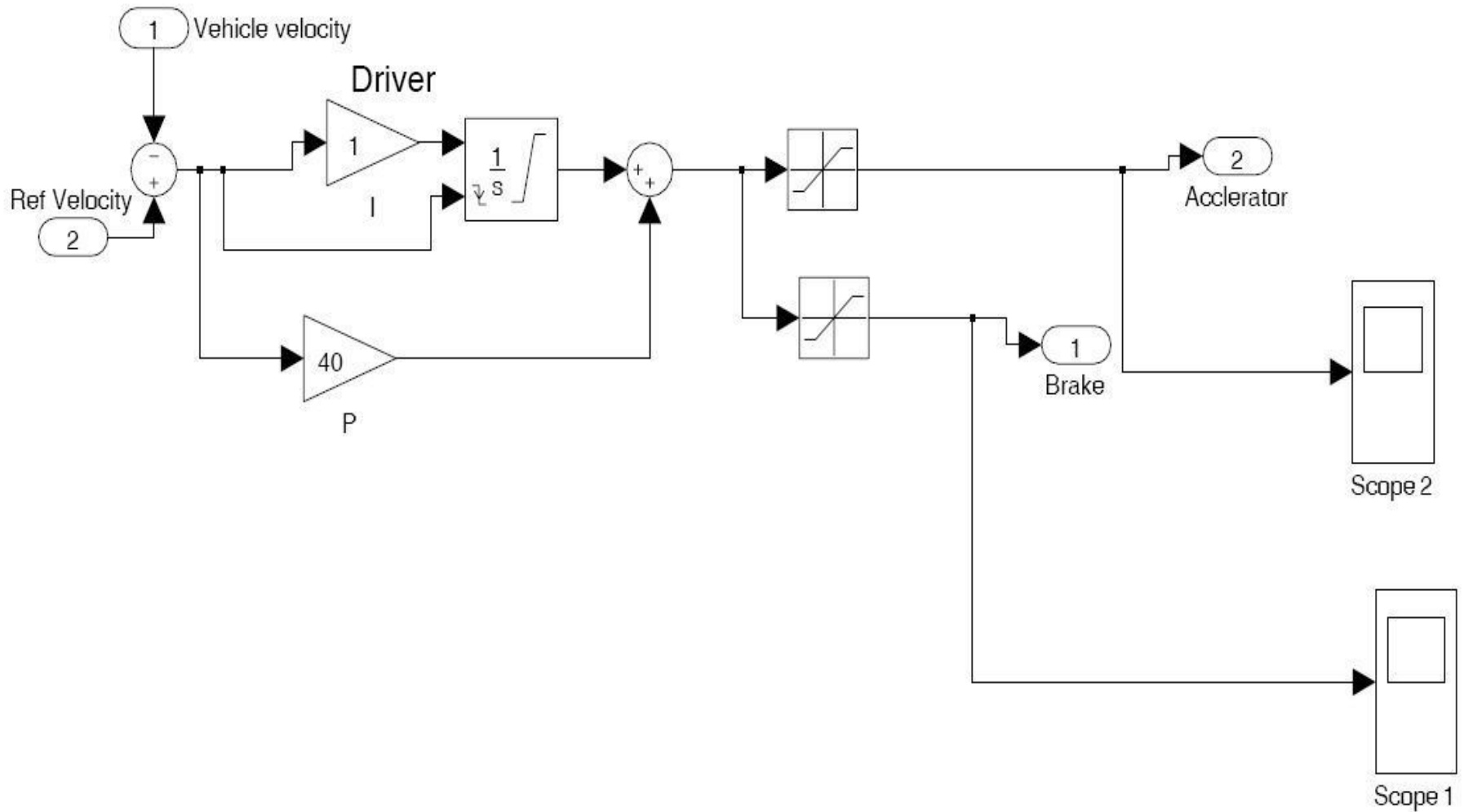


Regenerative Braking Block

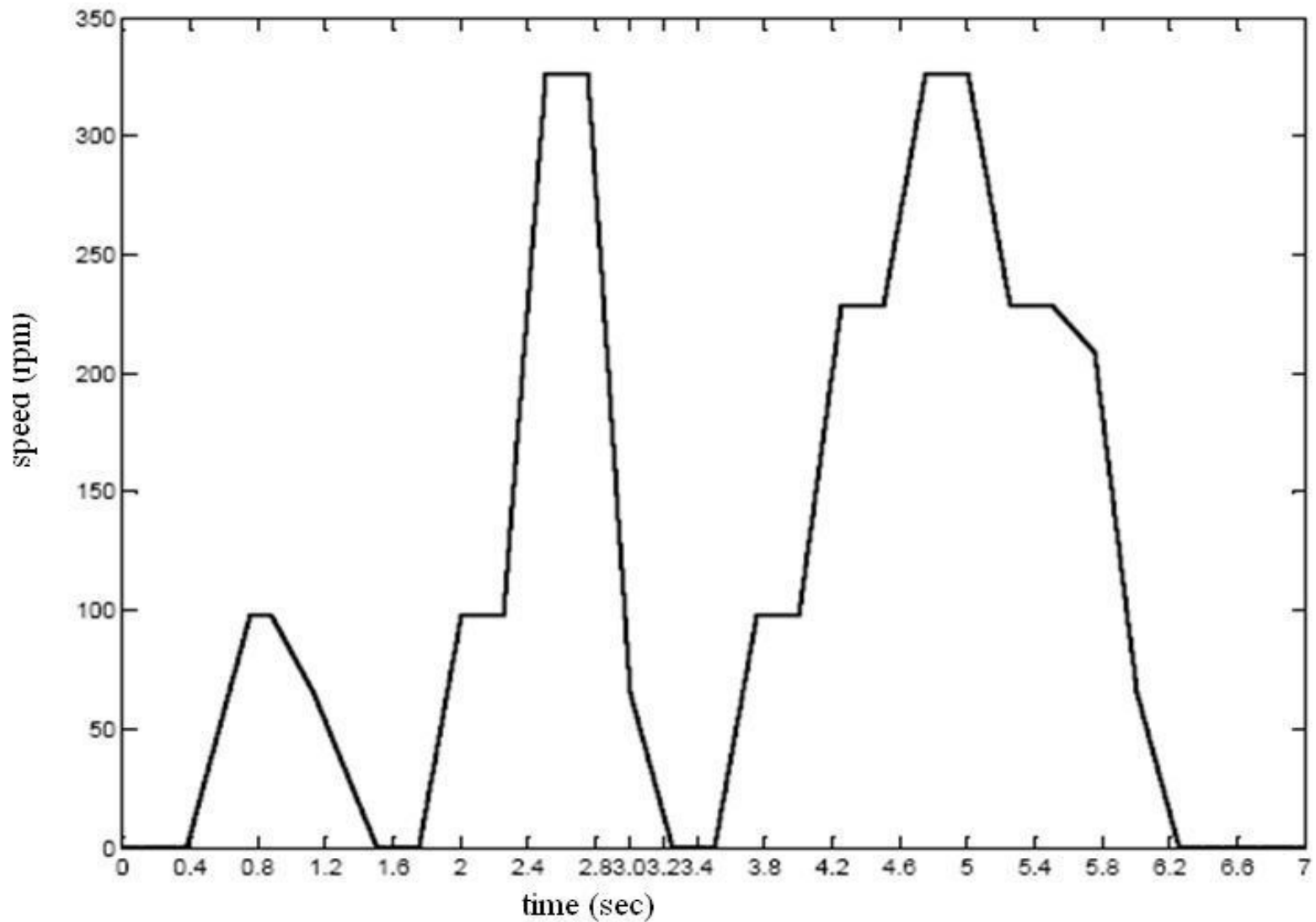
Braking=Regenerative Braking+ Mechanical braking



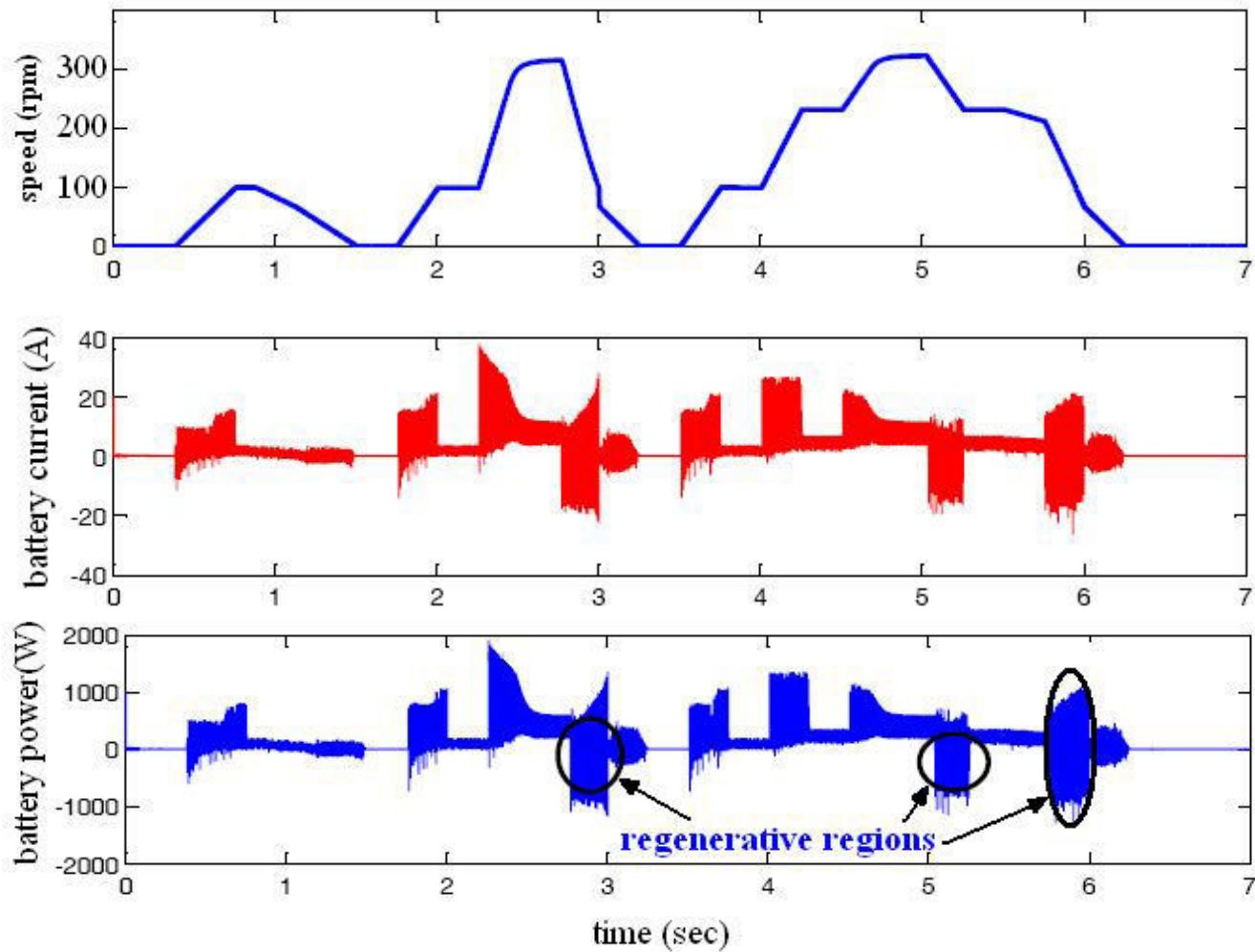
Driver Block



Simulation results

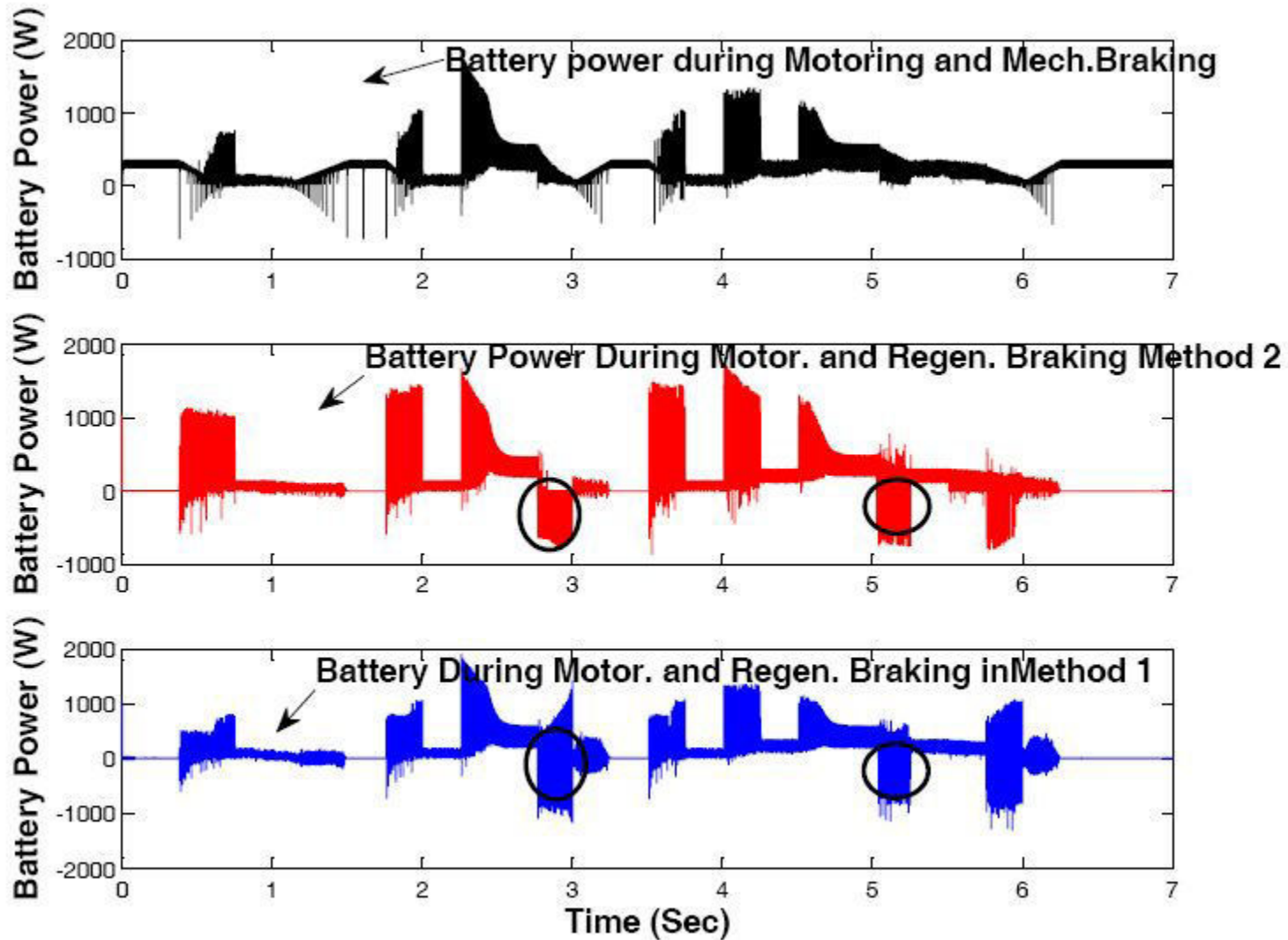


**Drive cycle with maximum vehicle
speed of 25 kmph (corresponding motor speed 330 rpm)**

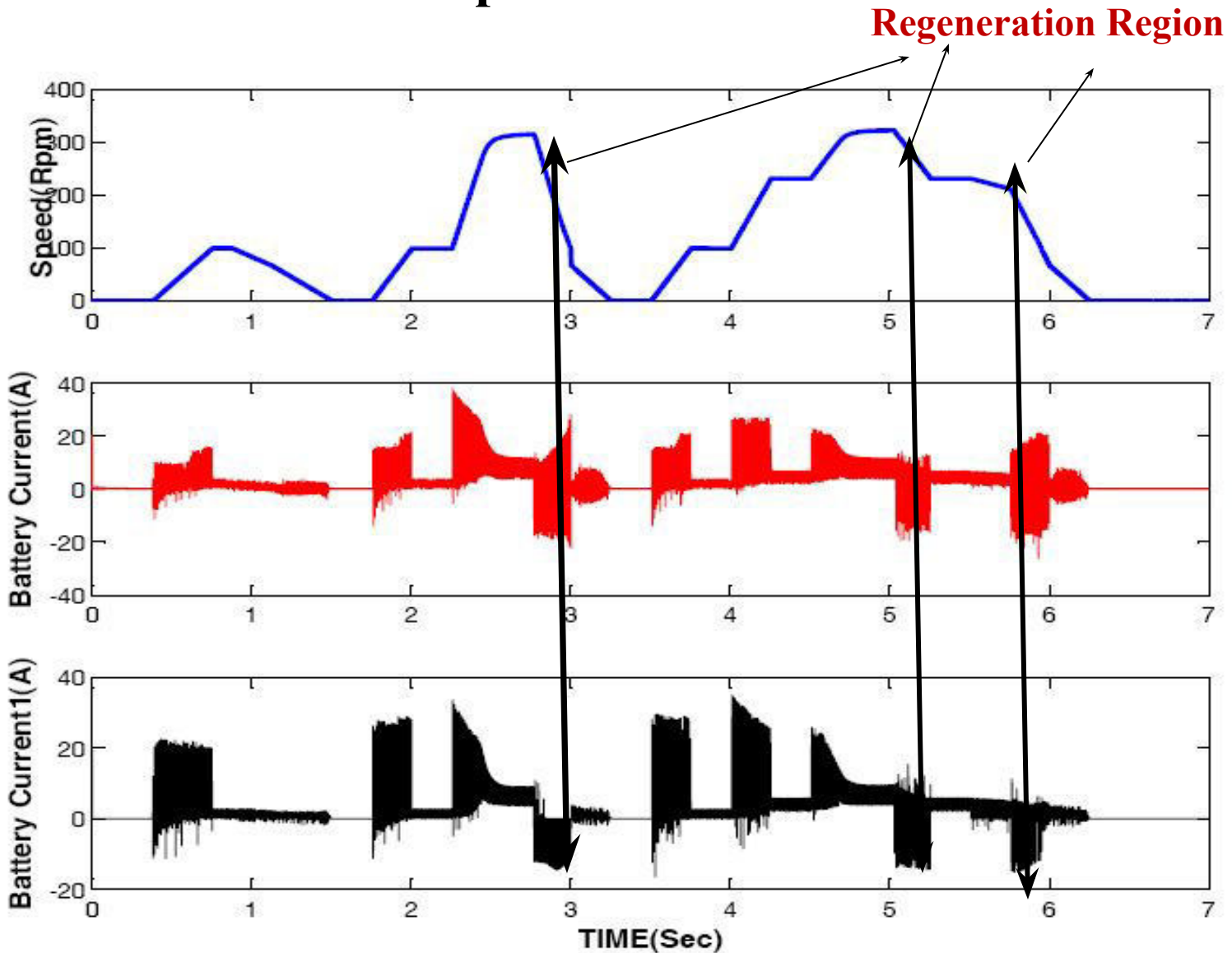


Battery power and current during combination of regenerative braking and mechanical braking

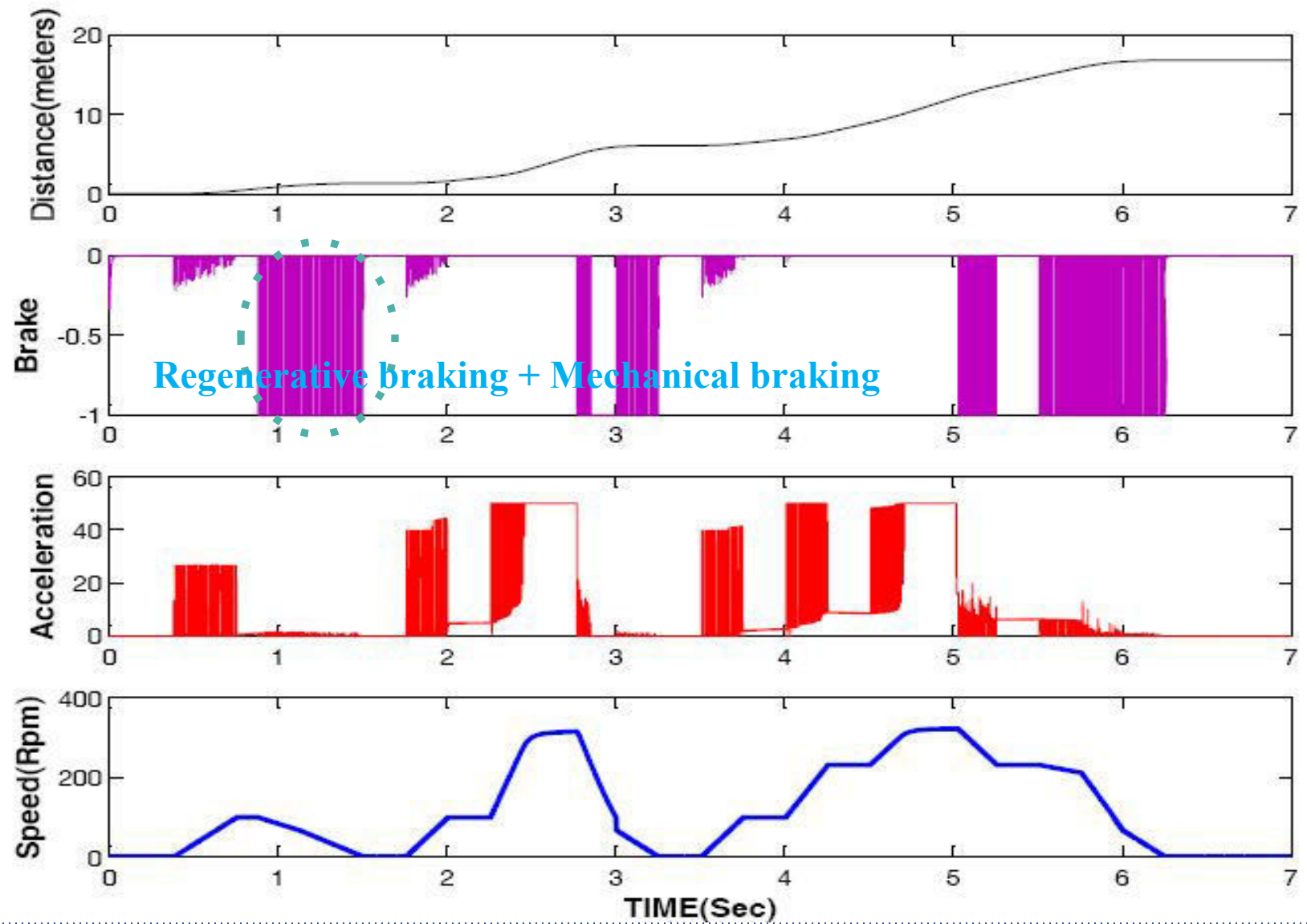
Powers comparison



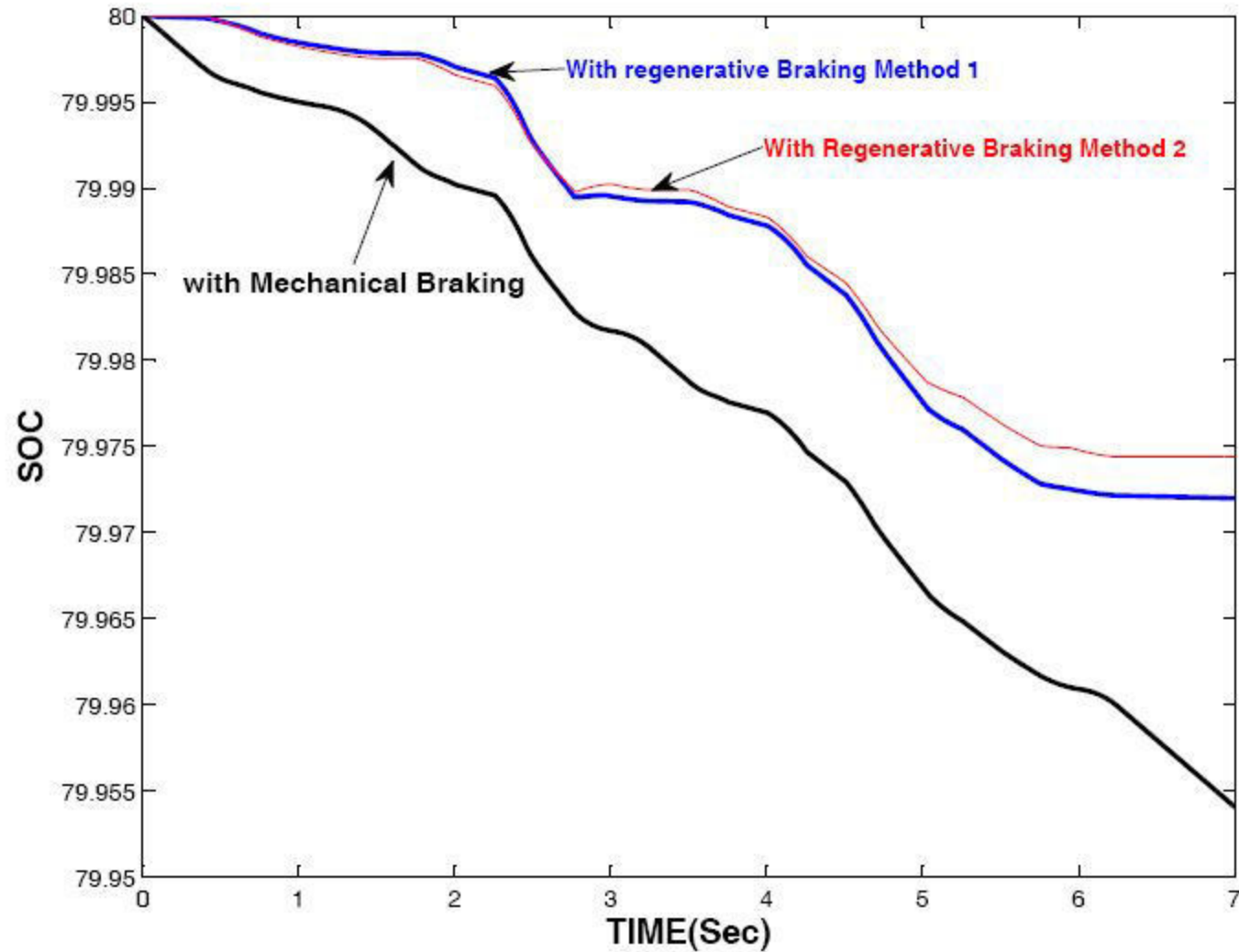
Powers Comparison in Two Methods



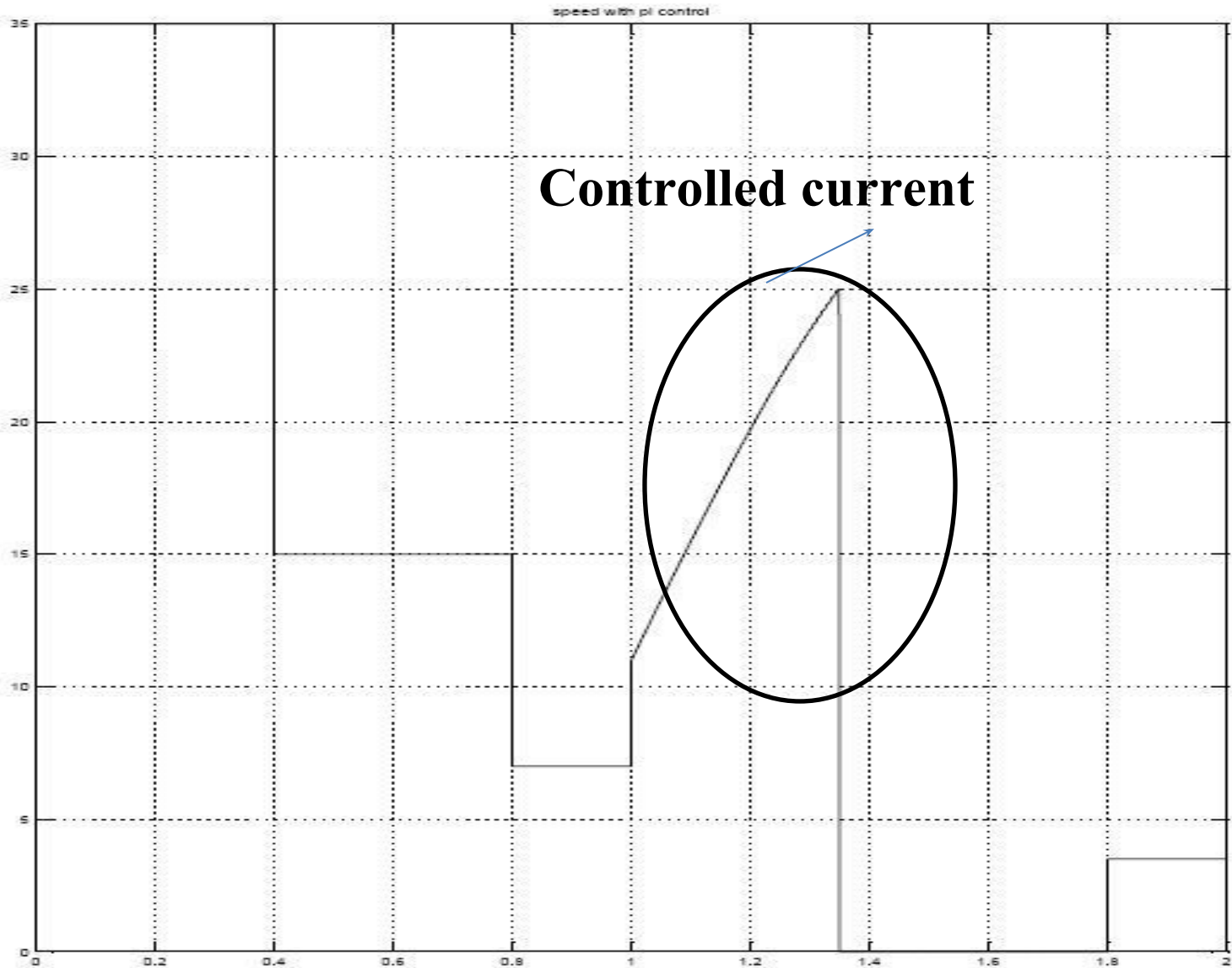
Accelerator and Brake Performance



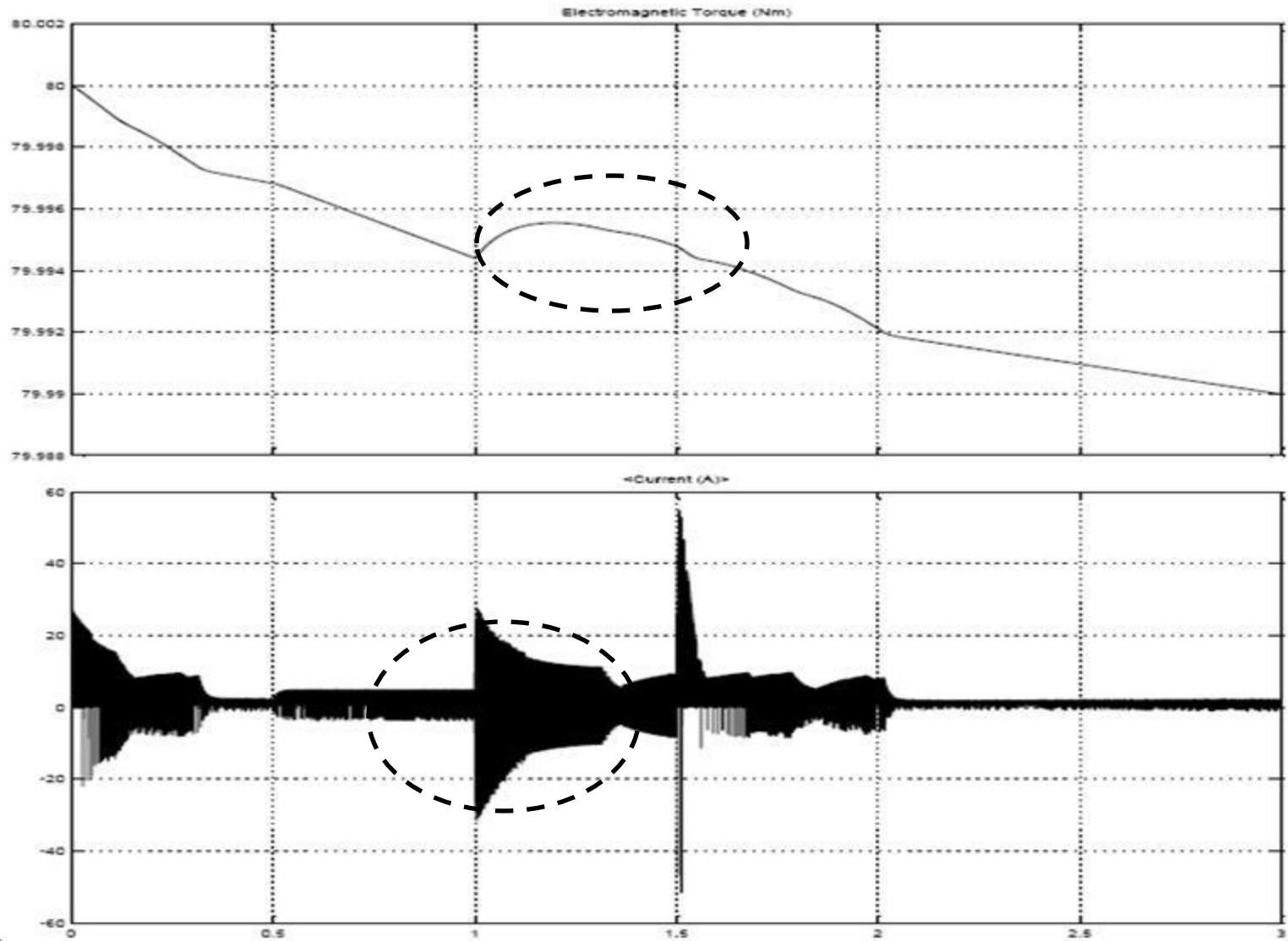
Soc Comparison

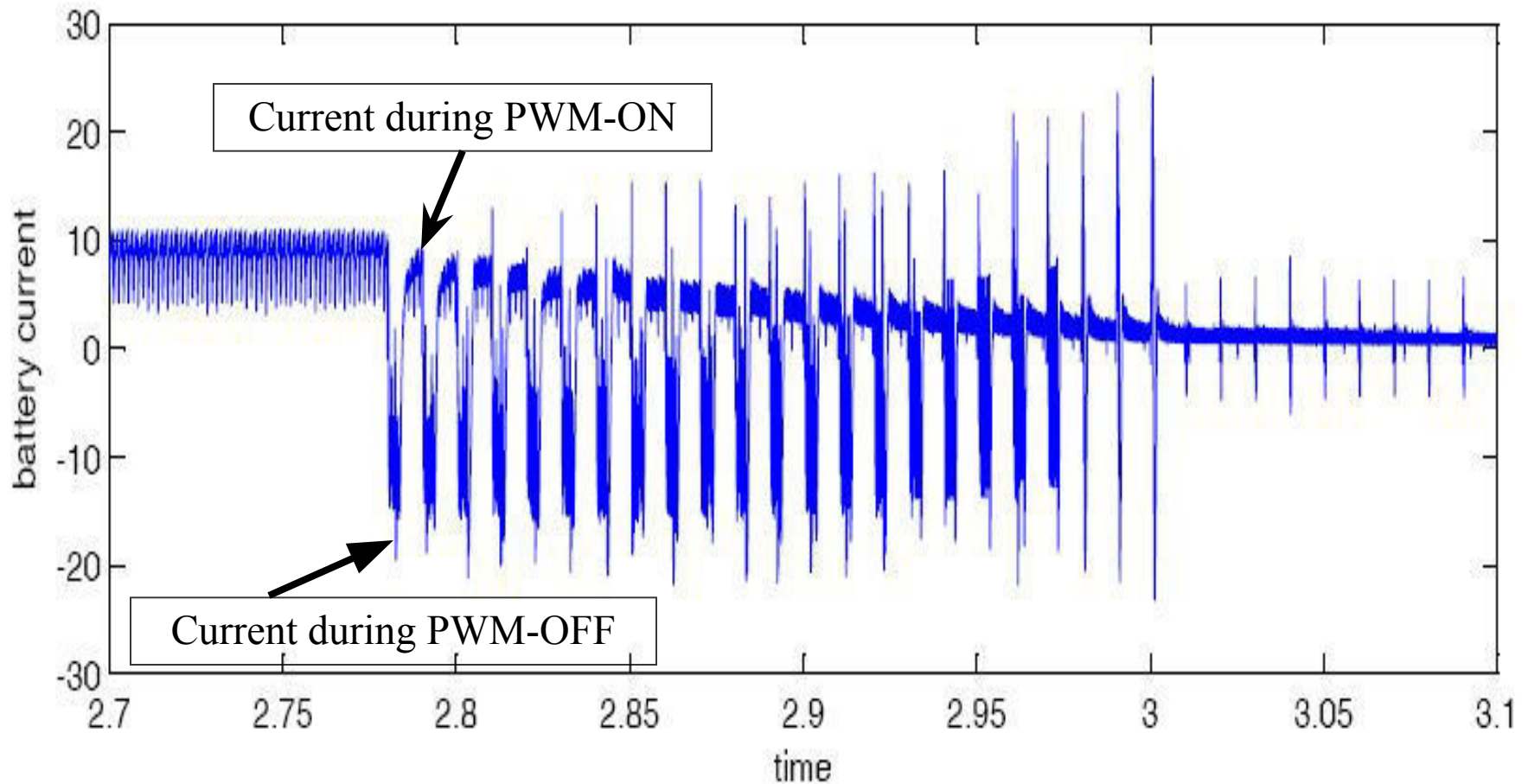


Reference current generation in RegenerativeBraking



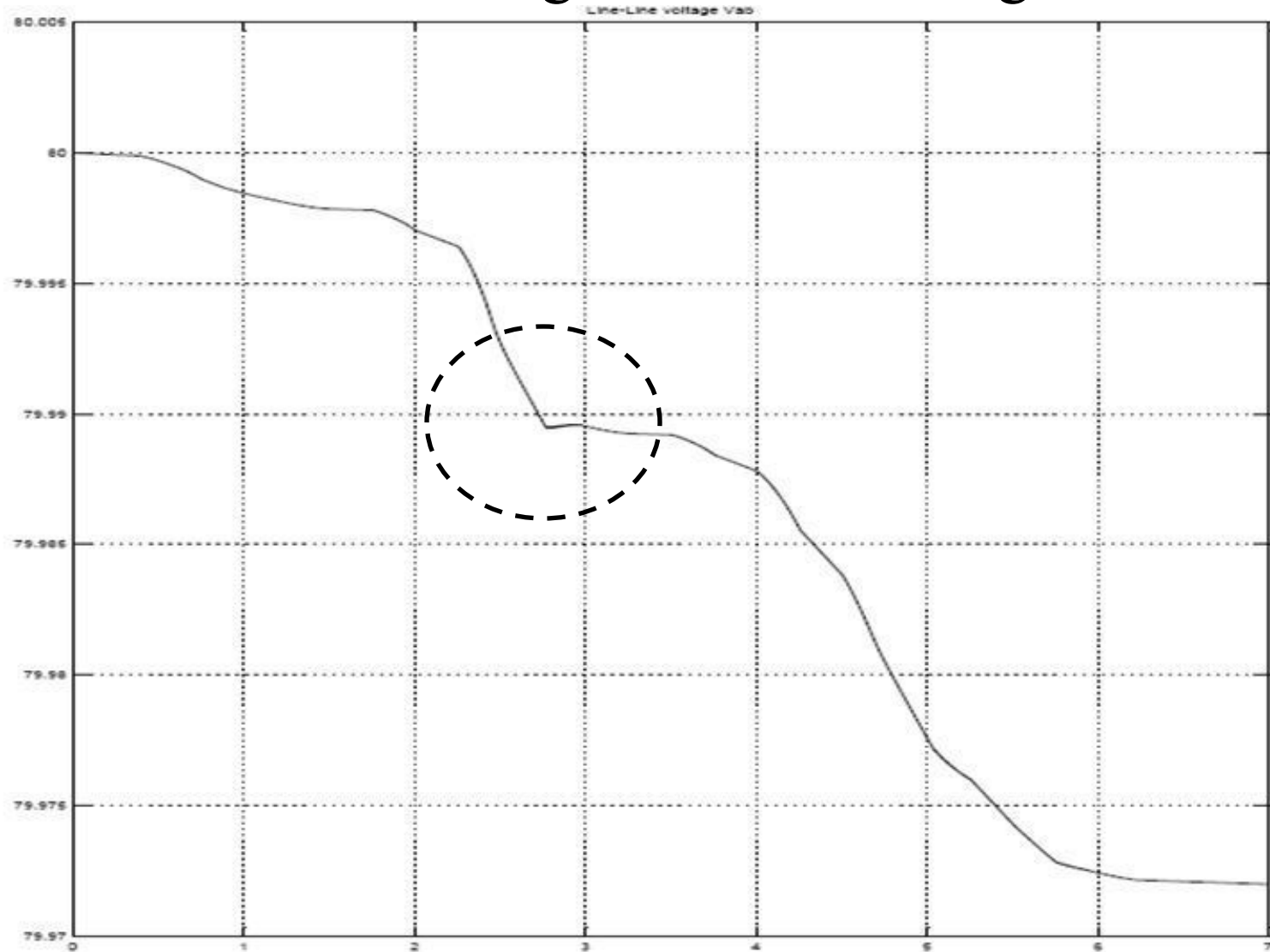
Soc and Power In Method 1



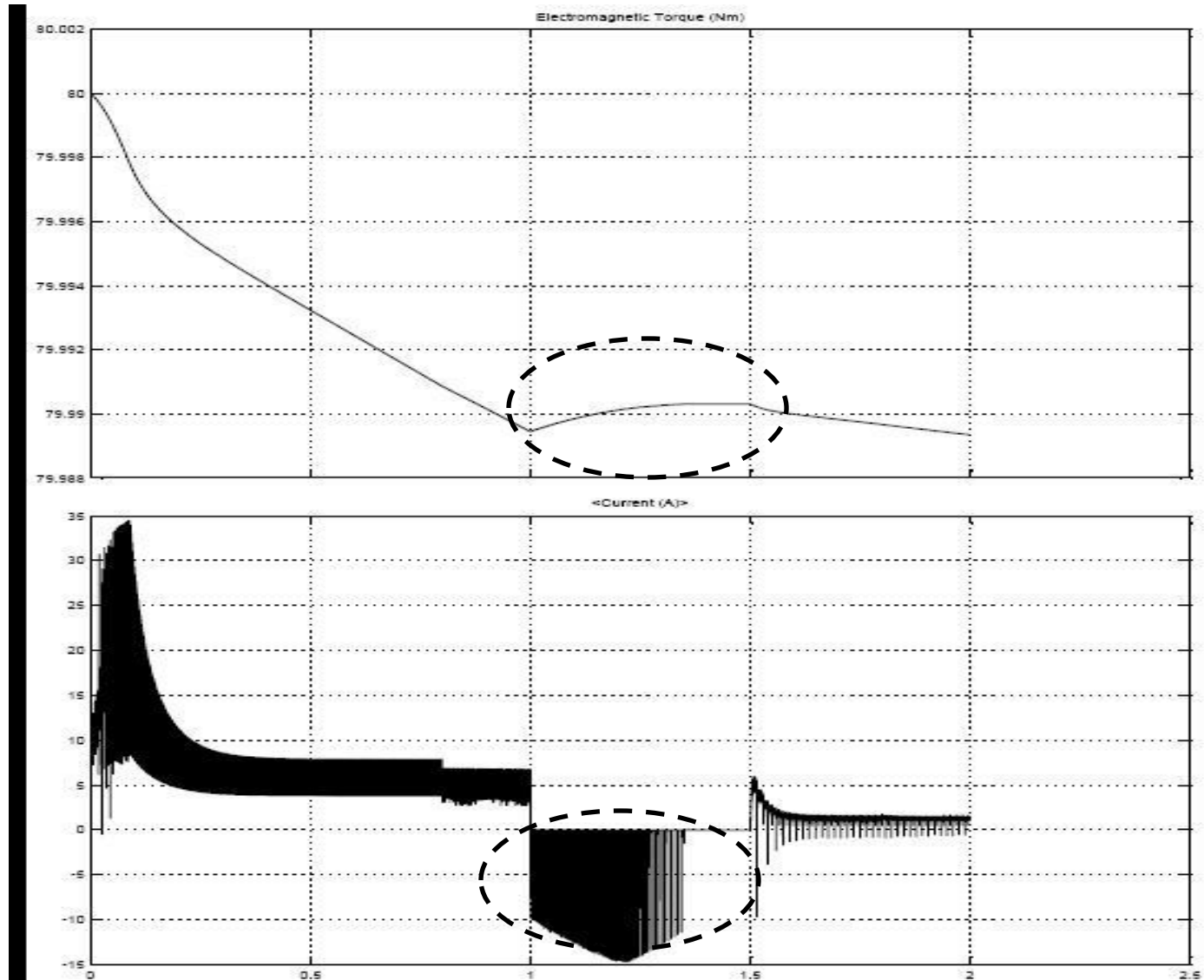


Battery current during regenerative braking

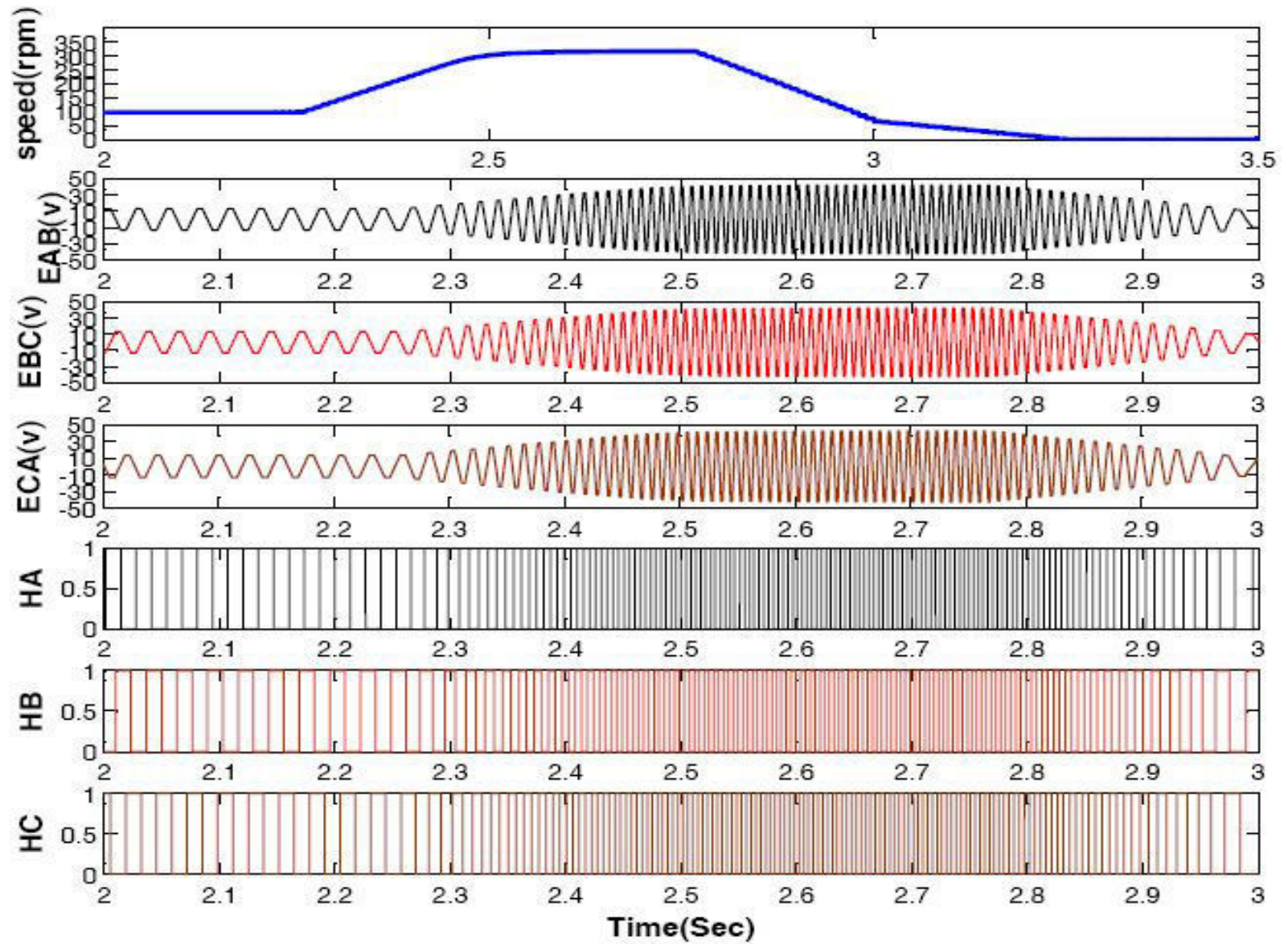
SOC In Regenerative Braking



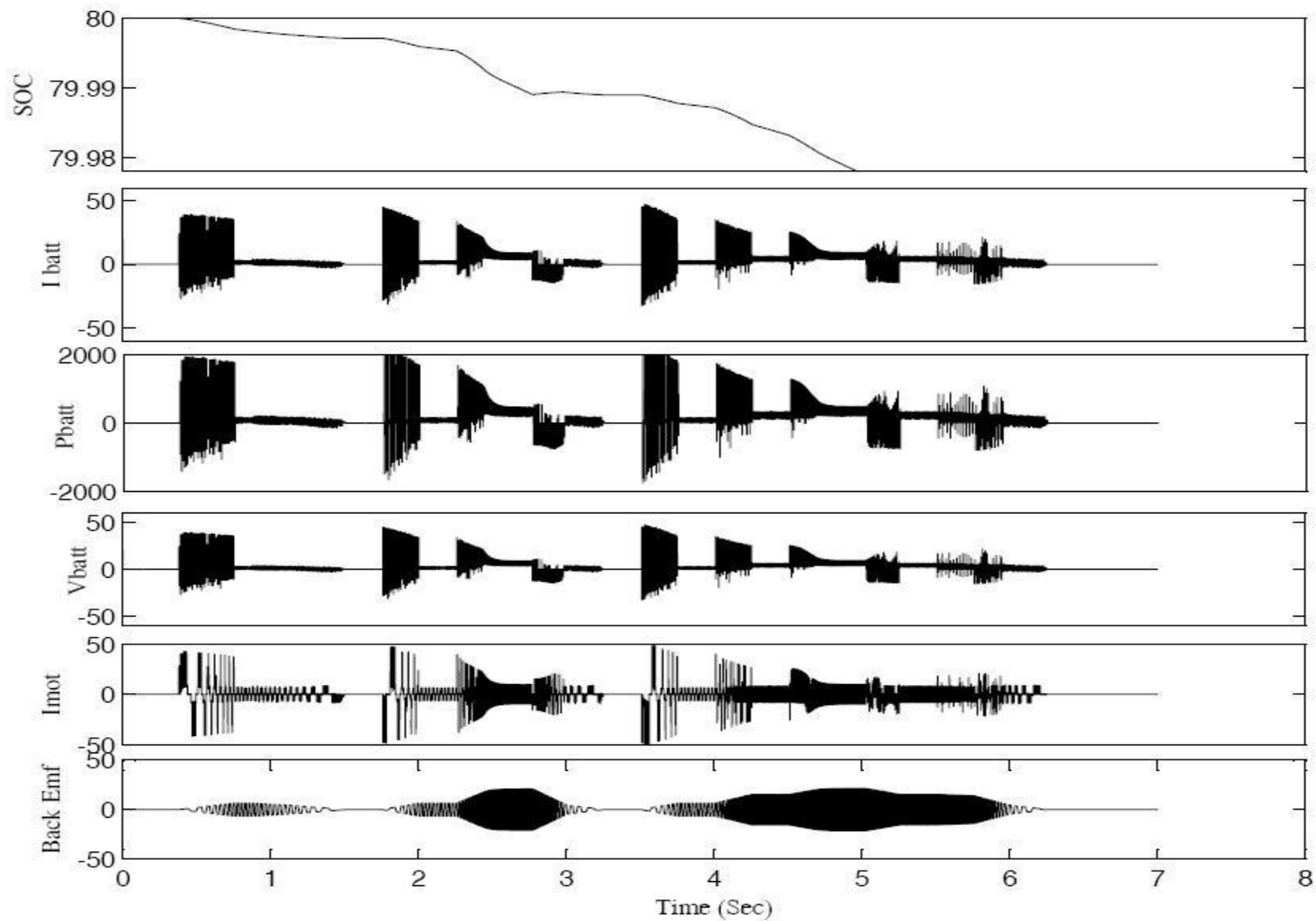
SOC and Power In Method2



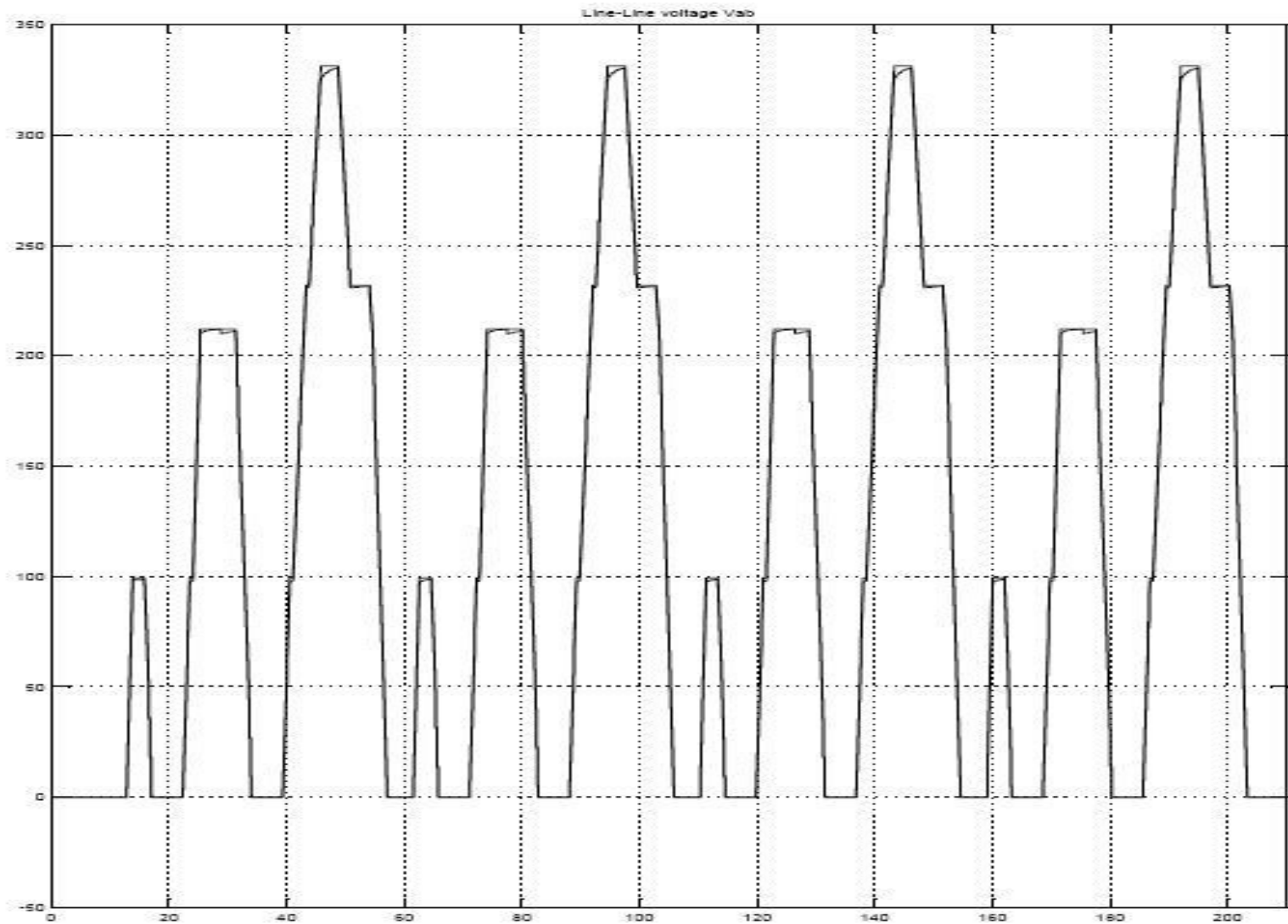
Halls and Back - EMF



Motor Current and Back-EMF In Method 2



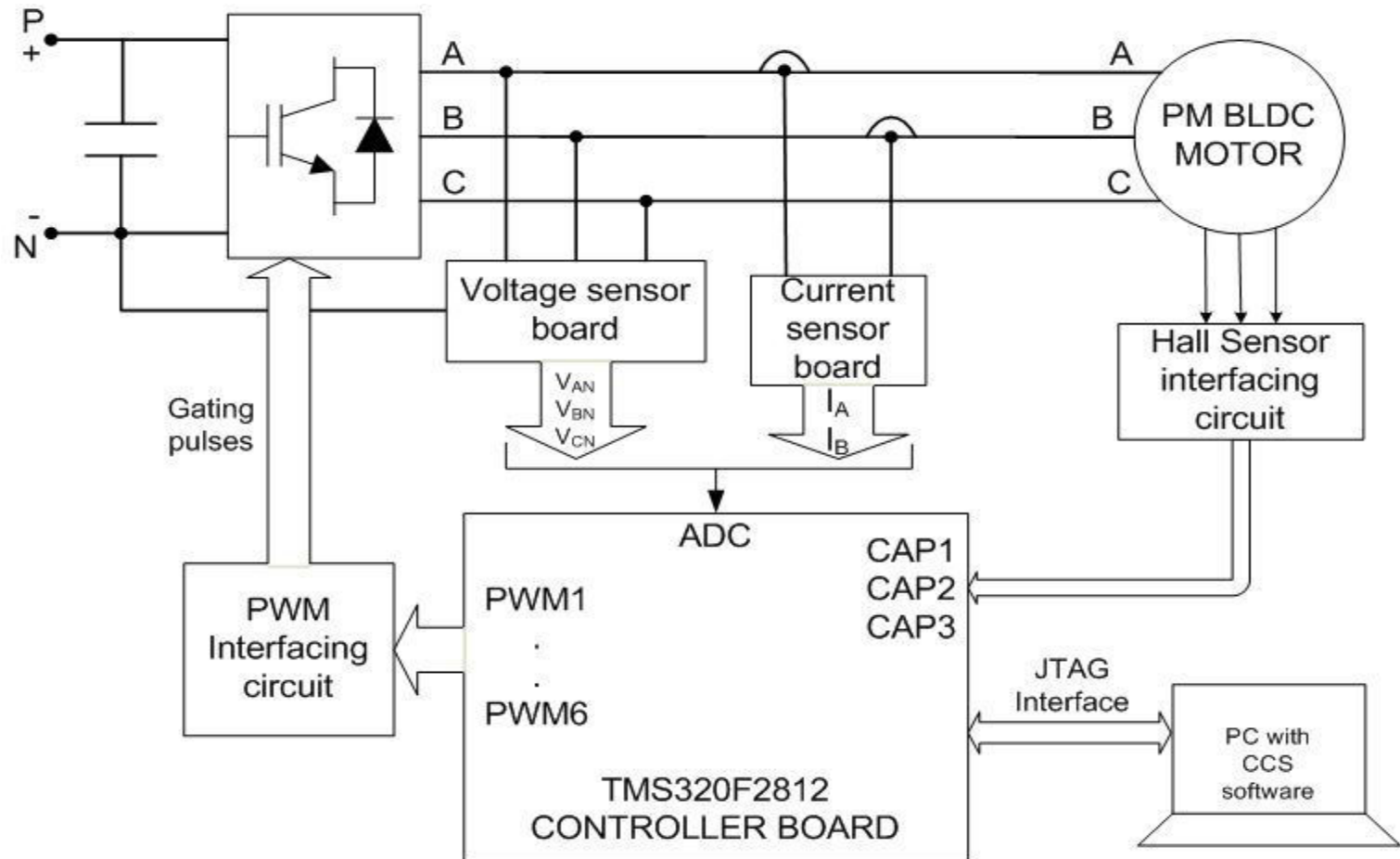
Drive cycle Performance



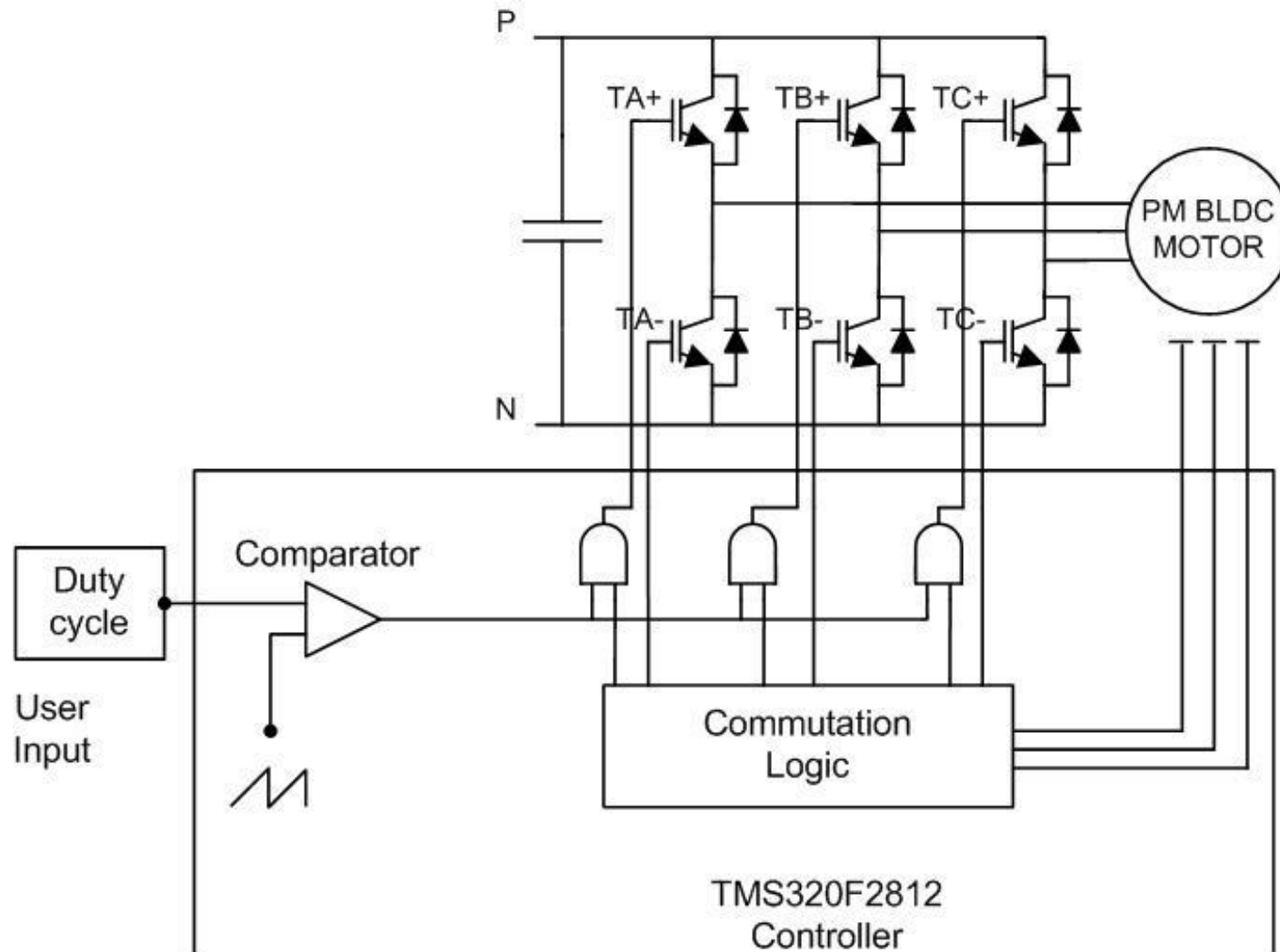
conclusion

- ❖ The line back-EMF based regeneration method presented in this paper delivers far better performance than the mechanical braking in two-wheeler EVs also. Further, the presented method is the simplest one among the known regenerative methods in terms of the simplicity of the system, ease of implementation and also the higher braking torque developed.
- ❖ In this method, a noticeable power is fed back to the battery. The range of the EV is obviously increased.

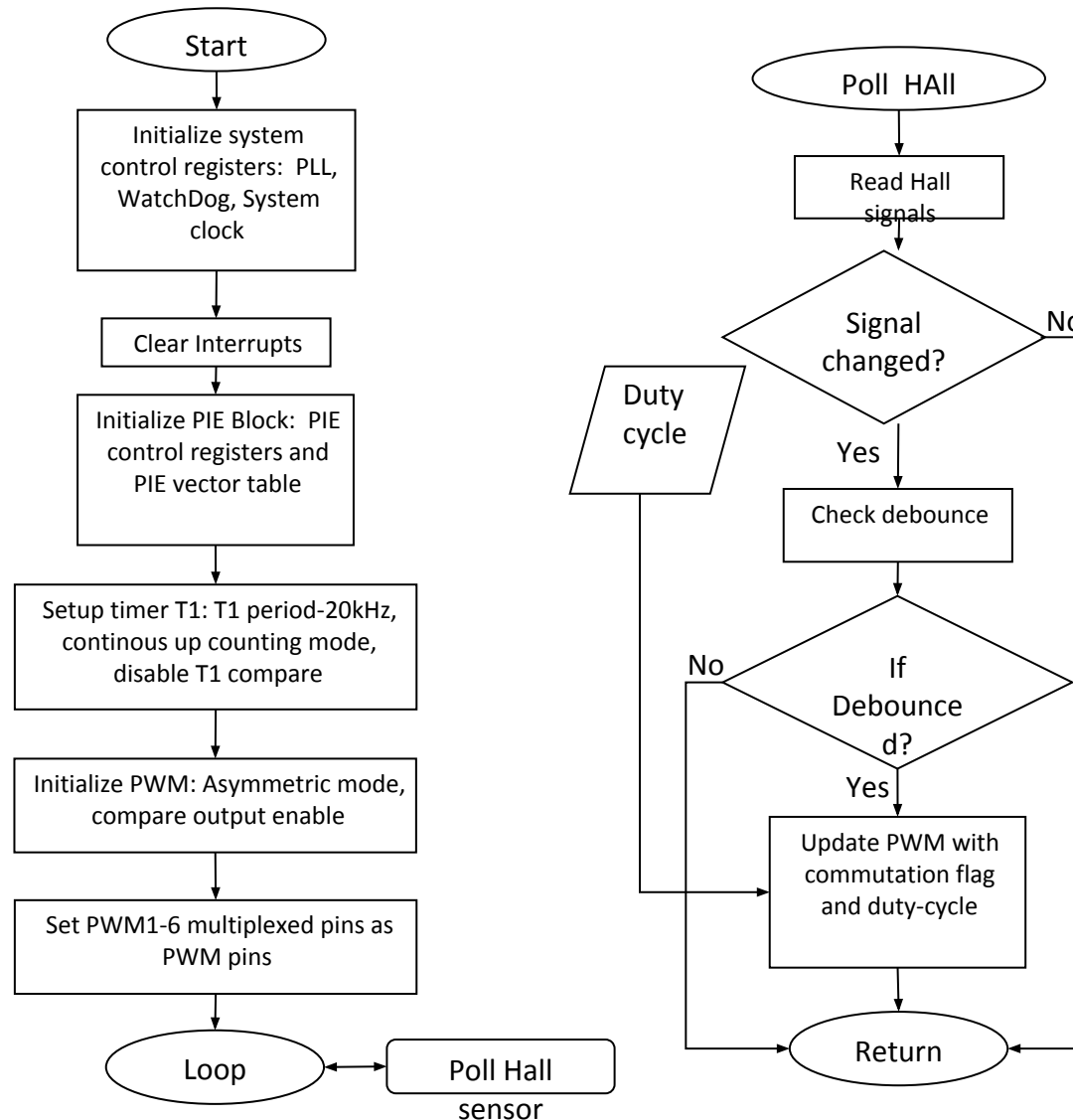
Hardware Implementation



Electric Two-Wheeler in Open-Loop mode



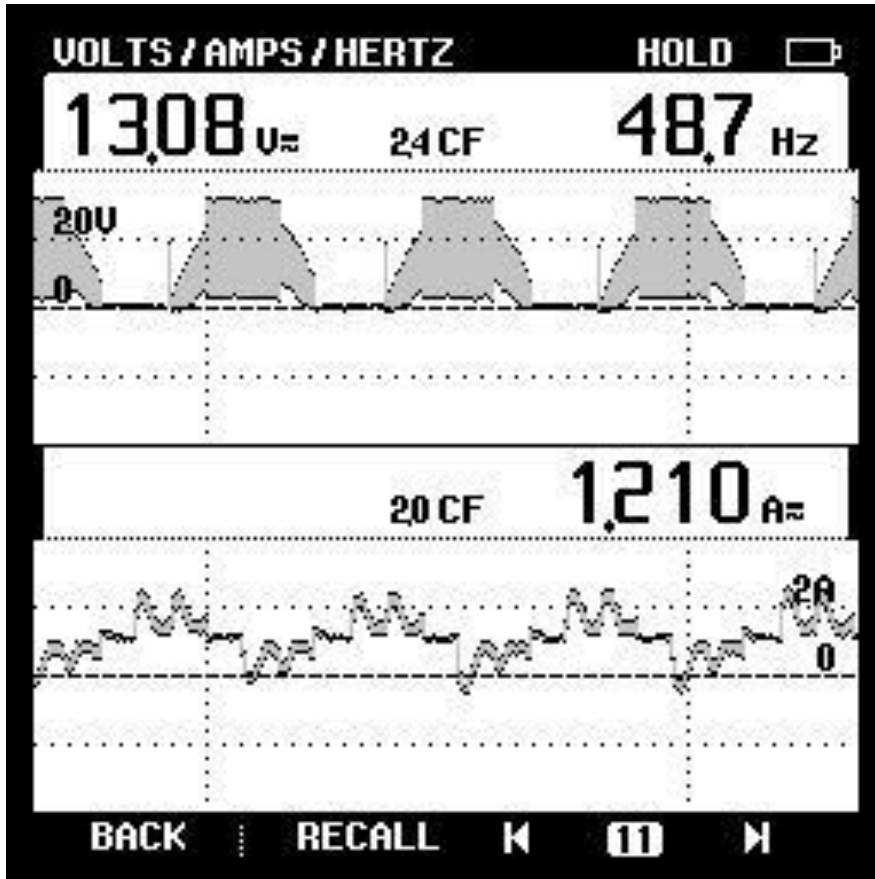
Flow-chart in open-loop mode



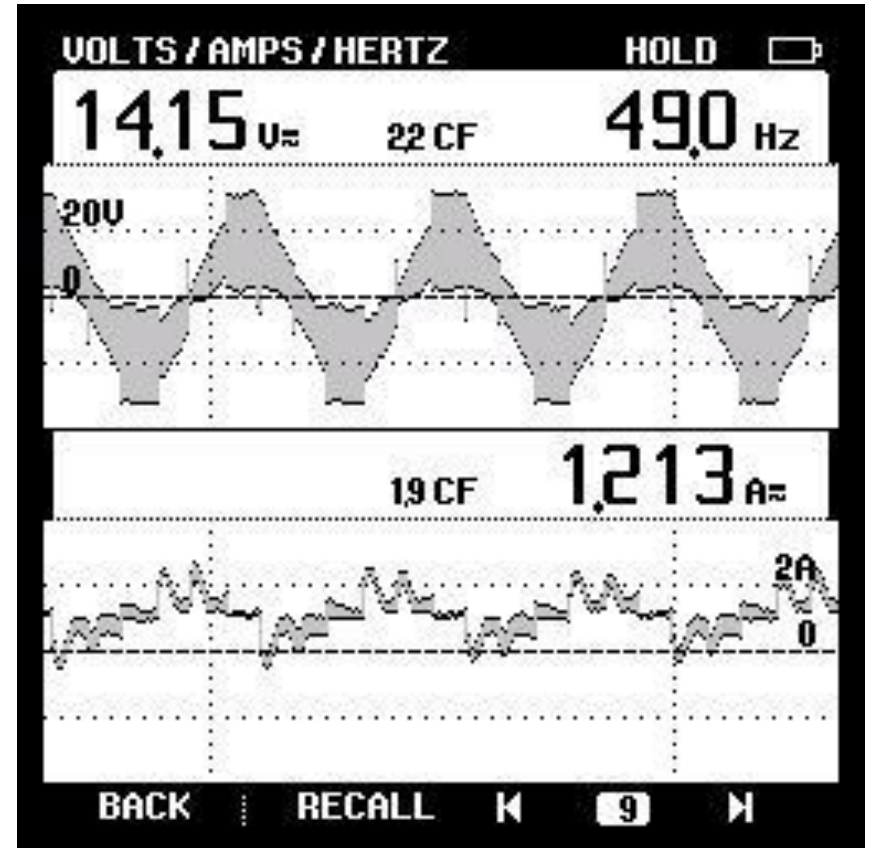
Hardware results

Open-loop Mode under No-Load

Dc link voltage=30v



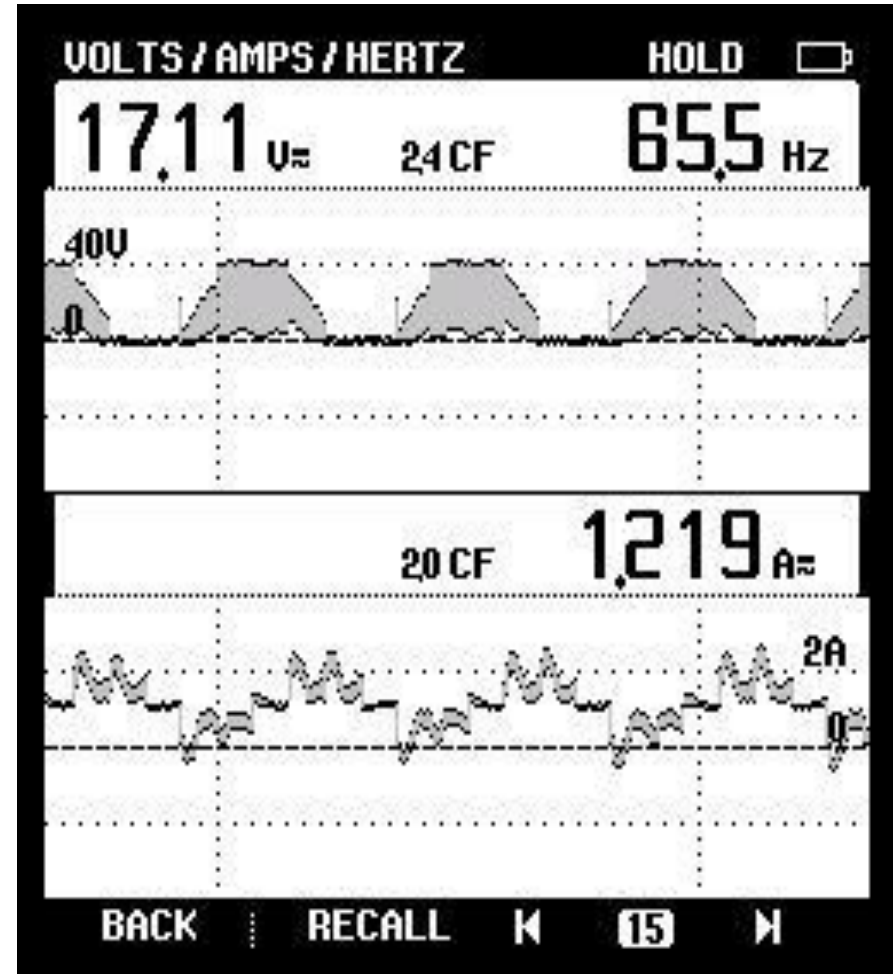
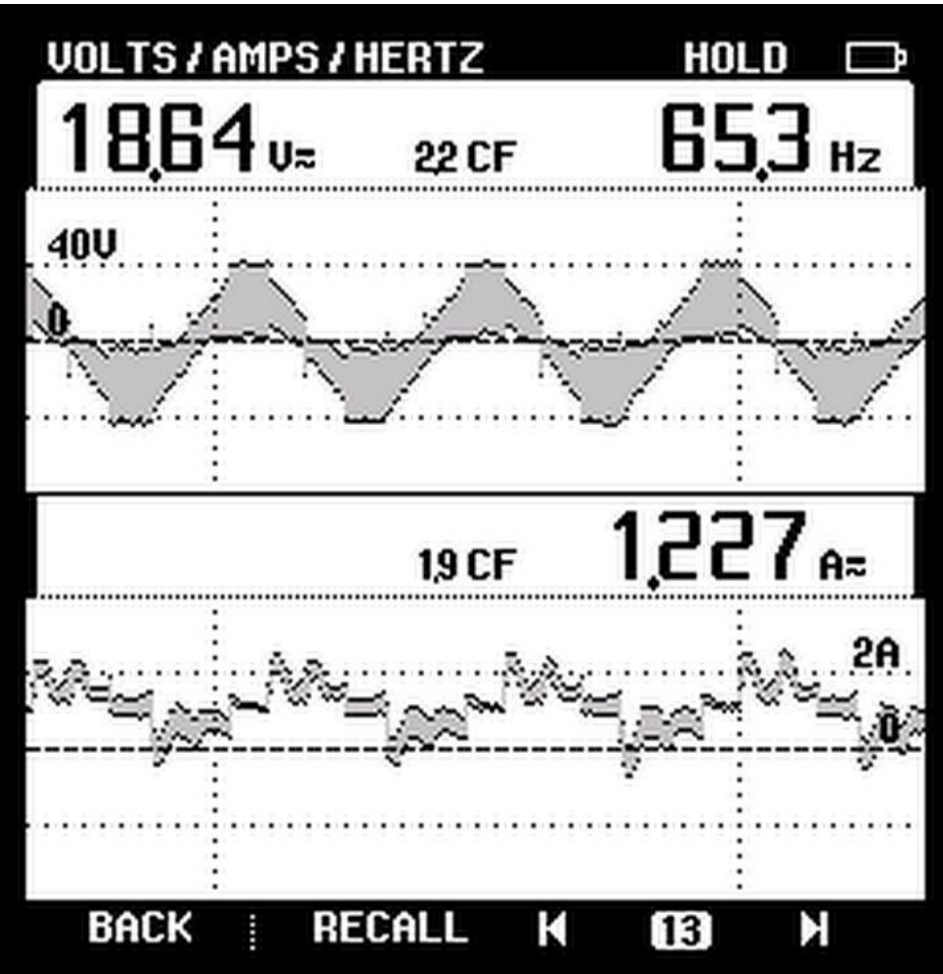
Phase voltage



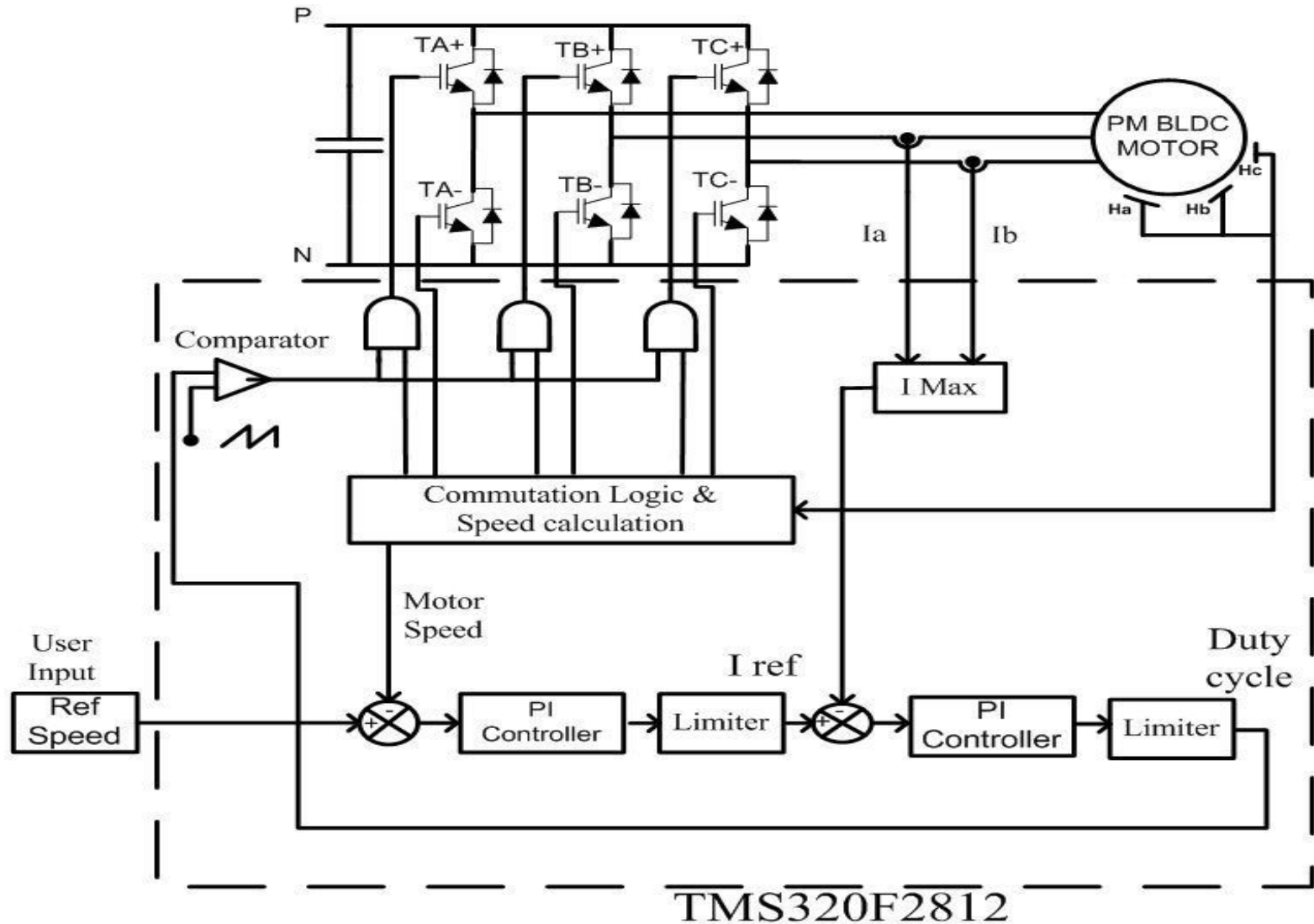
Line to line voltage

Open-loop Mode under No-Load

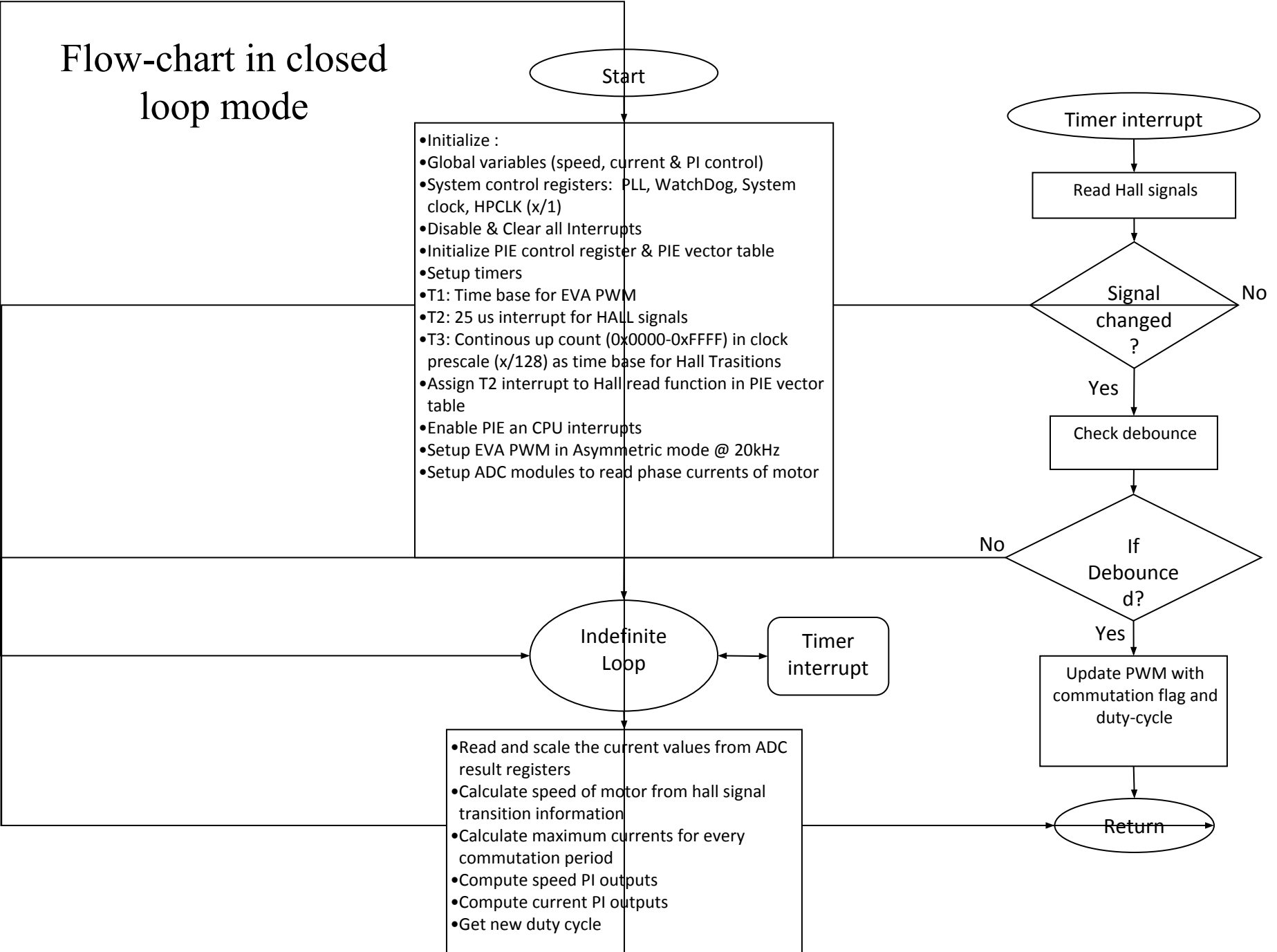
Dc link voltage=42v



Electric Two-Wheeler in closed-Loop mode



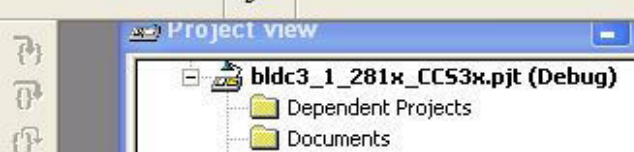
Flow-chart in closed loop mode





bldc3_1_281x_CCS3x.pjt

Debug



Watch Window

X

Name	Value	T.	R...
EnableFlag	1	u...	un...
Dcycle	0.3071692	f...	float
EvaRegs.T1CNT	14920	U.	un...
EvaRegs.ACTRA.all	0xFF3D	U.	hex
hall1.Revolutions	1	i...	dec
EvaRegs	{...}	s...	hex
EvaRegs.T3CNT	0xF84A	U.	hex
speed	100.0607	f...	float
spd	98.87653	f...	float
sped	100.0607	f...	float
t2	0.000680...	f...	float
ia	-0.9674001	f...	float
ib	0.02235007	f...	float
ic	0.3475001	f...	float
Imax	0.55515	f...	float
Ref_speed	100.0	f...	float
errorS	0.5100555	f...	float
integralS	0.00423346	f...	float
VirtualTimer	118	U.	un...
IsrTicker	29037	U.	un...

W... Bu... Bu... Bu... Wa...

Build

Channel... Channel...

RUNNING

POLITE REALTIME

C:\tidcs\DMC\c28\v32x\sys\bldc3_1_281x\cIQmath\src\bldc3_1.c

```

        Imax=ic;
    }
    else {
        if (ib>ic)
            Imax=ib;
        else
            Imax=ic;
    }

    //pi controller speed
    errorS=Ref_speed-speed;
    propS=kpS*errorS;
    integralS=kiS*errorS+integralS;
    if((errorS<=0)&&(integralS>0)) // to avoid windup effects
        integralS=0;
    if((errorS>=0)&&(integralS<0)) // to avoid windup effects
        integralS=0;

    if (integralS>100) //limiting the integral memory
        integralS=100;
    if (integralS<-100) //limiting the integral memory
        integralS=-100;
    // integral1= integralS;
    Iref=propS+integralS;
    if(Iref>Ilimit)
        Iref=Ilimit;
    if(Iref<0)
        Iref=0;
    //pi current controller
    errorI=Iref-Imax;
    propI=kpI*errorI;
    integralI=KiI*errorI+integralI;
    //Integral2=integralI;

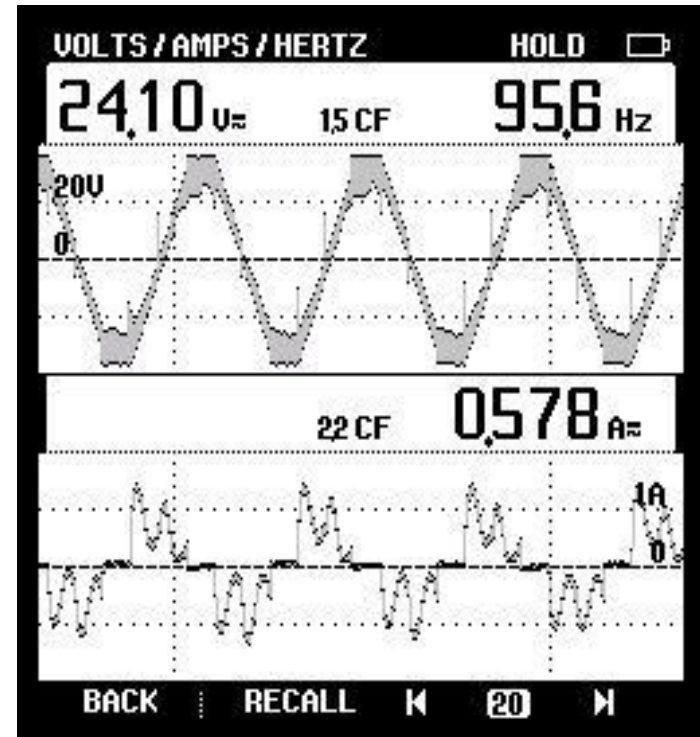
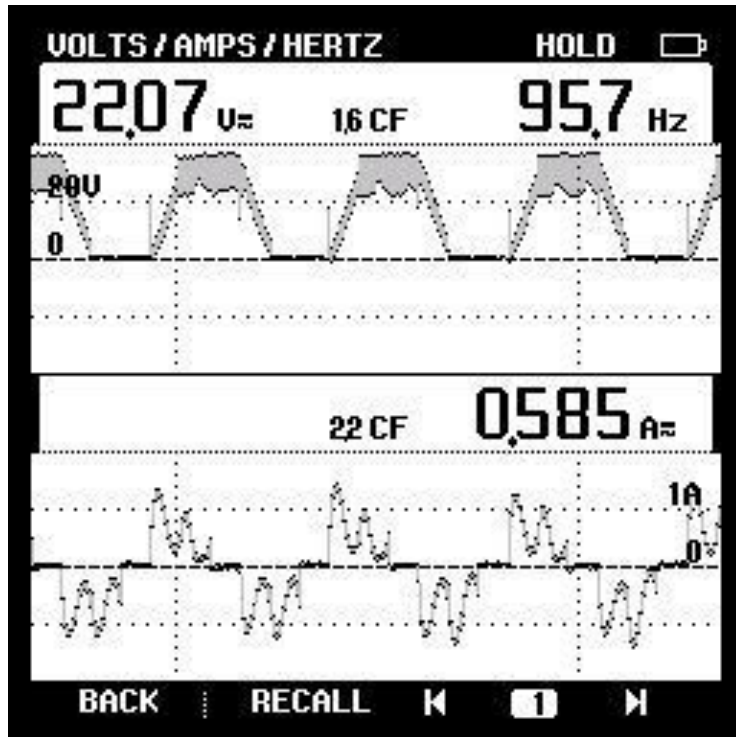
```

Hardware results of closed loop speed and current control

Input parameters		
D.C link voltage	35	V
3-Phase A.C Input	28.4	V
Reference speed	250	rpm
PI controller parameters		
Speed Loop	Kp=10	Ki=0.0001
Current loop	Kp=1	Ki=0

Results			
Reference speed	250	150	rpm
Motor phase voltage	22.07	14.77	V
Phase current peak	1.6	1.54	A
Frequency	95.7	57.5	Hz
Motor Speed	249.6	150	rpm

Line and Phase Back-EMFs

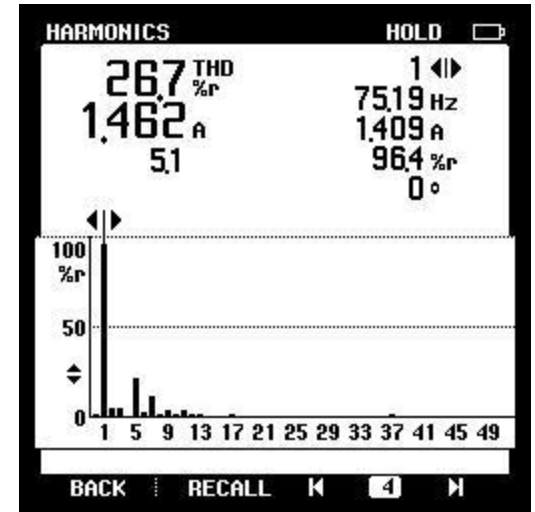
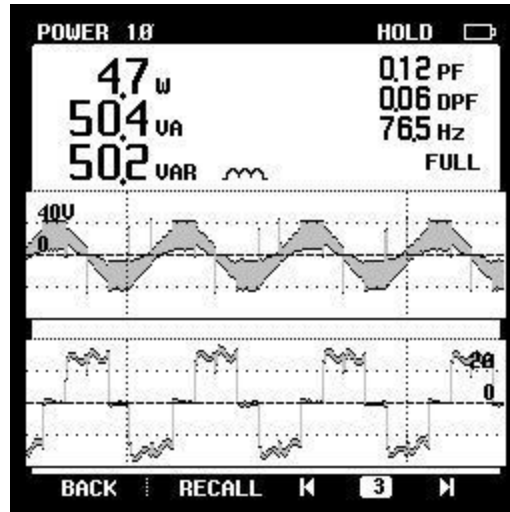
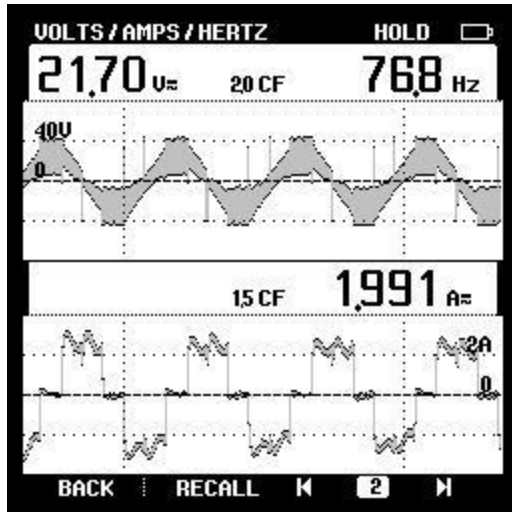


Load test on PM BLDC Hub Motor.

Sr. No.	Vbatt(V)	I batt(A)	Vdc(V)	Idc(A)	Vmotor(V)	Imotor(A)	power(W)	P.F	Vload (V)	Iload(A)	Pout(W)	Pin(W)	Efficiency
1	50	1	49.3	1	21.63	2	4.3	0.14	27.6	1.25	34.5	49.3	69.97
2	49.3	1.5	48.9	1.5	21.81	2.2	5	0.12	25.67	2	38.5	74.25	71.5
3	49.2	2	48.3	2	21.92	2.7	6	0.1	23.23	3	69.69	96.6	72.14
4	49.3	2.5	47.9	2.5	22.17	3.17	6.5	0.1	20.2	4	80.8	119.75	67.47

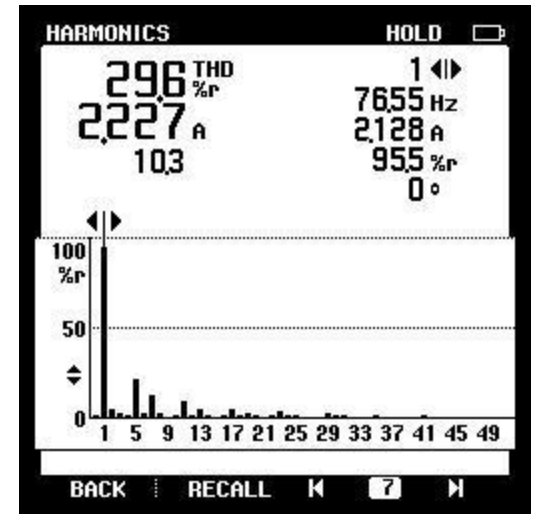
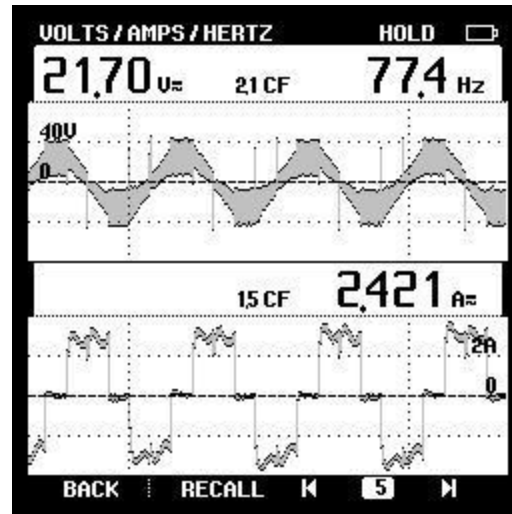
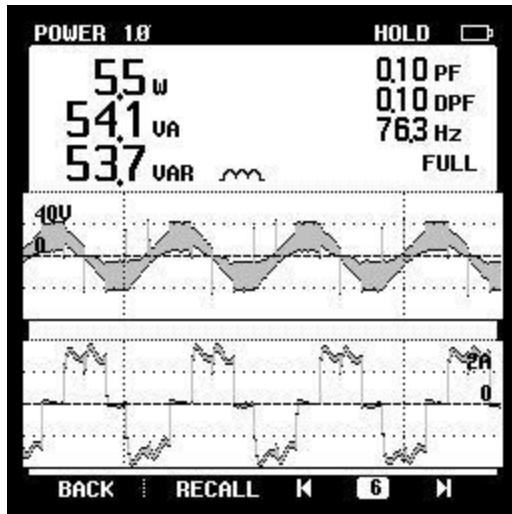
Load test at 200 rpm

Load test results



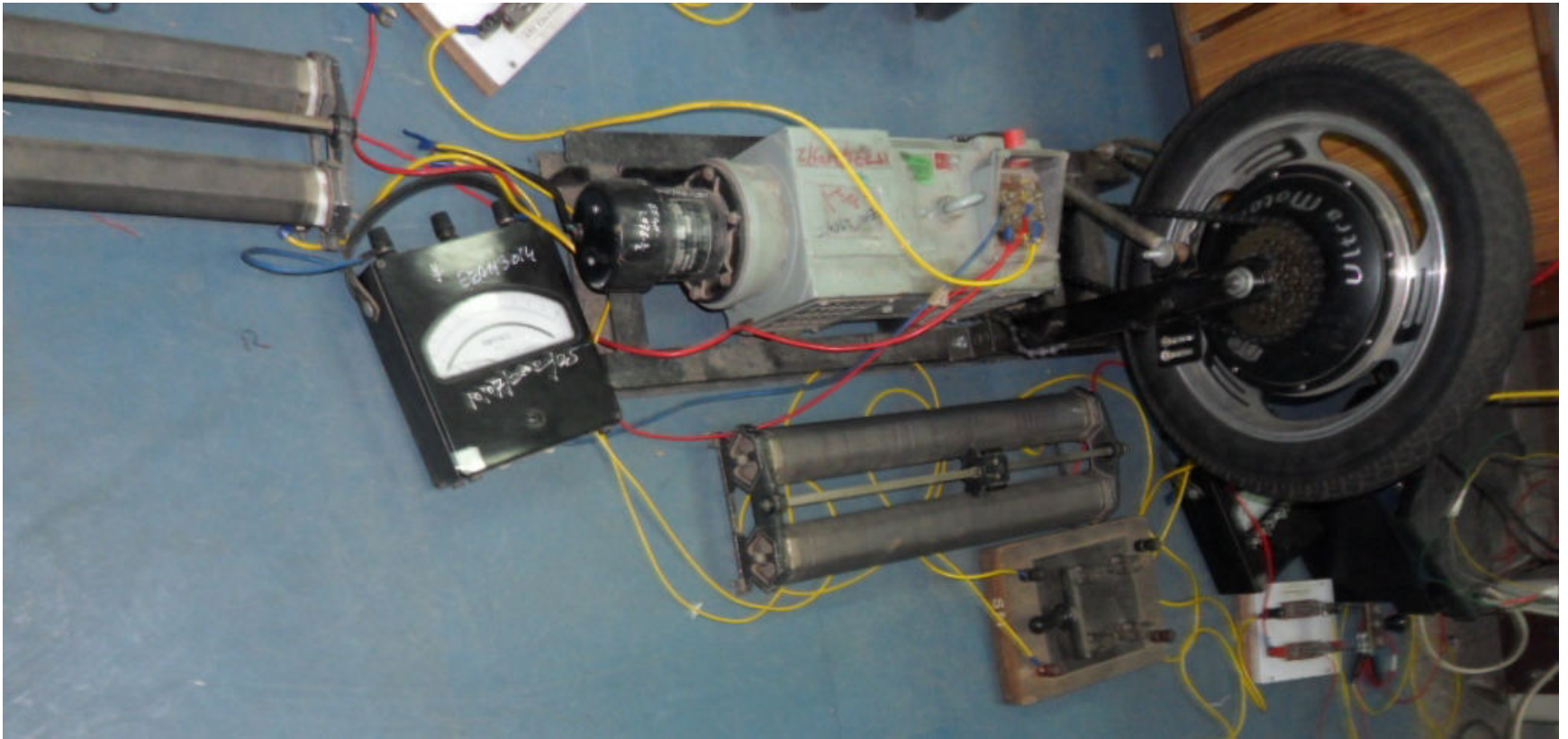
Motor Line voltage ,power and THD

Load test results

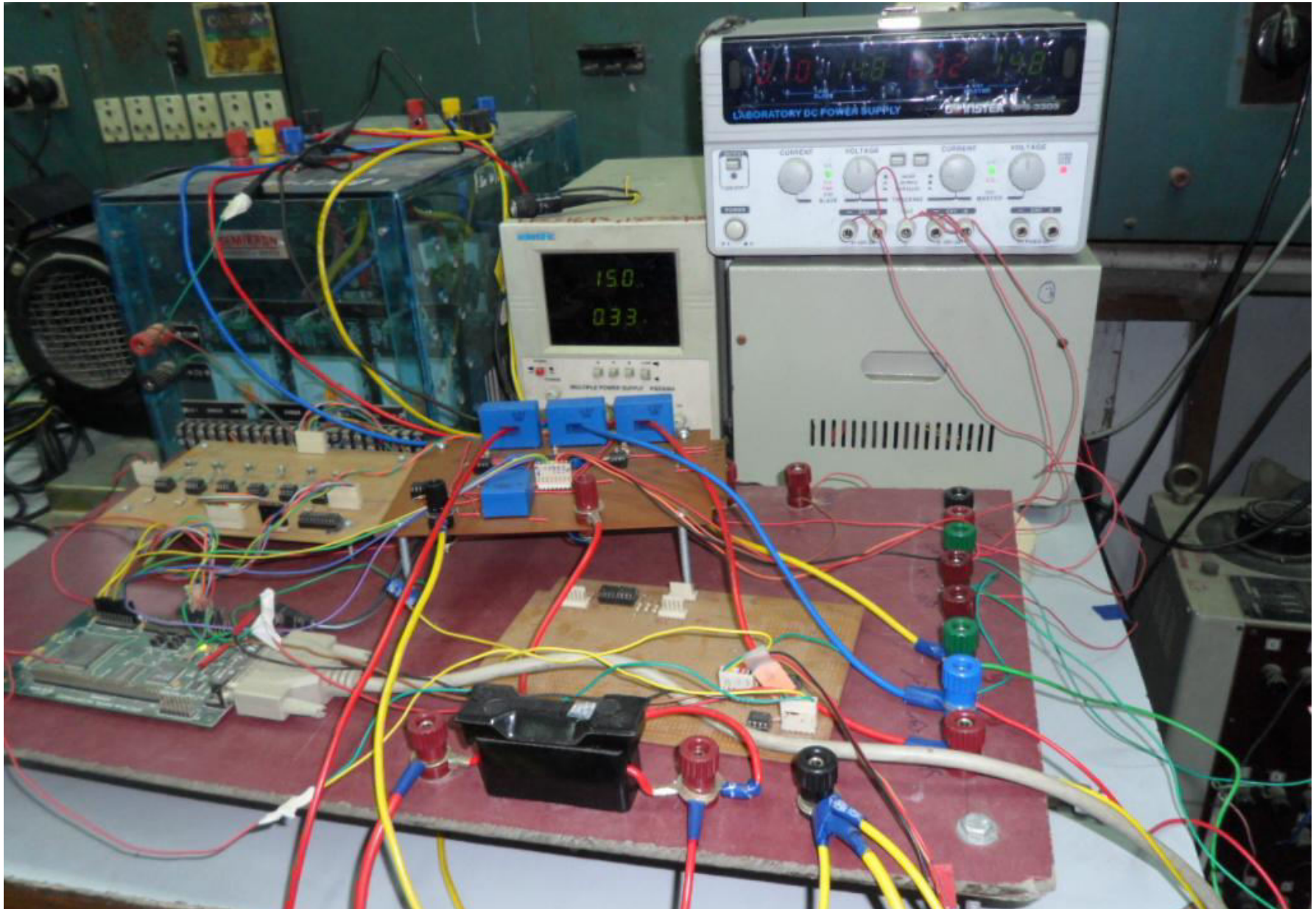


Motor Line voltage ,power and THD

PM BLDC Hub Motor load Set-up

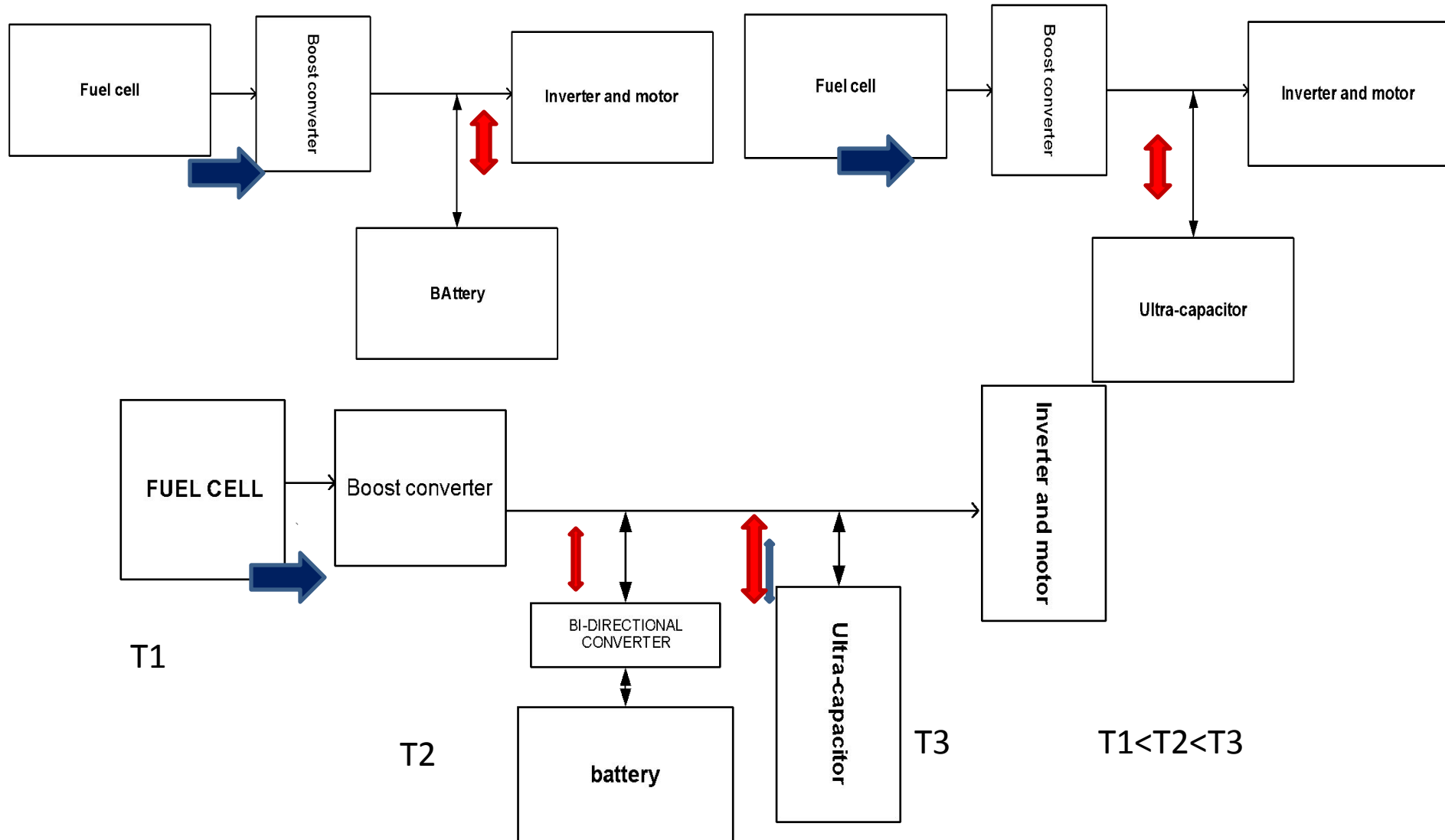


Control circuitry

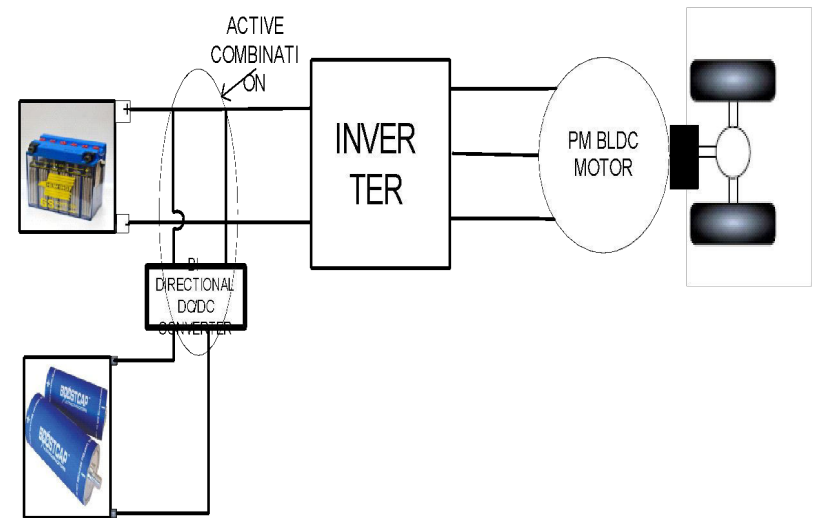
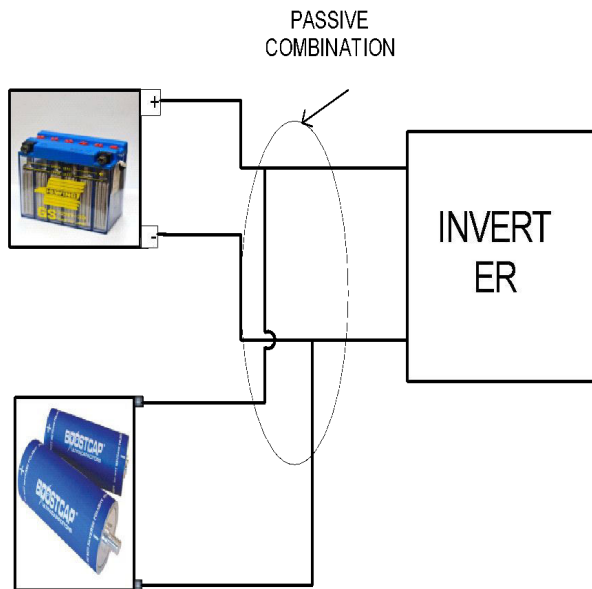
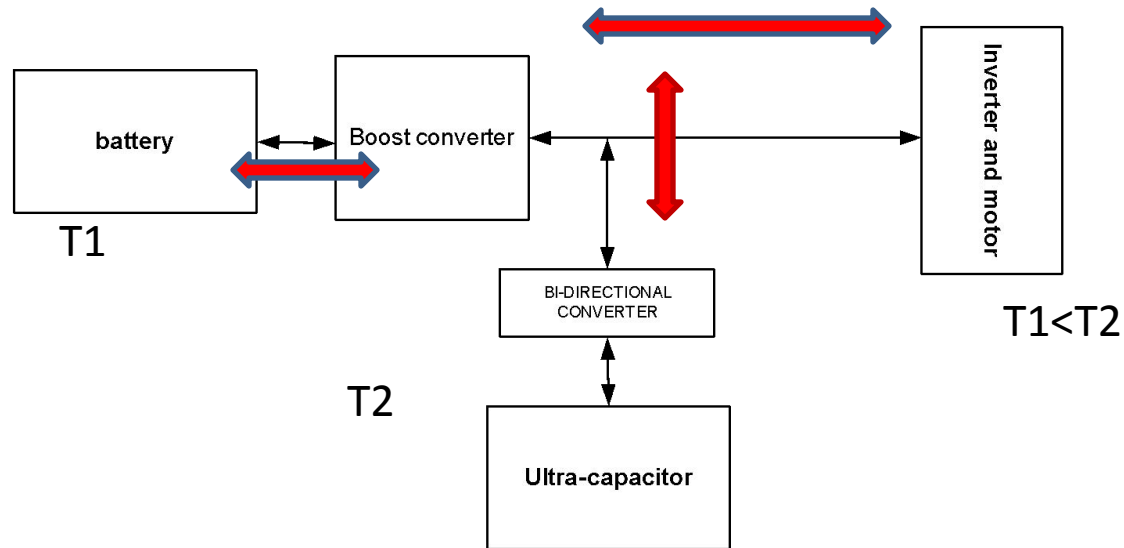


EV model with hybrid energy storage

FCV configurations



Hybrid battery vehicle topologies



Ultra-capacitor(UC) Modelling

Ultra –capacitor or Super capacitor or Electric double layer capacitors(EDLC's):

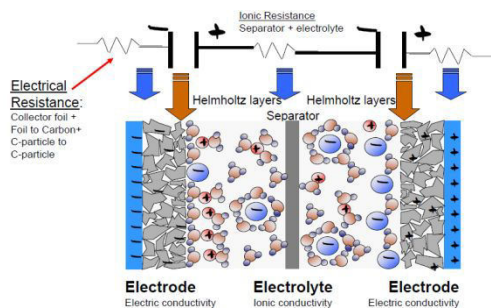
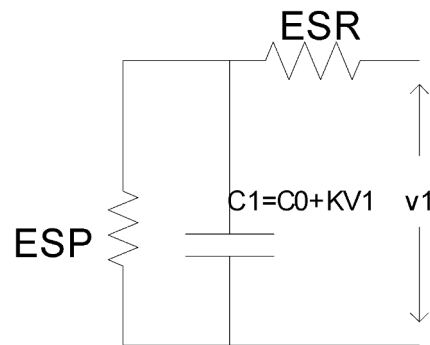
Ultra capacitors are selected as power buffers due to following properties

ESS Component	Specific Energy (Wh/kg)	Energy specific cost (\$/Wh)	Power specific cost (\$/kW)	Cycle Capability at 80% DOD # Cycles (Wh-cycles)
Ultracap	5	16	12	$>10^6$ 4×10^6
VRLA	30	0.12	80	3×10^2 7×10^3
NiMH	44	0.65	75	4×10^3 1.5×10^5
Lithium	70	0.50	75	JCS 2.5×10^3 1.4×10^5 A123 5×10^3 2.8×10^5 AltairNano 15×10^3 8.4×10^5

- Ultra capacitors are having high power density
- similar characteristics during charging and recharging process
- higher number of cycles

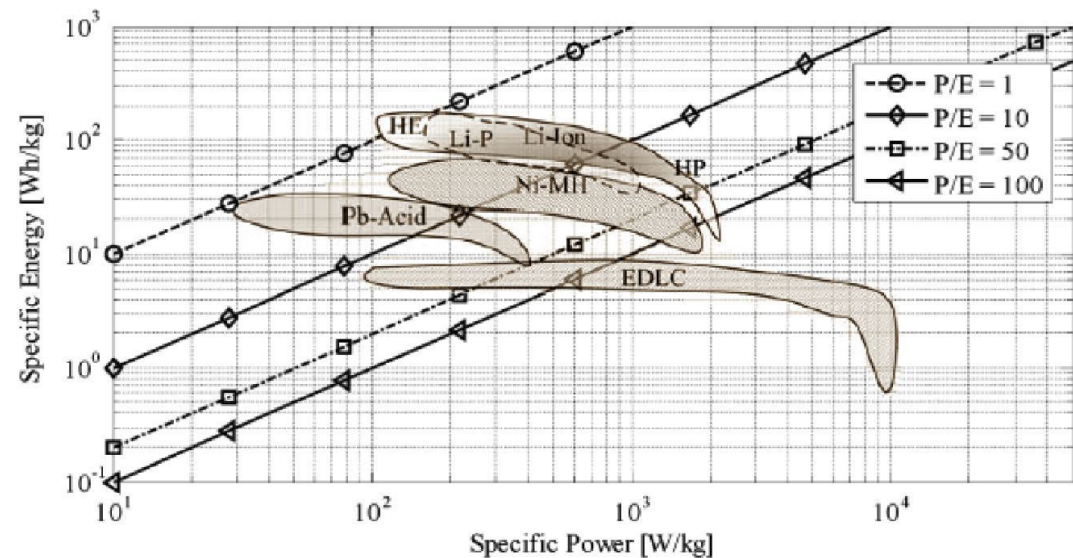
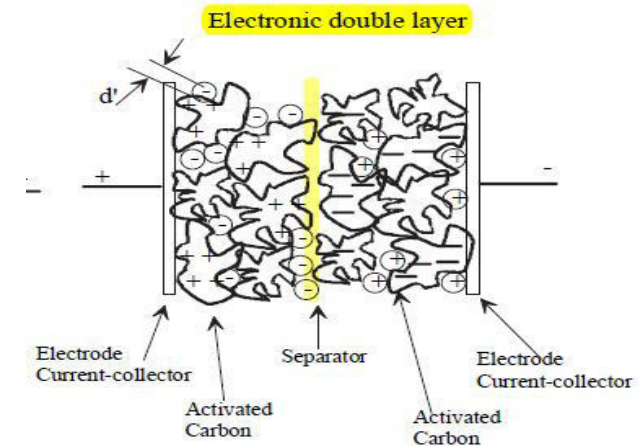
UC schematic

- EPR= represents self discharge (if super capacitor is operated in several hours it is effective)
- ESR= Represents loss due to charging and discharging
- $C1=C0+KV1$; voltage dependent variable capacitor



UC equivalent circuit

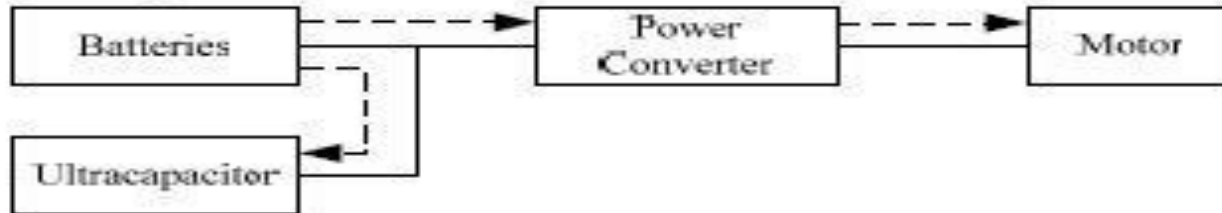
$$C = \frac{I}{V_{\max} - V_{\min}} (t + \tau)$$



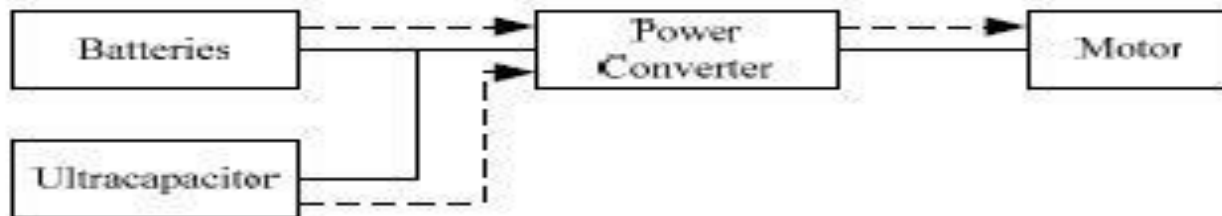
Ragone plots

Working principle of hybrid battery system

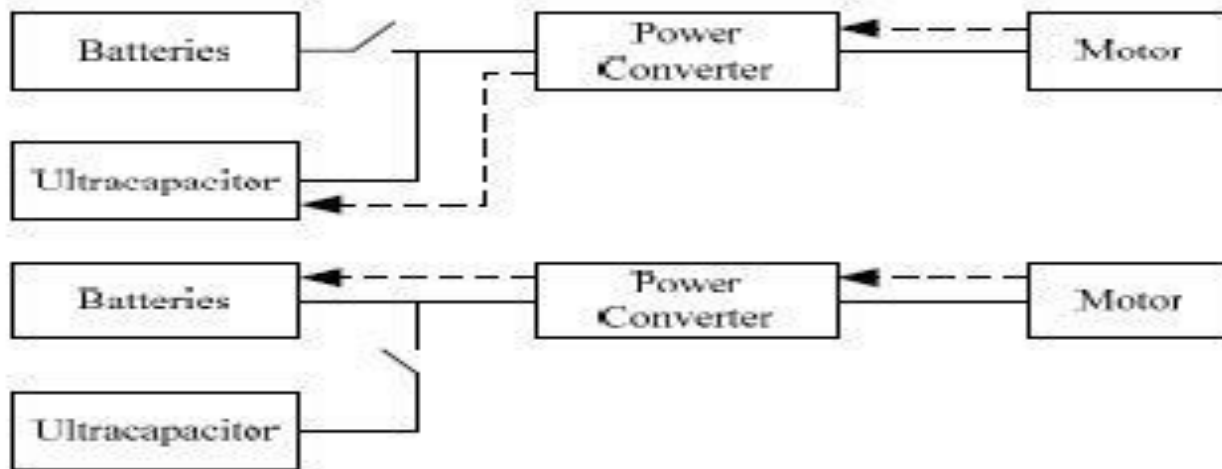
Normal Driving Conditions



Start / Accelerate / Climb Driving Conditions



Energy-Regenerative Braking Conditions



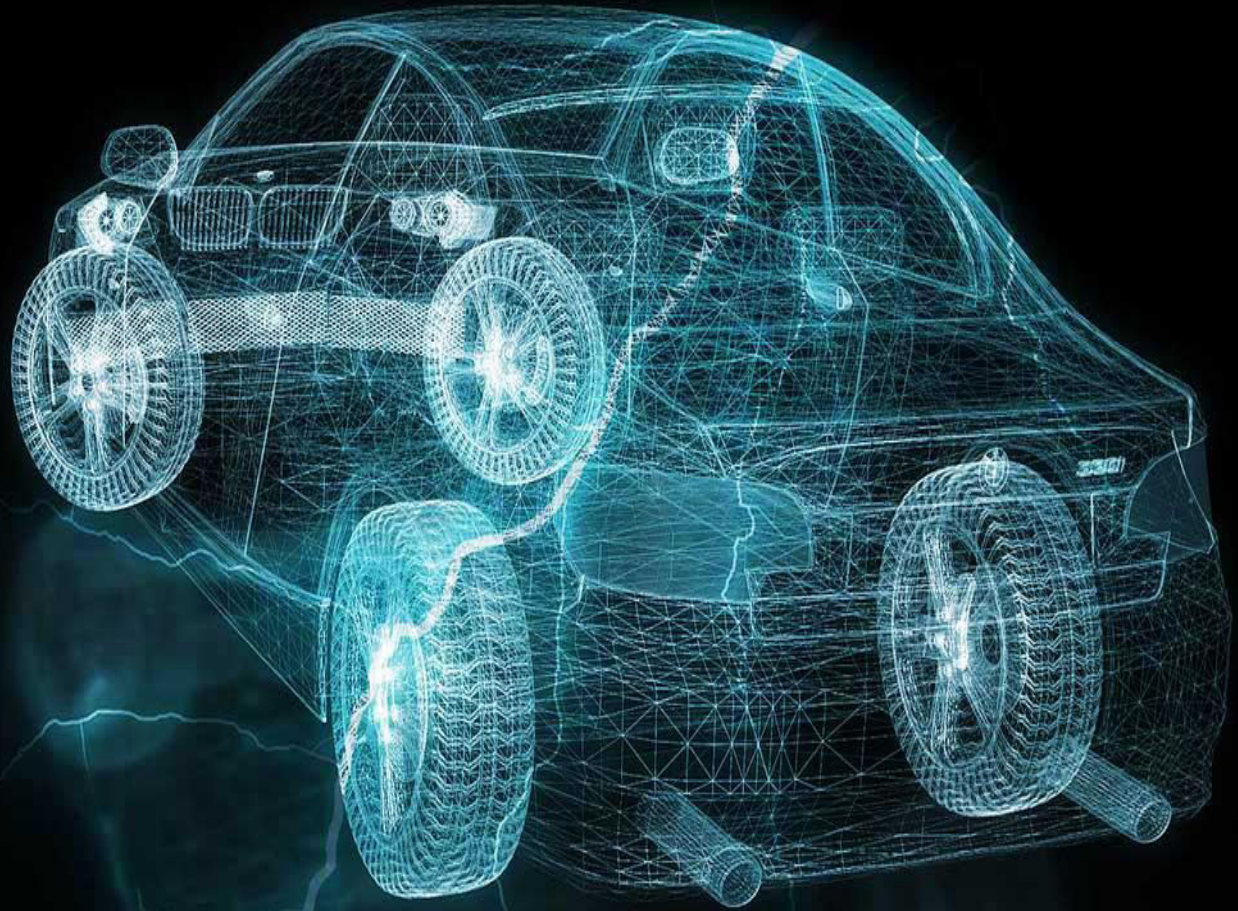
References

1. J. W. Dixon, and M. E. Ortizar, “Ultracapacitors + DC–DC Converters in Regenerative Braking System,” *IEEE Aerospace and Electronic Systems magazine*, Vol. 17, No. 8, pp. 16–21, August 2002.
2. J. Cao, B. Cao, Z. Bai and W. Chen,” Energy regenerative Fuzzy Sliding mode Controller design for Ultra capacitor –Battery Hybrid Power Electric Vehicle,” *Proceedings of the IEEE Int. Conf. on Mechatronics and Automation*, , pp. 1570–1575, August 2007.
3. J. Cao and B. Cao,”Fuzzy-logic - Based Sliding Mode Controller Design for Position -Sensorless Electric vehicle,” *IEEE Trans.Power Electron.* vol. 24, no. 10, pp. 2368–2378, October 2009.
4. M. Ye, Z. F. Bai, and B. Cao, “Robust $H_2/\text{Infinity}$ Control for Regenerative Braking of Electric Vehicles,” *Proceedings of the IEEE Int. Conf. on Control and Automation*, pp. 1366–1370, May/June 2007
5. J. Cao, B. Cao, Z. Bai and P. Xu , ” Regenerative – Braking Sliding mode Control of Electric Vehicle based on Neural network Identification,” *Proceedings of the IEEE Int. Conf. on Advanced Intelligent Mechatronics*, pp. 1219–1224, July 2008.

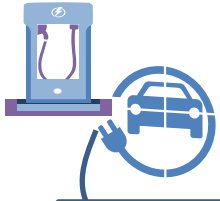
6. J. Cao, B. Cao, Z. Bai and P. Xu,” Neural network Self -adaptive PID control for Driving and Regenerative Braking of Electric Vehicle,” Proceedings of the IEEE Int. Conf.on Automation and Logistics, pp. 2029–2034, August 2007.
7. J. Cao, B. Cao, Z. Bai , P. Xu and X. Wu ,” Neural network control of Electric Vehicle based on Position –Sensor less Brushless DC Motor,” Proceedings of the IEEE Int. Conf. on Automation And logistics, pp. 2029–2034, August 2007.
8. C.-H. Chen and M.-Y. Cheng, “Implementation of a highly reliable hybrid electric scooter drive,” IEEE Trans. Ind. Electron., vol. 54, no. 5, pp. 2462–2473, Oct. 2007.
9. R. C. Becerra ,M. Ehsani, and T.M. Jahns, “Four-quadrant brushless ECM drive with integrated current regulation,” *IEEE Trans. Ind. Appl.*, vol. 28,no. 4, pp. 833–841, Jul./Aug. 1992. *Proceedings of the IEEE Int. Conf. on Automation and logistics*, pp. 2029–2034, August 2007

History of Electric Vehicles

History of Electric Vehicles

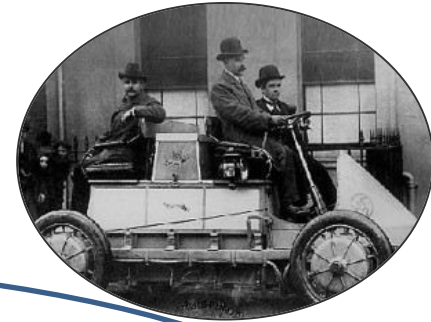


History of Electric Vehicles



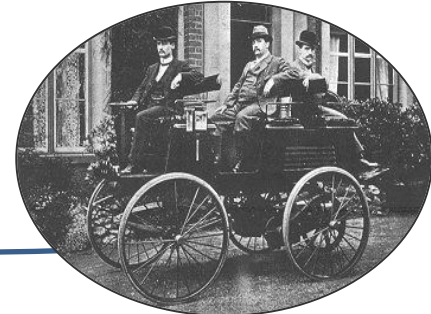
1837

Electric car begin their long history in Aberdeen, Scotland through inventor Robert Davidson. Later in 1841, he built a bigger electric train car.



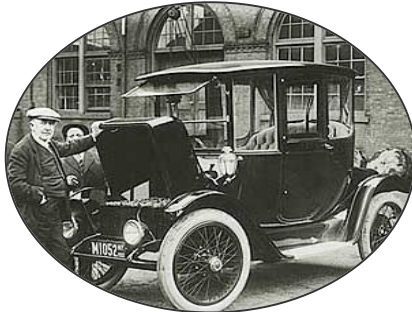
1884

After more than 40 years, inventor Thomas Parker creates the first manufacturing electric automobile in London.

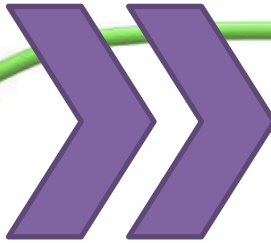


1890

The first electric car was produced in Iowa, U.S.A by William Morrison. The car is little more than an electrified wagon. This six-seater has a top speed of 14 mph.



Non-Chargeable
Batteries
1830s



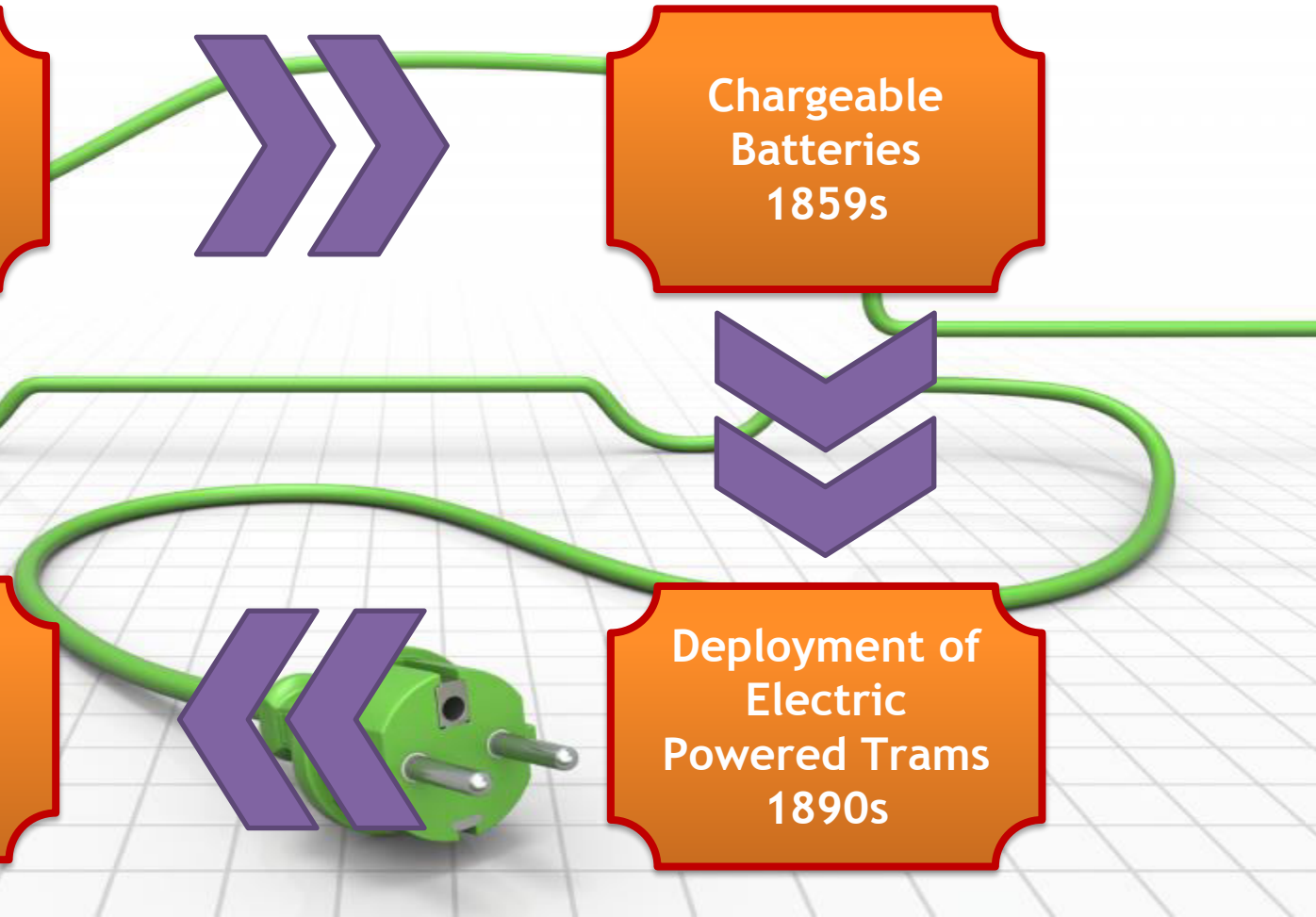
Chargeable
Batteries
1859s



Lithium Ion
Batteries Since
early
1990s



Deployment of
Electric
Powered Trams
1890s



- Electric Vehicles outsold Gasoline Cars 2:1 in the late 1890's
- 1834: Thomas Davenport invented the first electric car
- Pope Manufacturing Company
 - First large-scale operation in the US automobile industry
- 1903: First speeding ticket...in an electric vehicle



Source 9

1881

The first electric vehicle was built by Frenchman Gustave Trouvé. It was a tricycle powered by a 0.1 hp DC motor fed by lead–acid batteries. The whole vehicle and its driver weighed approximately 160 kg.

1883

A vehicle similar to this was built in by two British professors. These early realizations did not attract much attention from the public because the technology was not mature enough to compete with horse carriages. Speeds of 15 km/h and a range of 16 km were not exciting for potential customers.

The first commercial electric vehicle was Morris and Salom's Electroboat. This vehicle was operated as a taxi in New York City by a company created by its inventors. The Electroboat proved to be more profitable than horse cabs despite a higher purchase price (around \$3000 vs. \$1200). It could be used for three shifts of 4 h with 90-min recharging periods in between. It was powered by two 1.5 hp motors that allowed a maximum speed of 32 km/h and a 40-km range.

1897

The most significant technical advance of that era was the invention of regenerative braking by Frenchman M.A. Darracq. It is one of the most significant contributions to electric and hybrid electric vehicle technology as it contributes to energy efficiency more than anything else in urban driving.

In addition, among the most significant electric vehicles of that era was the first vehicle ever to reach 100 km/h. It was “La Jamais Contente” built by Frenchman Camille Jenatzy.

As gasoline automobiles became more powerful, more flexible, and, above all, easier to handle, electric vehicles started to disappear. Their high cost did not help, but it is their limited driving range and performance that really impaired them vs. their gasoline counterparts. The last commercially significant electric vehicles were released around 1905. During nearly 60 years, the only electric vehicles sold were common golf carts and delivery vehicles.

1945

three researchers at Bell Laboratories invented a device that was meant to revolutionize the world of electronics and electricity: the transistor. It quickly replaced vacuum tubes for signal electronics and soon the thyristor was invented, which allowed switching high currents at high voltages. This made it possible to regulate the power fed to an electric motor without the very inefficient rheostats, and allowed the running of AC motors at variable frequency.

1966

General Motors (GM) built the Electrovan, which was propelled by induction motors that were fed by inverters built with thyristors.

The most significant electric vehicle of that era was the Lunar Roving Vehicle, which the Apollo astronauts used on the Moon.

The vehicle itself weighed 209 kg and could carry a payload of 490 kg. The range was around 65 km.

The design of this extraterrestrial vehicle, however, has very little significance down on Earth.

The absence of air and the lower gravity on the Moon, and the low speed made it easier for engineers to reach an extended range with limited technology.

During the 1960s and 1970s, concerns about the environment triggered some research on electric vehicles.

However, despite advances in battery technology and power electronics, their range and performance were still obstacles.

The modern electric vehicle era culminated during the 1980s and early 1990s with the release of a few realistic vehicles by firms such as GM with the EV1 and PSA with the 106 Electric.

Although these vehicles represented a real achievement, especially when compared with early realizations, it became clear during the early 1990s that electric automobiles could never compete with gasoline automobiles for range and performance.

The reason is that in batteries the energy is stored in the metal of electrodes, which weigh far more than gasoline for the same energy content.

The automotive industry abandoned the electric vehicle to conduct research on hybrid electric vehicles.

After a few years of development, these are far closer to the assembly line for mass production than electric vehicles have ever been.

In the context of the development of the electric vehicle, it is battery technology that is the weakest, blocking the way of electric vehicles to market.

Great effort and investment have been put into battery research, with the intention of improving performance to meet the electric vehicle's requirement.

Unfortunately, progress has been very limited. Performance is far behind the requirement, especially energy storage capacity per unit weight and volume.

This poor energy storage capability of batteries limits electric vehicles only to some specific applications, such as at airports and railroad stations, on mail delivery routes, and on golf courses, etc.

In fact, basic study shows that electric vehicles will never be able to challenge liquid fueled vehicles even with the optimistic value of battery energy capacity.

In recent years, advanced vehicle technology research has turned to hybrid electric vehicles as well as fuel cell vehicles.

UNIT IV: Electric Propulsion Systems

Introduction to electric components used in hybrid and electric vehicles, Configuration and control of DC Motor drives, Configuration and control of Induction Motor drives, configuration and control of Permanent Magnet Motor drives, Configuration and control of Switch Reluctance Motor drives, drive system efficiency.

Electric Vehicle (EV) Configurations

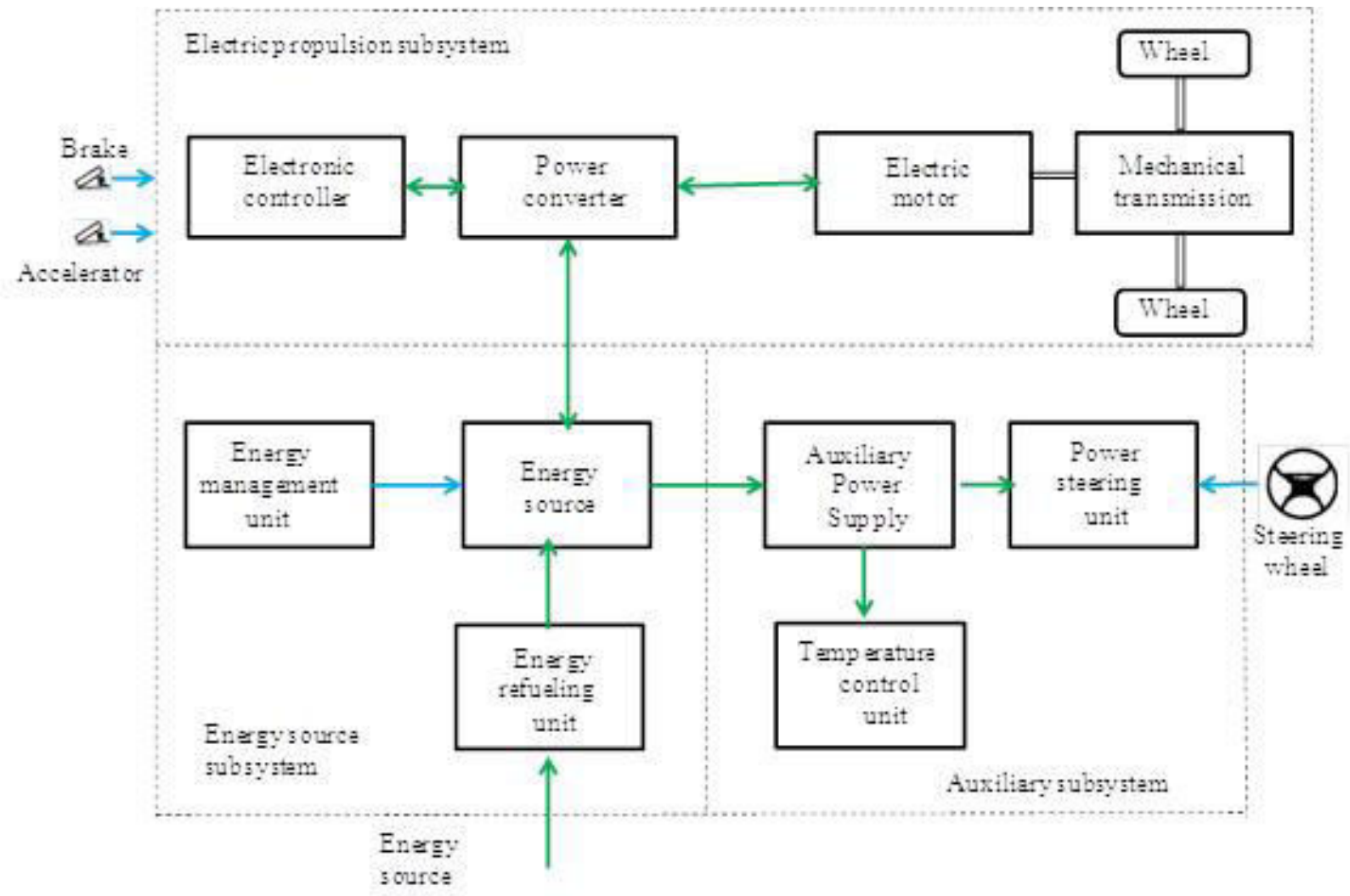
Compared to HEV, the configuration of EV is flexible. The reasons for this flexibility are:

- The energy flow in EV is mainly via flexible electrical wires rather than bolted flanges or rigid shafts. Hence, distributed subsystems in the EV are really achievable.
- The EVs allow different propulsion arrangements such as independent four wheel and in wheel drives.

The EV has three major subsystems:

- Electric propulsion
 - Energy source
 - Auxiliary system

General Configuration of a Electric Vehicle



The electric propulsion subsystem comprises of:

- The electronic controller
 - Power converter
 - Electric Motor (EM)
 - Mechanical transmission
 - Driving wheels

The energy source subsystem consists of

- The energy source (battery, fuel cell, ultracapacitor)
 - Energy management unit
 - Energy refueling unit

The auxiliary subsystem consists of

- Power steering unit
 - Temperature control unit
 - Auxiliary power supply

In **Figure 1** the black line represents the mechanical link, the green line represents the electrical link and the blue line represents the control information communication. Based on the control inputs from the brake and accelerator pedals, the electronic controller provides proper control signals to switch on or off the power converter which in turn regulates the power flow between the electric motor and the energy source. The backward power flow is due to regenerative braking of the EV and this regenerative energy can be stored provided the energy source is receptive.

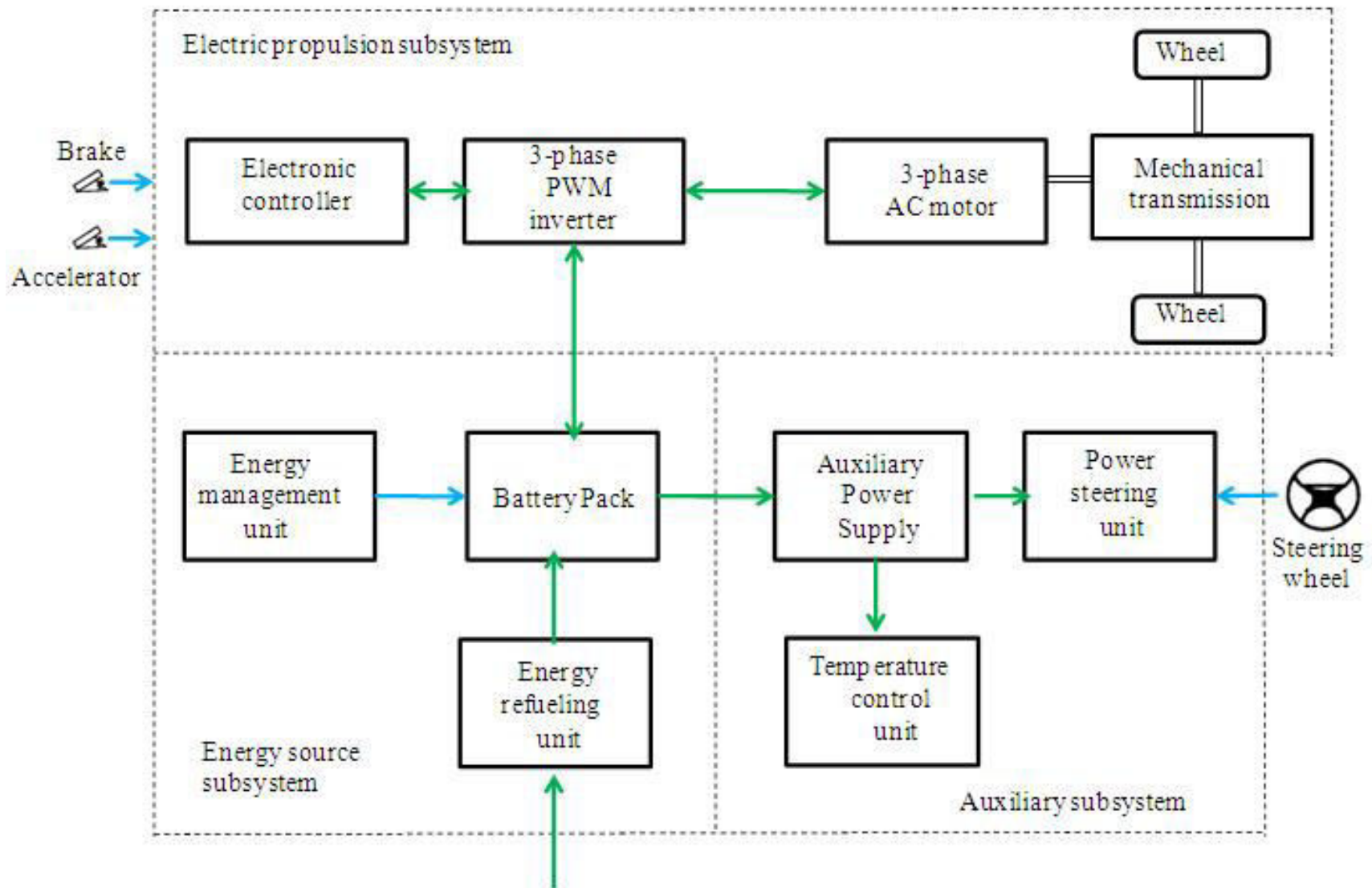
The energy management unit cooperates with the electronic controller to control regenerative braking and its energy recovery. It also works with the energy-refueling unit to control refueling and to monitor usability of the energy source.

The auxiliary power supply provides the necessary power with different voltage levels for all EV auxiliaries, especially the temperature control and power steering units.

In modern EV's configuration:

- Three phase motors are generally used to provide the traction force
- The power converter is a three-phase PWM inverter
- Mechanical transmission is based on fixed gearing and a differential
- Li-ion battery is typically selected as the energy source

Typical Configuration of a Electric Vehicle



Electric Vehicle (EV) Drivetrain Alternatives Based on Drivetrain Configuration

There are many possible EV configurations due the variations in electric propulsion and energy sources. Based on these variations, six alternatives are possible as shown in **Figure 3**. These six alternatives are

- EV configuration with clutch, gearbox and differential

- EV configuration without clutch and gearbox

- EV configuration with clutch, gearbox and differential

- EV configuration with two EM

- EV configuration with in wheel motor and mechanical gear

- EV configuration with in wheel motor and no mechanical gear

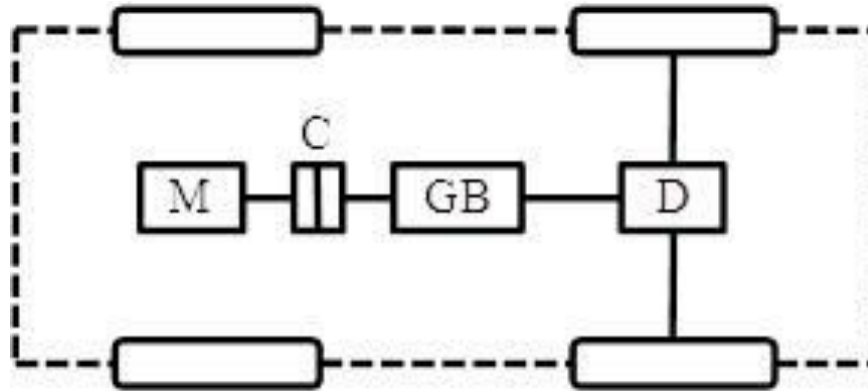


Figure 3a: EV configuration with clutch, gearbox and differential

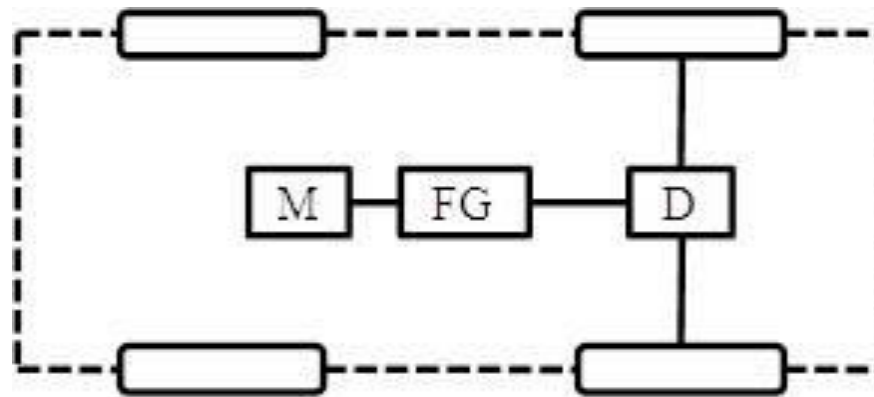


Figure 3b: EV configuration without clutch and gearbox

C: Clutch

D: Differential

FG: Fixedgearing

GB: Gearbox

EM: Electricmotor

- In **Figure 3a** a single EM configuration with gearbox (GB) and a clutch is shown. It consists of an EM, a clutch (C), a gearbox, and a differential (D). The clutch enables the connection or disconnection of power flow from EM to the wheels. The gear consists of a set of gears with different gear ratios. With the use of clutch and gearbox, the driver can shift the gear ratios and hence the torque going to the wheels can be changed. The wheels have high torque low speed in the lower gears and high-speed low torque in the higher gears.

- In **Figure 3b** a single EM configuration without the gearbox and the clutch is shown. The advantage of this configuration is that the weight of the transmission is reduced. However, this configuration demands a more complex control of the EM to provide the necessary torque to the wheels.

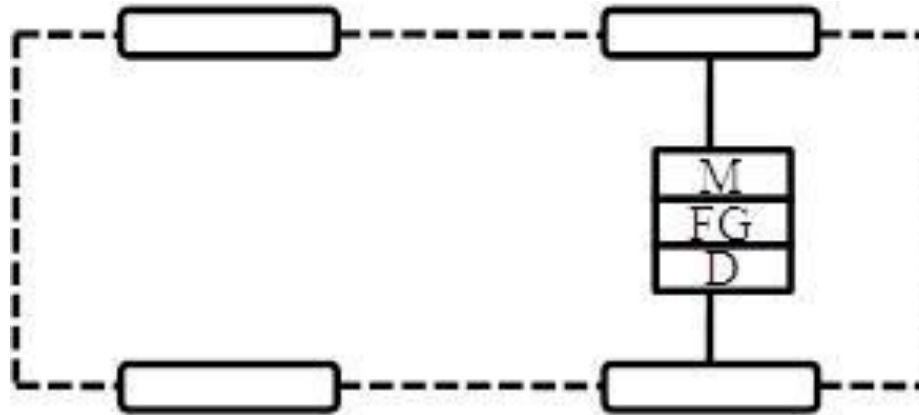


Figure 3c: EV configuration with clutch, gearbox and differential

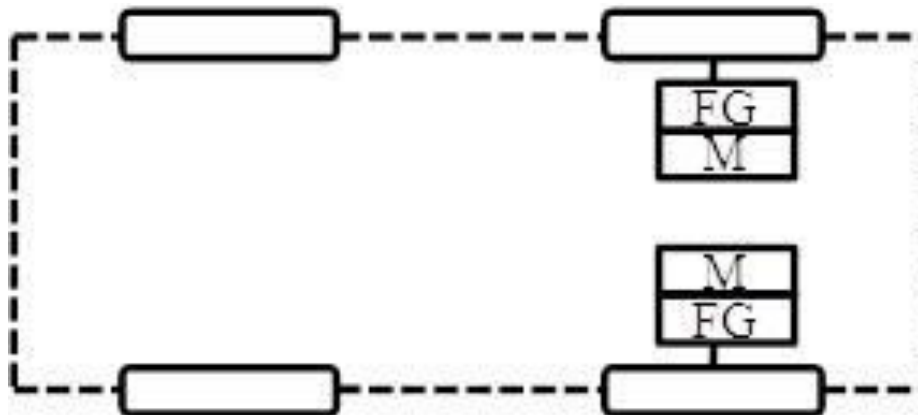


Figure 3d: EV configuration with two EM

C: Clutch

D: Differential

FG: Fixedgearing

GB: Gearbox

EM: Electricmotor

- **Figure 3c** shows a configuration of EV using one EM. It is a transverse front EM front wheel drive configuration. It has a fixed gearing and differential and they are integrated into a single assembly.

- In **Figure 3d** a dual motor configuration is shown. In this configuration the differential action of an EV when cornering can be electronically provided by two electric motors.

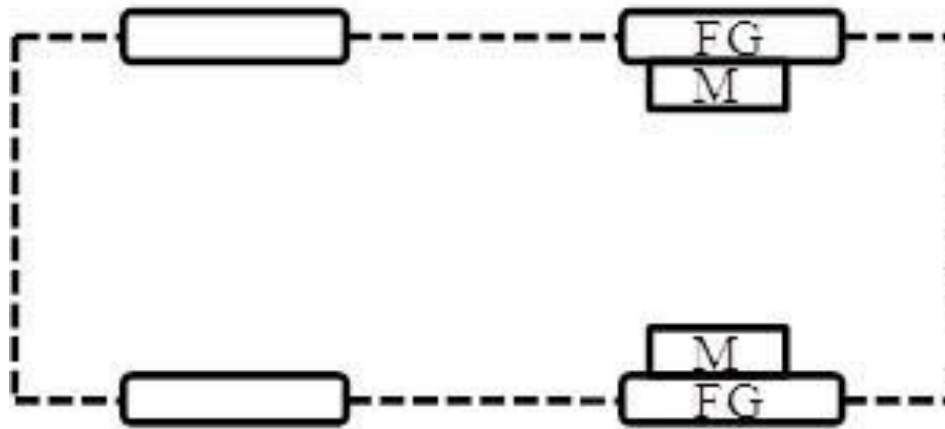


Figure 3e: EV configuration with in wheel motor and mechanical gear

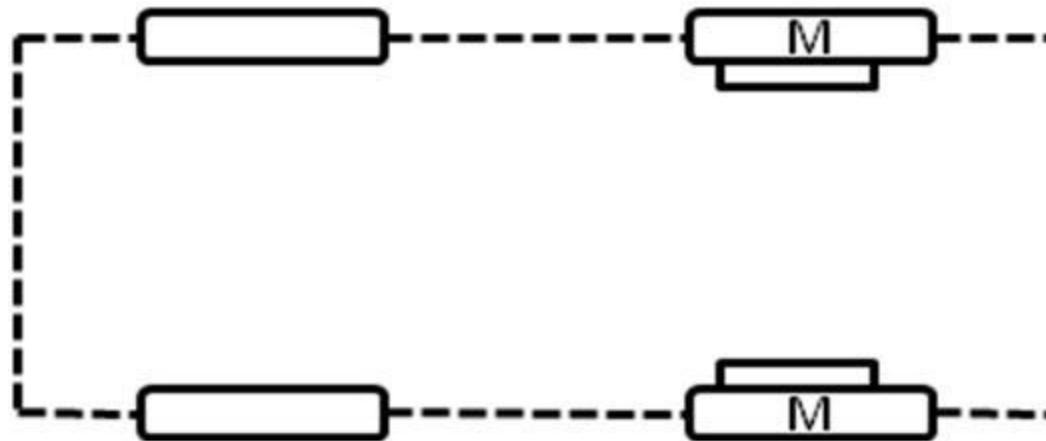


Figure 3f: EV configuration with in wheel motor and no mechanical gear

C: Clutch

D: Differential

FG: Fixedgearing

GB: Gearbox

EM: Electricmotor

- In order to shorten the mechanical transmission path from the EM to the driving wheel, the EM can be placed inside a wheel. This configuration is called in-wheel drive. **Figure 3e** shows this configuration in which fixed planetary gearing is employed to reduce the motor speed to the desired wheel speed.

- In **Figure 3f** an EV configuration without any mechanical gearing is shown. By fully abandoning any mechanical gearing, the in-wheel drive can be realized by installing a low speed outer-rotor electric motor inside a wheel.

Types of Motors used in Electric Vehicles

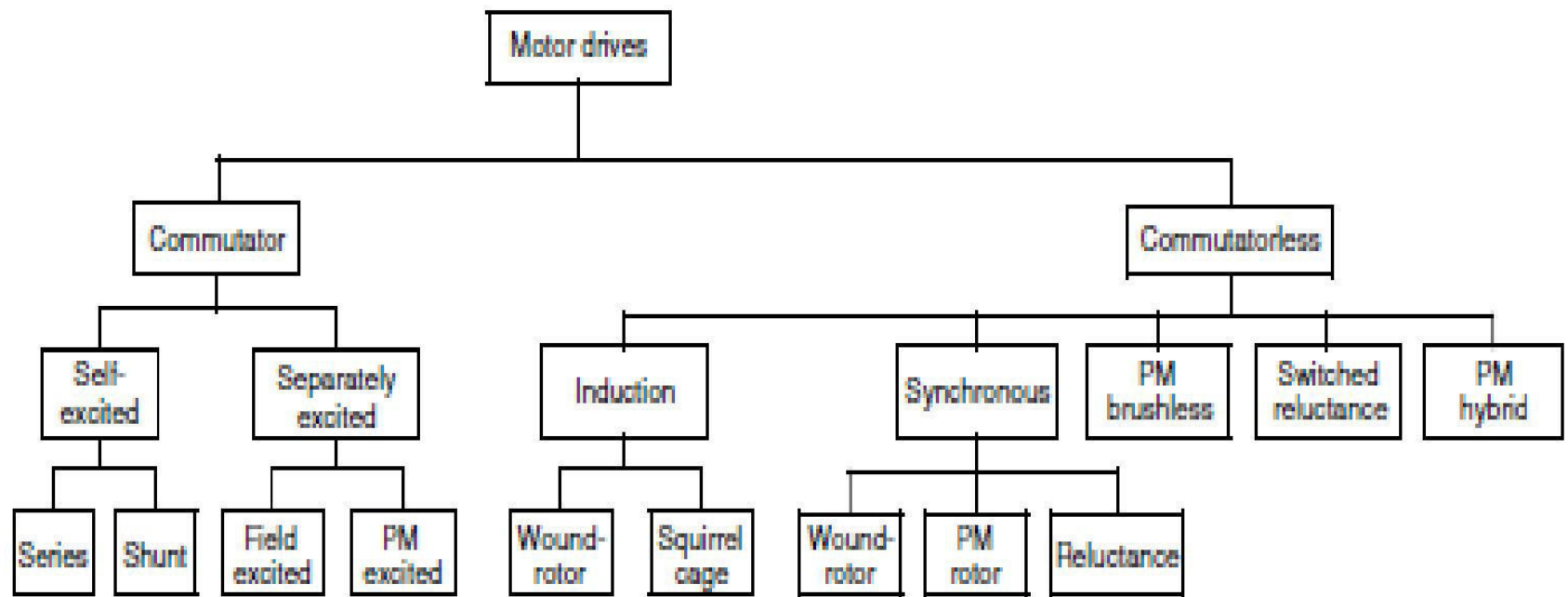
Electric motors can be categorized into two broad categories based on the kind of power source used for them:

AC Motors and DC Motors.

AC motors are generically powered using AC power sources(single phase or three phase) and are mostly used in Industrial and heavy duty applications where a lot of torque is required.

DC motors on the other hand are usually smaller and are used in battery (or plugged in DC sources) based applications where significantly less amount of work is required compared to AC motors.

The requirement for DC motors differs from one application to the other, as one application may require more torque and reduce speed while another may require more speed and reduced torque.



DC motors can be classified into three different categories as

1. Brushed DC Motor
2. Brushless DC Motors
3. Servo Motors.

Various types of Electric Motors used in Electric Vehicles

1. DC Series Motor
2. Brushless DC Motor
3. Permanent Magnet Synchronous Motor (PMSM)
4. Three Phase AC Induction Motors
5. Switched Reluctance Motors (SRM)

Factors to consider when selecting between the Brushless and Brushed DC Motors

1. Duty Cycle/ Service Life
2. Efficiency
3. Control/Actuation
4. Cost

DC Series Motor

High starting torque capability of the DC Series motor makes it a suitable option for traction application.

It was the most widely used motor for traction application in the early 1900s.

The advantages of this motor are easy speed control and it can also withstand a sudden increase in load.

The main drawback of DC series motor is high maintenance due to brushes and commutators.

Brushless DC Motors

Motors who do not adopt the use of brushes for commutation.

However, how the motor gets powered and how motion is achieved without brushes is the main aspect in this motors.



The armature which in the case of the brushed motor, rotates within the stator, is stationary in brushless motors and the permanent magnet, which in brushed motors is fixed, serves as the rotor in a brushless motor.



Stator for brushless DC motors is made up of coils while its rotor (to which the motor shaft is attached) is made up of a permanent magnet.

**Commutation algorithms for Brushless DC motors can be divided into two;
Sensor-based and senseless commutation.**

In sensor-based commutation, sensors (e.g hall sensor) are placed along the poles of the motor to provide feedback to the control circuitry to help it estimate rotor position. There are three popular algorithms employed for sensor-based commutation;

- ☐ Trapezoidal commutation
- ☐ Sinusoidal commutation
- ☐ Vector (or field-oriented) control.

Each of these control algorithm has its pros and cons and the algorithms can be implemented in different ways depending on the software and the design of the electronics hardware to make necessary changes.

In sensorless commutation on the other hand, instead of sensors being placed within the motors, the control circuitry is designed to measure the back EMF to estimate rotor position. This algorithm performs well and is at a reduced cost as the cost of the hall sensors is eliminated but its implementation is a lot more complex compared to the sensor based algorithms.

Permanent Magnet Synchronous Motor (PMSM)

- similar to BLDC motor which has permanent magnets on the rotor
- Similar to BLDC motors these motors also have traction characteristics like high power density and high efficiency.
- The difference is that PMSM has sinusoidal back EMF whereas BLDC has trapezoidal back
- Permanent Magnet Synchronous motors are available for higher power ratings.
- PMSM is the best choice for high performance applications like cars, buses.

Despite the high cost, PMSM is providing stiff competition to induction motors due to increased efficiency than the latter.

PMSM is also costlier than BLDC motors.

Most of the automotive manufacturers use PMSM motors for their hybrid and electric vehicles.

For example, Toyota Prius, Chevrolet Bolt EV, Ford Focus Electric, zero motorcycles S/SR, Nissan Leaf, Hinda Accord, BMW i3, etc use PMSM motor for propulsion.

Three Phase Induction Motors

The induction motors do not have a high starting torque like DC series motors under fixed voltage and fixed frequency operation. But this characteristic can be altered by using various control techniques like FOC or v/f methods.

By using these control methods, the maximum torque is made available at the starting of the motor which is suitable for traction application.

Squirrel cage induction motors have a long life due to less maintenance. Induction motors can be designed up to an efficiency of 92-95%.

Drawback of an induction motor is that it requires complex inverter circuit and control of the motor is difficult.

Merit: Adjusting the value of B in induction motors is easy when compared to permanent magnet motors. It is because in Induction motors the value of B can be adjusted by varying the voltage and frequency (V/f) based on torque requirements. This helps in reducing the losses which in turn improves the efficiency.

Induction motors are the preferred choice for performance oriented electric vehicles due to its cheap cost. The other advantage is that it can withstand rugged environmental conditions.

Switched Reluctance Motors (SRM)

Switched Reluctance Motors is a category of variable reluctance motor with double saliency. Switched Reluctance motors are simple in construction and robust. The rotor of the SRM is a piece of laminated steel with no windings or permanent magnets on it. This makes the inertia of the rotor less which helps in high acceleration.

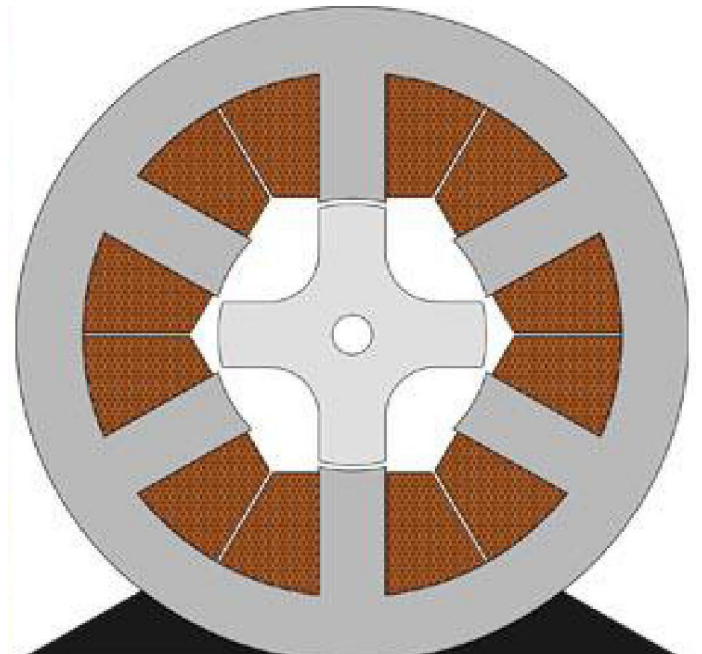
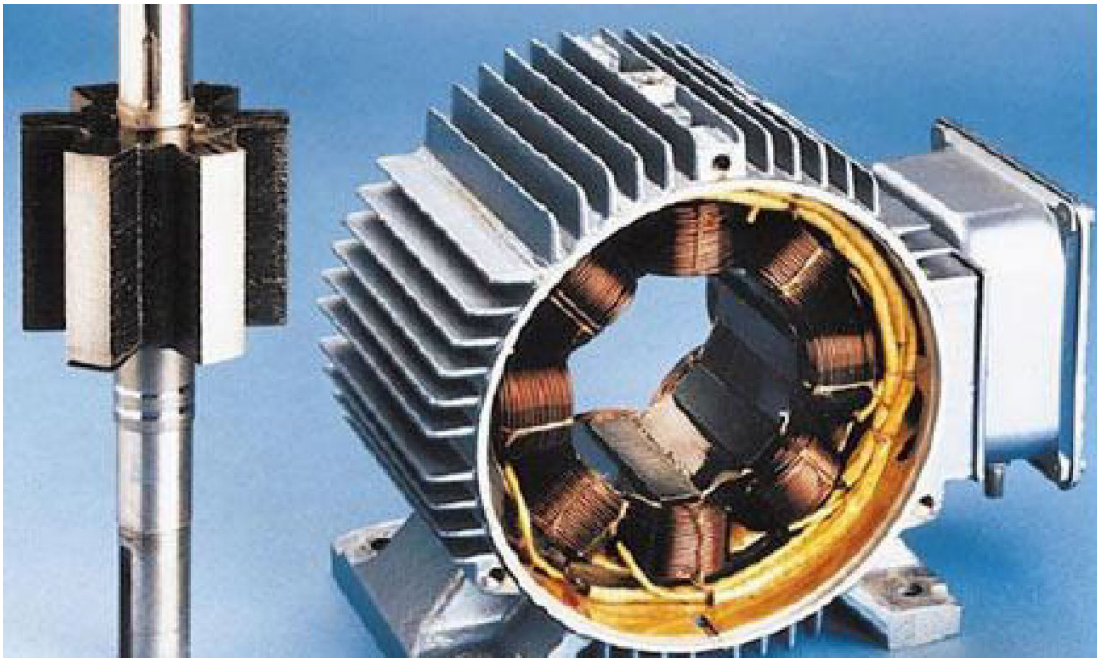
The robust nature of SRM makes it suitable for the high speed application. SRM also offers high power density which are some required characteristics of Electric Vehicles. Since the heat generated is mostly confined to the stator, it is easier to cool the motor.

Drawback of the SRM is

- Complexity in control and increase in the switching circuit.
It also has some noise issues.

Merit:

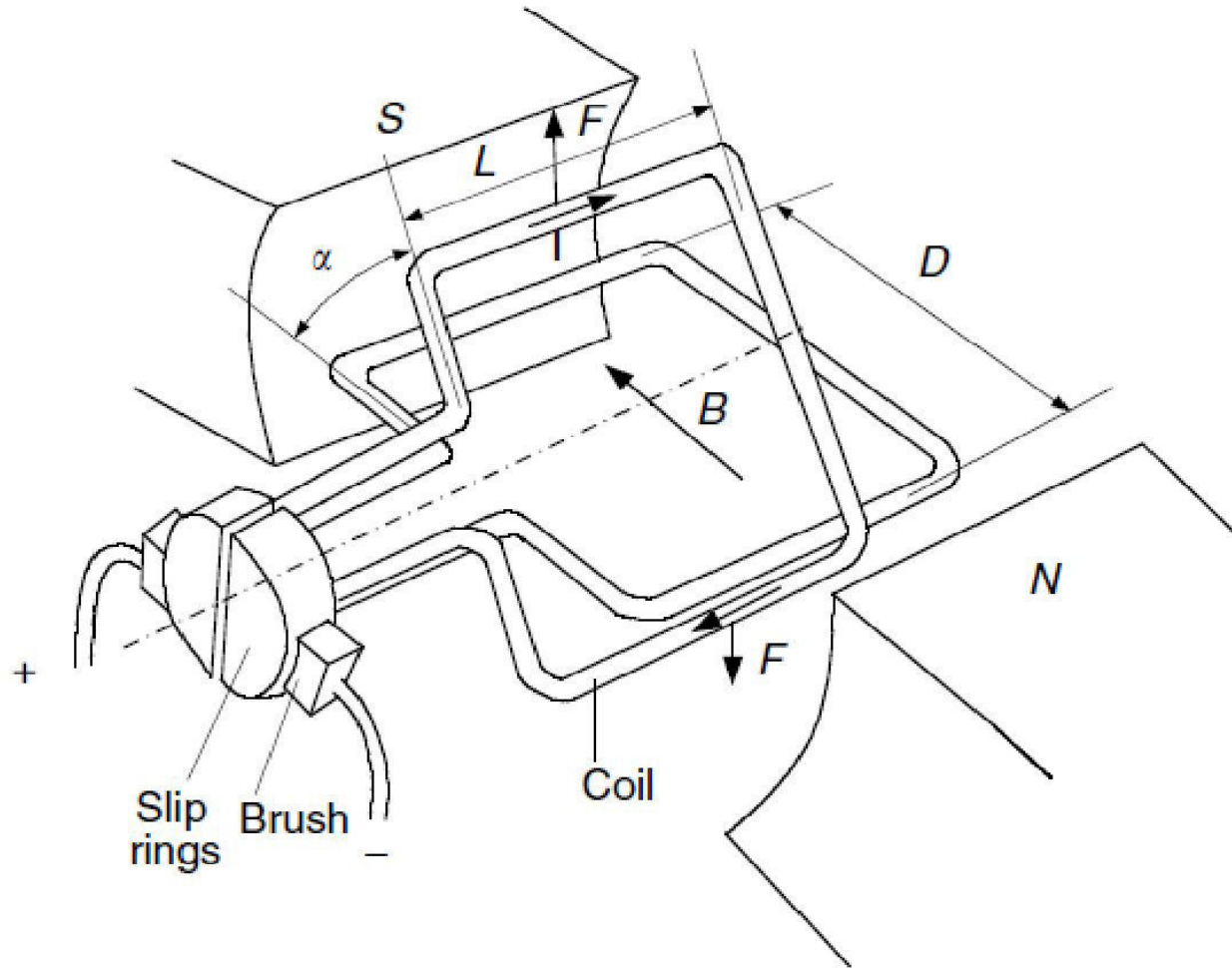
Once SRM enters the commercial market, it can replace the PMSM and Induction motors in the future.



DC Motor Drives

- ❖ Widely used in applications requiring adjustable speed, good speed regulation, and frequent starting, braking and reversing.
- ❖ Various DC motor drives have been widely applied to different electric traction.

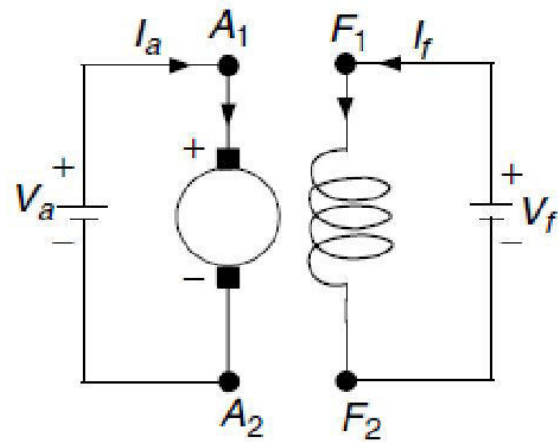
Principle of Operation



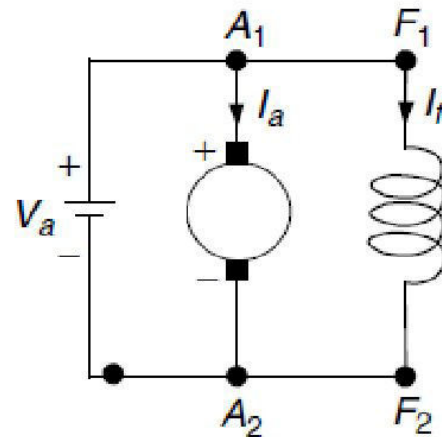
$$F = BIL$$

$$T = BIL \cos \alpha$$

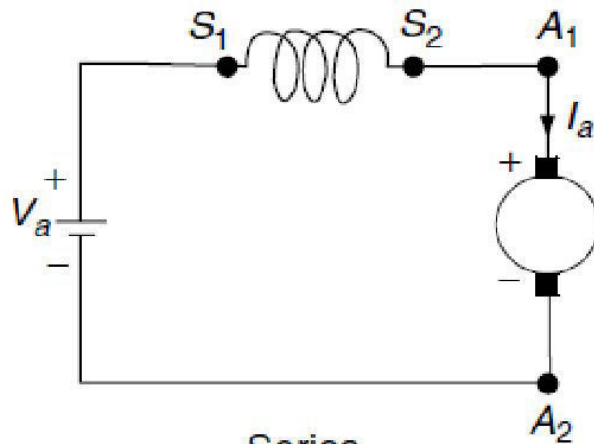
where α is the angle between the coil plane and magnetic field



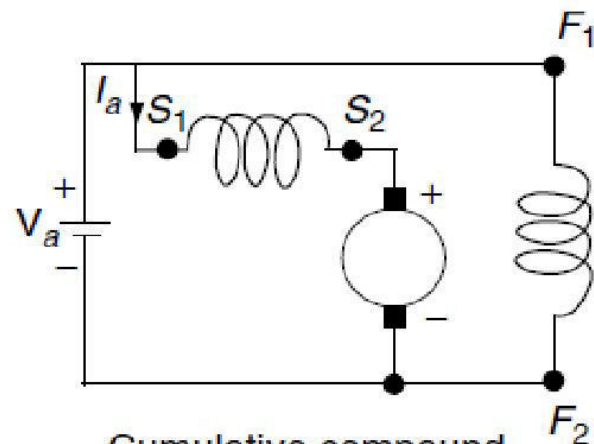
Separately



Shunt

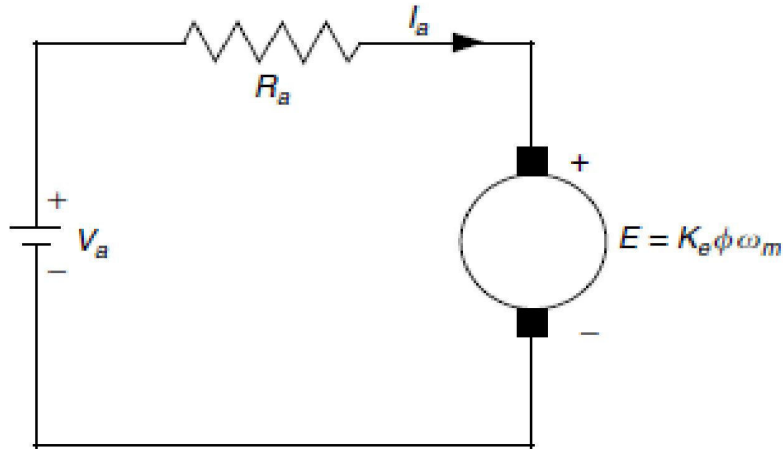


Series



Cumulative compound

Basic equations of a DC motor are



$$V_a = E + R_a I_a, \quad E = K_e \phi \omega_m$$

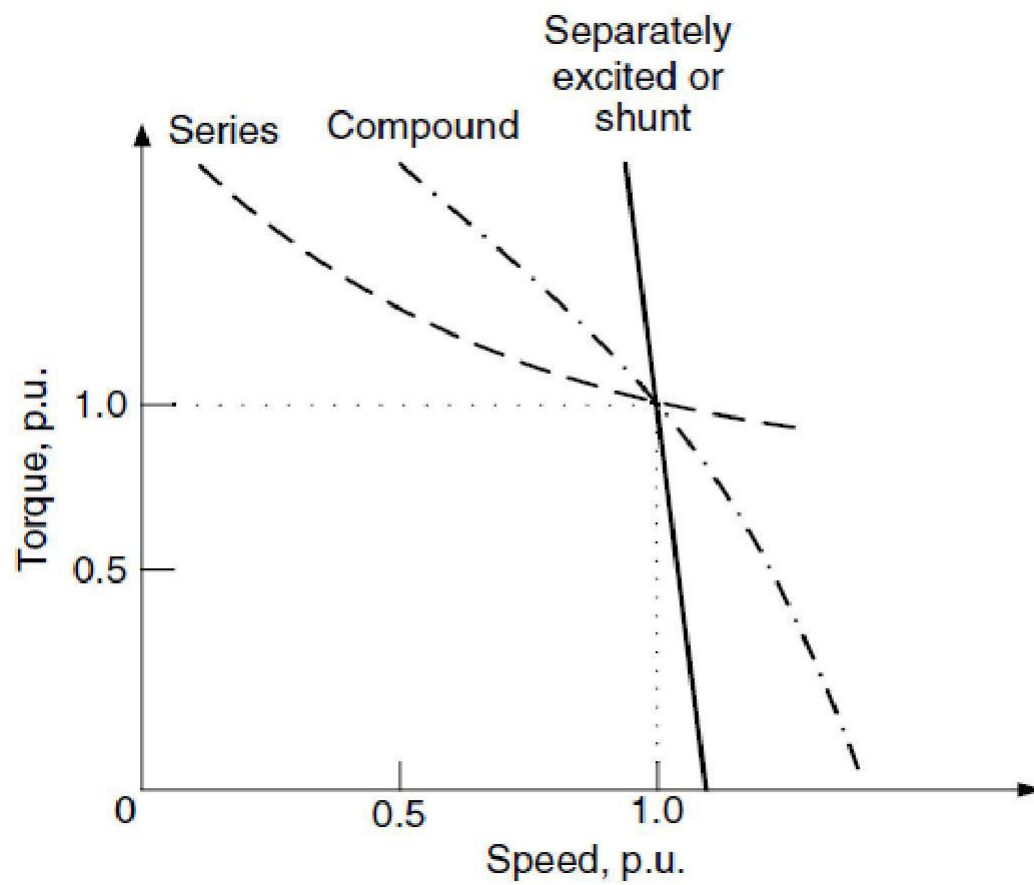
$$T = K_e \phi I_a$$

$$T = \frac{K_e \phi}{R_a} V - \frac{(K_e \phi)^2}{R_a} \omega_m$$

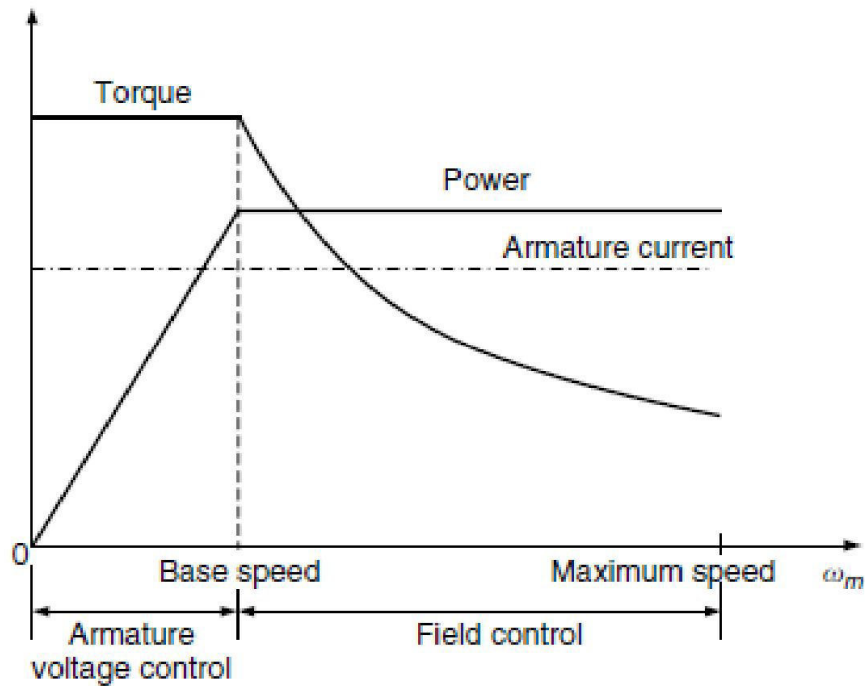
In the case of series motors, the flux is a function of armature current

$$\phi = K_f I_a$$

$$T = \frac{K_e K_f V_a^2}{(R_a + K_e K_f \omega_m)^2}$$



Combined Armature Voltage and Field Control

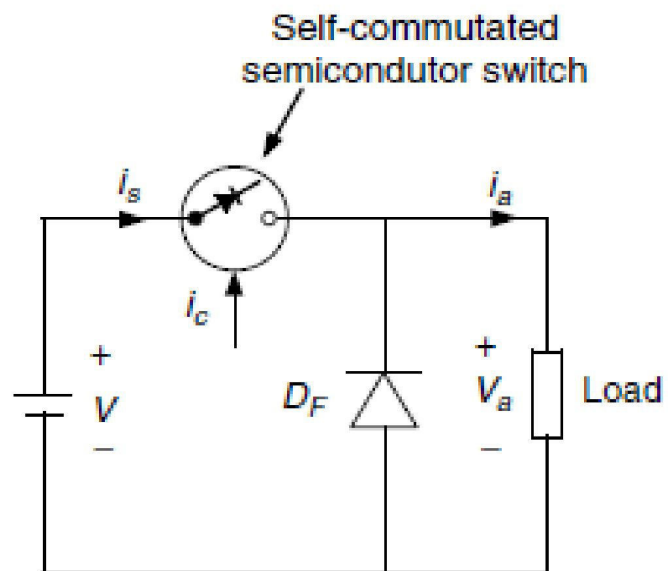


In EV and HEV applications, the most desirable speed–torque characteristic is to have a constant torque below a certain speed (base speed), with the torque dropping parabolically with the increase of speed (constant power) in the range above the base speed,

- In the range of lower than base speed, the armature current and field are set at their rated values, producing the rated torque.
- From equations , it is clear that the armature voltage must be increased proportionally with the increase of the speed.
- At the base speed, the armature voltage reaches its rated value (equal to the source voltage) and cannot be increased further.
- In order to further increase the speed, the field must be weakened with the increase of the speed, and then the back EMF E and armature current must be maintained constant.
- The torque produced drops parabolically with the increase in the speed and the output power remains constant

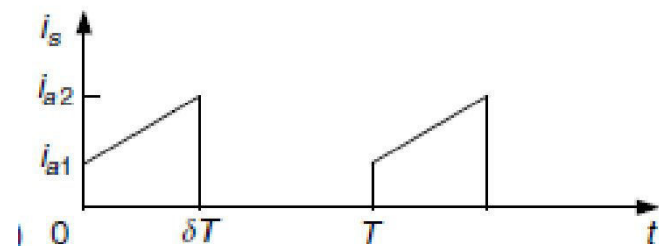
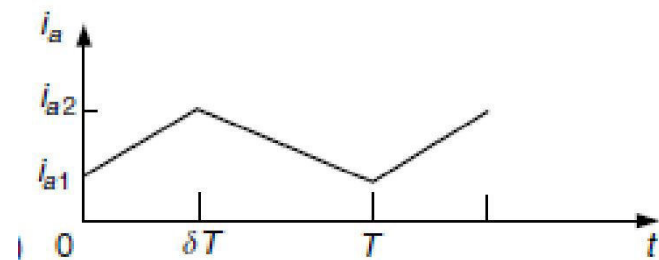
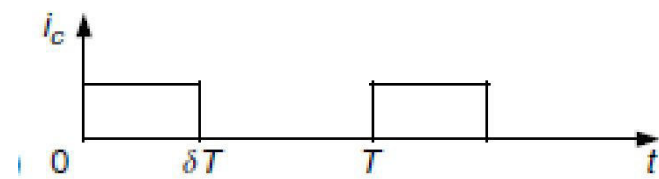
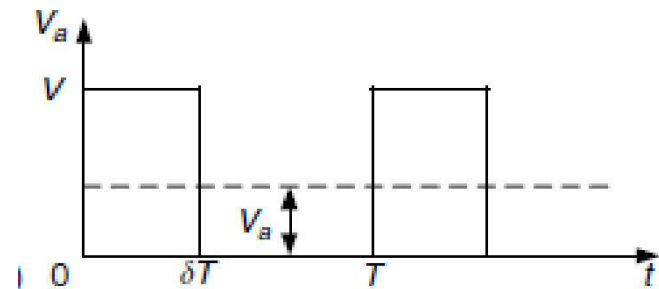
Chopper Control of DC Motors

- Choppers are used for the control of DC motors because of a number of advantages such as high efficiency, flexibility in control, light weight, small size, quick response, and regeneration down to very low speeds.
- Presently, the separately excited DC motors are usually used in traction, due to the control flexibility of armature voltage and field.
- For a DC motor control in open-loop and closed-loop configurations, the chopper offers a number of advantages due to its high operation frequency.



basic chopper circuit

$$V_a = \frac{1}{T} \int_0^T v_a dt = \frac{1}{T} \int_0^{\delta T} V dt = \delta V$$



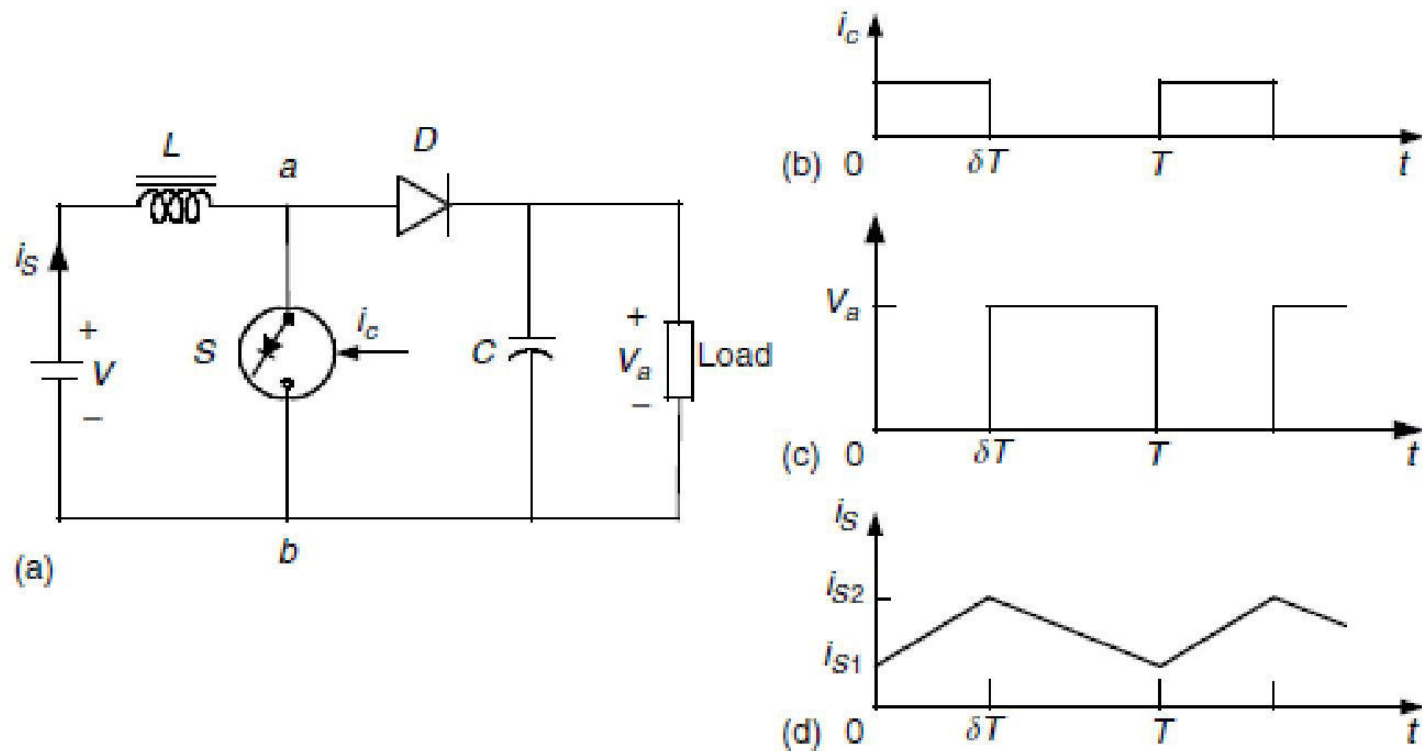
waveforms

The control technologies can be divided into the following categories:

1. Time ratio control (TRC).
2. Current limit control (CLC).

In TRC, also known as pulse width control, the ratio of on time to chopper period is controlled. The TRC can be further divided as follows:

1. Constant frequency TRC: The chopper period T is kept fixed and the on period of the switch is varied to control the duty ratio δ .
2. Varied frequency TRC: Here, δ is varied either by keeping t_{on} constant and varying T or by varying both t_{on} and T .

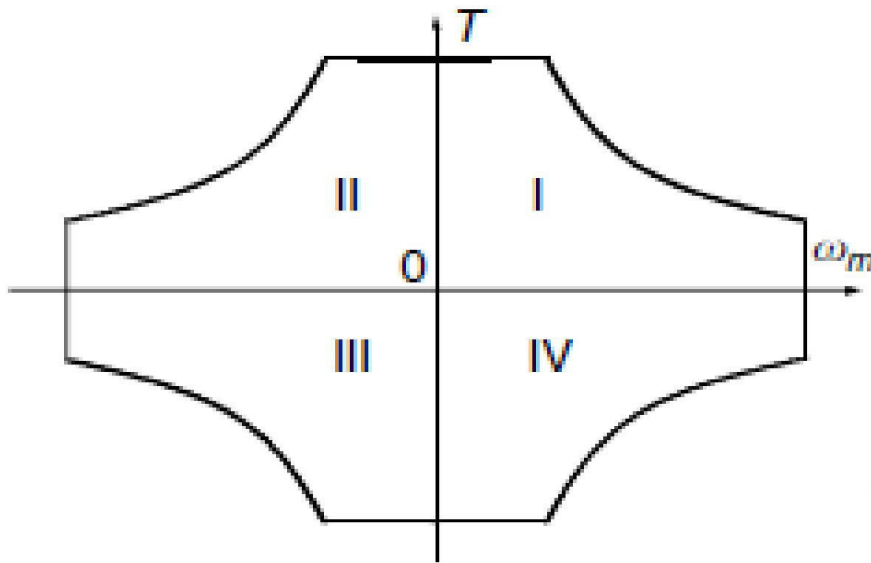


Principle of operation of a step-up (or class B) chopper: (a) basic chopper circuit; (b) to (d) waveforms

$$V_{ab} = \frac{1}{T} \int_0^T v_{ab} dt = V_a(1 - \delta).$$

$$V = V_a(1 - \delta) \text{ or } V_a = \frac{V}{1 - \delta}.$$

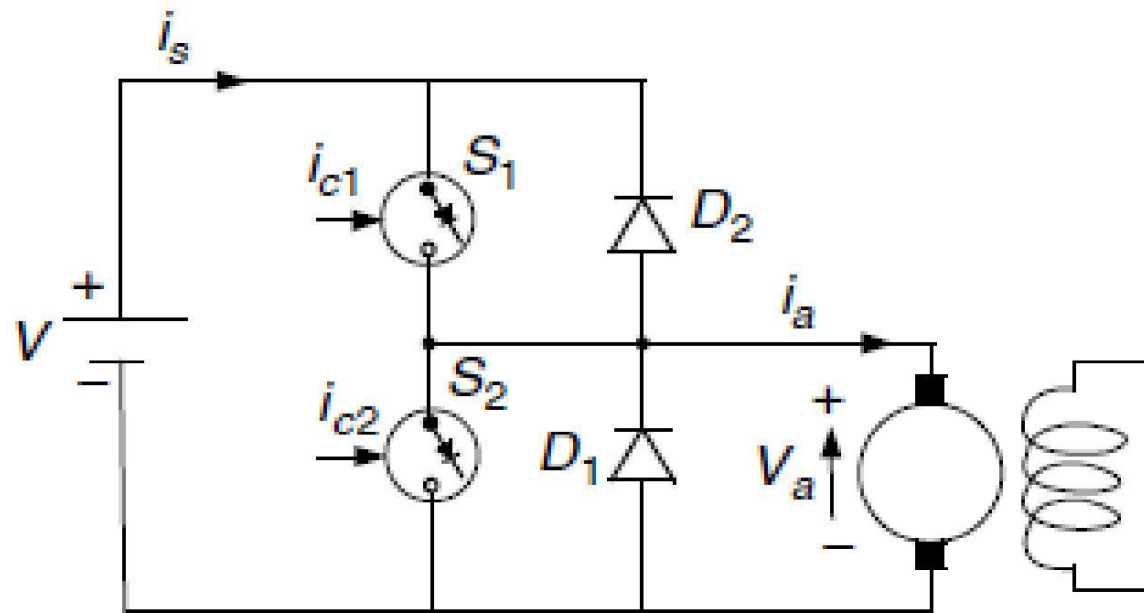
Multiquadrant Control of Chopper-Fed DC Motor Drives

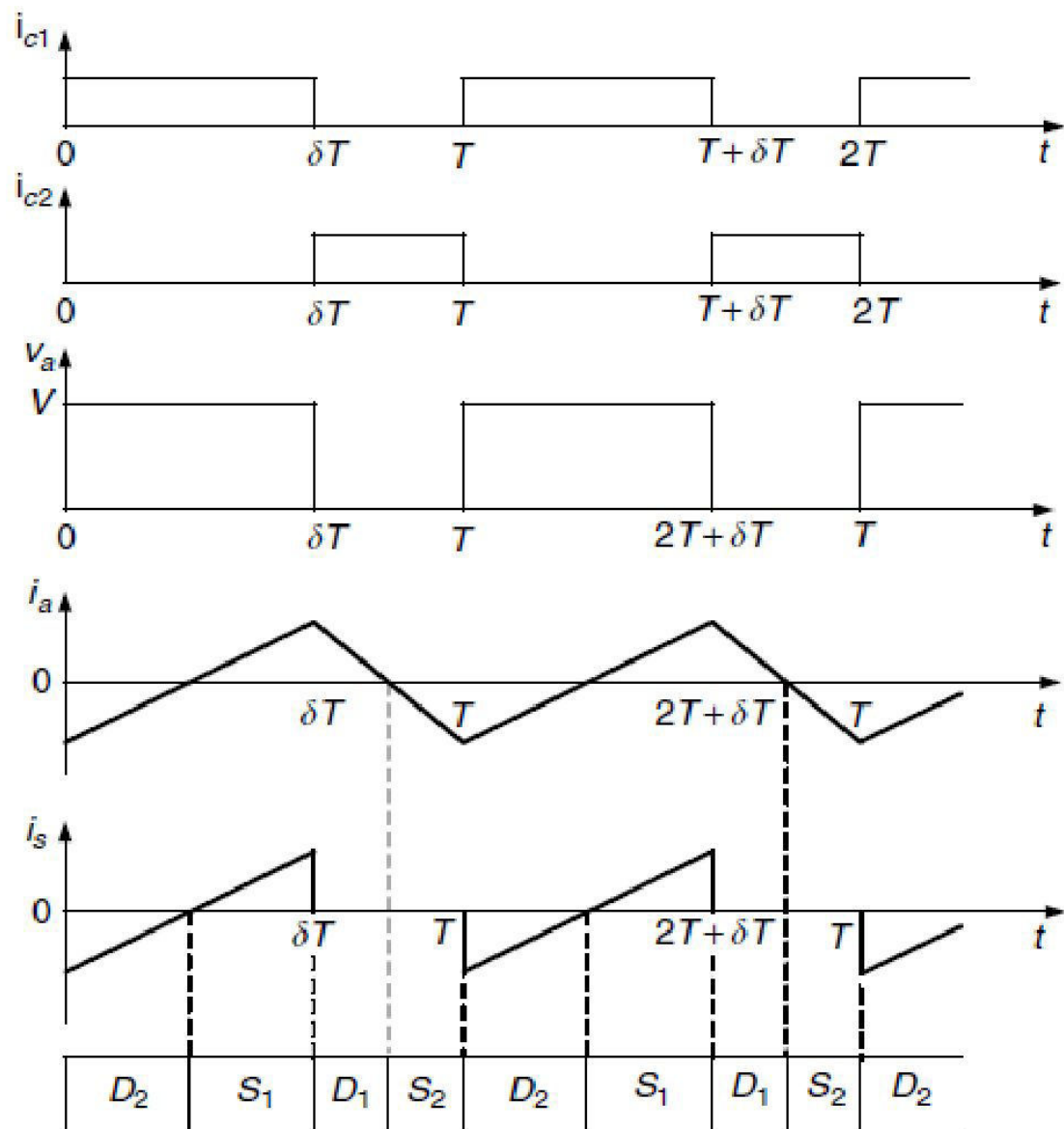


The application of DC motors on EVs and HEVs requires the motors to operate in multiquadrants, including forward motoring, forward braking, backward motoring, and backward braking

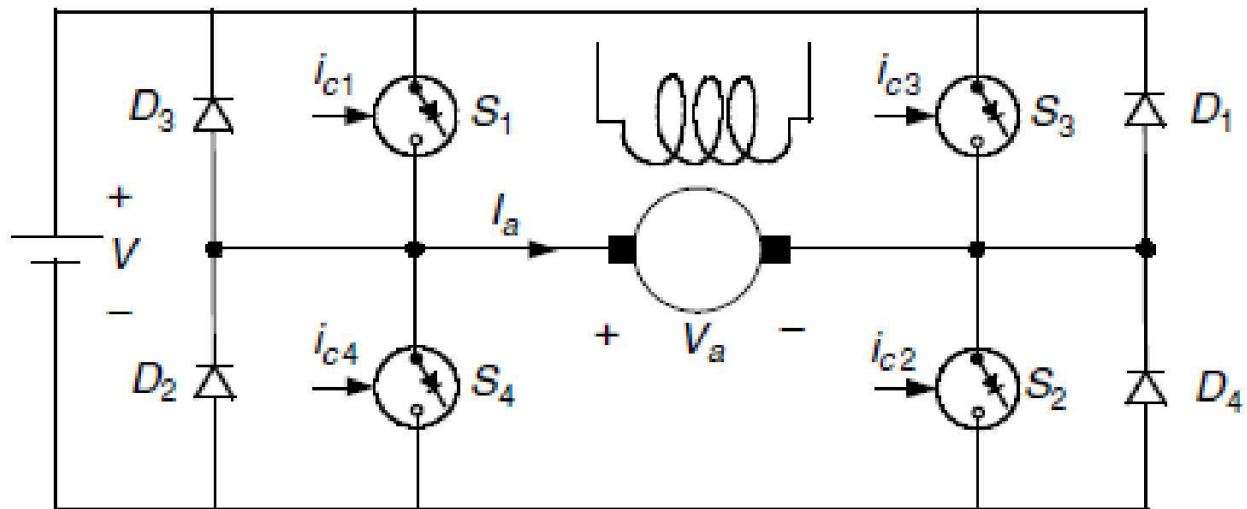
For vehicles with reverse mechanical gears, two-quadrant operation (forward motoring and forward braking, or quadrant I and quadrant IV) is required. However, for vehicles without reverse mechanical gears, four-quadrant operation is needed.

Class C Two-Quadrant Chopper

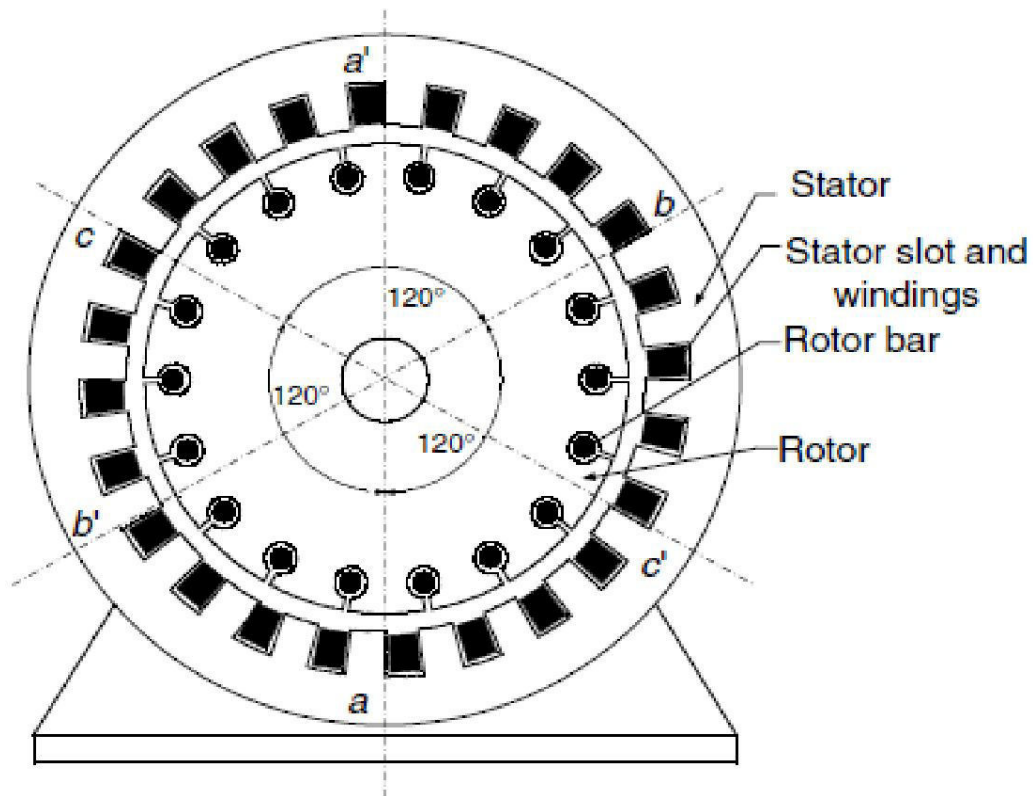




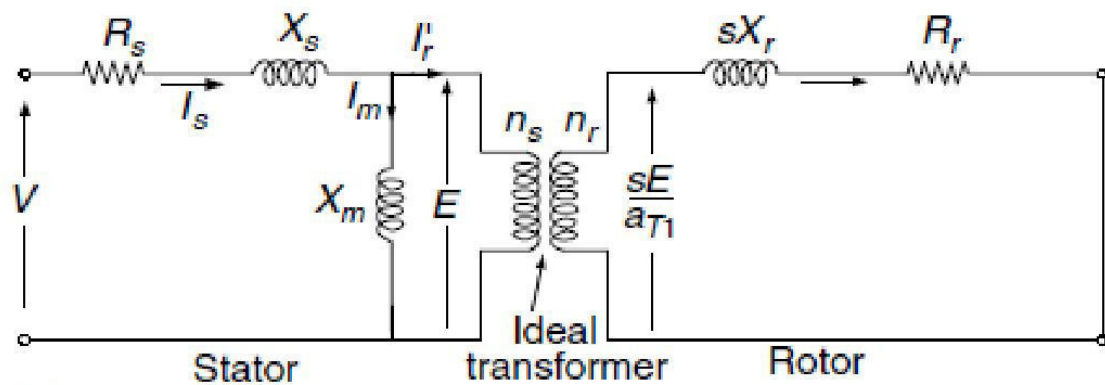
Four-Quadrant Operation



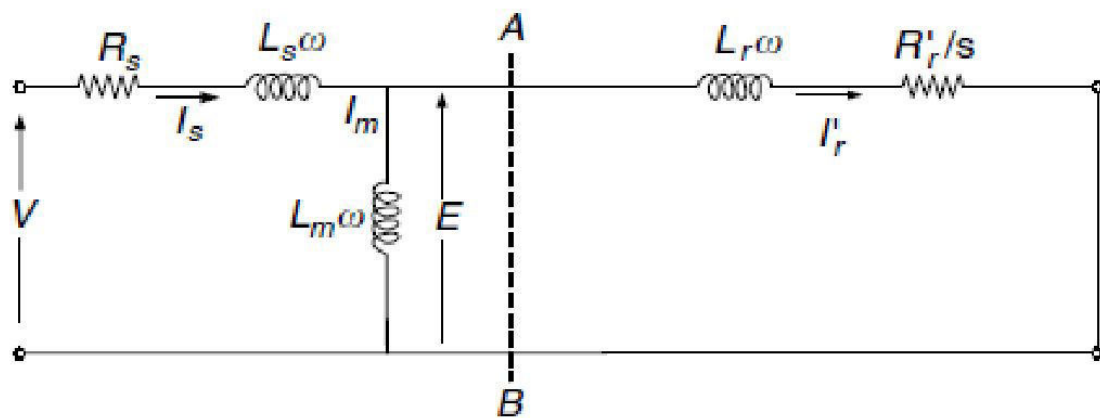
Induction Motor Drives



$$s = \frac{\omega_{ms} - \omega_m}{\omega_{ms}} = \frac{\omega_{sl}}{\omega_{ms}}$$



(a)



(b)

$$R'_r = a_{T1}^2 R_r \quad \text{and} \quad X'_r = a_{T1}^2 X_r.$$

$$Z_s = R_s + jL_s\omega,$$

$$Z_m = jL_m\omega,$$

$$Z_r = \frac{R'_r}{s} + jL_r\omega.$$

The driving-point impedance of the circuit is

$$Z = Z_s + \frac{Z_m Z_r}{Z_m + Z_r}.$$

Hence, the current I_s and I'_r can be calculated as

$$I_s = \frac{V}{Z}$$

and

$$I'_r = \frac{Z_m}{Z_m + Z_r} I_s.$$

The total electrical power supplied to the motor for three phase is

$$P_{elec} = 3I_r'^2 \frac{R_r'}{s}.$$

The mechanical power of the rotor can be obtained by subtracting the total power loss in the stator as

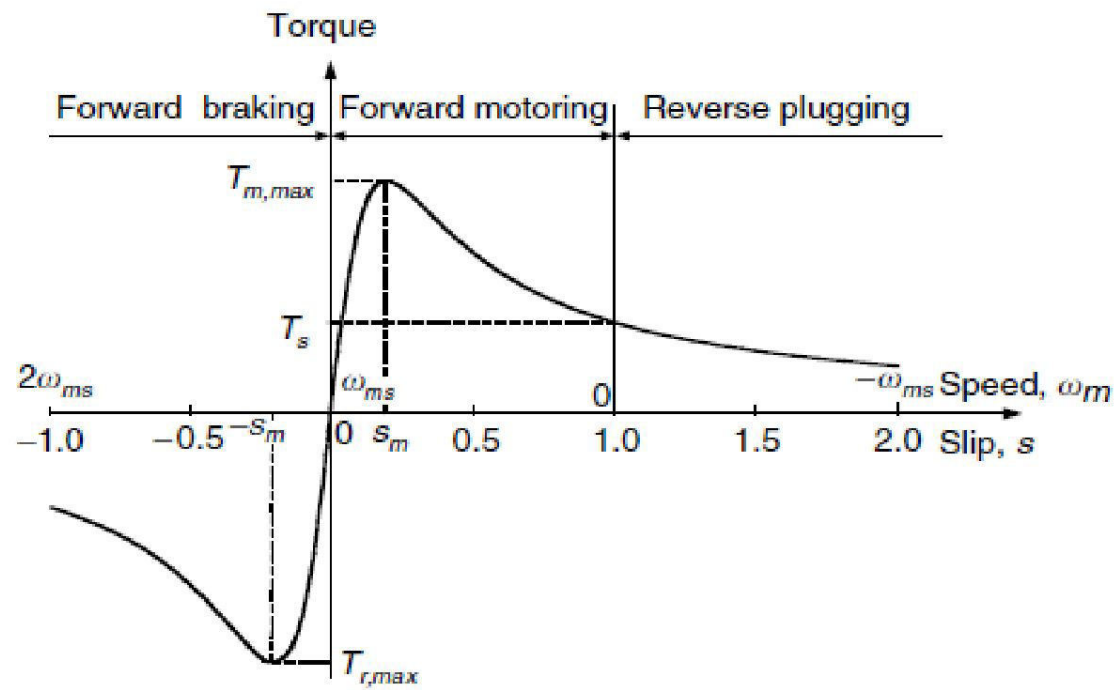
$$P_{mech} = P_{elec} - 3I_r'^2 R_r'.$$

The angular velocity of the rotor, ω_m , is

$$\omega_m = \frac{2}{p} \omega (1-s).$$

The torque developed by the motor can be determined by

$$T = \frac{P_{mech}}{\omega_m}.$$



Constant Volt/Hertz Control

For traction application, the torque–speed characteristic of an induction motor can be varied by simultaneously controlling the voltage and frequency, which is known as constant volt/hertz control.

From Equivalent ckt, the field current I_m should be kept constant and equal to its rated value. That

$$I_{mr} = \frac{E}{X_m} = \frac{E_{rated}}{\omega_r L_m}$$

The rotor current can be calculated as

$$I_r' = \frac{(\omega/\omega_r)E_{rated}}{jL_r\omega + R_r'/s}$$

The torque produced can be obtained as

$$T = \frac{3}{\omega} I_r'^2 R_r' / s = \frac{3}{\omega} \left[\frac{(\omega / \omega_r)^2 E_{rated}^2 R_r' / s}{(R_r' / s)^2 + (L_r \omega)^2} \right]$$

The slip s_m corresponding to the maximum torque is

$$s_m = \pm \frac{R_r'}{L_r \omega}.$$

And then, the maximum torque is

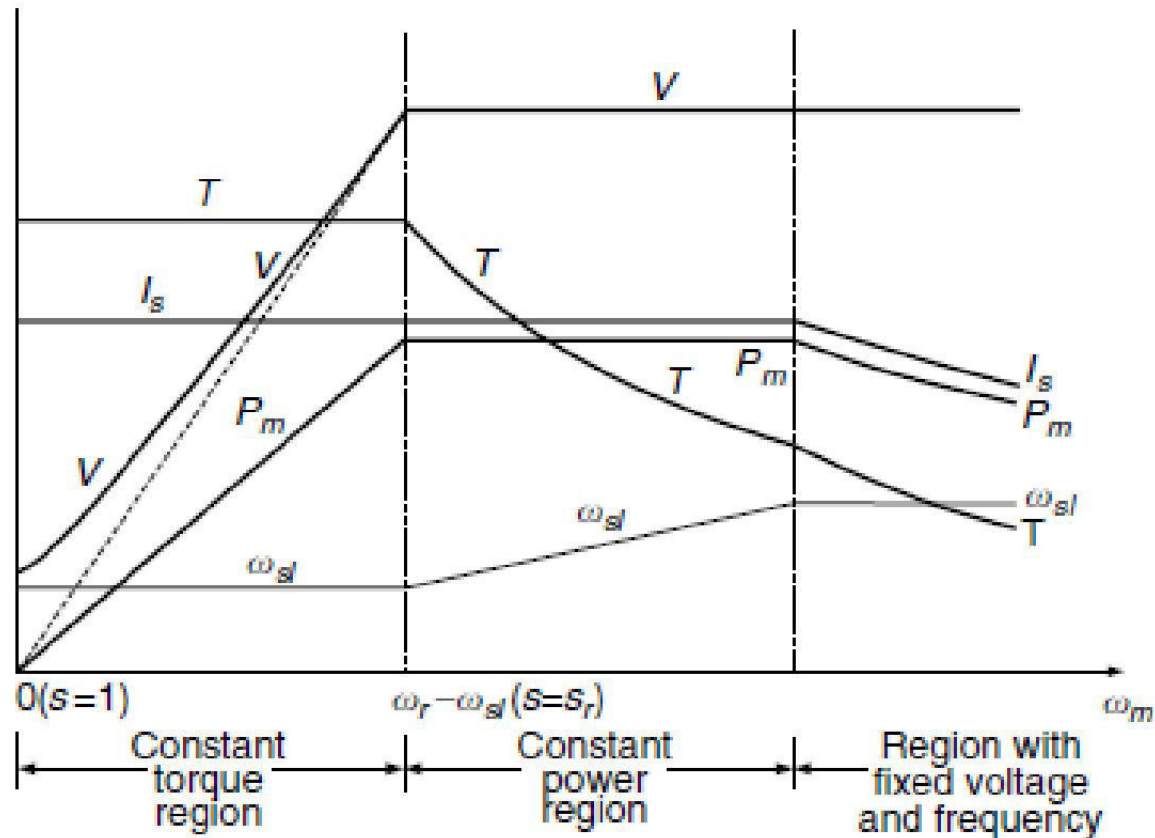
$$T_{max} = \frac{3}{2} \frac{E_{rated}^2}{L_r \omega_r^2}.$$

When motor speed is beyond its rated speed, the voltage reaches its rated value and cannot be increased with the frequency.

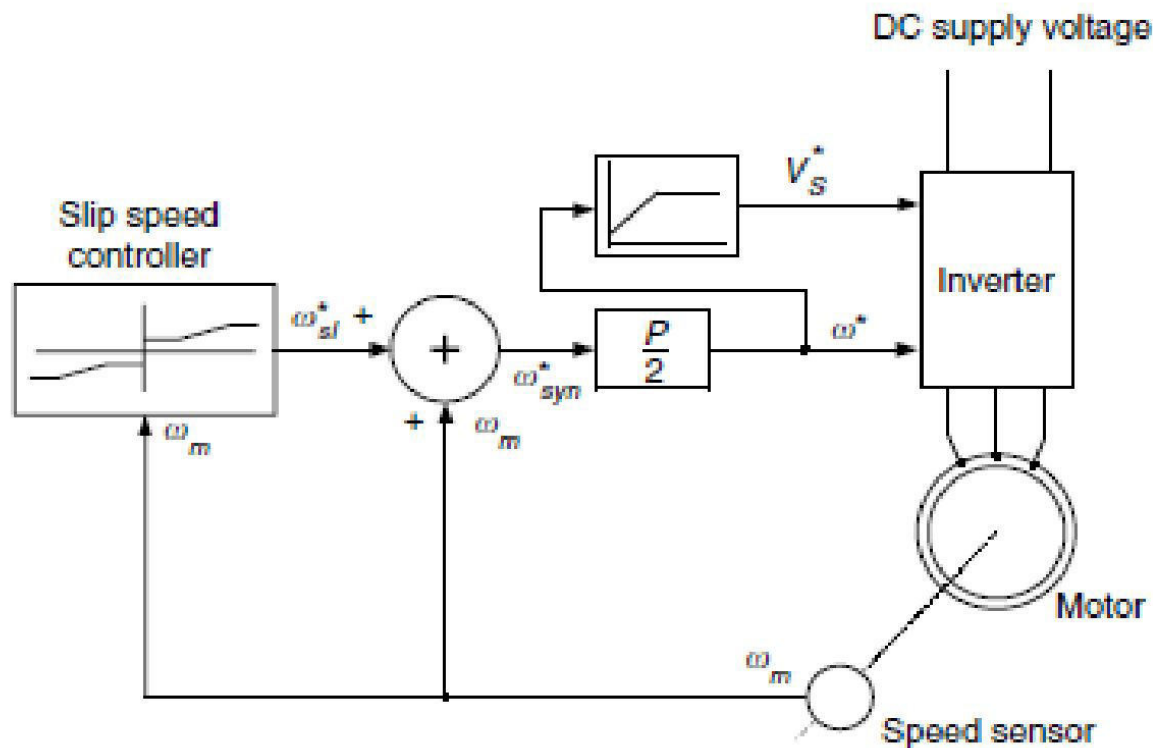
In this case, the voltage is fixed to its rated value and the frequency continuously increases with the motor speed.

The motor goes into the field weakening operation. The slip s is fixed to its rated value corresponding to the rated frequency, and the slip speed $\omega_{s/}$ increases linearly with motor speed. This control approach results in constant power operation

Operating variables varying with motor speed



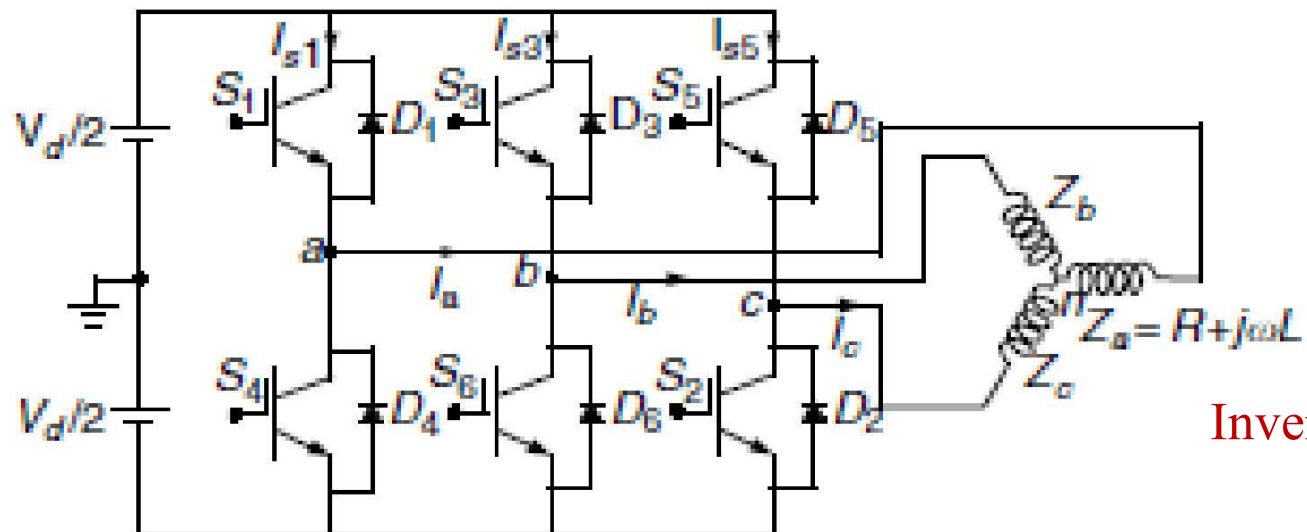
General configuration of constant V/f control



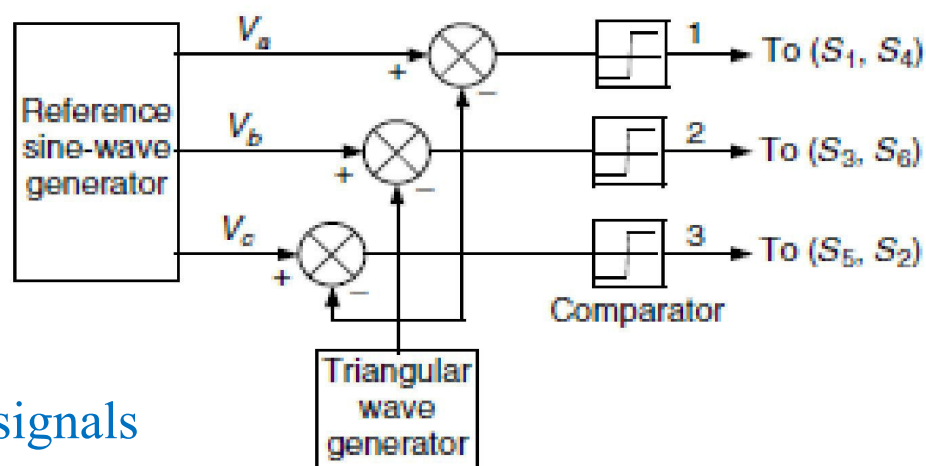
In traction application, speed control in a wide range is usually required and the torque demand in the high-speed range is low.

Control beyond constant power range is required.

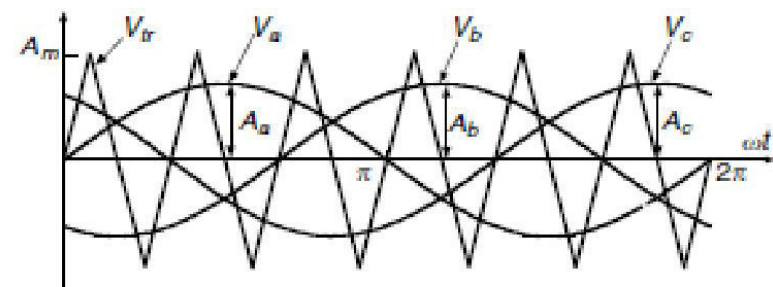
To prevent the torque from exceeding the breakdown torque, the machine is operated at a constant slip speed and the machine current and power are allowed to decrease



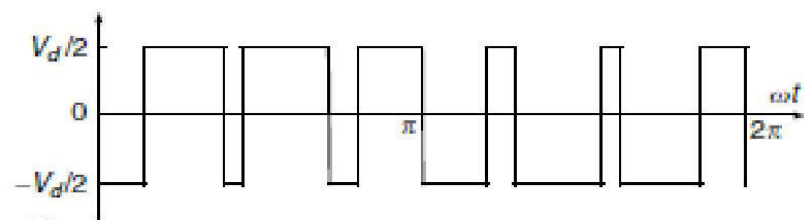
Inverter topology



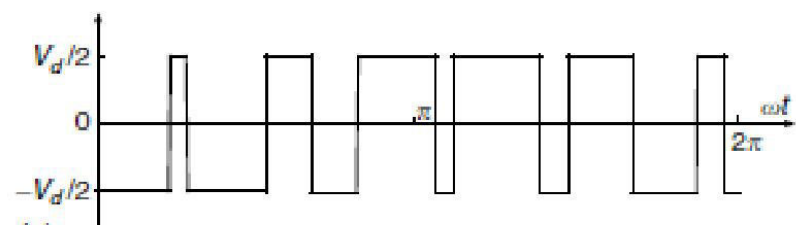
control signals



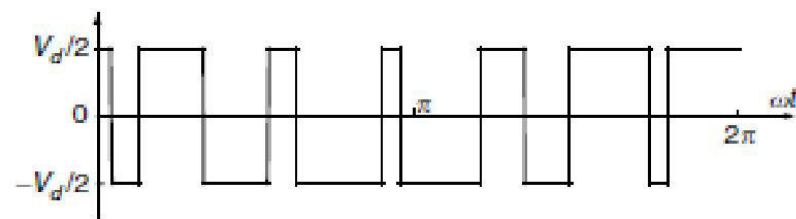
(c)



(d)



(e)



(f)

PERMANENT MAGNET MACHINES

Machines that use magnets to produce air-gap magnetic flux instead of field coils, as in DC commutator machines, or the magnetizing component of stator current, as in induction machines, are permanent magnet (PM) machines.

PM machines can be broadly classified into two categories:

- Synchronous machines (PMSMs): These machines have a uniformly rotating stator field as in induction machines. Induced waveforms are sinusoidal, and hence, dq transformation and vector control are possible.
- Trapezoidal or square-wave machines: These are also known as brushless DC or electronically commutated machines. Induced voltages are trapezoidal in nature. The stator field is switched in discrete steps with squarewave pulses.

Permanent Magnetic Brush-Less DC Motor Drives

A permanent magnet motor drive can be potentially designed with high power density, high speed, and high operation efficiency.

The major advantages of BLDC motor include:

High efficiency: BLDC motors are the most efficient of all electric motors. This is due to the use of permanent magnets for the excitation, which consume no power. The absence of a mechanical commutator and brushes means low mechanical friction losses and therefore higher efficiency.

Compactness: The recent introduction of high-energy density magnets (rare-earth magnets) has allowed achieving very high flux densities in the BLDC motor. This makes it possible to achieve accordingly high torques, which in turns allows making the motor small and light.

Ease of control: The BLDC motor can be controlled as easily as a DC motor because the control variables are easily accessible and constant throughout the operation of the motor.

- **Ease of cooling:** There is no current circulation in the rotor. Therefore, the rotor of a BLDC motor does not heat up. The only heat production is on the stator, which is easier to cool than the rotor because it is static and on the periphery of the motor.
- **Low maintenance, great longevity, and reliability:** The absence of brushes and mechanical commutators suppresses the need for associated regular maintenance and suppresses the risk of failure associated with these elements. The longevity is therefore only a function of the winding insulation, bearings, and magnet life-length.
- **Low noise emissions:** There is no noise associated with the commutation because it is electronic and not mechanical. The driving converter switching frequency is high enough so that the harmonics are not audible.

BLDC motor drives also suffer from some disadvantages such as:

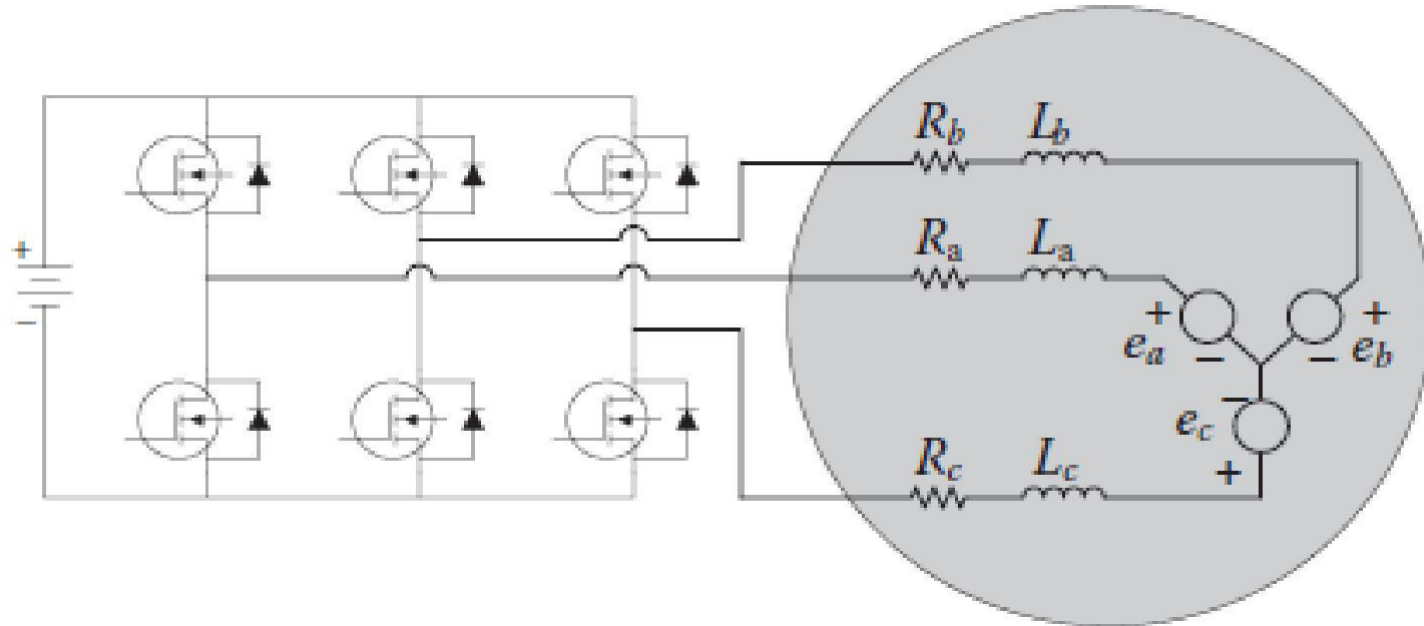
- **Cost:** Rare-earth magnets are much more expensive than other magnets and result in an increased motor cost.
- **Limited constant power range:** A large constant power range is crucial to achieving high vehicle efficiencies. The permanent magnet BLDC motor is incapable of achieving a maximum speed greater than twice the base speed.
- **Safety:** Large rare-earth permanent magnets are dangerous during the construction of the motor because they may attract flying metallic objects toward them. In case of vehicle wreck, if the wheel is spinning freely, the motor is still excited by its magnets and high voltage is present at the motor terminals that can possibly endanger the passengers or rescuers.

- Magnet demagnetization: Magnets can be demagnetized by large opposing mmfs and high temperatures. The critical demagnetization force is different for each magnet material. Great care must be exercised when cooling the motor, especially if it is built compact.
- High-speed capability: The surface-mounted permanent magnet motors cannot reach high speeds because of the limited mechanical strength of the assembly between the rotor yoke and the permanent magnets.
- Inverter failures in BLDC motor drives: Because of the permanent magnets on the rotor, BLDC motors present major risks in case of short circuit failures of the inverter. Indeed, the rotating rotor is always energized and constantly induces an EMF in the shortcircuited windings.

FUNDAMENTALS OF AC MOTOR CONTROL

- ❖ brushless DC (BLDC) machine (trapezoidal back EMF) control
- ❖ permanent magnet synchronous machines (PMSMs) called as brushless AC (BLAC) (sinusoidal back EMF) control

Fundamentals of BLDC machine torque Control

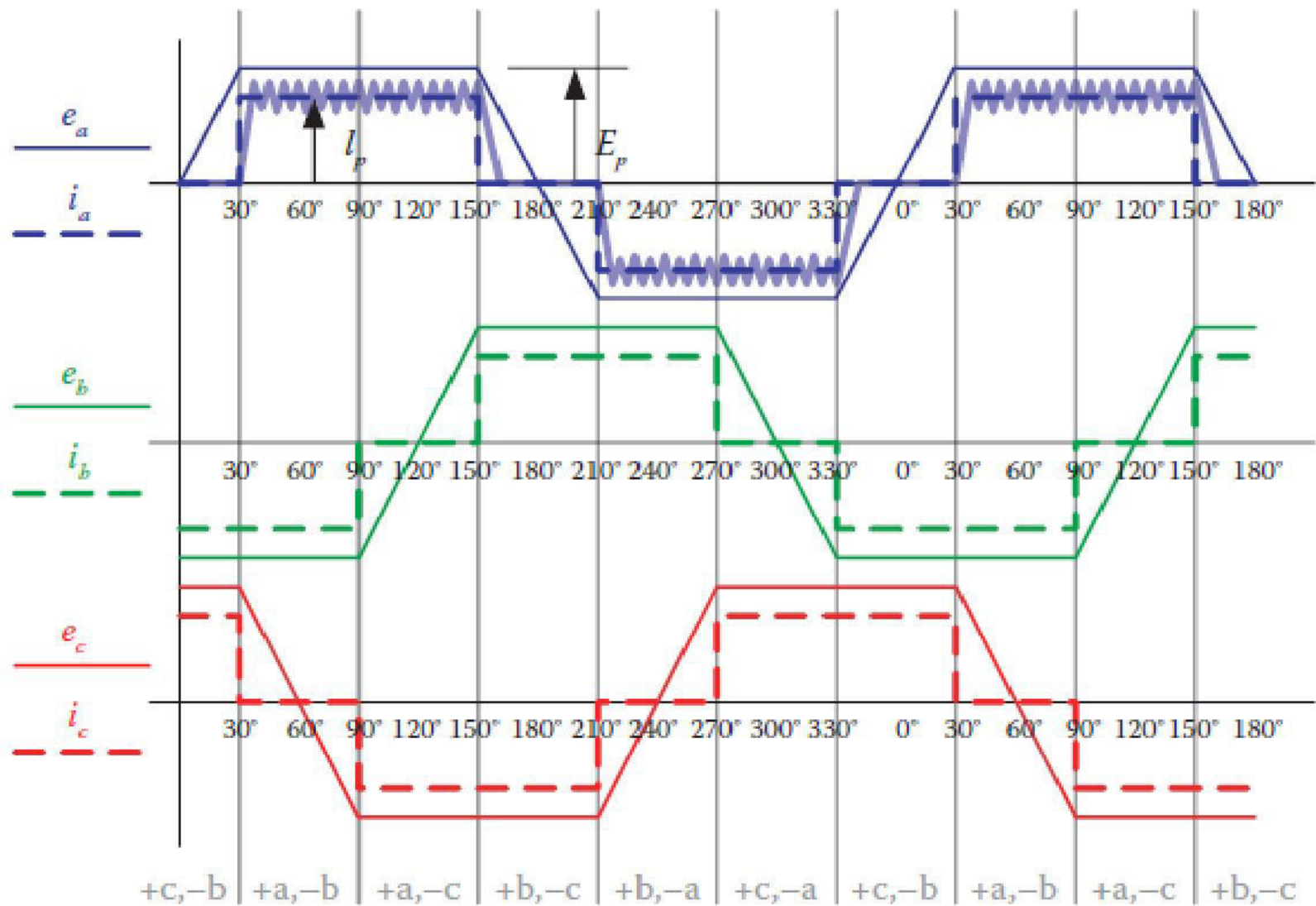


Equivalent circuit diagram of BLDC with inverter bridge

Typical BLDC machine has the PMs on the rotor (still producing the field) and has the armature windings on the stator that are electronically commutated through the inverter bridge.

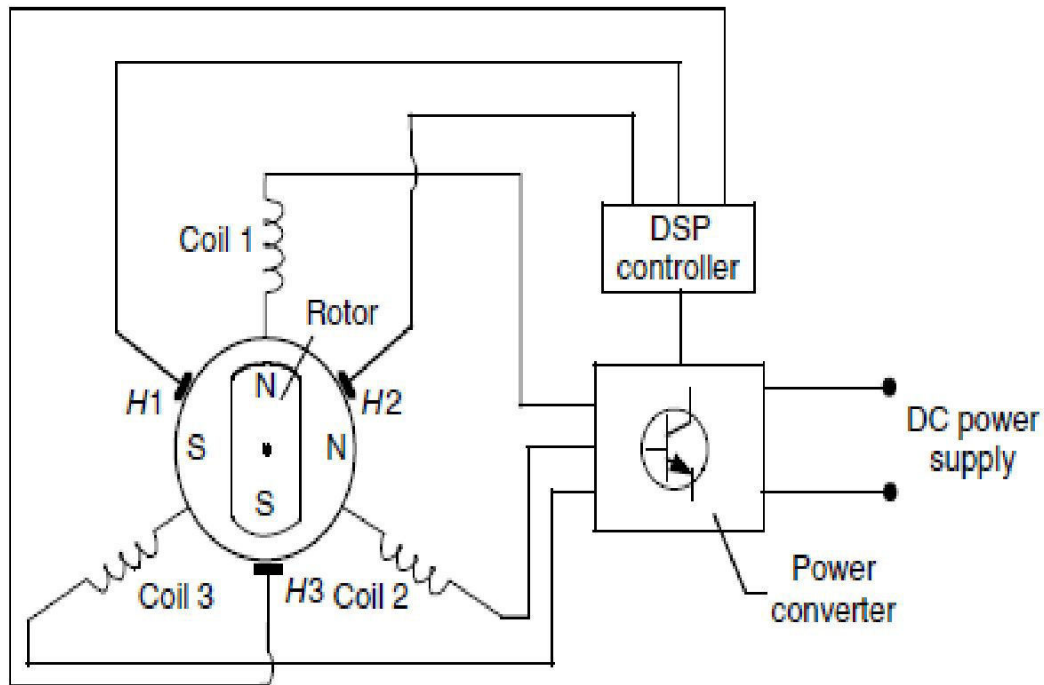
The BLDC machine operates by applying voltage and regulating current in two of the three phases at any one time. The third phase is open circuited during this time.

The machine is commutated between phases every 60 electrical degrees. Each phase is on for 120 electrical degrees



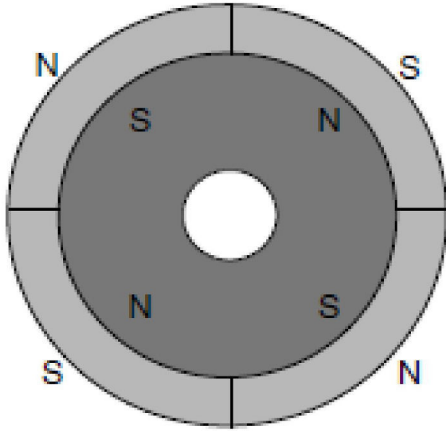
Voltage and current waveforms in a BLDC

Basic Principles of BLDC Motor Drives



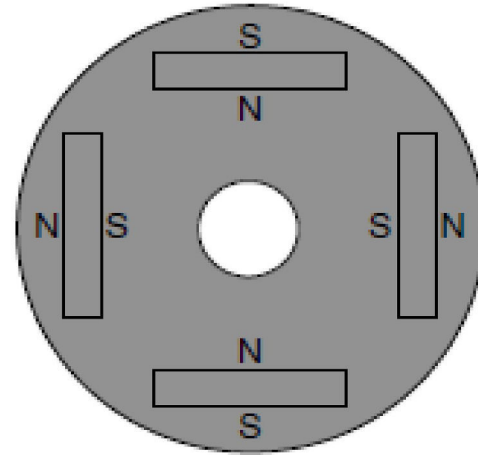
A BLDC motor drive consists mainly of the brush-less DC machine, a DSPbased controller, and a power electronics-based power converter, as shown in Figure. Position sensors $H1$, $H2$, and $H3$ sense the position of the machine rotor. The rotor position information is fed to the DSP-based controller, which, in turn, supplies gating signals to the power converter by turning on and turning off the proper stator pole windings of the machine. In this way, the torque and speed of the machines are controlled.

BLDC Machine Construction and Classification



surface-mounted PM rotor

Each permanent magnet is mounted on the surface of the rotor. It is easy to build, and specially skewed poles are easily magnetized on this surface-mounted type to minimize cogging torque. But there is a possibility that it will fly apart during high-speed operations.



interior-mounted PM rotor

Each permanent magnet is mounted inside the rotor. It is not as common as the surface-mounted type but it is a good candidate for high-speed operations.

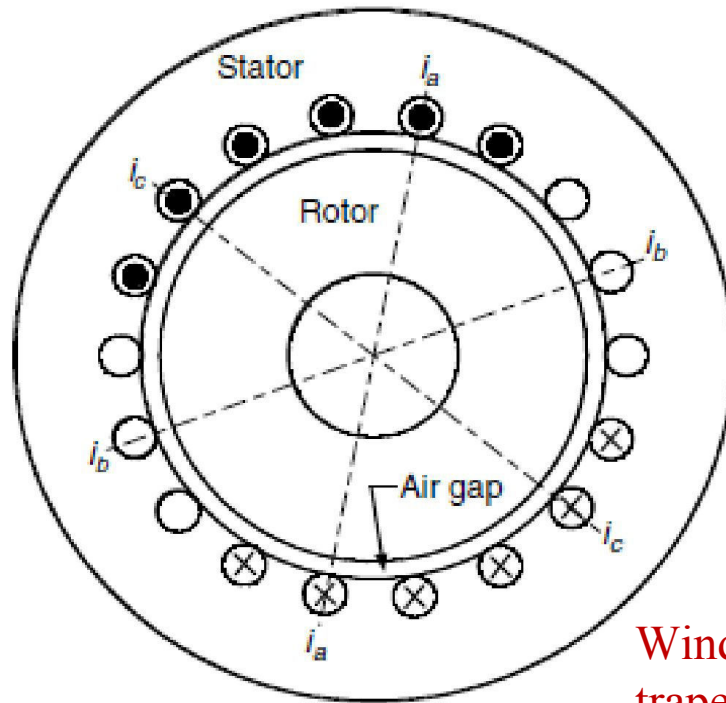
In the case of the stator windings, there are two major classes of BLDC motor drives, both of which can be characterized by the shapes of their respective back EMF waveforms: trapezoidal and sinusoidal.

The trapezoidal-shaped back EMF BLDC motor is designed to develop trapezoidal back EMF waveforms.

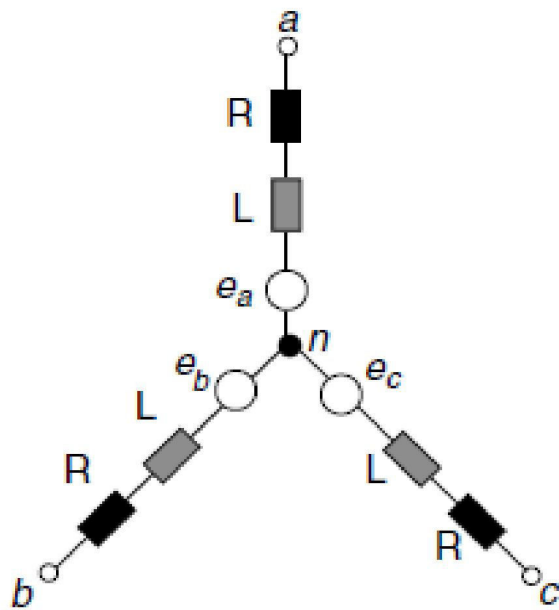
It has the following ideal characteristics:

1. Rectangular distribution of magnet flux in the air gap
2. Rectangular current waveform
3. Concentrated stator windings.

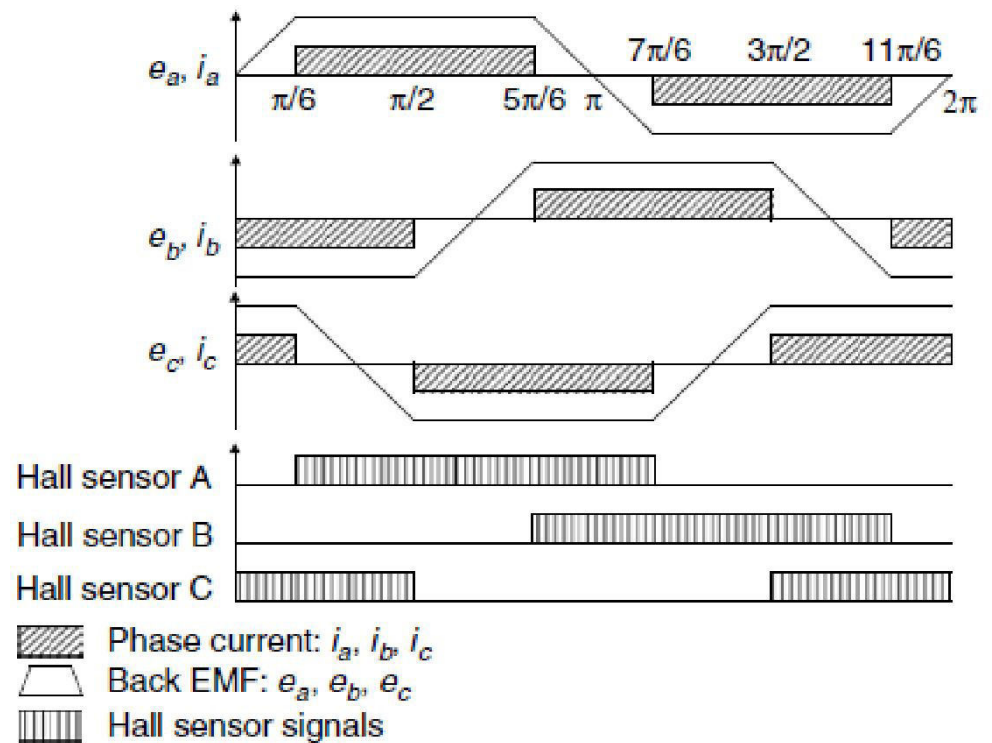
Excitation waveforms take the form of quasisquare current waveforms with two 60° electrical intervals of zero current excitation per cycle. The nature of the excitation waveforms for trapezoidal back EMF permits some important system simplifications compared to sinusoidal back EMF machines. In particular, the resolution requirements for the rotor position sensor are much lower since only six commutation instants are necessary per electrical cycle. Figure shows the winding configuration of the trapezoidal-shaped back EMF BLDC machine.



Winding configuration of the trapezoidal-shaped back EMF BLDC



Three-phase equivalent circuit



back EMFs, currents, and Hall sensor signals of a BLDC motor

Excitation waveforms take the form of quasisquare current waveforms with two 60° electrical intervals of zero current excitation per cycle. The nature of the excitation waveforms for trapezoidal back EMF permits some important system simplifications compared to sinusoidal back EMF machines. In particular, the resolution requirements for the rotor position sensor are much lower since only six commutation instants are necessary per electrical cycle.

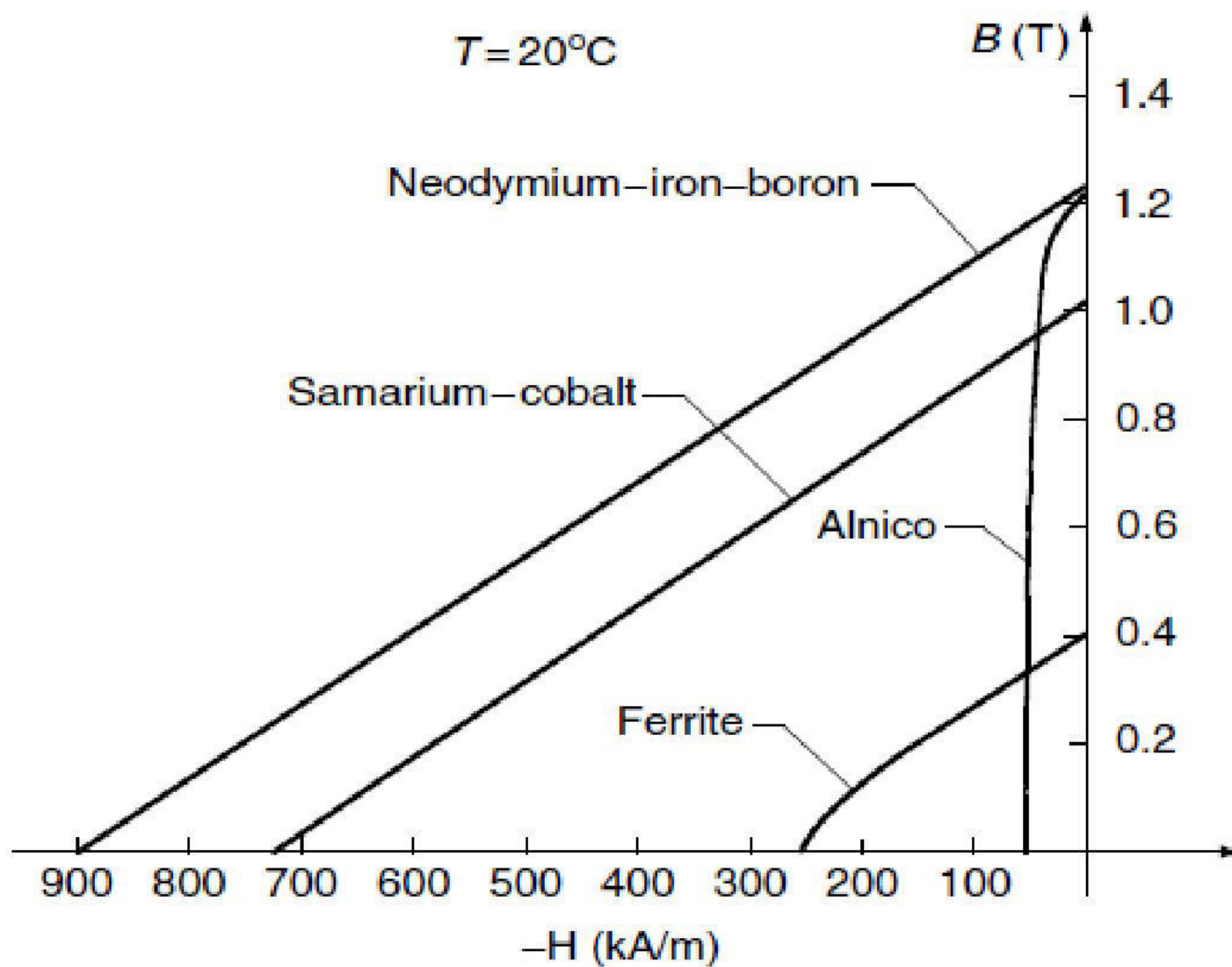
Figure shows an equivalent circuit and (b) shows trapezoidal back EMF, current profiles, and Hall sensor signals of the three-phase BLDC motor drive. The voltages seen in this figure, e_a , e_b , and e_c , are the line-to-neutral back EMF voltages, the result of the permanent-magnet flux crossing the air gap in a radial direction and cutting the coils of the stator at a rate proportional to the rotor speed.

The coils of the stator are positioned in the standard three-phase full-pitch, concentrated arrangement, and thus the phase trapezoidal back EMF waveforms are displaced by 120° electrical degrees. The current pulse generation is a “ 120° on and 60° off” type, meaning each phase current is flowing for two thirds of an electrical 360° period, 120° positively and 120° negatively. To drive the motor with maximum and constant torque/ampere, it is desired that the line current pulses be synchronized with the line-neutral back EMF voltages of the particular phase.

Properties of PM Materials

There are three classes of permanent magnet materials currently used for electric motors:

1. Alnicos (Al, Ni, Co, Fe)
2. Ceramics (ferrites), for example, barium ferrets $\text{BaO}6\text{Fe}_2\text{O}_3$ and strontium ferrite $\text{SrO}6\text{Fe}_2\text{O}_3$
3. Rare-earth materials, that is, samarium–cobalt SmCO and neodymium–iron–boron NdFeB .



Alnico

The main advantages of Alnico are its high magnetic remanent flux density and low-temperature coefficients. The temperature coefficient of its remanent magnetic flux density B_r , or remanence, is 0.02%/°C and the maximum service temperature is 520°C. These advantages allow quite a high airgap flux density and high operating temperature. Unfortunately, coercive force is very low and the demagnetization curve is extremely nonlinear. Therefore, it is very easy not only to magnetize but also to demagnetize Alnico. Alnico magnets have been used in motors having ratings in the range of a few watts to 150 kW.

Ferrites

A ferrite has a higher coercive force than that of Alnico, but at the same time has a lower remanent magnetic flux density. Temperature coefficients are relatively high, that is, the coefficient of B_r is $0.20\%/^{\circ}\text{C}$ and the coefficient of coercive field strength, H_c , or coercivity is $0.27\%/^{\circ}\text{C}$. The maximum service temperature is 400°C . The main advantages of ferrites are their low cost and very high electric resistance, which means that there are no eddy-current losses in the PM volume.

Rare-Earth PMs

During the last three decades, great progress regarding available energy density $(BH)_{max}$ has been achieved with the development of rare-earth PMs. The first generation of the rare-earth PMs based on the composition of samarium–cobalt (SmCo_5) was invented in the 1960s and has been produced commercially since the early 1970s. Today, it is a well-established hard magnetic material. SmCo_5 has the advantages of high remanent flux density, high coercive force, high-energy production, linear demagnetization curve, and low temperature coefficient. The temperature coefficient of B_r is 0.03 to 0.045%/°C and the temperature coefficient of H_c is 0.14 to 0.40%/°C. The maximum service temperature is 250 to 300°C. It is well suited for building motors with low volume and, consequently with, high specific power and low moment of inertia. The cost is the only drawback. Both Sm and Co are relatively expensive due to their supply restriction.

- With the discovery of a second generation of rare-earth magnets based on inexpensive neodymium (Nd) and iron in the recent years, remarkable progress with regard to lowering raw material cost has been achieved.
- NdFeB magnets, which are now produced in increasing quantities, have better magnetic properties than those of SmCo, but only at room temperature.
- The demagnetization curves, especially the coercive force, are strongly temperature dependent.
- The temperature coefficient of Br is 0.095 to 0.15%/°C and the temperature coefficient of H_c is 0.40 to 0.7%/°C.
- The maximum service temperature is 150°C and Curie temperature is 310°C.
- The latest grades of NdFeB have better thermal stability, enabling an increase in working temperature by 50°C, and offer greatly improved resistance to corrosion.

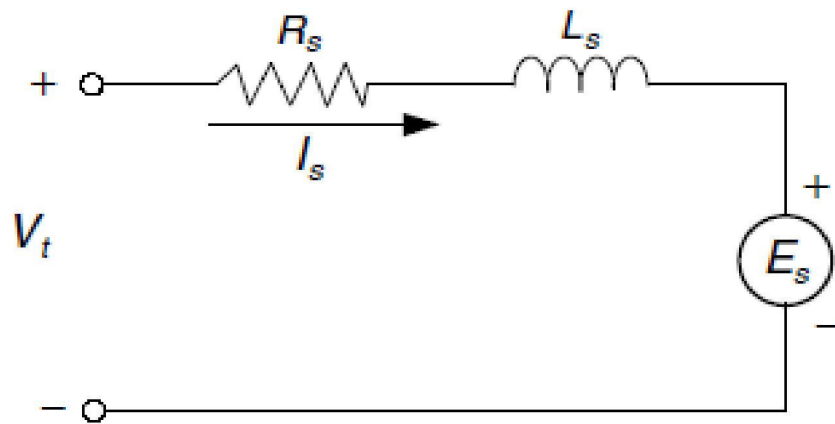
Performance Analysis and Control of BLDC Machines

Speed–torque performance is most important for traction and other applications. As in any other electric machine, the torque is produced by the interaction of magnetic field and current. The magnetic field is produced in BLDC by the permanent magnet and the current depends on the source voltage, control, and the back EMF, which is determined by the magnetic field and speed of the machine. To obtain the desired torque and speed at a given load, the current needs to be controlled.

Performance Analysis of BLDC

The performance analysis of the BLDC machines is based on the following assumptions:

1. The motor is not saturated
2. Stator resistances of all the windings are equal and self and mutual inductances are constant
3. Power semiconductor devices in the inverter are ideal
4. Iron losses are negligible.



Simplified equivalent circuit of BLDC motor

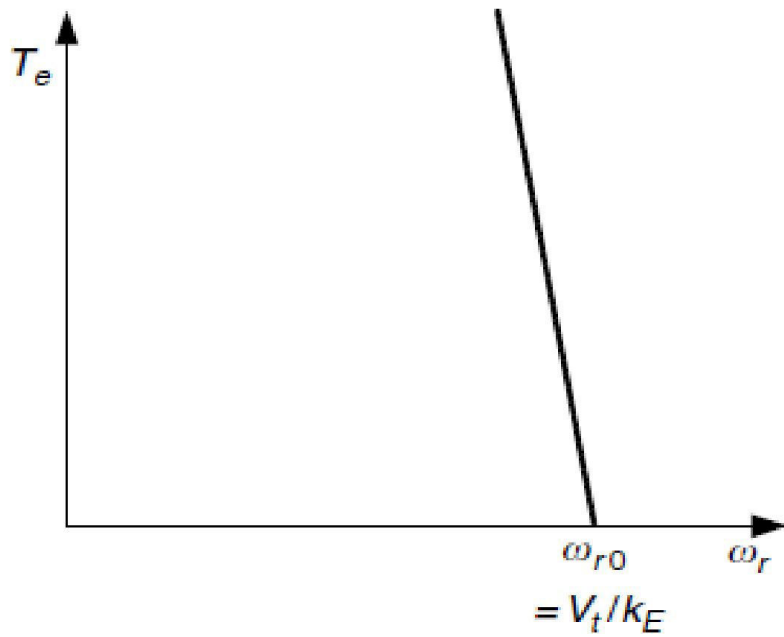
$$V_t = R_s I_s + L_s \frac{dI_s}{dt} + E_s$$

$$E_s = k_E \omega_r$$

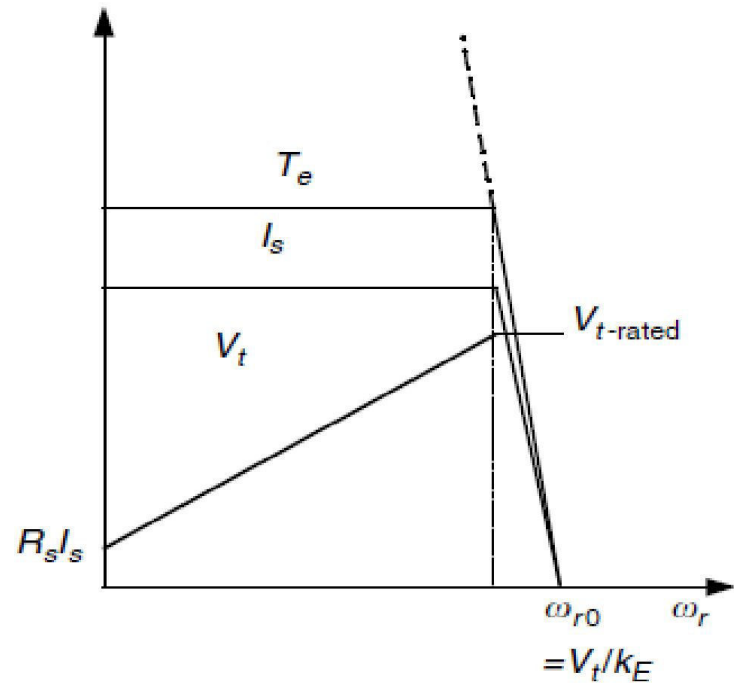
$$T_e = k_T I_s$$

$$T_e = T_L + J \frac{d\omega_r}{dt} + B \omega_r$$

$$T_e = \frac{(V_t - k_E \omega_r) k_T}{R_s}$$



Speed–torque curve at steady state
with constant voltage



Speed–torque curve at steady state
with variable voltage supply

Laplace forms as

$$V_t(s) = E_s(s) + (R_s + sL_s)I_s(s),$$

$$E_s(s) = k_E \omega_r(s),$$

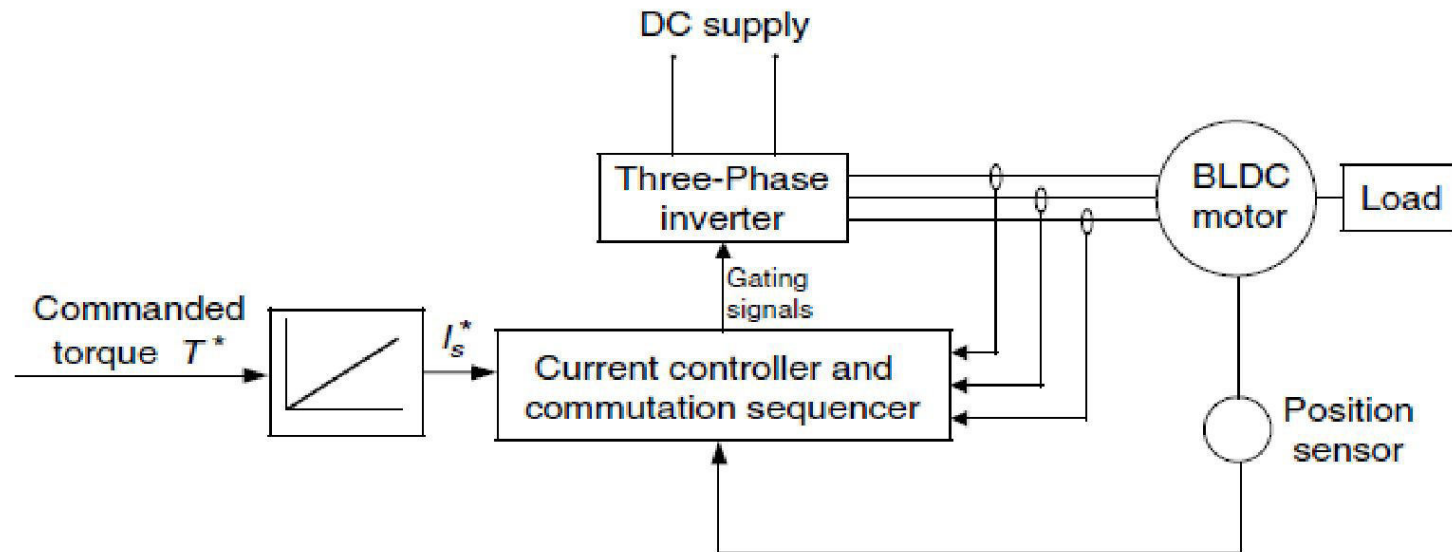
$$T_e(s) = k_T I_s(s),$$

$$T_e(s) = T_L(s) + (B + sJ)\omega_r(s).$$

Thus, the transfer function of the BLDC motor drive system is

$$\omega_r(s) = \frac{k_T}{(R_s + sL_s)(sJ + B) + k_T k_E} V_t(s) - \frac{R_s + sL_s}{(R_s + sL_s)(sJ + B) + k_T k_E} T_L(s)$$

Control of BLDC Motor Drives



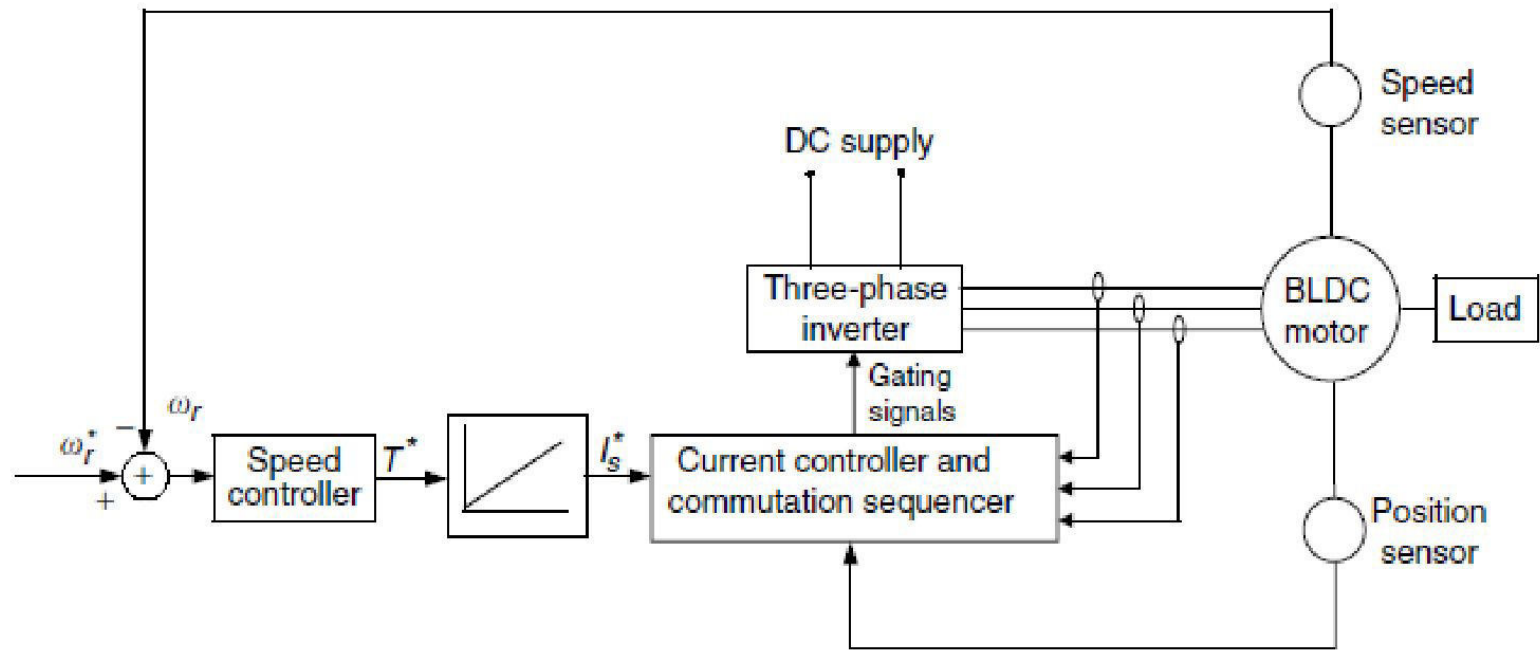
Block diagram of the torque control of the BLDC motor

The desired current I^* is derived from the commanded torque T^* through a torque controller. The current controller and commutation sequencer receive the desired current I^* position information from the position sensors, and perhaps the current feedback through current transducers, and then produces gating signals. These gating signals are sent to the three-phase inverter (power converter) to produce the phase current desired by the BLDC machine.

Many high-performance applications include current feedback for torque control. At the minimum, a DC bus current feedback is required to protect the drive and machine from overcurrents. The controller blocks, “speed controller” may be any type of classical controller such as a PI controller, or a more advanced controller such as an artificial intelligence control.

The “current controller and commutation sequencer” provides the properly sequenced gating signals to the “three-phase inverter” while comparing sensed currents to a reference to maintain a constant peak current control by hysteresis (current chopping) or with a voltage source (PWM)-type current control. Using position information, the commutation sequencer causes the inverter to “electronically commutate,” acting as the mechanical commutator of a conventional DC machine. The commutation angle associated with a brush-less motor is normally set so that the motor will commute around the peak of the torque angle curve.

Considering a three-phase motor, connected in delta or wye, commutation occurs at electrical angles, which are 30° (electrical) from the peaks of the torque–angle curves. When the motor position moves beyond the peaks by an amount equal to 30° (electrical), then the commutation sensors cause the stator phase excitation to switch to move the motor suddenly to 30° relative to the peak of the next torque–angle curve.



Block diagram of the speed control of the BLDC motor

Switched Reluctance Motor Drives

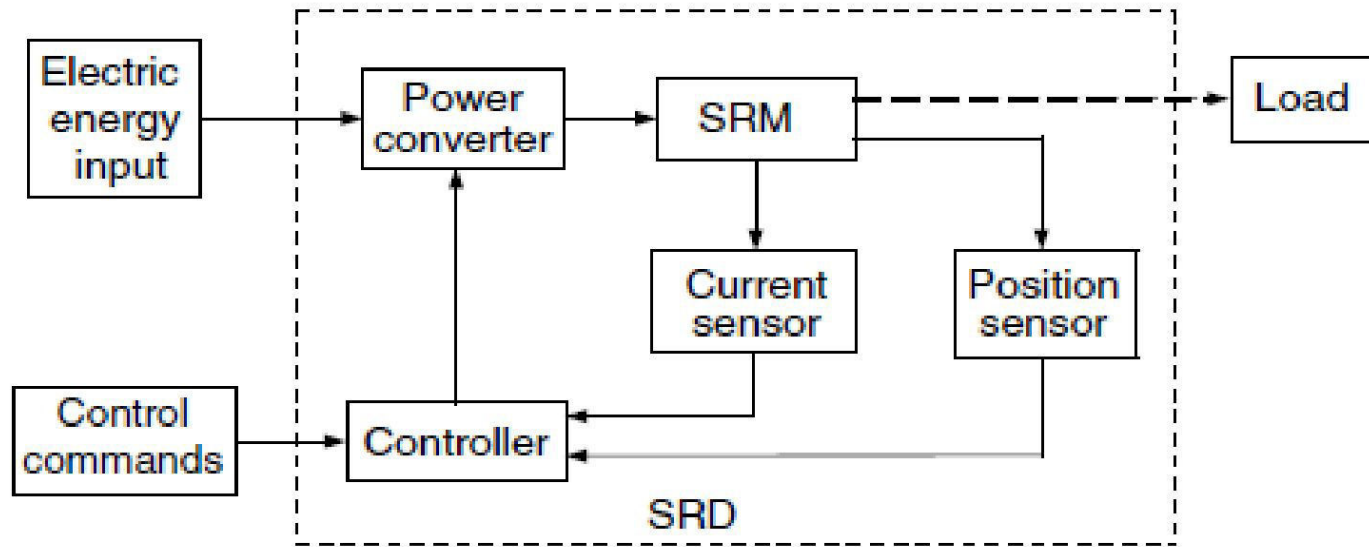
The switched reluctance motor (SRM) drive is considered to be an attractive candidate for variable speed motor drives due to its low cost, rugged structure, reliable converter topology, high efficiency over a wide speed range, and simplicity in control.

These drives are suitable for EVs, electric traction applications, automotive applications, aircraft starter/generator systems, mining drives, washing machines, door actuators, etc

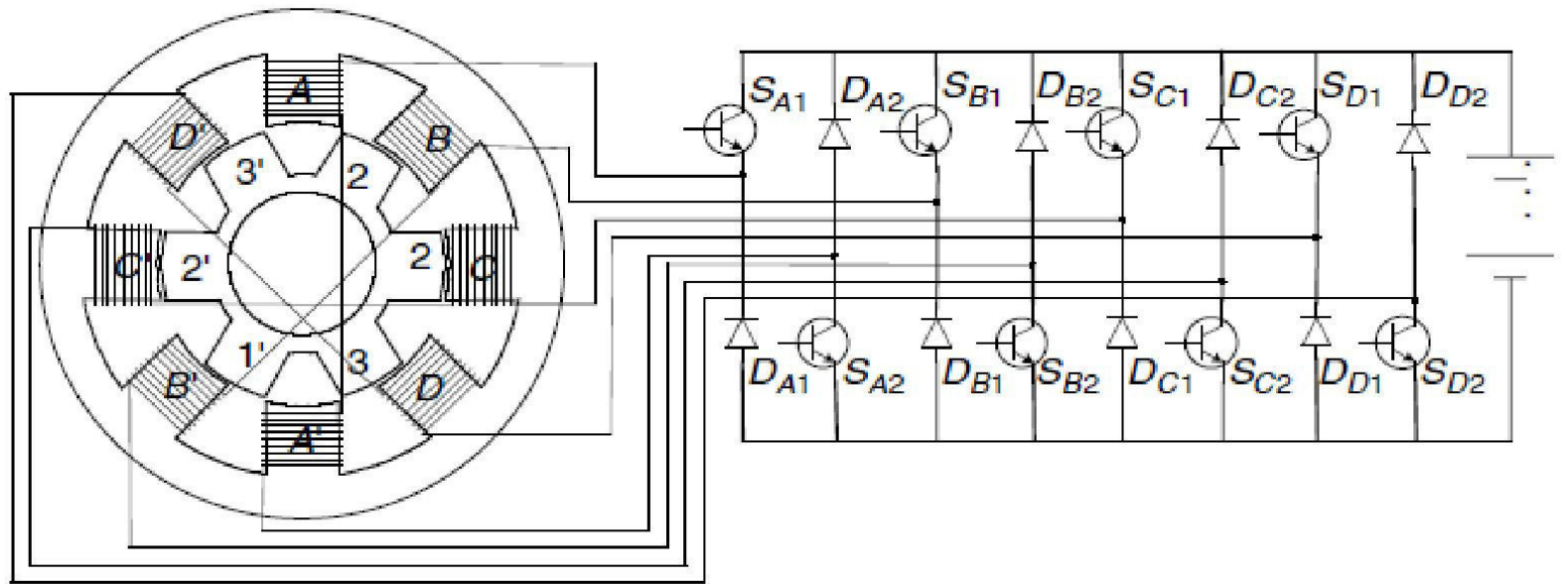
The SRM has a simple, rugged, and low-cost structure. It has no PM or winding on the rotor. This structure not only reduces the cost of the SRM but also offers high-speed operation capability for this motor. Unlike the induction and PM machines, the SRM is capable of high-speed operation without the concern of mechanical failures that result from the high-level centrifugal force.

In addition, the inverter of the SRM drive has a reliable topology. The stator windings are connected in series with the upper and lower switches of the inverter. This topology can prevent the shoot-through fault that exists in the induction and permanent motor drive inverter. Moreover, high efficiency over a wide speed range and control simplicity are known merits of the SRM drive

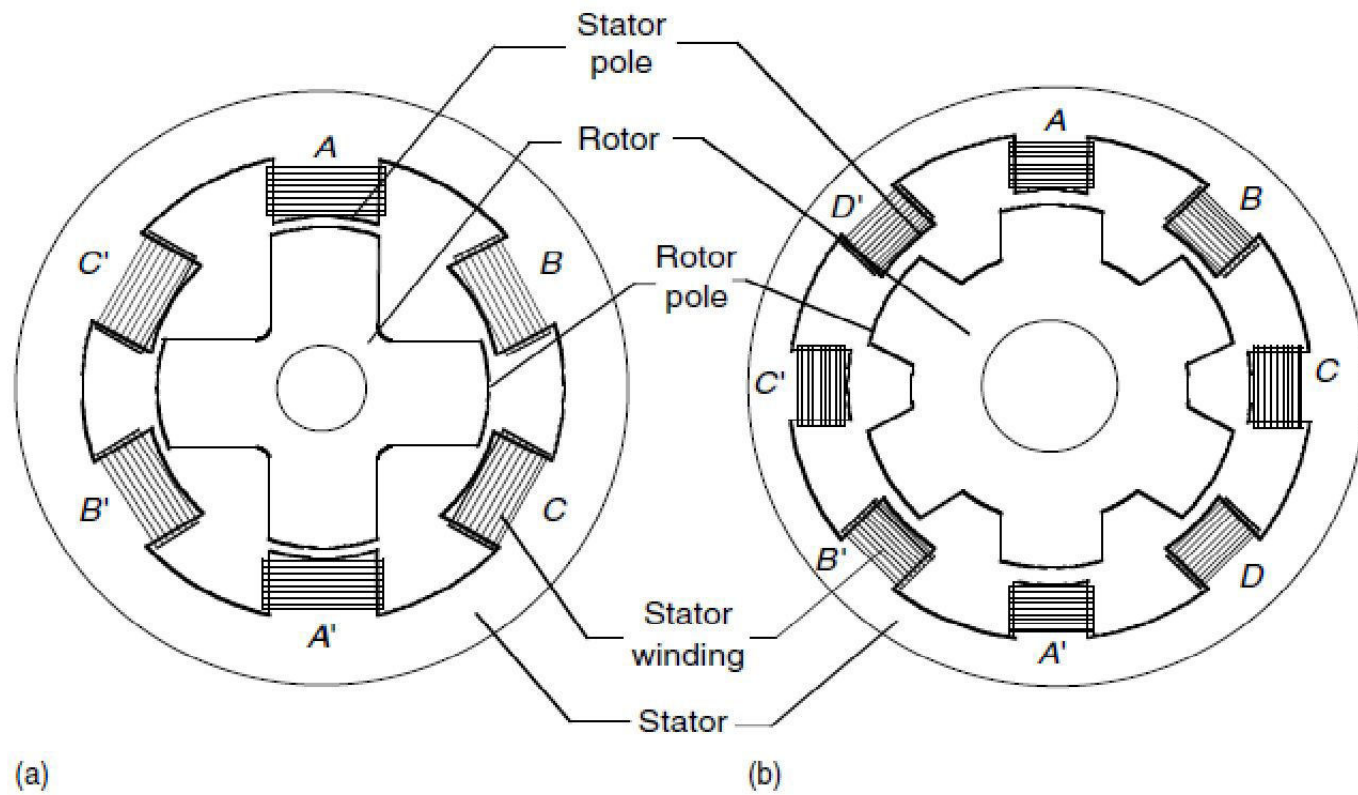
Basic Magnetic Structure of SRM



SRM drive system



SRM and its power supply



Cross-section of common SRM configurations: (a) a 6/4 SRM and (b) a 8/6 SRM

The SRM has salient poles on both the stator and rotor. It has concentrated windings on the stator and no winding or PM on the rotor. There are several configurations for SRM depending on the number and size of the rotor and stator poles. The configurations of the 8/6 and 6/4 SRM, which are more common, are shown in Figure

Due to its double saliency structure, the reluctance of the flux path for a phase winding varies with the rotor position. Also, since the SRM is commonly designed for high degree saturation at high phase current, the reluctance of the flux path also varies with the phase current. As a result, the stator flux linkage, phase bulk inductance, and phase incremental inductance all vary with the rotor position and phase current.

The phase voltage equation of the SRM is given by

$$V_j = Ri_j + \frac{d}{dt} \sum_{k=1}^m \lambda_{jk}$$

where m is the total number of phases, V_j is the applied voltage to phase j , i_j is the current in phase j , R is the winding resistance per phase, λ_{jk} is the flux linkage of phase j due to the current of phase k , and t is the time. The phase flux linkage, λ_{jk} , is given by

$$\lambda_{jk} = L_{jk}(i_k, \theta) i_k$$

where L_{jk} is the mutual inductance between phase k and phase j . Mutual inductance between phases is usually small compared to the bulk inductance and is neglected in equations.

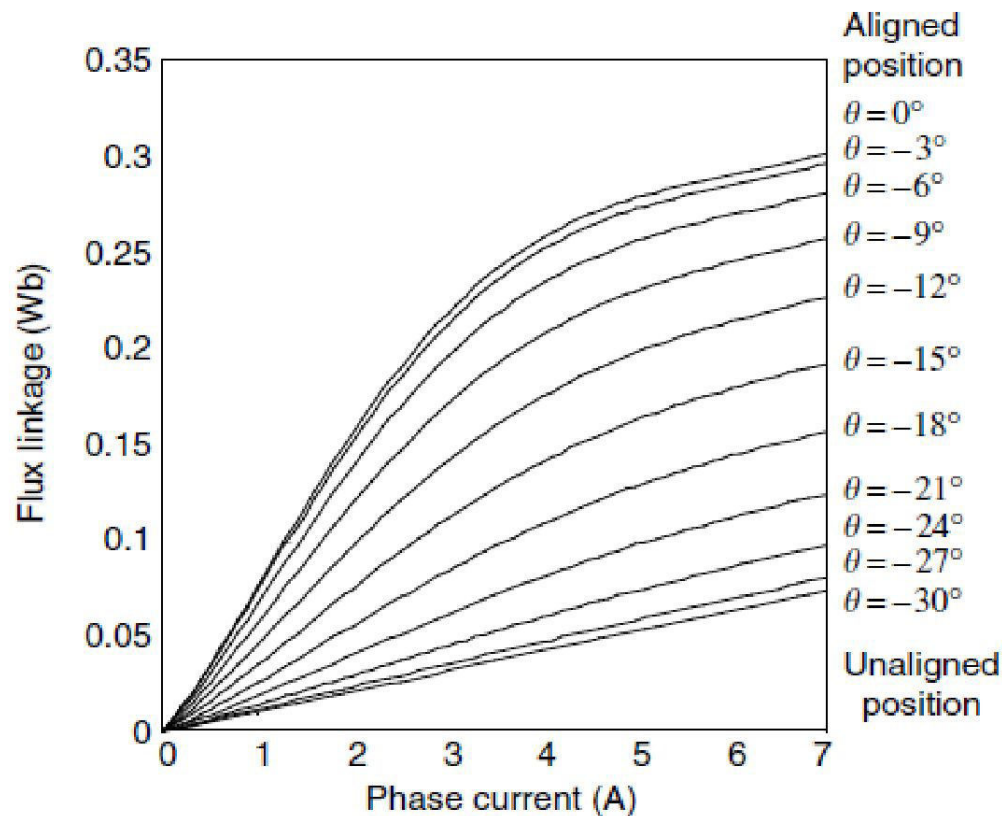
$$\begin{aligned}
V_j &= Ri_j + \frac{d}{dt} \sum_{k=1}^m \lambda_{jk} = Ri_j + \sum_{k=1}^m \left\{ \frac{\partial \lambda_{jk}}{\partial i_k} \frac{di_k}{dt} + \frac{\partial \lambda_{jk}}{\partial \theta} \frac{d\theta}{dt} \right\} \\
&= Ri_j + \sum_{k=1}^m \left\{ \frac{\partial (L_{jk} i_k)}{\partial i_k} \frac{di_k}{dt} + \frac{\partial (L_{jk} i_k)}{\partial \theta} \omega \right\} \\
&= Ri_j + \sum_{k=1}^m \left\{ \left(L_{jk} + i_k \frac{\partial L_{jk}}{\partial i_k} \right) \frac{di_k}{dt} + i_k \frac{\partial L_{jk}}{\partial \theta} \omega \right\}.
\end{aligned}$$

When only one phase is energized in the operation, the above equation can be written as

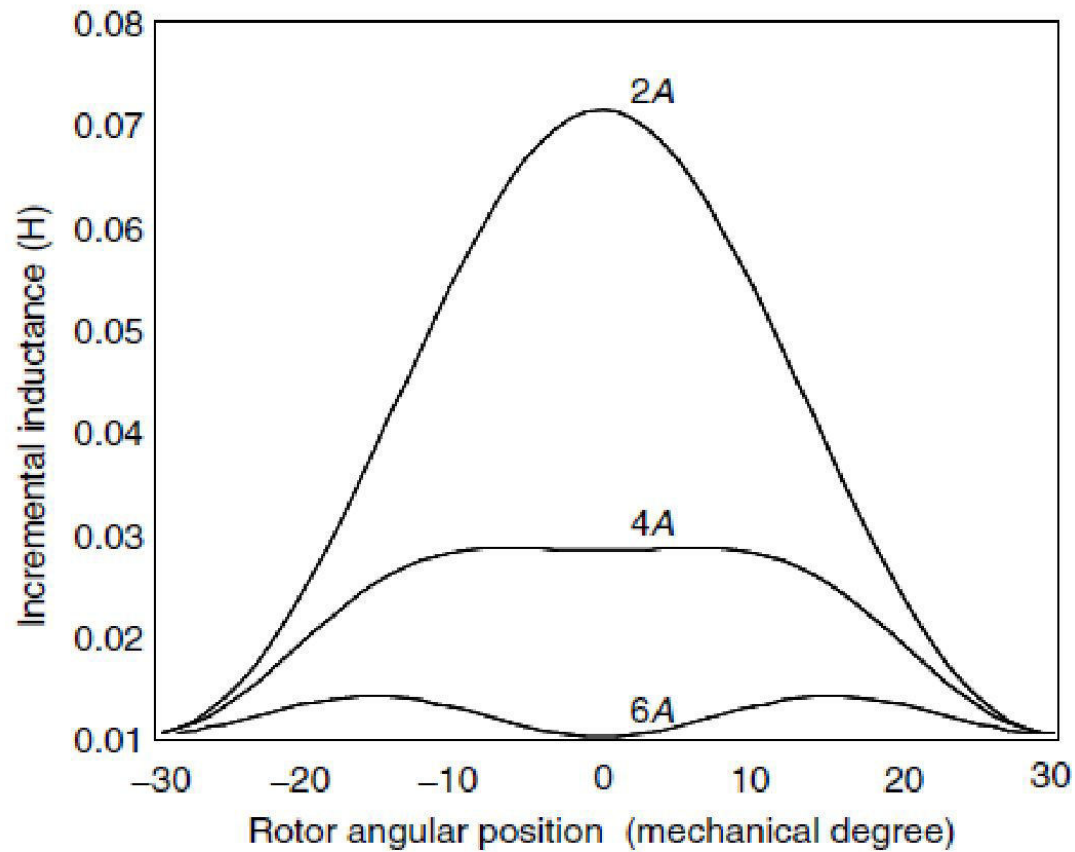
$$V_j = Ri_j + \left(L_{jj} + i_j \frac{\partial L_{jj}}{\partial i_j} \right) \frac{di_j}{dt} + i_j \frac{\partial L_{jj}}{\partial \theta} \omega.$$

Torque Production in SRM

Torque in SRM is produced by the tendency of the rotor to get into alignment with the excited stator poles. The analytical expression of the torque can be derived using the derivative of the coenergy against the rotor position at a given current.



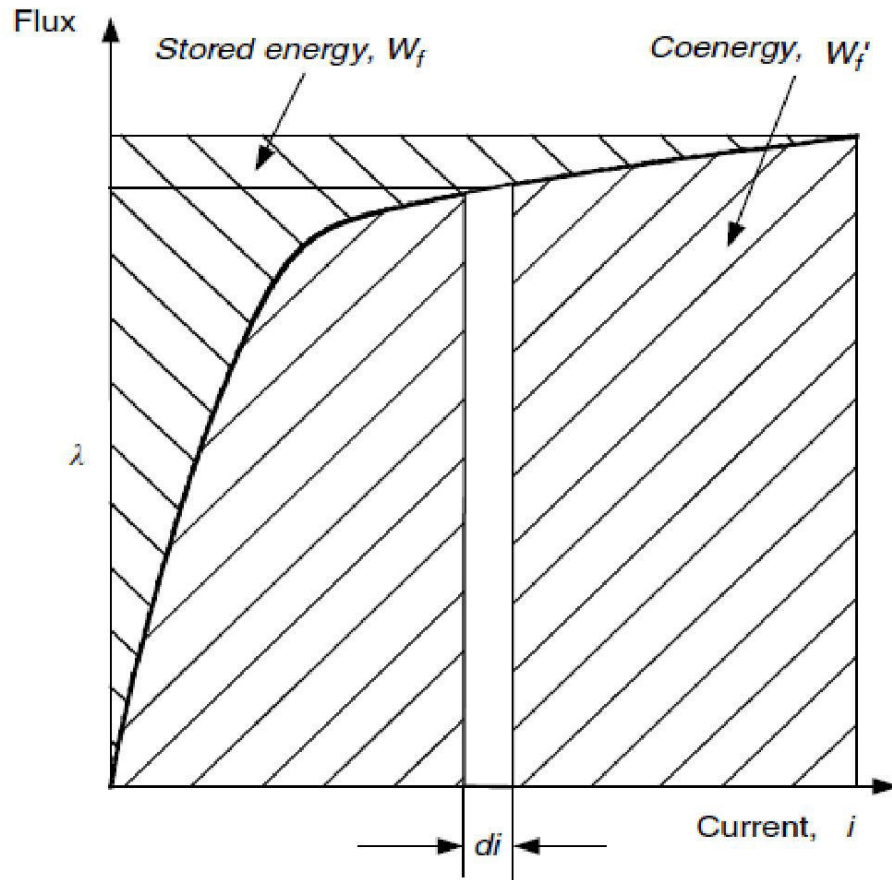
Variation of phase flux linkage with rotor position and phase current



Variation of phase incremental inductance with rotor position and phase current for a typical 8/6 SRM

Coenergy can be found from the definite integral:

$$W'_f = \int_0^i \lambda \, di$$



Stored field energy
and coenergy

The torque produced by one phase coil at any rotor position is given by

$$T = \left[\frac{\partial W'_f}{\partial \theta} \right]_{i=\text{constant}}$$

In the case of flux being linear with current, for example, in an unsaturated field, the magnetization curve in Figure would be a straight line and the co-energy would be equal to the stored field energy.

The instantaneous torque can be given as

$$T = \frac{1}{2} i^2 \frac{dL(\theta)}{d\theta}$$

where L is the unsaturated phase bulk inductance. In the case of a saturated phase, the torque cannot be calculated by a simple algebra equation; instead, an integral equation such as

$$T = \int_0^i \frac{\partial L(\theta, i)}{\partial \theta} i \, di$$

The output torque of an SRM is the summation of torque of all the phases

$$T_m = \sum_{i=1}^N T(i, \theta)$$

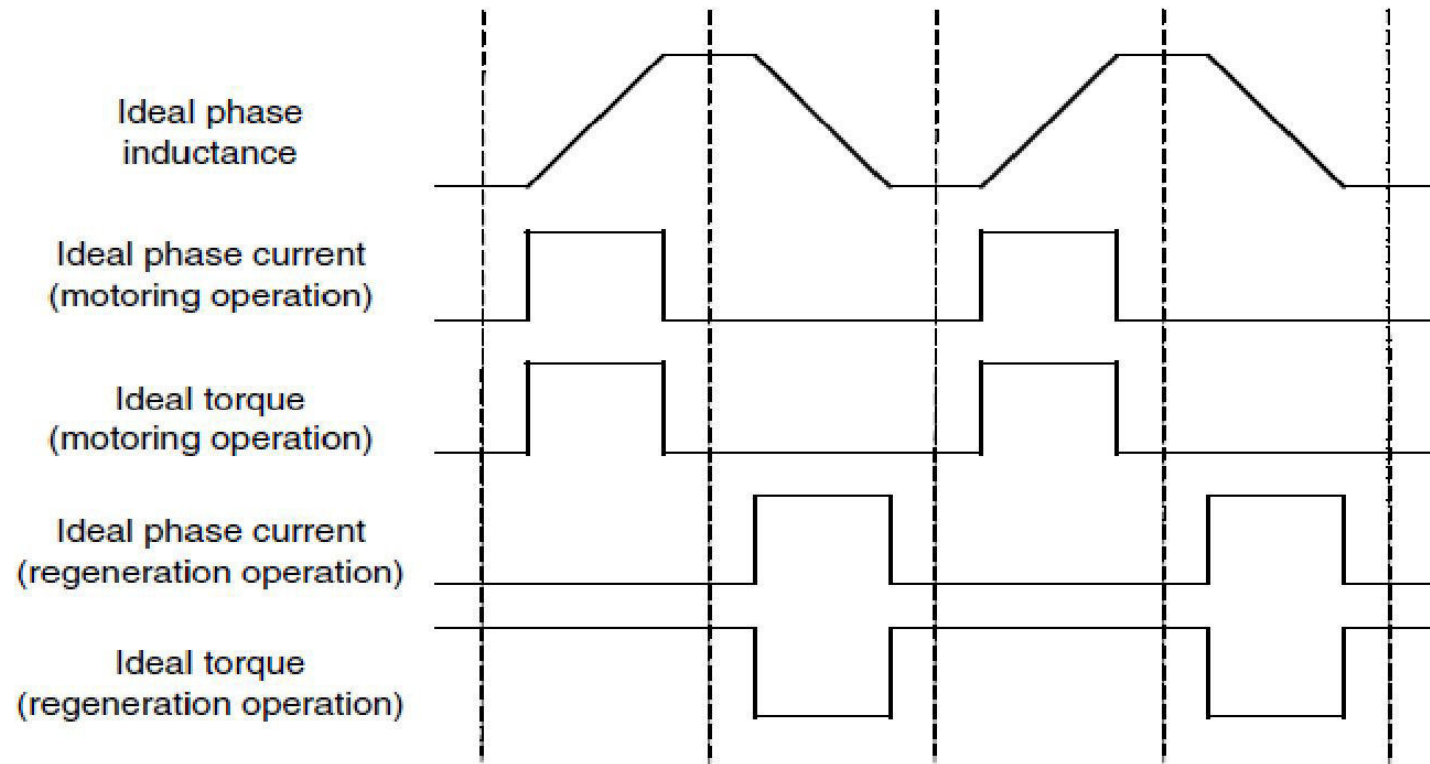
where T_m and N are the output torque and phase number of motor. The relation between the motor torque and mechanical load is usually given by

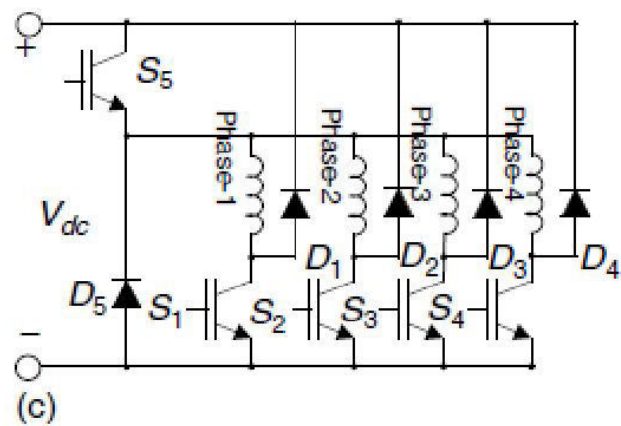
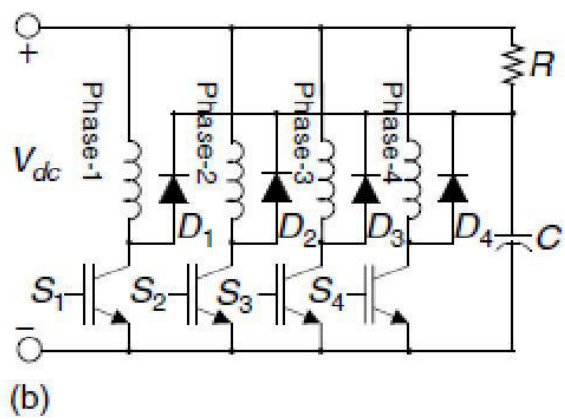
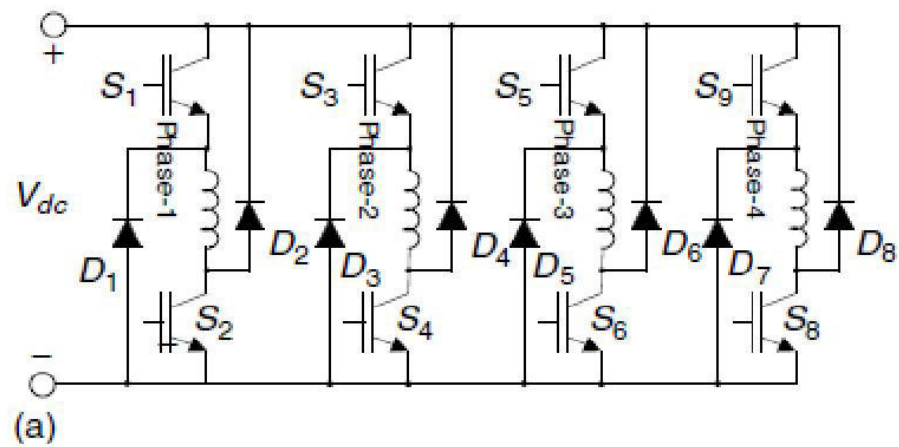
$$T_m - T_l = J \frac{d\omega}{dt} + B\omega$$

where J , B , and T_l are the moment of inertia, viscous friction, and load torque, respectively. The relation between position and speed is given by

$$\omega = \frac{d\theta}{dt}$$

SRM Drive Converter





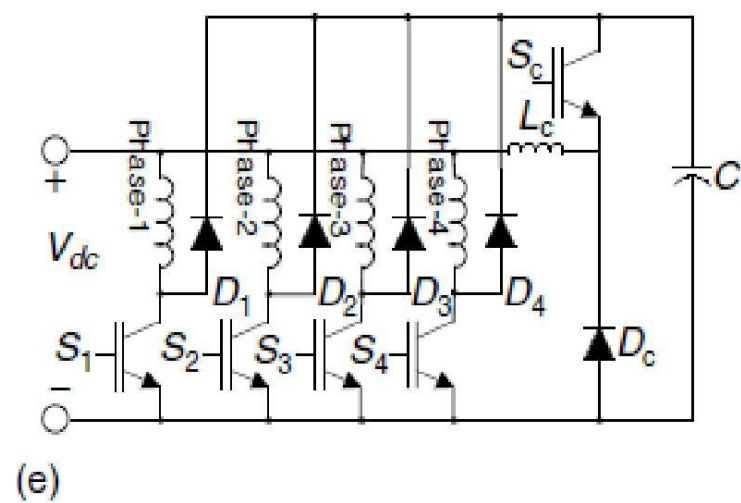
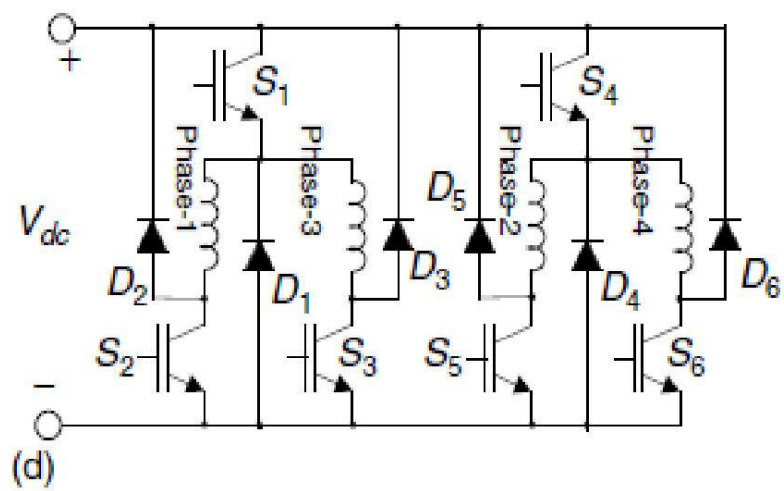


TABLE 3.1 Nominal Energy Density of Sources

Energy Source	Nominal Specific Energy (Wh/kg)
Gasoline	12,500
Natural gas	9350
Methanol	6050
Hydrogen	33,000
Coal (bituminous)	8200
Lead-acid battery	35
Lithium-polymer battery	200
Flywheel (carbon-fiber)	200

3.1 BATTERY BASICS

The batteries are made of unit cells containing the chemical energy that is convertible to electrical energy. One or more of these electrolytic cells are connected in series to form one battery. The grouped cells are enclosed in a casing to form a battery module. A battery pack is a collection of these individual battery modules connected in a series and parallel combination to deliver the desired voltage and energy to the power electronic drive system.

The energy stored in a battery is the difference in free energy between chemical components in the charged and discharged states. This available chemical energy in a cell is converted into electrical energy only on demand, using the basic components of a unit cell, which are the positive and negative electrodes, the separators, and the electrolytes. The electrochemically active ingredient of the positive or negative electrode is called the active material. Chemical oxidation and reduction processes take place at the two electrodes, thereby bonding and releasing electrons, respectively. The electrodes must be electronically conducting and are located at different sites, separated by a separator, as shown in [Figure 3.1](#). During battery operation, chemical reactions at each of the electrodes cause electrons to flow from one electrode to another; however, the flow of electrons in the cell is sustainable only if electrons generated in the chemical reaction are able to flow through an external electrical circuit that connects the two electrodes. The connection points between the electrodes and the external circuit are called the battery terminals. The external circuit ensures that most of the stored chemical energy is released only on demand and is utilized as electrical energy. It must be mentioned that only in an ideal battery does current flow only when the circuit between the electrodes is completed externally. Unfortunately, many batteries do allow a slow discharge, due to diffusion effects, which is why they are not particularly good for long-term energy storage. This slow discharge with open-circuit terminals is known as *self-discharge*, which is also used as a descriptor of battery quality.

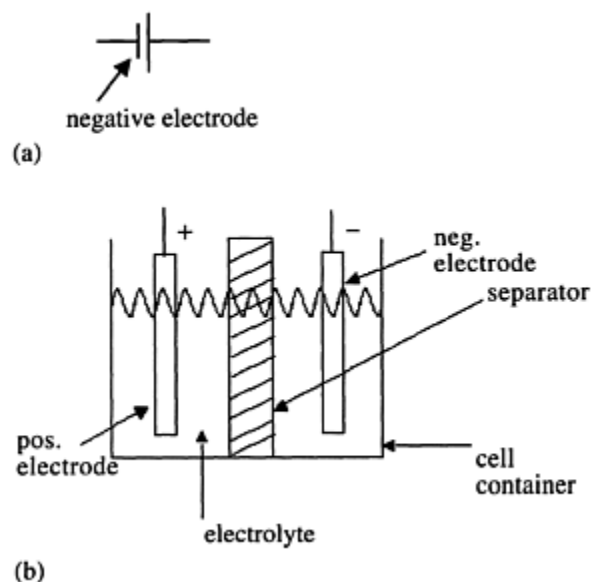


FIGURE 3.1 Components of a battery cell. (a) Cell circuit symbol; (b) cell cross-section.

The components of the battery cell are described as follows:

1. *Positive electrode:* The positive electrode is an oxide or sulfide or some other compound that is capable of being reduced during cell discharge. This electrode consumes electrons from the external circuit during cell discharge. Examples of positive electrodes are lead oxide (PbO_2) and nickel oxyhydroxide (NiOOH). The electrode materials are in the solid state.
2. *Negative electrode:* The negative electrode is a metal or an alloy that is capable of being oxidized during cell discharge. This electrode generates electrons in the external circuit during cell discharge. Examples of negative electrodes are lead (Pb) and cadmium (Cd). Negative electrode materials are also in the solid state within the battery cell.
3. *Electrolyte:* The electrolyte is the medium that permits ionic conduction between positive and negative electrodes of a cell. The electrolyte must have high and selective conductivity for the ions that take part in electrode reactions, but it must be a nonconductor for electrons in order to avoid self-discharge of batteries. The electrolyte may be liquid, gel, or solid material. Also, the electrolyte can be acidic or alkaline, depending on the type of battery. Traditional batteries such as lead-acid and nickel-cadmium use liquid electrolytes. In lead-acid batteries, the electrolyte is the aqueous solution of sulfuric acid [$\text{H}_2\text{SO}_4(\text{aq})$]. Advanced batteries currently under development for EVs, such as sealed lead-acid, nickel-metal-hydride (NiMH), and lithium-ion batteries use an electrolyte that is gel, paste, or resin. Lithium-polymer batteries use a solid electrolyte.

4. *Separator*: The separator is the electrically insulating layer of material that physically separates electrodes of opposite polarity. Separators must be permeable to the ions of the electrolyte and may also have the function of storing or immobilizing the electrolyte. Present day separators are made from synthetic polymers.

There are two basic types of batteries: primary batteries and secondary batteries. Batteries that cannot be recharged and are designed for a single discharge are known as primary batteries. Examples of these are the lithium batteries used in watches, calculators, cameras, etc., and the manganese dioxide batteries used to power toys, radios, torches, etc. Batteries that can be recharged by flowing current in the direction opposite to that during discharge are known as secondary batteries. The chemical reaction process during cell charge operation when electrical energy is converted into chemical energy is the reverse of that during discharge. The batteries needed and used for EVs and HEVs are all secondary batteries, because they are recharged during regeneration cycles of vehicle operation or during the battery recharging cycle in the stopped condition using a charger. All the batteries that will be discussed in the following are examples of secondary batteries.

The major types of rechargeable batteries considered for EV and HEV applications are:

- Lead-acid (Pb-acid)
- Nickel-cadmium (NiCd)
- Nickel-metal-hydride (NiMH)
- Lithium-ion (Li-ion)
- Lithium-polymer (Li-poly)
- Sodium-sulfur (NaS)
- Zinc-air (Zn-Air)

The lead-acid type of battery has the longest development history of all battery technology, particularly for their need and heavy use in industrial EVs, such as for golf carts in sports, passenger cars in airports, and forklifts in storage facilities and supermarkets. Research and development for batteries picked up momentum following the resurgence of interest in EVs and HEVs in the late 1960s and early 1970s. Sodium-sulfur batteries showed great promise in the 1980s, with high energy and power densities, but safety and manufacturing difficulties led to the abandonment of the technology. The development of battery technology for low-power applications, such as cell phones and calculators, opened the possibilities of scaling the energy and power of nickel-cadmium- and lithium-ion-type batteries for EV and HEV applications.

The development of batteries is directed toward overcoming significant practical and manufacturing difficulties. Theoretical predictions are difficult to match in manufactured products due to practical limitations. Theoretical and practical specific energies of several batteries are given in [Table 3.2](#) for comparison.

The characteristics of some of the more important battery technologies mentioned above are given in the following. The theoretical aspects of the lead-acid

TABLE 3.2 Specific Energy of Batteries

Battery	Specific Energy (Wh/kg)	
	Theoretical	Practical
Lead-acid	108	50
Nickel-cadmium		20–30
Nickel-zinc		90
Nickel-iron		60
Zinc-chlorine		90
Silver-zinc	500	100
Sodium-sulfur	770	150–300
Aluminum-air		300

battery will be discussed in detail first, followed by shorter descriptions of the other promising technologies.

3.2 LEAD-ACID BATTERY

Lead-acid batteries have been the most popular choice of batteries for EVs. Lead-acid batteries can be designed to be high powered and are inexpensive, safe, and reliable. A recycling infrastructure is in place for them. However, low specific energy, poor cold temperature performance, and short calendar and cycle life are among the obstacles to their use in EVs and HEVs.

The lead-acid battery has a history that dates to the middle of the 19th century, and it is currently a mature technology. The first lead-acid battery was produced as early as in 1859. In the early 1980s, over 100,000,000 lead-acid batteries were produced per year. The long existence of the lead-acid battery is due to the following:

- Relatively low cost
- Easy availability of raw materials (lead, sulfur)
- Ease of manufacture
- Favorable electromechanical characteristics

The battery cell operation consists of a cell discharge operation, when the energy is supplied from the battery to the electric motor to develop propulsion power, and a cell charge operation, when energy is supplied from an external source to store energy in the battery.

3.2.1 CELL DISCHARGE OPERATION

In the cell discharge operation ([Figure 3.2](#)), electrons are consumed at the positive electrode, the supply

of which comes from the negative electrode. The current flow is, therefore, out of the positive electrode into the motor-load, with the battery acting as the source.

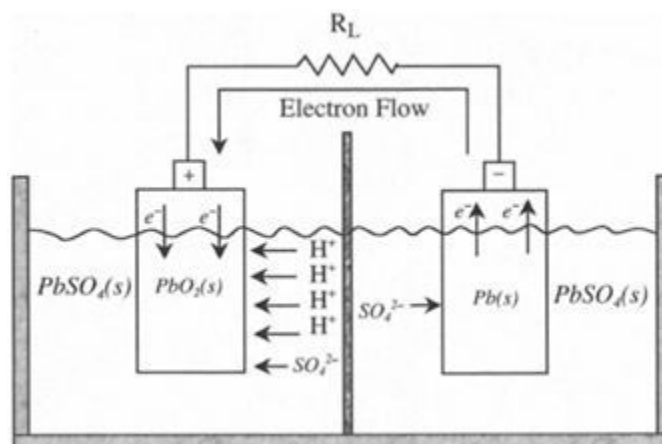
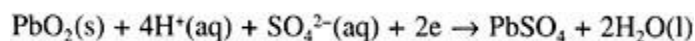


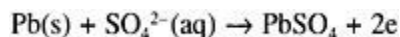
FIGURE 3.2 Lead-acid battery: cell discharge operation.

The positive electrode equation is given by:



A highly porous structure is used for the positive electrode to increase the $\text{PbO}_2(\text{s})$ /electrolyte contact area, which is about 50 to 150 m^2 per Ah of battery capacity. This results in higher current densities, as PbO_2 is converted to $\text{PbSO}_4(\text{s})$. As discharge proceeds, the internal resistance of the cell rises due to PbSO_4 formation and decreases the electrolyte conductivity as H_2SO_4 is consumed. $\text{PbSO}_4(\text{s})$ deposited on either electrode in a dense, fine-grain form can lead to sulfation. The discharge reaction is largely inhibited by the buildup of PbSO_4 , which reduces cell capacity significantly from the theoretical capacity.

The negative electrode equation during cell discharge is:



The electrons are released at the negative electrode during discharge operation. The production of $\text{PbSO}_4(\text{s})$ can degrade battery performance by making the negative electrode more passive.

The overall cell discharge chemical reaction is:

3.2.2 CELL CHARGE OPERATION

The cell charge operation ([Figure 3.3](#)) is the reverse of the cell discharge operation. During cell charging, lead sulfate is converted back to the reactant states of lead and lead oxide. The electrons are consumed from the external source at the negative electrode, while the positive electrode releases the electrons. The current flows into the positive electrode from the external source, thereby delivering

electrical energy

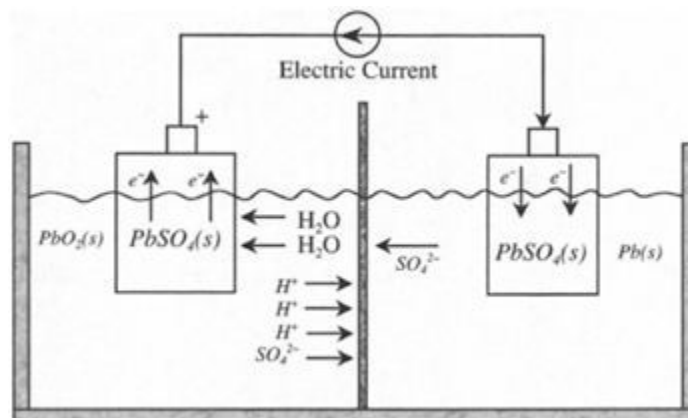
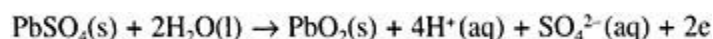
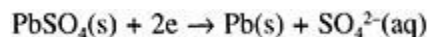


FIGURE 3.3 Lead-acid battery: cell charge operation.

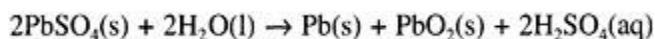
into the cell, where it gets converted into chemical energy. The chemical reaction at the positive electrode during cell charging is:



The chemical reaction at the negative electrode during cell charging is:



The overall chemical reaction during cell charging is:



Conventionally, lead-acid batteries are of flooded-electrolyte cells, where free acid covers all the plates. This imposes the constraint of maintaining an upright position for the battery, which is difficult in certain portable situations. Efforts in developing hermetically sealed batteries faced the problem of buildup of an explosive mixture of hydrogen and oxygen on approaching the top-of-charge or overcharge condition during cell recharging. The problem is addressed in the valve-regulated-lead-acid (VRLA) batteries by providing a path for the oxygen, liberated at the positive electrode, to reach the negative electrode, where it recombines to form lead-sulfate. There are two mechanisms for making sealed VRLA batteries, the gel battery, and the AGM (absorptive glass microfiber) battery. These types are based on immobilizing the sulfuric acid electrolyte in the separator and the active materials, leaving sufficient porosity for the oxygen to diffuse through the separator to the negative plate.¹

3.2.3 CONSTRUCTION

Construction of a typical battery consists of positive and negative electrode groups (elements) interleaved to form a cell. The through partition connection in the battery

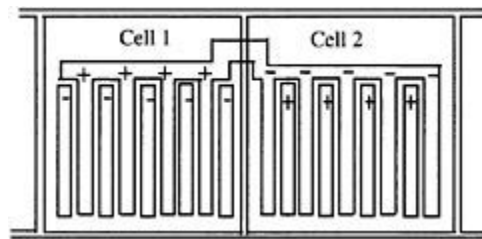


FIGURE 3.4 Schematic diagram of a lead-acid battery showing through-partition connection.

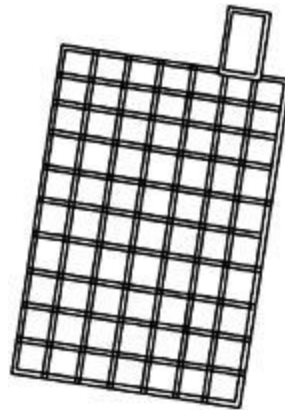


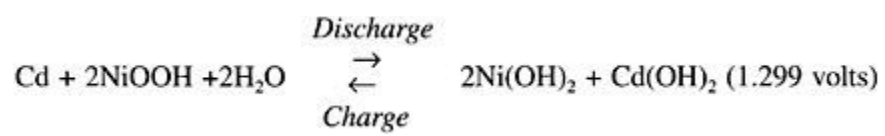
FIGURE 3.5 A lead-acid battery grid.

is illustrated in [Figure 3.4](#). The positive plate is made of stiff paste of the active material on a lattice-type grid, which is shown in [Figure 3.5](#). The grid, made of a suitably selected lead alloy, is the framework of a portable battery to hold the active material. The positive plates can be configured in flat pasted or tubular fashion. The negative plates are always manufactured as pasted types.

3.3 ALTERNATIVE BATTERIES

3.3.1 NICKEL-CADMIUM BATTERY

Nickel-cadmium (NiCd) and nickel-metal-hydride (NiMH) batteries are examples of alkaline batteries with which electrical energy is derived from the chemical reaction of a metal with oxygen in an alkaline electrolyte medium. The specific energy of alkaline batteries is lowered due to the addition of weight of the carrier metal. The NiCd battery employs a nickel oxide positive electrode and a metallic cadmium negative electrode. The net reaction occurring in the potassium hydroxide (KOH) electrolyte is:

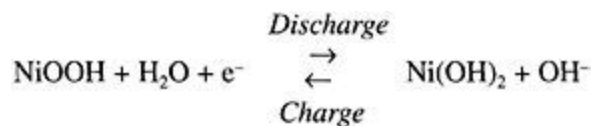


The practical cell voltage is 1.2 to 1.3 V, and the atomic mass of cadmium is 112. The specific energy of NiCd batteries is 30 to 50 Wh/kg, which is similar to that of lead-acid batteries. The advantages of NiCd batteries are superior low-temperature performance compared to lead-acid batteries, flat discharge voltage, long life, and excellent reliability. The maintenance requirements of the batteries are also low. The biggest drawbacks of NiCd batteries are the high cost and the toxicity contained in cadmium. Environmental concerns may be overcome in the long run through efficient recycling, but the insufficient power delivered by the NiCd batteries is another important reason for not considering these batteries for EV and HEV applications. The drawbacks of the NiCd batteries led to the rapid development of NiMH batteries, which are deemed more suitable for EV and HEV applications.

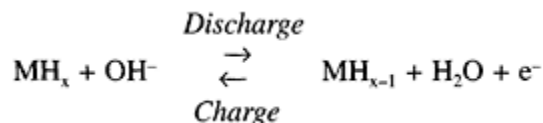
3.3.2 NICKEL-METAL-HYDRIDE (NiMH) BATTERY

The nickel-metal-hydride battery is a successor to the nickel-hydrogen battery and is already in use in production HEVs. In NiMH batteries, the positive electrode is a nickel oxide similar to that used in a NiCd battery, while the negative electrode is a metal hydride where hydrogen is stored. The concept of NiMH batteries is based on the fact that fine particles of certain metallic alloys, when exposed to hydrogen at certain pressures and temperatures, absorb large quantities of the gas to form the metal-hydride compounds. Furthermore, the metal hydrides are able to absorb and release hydrogen many times without deterioration. The two electrode chemical reactions in a NiMH battery are:

At the positive electrode,



At the negative electrode,



M stands for metallic alloy, which takes up hydrogen at ambient temperature to form the metal hydride MH_x . The negative electrode consists of a compressed mass of fine metal particles. The proprietary alloy formulations used in NiMH are known as AB_5 and AB_2 alloys. In the AB_5 alloy, A is the mixture of rare earth elements, and B is partially substituted nickel. In the AB_2 alloy, A is titanium or zirconium, and B is again partially substituted nickel. The AB_2 alloy has a higher capacity for hydrogen storage and is less costly. The operating voltage of NiMH is almost the same as that of NiCd, with flat discharge characteristics. The capacity of the NiMH

is significantly higher than that of NiCd, with specific energy ranging from 60 to 80 Wh/kg. The specific power of NiMH batteries can be as high as 250 W/kg.

The NiMH batteries have penetrated the market in recent years at an exceptional rate. The Chrysler electric minivan “Epic” uses a NiMH battery pack, which gives a range of 150 km. In Japan, NiMH battery packs produced by Panasonic EV Energy are being used in Toyota EV RAV-EV and Toyota HEV Prius. The components of NiMH are recyclable, but a recycling structure is not yet in place. NiMH batteries have a much longer life cycle than lead-acid batteries and are safe and abuse tolerant. The disadvantages of NiMH batteries are the relatively high cost, higher self-discharge rate compared to NiCd, poor charge acceptance capability at elevated temperatures, and low cell efficiency. NiMH is likely to survive as the leading rechargeable battery in the future for traction applications, with strong challenge coming only from lithium-ion batteries.²

3.3.3 LI-ION BATTERY

Lithium metal has high electrochemical reduction potential (3.045 V) and the lowest atomic mass (6.94), which shows promise for a battery of 3 V cell potential when combined with a suitable positive electrode. The interest in secondary lithium cells soared soon after the advent of lithium primary cells in the 1970s, but the major difficulty was the highly reactive nature of the lithium metal with moisture, restricting the use of liquid electrolytes. Discovery in the late 1970s by researchers at Oxford University that lithium can be intercalated (absorbed) into the crystal lattice of cobalt or nickel to form LiCoO_2 or LiNiO_2 paved the way toward the development of Li-ion batteries.³ The use of metallic-lithium is bypassed in Li-ion batteries by using lithium intercalated (absorbed) carbons (Li_xC) in the form of graphite or coke as the negative electrode, along with the lithium metallic oxides as the positive electrode. The graphite is capable of hosting lithium up to a composition of LiC_6 . The majority of the Li-ion batteries uses positive electrodes of cobalt oxide, which is expensive but proven to be the most satisfactory. The alternative positive electrode is based on nickel oxide LiNiO_2 , which is structurally more complex but costs less. Performance is similar to that of cobalt oxide electrodes. Manganese-oxide-based positive electrodes (LiMn_2O_4 or LiMnO_2) are also under research, because manganese is cheaper, widely available, and less toxic.

The cell discharge operation in a lithium ion cell using LiCoO_2 is illustrated in [Figure 3.6](#). During cell discharge, lithium ions (Li^+) are released from the negative electrode that travels through an organic electrolyte toward the positive electrode. In the positive electrode, the lithium ions are quickly incorporated into the lithium compound material. The process is completely reversible. The chemical reactions at the electrodes are as follows:

At the negative electrode,

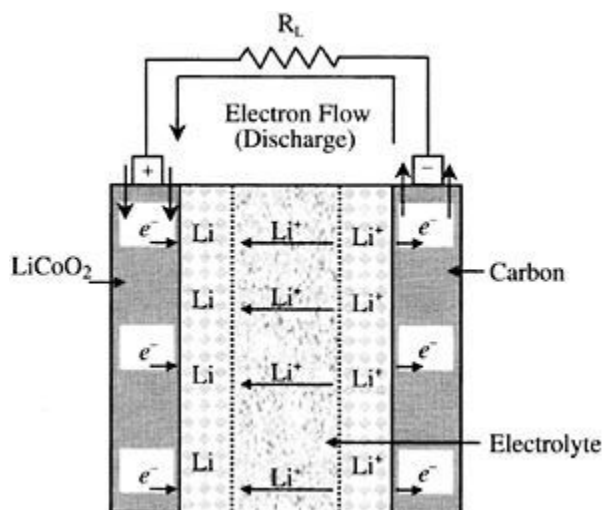
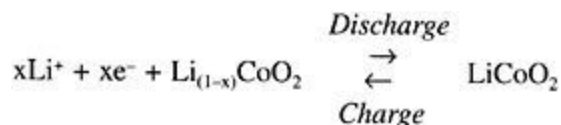


FIGURE 3.6 Lithium-ion cell.

At the positive electrode,



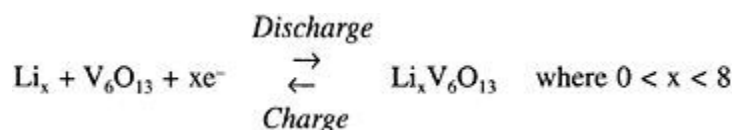
During cell charge operation, lithium ions move in the opposite direction from the positive electrode to the negative electrode. The nominal cell voltage for a Li-ion battery is 3.6 V, which is equivalent to three NiMH or NiCd battery cells.

Lithium-ion batteries have high specific energy, high specific power, high energy efficiency, good high-temperature performance, and low self-discharge. The components of Li-ion batteries are also recyclable. These characteristics make Li-ion batteries highly suitable for EV and HEV and other applications of rechargeable batteries.

3.3.4 LI-POLYMER BATTERY

Lithium-polymer evolved out of the development of solid state electrolytes, i.e., solids capable of conducting ions but that are electron insulators. The solid state electrolytes resulted from research in the 1970s on ionic conduction in polymers. These batteries are considered solid state batteries, because their electrolytes are solids. The most common polymer electrolyte is polyethylene oxide compounded with an appropriate electrolyte salt.

The most promising positive electrode material for Li-poly batteries is vanadium oxide V_6O_{13} .¹ This oxide interlaces up to eight lithium atoms per oxide molecule with the following positive electrode reaction:



Li-poly batteries have the potential for the highest specific energy and power. The solid polymers, replacing the more flammable liquid electrolytes in other type of batteries, can conduct ions at temperatures above 60°C. The use of solid polymers also has a great safety advantage in case of EV and HEV accidents. Because the lithium is intercalated into carbon electrodes, the lithium is in ionic form and is less reactive than pure lithium metal. The thin Li-poly cell gives the added advantage of forming a battery of any size or shape to suit the available space within the EV or HEV chassis. The main disadvantage of the Li-poly battery is the need to operate the battery cell in the temperature range of 80 to 120°C. Li-poly batteries with high specific energy, initially developed for EV applications, also have the potential to provide high specific power for HEV applications. The other key characteristics of the Li-poly are good cycle and calendar life.

3.3.5 ZINC-AIR BATTERY BATTERY

Zinc-air batteries have a gaseous positive electrode of oxygen and a sacrificial negative electrode of metallic zinc. The practical zinc-air battery is only mechanically rechargeable by replacing the discharged product, zinc hydroxide, with fresh zinc electrodes. The discharged electrode and the potassium hydroxide electrolyte are sent to a recycling facility. In a way, the zinc-air battery is analogous to a fuel cell, with the fuel being the zinc metal. A module of zinc air batteries tested in German Mercedes Benz postal vans had a specific energy of 200 Wh/kg, but only a modest specific power of 100 W/kg at 80% depth-of-discharge (see [Sections 3.4](#) and [3.5](#) for definitions of depth-of-discharge and specific power). With present-day technology, the range of zinc-air batteries can be between 300 to 600 km between recharges.

Other metal-air systems have been investigated, but the work has been discontinued due to severe drawbacks in the technologies. These batteries include iron-air and aluminum-air batteries, in which iron and aluminum are, respectively, used as the mechanically recyclable negative electrode.

The practical metal-air batteries have two attractive features: the positive electrode can be optimized for discharge characteristics, because the battery is recharged outside of the battery; and the recharging time is rapid, with a suitable infrastructure.

3.3.6 SODIUM-SULFUR BATTERY

Sodium, similar to lithium, has a high electrochemical reduction potential (2.71 V) and low atomic mass (23.0), making it an attractive negative electrode element for batteries. Moreover, sodium is abundant in nature and available at a low cost. Sulfur, which is a possible choice for the positive electrode, is also a readily available and low-cost material. The use of aqueous electrolytes is not possible due to the highly

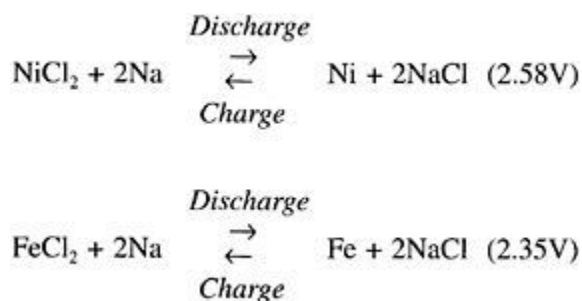
reactive nature of sodium, and because the natures of solid polymers like those used for lithium batteries are not known. The solution of electrolyte came from the discovery of beta-alumina by scientists at Ford Motor Company in 1966. Beta-alumina is a sodium aluminum oxide with a complex crystal structure.

Despite several attractive features of NaS batteries, there are several practical limitations. The cell operating temperature in NaS batteries is around 300°C, which requires adequate insulation as well as a thermal control unit. This requirement forces a certain minimum size of the battery, limiting the development of the battery for only EVs, a market that is not yet established. Another disadvantage of NaS batteries is the absence of an overcharge mechanism. At the top-of-charge, one or more cells can develop a high resistance, which pulls down the entire voltage of the series-connected battery cells. Yet another major concern is safety, because the chemical reaction between molten sodium and sulfur can cause excessive heat or explosion in the case of an accident. Safety issues were addressed through efficient design, and manufactured NaS batteries have been shown to be safe.

Practical limitations and manufacturing difficulties of NaS batteries have led to the discontinuation of its development programs, especially when the simpler concept of sodium-metal-chloride batteries was developed.

3.3.7 SODIUM-METAL-CHLORIDE BATTERY

The sodium-metal-chloride battery is a derivative of the sodium-sulfur battery with intrinsic provisions of overcharge and overdischarge. The construction is similar to that of the NaS battery, but the positive sulfur electrode is replaced by nickel chloride (NiCl₂) or a mixture of nickel chloride and ferrous chloride (FeCl₂). The negative electrode and the electrolyte are the same as in a NaS battery. The schematic diagram of a NaNiCl₂ cell is shown in [Figure 3.7](#). In order to provide good ionic contact between the positive electrode and the electrolyte, both of which are solids, a second electrolyte of sodium chloraluminate (NaAlCl₄) is introduced in a layer between NiCl₂ and beta-alumina. The NaAlCl₄ electrolyte is a vital component of the battery, although it reduces the specific energy of the battery by about 10%.³ The operating temperature is again high, similar to that of the NaS battery. The basic cell reactions for the nickel chloride and ferrous chloride positive electrodes are as follows:



The cells in a sodium metal chloride battery are assembled in a discharged state. The positive electrode is prefabricated from a mixture of Ni or Fe powder and NaCl

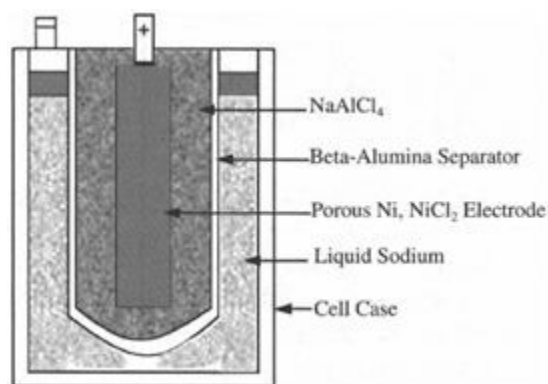


FIGURE 3.7 A sodium-nickel-chloride cell.

(common salt). On charging after assembly, the positive electrode compartment is formed of the respective metal, and the negative electrode compartment is formed of sodium. This procedure has two significant advantages: pure sodium is manufactured in situ through diffusion in beta-alumina, and the raw materials for the battery (common salt and metal powder) are inexpensive. Although iron is cheaper than nickel, the latter is more attractive as the metallic component because of fewer complications and a wider operating temperature range.

Sodium chloride batteries are commonly known as ZEBRA batteries, which originally resulted from a research collaboration between scientists from the United Kingdom and South Africa in the early 1980s. ZEBRA batteries have been shown to be safe under all conditions of use. They have high potential for being used as batteries for EVs and HEVs. There are several test programs utilizing the ZEBRA batteries.

3.4 BATTERY PARAMETERS

3.4.1 BATTERY CAPACITY

The amount of free charge generated by the active material at the negative electrode and consumed by the positive electrode is called the *battery capacity*. The capacity is measured in Ah (1 Ah=3600 C, or coulomb, where 1 C is the charge transferred in 1 s by 1 A current in the MKS unit of charge).

The theoretical capacity of a battery (in C) is:

where x is the number of moles of limiting reactant associated with complete discharge of the battery, n is the number of electrons produced by the negative electrode discharge reaction, and $F = Le_0$. L is the number of molecules or atoms in a mole (known as the Avogadro constant), and e_0 is the electron charge. F is the Faraday constant. The values for the constants are:

$$L = 6.022 \times 10^{23}$$

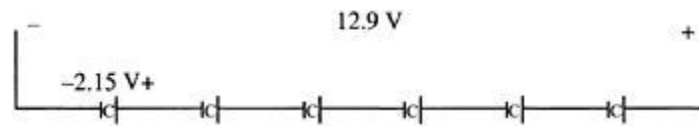


FIGURE 3.8 Battery cells connected in series.

and

$$e_0 = 1.601 \times 10^{-19} \text{ C}$$

$$\Rightarrow F = 96412.2 \text{ C/mol}$$

The theoretical capacity in Ah is:

$$Q_T = 0.278 F \frac{m_R n}{M_M} \quad (3.1)$$

where m_R is the mass of limiting reactant (in kg), and M_M is the molar mass of limiting reactant (in g/mol).

The cells in a battery are typically connected in series ([Figure 3.8](#)), and the capacity of the battery is dictated by the smallest cell capacity. Therefore, $Q_{T\text{battery}} = Q_{T\text{cell}}$.

3.4.2 DISCHARGE RATE

The *discharge rate* is the current at which a battery is discharged. The rate is expressed as Q/h rate, where Q is rated battery capacity, and h is discharge time in hours. For a battery that has a capacity of Q_T Ah and that is discharged over t , the discharge rate is Q_T/t .

For example, let the capacity of a battery be 1 Q=100 Ah. (1 Q usually denotes the rated capacity of the battery.) Therefore,

$$Q/5 \text{ rate is } \frac{100 \text{ Ahr}}{5 \text{ hr}} = 20 \text{ A}$$

and

3.4.3 STATE OF CHARGE

The *state of charge* (SoC) is the present capacity of the battery. It is the amount of capacity that remains after discharge from a top-of-charge condition. The battery

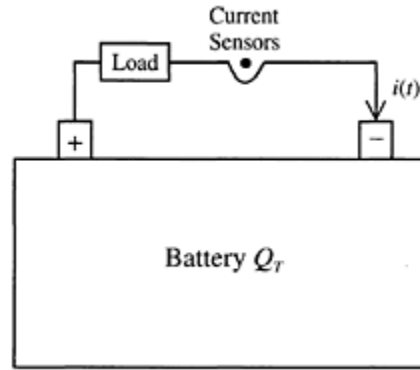


FIGURE 3.9 Battery *SoC* measurement.

SoC measurement circuit is shown in [Figure 3.9](#). The current is the rate of change of charge given by

$$i(t) = \frac{dq}{dt}$$

where q is the charge moving through the circuit. The instantaneous theoretical state of charge $SoC_T(t)$ is the amount of equivalent positive charge on the positive electrode. If the state of charge is Q_T at the initial time t_0 , then $SoC_T(t_0) = Q_T$. For a time interval dt ,

$$\begin{aligned} dSoC_T &= -dq \\ &= -i(t) dt \end{aligned}$$

Integrating from the initial time t_0 to the final time t , the expression for instantaneous state of charge is obtained as follows:

$$SoC_T(t) = Q_T - \int_{t_0}^t i(\tau) d\tau \quad (3.2)$$

3.4.4 STATE OF DISCHARGE

The *state of discharge (SoD)* is a measure of the charge that has been drawn from a battery. Mathematically, state of discharge is given as follows:

$$(3.3)$$

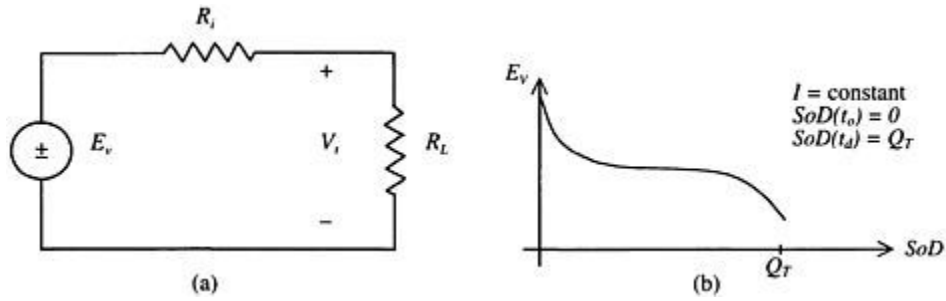


FIGURE 3.10 (a) Steady-state battery equivalent circuit. (b) Battery open circuit voltage characteristics.

3.4.5 DEPTH OF DISCHARGE

The *depth of discharge* (DoD) is the percentage of battery capacity (rated capacity) to which a battery is discharged. The depth of discharge is given by

$$\begin{aligned} \text{DoD}(t) &= \frac{Q_T - \text{SoC}_T(t)}{Q_T} \times 100\% \\ &= \frac{\int_a^t i(\tau) d\tau}{Q_T} \times 100\% \end{aligned} \quad (3.4)$$

The withdrawal of at least 80% of battery (rated) capacity is referred to as deep discharge.

3.5 TECHNICAL CHARACTERISTICS

The battery in its simplest form can be represented by an internal voltage E_v and a series resistance R_i , as shown in [Figure 3.10a](#). The internal voltage appears at the battery terminals as open circuit voltage when there is no load connected to the battery. The internal voltage or the open circuit voltage depends on the state of charge of the battery, temperature, and past discharge/charge history (memory effects), among other factors. The open circuit voltage characteristics are shown in [Figure 3.10b](#). As the battery is gradually discharged, the internal voltage decreases, while the internal resistance increases. The open circuit voltage characteristics have a fairly extended plateau of linear characteristics, with a slope close to zero. The open circuit voltage is a good indicator of the state of discharge. Once the battery reaches 100% DoD, the open circuit voltage decreases sharply with more discharge.

The battery terminal voltage ([Figure 3.11](#)) is the voltage available at the terminals when a load is connected to the battery. The terminal voltage is at its full charge voltage V_{FC} when the battery DoD is 0%. In the case of a lead-acid battery, it means that there is no more PbSO_4 available to react with H_2O to produce active material. V_{cut} is the battery cut-off voltage, where discharge of battery must be terminated.

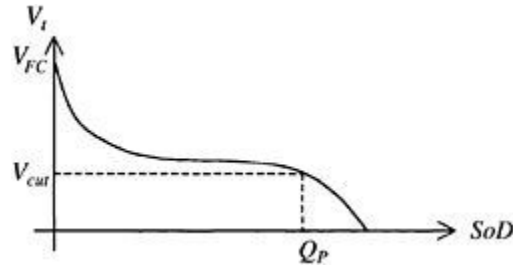


FIGURE 3.11 Battery terminal voltage.

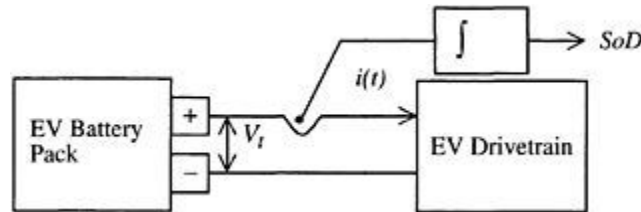


FIGURE 3.12 Battery *SoD* measurement.

In order to predict the range of an EV, the *SoC* or *DoD* can be used. However, the question is which one will be more accurate? The *SoC* and *DoD* are related as

$$SoC(t) = Q_T - SoD(t) \text{ (in Ah)}$$

$$DoD = \frac{SoD}{Q_T}$$

The reliability of *SoC* depends on reliability of Q_T , which is a function of discharge current and temperature, among other things. It will be difficult to use *SoC* for general discharge currents, because it is hard to predict Q_T . On the other hand, the *DoD* can be expressed more accurately, because it is expressed as a fraction of Q_T , and it is easier to measure *SoD* (Figure 3.12).

3.5.1 PRACTICAL CAPACITY

The *practical capacity* Q_P of a battery is always much lower compared to the theoretical capacity Q_T , due to practical limitations. The practical capacity of a battery is given as

(3.5)

where t_0 is the time at which the battery is fully charged [$SoD(t_0)=0$], and t_{cut} is the time at which the

battery terminal voltage is at V_{cut} . Therefore, $V_t(t_{cut})=V_{cut}$.

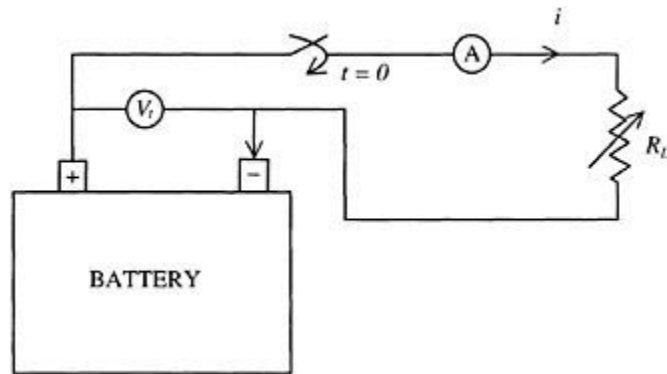


FIGURE 3.13 Battery capacity measurement.

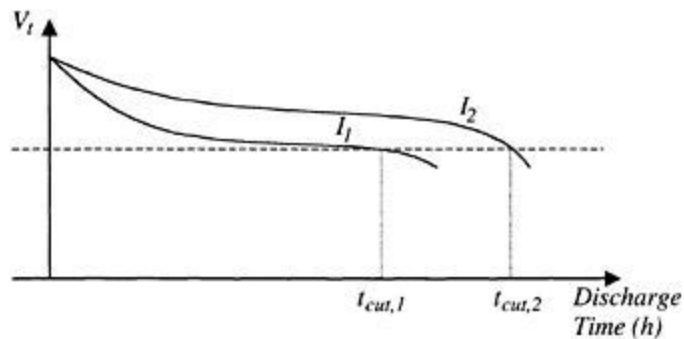


FIGURE 3.14 Constant current discharge curves.

3.5.1.1 Capacity Redefined

The practical capacity of a battery is defined in the industry by a convenient and approximate approach of Ah instead of coulomb under constant discharge current characteristics. Let us consider the experiment shown in [Figure 3.13](#), where the battery is discharged at constant current starting from time $t=0$. Current is maintained constant by varying the load resistance R_L until the terminal voltage reaches V_{cut} . The constant current discharge characteristics are shown qualitatively at two different current levels in [Figure 3.14](#). The following data are obtained from the experiment:

The results show that the capacity depends on the magnitude of discharge current. The smaller the

magnitude of the discharge current, the higher the capacity of the battery. To be accurate, when the capacity of a battery is stated, the constant discharge current magnitude must also be specified.

3.5.1.2 Battery Energy

The energy of a battery is measured in terms of capacity and discharge voltage. To calculate energy, the capacity of the battery must be expressed in coulombs. A measurement of 1 Ah is equivalent to 3600 C, while 1 V refers to 1 J (J for joule) of work required to move 1 C charge from the negative to positive electrode. Therefore, the stored electrical potential energy in a 12 V, 100 Ah battery is $(12)(3.6 \times 10^5) \text{J} = 4.32 \text{ MJ}$. In general, the theoretical stored energy is:

$$E_T = V_{bat} Q_T$$

where V_{bat} is the nominal no load terminal voltage, and Q_T is the theoretical capacity in C. Therefore, using Equation 3.1, we have

$$E_T = \left[\frac{1000 F n}{M_M} m_R \right] V_{bat} = 9.65 \times 10^7 \frac{n m_R}{M_M} V_{bat} \quad (3.6)$$

The practical available energy is:

$$E_p = \int_{t_0}^{t_{cut}} v_i dt \text{ Wh} \quad (3.7)$$

where t_0 is the time at which the battery is fully charged, t_{cut} is the time at which battery terminal voltage is at V_{cut} , v is the battery terminal voltage, and i is the battery discharge current. E_p is dependent on the manner in which the battery is discharged.

3.5.1.3 Constant Current Discharge

The battery terminal voltage characteristic is shown again in [Figure 3.15](#), indicating the midpoint voltage (MPV) at $t = 1/2 t_{cut}$. The extended plateau of the midpoint voltage can be represented by the straight-line equation $V_t = mt + b$, where m and b are the constants of the equation. We will replace the nonlinear terminal voltage characteristic of the battery by the extended plateau straight-line equation for simplicity. The energy of a battery with constant current discharge is

Let the average battery terminal voltage over discharge interval 0 to t_{cut} be $\langle v_t \rangle$. Therefore,

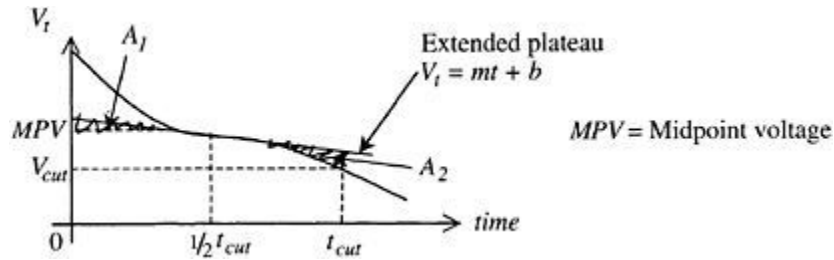


FIGURE 3.15 Midpoint voltage.

$$\langle v_t \rangle = \frac{1}{t_{cut}} \int_0^{t_{cut}} V_t dt = \frac{1}{t_{cut}} \left[A_1 + \int_0^{t_{cut}} (mt + b) dt - A_2 \right]$$

where A_1 and A_2 are the areas indicated in [Figure 3.15](#). We can assume that the areas A_1 and A_2 are approximately equal, $A_1 \cong A_2$. However, $m(1/2 t_{cut}) + b = MPV$ (MPV is midpoint voltage). This gives

$$\langle v_t \rangle = MPV \Rightarrow \int_0^{t_{cut}} V_t dt = t_{cut} MPV$$

Substituting,

$$E_t = I \cdot t_{cut} \cdot MPV = Q_t \cdot MPV \quad (3.8)$$

An empirical relation often used to describe battery characteristics is *Peukert's equation*. Peukert's equation relating constant current with t_{cut} is as follows:

$$t_{cut} = \frac{\lambda}{I^n} \quad (3.9)$$

where λ and n are constants. Substituting Peukert's equation in the energy equation,

3.5.1.4 Specific Energy

The *specific energy* of a battery is given by

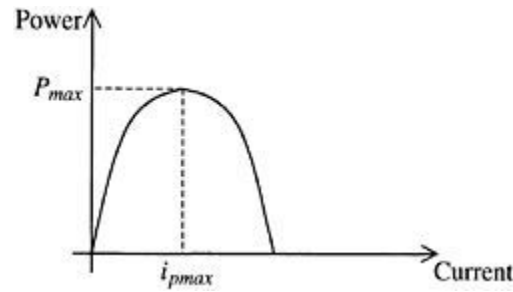


FIGURE 3.16 Battery power characteristics.

The unit for specific energy is Wh/kg. The theoretical specific energy of a battery is

$$SE_T = 9.65 \times 10^7 \times \frac{nV_{bat}}{M_M} \frac{m_R}{M_B} \quad (3.10)$$

If the mass of the battery M_B is proportional to the mass of the limiting reactant of the battery m_R , then SE_T is independent of mass. The specific energy of a lead-acid battery is 35 to 50 Wh/kg at Q/3 rate. Because E_P varies with discharge rate, the practical specific energy SE_P is also variable.

The term energy density is also used in the literature to quantify the quality of a battery or other energy source. Energy density refers to the energy per unit volume of a battery. The unit for energy density is Wh/liter.

3.5.2 BATTERY POWER

Battery power characteristics are illustrated in [Figure 3.16](#). The instantaneous battery terminal power is:

$$p(t) = V_t i \quad (3.11)$$

where V_t is the battery terminal voltage, and i is the battery discharge current. Using Kirchoff's voltage law for the battery equivalent circuit of [Figure 3.10a](#),

$$(3.12)$$

Substituting Equation 3.12 into Equation 3.11 yields:

$$(3.13)$$

Maximum power output is needed from the battery in fast discharge conditions, which occur when the electric motor is heavily loaded. Acceleration on a slope is such a condition, when the motor draws a lot of current to deliver maximum power required for traction. Using the maximum power transfer theorem in electric circuits,

the battery can deliver maximum power to a DC load when the load impedance matches the battery internal impedance. The maximum power is:

$$P_{\max} = \frac{E_v^2}{4 R_i}$$

Because E_v and R_i vary with the state of charge, P_{\max} also varies accordingly.

The performance of batteries to meet acceleration and hill climbing requirements can be evaluated with the help of rated power specifications, which are based on the ability of the battery to dissipate heat. *Rated continuous power* is the maximum power that the battery can deliver over prolonged discharge intervals without damage to the battery. These do not necessarily correspond to P_{\max} on the $p-i$ curve of battery characteristics. The *rated instantaneous power* is the maximum power that the battery can deliver over a short discharge interval without damage to the battery.

3.5.2.1 Specific Power

The specific power of a battery is

$$SP = \frac{P}{M_B} \text{ (units: Wh/kg)} \quad (3.14)$$

where P is the power delivered by the battery, and M_B is the mass of the battery. Typically, a lead-acid battery's maximum specific power is 280 W/kg (which corresponds to P_{\max}) at $DoD=80\%$. Similar to specific energy and energy density, power density refers to the power of the battery per unit volume, with units of W/liter.

3.5.2.2 Battery Pack Design

Batteries can be configured in series or in parallel configuration or in a combination thereof. Design depends on output voltage and discharge requirements. The series connection yields the required voltage, while the parallel connection delivers the desired capacity for the battery pack for minimum run time before recharging. The battery pack also includes electronics, which are typically located outside the battery pack. The electronic circuit of a multilevel battery pack controls charging and ensures reliability and protection against overcharge, overdischarge, short circuiting, and thermal abuse.

3.5.3 RAGONE PLOTS

In lead-acid and other batteries, there is a decrease in charge capacity (excluding voltage effects) with increasing currents. This is often referred to as the *Ragone* relationship and is described by *Ragone plots*. Ragone plots are usually obtained from constant power discharge tests or constant current discharge plots. Consider the experiment of [Figure 3.13](#), but this time, the current is adjusted by varying R_L

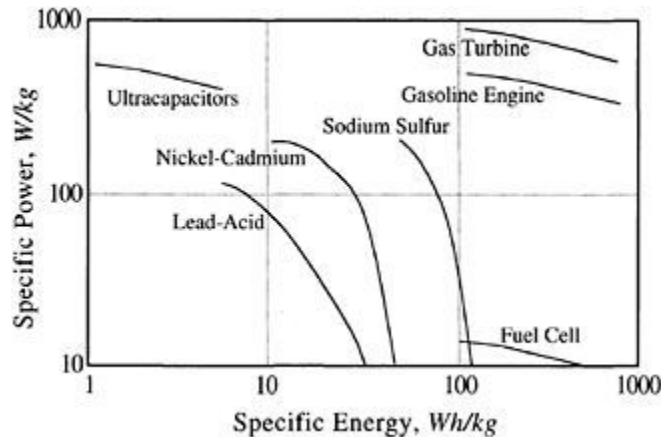


FIGURE 3.17 Specific power vs. specific energy (Ragone plots) of batteries, gasoline engine, and fuel cell.

such that the power output at the battery terminals is kept constant. The experiment stops when the battery terminal voltage reaches the cut-off voltage, i.e., $V_t = V_{cut}$. We assume that the battery is fully charged at $t=0$. The experiment is performed at several power levels, and the following data are recorded: power $p(t) = V_t i = P$, time to cut-off voltage t_{cup} , and practical energy $E_P = P t_{cut}$. The plot of SP vs. SE on log-log scale is known as the Ragone plot. The Ragone plots of some common batteries are shown in [Figure 3.17](#).

To a first-order approximation, we can use a linear Ragone plot (on a log-log scale) according to the following relationship between specific power and specific energy:

$$(SP)^n (SE) = \lambda \quad (3.15)$$

where n and λ are curve-fitting constants. The above is an alternative approach of using Peukert's equation to describe battery characteristics. The Ragone plots of several batteries, along with alternative energy sources and internal combustion (IC) engines, are given in [Figure 3.17](#) to give an idea about the relative power and energy capacities of these different units.

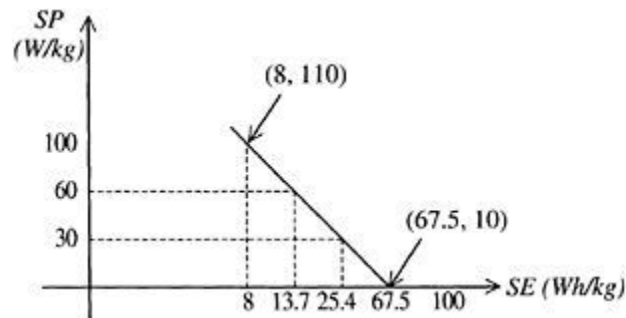
EXERCISE 3.1

The data given in [Table 3.3](#) are collected from an experiment on a battery with mass 15 kg. The data are used to draw the Ragone plot shown in [Figure 3.18](#). Using the data points (8,110) and (67.5,10), calculate the constants of Peukert's equation, n and λ .

Solution

TABLE 3.3 Data from Constant Power Discharge Test

P(W) (Measured)	t_{cut}(h) (Measured)	E_P (Wh) (Calculated)	SP (W/kg) (Calculated)	SE (Wh/kg) (Calculated)
150	6.75	(150)(6.75)=1013	150/15=10	1013/15=67.5
450	0.85	381	30	25.4
900	0.23	206	60	13.7
1650	0.073	120	110	8

**FIGURE 3.18** Ragone plot for Exercise 3.1.

3.6 TARGETS AND PROPERTIES OF BATTERIES

The push for zero-emission vehicles led to numerous research and development initiatives in the United States, Europe, and Japan. The California legislative mandates in the early 1990s led to the formation of the U.S. Advanced Battery Consortium (USABC) to oversee the development of power sources for EVs. The USABC established objectives focusing on battery development for mid-term (1995 to 1998) and long-term criteria. The purpose of the mid-term criteria was to develop batteries with a reasonable goal, while the long-term criteria were set to develop batteries for EVs, which would be directly competitive with IC engine vehicles (ICEVs). At the advent of the 21st century and following the developments in the 1990s, intermediate commercialization criteria were developed. The major objectives for the three criteria are summarized in [Table 3.4](#).

The two most developed battery technologies of today are lead-acid and nickel-cadmium batteries. However, these batteries will not be suitable for EVs, because the former store too little energy, while the latter have cost and toxicity problems. The future of the other batteries is difficult to predict, because these are mostly prototypes, where system design and performance data are not always available. The status of the promising batteries described in the previous section is summarized in [Table 3.5](#) from

information obtained from recent literature.

TABLE 3.4 USABC Objectives for EV Battery Packs

Parameter	Mid-Term	Commercialization	Long-Term
Specific energy (Wh/kg) (C/3 discharge rate)	80–100	150	200
Energy density (Wh/liter) (C/3 discharge rate)	135	230	300
Specific power (W/kg) (80% <i>DoD</i> per 30 s)	150–200	300	400
Specific power (W/kg), Regen. (20% <i>DoD</i> per 10 s)	75	150	200
Power density (W/liter)	250	460	600
Recharge time, h (20% 100% <i>SoC</i>)	<6	4–6	3–6
Fast recharge time, min	<15	<30	<15
Calendar life, years	5	10	10
Life, cycles	600 @ 80% <i>DoD</i>	1000 @ 80% <i>DoD</i> 1600 @ 50% <i>DoD</i> 2670 @ 30% <i>DoD</i>	1000 @ 80% <i>DoD</i>
Lifetime urban range, miles	100,000	100,000	100,000
Operating environment, °C	-30 to+65	-40 to+50	-40 to+85
Cost, US\$/kWh	<150	<150	<100
Efficiency, %	75	80	80

TABLE 3.5 Properties of EV and HEV Batteries

Battery Type	Specific Energy, Wh/kg	Specific Power, W/kg	Energy Efficiency, %	Cycle Life	Estimated Cost, US\$/KWh
Lead-acid	35–50	150–400	80	500–1000	100–150
Nickel-cadmium	30–50	100–150	75	1000–2000	250–350
Nickel-metal-hydride	60–80	200–300	70	1000–2000	200–350
Aluminum-air	200–300	100	<50	Not available	Not available
Zinc-air	100–220	30–80	60	500	90–120
Sodium-sulfur	150–240	230	85	1000	200–350
Sodium-nickel-chloride	90–120	130–160	80	1000	250–350
Lithium-polymer	150–200	350	Not available	1000	150
Lithium-ion	80–130	200–300	>95	1000	200

3.7 BATTERY MODELING

Peukert's equation is a widely accepted empirical relation among capacity (Q), discharge current (I), and time (t) or among specific power (SP), specific energy (SE), and time (t). Peukert's equation is used in developing a *fractional depletion model* (FDM) of batteries. The FDM of a battery can be used to predict the range of an EV. The FDM can be developed using the constant current discharge approach or the power density approach associated with the two forms of Peukert's equation.

3.7.1 CONSTANT CURRENT DISCHARGE APPROACH

Consider the constant current discharge experiment of [Figure 3.13](#). The battery is discharged under constant current condition from 100% capacity until cut-off voltage is reached. The load resistance R_L is varied to change the constant current level and also to maintain the current constant for each experiment. The I vs. t_{cut} data are used to fit Peukert's equation (Equation 3.9) with constant current:

$$I^n * t_{cut} = \lambda \quad (3.16)$$

where I is the constant discharge current; and λ , and n are curve-fitting constants, with $n = 1$ for small currents and $n = 2$ for large currents.

EXAMPLE 3.1

Find the curve-fitting constants n and λ , for Peukert's equation for the two measurements available from a constant current discharge experiment of a battery:

- (i) $(t_1, I_1) = (10, 18)$
- (ii) $(t_2, I_2) = (1, 110)$

Solution

Equation 3.16 is the Peukert's empirical formula using the constant current discharge approach. Taking logarithm of both sides of Equation 3.16:

$$\begin{aligned}\text{Log}_{10}(I^n * t_{cut}) &= \text{Log}_{10}(\lambda) \\ \Rightarrow \text{Log}_{10}(I) &= \frac{1}{n} \text{Log}_{10}(t_{cut}) + \frac{1}{n} \text{Log}_{10}(\lambda)\end{aligned}$$

Comparing with the equation for a straight line, $y=mx+b$, I vs. t_{cut} curve is linear on a log-log plot, as shown in [Figure 3.19](#). The slope of the straight line is

$$m = \frac{\Delta y}{\Delta x} = \frac{\log(I_1) - \log(I_2)}{\log(t_1) - \log(t_2)} = \frac{\log\left(\frac{I_1}{I_2}\right)}{\log\left(\frac{t_1}{t_2}\right)}$$

Therefore,

$$n = - \frac{\log\left(\frac{t_1}{t_2}\right)}{\log\left(\frac{I_1}{I_2}\right)}$$

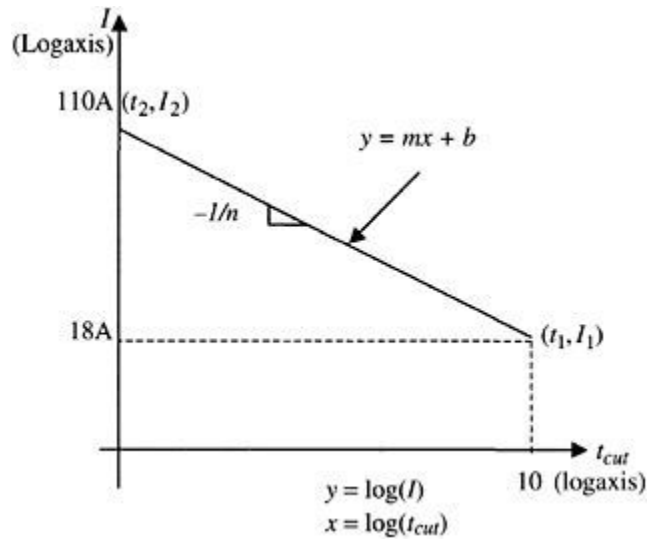


FIGURE 3.19 Plot of Peukert's equation using constant current discharge.

For the graph shown,

$$n = \frac{-1}{18/110} = 1.27 \quad [\because t_1 = 10t_2]$$

The other constant can now be calculated from Peukert's equation:

$$\lambda = 110^{1.27} * 1 = 3.91.4 \text{ Ah} \quad \text{or}$$

$$\lambda = 18^{1.27} * 10 = 392.8 \text{ Ah}$$

3.7.1.1 Fractional Depletion Model

Using Peukert's equation, we can establish the relationship between Q and I . The practical capacity of a battery is

Substituting into Peukert's equation:

Because $0 < n-1 < 1$, for $I > 1$, Q decreases as I increases.

From Section 3.4, we know that

$$SoD = \int i(\tau) d\tau$$

and

$$DoD = \frac{SoD}{Q(i)}$$

SoD is the amount of charge that the battery generates to the circuit. Assume that at $t=t_0$, the battery is fully charged. Let us consider a small interval of time dt . Therefore,

$$d(DoD) = \frac{d(SoD)}{Q(i)}$$

where

$$d(SoD) = i(t) dt$$

We know that $Q = I^{n-1}$ for constant current discharge. Let $Q = i^{n-1}$ for time varying current as well, for lack of anything better.

Therefore,

$$d(DoD) = \frac{idt}{\lambda/i^{n-1}} = \frac{i^n}{\lambda} dt$$

Integrating, we obtain,

$$\begin{aligned} \int_{t_0}^t d(DoD) &= \int_{t_0}^t \frac{i^n}{\lambda} dt \\ \Rightarrow DoD(t) - DoD(t_0) &= \int_{t_0}^t \frac{i^n}{\lambda} dt \end{aligned}$$

$DoD(t_0)=0$ if the battery is fully charged at $t=t_0$.

The *fractional depletion model* (FDM) is thus obtained as

(3.17)

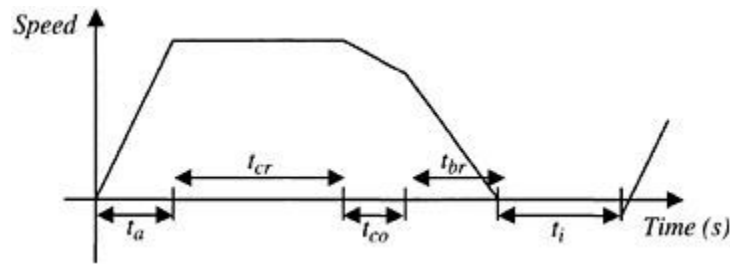


FIGURE 3.20 SAE J227a standard driving cycle.

The FDM based on current discharge requires knowledge of the discharge current $i(t)$. Therefore, this model to predict the EV range should be used when $i(t)$ is known.

3.7.2 STANDARD DRIVING CYCLES

The standard J227a driving cycle recommended by the Society of Automotive Engineers (SAE) is routinely used to evaluate the performance of EVs and energy sources. The SAE J227a has three schedules designed to simulate the typical driving patterns of fixed-route urban, variable-route urban, and variable-route suburban travels. These three patterns are the SAE J227a driving schedules B, C, and D, respectively. Each schedule has five segments in the total driving period:

1. Acceleration time t_a to reach the maximum velocity from start-up
2. Cruise time t_{cr} at a constant speed
3. Coast time t_{co} when no energy is drawn from the source
4. Brake time t_{br} to bring the vehicle to stop
5. Idle time t_i prior to the completion of the period

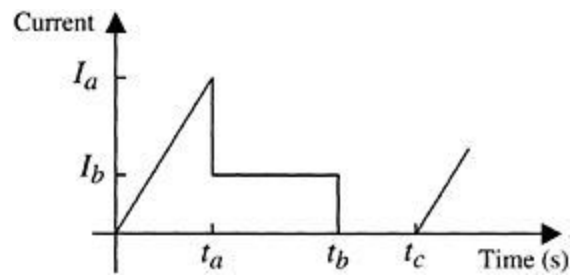
The driving cycle for J227a is shown in [Figure 3.20](#), with the recommended times for each of the schedules given in [Table 3.6](#). The figure drawn is slightly modified from the pattern recommended by the SAE. The J227a procedures specify only the cruise velocity and the time of transition from one mode to the other. The velocity profile at segments other than the cruising part is not fixed, and hence, the distance traversed during these other periods is also variable. In reality, the distances would depend on the design of the vehicle under consideration. For simplicity, straight-line approximations have been assumed in these schedules in this book.

EXAMPLE 3.2

The constant current discharge characteristics of the battery pack used in an EV are as follows:

TABLE 3.6 SAE J227a Standard Driving Schedules

Test Parameter	SAE J227a Schedules		
	B	C	D
Maximum speed, km/h	32	48	72
Acceleration time, t_a s	19	18	28
Cruise time, t_{cr} s	15	20	50
Coast time, t_{co} s	4	8	10
Brake time, t_{br} s	5	9	9
Idle time, t_i s	25	25	25
Total time, s	72	80	122
Approximate number of cycles per mile	4–5	3	1

**FIGURE 3.21** Pattern of current drawn from the battery.**TABLE 3.7 Current Data for the Driving Schedules**

Schedule J227a	I_a (A)	I_b (A)
B	100	35
C	216	54.6
D	375	88.7

The current drawn from the battery during test drives of the EV for the SAE schedule J227a has the profile shown in [Figure 3.21](#). The current magnitudes for the three SAE schedules are given in [Table 3.7](#).

Find the range of the EV for each of the three schedules.

Solution

Apply the FDM (Equation 3.17) to find the number of driving cycles for $DoD=100\%$. From FDM:

$$1 = \int_{t_0}^{t_{100\%}} \frac{i_n}{\lambda} dt \quad (3.18)$$

First, we need to determine λ and n from the given battery characteristics:

$$\frac{-1}{n} = -0.74 \Rightarrow n = 1.35$$

$$\frac{1}{n} \ln(\lambda) = 4.787 \Rightarrow \lambda = 645 * 3600 \text{ A} - \text{sec}$$

Therefore,

$$1 = \int_0^{t_{100\%}} \frac{i^{1.35}}{645 * 3600} dt$$

For Schedule B, the fraction depleted over one cycle is as follows:

$$\begin{aligned} DoD \text{ for 1 cycle} &\Rightarrow f_{cyc} = \int_0^{72} \frac{i^{1.35}}{645 * 3600} dt \\ &\Rightarrow f_{cyc} = 4.31 * 10^{-7} \left[\int_0^{19} \left(\frac{100t}{19} \right) dt + \int_{19}^{38} (35)^{1.35} dt \right] \\ &= 4.31 * 10^{-7} \left[9.41 \left(\frac{1}{2.35} \right) 119^{2.35} + 121.5(38 - 19) \right] \\ &\Rightarrow f_{cyc} = 2.74 * 10^{-3} \end{aligned}$$

Let N =the number of cycles required for 100% DoD , $DoD=1$:

$$\begin{aligned} \therefore 1 &= N * f_{cyc} \Rightarrow N = \frac{1}{f_{cyc}} \\ \therefore N &= \frac{1}{2.74 * 10^{-3}} = 365 \text{ cycles} \end{aligned}$$

From Table 3.6, the EV goes 1 mi in about four cycles for Schedule B.

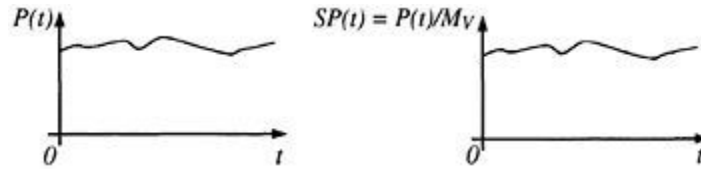


FIGURE 3.22 Power and specific power.

Therefore,

$$\text{EV Range} = \frac{365}{4} = 91 \text{ miles for Schedule B}$$

$$\text{Measured } N = 369 \Rightarrow \text{Error} = 1.08\%$$

J227a Schedule C: From FDM, $N=152$; EV range= $152/3=51$ mi.
(Measured, $N=184 \Rightarrow \text{Error}=17.4\%$.)

J227a Schedule D: From FDM, $N=41$; EV range= $41/1=41$ mi.
(Measured, $N=49 \Rightarrow \text{Error}=16.3\%$.)

3.7.3 POWER DENSITY APPROACH

Given a battery terminal power profile $p(t)$, the specific power $SP(t)$ profile can be obtained by dividing the power profile $p(t)$ by the total vehicle mass M_v . The battery is assumed to be fully charged at $t=0$. Let $f_r(t)$ be equal to the fraction of available energy provided by the battery from 0 to t , where $f_r(0)=0$, because $SoD(0)=0$. Now, consider the time interval dt over which a fraction of available energy df_r is provided by the battery:

$$df_r = \frac{dE}{E_{avail}} = \frac{\frac{dE}{M_v}}{\frac{dE_{avail}}{M_v}} = \frac{d(SE)}{SE_{avail}}$$

If dE is the energy provided by the battery to the electrical circuit over dt , and E_{avail} is the total available energy, then

Now E_{avail} is a function of instantaneous power, and we know that

Therefore,

$$SE_{avail} = f(SP)$$

We will use Peukert's equation to relate specific power and specific energy as follows:

$$(SP)^n * SE_{avail} = \lambda$$

Therefore,

$$df_r = \frac{SP}{\frac{\lambda}{(SP)^n}} dt = \frac{(SP)^{n+1}}{\lambda} dt$$

Integrating,

$$\begin{aligned} \int_{f_r(0)}^{f_r(t)} df_r &= \int_0^t \frac{(SP)^{n+1}}{\lambda} d\tau \\ \Rightarrow f_r(t) &= \int_0^t \frac{(SP)^{n+1}}{\lambda} d\tau \end{aligned} \quad (3.19)$$

Equation 3.19 is the FDM using the power density approach. If t is the time at which $x\%$ of available energy has been used, then

$$\frac{x}{100} = \int_0^t \frac{(SP)^{n+1}}{\lambda} d\tau$$

Note that

$$1 = \int_0^{t_{100\%}} \frac{(SP)^{n+1}}{\lambda} d\tau$$

At $t_{100\%}$, 100%, all of the available energy has been used by the system.

REFERENCES

1. Rand, D.A.J., Woods, R., and Dell, R.M., *Batteries for Electric Vehicles*, John Wiley & Sons, New York, 1998.

2. Dhameja, S., *Electric Vehicle Battery Systems*, Newnes (Elsevier Science), Burlington, MA, 2002.
3. Dell, R.M. and Rand, D.A.J., *Understanding Batteries*, Royal Society of Chemistry, United Kingdom, 2001.

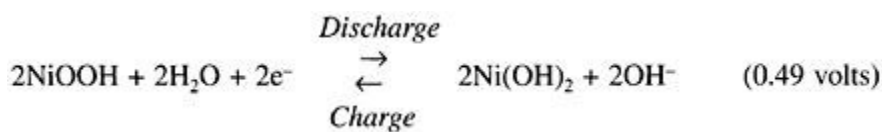
PROBLEMS

3.1

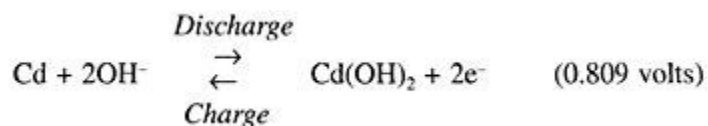
Estimate the weight of a 12 V, 100 Ah lead-acid battery by calculating the reactant masses participating in the overall chemical reaction. Assume that the mass of H₂O in the electrolyte is twice the mass of H₂SO₄. Neglect battery casing mass, electrode grid mass, separator mass, and current bus mass. (Note that $n=2$ for Pb and PbO₂, and $n=1$ for H₂SO₄.)

3.2

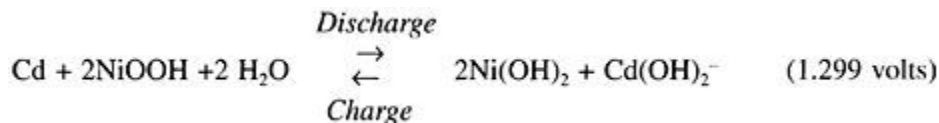
In the nickel-cadmium cell, nickel oxyhydroxide NiOOH is the active material in the charged positive plate. During discharge, it reduces to the lower valence state, nickel hydroxide Ni(OH)₂, by accepting electrons from the external circuit:



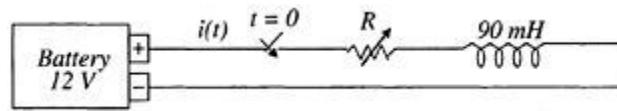
Cadmium metal is the active material in the charged negative plate. During discharge, it oxidizes to cadmium hydroxide Cd(OH)₂ and releases electrons to the external circuit:



The net reaction occurring in the potassium hydroxide (KOH) electrolyte is:



Estimate the weight of an 11.7 V, 100 Ah Ni-Cd battery. Neglect the mass of the KOH component of the electrolyte.

**FIGURE P3.3****3.3**

A 12 V battery is connected to a series RL load as shown in Figure P3.3. The battery has a rated capacity of 80 Ah. At $t=0$, the switch is closed, and the battery begins to discharge.

- Calculate and plot the battery discharge current, $i(t)$, if the steady state discharge rate is $C/2$. Neglect battery voltage drop.
- Calculate and plot $SoD(t)$ in Ah for $0 < t < 2$ h.
- Calculate and plot $SoC(t)$, assuming that at $t=0$ the battery is charged to rated capacity. Assume also that the rated capacity is the practical capacity.
- Calculate the time corresponding to 80% DoD .

3.4

Given below are constant power discharge characteristics of a 12 V lead-acid battery:

SP (W/kg)	SE (Wh/kg)
10	67.5
110	8

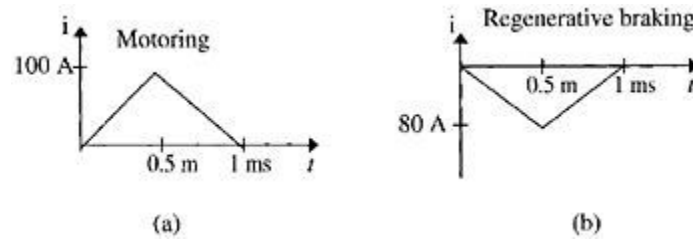
The battery characteristics are to be expressed in terms of Peukert's equation, which has the following form:

$$(SP)^n (SE) = \lambda \quad (n \text{ and } \lambda \text{ are curve fitting constants})$$

- Derive the constants n and λ , assuming a linear relationship between $\log(SP)$ and $\log(SE)$.
- Find the capacity Q_T of the battery if the theoretical energy density is $SE_T=67.5$ Wh/kg, given a battery mass of 15 kg.

3.5

An EV battery pack consists of four parallel sets of six series-connected 12 V, 100 Ah lead-acid batteries. One steady state motoring (discharge) cycle of battery current is shown in [Figure P3.5a](#). The steady-state regenerative braking (charge) cycle of the battery is shown in [Figure P3.5b](#).

**FIGURE P3.5**

- (a) Suppose no regenerative braking is employed. How much time does it take to reach 80% *DoD*?
 (b) If regenerative braking is employed such that for every 50 motoring cycles there is one regenerative braking cycle, how much time does it take to reach 80% *DoD*?

(Note: In this problem, neglect variation of capacity with discharge rate. Assume that the practical capacity is equal to the rated capacity.)

3.6

Given a lead-acid battery having the following empirical characteristics:

$$(SP)^9(SE) = 600 \text{ Ah}$$

where *SP* is specific power, and *SE* is specific energy. The EV parameters are as follows:

$$m = 700 \text{ kg}, M_B = 150 \text{ kg}, C_D = 0.2, A_F = 2 \text{ m}^2, C_0 = 0.009, \text{ and } C_1 = 0.$$

Also, take

$$\rho = 1.16 \text{ kg/m}^3, \text{ and } g = 9.81 \text{ m/s}^2$$

- (a) Derive and plot $F_{TR}(t)$ vs. t (assume level road).
 (b) Derive and plot $P_{TR}(t)$ vs. t .
 (c) Calculate the EV range based on the SAE J227a Schedule B driving cycle using the power density approach of the FDM. The SAE J227a driving cycle and the current profile of the EV are given in Figures P3.6a and P3.6b. (Assume no regenerative braking.)

FIGURE P3.6

This page intentionally left blank.

4 Alternative Energy Sources

The possible alternatives to batteries as portable energy sources that are being investigated today for electric vehicles (EVs) and hybrid electric vehicles (HEVs) and other applications are fuel cells and flywheels. Ultracapacitor technology has advanced tremendously in recent years, although it is unlikely to achieve specific energy levels high enough to serve as the sole energy source of a vehicle. However, ultracapacitors in conjunction with a battery or fuel cell have the possibility of being excellent portable energy sources with sufficient specific energy and specific power for the next generation of vehicles. These three alternative energy sources are covered in this chapter.

4.1 FUEL CELLS

A fuel cell is an electrochemical device that produces electricity by means of a chemical reaction, much like a battery. The major difference between batteries and fuel cells is that the latter can produce electricity as long as fuel is supplied, while batteries produce electricity from stored chemical energy and, hence, require frequent recharging.

The basic structure of a fuel cell ([Figure 4.1](#)) consists of an anode and a cathode, similar to a battery. The fuel supplied to the cell is hydrogen and oxygen. The concept of fuel cell is the opposite of electrolysis of water, where hydrogen and oxygen are combined to form electricity and water. The hydrogen fuel supplied to the fuel cell consists of two hydrogen atoms per molecule chemically bonded together in the form H_2 . This molecule includes two separate nuclei, each containing one proton, while sharing two electrons. The fuel cell breaks apart these hydrogen molecules to produce electricity. The exact nature of accomplishing the task depends on the fuel cell type, although what remains the same for all fuel cells is that this reaction takes place at the anode. The hydrogen molecule breaks into four parts at the anode due to the chemical reaction, releasing hydrogen ions and electrons. A catalyst speeds the reaction, and an electrolyte allows the two hydrogen ions, which essentially are two single protons, to move to the cathode through the electrolyte placed between the two electrodes. The flow of electrons from the anode to the cathode through the external circuit is what produces electricity. For the overall cell reaction to complete, oxygen or air must be passed over the cathode. The cathode reaction takes place in two stages. First, the bond between the two oxygen atoms in the molecule breaks and then each ionized oxygen atom grabs two electrons coming from the anode through the external circuit to become negatively charged. The negatively charged

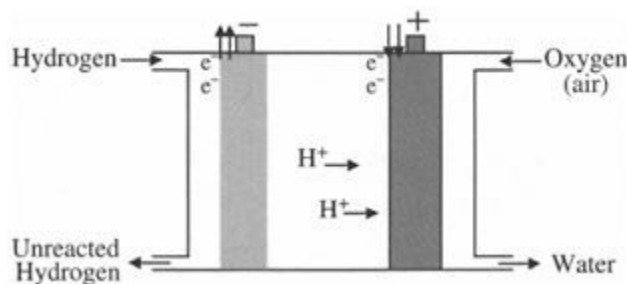
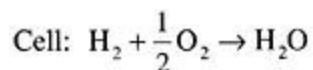
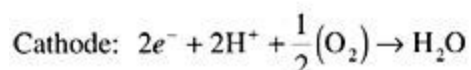
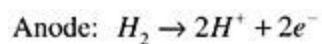


FIGURE 4.1 Basic fuel cell structure.

oxygen atoms are balanced by the positively charged hydrogen atoms at the cathode, and the combination produces H_2O commonly known as water. The chemical reaction taking place in a fuel cell is as follows:



The fuel cell was first developed for space applications as an alternative power source. The source was first used in a moon buggy and is still used in NASA's space shuttles. There has been tremendous interest in fuel cells in recent years for applications in other areas, such as EVs and stationary power systems. The research sponsored by several U.S. research agencies and corporations has attempted to improve cell performance with two primary goals: a desire for higher power cells, which can be achieved through higher rates of reaction, and the desire for fuel cells that can internally reform hydrocarbons and are more tolerant of contaminants in the reactant streams. For this reason, the searches have concentrated on finding new materials for electrodes and electrolytes. There are several different types of fuel cells, each with strengths and weaknesses. Low operating temperature is desirable for vehicle applications, despite the fact that higher temperatures result in higher reaction rates. Rapid operation and cogeneration capabilities are desirable for stationary applications. Cogeneration refers to the capability to utilize the waste heat of a fuel cell to generate electricity using conventional means.

4.1.1 FUEL CELL CHARACTERISTICS

Theoretically, fuel cells operate isothermally, meaning that all free energy in a fuel cell chemical reaction should convert into electrical energy. The hydrogen "fuel" in the fuel cell does not burn as in IC engines, bypassing the thermal to mechanical conversion. Also, because the operation is isothermal, the efficiency of such direct

electrochemical converters is not subject to the limitation of Carnot cycle efficiency imposed on heat engines. The fuel cell converts the Gibbs free energy of a chemical reaction into electrical energy in the form of electrons under isothermal conditions. The maximum electrical energy for a fuel cell operating at constant temperature and pressure is given by the change in Gibbs free energy:

$$W_{el} = -\Delta G = nFE \quad (4.1)$$

where n is the number of electrons produced by the anode reaction; F is Faraday's constant, equal to 96412.2 C/mol; and E is the reversible potential. The Gibbs free energy change for the reaction $\text{H}_2(\text{g}) + (1/2)\text{O}_2(\text{g}) \rightarrow \text{H}_2\text{O}(\text{l})$ at standard condition of 1 atmospheric pressure and 25°C is -236 kJ/mol or -118 MJ/kg. With $n=2$, the maximum reversible potential under the same conditions is $E_0=1.23$ V, using Equation 4.1. The maximum reversible potential under actual operating conditions for the hydrogen-oxygen fuel cell is given by the Nernst equation, as follows:¹

$$E = E_0 + \left(\frac{RT}{nF} \right) \ln \left[\frac{P_{\text{H}} \cdot P_{\text{O}}^{1/2}}{P_{\text{H}_2\text{O}}} \right] \quad (4.2)$$

where T is the temperature in Kelvin; R is the gas constant; and P_{H} , P_{O} , and $P_{\text{H}_2\text{O}}$ are the concentrations or partial pressures of the reactants and products.

The voltage-current output characteristic of a hydrogen-oxygen cell is illustrated in [Figure 4.2](#). The higher potentials around 1 V per cell are theoretical predictions that are not achievable in a practical cell. The linear region where the reduction in cell potential is due to ohmic losses is where a practical fuel cell operates. The resistive components in the cell limit the practical achievable efficiency of a fuel cell. The working voltage of the cell falls with an increasing current drain, knowledge that is important in designing fuel-cell-powered EVs and hybrid vehicles. Because cell potential is small, several cells are stacked in series to achieve the desired voltage. The major advantage of fuel cells is lower sensitivity to scaling, which means that fuel cells in the kW range have similar overall system efficiencies up to the MW range.

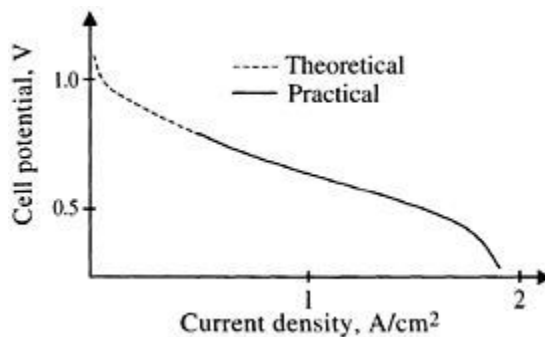


FIGURE 4.2 Voltage-current relationship of a hydrogen/oxygen cell.

4.1.2 FUEL CELL TYPES

The six major types of fuel cells are as follows: alkaline, proton exchange membrane, direct methanol, phosphoric acid, molten carbonate, and solid oxide. A short description of the relevant characteristics of each type in the context of vehicular and stationary applications is given below.^{2,3}

4.1.2.1 Alkaline Fuel Cell (AFC)

In an alkaline fuel cell (AFC), an aqueous solution of potassium hydroxide (KOH) is used as the electrolyte. Compared to some other fuel cells where acidic electrolytes are used, the performance of the alkaline electrolyte is as good as the acid electrolytes, while being significantly less corrosive toward the electrodes. Alkaline fuel cells have been in actual use for a long time, delivering electrical efficiencies of up to 60%. They require pure hydrogen as fuel and operate at low temperatures (at 80°C); therefore, they are suitable for vehicle applications. Residual heat can be used for heating, but the cell temperature is not sufficiently high to generate steam that can be used for cogeneration.

4.1.2.2 Proton Exchange Membrane (PEM)

The proton exchange membrane (PEM) fuel cells use solid electrolytes and operate at low temperatures (around 80°C). Nafion is an example of solid polymer electrolyte. These fuel cells are also known as solid polymer membrane fuel cells. The electrical efficiency of PEM fuel cells is lower than that of the alkaline cells (about 40%). However, a rugged and simple construction makes these types of fuel cells suitable for vehicle applications. The PEM fuel cell and the AFC are currently being considered for vehicle applications. The advantage of PEM cells is that they can tolerate impurity in the fuel, as compared to pure hydrogen which is needed in alkaline fuel cells.

4.1.2.3 Direct Methanol Fuel Cell (DMFC)

The direct methanol fuel cell (DMFC) is a result of research on using methanol as the fuel that can be carried on-board a vehicle and reformed to supply hydrogen to the fuel cell. A DMFC works on the same principle as the PEM, except that the temperature is increased to the range of 90 to 120°C such that internal reformation of methanol into hydrogen is possible. The electrical efficiency of DMFC is quite low at about 30%. This type of fuel cell is still in the design stages, because the search for a good electrocatalyst to reform the methanol efficiently and to reduce oxygen in the presence of methanol is ongoing.

4.1.2.4 Phosphoric Acid Fuel Cell (PAFC)

Phosphoric acid fuel cells (PAFC) are the oldest type with an origin that extends back to the creation of the fuel cell concept. The electrolyte used is phosphoric acid, and the cell operating temperature is about 200°C, which makes some cogeneration possible. The electrical efficiency of this cell is reasonable at about 40%. These types of fuel cells are considered too bulky for transportation applications, while higher efficiency designs exist for stationary applications.

4.1.2.5 Molten Carbonate Fuel Cell (MCFC)

Molten carbonate fuel cells, originally developed to operate directly from coal, operate at 600°C and

require CO or CO₂ on the cathode side and hydrogen on the anode. The cells use carbonate as the electrolyte. The electrical efficiency of these fuel cells is high at about 50%, but the excess heat can be used for cogeneration for improved efficiency. The high temperatures required make these fuel cells not particularly suitable for vehicular applications, but they can be used for stationary power generation.

4.1.2.6 Solid Oxide Fuel Cell (SOFC, ITSOFC)

Solid oxide fuel cells (SOFCs) use a solid ionic conductor as the electrolyte rather than a solution or a polymer, which reduces corrosion problems. However, to achieve adequate ionic conductivity in such a ceramic, the system must operate at very high temperatures. The original designs, using yttria-stabilized zirconia as the electrolyte, required temperatures as high as 1000°C to operate, but the search for materials capable of serving as the electrolyte at lower temperatures resulted in the “intermediate temperature solid oxide fuel cell” (ITSOFC). This fuel cell has high electrical efficiency of 50 to 60%, and residual heat can also be used for cogeneration. Although not a good choice for vehicle applications, it is at present the best option for stationary power generation.

The fuel cell features described above are summarized in [Table 4.1](#). The usable energy and relative costs of various fuels used in fuel cells are listed in [Table 4.2](#). The selection of fuel cells as the primary energy source in EVs and HEVs depends on a number of issues, ranging from fuel cell technology to infrastructure to support the system. Based on the discussion in this section, the choice of fuel cell for the vehicular application is an alkaline or proton exchange design, while for stationary applications, it will be the SOFC. The size, cost, efficiency, and start-up transient times of fuel cells are yet to be at an acceptable stage for EV and HEV applications. The complexity of the controller required for fuel cell operation is another aspect that needs further attention. Although its viability has been well-proven in the space program, as well as in prototype vehicles, its immature status makes it a longer-term enabling technology for an EV and HEV.

4.1.3 HYDROGEN STORAGE SYSTEMS

The options for storage of hydrogen play a critical role in the future development of infrastructure for fuel-cell-powered EVs and hybrid vehicles. The hydrogen gas at atmospheric pressure has a fairly low energy density and is not a suitable fuel for storage. Hydrogen could be stored as compressed or liquefied gas, or in a more advanced manner by using metal hydrides or carbon nanotubes. Gas storage in compressed form is an option that has been in use for a long time. In this method,

TABLE 4.1 Fuel Cell Types

Fuel Cell Variety	Fuel	Electrolyte	Operating Temperature	Efficiency	Applications
Phosphoric acid	H ₂ , reformat (LNG, methanol)	Phosphoric acid	~200°C	40–50%	Stationary (>250 kW)
Alkaline	H ₂	Potassium hydroxide solution	~80°C	40–50%	Mobile
Proton exchange membrane	H ₂ , reformat (LNG, methanol)	Polymer ion exchange film	~80°C	40–50%	EV and HEV, industrial up to –80 kW
Direct methanol	Methanol, ethanol	Solid polymer	90–100°C	~30%	EV and HEVs, small portable devices (1 W to 70 kW)
Molten carbonate	H ₂ , CO (coal gas, LNG, methanol)	Carbonate	600–700°C	50–60%	Stationary (>250 kW)
Solid oxide	H ₂ , CO (coal gas, LNG, methanol)	Yttria-stabilized zirconia	~1000°C	50–65%	Stationary

TABLE 4.2 Usable Energy and Cost of Fuels

Fuel	Usable Energy, MJ/kg	Relative Cost/MJ
Hydrogen:		
95% pure at plant	118.3	1.0
99% pure in cylinders	120	7.4
LPG (propane)	47.4	0.5
Gasoline	45.1	0.8
Methanol	21.8	3.3
Ammonia	20.9	3.6

a large amount of energy is required to compress the gas to a level that will make storage viable, usually at a pressure of several hundred atmospheres.⁴ Generation of liquid H₂ requires further

compression, along with refrigeration to cryogenic temperatures, and is not likely to become a viable means of storage for vehicle applications.

Advanced methods for H₂ storage include the use of metal hydrides or carbon nanotubes. Here, the gas is compressed to a lower pressure level (a few to a few tens of atmospheres) and fed into a container filled with a material that can absorb and release H₂ as a function of the pressure, temperature, and amount of stored

hydrogen in the system. The use of metal hydrides reduces the volumetric and pressure requirements for storage, because when fully loaded, these metal hydrides can contain twice as many hydrogen atoms than an equivalent volume of liquid hydrogen. The problem is that it is much heavier than the other solutions. However, current efforts are under way by several automakers to include this in the structure of the vehicle, which may result in an overall acceptable vehicle weight. The prospect of using carbon-nanotube-based materials for hydrogen storage is exciting, because it could eliminate most of the weight penalty. However, it should be noted that the properties of carbon nanotubes regarding their usefulness as H₂ storage materials is still controversial.

One of the myths that must be overcome to popularize fuel cell EVs is the safety of carrying pressurized hydrogen on board. The safety of hydrogen handling has been explored by commercial entities as well as public institutions, such as Air Products and Chemicals, Inc.⁵ and Sandia National Laboratories.⁶ The recommendations for its safe handling have been issued.⁵ In addition, the Ford report suggested that with proper engineering, the safety of a hydrogen vehicle could be better than that of a propane or gasoline vehicle.⁴

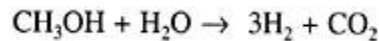
4.1.4 REFORMERS

Many in the automotive industry have been exploring the use of methanol, ethanol, or gasoline as a fuel and reforming it on-board into hydrogen for the fuel cell. The reformer is the fuel processor that breaks down a hydrocarbon, such as methanol, into hydrogen and other by-products. The advantage of this approach is the ease of handling of hydrocarbon fuel compared to hydrogen gas, substantiated by the difficulty in storage and generation of pure hydrogen.

The accepted methods of reforming technique for vehicular fuel cells are steam reforming, partial oxidation, and autothermal processing. The two types of steam reformers in use today use methanol and natural gas as the fuel. Gasoline can also be used as the fuel, but reforming it is an expensive and complex process. Methanol is the most promising fuel for reformers, because it reforms fairly easily into hydrogen and is liquid at room temperature. A brief description of how a methanol steam reformer works is given in the following.

The steam reformer is in fact part of a fuel processor that also includes a water-gas shift reactor.⁷ Steam reforming is carried out by supplying heat to a mixture of steam and fuel over a catalyst. In the case of natural gas, the mixture is fed to the reformer containing a catalyst (such as nickel) at a steam-to-carbon molar ratio of 3.5:1 and 760°C. The reformat is then passed through a low-temperature water-gas shift reactor containing a CuO-ZnO catalyst at 230°C. The process reduces the CO level to below 0.5%, which is essential since CO will poison the fuel cell anode platinum catalyst. The overall reactions in the steam reformer and the water-gas shift reactor are:

In the case of methanol, the mixture of methanol and fuel is reformed in the steam reformer using a catalyst of the transition metal oxide type at a steam-to-carbon molar ratio of 1.3:1 or higher and 250°C. The overall process reaction including the water-gas shift reaction is:



The major pollutant released as exhaust from the steam reformer is the green-house gas carbon dioxide (CO_2), although the concentration is minimal compared to that in the exhaust of internal combustion engines.

The argument for using reformers is that the infrastructure for the production and distribution of such fuel is already in place, although widespread conversion to methanol systems is not straightforward for methanol fuels due to high corrosivity.³ While hydrogen gas would lead to true zero-emission vehicles, it should be noted that reforming hydrocarbon fuels, including methanol and other possible biomass fuels, only shifts the source of emissions to the reformer plant. Other factors to consider are safety of methanol vs. hydrogen handling, including the fact that methanol is violently toxic, whereas hydrogen is innocuous. Methanol vapors tend to accumulate in enclosed spaces like those of gasoline leading to the formation of potentially explosive mixtures, whereas hydrogen will easily escape, even from poorly ventilated areas. The overall efficiency from the well to the wheel of methanol-based transportation will be comparable or even lower than that which can be achieved today from gasoline-based ICEVs.

4.1.5 FUEL CELL EV

A fuel cell EV consists of a fuel storage system that is likely to include a fuel processor to reform raw fuel to hydrogen, a fuel cell stack and its control unit, a power-processing unit and its controller, and the propulsion unit consisting of the electric machine and drivetrain. The fuel cell has current source type characteristics, and the output voltage of a cell is low. Several fuel cells have to be stacked in series to obtain a higher voltage level, and then the output voltage needs to be boosted in order to interface with the DC/AC inverter driving an AC propulsion motor, assuming that an AC motor is used for higher power density. The block diagram of a fuel cell EV system is shown in [Figure 4.3](#). The voltage and current values shown in the figure are arbitrary and are included to give an idea about the typical voltage ratings at different stages of the system. The power electronic interface circuit between the fuel cell and electric motor includes the DC/DC converter for voltage boost, DC/AC inverter to supply an AC motor, microprocessor/digital signal processor for controls, and battery/capacitors for energy storage. The time constant of the fuel cell stack is much slower than that of the electrical load dynamics. A battery storage system is necessary to supply the power during transient and overload conditions and also to absorb the reverse flow of energy due to regenerative braking. The battery pack voltage rating must be high in order to interface directly with the high-voltage DC link, which means that a large number of series batteries will be needed. Alternatively, a bidirectional DC/DC converter link can interface a lower voltage battery pack and the high-voltage DC bus. The battery pack can be replaced by ultracapacitors in a

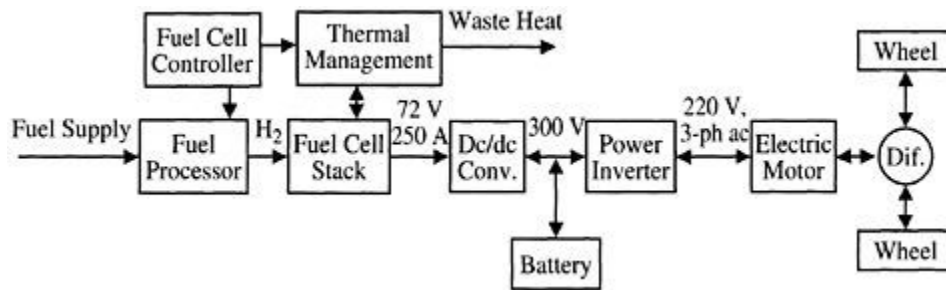


FIGURE 4.3 Fuel-cell-based EV.

fuel cell EV, although the technology is not yet ready to replace batteries. Ultra-capacitors will be discussed in the next section.

Fuel cell performance is sensitive to load variations because of the low voltage and high current output characteristics. The fuel cell controller using voltage and current feedback information regulates the flow of hydrogen into the fuel cell stack to achieve a reaction rate that delivers the required electrical power with minimum excess hydrogen vented. Attempts to draw more power out of the fuel cell without changing the flow rate deplete the concentration of hydrogen, which reduces the output voltage and may lead to damage to the fuel cell membrane.⁸ The fuel cell characteristic curves as a function of flow rate are shown in [Figure 4.4](#). When the hydrogen utilization rate approaches 100%, the cell goes into the current limit mode when it is dominated by high internal losses. The fuel cell controller must avoid operation in the current limit regime in order to maintain a decent efficiency of operation. The output power deliverability of the fuel cell stack reduces with a reduced flow rate of hydrogen, but if lower power is required for traction, then operating the fuel cell at a reduced flow rate minimizes wasted fuel. The ideal controller delivers fuel to the cell at exactly the same rate at which it is consumed by the cell to generate the electricity for the desired propulsion power. However, due to the slow response characteristics of the fuel cell, a reserve of energy is required to provide uninterrupted operation.

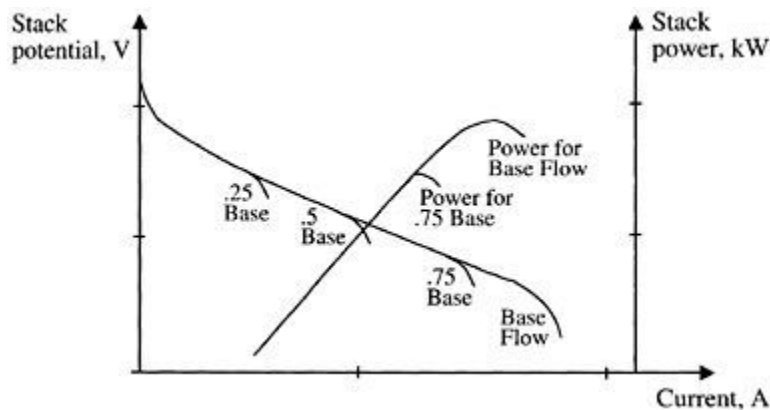


FIGURE 4.4 Fuel cell characteristics as a function of flow rate.

The by-product of the fuel cell reaction is water in the form of steam that exits the cell along with any excess hydrogen. The water vapor can be used for heating the inside of the vehicle, but the hydrogen that is vented out is a waste for the system.

EXAMPLE 4.1

The current drawn by an electric motor of a fuel cell EV for a SAE Schedule D J227A driving cycle is

$$I = \begin{cases} 9.36t + 1.42 + 1.482e^{-3t^3} \text{ A} & \text{for } 0 < t < 28 \\ 61.42 \text{ A} & \text{for } 28 < t < 78 \\ 0 \text{ A} & \text{otherwise} \end{cases}$$

The fuel flow rate for PEM fuel cell used in the vehicle is

$$N_f = \frac{405 I}{nF} \text{ gms/s}$$

- Calculate the amount of fuel (hydrogen) needed for one cycle of Schedule D.
- Calculate the range of the vehicle using Schedule D for the storage capacity of 5 kg of hydrogen.

Solution

- The fuel flow rate from the given equation is

$$N_f = \begin{cases} 0.01964t + 3.11e^{-6t^3} & 0 < t < 28 \\ 0.1289 & 28 < t < 78 \\ 0 & \text{otherwise} \end{cases}$$

The amount of fuel (hydrogen) needed in one cycle can be obtained by integrating the $N_f(t)$ for $t=0$ s to $t=78$ s.

Using numerical integration, we can show that

$$\int_0^{78} N_f(t) dt = 15.10 \text{ gms}$$

- For Schedule D, one cycle is equivalent to 1 mi. Therefore, 5 kg of hydrogen will give a range of $5000/15.1=331$ mi.

4.2 SUPERCAPACITORS AND ULTRACAPACITORS

Capacitors are devices that store energy by the separation of equal positive and negative electrostatic charges. The basic structure of a capacitor consists of two conductors, known as plates, separated by a dielectric, which is an insulator. The power densities of conventional capacitors are extremely high

($\sim 10^{12}$ W/m³), but the energy density is very low (~ 50 Wh/m³).⁹ These conventional capacitors are commonly known as “electrolytic capacitors.” They are widely used in electrical circuits as intermediate energy storage elements for time constants that are of a completely different domain and are of much smaller order compared to the energy storage devices that are to serve as the primary energy sources for EVs. The capacitors are described in terms of capacitance, which is directly proportional to the dielectric constant of the insulating material and inversely proportional to the space between the two conducting plates. The capacitance is measured by the ratio of the magnitude of the charge between either plate and the potential difference between them ($C=q/V$).

Supercapacitors and ultracapacitors are derivatives of conventional capacitors, where energy density has been increased at the expense of power density to make the devices function more like a battery. Power density and energy density of supercapacitors and ultracapacitors are of the order of 10^6 W/m³ and 10^4 Wh/m³, respectively. Energy density is much lower compared to those of batteries (~ 5 to 25×10^4 Wh/m³), but the discharge times are much faster (110 s compared to $\sim 5 \times 10^3$ s of batteries), and the cycle life is much more ($\sim 10^5$ compared to 100 to 1000 of batteries).⁹⁻¹¹

Supercapacitors contain an electrolyte that enables the storage of electrostatic charge in the form of ions, in addition to conventional energy storage in electrostatic charges, like in an electrolytic capacitor. The internal functions in a supercapacitor do not involve electrochemical reaction. The electrodes in supercapacitors are made of porous carbon with high internal surface area to help absorb the ions and provide a much higher charge density than is possible in a conventional capacitor. The ions move much more slowly than electrons, enabling a much longer time constant for charging and discharging compared to electrolytic capacitors.

Ultracapacitors are versions of electrolytic capacitors that use electrochemical systems to store energy in a polarized liquid layer at the interface between an ionically conducting electrolyte and an electrically conducting electrode. Energy storage capacity is increased by increasing the surface area of the interface, similar to that in a supercapacitor. Electrochemical (also known as Faradaic) reactions in ultracapacitors are confined to the surface layers and, hence, are fully reversible with a long cycle life.

Current research and development aim to create ultracapacitors with capabilities in the vicinity of 4000 W/kg and 15 Wh/kg. The possibility of using supercapacitors and ultracapacitors as primary energy sources is quite far reaching, although it is likely that these can be improved to provide sufficient energy storage in HEVs. On the other hand, supercapacitors and ultracapacitors with high specific power are suitable as an intermediate energy transfer device in conjunction with batteries or fuel cells in EVs and HEVs to provide sudden transient power demand, such as during acceleration and hill climbing. The devices can also be used efficiently to capture recovered energy during regenerative braking.

4.3 FLYWHEELS

The flywheel is the kind of energy supply unit that stores energy in mechanical form. Flywheels store kinetic energy within a rotating wheel-like rotor or disk made of composite materials. Flywheels have a long history of usage in automobiles, being routinely used in all of today’s IC engines to store energy and smooth the power delivered by abrupt pulses of the engine. However, the amount of energy storage required in flywheels of IC engines is small and is limited by the need of the vehicle to accelerate rapidly. The flywheel is currently being looked into for use in a number of different capacities. Flywheels can be used in HEVs with a standard IC engine as a power assist device. Alternatively,

flywheels can be used to replace chemical batteries in EVs to serve as the primary energy source or could be used in conjunction with batteries. However, technological breakthroughs in increasing the specific energy of flywheels are necessary before they can be considered as the energy source for EVs and HEVs. The flywheels of today are quite complex, large, and heavy. Safety is also a concern with flywheels.

The flywheel design objective is to maximize energy density. The energy U stored in the flywheel is given by

$$U = \frac{1}{2} J \omega^2$$

where J is the polar moment of inertia, and ω is the angular velocity. Energy storage is increased by spinning at higher velocities without increasing the inertia, which is directly proportional to mass. Increasing angular velocity, in turn, increases centrifugal stress, which must not exceed failure stress with a given factor of safety. Stored energy per unit mass can be expressed as follows:

$$\frac{U}{m} = k \frac{\sigma}{\rho}$$

where k is a constant depending on the geometry, σ is the tensile strength, and ρ is the density of the material. Therefore, the material to be used in a flywheel must be lightweight with high tensile strength, conditions that are satisfied by composite materials.

Flywheels have several advantages as an energy source, the most important of which is the high specific power. Theoretically, specific power of fly wheels has been shown to be of the order of 5 to 10 kW/kg, with a specific power of 2 kW/kg being easily achievable without exceeding safe working stresses. Other performance features that make flywheels attractive can be attributed to their mechanical nature. Flywheels are not affected by temperature extremes. There are no concerns with toxic chemical processing and disposal of waste materials, making flywheels

environmentally friendlier than chemical batteries. Flywheel energy storage is reliable in that it possesses excellent controllability and repeatability characteristics. The state of charge in flywheels is precisely known at all times through measurement of the rotational speed. The energy conversion process to and from the flywheel approaches 98%, compared to 75 to 80% of batteries. The service life of a flywheel is many times that of a battery, with little maintenance required. The charging of flywheels is a fraction of that required by batteries and can be less than 10 min for full recharge in a flywheel charging station. The ability to absorb or release a high amount of power in a short period of time also aids the regenerative braking process.

Despite several advantages, there are still a number of significant drawbacks with flywheels. The major difficulty in implementing a flywheel energy storage system is in the extra equipment needed to operate and contain the device. The extras are particularly difficult in EV and HEV applications, where the extra weight and expense make a big difference. In order to reduce windage losses, the flywheel needs to be enclosed in a vacuum chamber. The vacuum condition adds additional constraints on the bearings, because liquid-lubricated bearings do not survive in vacuum. The alternative is to use magnetic bearings, which are in a development stage. The biggest extra weight in flywheels comes from the safety containment vessel, which is required for protection from the dangerous release of sudden energy and material in the case of a burst failure.

A flywheel, similar to a battery, goes through charge and discharge processes in order to store and extract energy, which earned it the name “electromechanical battery.” The rotor’s shaft is coupled with a motor and generator, which, during charging, spin the rotor to store the kinetic energy and, during discharging, convert the stored energy into electric energy. Interface electronics is necessary to condition the power input and output and to monitor and control the flywheel. Modern flywheels are made of composite materials, such as carbon fiber, instead of steel to increase the energy density, which can be up to 200 Wh/kg. A composite material flywheel has the additional advantage in that it disintegrates in the form of a fluid, as compared to large metallic pieces for a steel-made flywheel, in the case of a catastrophic burst.

REFERENCES

1. Appleby, A.J. and Foulkes, F.R., *Fuel Cell Handbook*, Van Nostrand Reinhold, New York, 1989.
2. Andrews, N., Poised for growth: DG and ride through power, *Power Quality*, January/February, 10–15, 2002.
3. Laughton, M.A., Fuel cells, *Power Eng. J.*, February, 37–47, 2002.
4. Ford Motor Co., Direct-Hydrogen-Fueled Proton-Exchange-Membrane Fuel Cell System for Transportation Applications: Hydrogen Vehicle Safety, Report DOE/CE/50389–502, Directed Technologies Inc., Arlington, VA, May, 1997.
5. Linney, R.E. and Hansel, J.G., Safety considerations in the design of hydrogenpowered vehicles, Part 2, *Hydrogen Energy Progress XI: Proc. 11th World Hydrogen Energy Conf.*, Stuttgart, Veziroglu, T.N. et al., Eds., International Association for Hydrogen Energy, Coral Gables, FL, 1996.

IV B.Tech I Semester Regular Examinations, November/December 2022

ELECTRICAL AND HYBRID VEHICLES
(Electrical and Electronics Engineering)

Time: 3 hours

Max Marks: 70

Instructions:

1. Question paper comprises of **Part-A** and **Part-B**
2. **Part-A** (for 20 marks) must be answered at one place in the answer book.
3. **Part-B** (for 50 marks) consists of **five questions with internal choice**, answer all questions.

PART – A

(Answer ALL questions. All questions carry equal marks)

10 *

2 = 20 Marks

- | | | | | |
|-------|--|-----|-----|-----|
| 1. a. | List out the power control strategies of hybrid electric drive train. | [2] | CO1 | BL1 |
| b. | What are the various electric drive train topologies? | [2] | CO1 | BL1 |
| c. | Analyze the different factor involved in the braking performance of the vehicle. | [2] | CO2 | BL2 |
| d. | Identify the different factors effect the movement of vehicle. | [2] | CO2 | BL2 |
| e. | Classify hybrid electric drive trains. | [2] | CO3 | BL1 |
| f. | Define hybrid traction. | [2] | CO3 | BL1 |
| g. | Define induction motor drives. | [2] | CO4 | BL1 |
| h. | Define permanent magnet motor drives. | [2] | CO4 | BL1 |
| i. | Define super capacitor. | [2] | CO5 | BL1 |
| j. | What is meant by fuel cell? | [2] | CO5 | BL1 |

PART – B

(Answer ALL questions. All questions carry equal marks)

5 *

10 = 50 Marks

- | | | | | |
|----|---|------|-----|-----|
| 2. | Explain about electric traction systems and advantages. | [10] | CO1 | BL2 |
|----|---|------|-----|-----|

OR

- | | | | | |
|----|---|------|-----|-----|
| 3. | Explain the parallel configurations of hybrid drive train with neat diagram? | [10] | CO1 | BL3 |
| 4. | (a) Explain the fully controllable hybrid brake system. | [10] | CO2 | BL2 |
| | (b) Explain the brake system of EV, HEV, and FCV- parallel hybrid braking system. | | | |

OR

5. (a) Explain the power train tractive effort and vehicle speed, vehicle power plant and transmission characteristics. [10] CO2 BL3
(b) Analyze the operation of hydrodynamic transmission from its performance characteristics.

6. (a) What are the social impacts of hybrid electric vehicles? [10] CO3 BL2
(b) What are the environmental impacts of hybrid electric vehicles?

OR

7. Explain about the history of hybrid electric vehicles. [10] CO3 BL2
8. (a) Classify the electric motor drives for electric vehicles and hybrid electric vehicles. [10] CO4 BL2
(b) What are the benefits of induction motors drives used in hybrid electric vehicles?

OR

9. List out the control methods and block diagram of switch reluctance motors used in hybrid electric vehicles. [10] CO4 BL3
10. Describe the basic principle of various energy storage systems in hybrid electric vehicles. [10] CO5 BL4

OR

11. Explain about [10] CO5 BL2
(i) Fuel cell
(ii) Fly wheel.

**ELECTRIC AND HYBRID VEHICLES
ASSIGNMENT**

1.	compare the difference of energy sources used in EVs and EHV's .?
2.	Write the Role of electrifying the transportation system to reduce global warming
3.	Explain about Rolling Resistance and Aerodynamic Drag?
4.	Draw the layout of a EV and discuss the characteristics.
5.	Illustrate the power flow control in hybrid electric drive train
6.	Explain the battery and fuel cell?
7.	Draw and explain the block diagram of switched reluctance motor drive system
8.	Explain the working Principle of PM Brushless DC motor
9.	Distinguish between Super capacitor based energy storage and Fuel cell based energy storage
10.	Briefly explain about different energy storage systems used in EVs?

ELECTRIC AND HYBRID VEHICLES ASSIGNMENT

Unit-I

1. compare the difference of energy sources used in EVs and EHV's .?

Specifications	Hybrid Vehicles	Electric Vehicles
Power/Fuel Source	Electricity and Fossil Fuel (Petrol and Diesel)	Electricity Through Battery Pack (DC)
Engine	Internal Combustion Engine (ICE) and Electric Motor(s)	Electric Motor(s)
Fuel Efficiency	Combination of ICE and Battery Range	Depends on Battery Range
Emission Levels	Higher Compared to Electric Cars	Lower Compared to ICE and Hybrid Cars
Price Range	Similar to Conventional ICE Cars	High
Charging	Not Needed	Needed

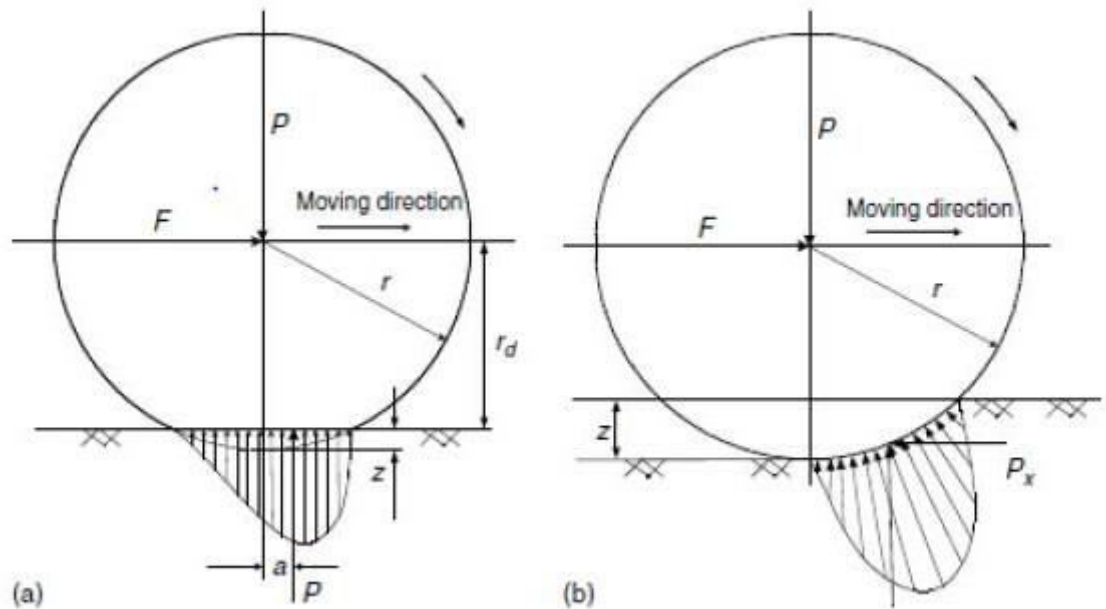
2. Write the Role of electrifying the transportation system to reduce global warming.

Electrification is widely considered an attractive solution for reducing the oil dependency and environmental impact of road transportation. Many countries have been establishing increasingly stringent and ambitious targets in support of transport electrification. While transport electrification alone would not contribute to climate change mitigation, it is interesting to note that switching to electrified road transport under the sustainable shared socioeconomic pathways permitted an optimistic outlook for a low-carbon transition, even in the absence of a decarbonized power sector. Another interesting finding was that the stringent penetration of electric vehicles can reduce the mitigation cost generated by the 2 °C climate stabilization target, implying a positive impact for transport policies on the economic system. With technological innovations such as electrified road transport, climate change mitigation does not have to occur at the expense of economic growth. Because a transport electrification policy closely interacts with energy and economic systems, transport planners, economists, and energy policymakers need to work together to propose policy schemes that consider a cross-sectoral balance for a green sustainable future. Transportation is a growing source of the global greenhouse gas emissions that are driving climate change, accounting for 23% of energy-related carbon dioxide emissions worldwide in 2019 and 29% of all greenhouse gas emissions in the U.S.

Unit-II

3. Explain about Rolling Resistance and Aerodynamic Drag?

The rolling resistance of tires on hard surfaces is primarily caused by hysteresis in the tire materials.

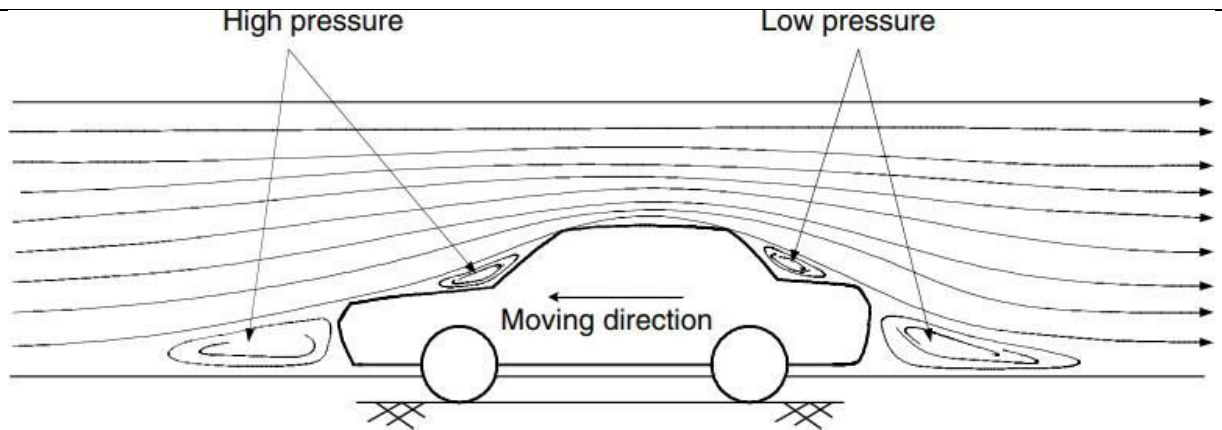


This is due to the deflection of the carcass while the tire is rolling. The hysteresis causes an asymmetric distribution of ground reaction forces. The pressure in the leading half of the contact area is larger than that in the trailing half, as shown in Figure (a). This phenomenon results in the ground reaction force shifting forward. This forwardly shifted ground reaction force, with the normal load acting on the wheel center, creates a moment that opposes the rolling of the wheel. On soft surfaces, the rolling resistance is primarily caused by deformation of the ground surface as shown in Figure (b). The ground reaction force almost completely shifts to the leading half.

Aerodynamic Drag

A vehicle traveling at a particular speed in air encounters a force resisting its motion. This force is known as aerodynamic drag. The main causes of aerodynamic drag are:

- shape drag
- skin friction



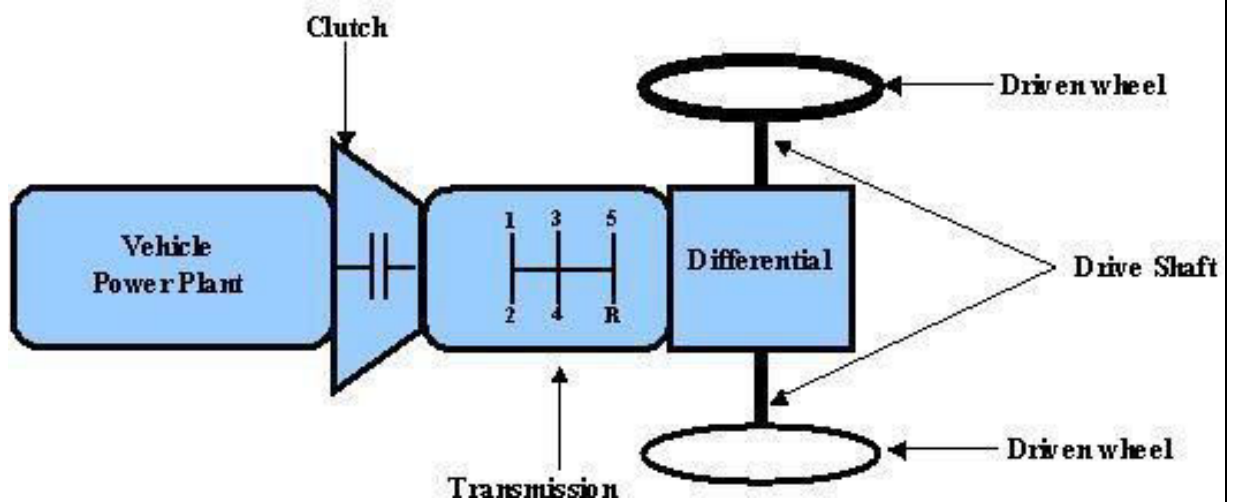
Shape drag

The shape drag is due to the shape of the vehicle. The forward motion of the vehicle pushes the air in front of it. However, the air cannot instantaneously move out of the way and its pressure is thus increased. This results in high air pressure in the front of the vehicle. The air behind the vehicle cannot instantaneously fill the space left by the forward motion of the vehicle. This creates a zone of low air pressure. Hence, the motion of the vehicle creates two zones of pressure. The high pressure zone in the front of the vehicle opposes its movement by pushing. On the other hand, the low pressure zone developed at the rear of the vehicle opposes its motion by pulling it backwards.

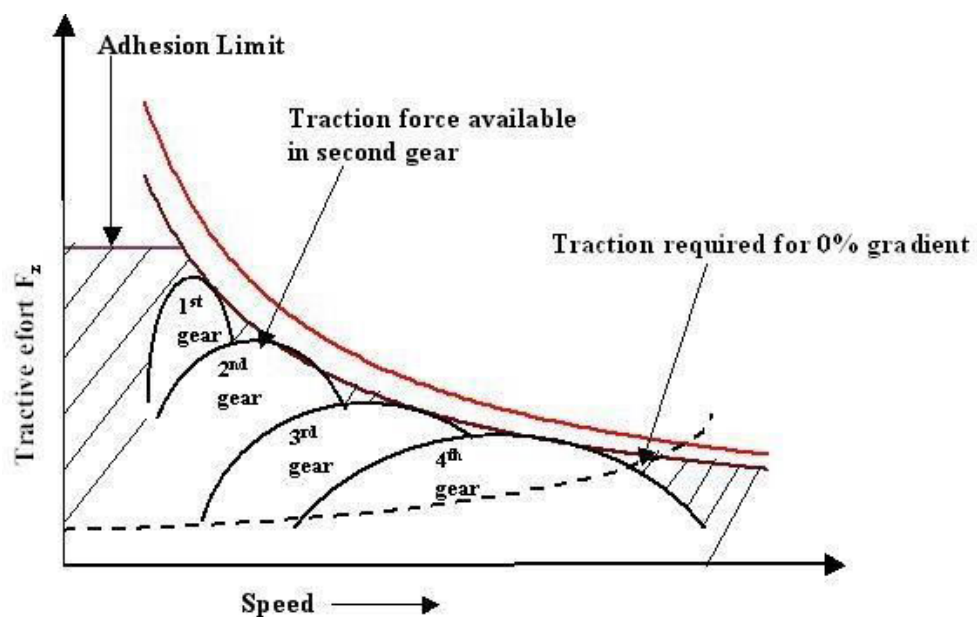
Skin friction

The air close to the skin of the vehicle moves almost at the speed of the vehicle while the air away from the vehicle remains still. Between these two layers (the air layer moving at the vehicle speed and the static layer) the molecules move at a wide range of speeds. The difference in speed between two air molecules produces friction. This friction results in the second component of aerodynamic drag and it is known as skin friction.

4. **Draw the layout of a ev and discuss the characteristics.**
- General lay out of a EV: It consists of a power plant, a clutch in a manual transmission or a torque converter in automatic transmission, a gear box, final drive, differential shaft and driven wheels



Transmission characteristics:



Unit-III

5. Illustrate the power flow control in hybrid electric drive train.

Power Flow Control in Series Hybrid

- Power Flow Control in Parallel Hybrid
- Power Flow Control Series-Parallel Hybrid
- Power Flow Control Complex Hybrid Control

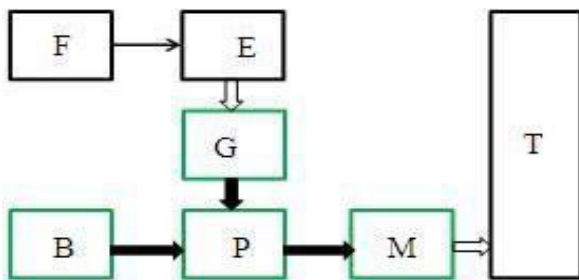
Power Flow Control in Series Hybrid

Figure 1a: Mode 1, normal driving or acceleration

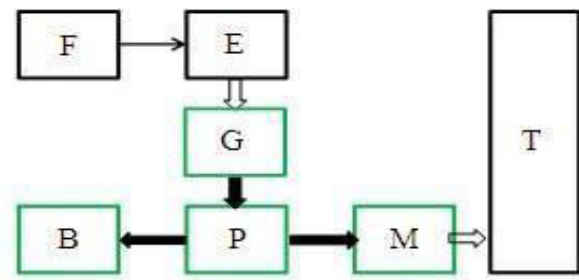


Figure 1b: Mode 2, light load

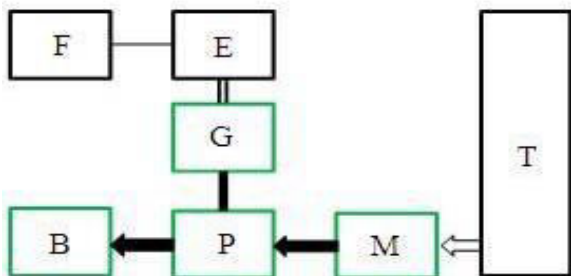


Figure 1c: Mode 3, braking or deceleration

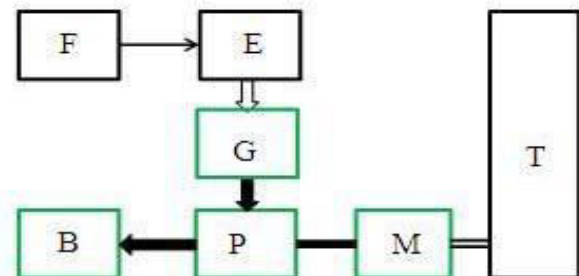


Figure 1d: Mode 4, vehicle at stop

B: Battery
E: ICE
F: Fuel tank
G: Generator
M: Motor
P: Power Converter

— Electrical link
— Hydraulic link
= Mechanical link

T: Transmission (including brakes, clutches and gears)

6. Explain the battery and fuel cell?

A fuel cell is an electrochemical device that continuously generates electricity without the need for any intermediate energy conversion. Hydrogen fuel cells work like batteries, but they do not need any recharging as they produce electricity if there is a supply of H₂ and O₂ as fuels. A fuel cell is made up of a negative electrode (anode), and a positive electrode (cathode) sandwiched around an electrolyte. Hydrogen is fed to the anode, and the air is fed to the cathode. In a hydrogen fuel cell, a catalyst at the anode separates hydrogen molecules into protons and electrons, the electrons go through an external circuit, creating a flow of electricity. The protons migrate through the electrolyte to the cathode, where they unite with oxygen and electrons to produce water and heat.

The expectation from the market is to have safe, green, sustainable, and reliable automobiles with minimal or no wait time for refuelling/recharging like ICE vehicles. However, the current technology is not adequate to cater to these needs. The challenges include a lack of adequate infrastructure (Refuelling stations), Hydrogen produced from fossil fuels which

nullifies the effort to move to greener mobility and would require huge investments to produce green hydrogen through renewable resources. Also, the quantity of hydrogen currently produced is less as it is currently being produced only for industrial purposes and

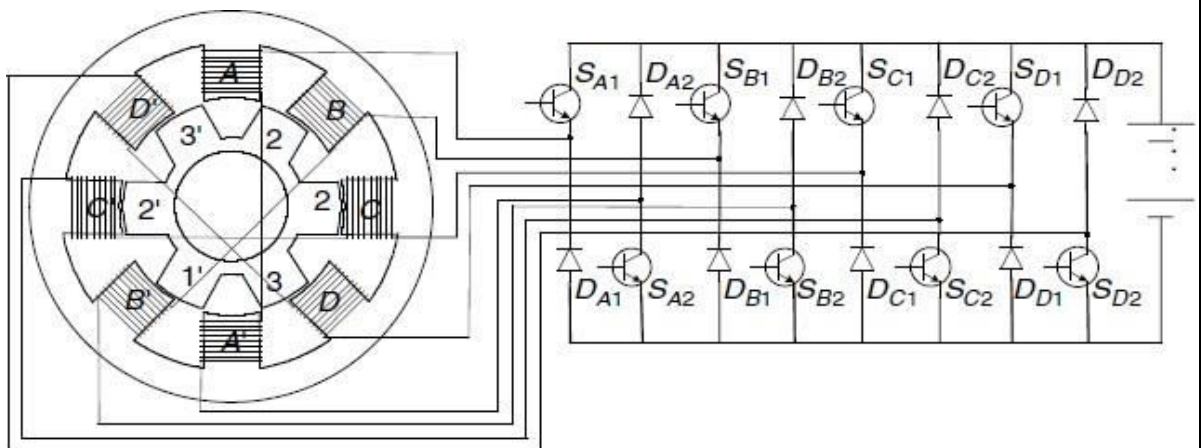
would require additional funds to increase the production to cater to demands from the automobile sector.

Unit-IV

7. Draw and explain the block diagram of switched reluctance motor drive system

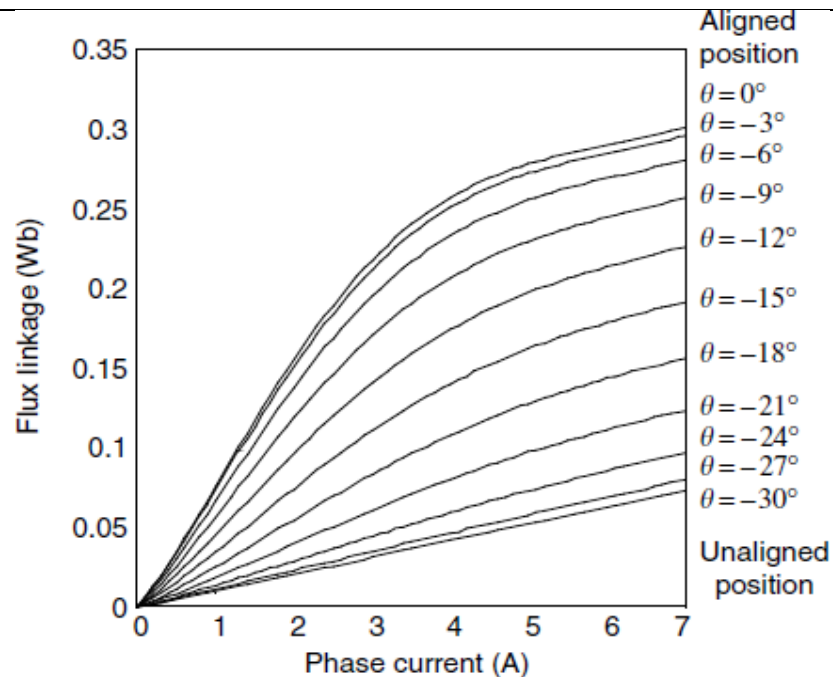
The SRM has a simple, rugged, and low-cost structure. It has no PM or winding on the rotor. This structure not only reduces the cost of the SRM but also offers high-speed operation capability for this motor. Unlike the induction and PM machines, the SRM is capable of high-speed operation without the concern of mechanical failures that result from the high-level centrifugal force.

In addition, the inverter of the SRM drive has a reliable topology. The stator windings are connected in series with the upper and lower switches of the inverter. This topology can prevent the shoot-through fault that exists in the induction and permanent motor drive inverter.



The SRM has salient poles on both the stator and rotor. It has concentrated windings on the stator and no winding or PM on the rotor. There are several configurations for SRM depending on the number and size of the rotor and stator poles.

Due to its double saliency structure, the reluctance of the flux path for a phase winding varies with the rotor position. Also, since the SRM is commonly designed for high degree saturation at high phase current, the reluctance of the flux path also varies with the phase current. As a result, the stator flux linkage, phase bulk inductance, and phase incremental inductance all vary with the rotor position and phase current.



Torque in SRM is produced by the tendency of the rotor to get into alignment with the excited stator poles. The analytical expression of the torque can be derived using the derivative of the co-energy against the rotor position at a given current.

8. Explain the working Principle of PM Brushless DC motor

BLDC motor works on the principle similar to that of a **Brushed DC motor**. The Lorentz force law which states that whenever a current carrying conductor placed in a magnetic field it experiences a force. As a consequence of reaction force, the magnet will experience an equal and opposite force. In the BLDC motor, the current carrying conductor is stationary and the permanent magnet is moving. When the stator coils get a supply from source, it becomes electromagnet and starts producing the uniform field in the air gap. Though the source of supply is DC, switching makes to generate an AC voltage waveform with trapezoidal shape. Due to the force of interaction between electromagnet stator and permanent magnet rotor, the rotor continues to rotate.

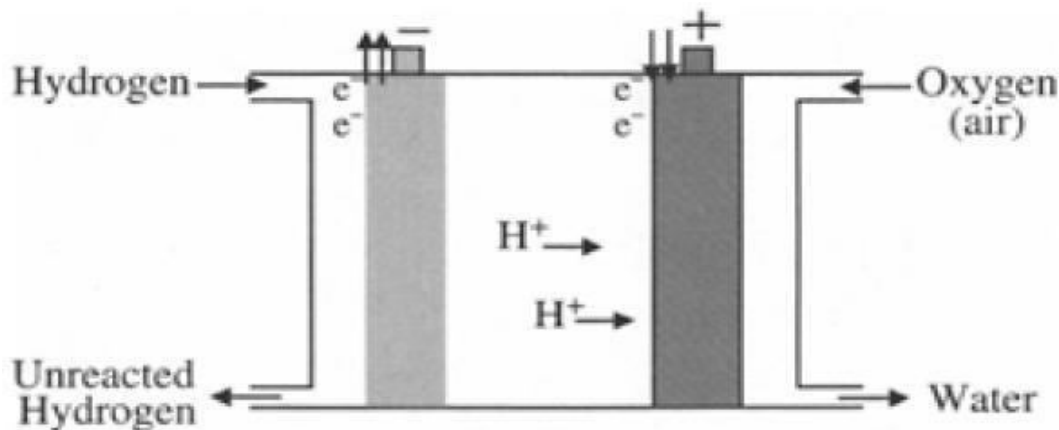
Unit-V

9. Distinguish between Super capacitor based energy storage and Fuel cell based energy storage

There are a number of requirements for energy storage applied in an automotive application, such as specific energy, specific power, efficiency, maintenance management, cost, environmental adaptation and friendliness, and safety. For allocation on an EV, specific energy is the first consideration since it limits the vehicle range. On the other hand, for HEV applications specific energy becomes less important and specific power is the first consideration, because all the energy is from the energy source (engine or fuel cell) and sufficient power is needed to ensure vehicle performance, particularly during acceleration, hill climbing, and regenerative braking.

(b) A fuel cell is an electrochemical device that produces electricity by means of a chemical

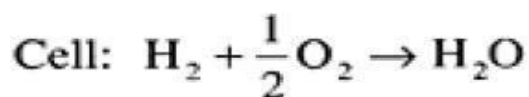
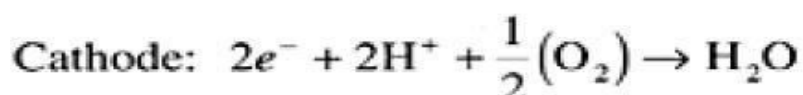
reaction, much like a battery.



The major difference between batteries and fuel cells is that the latter can produce electricity as long as fuel is supplied. Batteries produce electricity from stored chemical energy and, hence, require frequent recharging.

The basic structure of a fuel cell consists of an anode and a cathode, similar to a battery. The fuel supplied to the cell is hydrogen and oxygen. The concept of fuel cell is the opposite of electrolysis of water, where hydrogen and oxygen are combined to form electricity and water.

The chemical reaction taking place in a fuel cell is as follows:



10. Briefly explain about different energy storage systems used in EVs?

With the development of energy storage technology, the main energy storage technology can be divided into the following categories. According to the classification of technology, it is divided into four categories: Physical storage (such as pumped storage, compressed air energy storage, flywheel energy storage, etc.), chemical energy storage (such as sodium sulfur batteries, flow batteries, lead-acid batteries, nickel-cadmium batteries, supercapacitor, etc.), Energy Storage (superconducting magnetic energy storage, etc.) and the phase change energy storage (ice storage, etc.). Large-capacity, high-density, high-efficiency, low-cost and long service life of the storage energy technology is undoubtedly the most ideal, but so far there is not a kind of

energy storage technology can satisfy these conditions simultaneously. Therefore, it is necessary for all storage technology choice suitable application field, namely the right selection of energy storage. Under normal circumstances, when the selection of energy storage system, the economy, security and stability, and the capacity of the energy storage system should be considered. It can be predicted that the future power grid will be presented with a situation of energy storage, and the largest proportion of clean energy, fossil energy is used as auxiliary. The rational allocation of the load control system, and complemented by high-performance power electronic devices, flexible transmission, distributed power supply, demand response, efficient control of the new clean energy development model systems and other advanced technologies.

IV B.Tech I Semester Regular Examinations, December 2021
ELECTRICAL AND HYBRID VEHICLES
 (Electrical and Electronics Engineering)

Time: 3 hours

Max Marks: 70

< **Note:** Type the questions in the given format only, Times New Roman font , size 12 >

Instructions:

1. Question paper comprises of **Part-A** and **Part-B**
2. **Part-A** (for 20 marks) must be answered at one place in the answer book.
3. **Part-B** (for 50 marks) consists of **five questions with internal choice**, answer all questions.

PART – A

(Answer ALL questions. All questions carry equal marks)

10 * 2 = 20 Marks

1. a.	Why a gear system is needed for an ICE?	[2]	CO1	BL1
b.	Sketch the ideal torque-speed characteristics required for an electric/hybrid vehicle power plant.	[2]	CO1	BL1
c.	Define Maximum Tractive Effort	[2]	CO2	BL1
d.	What are the important subsystems in an electric/hybrid vehicle?	[2]	CO2	BL1
e.	Explain the working principle of a fuel-cell.	[2]	CO3	BL1
f.	Compare conventional vehicle with Hybrid electric vehicle.	[2]	CO3	BL1
g.	Classify the electric motors drives for EV and HEV application.	[2]	CO4	BL1
h.	What are the desired features of motors used for electric vehicles?	[2]	CO4	BL1
i.	Explain the terms specific power and energy efficiency of a battery.	[2]	CO5	BL1
j.	What are the sizing constraints for the electric motor?	[2]	CO5	BL1

PART – B

(Answer ALL questions. All questions carry equal marks)

5 * 10 = 50 Marks

2.	Write short notes on fuel efficiency analysis in hybrid electric drive-trains.	[10]	CO1	BL2
----	--	------	-----	-----

OR

3.	Enlist the different architectures of hybrid electric drive train and explain the series hybrid electric drive train	[10]	CO1	BL1
4.	Explain the term rolling resistance and aerodynamic drag in vehicles and derive the expression for vehicle translational speed from fundamentals.	[10]	CO2	BL4

OR

5.	State and explain the dynamic equation of vehicle motion	[10]	CO2	BL3
----	--	------	-----	-----

6.	Explain the different power flow control modes of a typical parallel hybrid system with the help of block diagrams.	[10]	CO3	BL2
OR				
7.	What are the social and environmental impacts of hybrid vehicles?	[10]	CO3	BL2
8.	Draw and explain the block diagram of switched reluctance motor drive system.	[10]	CO4	BL3
OR				
9.	Explain the four-quadrant chopper control of dc motor.	[10]	CO4	BL4
10.	What are factors affecting the performance of batteries used in EVs? Explain Each factor in detail.	[10]	CO5	BL2
OR				
11.	Explain fuel cell and flywheel as energy source elements in electric and hybrid electric vehicle	[10]	CO5	BL2



IV B.Tech I Sem (EEE) Result Analysis

Academic Year: 2022-23

Total No. of Students Registered: 129

Course	Total No. of Students appeared	Total No. of Students Passed	No. of Students Failed	Count of Students with Grade Point					
				GP (10)	GP (9)	GP (8)	GP (7)	GP (6)	GP (5)
DBMS	59	50	09	00	01	07	19	27	07
PS-III	129	125	04	01	12	37	35	32	08
ED	129	127	02	04	45	4	22	08	01
EHV	129	126	03	11	17	32	47	13	06
HVE	129	126	03	01	18	32	41	25	09
ED Lab	129	129	00	71	26	21	06	05	00
PW Lab	129	129	00	16	52	37	15	09	00
ROBOTICS	70	70	00	13	21	17	05	03	00

Arrears Position – IV year / I Semester

No. of students	All Pass	One Arrear	Two Arrears	Three Arrears	More than three arrears	Overall % of pass
129	119	06	00	02	02	92%

Performance overall Class Three Toppers

ROLL NO.	NAME	SGPA
19241A0252	Suchismita Das	8.96
19241A0236	Nimmanagoti Sowmya	8.79
19241A0250	Saraswathi Srikari	8.63

Class coordinator

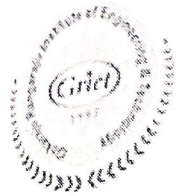
HOD, EEE

IV B.Tech - I Sem (EEE)

SECTION	Courses	DBMS	PS-III	ED	EHV	HVE	ED Lab	PW	ROBOTICS
	Course codes	GR18A2068	GR18A4012	GR18A4013	GR18A4014	GR18A4021	GR18A4022	GR18A4061	GR18A4079
A	TOTAL	36	63	63	63	63	63	63	23
	PASS	33	61	62	61	61	63	63	23
	PASS (%)	91.66	96.82	98.41	96.82	96.82	100	100	100
	FACULTY NAME	D Swathi	Dr P Srividya Devi	Dr D S N M Rao	D Srinivasa Rao	A Vinay Kumar	P Ravikanth /Dr DSNM Rao	A Vinay Kumar/ D Srinivasa Rao	Dr Anitha
	FACULTY ID		931	1598	1598	881	1178/1598	881/1598	944
B	TOTAL	23	66	66	66	66	66	66	47
	PASS	17	64	65	64	65	66	66	47
	PASS (%)	73.91	96.96	98.48	96.96	98.48	100	100	100
	FACULTY NAME	D Swathi	P Prashanth Kumar	Dr D S N M Rao	D Srinivasa Rao	A Vinay Kumar	D Karuna Kumar/ V Usha Rani	M N Sandhya Rani / G Sandhya Rani	Dr Anitha
	FACULTY ID		1055	1598	1598	881	760 /1045	882/888	944

Class coordinator

HOD, EEE

**GOKARAJU RANGARAJU INSTITUTE OF ENGINEERING AND TECHNOLOGY**

Approved By AICTE, Affiliated to JNTUH, Autonomous Under UGC

Nizampet Road, Bachupally, Kukatpally, Hyderabad - 500090, Telangana, India

Tel: 7207344440, Email: info@griet.ac.in, www.griet.ac.in

STUDENT FEEDBACK

Faculty : DAVU. SRINIVASA RAO
 Subject : Electrical And Hybrid Vehicles (B.Tech, IV/IV B.Tech I Semester, EEE Sec-A)
 Academic Year : 2022 - 2023
 Phase : Phase-2

Sl.No	Question	Excellent	Good	Average	Poor	Q.Wise Total	Q.Wise %
1	Preparation and delivery of the lessons by the teacher	21	16	1	1	135	87.00
2	Subject Knowledge	20	16	2	1	133	85.00
3	Clarity in Communication	19	16	3	1	131	84.00
4	Using Modern Teaching Aids of ICT	19	16	3	1	131	84.00
5	Creating interest on the course in the class	18	16	4	1	129	83.00
6	Maintaining discipline in the class	18	17	2	2	129	83.00
7	Encouraging and clearing doubts in the class	17	20	1	1	131	84.00
8	Punctuality	19	16	3	1	131	84.00
9	Accessibility of the teacher	18	17	2	2	129	83.00
10	Overall grading of the teacher	19	16	2	2	130	83.00
Total		188	166	23	13		
Total Points		752	498	46	13	1309	84.00

No.Of Students Posted	39
Total Percentage Awarded to The Faculty	84.00
Grade of Faculty	Good

*Excellent (4) : $\geq 90\%$ *Good (3) : $\geq 75\%$ & $< 90\%$ *Average (2) : $\geq 60\%$ & $< 75\%$

*Poor (1) : Below 60 %

Formula: Total Obtained Points/(Max Points(i.Excellent-4) * No.Of.Students * NoOfQuestions)



Gokaraju Rangaraju Institute of Engineering and Technology

(Autonomous)

Bachupally, Kukatpally, Hyderabad – 500 090

Direct Internal CO Attainments

Academic Year	2022-23	Department		Electrical and Electronic Engineering			
Year - Semester	IV- I	Course Name :		Electrical and Hybrid Vehicles			
		Mid -I					
	Q.No 1(a)	Q.No 1(b)	Q.No 2	Q.No 3	Q.No 4(a)	Q.No 4(b)	Objective Marks
Enter CO Number → 1,2,3,4,5,6,7	1	1	2	3	2	3	1,2,3
Marks →	3	2	5	5	3	2	5

Name of the Programme	B.Tech					
Course Code	GR18A4014		Section	A & B		
Mid-II						
Q.No 1	Q.No 2	Q.No 3(a)	Q.No 3 (b)	Q.No 4(a)	Q.No 4 (b)	Objective Marks
3	4	4	4	5	5	3,4,5
5	5	3	2	3	2	5

Assignment Marks					Assessment
I	II	III	IV	V	Marks
1,2	2,3	3,4	4,5	5,1	1,2,3,4,5
5	5	5	5	5	5

S.No/Roll No.	Note : Enter Marks Between Two Green rows. Another Note : Additional Columns if Required should be inserted after column H and appropriately rename the Q. Nos. For Calculations consult Departments CO-PO Incharge													
First Record / 1	3	2	3			3		3		3		3		3
2	3	2	5			3		2		3				
3	3	2	3			3		2		2				
4	2	2		3	2	2		3						
5	3	2		4	2	2		2						
6	3	2	5	4						2				
7	1	2	3		3	2		2						
8	2	2		3	1	1		2						
9	3	2			1	0		3						
10	3	2	5		3	2		2						
11	3			4	2	2		2						
12	3	2	3					3						
13	3	2	5		3	2		3						
14	3	2	3		3	2		2						
15	2	2		3	2	2		3						
16	2	2	3					2						
17	3	2	3		2	2		3						
18	3	2	4		3	1		4						
19	2	2	3		2	1		3						
20	3	2			3	2		2						
21	3	2	5		2	2		2						
22	2	2			1	2		2						
23	2	2	3		3	1		4						
24	2	2	2		2	2		4						
25	3	2	5		3	2		3						
26	AB	AB	AB	AB	AB	AB		AB						
27	3	2	3		3	2		3						
28	3	2				1		2						
29	3	2			3	2		2						
30	2	2			3	1		3						
31	3		3		3			2						
32	2	2			1	2		2						
33	3	2		4	2	2		4						
34	2	2	2		2	2		3						
35	3	2	5		3	2		3						
36	2	2	5		3	2		4						
37	3	2						2						
38	3	2			3			2						
39	AB	AB	AB	AB	AB	AB		AB						
40	3	2	4		3	2		3						
41	3	2	3		2	2		3						
42	3	2			3			3						
43	3	2	4		2	2		2						
44	3	2	5		3	2		1						
45	3	2			3			2						
46	3	2	4		3	2		2						
47	3	2	3		3	1		3						
48	3	2	5		3	2		2						
49	3	2	4		3	2		2						
50	3	2	5		3	2		2						
51	3	2		5	3	2		2						

123	2	2	2		2	2	2		3	3	3	2			4	4	4	4	4	5
124	3	2	4		2	2	2		4	4	3	2			4	5	5	5	5	4
125	3	2		2	3	1	3			2	2	2	2	2	4	3	3	3	3	3
126	AB	AB	AB	AB	AB	AB	AB			2	4	2	3	2	4	4	4	4	4	4
127	2	2	2		2	2	2				3	2			4	3	3	3	3	4
128			4	2			3			3	3	2	2	2	4	4	4	4	4	4
Last Record	3	2	5		2		2				3	2	3	2	4	3	3	3	3	4

if your class strength is > 60 then *insert rows above the green row(last record)*, Similarly *delete the empty rows above green row* if the class strenght is < 60)

Total number of students appeared for the examination (NST)	129	129	129	129	129	129	129		129	129	129	129	129	129	129		129	129	129	129	129	129
Total number of students attempted the question (NSA)	115	113	66	38	100	96	120		85	115	117	109	49	46	126		129	129	129	129	129	129
Attempt % (TAP) = (NSA/NST)*100	89.15	87.60	51.16	29.46	77.52	74.42	93.02		65.89	89.15	90.70	84.50	37.98	35.66	97.67		100.00	100.00	100.00	100.00	100.00	100.00
Total number of Students who got more than 60% marks (NSM)	115	113	61	30	100	95	52		73	101	117	107	49	46	124		129	129	129	129	129	129
Attainment % (TMP) = (NSM/NSA)*100	100.00	100.00	92.42	78.95	100.00	98.96	43.33		85.88	87.83	100.00	98.17	100.00	100.00	98.41		100.00	100.00	100.00	100.00	100.00	100.00
Score(S)	3	3	3	3	3	3	1		3	3	3	3	3	3	3		3	3	3	3	3	3

Note : CO attainment is considered to be zero if the attempt % is less than 30%

CO Validation	1	1	2	3	2	3	1,2,3		3	4	4	4	5	5	3,4,5		1,2	2,3	3,4	4,5	5,1	1,2,3,4,5
Course Outcome	CO1	CO1	CO2	CO3	CO2	CO3	CO1,CO2,CO3		CO3	CO4	CO4	CO4	CO5	CO5	CO3,CO4,CO5		CO1,CO2	CO2,CO3	CO3,CO4	CO4,CO5	CO5,CO1	CO1,CO2,CO3,CO4,CO5
Marks (Y)	3	2	5	5	3	2	5		5	5	3	2	3	2	5		5	5	5	5	5	5
No. of COs Shared (Z)	1	1	1	1	1	1	3		1	1	1	1	1	1	3		2	2	2	2	2	5
Y/Z	3	2	5	5	3	2	1.666666667		5	5	3	2	3	2	1.666667		2.5	2.5	2.5	2.5	2.5	1
S*Y/Z	9	6	15	15	9	6	1.666666667		15	15	9	6	9	6	5		7.5	7.5	7.5	7.5	7.5	3

CO1	1	1	0	0	0	0	1		0	0	0	0	0	0	0		1	0	0	0	1	1
CO2	0	0	1	0	1	0	1		0	0	0	0	0	0	0		1	1	0	0	0	1
CO3	0	0	0	1	0	1	1		1	0	0	0	0	0	1		0	1	1	0	0	1
CO4	0	0	0	0	0	0	0		0	1	1	1	0	0	1		0	0	1	1	0	1
CO5	0	0	0	0	0	0	0		0	0	0	0	1	1	1		0	0	0	1	1	1

Weighted Average for Attainment relevance (Internal CODn)	CO1	CO2	CO3	CO4	CO5
	2.74	2.79	2.84	3.00	3.00

!!

!! Caution !! For CO Values < 2.1 should be justified with Remedial Action Report.